K8-10278

MM

TP9308E

CA1
DTC 800
88
L33
c.2

LINEAR INDUCTION MOTORS
AND
THEIR CONTROL SYSTEMS

BY

K. VOLLENWYDER, W.J. BALLANTYNE, L. PATTISON

UTDC INC.

Library and Information Centre /
Centre de Documentation (GSLA)
RECEIVED - REÇU LE
NOV 18 1988
Transport Canada / Transports Canada

PREPARED FOR:	**TRANSPORT CANADA, TRANSPORTATION DEVELOPMENT CENTRE**
D.S.S. FILE NO:	**11SD.T8200-5-5565**
UTDC INC. REPORT NO:	**454 991 001**
DATED:	**MARCH 31, 1988**

398470

K7-10269

DISCLAIMER

The contents of this report reflect the views of the contractor and not necessarily the official views of the Transportation Development Centre of Transport Canada.

Un sommaire en français de ce document est inclus avant la table des matières.

Transport Canada Transports Canada
Development Développement

REPORT DOCUMENTATION FORM

1. Transport Canada Report No.
TP9308E

2. TDC Project No.
6598/6599

3. Recipient's Catalogue No.

4. Title and Subtitle
LINEAR INDUCTION MOTORS AND THEIR CONTROL SYSTEMS

5. Report Date
March 31, 1988

6. Performing Organization Report No.
454-991-001

7. Author(s)
K. Vollenwryder, W.J. Ballantyne, L. Pattison

8. Transport Canada File No.
D1465-427-2

9. Performing Organization Name and Address
UTDC Inc.
P.O. Box 70, Station 'A'
Kingston, Ontario
K7M 6P9

10. DSS File No.
T8200-5-5565

11. DSS or Transport Canada Contract No.
11SD.T8200-5-5565

12. Sponsoring Agency Name and Address
Transportation Development Centre (TDC)
200 René-Lévesque Blvd. West
Suite 601, West Tower
Montreal, Quebec H2Z 1X4

13. Type of Report and Period Covered
Final

14. Sponsoring Agency Code

15. Supplementary Notes

16. TDC Project Officer
C.A. Versailles

17. Abstract
The purpose of this projct was to advance the technology of LIT (Linear induction motors in track) propulsion, improve linear induction motor (LIM) design techniques and identify new applications for LIT propulsion. A variable voltage, fixed frequency (60 Hz) intelligent LIM control module was designed and constructed. A network of these controllers operates under the supervision of a host computer. The host performs routing control and general housekeeping tasks, leaving time-critical tasks to the control modules. A network comprising a host and several LIM control modules was successfully tested. Replacement of the variable voltage, fixed frequency LIM power supplies used in the LIM control module by variable voltage, variable frequency (VVVF) supplies was investigated. Simulation and limited testing indicated that a significant gain in performance could be obtained by using the VVVF supplies. Several LIMs were tested using a pulse width modulated (PWM) voltage source inverter, over a wide range of speeds and supply frequencies. The experimental results were compared with predictions generated by a new mathematical LIM model. The model predicted machine behaviour, including the speed dependent end effect, over a wide range of operating conditions. The system requirements for several new LIT applications were identified, including airport baggage handling and people mover system. Valuable experience gained during this project will allow better LIM and LIT design and increased technical performance and capability.

18. Key Words
Linear Induction Motors. Control Systems.

19. Distribution Statement
A limited number of copies are available from the Transportation Development Centre.

20. Security Classification (of this report)
Unclassified

21. Security Classification (of this page)
Unclassified

22. No. of Pages
432

23. Price

TDC/CDT 79-005
Rev 86

Canada

Transports Canada Transport Canada
Développement Development

FORMULE DOCUMENTAIRE DU RAPPORT

1. Nº du rapport Transports Canada: TP9308E

2. Nº de l'étude — CDT: 6598/6599

3. Nº de catalogue du destinataire:

4. Titre et sous-titre: LINEAR INDUCTION MOTORS AND THEIR CONTROL SYSTEMS

5. Date du rapport: 31 mars 1988

6. Nº du rapport de l'organisme exécutant: 454-991-001

7. Auteur(s): K. Vollenwryder, W.J. Ballantyne, L. Pattison

8. Nº de dossier Transports Canada: D1465-427-2

9. Nom et adresse de l'organisme exécutant:
UTDC Inc.
B.P. 70, Succursale 'A'
Kingston, Ontario
K7M 6P9

10. Nº de dossier — ASC: T8200-5-5565

11. Nº de contrat — ASC ou Transports Canada: 11SD.T8200-5-5565

12. Nom et adresse de l'organisme parrain:
Centre de développement des transports (CDT)
200 ouest boul. René-Lévesque
Suite 601, Tour ouest
Montréal, Québec H2Z 1X4

13. Genre de rapport et période visée: Final

14. Code de l'organisme parrain:

15. Remarques additionnelles:

16. Agent de projet — CDT: C.A. Versailles

17. Résumé La recherche avait pour objectif de faire progresser la technologie du moteur linéaire à induction dont les parties actives sont encastrées dans le sol, de lui trouver de nouvelles applications et d'améliorer les techniques d'étude de ces moteurs. Une électronique de commande "intelligente" à tension variable et à fréquence fixe (60 Hz) a été conçue et réalisée, le réseau formé par l'ensemble de ces régulateurs étant placé sous la surveillance d'un ordinateur central. Celui-ci commande les acheminements et gère les opérations de servitude générales, laissant eux-mêmes aux régulateurs les fontions oû le temps est un facteur capital. Un réseau formé d'un ordinateur central et de plusieurs régulateurs a été essayé avec succès. L'idée de remplacer une alimentation à fréquence fixe par une autre à fréquence variable, tout en gardant la tension variable, a été étudiée en simulation et soumise à des essais de portée limitée. Il a été montré que les performances pouvaient être considérablement accrues grâce à une alimentation à tension et fréquence variables. Des essais ont été faits à l'aide d'un onduleur à modulation de largeur d'impulsions, dans une vaste gamme de vitesses et de fréquences d'alimentation. Les résultats de ces expérimentations ont été comparés aux résultats théoriques produits par un nouveau modèle mathématique permettant de simuler les moteurs linéaires à induction. Celui-ci a donné une bonne approximation des valeurs réelles, compte tenu même des effets d'extrémités liés à la vitesse, dans une vaste plage de variation des conditions d'exploitation. Les exigences imposées par diverses applications nouvelles ont été identifiées, notamment un système de convoyage de bagages et de transport hectométrique de personnes dans les aéroports. La recherche a permis d'élargir le champ des connaissances et débouchera sur des performances et des aptitudes améliorées dans le domaine des moteurs linéaires à induction.

18. Mots-clés:
Moteurs à induction linéaires.
Systèmes de contrôle.

19. Diffusion: Le Centre de développement des transports dispose d'un nombre limité d'exemplaires

20. Classification de sécurité (de ce rapport): non classifié

21. Classification de sécurité (de cette page): non classifiée

22. Nombre de pages: 432

23. Prix:

CDT/TDC 79-005
Rev 86

Canada

ACKNOWLEDGEMENT

The research and development program for linear induction motors and their control systems has been carried out under a contract awarded by the Department of Supply and Services on behalf of the Transportation Development Centre. The help of Transport Canada staff and Queen's University is gratefully acknowledged.

SUMMARY

Of the various forms of linear electric propulsion that have been introduced over the past several decades, the linear induction motor (LIM) has been found the most practical for low and medium speed vehicle-drive applications.

Various configurations of LIM are possible. Some feature the "double-sided" topology in which a magnetic field and reactive surface are present on two faces of the motor. More common for vehicular applications, however, is the single-sided variety, which has proven much simpler to integrate into vehicle/track designs.

Two basic configurations of the single-sided LIM are used for vehicle propulsion. One has the active, or primary, part of the motor fixed to the vehicle, and the passive, or secondary, part fixed to the track. This configuration was adopted by UTDC for use on the Intermediate Capacity Transit System (ICTS) vehicles.

The other LIM configuration uses a series of primaries in the track and a passive secondary fixed to the vehicle. UTDC has identified potential applications for this form of propulsion in areas such as airports, industrial handling systems and people moving. The attractive aspects of this technology, referred to as LIT (LIM-in-Track), derive from three of its key features:

1) The vehicles carry no active propulsion equipment.

2) No power-collector rail is required for wayside-to-vehicle power transmission.

3) Control of vehicle motoring and braking is inherently "distributed" through the system.

The special features of LIT propulsion have long been recognized, and a number of system products based on LIT have been developed by various companies around the world. In 1984, UTDC decided that the application scope for LIT was sufficiently greater than that being addressed by the current state-of-the-art as to warrant a comprehensive technology development effort. With the assistance of Transport Canada's Transportation Development Centre (TDC), it embarked on the "Linear Induction Motors and Their Control Systems" program.

The UTDC/TDC program covered a wide range of topics pertinent to the technology of LIT and its application:

Chapter 2 reviews the history of LIM propulsion and identifies the areas of LIT application that continue to hold promise.

Chapter 3 goes into some detail describing four areas of potential application and compares and contrasts the specific requirements imposed by each on the LIT propulsion and control system.

SUMMARY (Cont'd)

Chapter 4 highlights a number of practical design considerations which arise from the general LIT approach.

Chapter 5 details the specific design considerations for fixed and variable frequency LIMs and supports these with descriptions of the analytical and experimental facilities developed under the program.

Chapter 6 explores the potential of "expert system" software as a LIM design aid.

Chapter 7 presents the concept of distributed control in LIT systems and shows how this concept may be used to advantage to provide many system functions.

Chapters 8 through 11 review the areas of component development which were covered under the program. Power control and communications approaches are compared generally, and two specific LIM controller designs are described.

Chapter 12 examines the trade-off between the fixed frequency and the variable frequency control approach and makes some observations about the suitability of each in general.

Chapter 13 provides a look into the theory and application of LIM slip power recovery. Issues of design practice and technical feasibility are reviewed, and proposed uses are presented.

As a result of the program, a number of important conclusions were able to be formulated; these are summarized below.

RANGE OF APPLICATION

The basic LIT propulsion and control concepts described in this report are technically able to meet a very wide range of performance requirements.

The four applications specifically reviewed were:

1) a low speed industrial transport system
2) a high speed airport baggage transporter
3) an airport people-mover
4) a container handling system

In each case, LIT with distributed control seems highly appropriate.

In fact, one might be at a loss to suggest any other technology that could satisfy the requirements of all four areas. Wheel adhesion limitations eliminate self-powered, wheel-driven alternatives. The power-rail hazard potential eliminates LIM-on-board, and belt or roller conveyor systems cannot achieve the required speeds.

SUMMARY (Cont'd)

While the four application areas studied exhibited widely varying requirements in terms of speeds, masses, grades and system lengths, they do not appear significantly different in terms of required functions. It is therefore likely that the key elements of the system, i.e. LIM controllers, communications network, sensors, etc., could be designed as "universal", mass-producable components.

LIM DESIGN

Design studies highlight the fact that there are key trade-offs in the areas of stator weight, and real and reactive power consumption. Assuming that appropriate weighting figures can be applied to these, optional designs may be sought so long as variable frequency (VF) control is employed. Fixed frequency (FF) control severely restricts opportunities to optimize.

There appears to be less to be gained by adapting VF control for "small" LIMs than for "big" LIMs. Below the range of 2-3 kN and 5% duty cycle, it is not possible to effectively exploit longer pole pitch in a design; hence, a key advantage of the VF approach is lost.

Above this range, LIMs designed for VF control are significantly better than FF-controlled LIM designs in terms of real and reactive power consumption.

Defining a methodology for LIM design has proven very difficult. A first step is to achieve an even balance of thermal and magnetic loading over the expected range of operating speeds and frequencies. Beyond this, judgement is required to achieve the appropriate trade-off balance of stator weight, reaction plate weight, real power and apparent power consumption. The trade-offs can be quite dramatic. For example, one design comparison was made in which a 29% stator weight increase resulted in a factor of two reduction in apparent power consumption.

Expert system software would not provide "answers" to trade-off dilemmas, but it may play a role in the "coaching" of inexperienced designers by explicitly highlighting the trade-off issues corresponding to any given step in the design process. For example, at the point where the designer selects a top cap depth the expert system might "suggest" that he try two slightly different depths and observe the sensitivities of weight, apparent power, etc. to this parameter.

MODELLING

The LIM model presented in this report predicts trends and performance reasonably well so long as the designs it models do not exhibit strong magnetic saturation or lateral edge effects. While better predictive tools are definitely available, it must be stressed that the utility of a model is determined as much or more by its "accessibility" as by its accuracy. Models that use involved mathematical constructions and which fail to link the abstract formulations with suitable physical pictures are likely to be more a hindrance than a help.

SUMMARY (Cont'd)

A technique which proved very useful was to augment the simple LIM model when necessary with Finite Element Analysis (FEA). FEA, when correctly employed and interpreted, can produce a very accurate picture of the electromagnetic behaviour of a given LIM design. However, setting up the model and running variant design cases is relatively cumbersome. A combination of the simpler model and FEA works better than either alone.

DISTRIBUTED PROPULSION CONTROL

It is hard to overstate the significance of the distributed control concept in LIT applications. Besides resulting in an extremely robust arrangement in terms of failure tolerance, distributed control simplifies communications, health monitoring and multi-vehicle management. The costs of implementing distributed control have been kept within reason by adopting hardware developed for the industrial automation market. A future development area would be a version of the distributed network specifically tailored to LIT applications.

POWER CONTROL

The advance in the state of power semiconductor technology over the past decade has been quite rapid. Nevertheless, the cost differential between fixed and variable frequency LIM control is still largely due to the differences in switching devices and associated circuitry. It is not at all unreasonable to expect that this differential will grow narrower over the coming decade as the applications of force-commutated power devices grow and demand increases. In the meantime, fixed frequency control is likely to prove most cost-effective for "low-end" applications. It is recommended however that development of a variable frequency design be continued for use in large applications, e.g. above 3 kN thrust.

SLIP POWER APPLICATIONS

The slip power recovery concept has been analyzed to the point where it appears technically feasible for applications such as the supply of 2 kW auxiliary loads on a people-mover vehicle. There is some concern, however, about the weight of batteries which may be required to be compatible with expected charging rates. This concern may be alleviated somewhat by employing "smart" load management control and/or advanced battery-charging techniques.

Automated steering control supplied by slip power seems a worthwhile application as it provides a new degree of functionality, namely guidance.

The continued development of slip power recovery is recommended, but should focus on the issues of battery-charging and load management in order to determine whether these areas have reasonable technical solutions.

SOMMAIRE

Le moteur à induction linéaire s'est révélé l'application la plus réussie de toutes les variantes de convertisseur électromécanique linéaire développées au cours des dernières décennies, du moins dans le domaine de la traction aux vitesses allant de faibles à moyennes.

Il en existe plusieurs variantes : le moteur linéaire à double inducteur comprenant une armature magnétique et une surface de réaction de chaque côté du moteur ainsi que le moteur linéaire à inducteur simple, plus répandu et plus simple à utiliser en traction électrique guidée.

De ce dernier, il existe deux architectures de base. La première où les primaires (partie active du moteur) sont embarquées, alors que les secondaires (partie passive) sont fixées au sol. Cette architecture est celle que l'UTDC a adoptée pour son système de transport de capacité intermédiaire.

Dans la seconde architecture, les primaires, elles, sont encastrées dans le sol, alors que les secondaires sont embarquées. L'UTDC lui a trouvé bon nombre d'applications, notamment le transport hectométrique de personnes, le transport aéroportuaire et les chaînes de montage. Les grands atouts de cette technique sont les trois suivants :

1) Aucune partie active à bord du véhicule.
2) Absence de rail d'alimentation en bordure de voie.
3) Électronique de traction-freinage répartie dans le système.

Ces avantages sont reconnus depuis longue date et un certain nombre de systèmes ont été réalisés mondialement. En 1984, se rendant compte que le potentiel de cette technique était loin d'être exploité à fond, l'UTDC s'est dit prête à lancer une campagne de recherche technologique approfondie, avec le concours financier du Centre de développement des transports (CDT), de Transports Canada. C'est de cette initiative qu'est né le programme de recherche sur les moteurs linéaires à induction et leurs systèmes de commande.

Ce programme conjoint UTDC/CDT a couvert une vaste gamme de sujets touchant la technologie proprement dite et ses applications.

Chapitre 2 :	Rappel historique et créneaux prometteurs.
Chapitre 3 :	Détails sur les quatre domaines d'application possibles et exigences techniques de chacun d'eux.
Chapitre 4 :	Considérations d'ordre pratique devant être prises en compte dans l'étude d'un moteur linéaire à induction au sol.
Chapitre 5 :	Considérations propres aux alimentations à fréquence fixe et variable et description des installations d'étude analytique et expérimentale réalisées dans le cadre du programme.
Chapitre 6 :	Potentiel d'un système expert appliqué à l'étude d'un moteur linéaire à induction.
Chapitre 7 :	Idée de la commande électronique répartie et son utilité pour nombre de fonctions.

SOMMAIRE

Chapitre 8 : à 11	Mise au point des composants étudiés dans le cadre du programme. Considérations sur l'électronique de commande et les communications. Description de régulateurs.
Chapitre 12 :	Arbitrage entre deux types d'alimentation (à fréquence fixe et à fréquence variable). Avantages et inconvénients respectifs.
Chapitre 13 :	Aperçu de la théorie de la récupération des pertes de puissance dues au glissement et des applications possibles. Pratique et faisabilité techniques. Utilisations possibles.

Le programme de recherche a débouché sur d'importantes conclusions, dont voici les grandes lignes.

DOMAINES D'APPLICATION

Le moteur linéaire à induction au sol et son système de commande décrits dans ce rapport permettent de satisfaire à une vaste gamme de besoins, plus particulièrement dans les quatre applications suivantes :

1) système de transport faible vitesse dans les usines,
2) système de convoyage de bagages grande vitesse dans laes aéroports,
3) système aéroportuaire de transport hectométrique de personnes,
4) manutention de conteneurs.

Dans chaque cas, une électronique de commande répartie semble être la plus appropriée.

En fait, il serait plutôt difficile de trouver une autre technologie pouvant satisfaire aux besoins définis pour l'ensemble de ces quatre applications. La faible adhérence roue-rail élimine les systèmes automoteurs sur roues; le danger du rail d'alimentation, le système à partie active embarquée; les vitesses élevées à réaliser, les systèmes de convoyage à courroie ou à rouleaux.

Bien que ces quatre applications imposent des contraintes et des exigences très variées sur le plan des vitesses, masses, rampes et distances, elles ne semblent pas trop s'écarter les unes des autres pour ce qui touche les fonctions. Aussi, pense-t-on qu'il sera possible de concevoir des systèmes dont les principaux organes (régulateurs, réseau de communications, capteurs, etc.) pourraient être standardisés, donc susceptibles de fabrication série.

DÉMARCHE D'ÉTUDE

La démarche d'étude concernant le moteur linéaire à induction a révélé la nécessité d'effectuer des arbitrages serrés entre masses statoriques, d'une part, et puissances actives et réactives consommées, d'autre part. À supposer qu'il soit possible de pondérer chacun des ces paramètres, diverses options pourront être dégagées dans la mesure où elles sont assorties d'une alimentation à fréquence variable. La faiblesse d'une alimentation à fréquence fixe est d'hypothéquer sérieusement l'optimisation des systèmes étudiés.

SOMMAIRE

Cependant, les gains apportés par une alimentation à fréquence variable s'amenuisent à mesure que les puissances mises en oeuvre baissent. Au-dessous de 2 à 3 kN et d'un facteur d'utilisation de 5 p. 100, le paramètre d'un pas polaire allongé perd de son efficacité, d'où la perte d'un des grands avantages de l'alimentation à fréquence variable.

Par contre, au-dessus de ces valeurs, cette dernière devient de plus en plus intéressante, notamment sous le rapport de la puissance active et apparente consommée.

La définition de moteurs linéaires à induction semble échapper à une démarche méthodologique raisonnée, mais on sait que, en première analyse, les charges thermique et magnétique devront être équilibrées dans la plage prévue de variation des vitesses et des fréquences de fonctionnement. Au-delà, un arbitrage serré s'imposera entre masse statorique, masse des plaques de réaction et puissances active et apparente consommées. Cela peut donner des résultats inattendus. Dans un cas cité en exemple, une augmentation de 29 p. 100 de la masse statorique s'est traduite par une réduction de moitié de la puissance apparente consommée.

Pour s'en sortir, il ne saurait être question de s'en remettre à un système expert qui ne pourrait faire mieux que de guider les projeteurs encore inexpérimentés, en mettant en évidence les conséquences découlant de chaque étape du processus et, donc, les arbitrages qui s'imposent. À supposer, par exemple, que l'ingénieur opte pour une épaisseur de chape donnée, le système expert lui "conseillera" dans ce cas d'étudier plutôt deux épaisseurs distinctes, et de vérifier la sensibilité d'autres paramètres (masse, puissance apparente, etc.) à ce paramètre-là.

MODÉLISATION

Le modèle mathématique proposé dans le rapport a donné de bonnes approximations des performances et des tendances à condition que les concepts simulés ne se caractérisent pas par une saturation magnétique élevée ou par un effet de largeur finie important. Bien qu'il soit possible d'améliorer la qualité des techniques de prévision, il faut garder à l'esprit que l'utilité d'un modèle dépend autant, sinon plus, de sa facilité de mise en oeuvre que de la précision dont il est capable. Un modèle mathématique complexe et abstrait risque de poser plus de problèmes qu'il n'en résoud.

Une technique qui s'est révélée utile a été de compléter chaque fois que nécessaire, le modèle de base au moyen d'une analyse par la méthode des éléments finis. Cette analyse menée avec beaucoup de rigueur tant au niveau de maillage que de l'interprétation des résultats permet de visualiser avec un degré élevé de précision le comportement électromagnétique du concept étudié. Cependant, l'étude cas par cas par cette seule méthode pourra se révéler fastidieuse. On obtiendra de meilleurs résultats en combinant ensemble le modèle de base et la méthode des éléments finis qu'en utilisant séparément chacune de ces deux méthodes.

SOMMAIRE

ÉLECTRONIQUE DE COMMANDE RÉPARTIE

L'importance de ce facteur est capitale car, en plus de permettre au système de résister aux défaillances de toutes sortes, une électronique de commande répartie simplifie les communications et facilite les procédures de surveillance générale du réseau et de gestion du trafic. Quant au coût, il a pu être gardé dans des limites raisonnables en empruntant à l'automatisation industrielle les matériels qui y snt utilisés. Un projet futur pourrait être l'étude d'une électronique de commande répartie, conçue exprès pour les applications envisagées des moteurs linéaires à induction au sol.

ALIMENTATION

Les progrès réalisés dans le domaine de l'électronique au cours de la dernière décennie ont été très rapides. Néanmoins, l'écart de coût entre une électronique de commande à alimentation à fréquence fixe et une autre à fréquence variable est surtout tributaire du type de commutation adopté et des circuits connexes. Il n'est pas impossible qu'à l'avenir cet écart s'amenuise à mesure que les applications faisant appel à une alimentation à commutation forcée se multiplient. Entre-temps, l'alimentation à fréquence fixe demeurera économique dans les applications de faible puissance. Cependant, la recherche sur l'alimentation à fréquence variable n'en devra pas moins se poursuivre pour les applications d'une puissance supérieure à 3 kN.

RÉCUPÉRATION

L'idée d'utiliser le courant récupéré par l'élimination des pertes de puissances dues au glissement a été poussée au point qu'elle devient maintenant faisable dans certaines applications. Exemple, alimenter en courant 2 kW les circuits électriques de servitude à bord d'un système de transport hectométrique. Reste à décider ce que devrait être la masse des batteries nécessaires en fonction du régime de charge auquel elles seront soumises. Une solution partielle serait d'utiliser des méthodes rationnelles de gestion de la puissance appelée, ou des techniques avancées de charge, ou les deux.

Auto-guidage. Des systèmes d'auto-guidage alimentés par le courant récupéré semblent promis à un bel avenir.

Il est recommandé de poursuivre l'idée de récupérer les pertes de puissance dues au glissement, mais en s'attaquant d'abord aux deux domaines de la charge des batteries et de la gestion de la puissance appelée, afin de vérifier si les problèmes posés sont susceptibles de solution technique.

TABLE OF CONTENTS

Section		Page No.
1.0	INTRODUCTION	1
1.1	PROGRAM OBJECTIVES	1
1.2	ORGANIZATION OF REPORT	2
2.0	BACKGROUND	3
2.1	HISTORICAL	3
2.2	LIM-IN-TRACK VS LIM-ON-BOARD	3
2.3	APPLICATIONS SCOPE	4
2.4	TECHNICAL AND COST CHALLENGES	5
3.0	REVIEW OF TYPICAL SYSTEM FUNCTIONAL AND PERFORMANCE REQUIREMENTS	7
3.1	INDUSTRIAL HANDLING SYSTEMS	7
3.2	AIRPORT BAGGAGE TRANSPORT SYSTEMS	14
3.3	PEOPLE MOVING SYSTEMS	17
3.4	CONTAINER HANDLING SYSTEMS	20
3.5	SECTION SUMMARY	21
4.0	DESIGN ISSUES PECULIAR TO LIT SYSTEMS	24
4.1	AIRGAP CONTROL AND GEOMETRICAL CONSTRAINTS	24
4.2	"BOOST/COAST" DESIGN	26
4.3	POWER FAILURE	28
4.4	SINGLE POINT FAILURE AVOIDANCE	32
4.5	POWER DISTRIBUTION AND PROTECTION	32
4.6	VEHICLE SENSING	32
5.0	LIM MODELLING, EXPERIMENTS AND DESIGN	37
5.1	REVIEW OF LIM DESIGN ISSUES	37
5.2	ANALYTICAL MODEL DEVELOPMENT	48
5.3	EXPERIMENTAL FACILITY	67
5.4	EXPERIMENTAL RESULTS SUMMARY	73
5.5	MODEL PREDICTIONS	75
5.6	FIXED VS. VARIABLE FREQUENCY LIM PERFORMANCE COMPARISONS	75
6.0	LIM DESIGN AND "EXPERT SYSTEM" SOLUTIONS	90
6.1	THE LIM DESIGN PROBLEM EXPLORED	90
6.2	EXPERT SYSTEM TECHNOLOGY	90
6.3	FUTURE IMPLEMENTATION OF A LIM DESIGN EXPERT SYSTEM	91

TABLE OF CONTENTS

Section		Page No.
7.0	DISTRIBUTED PROPULSION CONTROL CONCEPT	93
7.1	OVERVIEW	93
7.2	VELOCITY AND POSITIONING CONTROL	93
7.3	MULTI-VEHICLE MANAGEMENT	99
7.4	DESTINATION AND STATION CONTROL	103
7.5	HEALTH MONITORING	106
8.0	POWER SEMICONDUCTOR TECHNOLOGY	107
8.1	INTRODUCTION	107
8.2	POWER SEMICONDUCTOR DEVICES	107
8.3	AC VOLTAGE CONTROLLER	111
8.4	VOLTAGE SOURCE INVERTER	114
8.5	ALTERNATIVE SCHEMES	118
8.6	FUTURE DEVELOPMENTS	120
9.0	COMMUNICATIONS	122
9.1	COMMUNICATIONS APPROACHES	122
9.2	COMMUNICATIONS FUNCTIONAL AND CONTROL REQUIREMENTS	129
9.3	SUITABILITY OF "BITBUS" DISTRIBUTED INTELLIGENCE NETWORK	129
9.4	SECTION CONCLUSION	131
10.0	LIM VOLTAGE CONTROL MODULE	132
10.1	SYSTEM DESCRIPTION	132
10.2	FIELD EXPERIENCE	159
10.3	FUTURE REFINEMENTS	163
11.0	LIM FREQUENCY CONTROL MODULE	166
11.1	THE LFCM	166
11.2	LFCM CONTROL SOFTWARE	166
11.3	MICRO-CONTROLLER INVERTER INTERFACE	173
11.4	TESTING THE LFCM	173
11.5	SPEED AND POSITION SENSING	186
11.6	TESTING OF LFCM AND MOTOR COMBINATION	191
12.0	FIXED FREQUENCY VERSUS VARIABLE FREQUENCY SYSTEM TRADE-OFF	198
12.1	POWER DISTRIBUTION	198
12.2	POWER CONDITIONING UNITS	199
12.3	LIM AND REACTION RAIL	199
12.4	CONCLUSIONS	200

TABLE OF CONTENTS

Section		Page No.
13.0	SLIP POWER APPLICATIONS	201
13.1	THEORETICAL PRINCIPLES	202
13.2	ANALYSIS OF TYPICAL SLIP POWER AVAILABILITY	206
13.3	PRACTICAL SYSTEM DESIGN	210
13.4	BATTERY CHARGING WITH SLIP POWER RECOVERY	213
13.5	AUTOMATIC GUIDANCE SYSTEM	215
14.0	CONCLUSIONS AND RECOMMENDATIONS	223
14.1	RANGE OF APPLICATION	223
14.2	LIM DESIGN	223
14.3	MODELLING	224
14.4	DISTRIBUTED PROPULSION CONTROL	224
14.5	POWER CONTROL	224
14.6	SLIP POWER APPLICATIONS	225
REFERENCES		226
APPENDIX A-1	DERIVATION OF MINIMUM ENTRY SPEED TO A VERTICAL TRANSITION	
APPENDIX A-2	DERIVATION OF THE FORMULA FOR THE RMS FEEDER CURRENT IN L.I.T. SYSTEMS	
APPENDIX A-3	STATOR SURFACES POWER DENSITY	
APPENDIX A-4	REACTION PLATE POWER	
APPENDIX A-5	LIM EQUIVALENT NETWORK COMPUTER MODEL	
APPENDIX A-6	"FLUX BUNCHING" IN THE LIM CORE	
APPENDIX A-7	FLUX DENSITY ESTIMATION FORMALAE	
APPENDIX A-8	VERTICAL FORCE	
APPENDIX A-9	SLIP FREQUENCY MAPPING	
APPENDIX B	SENSING, CONTROL & COMMUNICATION FOR IN-TRACK LIM DRIVES	

LIST OF FIGURES

Page No.

Figure 3.1 LIM-In-Track System for Industrial Handling 9
Figure 3.2 "Flat Floor" LIT System 10
Figure 3.3 Comparison of Loop and Shuttle Layouts 11
Figure 3.4 LIT Airport Baggage Transport System 15
Figure 3.5 LIT-Propelled Vehicle for "People-Moving" 19
Figure 3.6 Carrier Concept for LIT Container Handling System 22

Figure 4.1 Approaches to Propulsion on Vertical Curves 27
Figure 4.2 Boost/Coast Propulsion Concept 29
Figure 4.3 Wayside Brake Assembly 30
Figure 4.4 Permanent Magnet Decelerator 31
Figure 4.5 Single line diagrams of a LIT Power Distribution System 34
Figure 4.6 Vehicle Presence Detection Arrangement for Boost-Coast Systems 36

Figure 5.1 LIM Thrust vs. Speed Characteristics 40
Figure 5.2 Simple Duty Cycle 41
Figure 5.3 Typical Duty Cycle 41
Figure 5.4 Typical Temperature Rise Power Density Characteristics for a LIM Stator 43
Figure 5.5 Typical Temperature Rise vs. Power Density Characteristic for a Reaction Plate 45
Figure 5.6 Consideration Which Influence the Design of LIMs 47
Figure 5.7 Common Lumping Transformations 50
Figure 5.8 Effects Modelled by Equivalent Circuit Parameters 51
Figure 5.9 Section of an Infinitely Extended Machine 53
Figure 5.10 Core-Flux Modulation Due to Finite Core Length 56
Figure 5.11 Average Primary Surface Current Density Showing Effect of Half-filled End Slots 56
Figure 5.12 Transient Condition Resulting from the Sudden Introduction of Unenergized Conductor in the Airgap Field 57
Figure 5.13 Instantaneous Airgap Flux Distribution of a Moving LIM showing the "Entry-End Effect" 57
Figure 5.14 Fourier Representation of Motor mmf Distributions 58
Figure 5.15 Development of the LIM Equivalent Network 60
Figure 5.16 Airgap Flux Density Distributions as Determined by LIM Equivalent Network Computer Model 61
Figure 5.17 Comparison of Finite Element Analsysi with LEN Predictions 65
Figure 5.18 Difference in Peak Flux Density Between Actual and Sinusoidal Waveforms 66
Figure 5.19 Typical Vertical Force vs. Slip Frequency Characteristic (LEN Production and Experimental Results) 68
Figure 5.20 LIM Dynamic Test System 70
Figure 5.21 Test Stand Illustration 71

LIST OF FIGURES (Cont'd)

Page No.

Figure 5.22 Schematic Data Reduction 72
Figure 5.23 Test System Block Diagram Indicating Measured and Derived Information 74
Figure 5.24 Sample LIM Test Results 76-77
Figure 5.25 Model/Test Comparison Sample @ 1 m/s 78
Figure 5.26 Model/Test Comparison Sample @ 3 m/s 79
Figure 5.27 Model/Test Comparison Sample @ 5 m/s 80
Figure 5.28 Model/Test Comparison Sample @ 7 m/s 81
Figure 5.29 Model/Test Comparison Sample @ 9 m/s 82
Figure 5.30 Comparison of VF VS FF LIM Performance: Thrust Per Apparent Power 85
Figure 5.31 Comparison of VF VS FF LIM Performance: Thrust Per Input Real Power 86

Figure 7.1 Distributed Propulsion Control System Overview 94
Figure 7.2 LIT Velocity Loop with Centralized Control and Power Switching 96
Figure 7.3 LIT Velocity Loop with Centralized Control and Distributed Power Switching 97
Figure 7.4 LIT Distributed Velocity Control Configuration 98
Figure 7.5 Fixed Block Scheme Employing Local Cross-Connected Block Controllers 101
Figure 7.6 Trailing Block Scheme Employing Local Cross-Connected LIM Controllers 102
Figure 7.7 Merge Protection Scheme Employing Local Cross-Connected LIM Controllers 104
Figure 7.8 Destination/Routing Control 105

Figure 8.1 Switching Frequency and KVA Capability of the Power Semi-conductor Devices 108
Figure 8.2 Standard Symbols of the Power Semi-conductor Devices 109
Figure 8.3 Single Phase ACVC 112
Figure 8.4 Typical ACVC Waveforms for Resistive Loads 113
Figure 8.5 Typical BJT Three Phase Voltage Service Inverter (VSI) 115
Figure 8.6 Pulse Width Modulation Waveforms 116
Figure 8.7 Single-Triangle Comparison Method for Generating PWM Waveform 117
Figure 8.8 Three Phase Cyclo-Converter 119
Figure 8.9 Three Phase Power Control Circuit 121

Figure 10.1 LIM-In-Track Propulsion Configuration 133
Figure 10.2 LVCM Sensor Arrangement 135
Figure 10.3 LVCM Power Section 137
Figure 10.4 Gate Signal Timing and Related Logic 139
Figure 10.5 Gate Signal Conditioning 141
Figure 10.6 Sensor Handling Logic 143
Figure 10.7 LVCM Function Block Diagram 147
Figure 10.8 Overall Velocity Distance Profile and Corresponding LVCM Demand Profiles 148

LIST OF FIGURES (Cont'd)

Page No.

Figure 10.9 Velocity Controller 151
Figure 10.10 Position 152
Figure 10.11 Jerk Limit Principal 154
Figure 10.12 LIM thrust vs. Firing Delay 156
Figure 10.13 Firing Delay vs. Control Signal 156
Figure 10.14 Prototype Industrial Handling System 161

Figure 11.1 Regular Sampling 168
Figure 11.2 PI - Current Control Process 170
Figure 11.3 Airgap Variation Effects on Speed Determination 172
Figure 11.4 Microcontroller Inverter Interface 174
Figure 11.5 Inverter/Load Simulator 176
Figure 11.6 Load Simulation Development 177
Figure 11.7 Current Controller Step Response - Small K 179
Figure 11.8 Current Controller Step Response - Increased 180
Figure 11.9 Current Controller Step Response - Demand 0-256-80 181
Figure 11.10 Current Controller Steo Response - Demand 256-0 Units 182
Figure 11.11 Current Loop Response - 0-80-256 Demand 183
Figure 11.12 Current Controller - Steady State Operation 184
Figure 11.13 Unbalanced Load - Steady State 185
Figure 11.14 Unbalanced Load - Transient 187
Figure 11.15 Transient Frequency Change 188
Figure 11.16 Transient Phase Sequence Reversal 189
Figure 11.17 Speed and Distance Signals At 3 m/s 190
Figure 11.18 Speed and Distance Signals Under Acceleration 192
Figure 11.19 Position Signal as Vehicle Enters Control Zone, Stops and Exits 193
Figure 11.20 Simulated LFCM Speed Control 196
Figure 11.21 Position control 197

Figure 13.1 Relationships Between Variables in Slip Power Recovery 205
Figure 13.2 Example Slip Power Availability 208
Figure 13.3 Surface - Wound Reaction Plate 211
Figure 13.4 Slip Power Recovery System Circuit Concept 212
Figure 13.5 a Two Wire Magnetic Field Pattern 217
Figure 13.5 b Single Wire Magnetic Field Pattern 217
Figure 13.6 a Single Loop Antenna 217
Figure 13.6 b Dual Loop Antenna 217
Figure 13.6 c Multi Loop Antenna 218
Figure 13.7 a Even Pole Pitch Antenna Length 218
Figure 13.7 b Antenna Chording in Curving 218
Figure 13.8 Antenna Filtering 219
Figure 13.9 Wire Guided Vehicle Path Selection 220
Figure 13.10 Wire Guided Vehicle Utilizing Slip Power Recovery 221

LIST OF TABLES (Cont'd)

		Page No.
Table 3.1	Typcial Specifications for LIM-In-Track Systems	23
Table 4.1	Typical LIM Airgap Budget	25
Table 4.2	Signle-Point Failure Avoidance Design	33
Table 5.1	Parameter Variations Which Affect Thrust Performance	38
Table 5.2	Correspondence Between Equivalent Network Elements and Motor	54
Table 5.3	Practical Features in Induction Motors	55
Table 5.4	Comparison of Various LIMs Designed to Satisfy Common Performance Criteria	88
Table 9.1	Communications Networks: Physical Signalling Approaches	124
Table 9.2	Communications Networks: Bus Access Methods	126-127
Table 9.3	Communications Networks: Data Encoding	128
Table 9.4	Communications - Dependent Functions	130
Table 10.1	LIM Voltage Control Module Functional Overview	134
Table 10.2	LVCM Signals, Constant and Logic Variables	145
Table 13.1	Relationship Between Variables in Wheel Slip Analogy of LIM Behaviour	203

1.0 INTRODUCTION

The "Linear Induction Motors and Their Control Systems" program was conceived as a multi-sided approach to the development of LIM-in-Track (LIT) technology. The program follows an earlier TDC-sponsored program entitled "Design, Construction and Testing of a Linear Induction Motor Powered by Commercial Frequency (60 Hz)". In that program, the basic characteristics of in-track LIMs using 60 Hz supply frequency were investigated both analytically and experimentally.

In the latest program, the scope was incresed to include a broad treatment of the LIM control issues; i.e. to consider the potential and design implications of variable-frequency as opposed to fixed-frequency control, to investigate approaches to multi-vehicle control, and to further develop the concept of LIM slip power recovery.

Besides covering a wider range of topics than the previous program, "LIMs and Their Control Systems" maintained a more highly-defined applications focus, and drew extensively from "real world" design and opertional information provided by other UTDC programs.

1.1 PROGRAM OBJECTIVES

The program objectives were as follows:

1) To advance the concept of LIM-In-Track (LIT) propulsion from the current state-of-the-art by introducing key technological elements:
   - "Intelligent" LIT propulsion modules featuring advanced sensing, control and communications functions
   - an improved thermal and electromagnetic LIM design
   - a versatile multi-vehicle, multi-path command and control strategy
2) To determine the potential of variable-frequency power control as a replacement to fixed frequency control for a range of LIT applications.
3) To extend the range of potential LIT applications through the performance and functional improvements gained through 1) and 2) above.
4) To investigate the potential uses of LIM slip power recovery in LIT systems.
5) To further develop design tools and a design database for in-track LIMs.

1.2 ORGANIZATION OF REPORT

The "LIMs and Their Control Systems" program covered a wide range of topics relating to LIT technology. This report attempts to present these topics in a manner which builds concept upon concept, showing (hopefully) that LIT is not merely a means of propulsion but a complete system philosophy.

Chapter 2 reviews the history of LIM propulsion and identifies the areas of LIT application that continue to hold promise.

Chapter 3 goes into some detail describing four areas of potential application and compares and contrasts the specific requirements imposed by each on the LIT propulsion and control system.

Chapter 4 highlights a number of practical design considerations which arise from the general LIT approach.

Chapter 5 details the specific design considerations for fixed and variable frequency LIMs and supports these with descriptions of the analytical and experimental facilities developed under the program.

Chapter 6 explores the potential of "expert system" software as a LIM design aid.

Chapter 7 presents the concept of distributed control in LIT systems and shows how this concept may be used to advantage to provide many system functions.

Chapter 8 through 11 review the areas of component development which were covered under the program. Power Control and Communications approaches are compared generally, and two specific LIM controller designs are described.

Chapter 12 examines the trade-off between the fixed frequency and variable frequency control approach and makes some observations about the suitability of each in general.

Chapter 13 provides a look into the theory and application of LIM Slip Power Recovery. Issues of design practice and technical feasibility are reviewed, and proposed uses are presented.

2.0 BACKGROUND

2.1 HISTORICAL

The first patents for linear motor propulsion of vehicles date back to the turn of the century, and even at that time, both the in-track stator and vehicle-borne stator approaches had been identified.

It was not until the 1960's, when technology had caught up to the visionaries of earlier years, that full-scale working prototypes of linear-powered vehicles were built. Even then, the state of technology was not such that these systems could be considered practical.

By the mid-1970's, solid-state power conversion technology had matured to the point that systems employing Linear Induction Motor (LIM) technology were quite feasible. Companies in Germany, France, Great Britain and the U.S. were developing transportation systems products based on LIM technology for various markets, including Personal Rapid Transit (PRT), Intercity Rail, Industrial Handling, Airport Transit and Airport Baggage Transport. Of the many companies that ventured in to the area, few carried through to the point of actual sales, and today, virtually all of the original promotors have abandoned the technology.

The 1980's saw some new activity in the technology and marketing of LIM-based systems. The Urban Transportation Development Corporation has had promising beginnings with their Intermediate Capacity Transit System, and have recently introduced LIM-in-Track systems for Industrial and Airport Handling.

Bombardier Ltd. markets a LIM-in-Track People Mover technology originally developed in the U.S. by Wedway Enterprises, and Boeing Airport Equipment Ltd. is marketing a LIM-in-Track baggage handling system developed in the late sixties and early seventies by Docutel Ltd. of Texas. There is also considerable activity in Japan, where Hitachi Ltd. and Mitsubishi Heavy Industries are marketing LIM-on-board vehicles as "mini-subways" and Toshiba Ltd. has developed systems for specialized industrial handling.

It is hard to predict whether LIM-based transportation will continue to succeed in any or all of the applications for which it is currently targeted, but if the imitation of one company by others is an indicator, then it would seem that at least in the Urban Transit, Industrial and Airport markets there is some promise.

2.2 LIM-IN-TRACK VS LIM-ON-BOARD

The differences between LIM-on-Board (LOB) and LIM-in-Track (LIT) configurations in terms of practical design issues are rather numerous. The most obvious differences arise because in LIT the vehicle carries no propulsion equipment. The resulting advantages span a wide range of issues; for example:

- reduced vehicle height - smaller guideway/tunnel cross-section
- reduced vehicle weight - lighter guideway
- no power collector - all-season reliability/no hazard potential
- increased thrust-weight ratio - steeper grade climbing/higher acceleration

Less obvious, but at least as important, are the differences which arise because propulsion is wayside-based, i.e. fixed to the track:

- fixed LIM stators - simpler LIM design, longer LIM life, lower maintenance
- wayside controllers - eliminate wayside/vehicle communications
- inherent "block" definition - simpler train control

It is especially in the area of train control that LIT may have the most profound implications. The functional structure, or "architecture" of the LIT approach presents an opportunity to adopt a distributed control philosophy. Distributed control architectures are becoming increasingly popular in industrial automation, marine, and aerospace systems because they simplify communications requirements, improve fault-tolerance, and provide superior control and monitoring capabilities than centralized control architectures. Chapter 7 explains the distributed propulsion control concept in more detail.

While the LIT configuration has advantages over the LIM-on-board configuration it is clearly not without certain disadvantages. The first, and most serious weakness is on account of the proliferation of LIMs and control elements within any system. Even in systems which employ high vehicle densities, the utilization of any given LIM and its associated control equipment is quite small in terms of "active" versus "standby" time. Low equipment utilization generally implies a higher cost than a competing system might offer.

Secondly, LIT technology at the present time provides considerably lower electromechanical efficiency (e.g. 3 to 6 times lower) than can be achieved with LOB technology.

2.3 APPLICATIONS SCOPE

In the area where LOB systems have proven to be marketable, (i.e. Urban Transit), LIT systems would appear uncompetitive. The particular advantages LIT offers could only be partially exploited in such applications and would not likely offset the cost differential.

There may be areas of application however, where LIT would be more appropriate than LOB. These are applications which exhibit one or more of the following characteristics:

- Short distances (100 - 10,000 metres)
- Steep grades (above 8%)
- Requirement for no exposed power (e.g. safety issues)
- High system availability requirements (e.g. 98.6%)
- High vehicle densities (e.g. 1 vehicle/10 metres)

LIT systems can be applied over a fairly wide range of speed, distance and load capability requirements. Speeds can be very low (e.g. 0.1 m/s) or relatively high (e.g. 10 m/s). Distances are not physically limited, but since propulsion equipment costs grow proportionally, longer systems (1-5 km) become less competitive with LOB. Mass carried can be tens, or tens of thousands of kilograms.

It is difficult to generalize about which operating ranges and applications are most favourable for LIT. Chapter 3 reviews four types of application that represent various combinations of speed, distance and load. The suitability of LIT versus LOB (or versus any other type of transport), for each of these applications is in some cases quite obvious (e.g. Industrial Handling and Airport Baggage Transport). In other cases the competitive advantage is less apparent. It is not the intention of Chapter 3 to draw firm conclusions about which applications are best handled by LIT, but rather to illustrate how the unique features of LIT can fit a broad range of requirements.

2.4 TECHNICAL AND COST CHALLENGES

As was mentioned in Section 2.2, the LIT concept, by its nature, involves the use of large numbers of LIMs and controllers, which are grossly under utilized. High component count and low utilization hardly seem like good engineering practice, but to a certain extent, these very things can be exploited to help improve the cost picture.

Firstly, the large numbers of LIMs and control elements suggest that these components could be value-engineered for large-scale production. LIMs, for example, would lend themselves well to automated winding. Controllers could be made cheaper and more compact through use of custom VLSI (Very Large Scale Integration) chips, automated PC board assembly, and custom packaging.

Secondly, the low utilization factor means, at least for the LIM stators and power circuits, substantial decrease in thermal stresses, allowing LIMs to be smaller than their LOb counterparts for the same thrust rating, and power devices to be downsized.

Value-engineering will go a long way to reducing the cost of LIT technology thereby opening doors to more applications. However, the problem of cost may also be attached at a more fundamental level.

Specifically, the approaches to the design of the LIM and its controller. The program focusses primarily on this point and explores in some detail the cost/performance issues involved in competing approaches, namely fixed frequency (FF) control and variable frequency (VF) control.

3.0 REVIEW OF TYPICAL SYSTEM FUNCTIONAL AND PERFORMANCE REQUIREMENTS

As indicated in the previous chapter, the applications scope for LIM-in-Track propulsion is rather extensive.

This chapter is a review of some of the particular requirements that are found in a broad range of target applications, and an indication of how these requirements drive the propulsion system design specifications.

It is impossible to be precise about "typical" system requirements, so it must be borne in mind when reading the following subsections that any statements made or figures offered are merely intended to give a rough idea of what a given LIT system might be.

The section closes with a summary table which compares four distinct application areas.

3.1 INDUSTRIAL HANDLING SYSTEMS

Spurred by competition from Japan and Europe, the North American manufacturing industry has seen fit to modernize the technology for making, moving and storing its materials and products.

Industrial robots are among the most noticed of the new manufacturing technologies. Also, materials transport systems have become increasingly automated and "flexible".

In the past, means of automated industrial materials handling included belt- or roller-conveyor systems, overhead monorail systems and chain-in-floor tow systems. Whenever flexibility and/or interfacing requirements became too challenging for these technologies, manned forklift trucks provided a simple, though costly, solution.

The 1980's saw the emergence of Automated Guided Vehicle Systems (AGVS) as a practical alternative to manned forklift handling. The AGVS employs battery-powered, wire-following vehicles which can receive, transport and transfer unit loads automatically. Typical systems incorporate from only a few to a hundred or more vehicles. They are relatively simple to integrate into plant or warehouse facilities, and are quite flexible and expandable in terms of layout.

While AGV systems possess many desirable features, they also suffer certain limitations. For example, the vehicles are battery-powered and typically must be able to operate for six to eight hours before recharging. This limits their maximum speed, gradability and load-carrying capacity.

Furthermore, because the vehicles are technically sophisticated and complex, systems with large numbers of vehicles (ie. high throughput) become prohibitively expensive compared to conventional technologies.

LIM-in-Track (LIT) technology is inherently less flexible than AGVS technology because of the requirement for LIMs in the plant floor. Nevertheless, it will provide similar functions to the AGVS and does not share the limitations in performance. Indeed the speed, gradability, load capacity and throughput potential far exceed typical AGVS specifications. Figure 3-1 is an illustration showing a vehicle and loading station in a typical LIT industrial application.

3.1.1 System Requirements

3.1.1.1 Physical

Handling systems which are to be retrofitted into existing plants are generally required to be non-obstructive to cross traffic. Elevated track can be a solution but usually requires steep inclines or vertical lifts. "Flat floor" arrangements are a solution when it is practical to excavate enough floor to flush-mount the LIMs to the surface. Figures 3-1 and 3-2 illustrate this approach.

3.1.1.2 System Length and Layout

Manufacturing and warehousing facilities typically transport material distances of 1 kilometer or less, however, the number of serviced locations can be large (eg. ten) and the routing layout complex. AGV systems generally use one or more unidirectional continuous loops. LIT systems may be configured in the same way, but can also operate as a bi-directional shuttle. Figure 3-3 illustrates how either a "loop" or "shuttle" layout can serve the same requirement.

3.1.1.3 Throughput

The throughput of a handling system is the average vehicle speed multiplied by the vehicle traffic density. In typical AGVS installations economic considerations limit vehicle densities to about 6 vehicles per 100 m. Speeds are typically less than 1 m/s, hence throughputs of AGV systems seldom range beyond 200 loads per hour, and are more typically, less than 50 loads per hour.

Beyond 200 loads per hour, powered-roller conveyor (PRC) systems are common. LIT handling systems could achieve throughputs approaching PRC by exploiting the inherent high speed capability, but even at low to moderate speeds LIT could surpass AGV figures by using high vehicle densities: for example, 10 vehicles per 100 m.

3.1.1.4 Load Capacity

The range of weights for typical unit loads is from 300 kg. to 2,000 kg. The low end represents palletized or packaged product which may

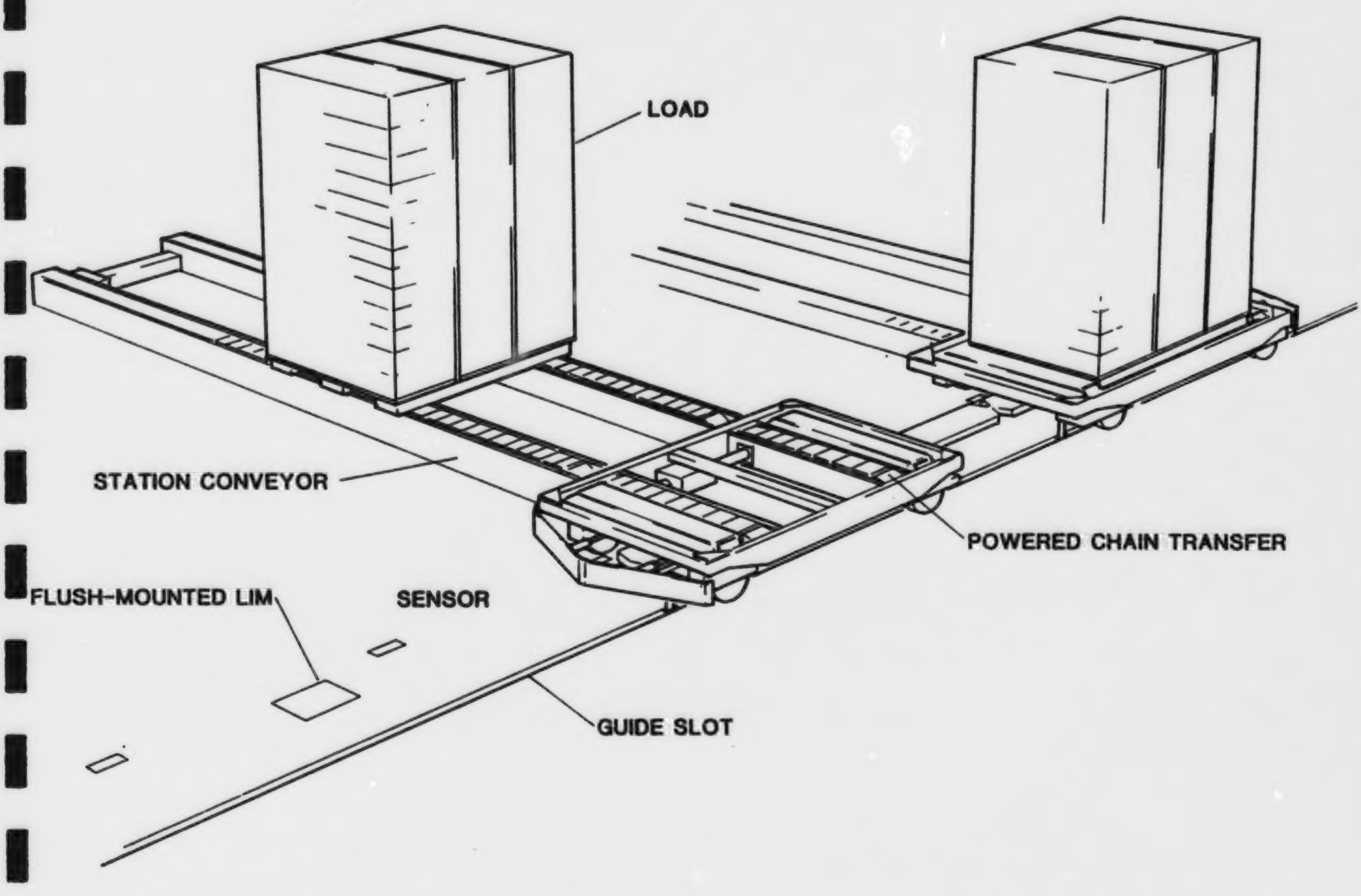
LOAD
STATION CONVEYOR
POWERED CHAIN TRANSFER
FLUSH-MOUNTED LIM
SENSOR
GUIDE SLOT

FIGURE 3-1: LIM-IN-TRACK SYSTEM FOR INDUSTRIAL HANDLING

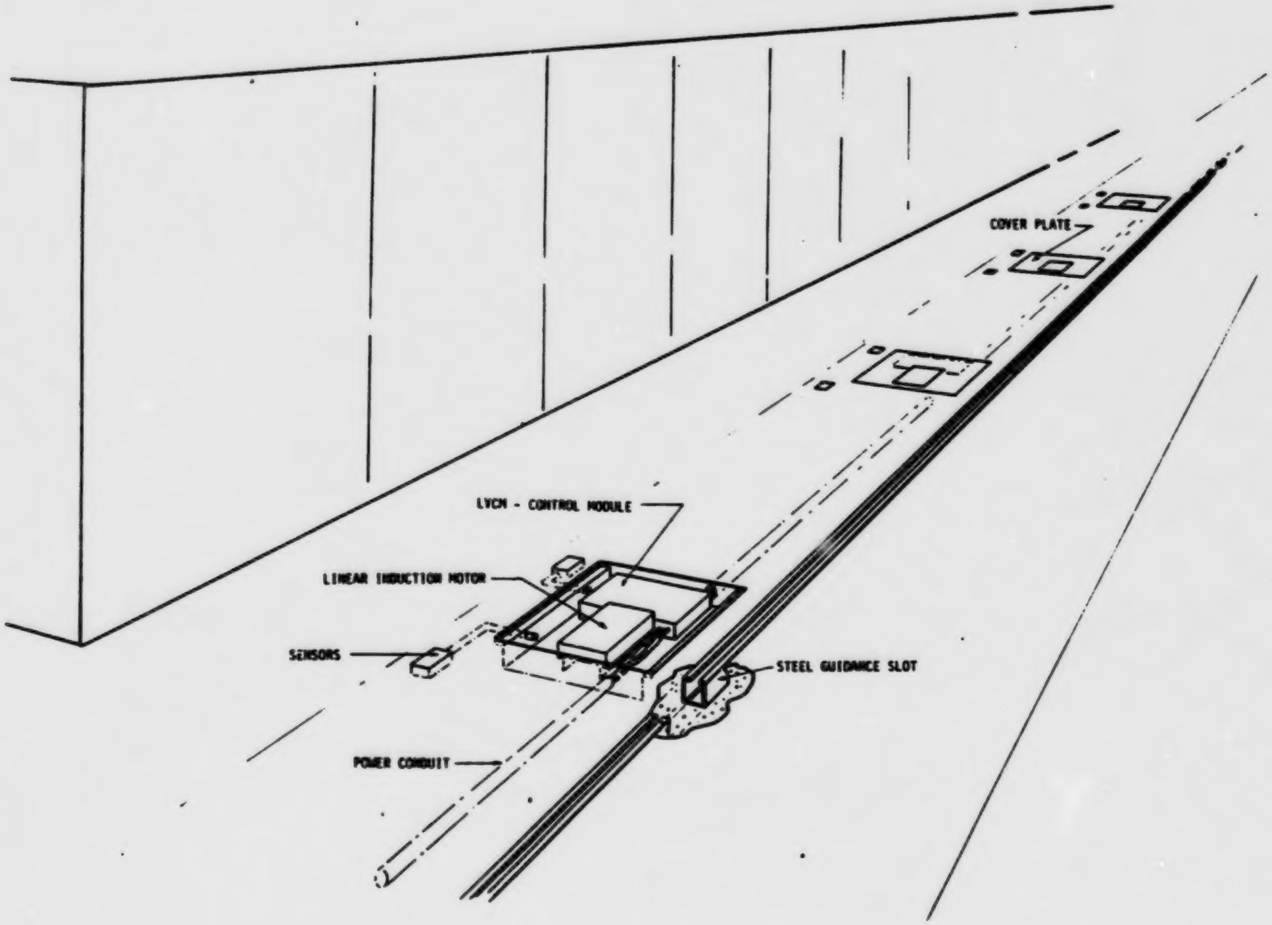
COVER PLATE
LVCM - CONTROL MODULE
LINEAR INDUCTION MOTOR
SENSORS
STEEL GUIDANCE SLOT
POWER CONDUIT

FIGURE 3-2: "FLAT FLOOR" LIT SYSTEM

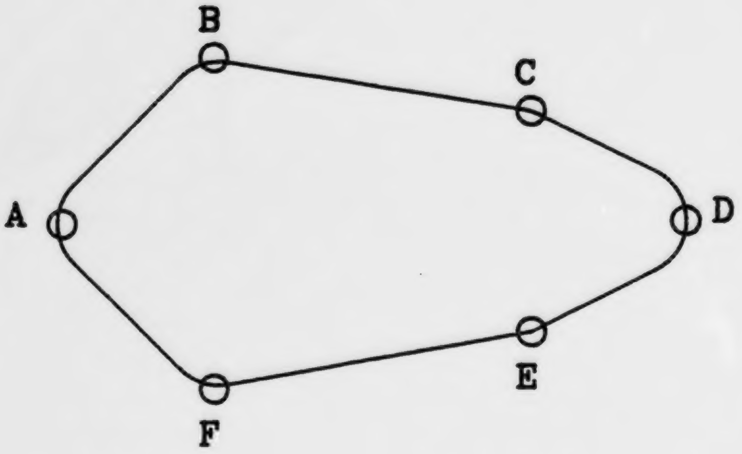

A. Loop System

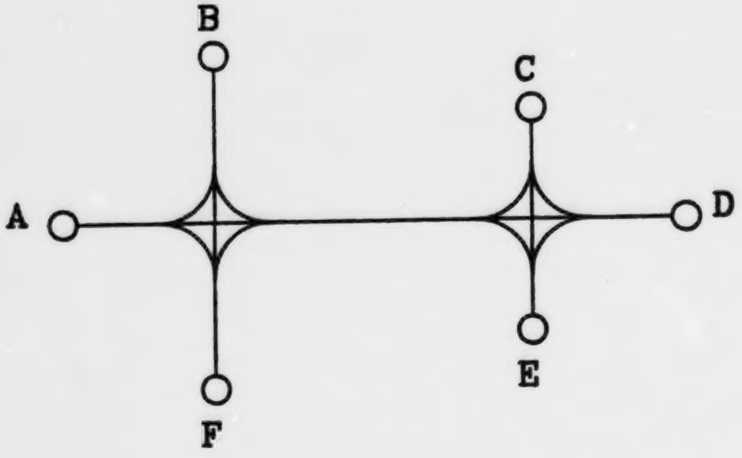

B. Shuttle System

FIGURE 3-3: COMPARISON OF LOOP AND SHUTTLE LAYOUTS

require further transportation and distribution after leaving the plant. The high end is typically material which is fed into the plant.

3.1.1.5 System Availability

Many manufacturing facilities, especially those which are highly automated, operate around the clock. In many cases this situation exists because it is simply too costly to stop production. Clearly, such operations demand high availability from their handling systems, or at the very least, minimum time to recover from system failures.

A typical system availability requirement is 98% with maximum time to restore of 4 hours. Depending on the nature of the operation, these figures will vary considerably. Availability figures in excess of 98% are rare in the manufacturing industry.

3.1.2 Functional Requirements

3.1.2.1 Destination Control

Many industrial handling systems service multiple pick-up and/or drop-off points. This generates a requirement for path-switching capability and control of vehicle routing, which in more sophisticated systems may involve real-time vehicle tracking or wayside-based vehicle identification.

3.1.2.2 Grade Climbing

Elevation changes are common in factory and warehouse operations. Vertical lifts are sometimes used to cope with elevation changes if space is tight and throughput and reliability considerations permit. Alternatively, inclined track or guideway is used. AGVs can negotiate inclines of about ten percent, but the additional propulsion load imposed by grades shortens the length of operating time between battery-charging intervals.

LIT systems can easily negotiate ten percent grades and steeper, since traction is not dependent on wheel adhesion. Moreover, unlike AGVs which must carry their own propulsion and energy supply, LIT vehicles receive propulsion from the track, so there are no particular weight penalties or operational complications introduced by grades.

3.1.2.3 Curving

In order to minimize the amount of floor space taken up by the handling system guidepath, the smallest practical curving radii are required. In LIT systems a 3 or 4 metre mean curving radius is typical.

3.1.2.4 Safety

In systems where some or all of the guidepath is exposed to unregulated cross-traffic, speeds must be kept below about 1.3 m/s so that a brake-activating bumper mechanism can stop the vehicle within the length of the bumper extension.

A second typical safety-related requirement is that all vehicles in the system be stoppable by activation of a "panic button".

3.1.2.5 Operating Modes

Most automated handling systems require various modes of automatic or semi-automatic operation in order to facilitate peculiar situations which can arise. These may involve, for example, changes in speed limits, routing or stopping locations. Stemming from this requirement is the requirement for a simple, "fool-proof" operator interface which will permit mode-selection.

3.1.3 Performance Requirements

3.1.3.1 Speed

Speed requirements for industrial handling systems are generally in the order of 1 to 2 m/s, but can be higher (eg. 4 to 5 m/s) where dedicated right-of-ways are provided.

3.1.3.2 Speed Regulation

Where speed is limited due to safety considerations, good regulation (eg. ±5 percent of the nominal value) is required.

3.1.3.3 Thrust

Thrust requirements for cruising typically range from 300 N to 600 N. On grades, thrust levels from 2 kN to 6 kN are typical.

3.1.3.4 Duty Cycle

The duty cycle of a given LIM stator is the ratio of the time that it is "on" to the period of its repetitive cycle. Duty cycle is a direct function of vehicle traffic density. Typically, it ranges from 0.03 to 0.10.

3.1.3.5 Positioning Accuracy

Vehicles must interface at pick-up and drop-off points with automatic load transfer stations. Positioning accuracies of ±3 cm are required for proper load transfer.

3.2 AIRPORT BAGGAGE TRANSPORT SYSTEMS

The opportunities for reducing labour costs through automation are as prevalent for airport operations as they are in the manufacturing industry. The baggage handling function is one which is being increasingly automated. Of course, baggage conveyors and carousels have been used at check-in and claim areas respectively, for several decades. More recently, high speed transport links between terminals are being designed into new airports.

In the late 1960's, Docutel Ltd. of Texas developed an LIT-based system under a development program sponsored by the U.S. Airlines. Since then, the system has proven itself in applications at JFK and Atlanta. UTDC Inc. has developed designs for a similar, but technologically-updated version to be introduced in Changi Singapore before the end of the decade. Figure 3-4 shows a typical Airport Baggage Transport System.

3.2.1 System Requirements

3.2.1.1 Physical

Floor-mounted, bolt-together track modules are generally acceptable. Such modules can be fastened to existing or newly-poured concrete floor. Accommodation for cross-traffic is limited to special regulated-access crossings.

3.2.1.2 System Length and Layout

Typical systems include two or more terminals connected by links of the order of 1 kilometre. Stopping points can number from ten upward. Track layouts generally employ a unidirectional loop. A typical system layout is shown in Figure 3-4.

3.2.1.3 Throughput

In airport baggage transport systems, there is often a requirement for handling temporary peaks which exceed the nominal average throughput by several times. These peak loads exist because baggage is fed into the system in concentrated "lumps" (ie. when an aircraft lands). Smoothing the peak loading can only be achieved at the expense of transit time, and there are clear limits to how long this can be if arriving passengers are to claim their bags within reasonable time after disembarking.

Of course, there are other scenarios which can be less time-critical, such as the flow of baggage between connecting flights or from the check-in counter to a departing flight. Nevertheless, high peak throughput capability is a standard requirement. Somewhere between 20 and 40 bags per minute is typical.

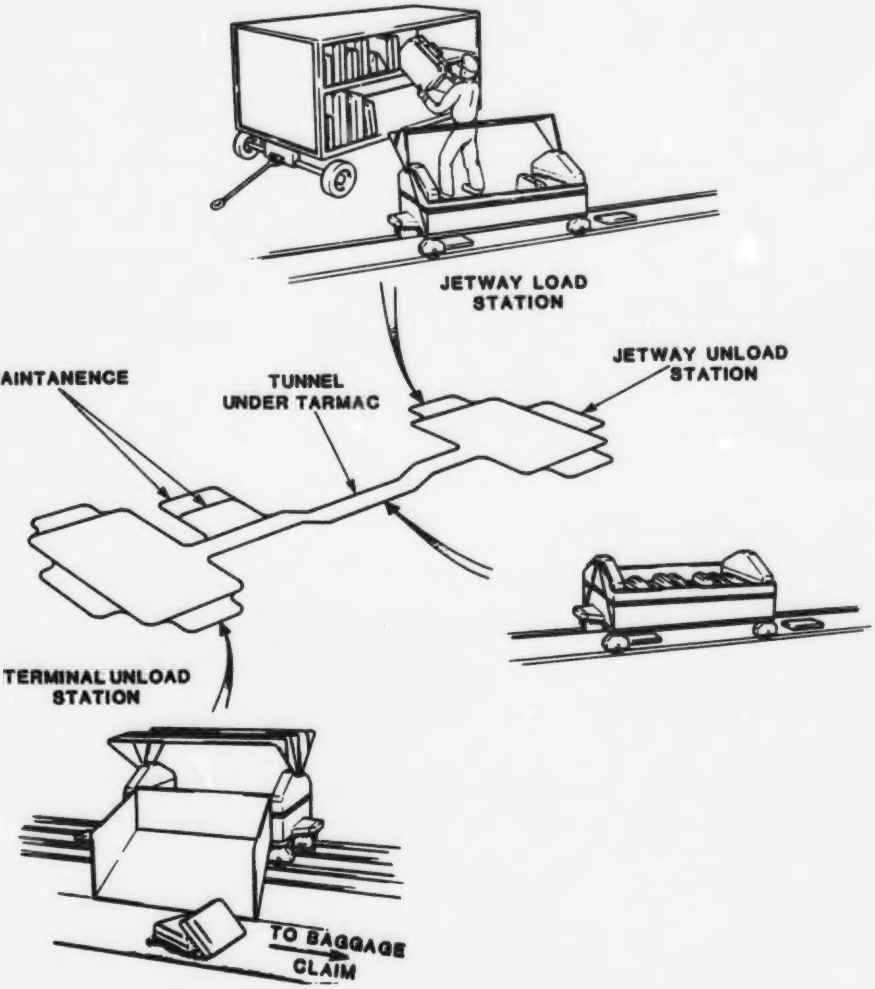
JETWAY LOAD STATION
JETWAY UNLOAD STATION
MAINTANENCE
TUNNEL UNDER TARMAC
TERMINAL UNLOAD STATION
TO BAGGAGE CLAIM

FIGURE 3-4: LIT AIRPORT BAGGAGE TRANSPORT SYSTEM

3.2.1.4 Load Capacity

The original Docutel system requirement called for small vehicles carrying 4 to 6 luggage pieces each. More recent specifications have increased this load to 10 bags or approximately 300 kg.

3.2.1.5 System Availability

Airport systems are generally not required to be available on a 24 hour basis. However, during the normal operating hours, the "full performance" availability requirement is typically 96 percent or greater. A back-up system (usually a truck or towmotor) ensures that bags will continue to move if the handling system fails.

3.2.2 Functional Requirements

3.2.2.1 Destination Control

As in industrial handling systems, baggage transport systems generally have multiple pick-up and drop-off points. In addition, vehicles may be routed to and from a storage/maintenance area. The destination/routing control requirement demands real-time vehicle identification and path-switching functions.

3.2.2.2 Grade Climbing

Inclines in typical baggage transport systems are 30 degrees (60 percent). By comparison to other types of transport, these are steep grades. The requirement is generated by the need for part of the system to be routed deep below ground, ie. under the airport tarmac.

3.2.2.3 Curving

Curving radii are typically 5 m.

3.2.2.4 Safety

Due to system length and throughput requirements, vehicle speeds are too high for bumper-activated brakes to be effective. It is therefore necessary to provide for dedicated guideway with restricted access.

3.2.3 Performance Requirements

3.2.3.1 Speed

Due to the requirement for high peak throughput and low transit time, speeds must be as high as is practical. This is about 10 m/s on straight, level track and 5 m/s through curves and switches.

3.2.3.2 Speed Regulation

Regulation of speed is required in order to avoid traffic "bunching" during peak throughput periods, and to ensure that speeds approaching and exiting inclined track sections are near the design targets. Regulation of ±10% of nominal is generally adequate.

3.2.3.3 Thrust

The high speeds used in baggage transport systems permit "boost/coast" propulsion, in which vehicles receive propulsive force at intervals rather than continuously. During these brief "bursts" of propulsion the vehicle must be accelerated to regain the speed that it lost since the last "burst". If the vehicle were required to stop, say in response to an emergency shut-down command, then the same LIM stator normally used to maintain cruise velocity would be required to accelerate the vehicle from standstill to a high enough speed to make it over the spanning interval to the next LIM.

In typical systems the LIM stators must be capable of providing 1 kN force at 10 m/s and 3 kN at standstill.

On grades, the LIM stators must provide sufficient thrust to overcome both gravitational and drag forces. Section 4.1 describes other considerations related to grade entry and exit transitions. The resulting thrust requirement is typically in the range of 2 kN to 3 kN.

3.2.3.4 Duty Cycle

Typical duty cycles are 0.03 or smaller for baggage transport applications.

3.2.3.5 Positioning Accuracy

As in industrial systems, required positioning accuracy of ±3 cm is typical.

3.3 PEOPLE MOVING SYSTEMS

The "low end" of automated public transit systems in terms of distance and capacity are known as "People Movers". There are several suppliers of People Mover systems worldwide. Airports are the primary market, but some of these systems have been sold to cities for application in congested downtown areas.

The first People Mover (PM) system to use LIT technology was known as WEDway and has been applied successfully at Disney World in Orlando and as an Airport People Mover (APM) in Houston [1]. The WEDway system has demonstrated high availability, but is somewhat limited in capacity and is not suitable for all-season operation.

UTDC Inc. is developing an LIT-based People Mover which uses larger, articulated vehicles and higher speeds to improve capacity, and a unique steel-wheel on steel-rail suspension to permit operation in ice and snow [2]. The vehicle is illustrated in Figure 3-5.

3.3.1 System Requirements

3.3.1.1 Physical

While there are some APM systems which operate indoors only, People Movers generally should be capable of outdoor operation in all weather. Typically, systems operate on dedicated, restricted guideway.

3.3.1.2 System Length and Layout

PM systems are seldom longer than 5 km. Both bi-directional "shuttle" and unidirectional "loop" arrangements are common.

3.3.1.3 Throughput

PM capacities are in the range of 1,000 to 3,000 passengers per hour per direction. Vehicles sized for 40 to 60 passengers are typical, so headways would need to range from about 60 s to 150 s.

3.3.1.4 Load Capacity

Maximum passenger loading per vehicle is typically 3,000 kg.

3.3.1.5 System Availability

APM systems generally require availability (during operating hours) of greater than 99.5 percent. People Movers for other applications would have similar availability requirements.

3.3.2 Functional Requirements

3.3.2.1 Destination Control

In general, PM systems are configured so as not to require destination control. Vehicles stop at each station along a fixed route with no variation. This approach eliminates a certain amount of control complexity.

3.3.2.2 Grade Climbing

Grades in PM systems would seldom exceed 8 percent.

3.3.2.3 Curving

Minimum curve radii for PM systems are typically 20 m.

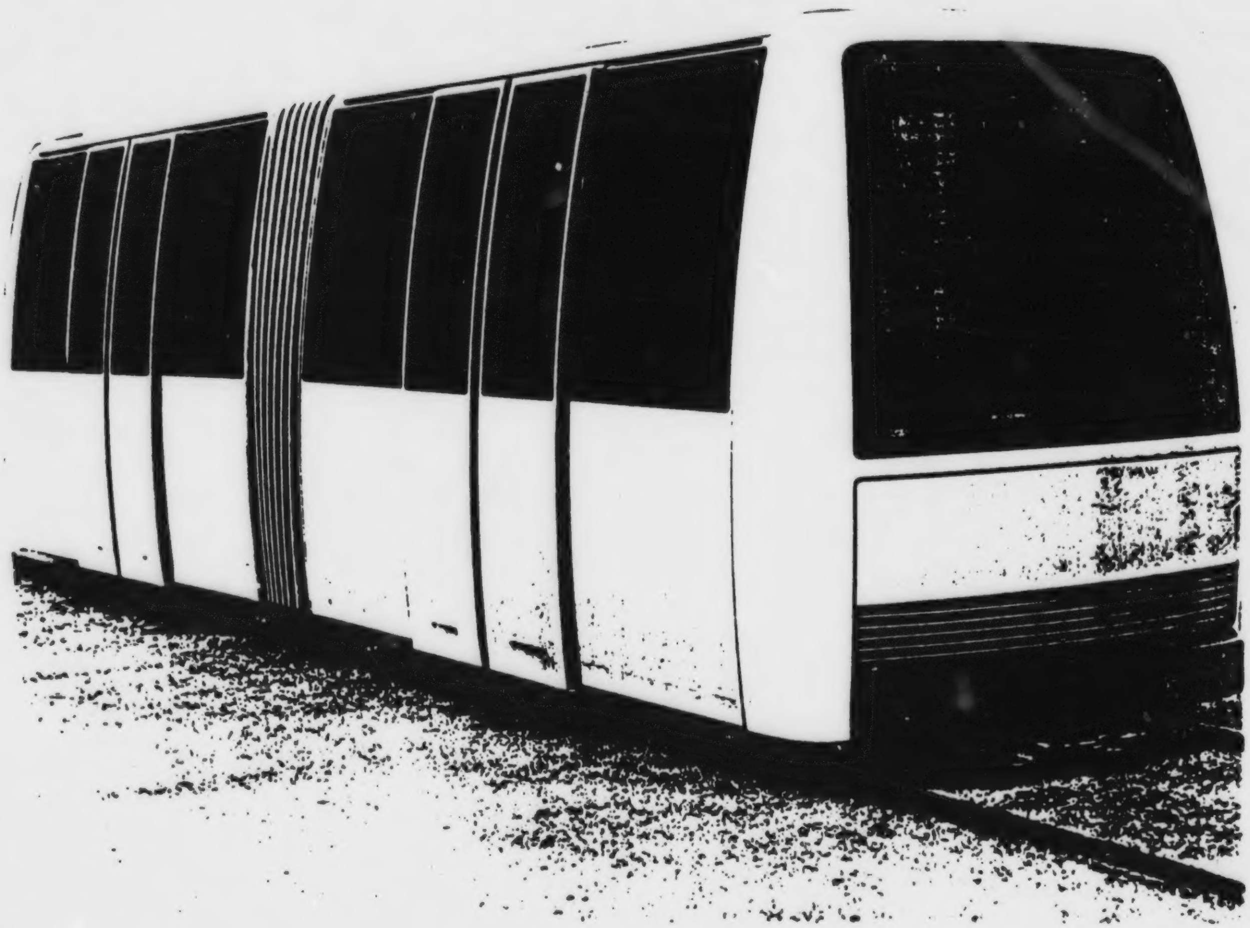

FIGURE 3-5: LIT - PROPELLED VEHICLE FOR "PEOPLE-MOVING"

3.3.2.4 Safety

Safety requirements for PM systems are more extensive than for material or baggage handling systems. All subsystems which relate to safety must be designed to be fail safe. In some cases this may lead to a requirement for redundant back-up systems and failure detection systems. For example, the loss of LIM braking effort must be detected and alternative braking immediately initiated.

3.3.3 Performance Requirements

3.3.3.1 Speed

Maximum speeds for PM systems are typically 12 m/s or less. Regulation of ±10 percent is adequate.

3.3.3.2 Acceleration and Jerk

Passenger comfort considerations limit the acceleration to 1 m/s^2. The rate of change of acceleration typically should not exceed 1 to 1.3 m/s^3.

3.3.3.3 Thrust

Typical acceleration thrust requirements are 4 kN. Cruise thrust 1 kN and grade-climbing thrust 5 kN.

3.3.3.4 Duty Cycle

LIM duty cycle is dependent on its location and on the system headway. Worst case duty cycle would be for a "station" LIM stator in a low headway system. For example, a 10 m long vehicle would present itself to a station LIM stator for a total of about 9 seconds (4.5 stopping, 4.5 starting) every 60 seconds giving a duty cycle of 0.2. In contrast a "cruise" LIM would only be "on" for 1 s in every 60 s for a duty cycle of less than 0.02.

3.3.3.5 Positioning Accuracy

Many PM systems employ "station doors", which require vehicles to be accurately aligned with preset stopping points at the station platform. Stopping accuracies of ±3 cm are typical.

3.4 CONTAINER HANDLING SYSTEMS

UTDC has recently conceived a scheme for moving shipping containers between port terminals and the train loading/unloading facility. The system concept employs LIT propulsion to carriers which are essentially railway flatcars equipped with reaction plates. The track is standard railway, mostly at grade, but elevated to create an overpass where required. Figure 3-5 illustrates the system and vehicle concept.

3.4.1 System Requirements

System requirements are at the time of writing, still being developed and detailed. Some of the figures coming out of the present UTDC system concept appear in the table introduced in the next subsection.

3.5 SECTION SUMMARY

The applications presented in this section illustrate the broad range of characteristics and performance that can be required of the basic LIT technology. Table 3-1 summarizes the typical specifications required in the four application areas.

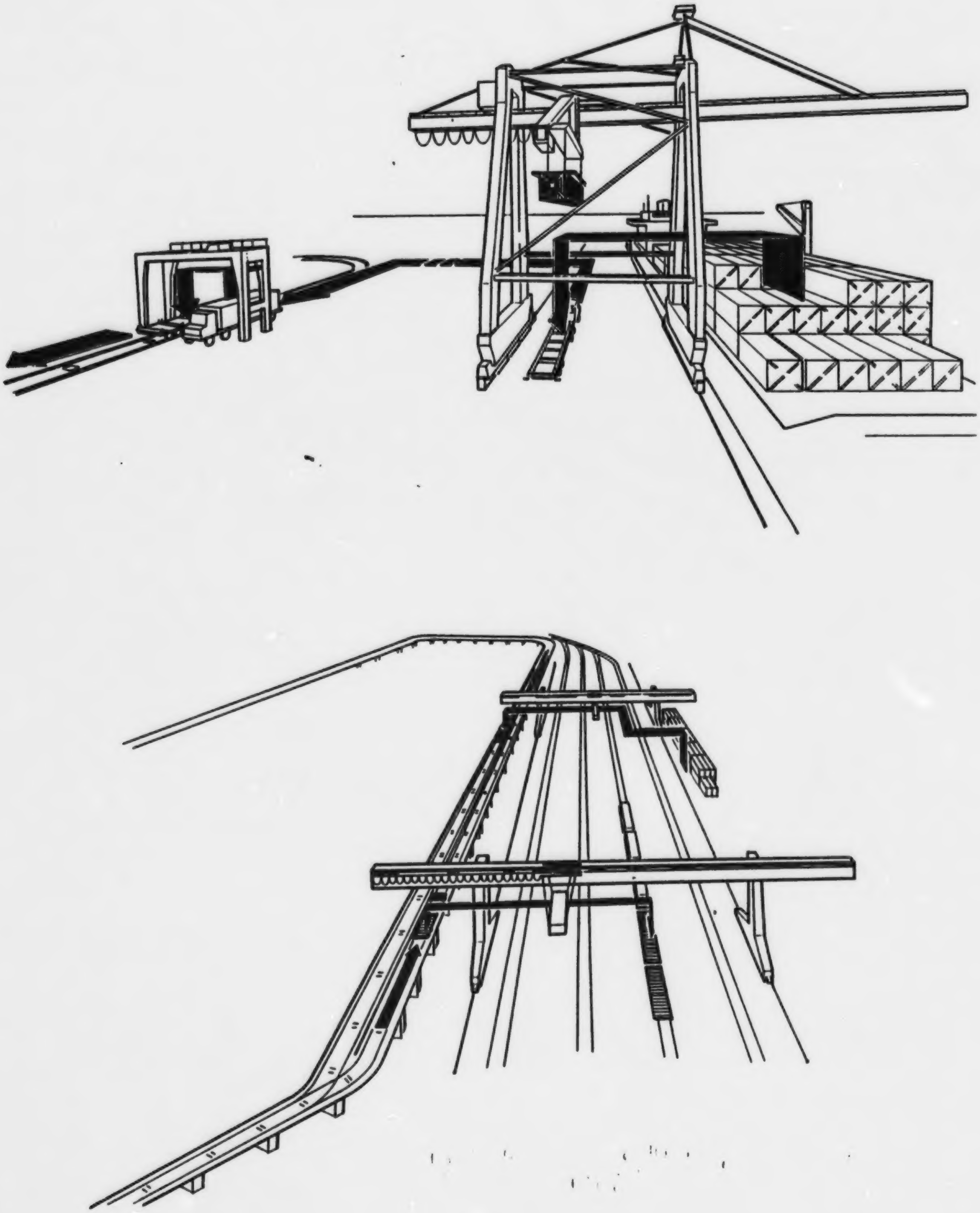

FIGURE 3-6: CARRIER CONCEPT FOR LIT CONTAINER HANDLING SYSTEM

TABLE 3-1: TYPICAL SPECIFICATIONS FOR LIM-IN-TRACK SYSTEMS

	INDUSTRIAL HANDLING	AIRPORT BAGGAGE TRANSPORT	PEOPLE MOVING	CONTAINER HANDLING
OPERATING REQUIREMENT				
Daily Service	16-24 hours	16-20 hours	16-20 hours	16-24 hours
Guidepath Environment	Comb. Shared/Ded	Dedicated	Dedicated	Dedicated
Availability	95%-98%	95%-98%	99.5%	99.5%
Throughput (1)	50-250 loads/hr	20-40 bags/min.	1000-5000	40-50 contners
Max. Time to Restore	4-8 hours	4-8 hours4-8	1 hour	1-4 hours
SYSTEM LAYOUT				
Configuration	Unidir. loop or Bi-dir Shuttle	U/D Loop	U/D Loop or B/D Shuttle	B/D Shuttle
Round Trip Distance	300-1000 m	3000-6000 m	1000-5000 m	15-20 km
No. of Branch Points	1-10	5-15	none	10-20
No. of Stopping Points (2)	2-10	20-60	2-10	
Elevation Change	5-10 m	10-20 m	5-10 m	15-20 m
TRACK DESIGN				
Configuration	Flat Floor or Elevated Track	At-grade and Elevated Track	Steel Rail, Cncrt Guideway	Steel Rail
Min. Curve (Horiz.)	3.5 m	5 m	20 m	75 m
Min. Curve (Vert.)	10 m	3 m	300 m	300 m
Max. Incline	10-18%(6-10 deg)	25-60%(14-30deg	8% (5 deg.)	5% (3 deg.)
VEHICLE				
Configuration	Two-car articulated	Single car	Two-car articulated	Modified Rail-way car
Length	5 m	2 m	7 m	15 m
Mass (Empty)	1,000 kg	300 kg	4,000 kg	15,000 kg
Mass (Loaded)	1,500-4,000 kg	600 kg	7,000 kg	35,000 kg
CONTROL				
Min. Headway	30 sec.	30 sec.	60 sec.	70 sec.
Acceleration	1 m/s^2	4 m/s^2	1 m/s^2	0.3 m/s^2
Positioning	± 3 cm	± 3 cm	± 3 cm	± 20 cm
PROPULSION (CRUISE)				
Stator Spacing	Vehicle length	Several vehicle lengths	Vehicle len.	Several vehicle lengths
Thrust	300-600 N	1,000-2,000 N	2,000-3,000 N	3,000-5,000 N
Duty Cycle	3-10%	1-4%	1-4%	1-4%
Speed	1-3 m/s^2	5-10 m/s^2	10-12 m/s^2	7-10 m/s^2
PROPULSION (SLOPE)				
Stator Spacing	½ vehicle length	½ veh. length	½ veh. length	½ veh. length
Thrust	2,000-6,000 N	2,000-3,000 N	4,000-5,000 N	5,000-6,000 N
Duty Cycle	3-10%	1-4%	1-4%	1-4%
Speed	1-3 m/s^2	5-10 m/s^2	10-12 m/s^2	7-10 m/s^2
PROPULSION (STATION)				
Stator Spacing	½ vehicle length	½ veh. length	½ veh. length	½ veh. length
Thrust	1,000-3,000 N	2,000-3,000 N	3,000-4,000 N	4,000-6,000 N
Duty Cycle	6-20%	2-8%	2-8%	3-12%

Notes: (1) Throughput expressed in application-specific terms. See "Min. Headway" for comparison reference.
(2) Does not include stops in live buffer storage areas (eg. queuing zones).

4.0 DESIGN ISSUES PECULIAR TO LIT SYSEMS

4.1 AIRGAP CONTROL AND GEOMETRICAL CONSTRAINTS

A distinct feature of LIM-driven vehicles as compared with conventional wheel-driven vehicles is the requirement for a reaction plate, and the small gap which separates it from the LIM stator. One might be inclined to ask: "How small must the airgap be?". The answer: "As small as is practical.". LIM performance is strongly airgap-dependent, that is, smaller gaps mean smaller LIMs, smaller controllers and less Volt-Ampere consumption. Of course, there are practical limits to how small the gap can be. Mechanical deflections, design tolerances, thermal distortion and wheel-wear mitigate against absolute gap control. Moreover, one must recognize that having settled on a nominal gap there are considerations relating to track geometry. Specifically, the handling of gap control requirements in the vicinity of vertical transistions, ie. at the entrance and exit to grades and superelevated (banked) curves. The following subsections address these issues in greater detail.

4.1.1 Airgap "Budget"

Table 4-1 provides a typical breakdown of the variables which affect the airgap tolerance. The purpose of the breakdown is primarily to identify these variables, not to quantify them. The actual contributions of each will of course be determined by the particular designs, installation practices and maintenance practices which are employed in a given case. The numbers used are typical of UTDCs experience, which suggests that a nominal gap of about 5-6 mm is practical for polyurethane-tired vehicles running on "I-beam" track or concrete floor. It should be noted however that the WEDway APM system employs a 4 mm gap while the Docutel BTS system specifies only slightly more than 2 mm. The tradeoff for a smaller gap is more performance at the cost of stiffer (and heavier) vehicle and track designs, increased maintenance (adjustment and wheel replacement) and occasional damage due to stator/reaction plate interference.

4.1.2 Track Geometry Issues

Vertical track curvature of either positive or negative radius (ie. at transitions to an inclined section) present a special problem to vehicles which carry reaction plates, since the plate, in chording the arc of the curve, does not present a fixed, uniform airgap to a stator located on the arc. There are at lest three ways to address this issue, but none are of universal utility. Their suitability depends on the specific application.

The first approach is simply to tolerate the airgap variations caused by vertical curve chording. So long as the vertical curve radius is very large compared to the vehicle wheelbase, chording on both positive and negative curves produces minor gap changes, and

CAUSE	ITEM	GAP CHANGE mm
Deflection Due to LIM Vertical Forces	o Wheel	-0.2
	o Track	-0.1
	o Chassis	-0.1
	o Reaction Plate	-0.2
Distortion Due to Thermally-Induced Forces	o Stator	-0.1
	o Reaction Plate Top Cap	-0.4
	o Reaction Plate Back Iron	-0.1
Design Tolerances	o Track Surface Flatness	±1.0
	o Stator Surface Flatness	±0.2
	o Reaction Plate Surface Flatness	±0.5
Installation Adjustment	o Reaction Plate	±1.0
	o Stator	±0.5
Wear	o Wheels	-1.0
	Minimum gap = nominal	-5.4
	Maximum gap = nominal	+1.0

TABLE 4-1: TYPICAL LIM AIRGAP BUDGET

LIM thrust can be maintained. This approach is reasonable in People Mover systems where grades are typically 8 percent or less, and where vertical curve radii are limited by speed and passenger comfort criterion to 200 m or more.

In Industrial and Airport Handling systems, grades are steeper and "comfort" is not a criterion. Indeed, in order to minimize the length required to change elevations, steep grades and small vertical curve radii are demanded. With typical vehicle/track geometries it is totally impractical to place LIM stators along the arc of the curved transition. However, if vehicle speed entering the transition is sufficiently high, the vehicle will have enough kinetic energy to coast through the transition thereby eliminating the need for stators. Appendix A-1 develops a formula for determining the minimum required speed for a vehicle of a given wheelbase entering a transition of given radius and angular elevation such that it will coast to the next LIM stator.

In some applications, vertical transitions are such as to prohibit stator placement, but vehicle speeds are too low to allow coast-through. A solution which has proven practical is to couple two or more vehicles by employing a continuous, "articulated" reaction plate. The resulting extra-long vehicle spans the transition sector so that stator coverage is continuous and propulsion is maintained.

Figures 4-1 a-c illustrate the three approaches to the vertical curve issue. The positive radius case is shown, but similar principles apply the negative radius case (ie. at the "top" of the grade).

Another track-geometry issue which is rather complicated is handling transitions into superelevated curves. In materials transport systems, such geometries are avoidable, but in People Mover systems, banking is often necessary. While airgap considerations pose potential problems here, a more serious issue is the mechanical design of the suspension and reaction rail, which typically have little torsional compliance. In practice, the rate of track twist must be kept small enough to avoid wheel-lifting.

4.2 "BOOST/COAST" DESIGN

In systems which do not carry passengers (ie. no "comfort" criterion) and which have sufficiently high cruising speeds, it is cost-saving to place LIM stators at distances several times greater than the vehicle length. This results in non-continuous propulsion, hence a variation in speed about some average value. Nevertheless, the performance is often more than adequate.

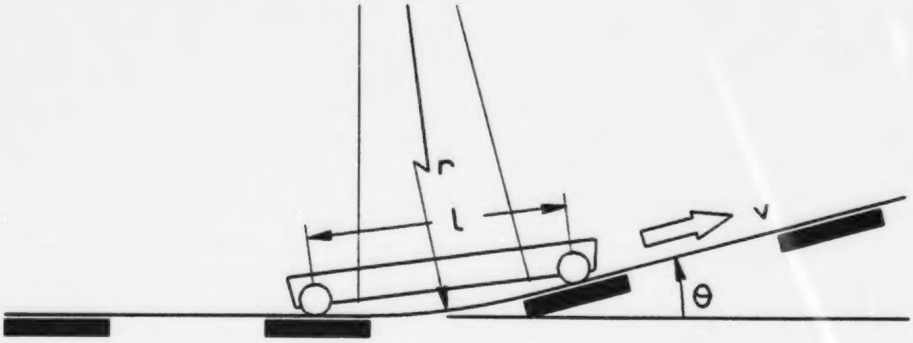

A) CONTINUOUS STATOR COVERAGE FOR LARGE-RADIUS CURVES

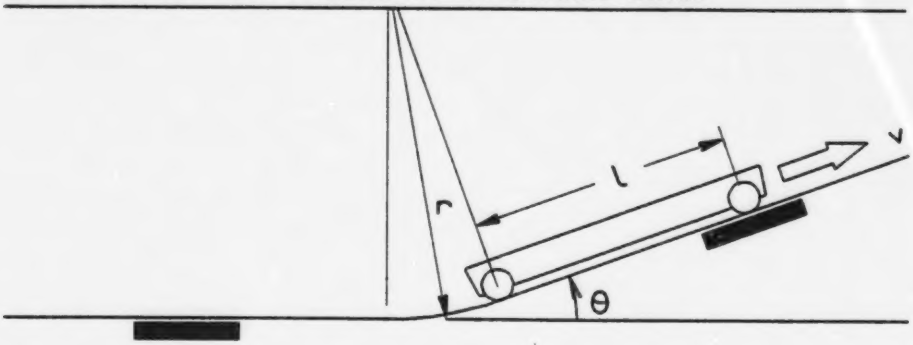

B) COAST THROUGH APPROACH FOR SMALL-RADIUS CURVES

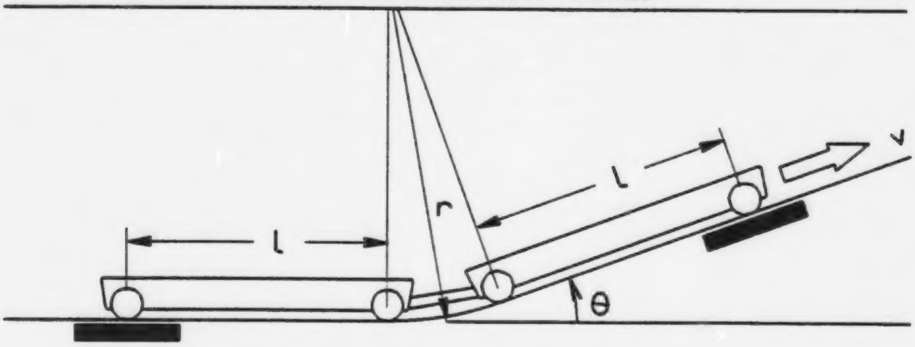

C) COUPLED-VEHICLE APPROACH FOR CONTINUOUS COVERAGE

FIGURE 4-1: APPROACHES TO PROPULSION ON VERTICAL CURVES

Figure 4-2 is a speed vs. distance graph showing the concept of boost/coast LIM propulsion. The curve labelled "1" is the normal case: Through the "boost" zone the vehicle is over a LIM stator and is accelerated to a higher speed. Through the "coast" zone the vehicle slows down due to drag forces. If the next LIM stator and its associated controller are functional, the kinetic energy lost while coasting will be restored so as to maintain a steady average speed. If this LIM fails to thrust, the vehicle will continue to lose speed as shown on curve "2".

It is generally an important consideration in systems employing the "boost/coast" principle to design in the capability to "coast through" at least one failed LIM. In other words the LIM spacing must be sufficiently close to ensure that the vehicle speed will not have dropped to zero over the distance spanning three LIM stators.

Curve "3" shows the speed increase imparted by the third LIM to a vehicle which has coasted to below normal speed. Note that there may not be sufficient extra thrust capability in a LIM to fully restore the vehicle's normal speed after only one boost, but subsequent boosts will do so.

The "boost/coast" principle is useful in systems which have long, level, high speed sections. In UTDC's experience, vehicle speeds of 4 m/s and higher can be considered suitable.

4.3 POWER FAILURE

In LIT systems, failure of main power results in total loss of propulsion, and just as seriously, loss of LIM braking. The situations of concern are power failures which occur at the moment a vehicle is ascending or descending a grade, or approaching a station stop. The means which have been devised to deal with these situations are described in the following sections.

4.3.1 Wayside Brakes

Figure 4-3 is an illustration of a wayside friction brake assembly. It is spring-applied and pneumatically-released. The jaws close on a vertical rail which is fixed to the vehicle. The ends of the friction plates are flared so as to allow a slightly misaligned brake rail to enter a closed brake without damage.

Wayside brakes are located on grades and approaching station stops. Failure of power will result in immediate closure of the brakes thereby avoiding a runaway vehicle situation.

4.3.2 Permanent Magnet Decelerators (PMD)

Electromagnetic braking can be achieved by passive means employing stator-like devices which use permanent magnets rather than energized windings to provide a magnetic field. (Refer to Figure 4-4.) A reaction plate passing over such a device will see induced

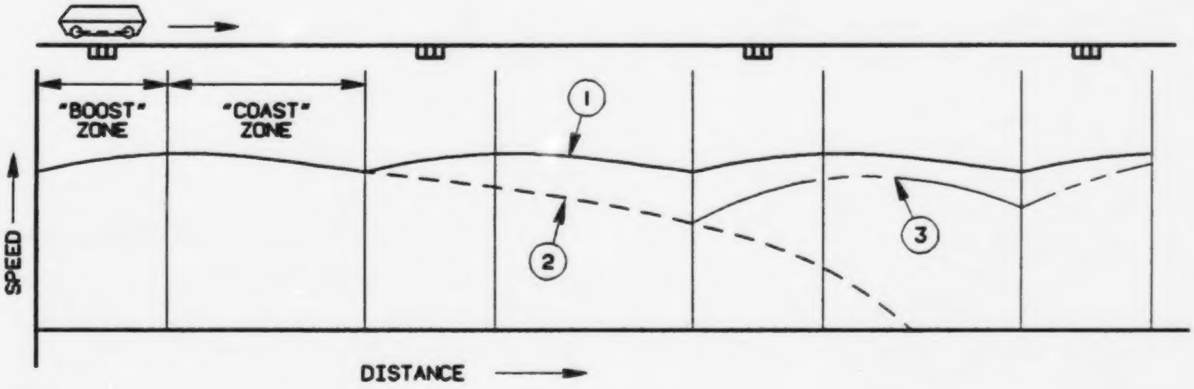
"BOOST" ZONE
"COAST" ZONE
①
②
③
SPEED
DISTANCE

FIGURE 4-2: BOOST/COAST PROPULSION CONCEPT

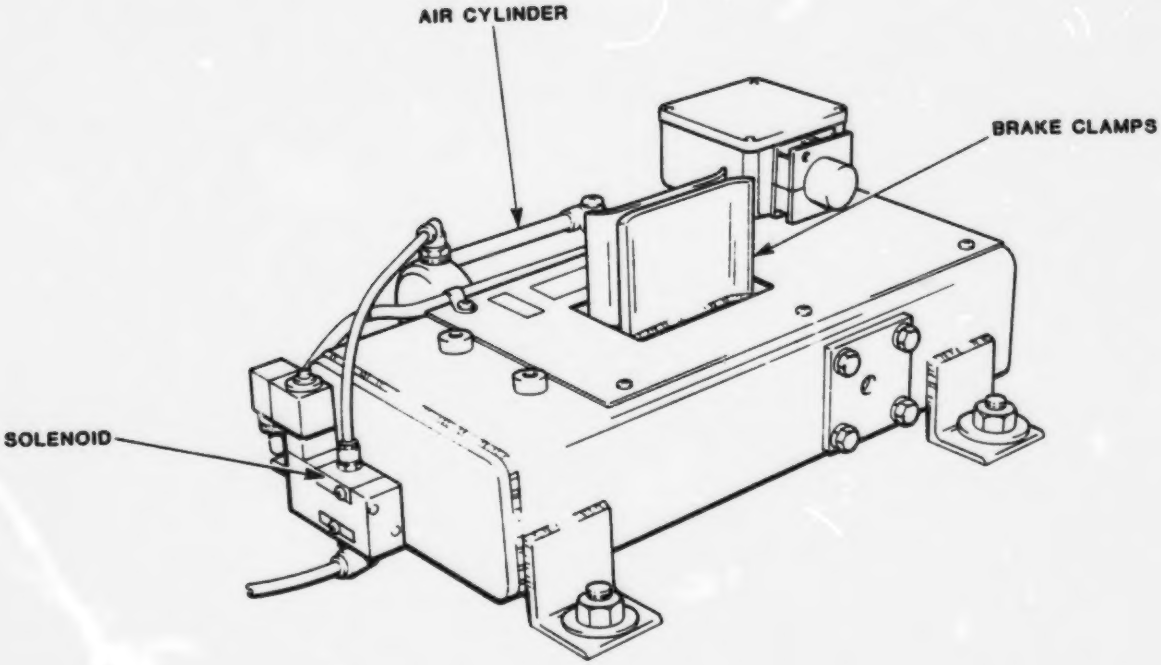
AIR CYLINDER
BRAKE CLAMPS
SOLENOID

FIGURE 4-3: WAYSIDE BRAKE ASSEMBLY

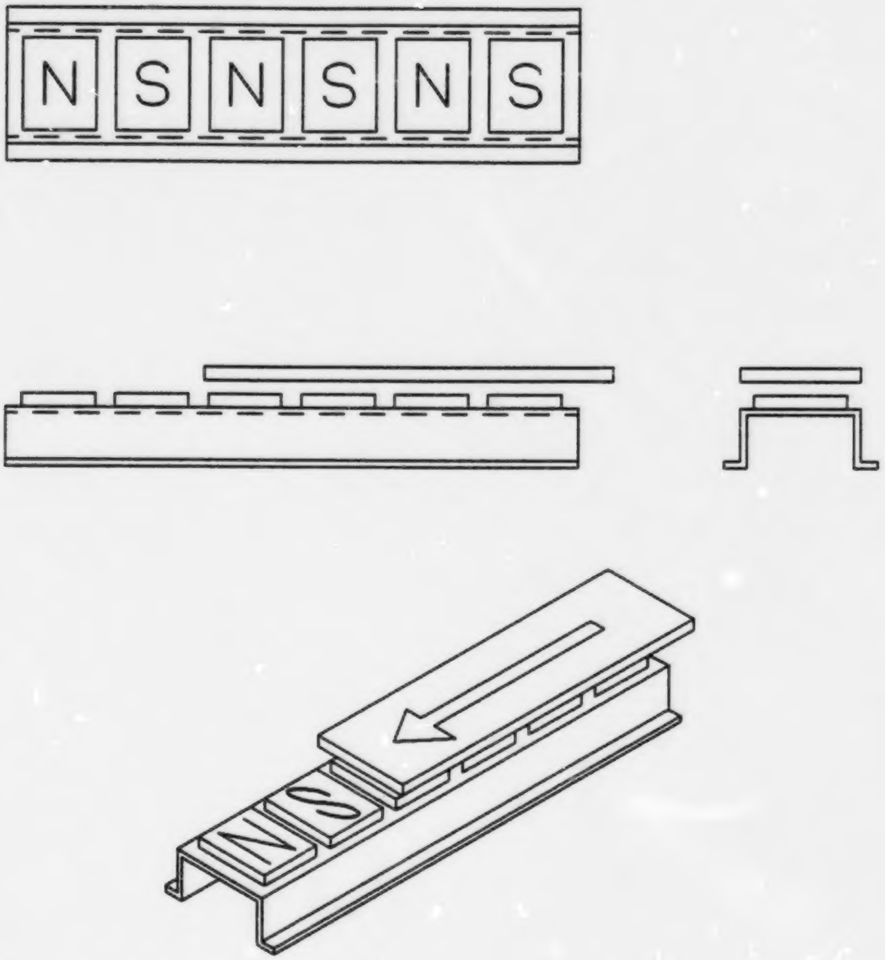

FIGURE 4-4: PERMANENT MAGNET DECELATOR

currents which will interact with the magnetic flux so as to cause braking action. The braking effect diminishes as speed approaches zero, so PMDs cannot actually bring a moving vehicle to a stop. However, they can be used quite effectively in areas where the vehicle would normally need braking to reduce speed or to avoid overspeed. For example, on descending slopes.

PMDs require no power and are therefore effective even during a power failure. However, since they cannot be "turned off" they are seldom if ever useful in bi-directional systems.

4.4 SINGLE POINT FAILURE AVOIDANCE

In systems of which high reliability is demanded, functionality should not be lost due to the failure of any one component or subsystem. In LIT systems, the inherent redundancy of the distributed propulsion control architecture simplifies the realizing of this goal. However, some guiding principles apply. Table 4-2 highlights these.

4.5 POWER DISTRIBUTION AND PROTECTION

Figure 4.5 is a single-line schematic diagram of a typical LIT power distribution system. Individually fed subsections permit maintenance of a section without impacting the whole system. The loads, which are the LIM stators, are often distributed over several tens of meters between feed points. Since the LIMs are "on" cyclically and intermittently, their loading effect must be calculated based on a root-mean-square determination of the current drawn by each controller (for description of current cycle, see Figure 5-3).

The formula for the determination of the load current of the cables is explained in Appendix A-2. Note that the distribution line carries the most current closest to the feed point. As the distance increases away from the feed, the distribution cables carry less current.

One might propose as a cost saving measure that the size of the power cables could be reduced for sections that see less current, i.e., that the cable diameter could be lowered by a "step" at each interload link as the distance from the feed point increases. Unfortunately, this approach cannot be employed. The circuit breaker that protects the power distribution line must be sized for the current seen at the feed point. It would therefore not serve to protect cable any smaller than that used at the feed point, i.e., while the smaller cable may be suitable in terms of its normal current handling capacity, it would not be adequately protected in the fault condition.

PROPULSION	Grades	Extra-close spacing is usually required to ensure coast-through capability on ascending slopes.
	Curves	High drag and low speeds are typical, so close spacing may be necessary to ensure coast-through capability.
	Station-Stops	Two LIM/controller sets are required under a stopped vehicle to ensure re-start.
SUPERVISORY SYSTEM	Master Computer & Data Link (Option 1)	System should remain functional (perhaps with degraded performance and no monitoring) for a temporary period following the loss of either the master computer or communications bus.
	Master Computer & Data Link (Option 2)	If system function is highly dependent on Central Control functions, then a standby computer and communications link should be switched in. Automatic failure detection and changeover is preferred to manual.

TABLE 4-2: SINGLE-POINT FAILURE AVOIDANCE DESIGN PRINCIPLES FOR LIT SYSTEM

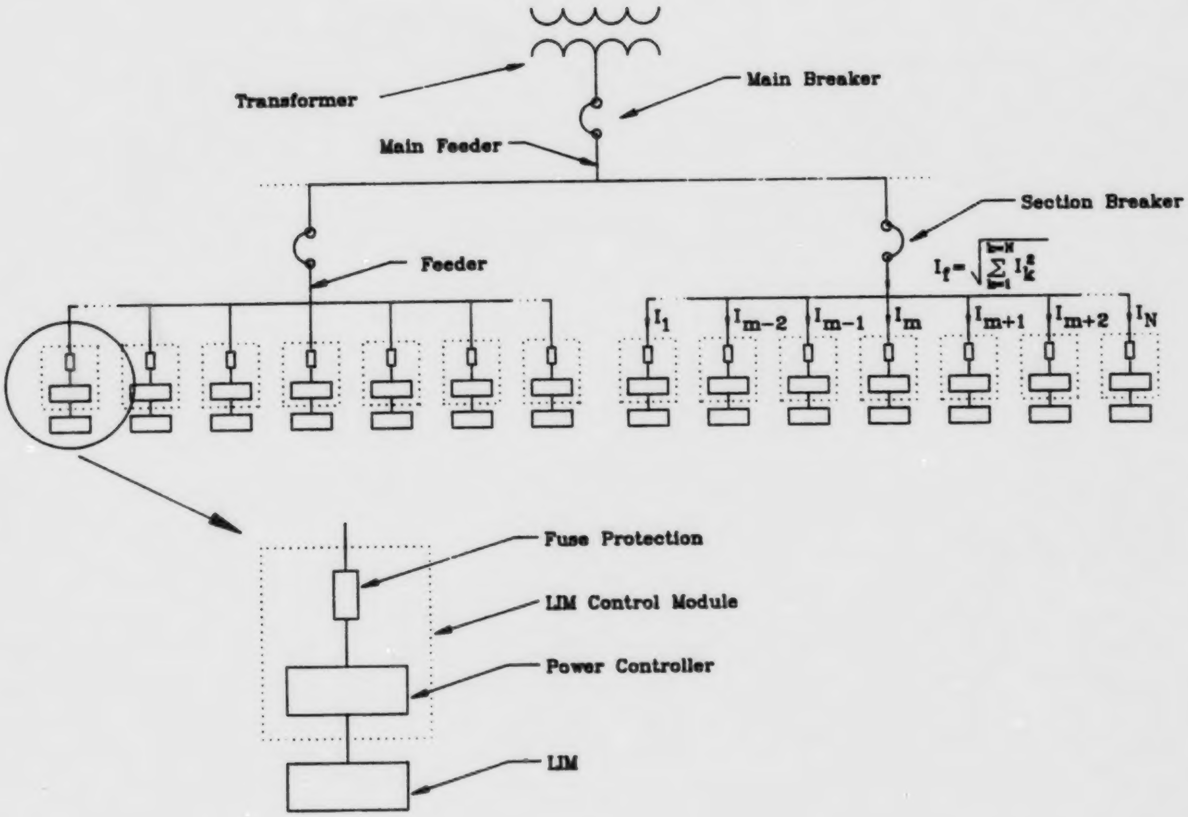
Transformer
Main Breaker
Main Feeder
Section Breaker
Feeder
$I_f = \sqrt{\sum_{k=1}^{k=N} I_k^2}$
I_1
I_{m-2}
I_{m-1}
I_m
I_{m+1}
I_{m+2}
I_N
Fuse Protection
LIM Control Module
Power Controller
LIM

FIGURE 4-5: SINGLE LINE DIAGRAMS OF A LIT POWER DISTRIBUTION SYSTEM

4.6 VEHICLE SENSING

Because LIT systems control vehicles from the wayside, the sensing of vehicle position and velocity is wayside-based. The sensor and processing described in Section 10 is able to detect the position and velocity of a vehicle passing over it, but in systems which employ the "boost-coast" control strategy described in Section 4.2, there would be a distance between LIMs in which the supervisory system could not know the vehicle position or velocity for lack of sensors. These "blind spots" are significant if the vehicle happens to stop between LIMs; an eventuality that must be accommodated for in the automatic control system.

Figure 4-6 illustrates one approach to managing the "blind spot" problem. It requires a "detect" output from the LIM controller that indicates that the controller "sees" a vehicle. This output latches "on" the moment a vehicle is detected. The signal is passed to a "clear" input on the previous LIM controller, which resets its own "detect" output. In this manner, the location of the vehicle can always be known to within the distance between any two LIMs, and should the vehicle stop, it will not become "invisible" to the automatic control system.

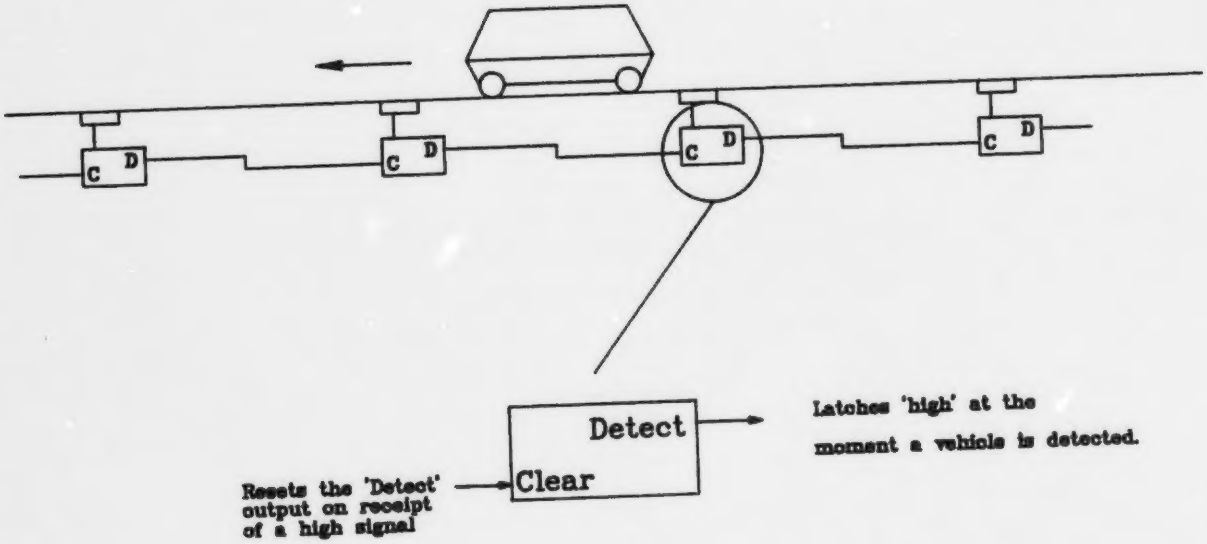
C
D
C
D
C
D
C
D
Detect
Clear
Latches 'high' at the moment a vehicle is detected.
Resets the 'Detect' output on receipt of a high signal

FIGURE 4-6: VEHICLE PRESENCE DETECTION ARRANGEMENT FOR BOOST-COAST LIT SYSTEMS

5.0 LIM MODELLING, EXPERIMENTS AND DESIGN

5.1 REVIEW OF LIM DESIGN ISSUES

In this section an overview of the LIM design problem is presented. The topic is approached from three sides: the first side is a review of the basic performance requirements typical of LIT applications and identifies some practical considerations. The second side concerns the physical factors that constrain the design, i.e. which prescribe the limits and trade-offs relating to form, material quantities, power consumption and control requirements.

Finally, the notion of design optimization is explored, and some typical optimization criteria are identified.

5.1.1 Performance Requirement

What is required of a given LIM stator operating in a LIT system? Clearly it must provide propulsion or braking effort to vehicles that pass over it. The requirement is most simply stated as a Thrust at some Speed for some Duty Cycle. The following sub-sections consider these three parameters.

5.1.1.1 Thrust

In most LIT systems it is necessary to specify a "nominal operating" thrust and a "peak" thrust. The former is determined by the normal operating case, be it cruising, accelerating, decelerating, grade-ascending or grade-descending. "Peak" thrust is designed-in as "headroom" or reserve thrust capacity and is sometimes associated with a "one time" system failure-recovery scenario such as accelerating a vehicle from a dead start in what would normally be a cruise section.

Care must be taken to choose the "nominal" thrust for worst-case operating conditions if those conditions are likely to persist for more than a few hours. (The stator thermal time-constant is long enough that thrust higher than nominal can be tolerated for an hour or so, so long as subsequent operation is lighter than nominal.)

For example, a typical "worst-case nominal" thrust design target would need to address all of the operating parameter variations which 1) diminish the normal thrust capability of the stator and 2) increase the basic thrust requirement of the vehicle. Thesevariations are case-dependent, but almost any system is subject to at least a few parameter variations. Some of the more sensitive of these are listed in Table 5-1.

5.1.1.2 Thrust vs. Speed

The characteristic performance of any motor is speed dependent, though sometimes it is possible through appropriate control of the

PARAMETER	SENSITIVITY OF THRUST TO PARAMETER CHANGE
Mechanical Airgap	Thrust lost of 10% per mm of increase off nominal is typical of short-pitch, fixed-frequency LIMs. Longer pole pitch reduces sensitivity to gap changes.
Supply Voltage	Max. Thrust is diminished by the square of the reduction in supply voltage off nominal.
Top Cap Temp.	Depending on design, higher temperatures can mean more, or less, maximum thrust capability. Usually, for fixed-frequency LIMs, accelerating thrust is diminished while braking thrust increases.

TABLE 5-1: PARAMETER VARIATIONS WHICH AFFECT THRUST PERFORMANCE

supply to make the thrust appear not to be, if such a characteristic is desirable.

In the case of LIMs with closed-loop speed control, the "natural" voltage-driven or current-driven thrust vs. speed characteristic does not hold a great deal of significance except in the limits that it presents to operation beyond a given speed. For example, Figure 5-1 a indicates this limit in the characteristic of a voltage-controlled, fixed frequency LIM. Beyond point "A", thrust falls with increasing speed until at point "B" thrust is zero. (The negative-slope of the curve between "A" and "B" is sometimes exploited as a means to regulate speed in the absence of a closed loop controller.)

In Figure 5-1 b the envelope of a "family" of fixed-frequency, current-controlled thrust/speed curves is shown.

Note the point "C" at which the voltage required to maintain constant current exceeds the voltage limits of the variable-frequency supply. Beyond this point voltage is held at the limiting value and thrust diminishes with increasing speed. Point "D" represents the upper limit to speed imposed by the maximum operating frequency of the supply.

5.1.1.3 Duty Cycle

The duty cycle is the averaged proportion of time the LIM stator is "on". It is intended as some measure of the thermal load to which the stator is subjected. Duty Cycle is straightforward to calculate and employ when the stator "on/off" cycle is the simple type shown on Figure 5-2, but the concept loses its utility for more complicated cycles such as is shown in Figure 5-3. For these situations the root-mean-square current must be calculated first and an "effective" duty cycle derived.

5.1.2 Physical Constraints

The progress made in the engineering of electrical machines over the past century has largely been due to steady efforts at pushing back the barriers imposed by material properties, and more recently, by advances in techniques for controlling electrical power by means of solid-state electronics. Notwithstanding the progress in these areas, physical constraints are as much as ever a concern of the design engineer, who must attempt not only to design within the constraints, but to gain maximum utility from the materials and energy used.

5.1.2.1 Power Supply

The power semi-conductor devices which are employed in circuits for controlling LIMs are subject to limitations in voltage withstand capability and current handling capacity. There are other

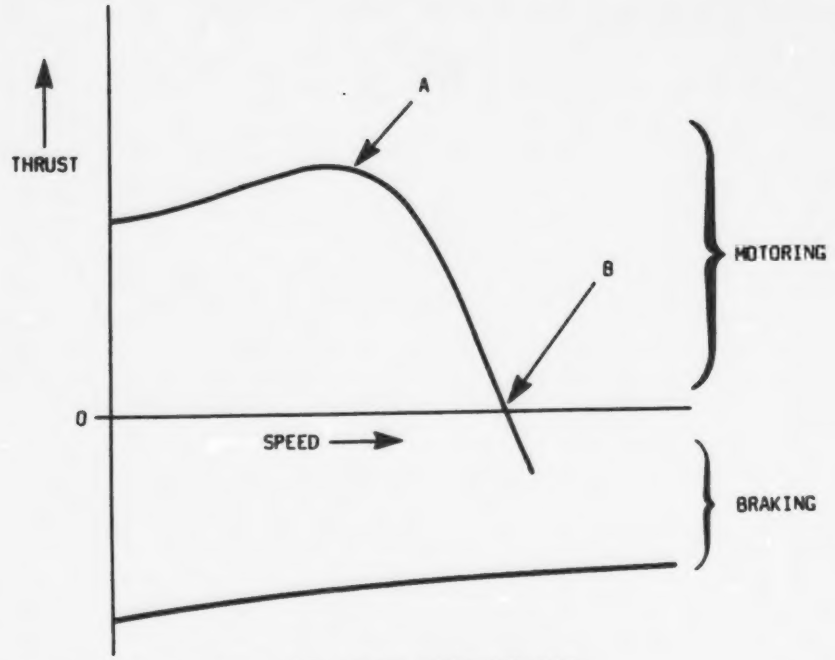

a) FIXED-FREQUENCY, VOLTAGE-DRIVEN CHARACTERISTIC

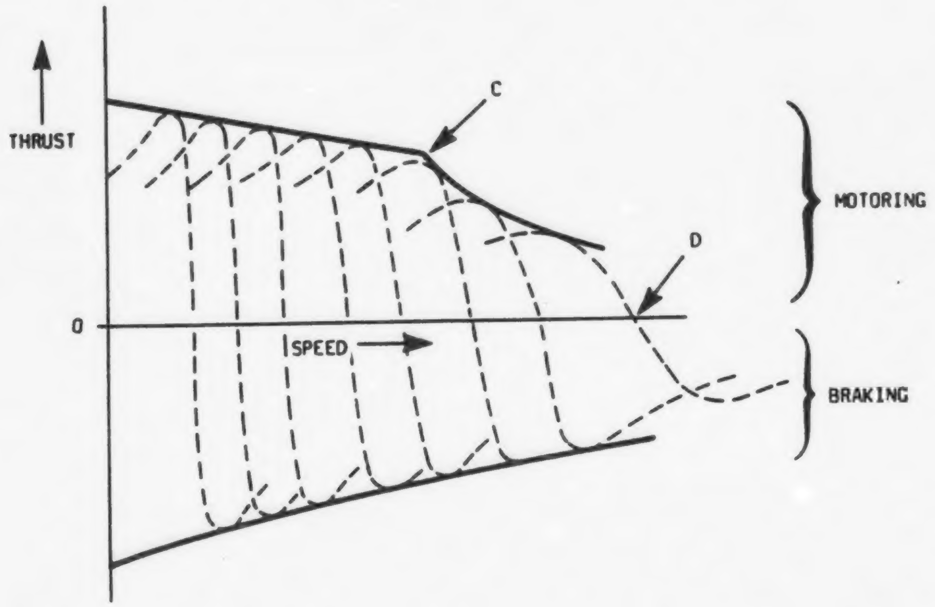

FIGURE 5-1: LIM THRUST VS. SPEED CHARACTERISTICS

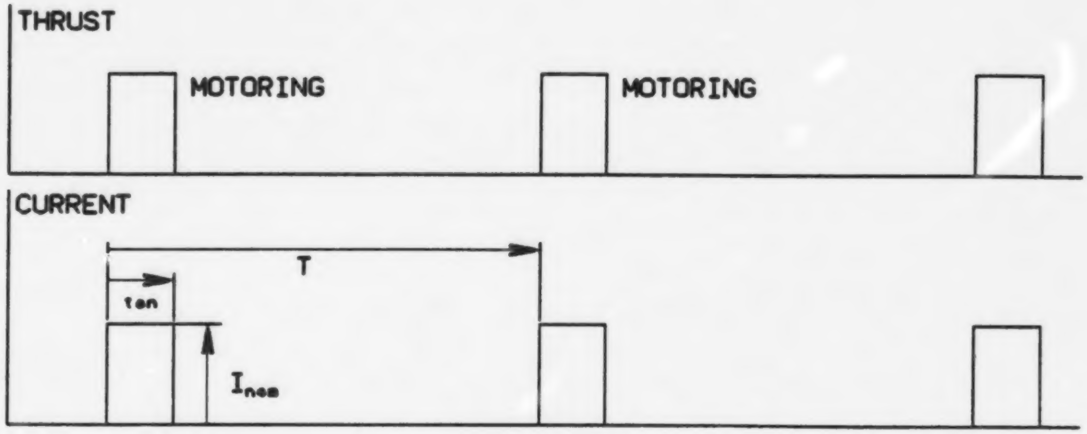
THRUST
MOTORING
MOTORING
CURRENT
T
ton
I_{nom}

D = DUTY CYCLE = $\frac{t_{on}}{T}$ EFFECTIVE CURRENT = $I_{rms} = \sqrt{D}\, I_{nom}$

FIGURE 5-2: SIMPLE DUTY CYCLE

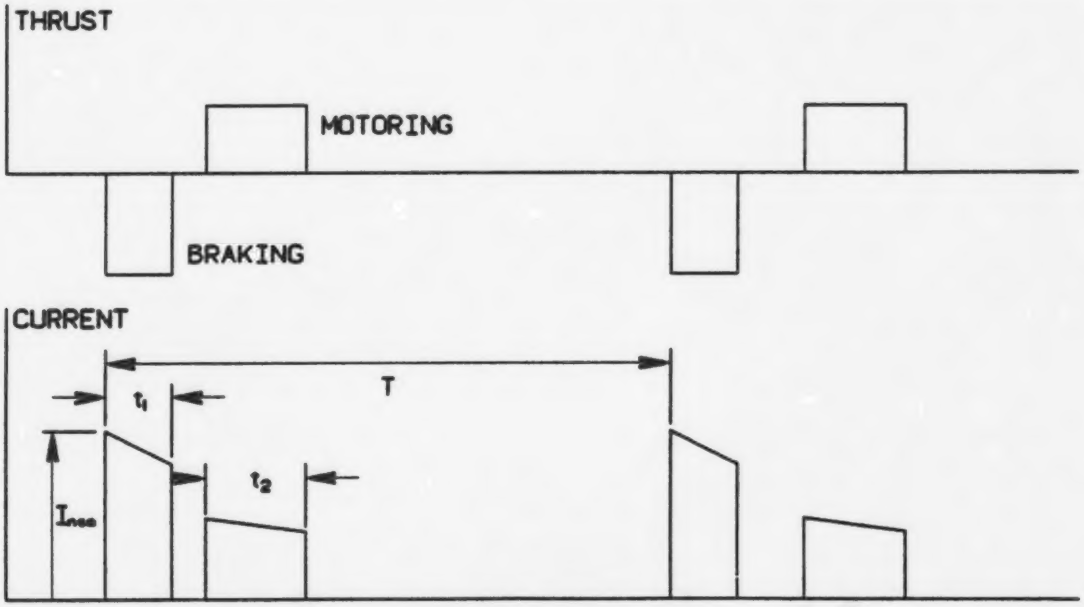
THRUST
MOTORING
BRAKING
CURRENT
T
t_1
t_2
I_{nom}
TIME

D_{eff} = EFFECTIVE DUTY CYCLE = $\left(\frac{I_{rms}}{I_{nom}}\right)^2$

FIGURE 5-3: TYPICAL DUTY CYCLE

limitations which must be understood for such circuits to be correctly designed, but it is voltage and current limits that place the upper boundary on the thrust that can be produced by a LIM.

Fixed frequency LIM designs employ silicon-controlled rectifiers (SCR's) in the power circuit. For this type of circuit, SCR's are available in an anti-parallel connected, plastic-encapsulated package. These components permit a simple, low cost, compact, physical construction and are suitable for use in applications of up to 600 V, 150 A. Higher current devices are available in "puck" packages.

Variable frequency applications employ either Gate- Turn-Off (GTO) Thyristor or Bipolar Junction Transistor (BJT) devices as the switching element and power diodes as the non-switched (freewheel) element. Both GTOs and BJTs are also available in plastic packages with integrated diode. In the case of GTOs, 600 V, 200 A is about the practical limit for the plastic package. The BJT limit is somewhat lower at about 350 V, 200 A.

It is likely that power-semiconductor ratings will continue to improve over the coming years, but historically, the relative costs of devices has been more or less a direct function of their volt ampere rating, and will probably remain that way.

5.1.2.2 Stator Thermal Limits

Modern insulating materials typically have operating temperature limits of around 180°C depending on the classification of the material used. The LIM stator must therefore be designed accordingly.

The temperature rise above ambient for a given LIM stator can be estimated from a knowledge of the root-mean-square slot current density, J (A/mm^2), the root-mean-square surface current loading, A (A/mm), and the resistivity of the winding material (usually copper). Appendix A-3 shows that the product of these three terms yields the power per unit of stator face area. Experiments indicate that temperature rise is proportional to stator face power density and that the constant of proportionality is about $30°C/kW/m^2$. Figure 5-4 is a graph of temperature rise vs. power density based on tests made on a typical LIM stator. (Note that at temperatures beyond 100°C the curve begins to deviate slightly from the linear projection).

If it is assumed that the LIM will operate in a maximum ambient temperature of 40°C, and that a 10°C "margin" is required on top of that, then a 130°C rise is the maximum allowable if the winding temperature is to be kept below the safe operating limit of 180°C. From the graph it is seen that this corresponds to a stator face power density of 5 kW/m^2.

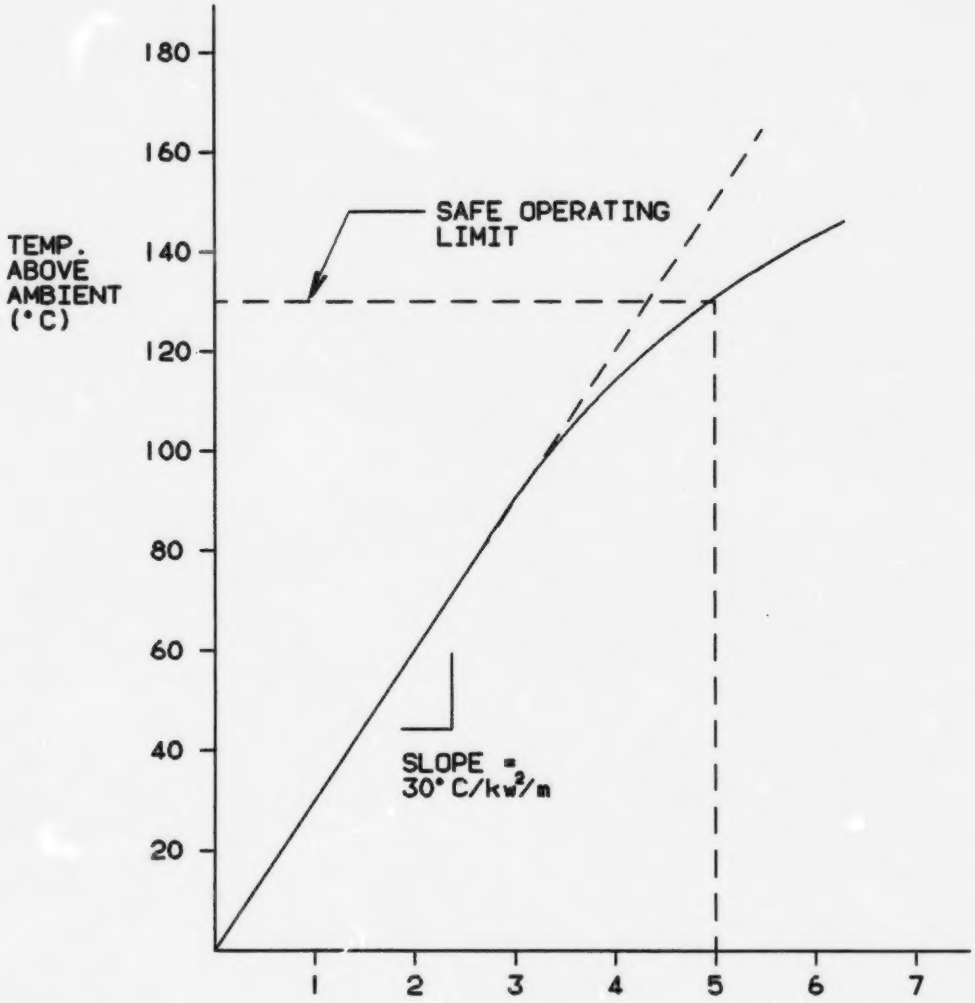

FIGURE 5-4: TYPICAL TEMPERATURE RISE POWER DENSITY CHARACTERISTICS FOR A LIM STATOR

The resistivity of copper wire is about 2.8 microhm-cm at these temperatures. Working back, one can state the thermal limit in terms of the JA product as 180 A^2/mm^3 which is a convenient number to remember, since it corresponds to the operating temperature limit of 180°C.

5.1.2.3 Stator Magnetic Limits

The stator Magnetic limits are based on the saturation characteristic of electrical steel, which exhibits a trend toward diminishing magnetic permeability as flux densities approach and exceed about 1.8 Tesla.

If part of the LIM magnetic circuit operates at flux densities above this range, the effectiveness of the LIM at producing thrust is reduced.

Good design practice is to choose the LIM core geometry so that flux densities are neither "too high" or "too low", since high densities result in reduced performance and low densities imply a "waste" of steel and a corresponding extra weight and cost.

Magnetic loading is more difficult to estimate than thermal loading, and requires an analytical model like the one described in Section 5.2.

5.1.2.4 Reaction Plate Thermal Limits

Like the LIM stator, the temperature rise of the reaction plate can be related to the power dissipated per unit face area. The power in the reaction plate may be calculated by application of the formula found in Appendix A-4. With this formula, power vs. time profiles can be constructed either manually or by computer simulation. The time-averaged power can then be calculated, and the reaction plate face power density determined by simply dividing by the reaction plate length and width.

The temperature rise characteristic as a function of power density for a typical reaction plate is shown in Figure 5-5. Note that airflow velocity makes a significant difference to the temperature rise. Since the reaction plate moves, there will be some airflow in practice. The actual amount will depend on the particular operating speeds.

5.1.3 Design Optimization Criteria

Once the basic performance requirements of thrusts, speed and duty cycle are established, the design task becomes one of choosing a geometrical configuration and control strategy that satisfies these requirements in a way that results in the most satisfactory overall system. Of course, the stated task is only possible if one has an understanding of how the design and control parameters can be

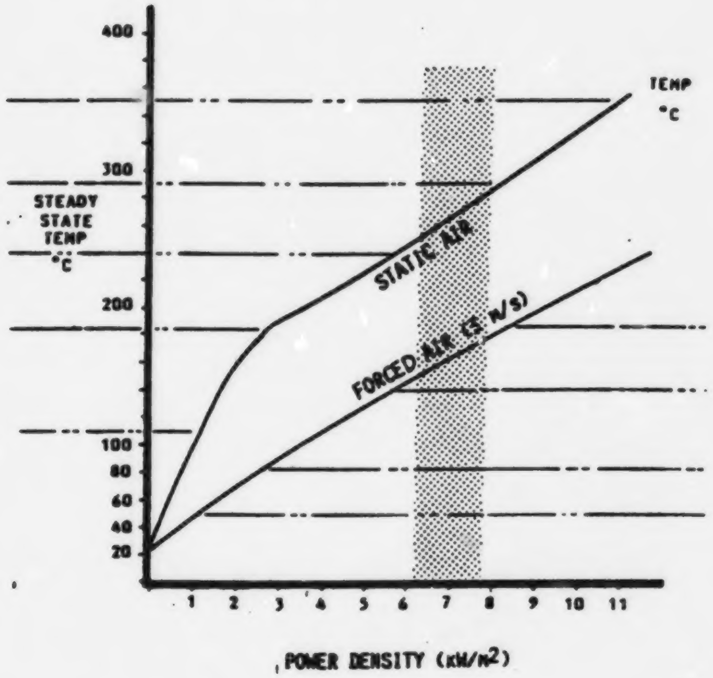

FIGURE 5-5: TYPICAL TEMPERATURE RISE VS POWER DENSITY CHARACTERISTIC FOR A REACTION PLATE

manipulated and to what effect, and some criteria by which a design can be judged relative to other candidate designs. System issues and the optimization criteria that arise from them are notoriously difficult to quantify accurately, so a true optimum is seldom if ever, achieved. Nevertheless, even a qualitative identification of the system issues can lead to a more intelligent LIM design.

The following subsections identify some issues that are universal for LIT systems. The relative importance of each of these will vary with the specific application. Most of the system issues derive from six design-related considerations which are highlighted in Figure 5-6.

5.1.3.1 Apparent Power

The amount of apparent power (VA) consumption of the LIM can be traded off against other issues, i.e., control complexity, stator size, real power and airgap.

In a fixed frequency system utilizing DC Power Distribution, apparent power is quite important because it impacts on the cost of the controllers, power distribution cables, circuit breakers and distribution transformers. Also, Power Utilities charge an additional rate for reactive power consumption.

In a variable frequency system, apparent power has a much smaller impact. Only the controller cost is sensitive to apparent power.

5.1.3.2 Real Power

In fixed frequency systems, Real Power is a relatively small proportion of the Apparent Power, and therefore does not, in itself, influence the cost of the power distribution or power controllers. In variable frequency systems, Real Power determines the size of the cables, D.C. breakers, rectifiers and transformers.

5.1.3.3 Control Complexity

Fixed frequency LIM control is simpler than variable frequency control, but results in considerably higher apparent power consumption (refer to Chapter 12). In "big" applications (e.g., LIMs of 3000 N thrust and higher) VF control can result in smaller stator size.

5.1.3.4 Stator Size

Minimization of stator size can be important in many LIT systems because LIM stators can represent a relatively large proportion of the system overall cost. Unfortunately, minimum stator size is achieved at the expense of real and apparent power consumption.

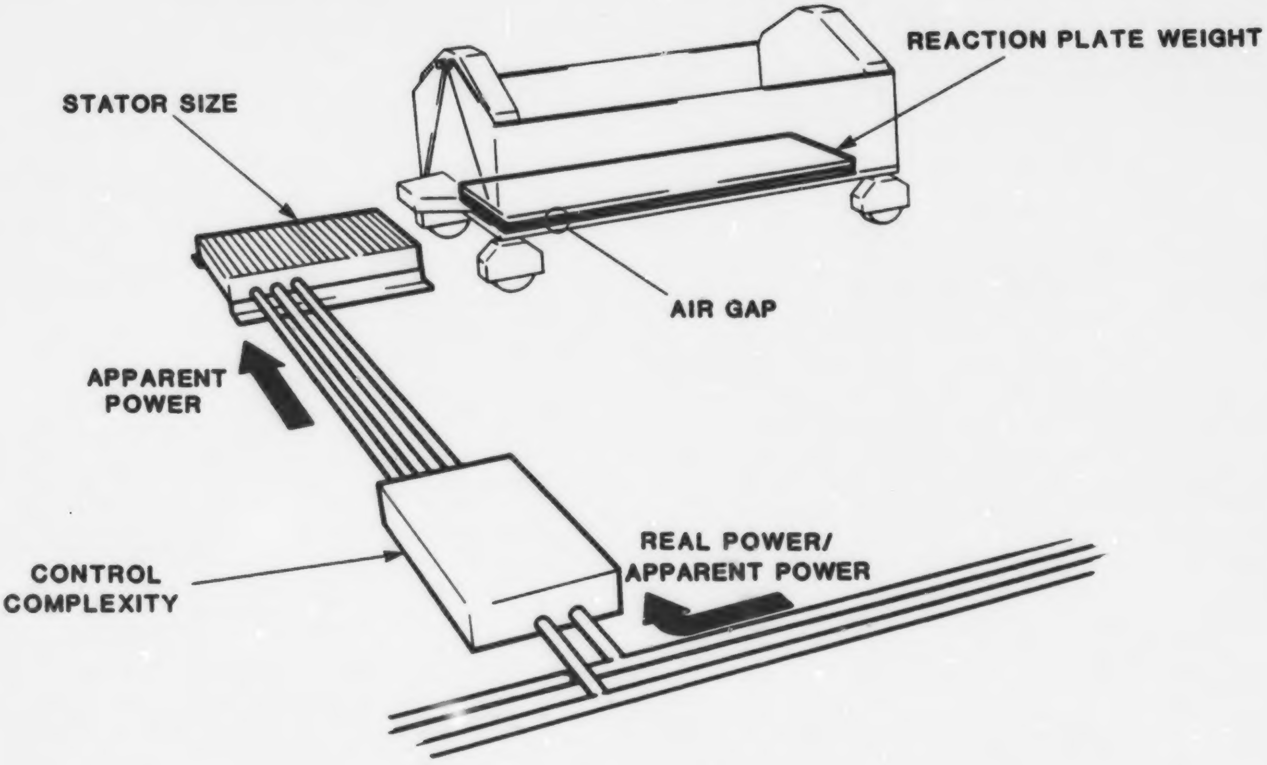
REACTION PLATE WEIGHT
STATOR SIZE
AIR GAP
APPARENT POWER
CONTROL COMPLEXITY
REAL POWER/ APPARENT POWER

FIGURE 5-6: CONSIDERATIONS WHICH INFLUENCE THE DESIGN OF LIMS

5.1.3.5 Reaction Plate Weight

The weight of the reaction plate is important in most systems because it represents a significant portion of the overall vehicle weight. Obviously, systems with many stations and/or steep grades are particularly sensitive since additional vehicle weight reflects back into the sizing of the LIM stators, power controllers and distribution system.

Reaction plate weight is minimized at the expense of real and apparent power consumption and stator size.

5.1.3.6 Airgap

As stated in section 4.1.1 the selection of a nominal airgap impacts on mechanical design, installation and maintenance. The cost of larger airgaps is increased real and apparent power consumption and larger stator size.

5.1.3.7 Commonality

While in principle one might conceive of optimizing the stator design for every location in the track, practical considerations dictate that only a limited number of unique stator types are used in any one system. The choice of how many different types of stator to use becomes an optimization exercise in itself. The trade-off for fewer types is stator size, since forcing commonality is likely to imply that most of the stators are overdesigned. On the other hand, more types leads to an increased spares inventory and possibly higher unit costs.

5.2 ANALYTICAL MODEL DEVELOPMENT

As a means of gaining insight into the behaviour of LIMs and the sensitivity of their performance to design and control parameters, analytical models are essential. A good model, besides having predictive power, should augment one's qualitative insight. That is to say, it should help one to better "visualize" the physical interactions behind the behaviour.

In this section, a picture of LIM behaviour is developed by means of analogical and intuitive reasoning. The "picture" is a conceptual model, offering qualitative insights. It should help clarify some of the notions which were used in developing the LIM Equivalent Network model, a listing of which appears in Appendix A-5.

5.2.1 Equivalent Network Models

In many fields of engineering, especially in the context of teaching, principles of circuit theory are used to explain behaviour in various kinds of physical systems. For example, plane waves (fluid, acoustic or electromagnetic) are often studied by using a transmission-line analogy, and thermodynamic and heat-transfer problems are sometimes formulated as a thermal equivalent network.

The property of electric networks which is found useful is that they are, practically speaking, one-dimensional. In other words, the quantities of interest have no shape or direction. The simplicity of description offered by the electric network analogue is sufficient reason to adopt it as a format for engineering models.

To arrive at a network-type model of a physical system, multiple, distributed effects are condensed into single elements. This process is termed "lumping", and employs transformations designed to partition the system into discrete regions of uniform behaviour. A number of such transformations have been developed for, or adapted to, the study of electrical machines. Figure 5-7 schematically illustrates some of the more well-known of these.

5.2.2 Classical Induction Motor Equivalent Network

The classical induction motor equivalent network introduced by C.P. Steinmetz in 1897 is an excellent starting point for understanding LIM behaviour [3]. Figure 5-8 and Table 5-2 indicate the correspondence between the lumped circuit elements and the "real" effects that they model.

It is important to recognize that not only is the equivalent network capable of representing the electrical behaviour as measured at the motor terminals, but can be employed to determine certain thermal and electromagnetic behaviour of the motor as well. This is possible because the analogical relationships that link the network to the physical motor can be quantitatively expressed. The LIM Equivalent Network model listed in Appendix A-5 exploits these analogies to determine flux densities in the airgap, teeth, stator core and reaction plate core and the thermal loading in the stator.

5.2.3 The Airgap Field

When the primary winding of an induction motor is fed with polyphase current, a time-varying magnetic field is established in the airgap. The major field component is normally-directed, sinusoidally distributed, and travels, wave-like, along the axis of motor motion.

The airgap magnetic field wave induces electric current in the conducting material of the motor secondary. Under the primary stack, this current is transverse to motion, sinusoidally distributed, and travels with the same wave-velocity as the airgap field.

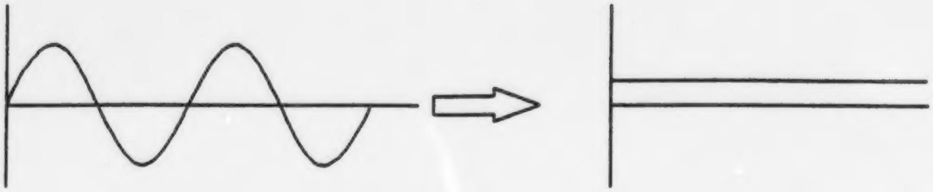

A) "ROOT MEAN SQUARING" REPLACES A SINUSOIDAL CURRENT OR MMF WAVE WITH A UNIFORMLY DISTRIBUTED "EFFECTIVE VALUE"

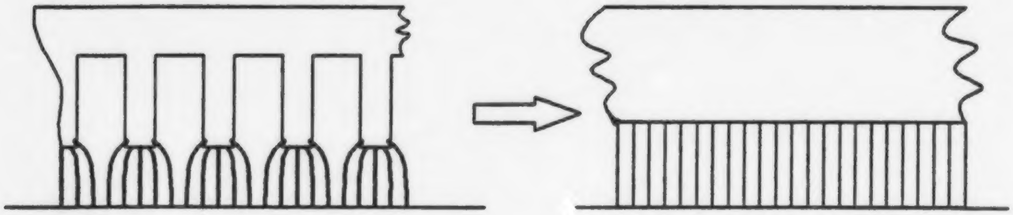

B) THE "CARTER FACTOR" REPLACES THE SLOTTED AIR GAP WITH A SMOOTH "EFFECTIVE GAP"

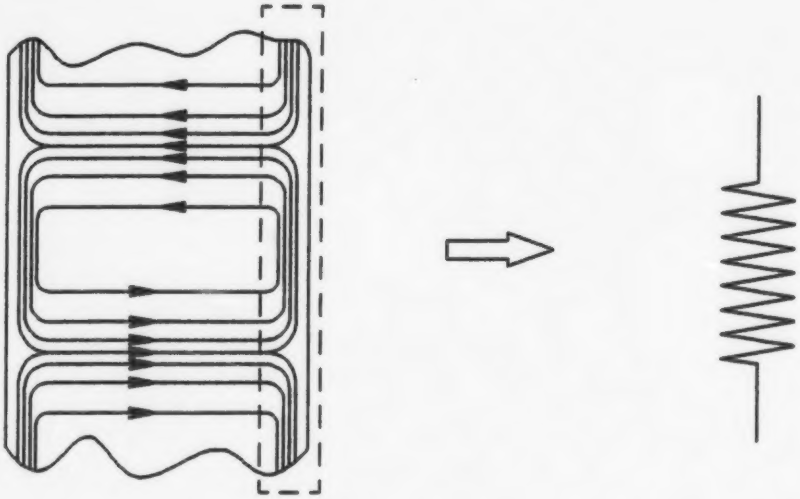

C) THE "RUSSELL-NORSWORTHY FACTOR" LUMPS THE DISTRIBUTED LATERAL EDGE EFFECT INTO A SINGLE FACTOR

FIGURE 5-7: COMMON LUMPING TRANSFORMATIONS

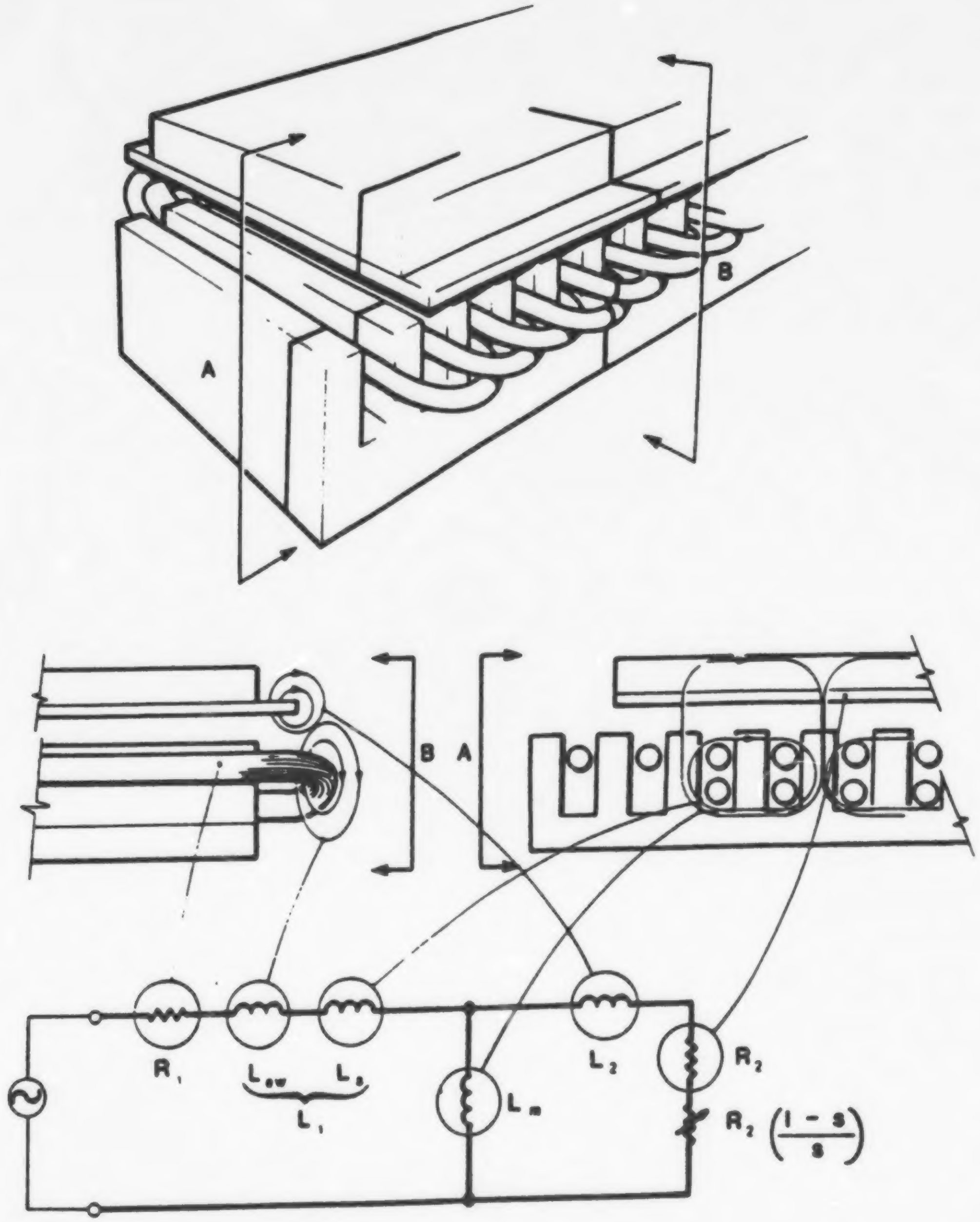
A
B
B
A
R_1
L_{ew}
L_s
L_1
L_m
L_2
R_2
$R_2\left(\frac{1-s}{s}\right)$

FIGURE 5-8: EFFECTS MODELLED BY EQUIVALENT CIRCUIT PARAMETERS

Many theories of the induction motor [4] begin this development by presuming an "infinitely extended machine", which possesses flux- and current-density distributions as described above, and as illustrated in Figure 5-9.

The finite-length geometries of practical machines complicate this conception, and it is thus necessary to "add on" various effects. Some of these, and their causes, are listed in Table 5-3.

5.2.4 LIM End-Effects

Geometrically, a rotary motor has peripheral length proportional to its diameter. A common analytical procedure is to map the radial geometry onto a cartesian reference, so that, conceptually, the motor is "linear", and part of an "infinitely long" machine. This image of the rotary motor has led investigators to coin phrases such as "short stator" or "finite core" as descriptions of the LIM.

There are a number of effects which have been identified as due to the LIM's "finite length". For example, Laithwaite [11] and Appendix A-6 explain why the time averaged core-flux-density distribution of the LIM is "modulated" due to the finite length of the primary iron (See Figure 5-10). Also, most references note the reduced surface current-density at the LIM primary ends due to the "half-filled end-slots" which are a characteristic of designs with the common, double-layered winding (See Figure 5-11). Yet another end-effect is the energy loss associated with the secondary currents which trail behind the travelling "active zone", or moving primary.

The end-effect which has the most degrading influence on LIM performance is due to the electro-dynamic response of the LIM as it passes over "new", or unenergized material in the secondary. The behaviour may be appreciated by picturing a stationary, current-fed LIM with the secondary conducting top-cap removed. If the top-cap is suddenly reintroduced, a transient current will develop in the conducting material, as shown in Figure 5-12, causing an opposing mmf, and a temporary cancellation of the airgap flux. A moving LIM sees a similar transient condition as elemental areas of new material enter the influence of the primary field. The aptly-named "entry-end effect" is the distortion in the airgap flux distribution resulting from this continuously occurring transient condition (See Figure 5-13).

5.2.5 Fourier Series Representation of the "Short Machine"

The speed-dependent, exponentially-modulated flux- and induced current-density distributions of the LIM preclude the use of a "uniform field" model unless a suitable transformation is introduced. One such transformation employs a Fourier-series

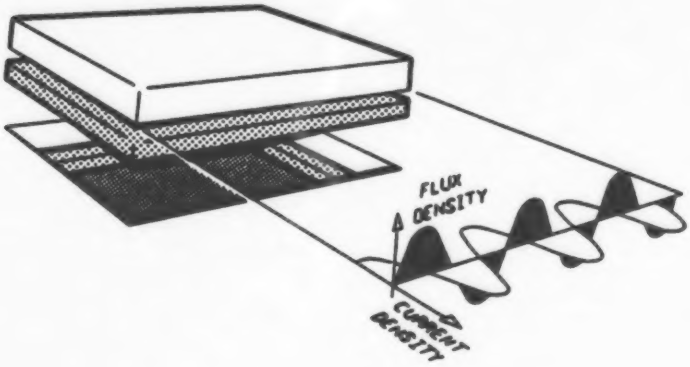
FLUX DENSITY
CURRENT DENSITY

FIGURE 5-9: SECTION OF AN INFINITELY EXTENDED MACHINE

Network Element	Symbol	Analogical Link to Physical Motor
1. Primary Resistance	R_1	o current through R_1 is equivalent to the per phase current measured at the motor terminals o power dissipated in R_1 is equivalent to 1/n of the power dissipated in the stator of an n phase motor
2. Endwinding Inductance	L_{ew}	o current through L_{ew} corresponds to the endwinding leakage flux linking the stator coils
3. Slot Leakage Inductance	L_s	o current through L_s corresponds to the cross-slot and tooth-tip leakage flux linking the stator coils
4. Magnetizing Inductance	L_m	o current through L_m corresponds to the flux linking the stator coils with the reaction plate top cap
5. Secondary Leakage Inductance	L_2	o current through L_2 corresponds to the leakage flux linking the reaction plate top cap currents
6. Secondary Resistance	R_2	o power dissipated in R_2 is equivalent to 1/3 of the power dissipated in the reaction plate top cap

TABLE 5-2: CORRESPONDENCE BETWEEN EQUIVALENT NETWORK ELEMENTS AND MOTOR

FEATURE	EFFECTS	REFERENCES
Slotted primary	1. Increased gap reluctance 2. Stationary harmonic fields 3. Leakage fields	[5] [6] [7]
Winding distribution	Travelling harmonic fields	[6]
Long gap/Short pole pitch	Introduction of tangentially-directed flux in the air gap (pole-to-pole leakage)	[4]
Primary end windings	Leakage fields	[7]
Secondary lateral edges	1. Introduction of longitudinally directed current 2. Secondary leakage fields	[8] [9]

TABLE 5-3: PRACTICAL FEATURES IN INDUCTION MOTORS

The references in the above table offer descriptions and methods which are commonly applied as "corrections" to network-type models. Each approach is based on the application of superposition and on the assumption of steady-state, principles which facilitate the creation of regions of uniformity, leading to the formulation of "lumped" corrections.

The concept of the uniform, corrected, airgap field is often adequate for studying rotary induction motor behaviour. An exception is found in the linear induction motor, which, unlike the rotary motor, has ends normal to the axis of motion. Intuition suggests that the resulting discontinuities in the airgap field could influence behaviour to a significant degree. Practical experience has shown this to be true, and several theories of LIM end-effects have been proposed.

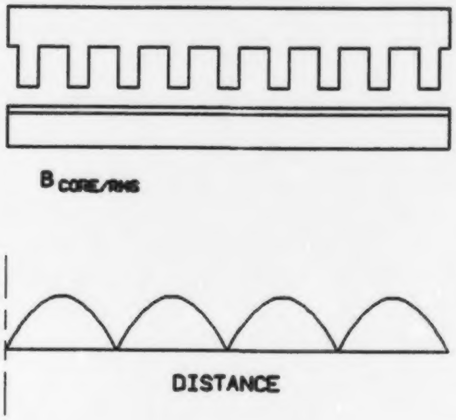
B CORE/RMS
DISTANCE

FIGURE 5-10: CORE-FLUX MODULATION DUE TO FINITE CORE LENGTH

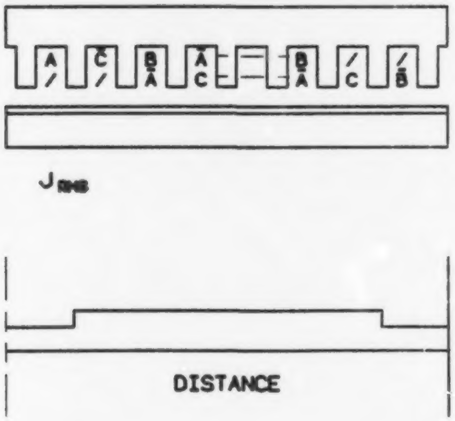
A
C̄
B̄
A
Ā
C
B̄
A
C
B̄
J RMS
DISTANCE

FIGURE 5-11: AVERAGE PRIMARY SURFACE CURRENT DENSITY SHOWING EFFECT OF HALF-FILLED END SLOTS

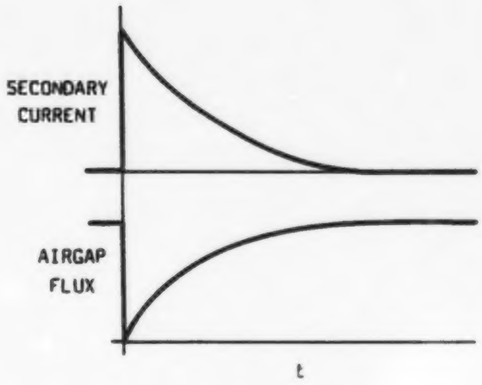

FIGURE 5-12: TRANSIENT CONDITION RESULTING FROM THE SUDDEN INTRODUCTION OF UNENERGIZED CONDUCTOR IN THE AIRGAP FIELD

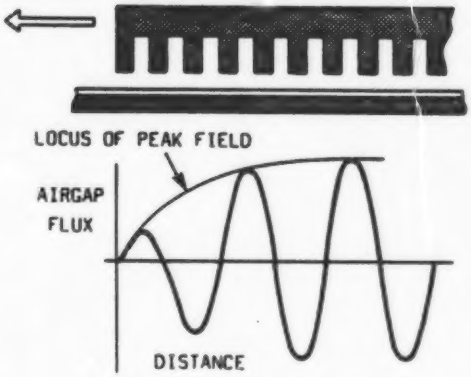
LOCUS OF PEAK FIELD
AIRGAP FLUX
DISTANCE

FIGURE 5-13: INSTANTANEOUS AIRGAP FLUX DISTRIBUTION OF A MOVING LIM SHOWING THE "ENTRY-END EFFECT"

representation of the airgap field distribution (See for example [10]). In this representation the "short" machine is equivalently expressed as the contributions from numerous "infinite" machines, assuming that the principle of superposition holds, and that steady-state conditions exist.

Fourier techniques have long been used in the analysis of conventional electrical machine. This fact is reflected in much of the technical language used in the literature. For example, the terms "space harmonic" and "winding fundamental" are common. There is a distinction which must be made, however, between the usual application of the Fourier method, and the one intended here. That is, in the analysis of conventional motors, the Fourier components, or "harmonics", exist only at integral multiples of the winding fundamental, as illustrated in Figure 5-14. In contrast, the Fourier representation of a finite length LIM will contain "sideband harmonics" clustered about the winding fundamental and its multiples.

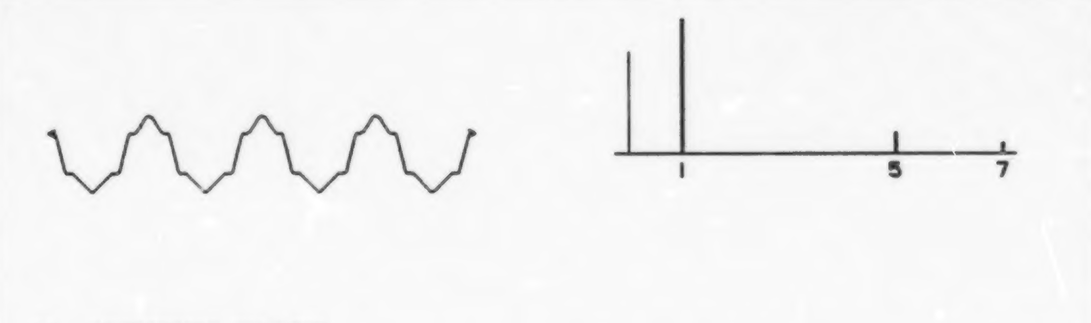

A) "INFINITE" MACHINE

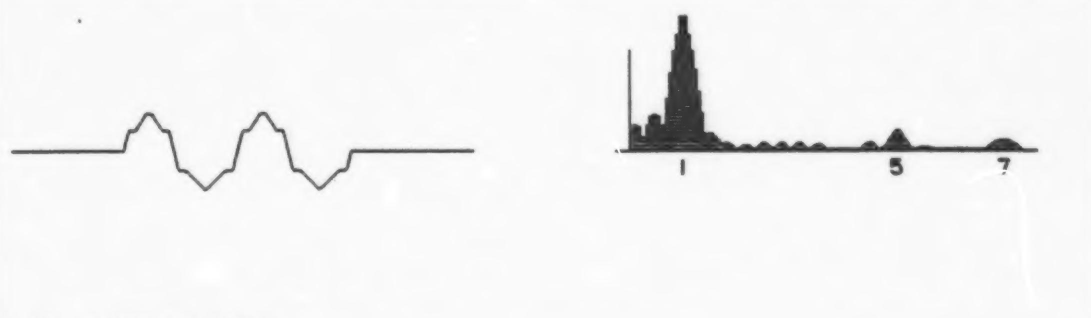

B) "SHORT MACHINE

FIGURE 5-14: Fourier Representation of Motor mmf Distributions

5.2.6 The LIM Equivalent Network

The Fourier-series/travelling-wave model is a suitable basis from which to develop a lumped-parameter, electrical-network representation of the LIM. Note that a single travelling wave of the series can be regarded in the same way as the field of a rotary motor. Since a rotary motor can be described adequately (in steady-state) by an equivalent network; then a linear motor can be described by the superposition of many such networks, each having a relationship to the amplitude, wavelength and velocity of the associated component wave. The development of the LIM equivalent network is illustrated in Figure 5-15.

5.2.7 Airgap Field Reconstruction

At conditions of zero velocity the secondary branches of the LIM Equivalent Network each see unity slip. At any other velocity the various harmonic slips take on unique values, and consequently the distribution of currents through the harmonic magnetizing inductances changes as a function of velocity.

Recalling the analogy between magnetizing branch current and airgap flux, one might suppose that this velocity-dependent redistribution of the currents is somehow linked to the airgap field distortion known as the LIM entry-end effect.

Since each magnetizing branch current may be quantitatively related to a harmonic flux wave, and since the principle of superposition is assumed, it would seem possible to construct the LIM airgap flux wave for any given velocity by summing together the harmonic components. Basically, the procedure involves firstly determining the harmonic currents by solving the network equations for given conditions of terminal voltage and LIM speed. Secondly, the harmonic currents (amplitude and phase) are transformed to harmonic mmfs, which are expressed as a series of space-waves, each component having an amplitude, wavelength and phase-displacement. Summing together these wave functions results in an mmf distribution which is then converted to a flux density distribution. Figure 5-16 a) and b) show examples of computed distributions for a LIM at 15 m/s and standstill respectively. The computer program provides a means of "freezing" the flux density wave at any instant in the A.C. supply cycle. Several "snapshots" were overlayed to indicate the average envelope of the flux density distribution.

5.2.8 Flux Density Estimation

As mentioned earlier in Section 5.1.2.3, it is important to design the LIM magnetic circuits to operate at flux densities which are neither "too high" nor "too low" for any portion of the stator or reaction plate steel.

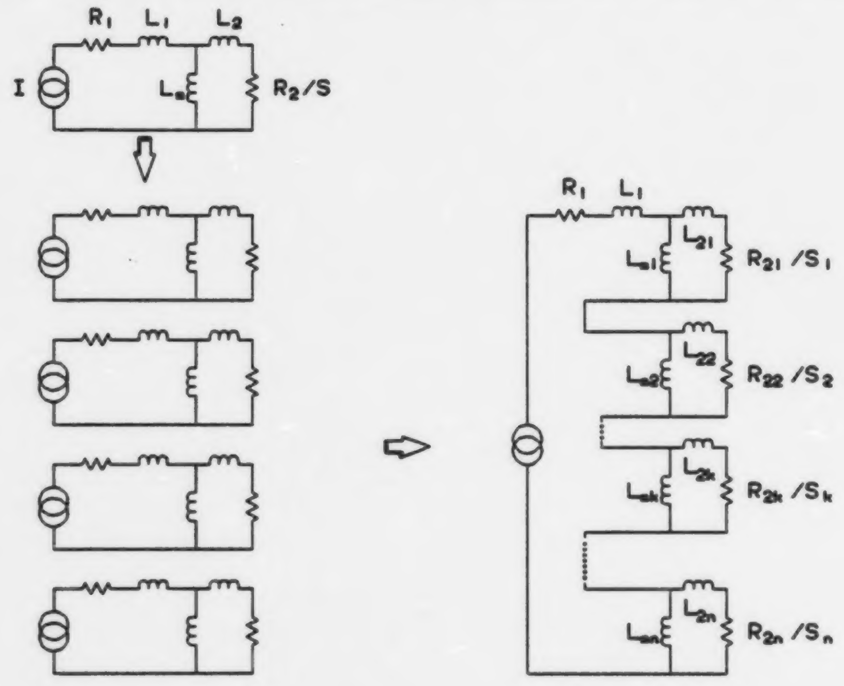
R1
L1
L2
I
Lm
R2/S
R1
L1
L21
Lm1
R21 /S1
L22
Lm2
R22 /S2
L2k
Lmk
R2k /Sk
L2n
Lmn
R2n /Sn

FIGURE 5-15 DEVELOPMENT OF THE LIM EQUIVALENT NETWORK

SYMBOL	ACCOUNTS FOR ....
R_1	PRIMARY WINDING RESISTANCE
L_1	PRIMARY ENDWINDING - AND SLOT-LEAKAGE
L_{1K}	GAP LEAKAGE COMPONENT OF THE Kth SPACE HARMONIC FIELD
L_{MK}	MAGNETIZING COMPONENT OF THE Kth SPACE HARMONIC FIELD
L_{2K}	SECONDARY LEAKAGE OF THE Kth SPACE HARMONIC FIELD
R_{2K}	SECONDARY RESISTANCE TO THE Kth SPACE HARMONIC CURRENT-DENSITY
S_K	SLIP OF THE Kth SPACE HARMONIC FIELD

FIGURE 5-15: DEVELOPMENT OF THE LIM EQUIVALENT NETWORK

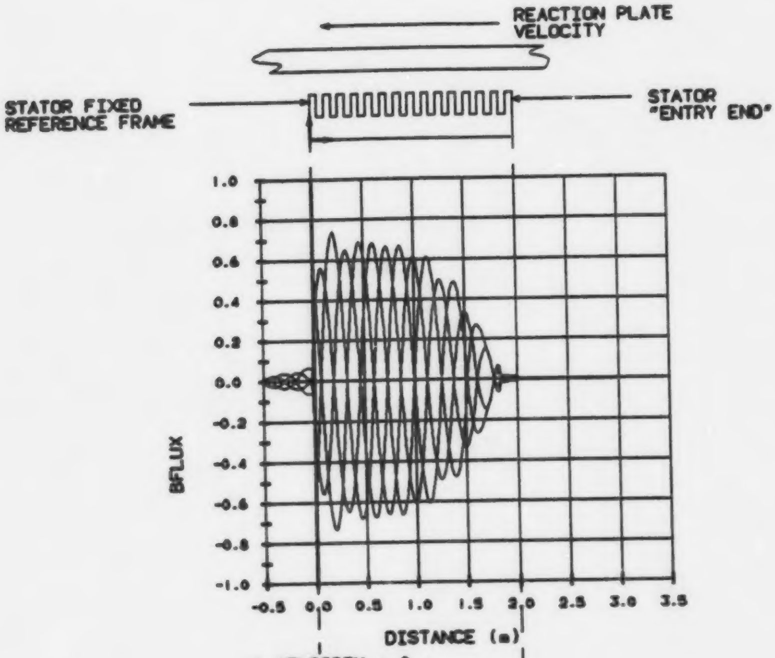

a) VELOCITY = 0

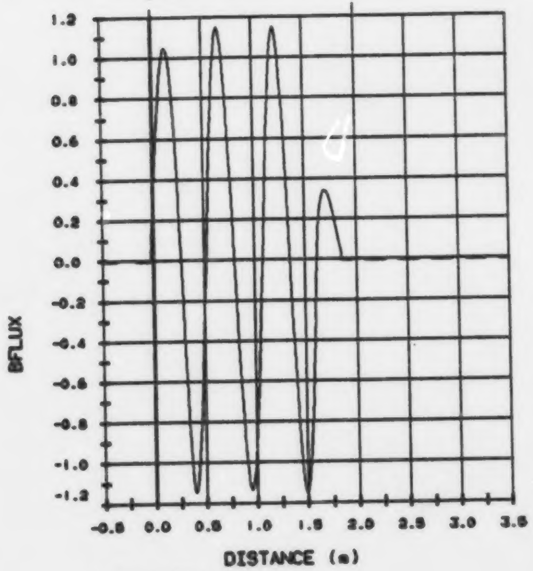

b) VELOCITY = 15 m/s

FIGURE 5-16: AIRGAP FLUX DENSITY DISTRIBUTIONS AS DETERMINED BY LIM EQUIVALENT NETWORK COMPUTER MODEL

Flux density in the airgap may be determined by the approach outlined in Section 5.2.7, but it is in the stator teeth and core and reaction plate core that we desire to check the design flux densities to ensure that saturation limits are avoided. Therefore, a means of estimating these would be useful.

It must be kept in mind that flux in any part of the LIM is time-varying, since the windings are excited with alternating current. When we refer to flux density, therefore, we choose either to represent the peak, or the rms flux density by single values.

Additionally, we should recognize that flux in the airgap is, at any given instant, sinusoidally distributed. Again, we may refer to either the peak or rms value of flux density, though in this case the root-mean-square is based on distance, not time.

5.2.8.1 Pole Flux

An estimation of the stator and reaction plate core flux densities begins with the notion of Pole Flux. Pole Flux is a lumped quantity derived by integrating the airgap flux density distribution over one-half cycle and laterally across the width of the stator. We assume that this flux completes a closed circuit through the stator and reaction plate cores to produce the next half-cycle of the airgap flux density distribution, i.e. the adjacent pole.

For the imaginary "infinitely-extended" LIM, every pole (i.e. every half-cycle of the airgap flux distribution) contains the same amount of flux. Real LIMs, however, exhibit the entry-end-effect described in Section 5.2.4, which means that poles near the leading end of the stator contain less flux than the poles near the trailing end. It is therefore necessary either to analyze pole-by-pole, or to establish a "representative" pole flux based on the effective, or rms flux density over the complete stator length.

The former approach while possible, is quite tedious, and many times, unnecessary. The latter is useful for getting a rough idea of the magnetic loading of the core, so long as it is appreciated that the flux densities at the entry end are somewhat less, and at the exit end somewhat more, than the prediction indicates.

The model LEN (Appendix A-5) creates an effective gap flux density by root-mean-squaring the distribution it constructed according to the method outlined in Section 5.2.7. The representative pole flux is then determined according to the formula derived in Appendix A-7.

5.2.8.2 Reaction Plate Core Flux Density

It is assumed that the pole flux flows uniformly through any given lateral cross section of the reaction plate core. Longitudinally, the flux density distribution follows the envelope created by the "flux bunching" effect described in Appendix A-6. The flux density we are most interested in representing is located at the highest point on this envelope, and at the instant in time at which it is at its peak value. These requirements are automatically satisfied by using the Pole Flux.

The reaction plate core flux density is simply calculated by dividing the Pole Flux by the width and depth of the reaction plate back iron.

5.2.8.3 Stator Core Flux Density

The stator core, like the reaction plate core, carries the pole flux, but in addition, it carries the slot leakage flux. The two fluxes must therefore be combined and divided by the width and depth of the stator core to determine the core flux density. Appendix 5E develops a formula for slot leakage flux based on the current flowing in the slot leakage inductance.

5.2.8.4 Tooth Tip Flux Density

The flux in the airgap flows from the tips of the stator teeth. If we assume that all the flux "funnels through" the ends of the teeth, and none comes from the slot opening, then we can calculate the density in the tooth tip by scaling the gap flux density up by the ratio of the slot pitch to the tooth width. Here, it is the peak airgap flux density which we choose as the basis for calculation.

5.2.9 Flux Density Estimate Assumptions

A number of simplifying assumptions are made in order to estimate the flux densities as outlined in the previous sub-sections. Firstly, it should be recognized that the airgap flux distribution and the slot leakage flux, upon which the estimates are based, were derived from the currents and inductances of the equivalent network, which are themselves approximations. Secondly, a number of assumptions were made about the way flux flows in the magnetic structures of the stator and reaction plate. For example, the ideas that flux is spread with uniform density through a lateral core section, or that flux enters or exits only the end face of a stator tooth tip, are simplified descriptions of the real behaviour.

5.2.9.1 Comparison with FEA Predictions

In order to get an idea of how well the flux densities are estimated by the methods described in Section 5.2.8, LEN predictions were compared to finite element analysis (FEA) predictions. (FEA offers a more realistic representation of magnetic fields, but setting up an FEA model, running the program, and interpreting the computational output is many times more time-consuming than LEN.)

The LIM chosen for the comparison study has a pole pitch of 57 mm. This is about as short as is ever used in practice, and would normally be employed in fixed-frequency (i.e. 60 Hz) applications. The interesting feature of short pole-pitch LIMs is the degree of cross-slot flux leakage exhibited. This flux contributes to the flux in the stator core but not the reaction plate core, and provides a good test for the prediction methods.

It must be pointed out that the FEA results, while offering a meaningful comparison, are by no means a perfect representation of the real behaviour. This is because, in order to obtain reasonable mesh resolution, only one wavelength of the LIM was modelled, and this was assumed to be a section of an infinitely-extended machine. Consequently, the FEA results do not reflect either of the effects related to finite stator length, i.e. the "flux bunching" effect described in Appendix A-6 and the entry-end effect described in Section 5.2.4. The former deficiency is compensated for by doubling the portion of flux not contributed by slot leakage in both the stator and reaction plate cores. The legitimacy of this approach rests on the observation that "flux bunching" creates peak densities twice those of an infinitely-extended LIM when slot leakage is ignored, but the leakage paths themselves are no different for the finite LIM than for the infinite LIM, and therefore the leakage flux contribution should not be doubled.

The second deficiency of the FEA model, i.e. that it ignores the entry-end effect, is not relevant for this comparison case since the results are for zero-speed conditions.

The comparisons of peak flux densities in the reaction plate core, stator core and stator tooth tip appear in Figure 5-17. The flux densities are calculated for a constant stator current over a range of slip frequencies. Note that both methods predict a trend to reduced flux density with increasing slip frequency. The relative change in the stator core is not nearly so pronounced as it is in the reaction plate core or tooth tip. This is due to the influence of the slot leakage flux, which unlike the pole flux is not attenuated by the eddy currents which flow in the reaction plate top cap.

The comparisons indicate differences in the order of 20% between LEN and FEA predictions at low slip frequencies. These differences can be explained by reviewing the formulation of the "representative pole flux" in LEN: The root-mean-square calculation preceding the calculation of the "representative pole flux" effectively eliminates any higher order space harmonics which exist in the gap flux density distribution. This smooths out localized peaks as shown in Figure 5-18, thereby leading to errors in determining the "true" peak value.

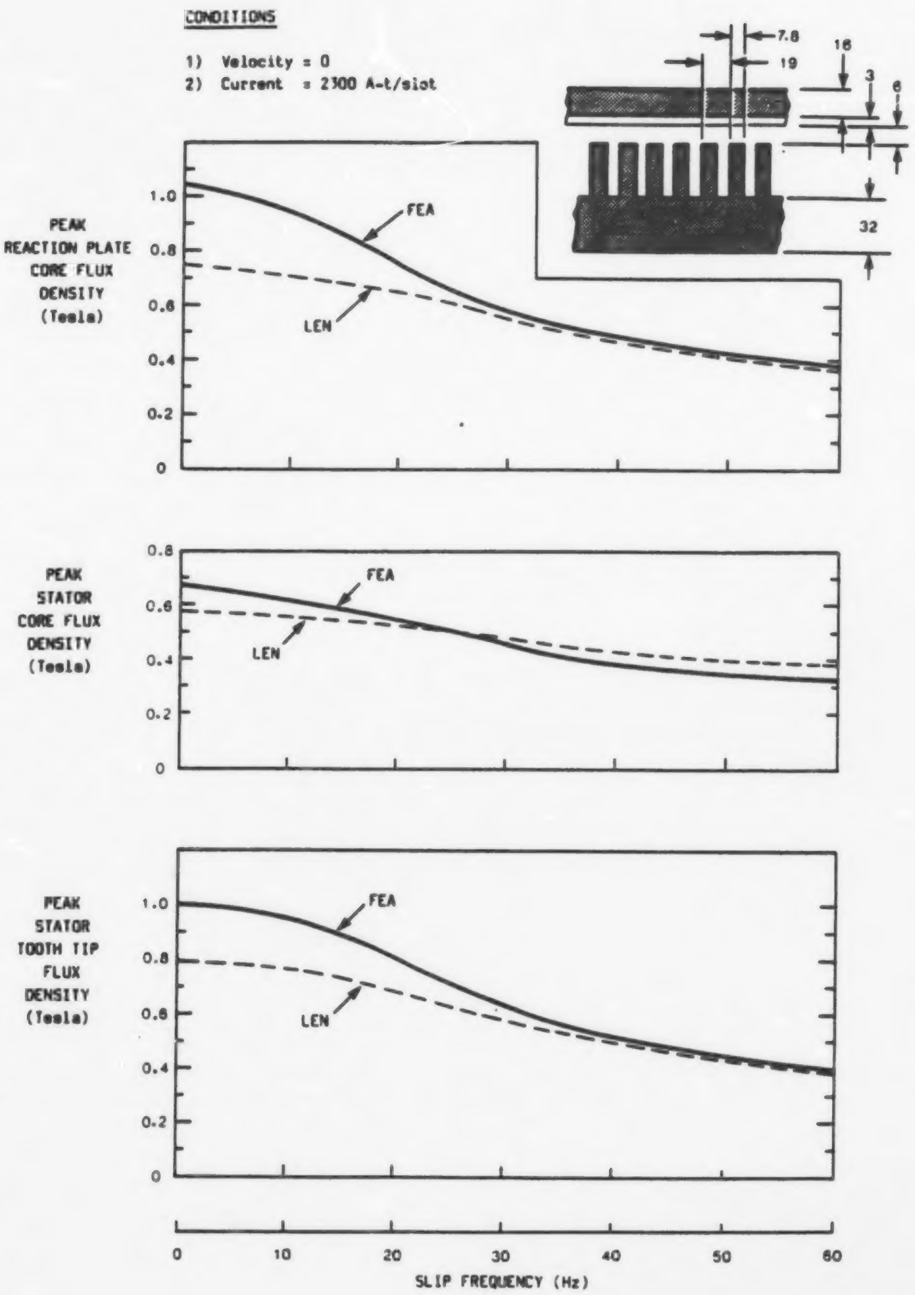

FIGURE 5-17: COMPARISON OF FINITE ELEMENT ANALYSIS WITH LEN PREDICTIONS

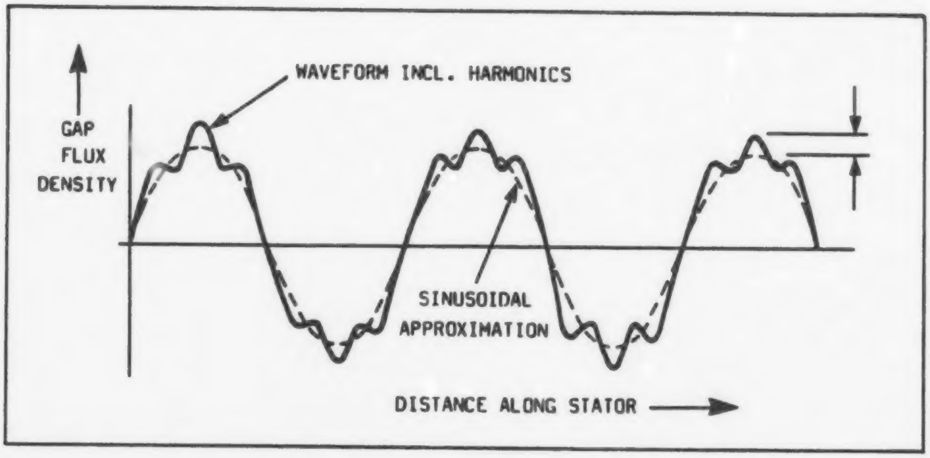
WAVEFORM INCL. HARMONICS
GAP FLUX DENSITY
SINUSOIDAL APPROXIMATION
DISTANCE ALONG STATOR

FIGURE 5-18: DIFFERENCE IN PEAK FLUX DENSITY BETWEEN ACTUAL AND SINUSOIDAL WAVEFORMS

The inability of the flux density estimation method used in LEN to resolve the peaks due to space harmonics is not a shortcoming: These peaks are of little significance in the performance of the LIM, and using these values in the context of evaluating magnetic design would be unnecessarily conservative.

5.2.10 Vertical Force Estimation

Besides producing force along the axis of motion, the LIM exhibits a vertical force reacted between the stator and reaction plate. This force actually has two components, one attractive, the other repulsive. The net force being the combination of the two.

The attractive component of the vertical force is due to the magnetic coupling between the iron portions of the stator and reaction plate members.

The repulsive component is due to the interaction of the stator and reaction plate currents.

Depending on the particular design and operating slip frequency, one or the other of these component forces will dominate. At zero slip frequency the repulsive component is always nil and the net vertical force must be attractive. At high slip frequencies the repulsive component grows larger and in some LIM designs will exceed the attractive component so as to result in a net repulsive, or lifting force.

Appendix A-8 derives formulae for vertical force estimation based on the LIM Equivalent Network. The attractive component uses a fairly straightforward theory, however the repulsive component is more difficult to analyze and depends on an empirical factor derived from tests. Figure 5-19 shows some typical vertical force vs. slip frequency characteristics.

5.3 EXPERIMENTAL FACILITY

The dynamic test facility which was designed and built for the 60 Hz Program was used for the LIM & Controls variable frequency tests. The facility is described in Volume I, Appendix 3 of the Dynamic Experiment Report for the 60 Hz LIM project, Report Number 453-610-003.

Since the 60 Hz tests, the track has been enclosed and the LIM powering the secondary carriage has been converted from a delta to a wye connection. Otherwise it is as described in the 60 Hz program report.

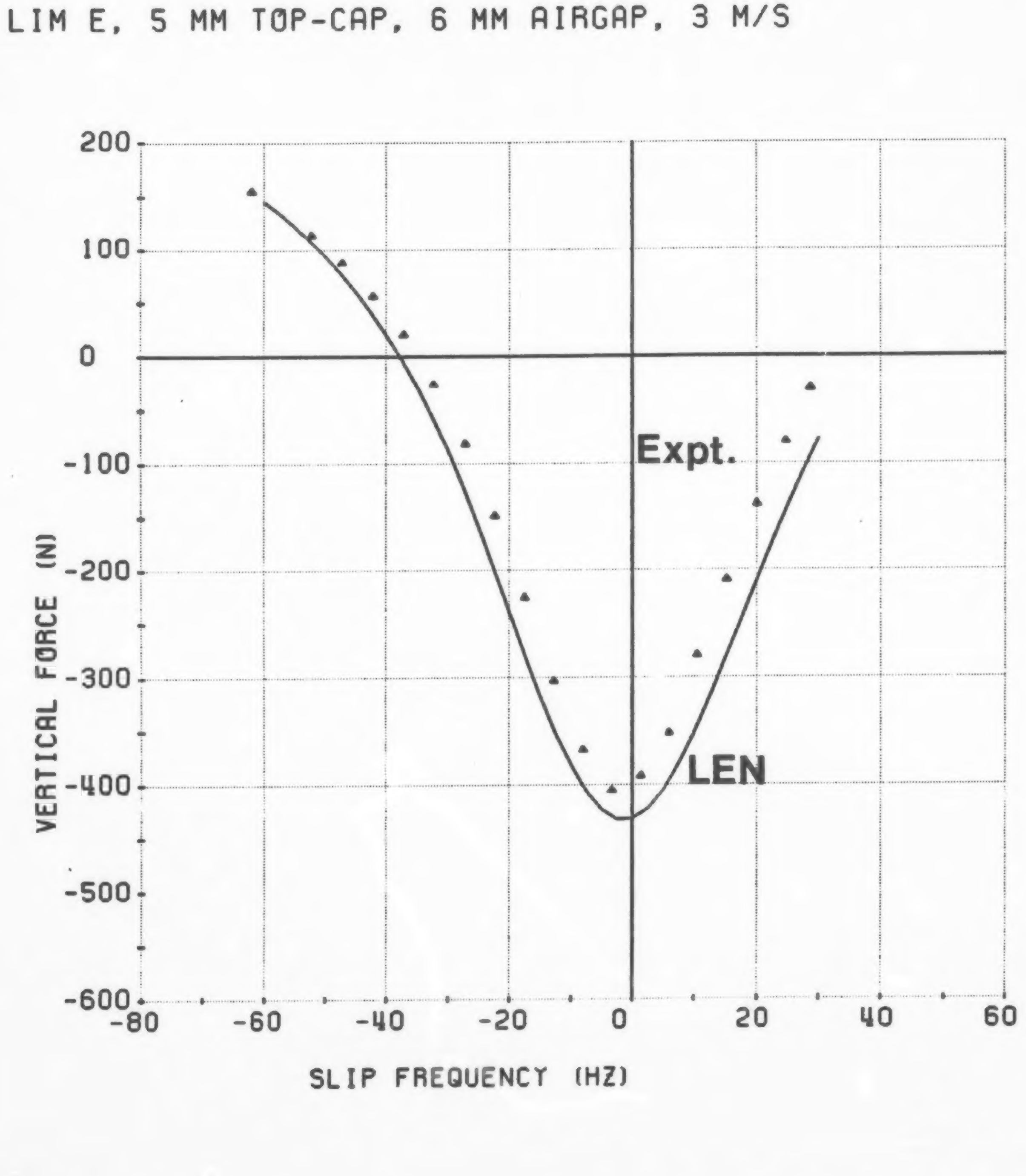

FIGURE 5-19: TYPICAL VERTICAL FORCE VS. SLIP FREQUENCY CHARACTERISTIC (LEN PREDICTION AND EXPERIMENTAL RESULTS)

As shown schematically in Figure 5-20, the LIM test facility features:

1. A 3 phase/2 phase voltage source, current controlled PWM inverter capable of supplying 1-100A at 1-60 Hz.

2. A stationary test LIM Primary instrumented for voltage, current, vertical force, thrust and mechanical gap. See the test stand illustration in Figure 5-21.

3. A test LIM secondary supporting carriage including wheels for suspension, guidance, and anti-lift, drive LIM, power collector assembly, target rail for optical speed sensing system and magnetic targets for magnetic position sensing sytem.

4. A variable voltage 60 Hz LIM-drive system for regulation of carriage speed.

5. Magnetic sensors for determining carriage position.

6. An "I-Beam" integral track/drive LIM secondary.

7. LIM test instrument (custom-designed multi-channel signal conditioner).

8. Fourteen-channel analog data recorder.

9. Digital data acquisition/storage/processing system.

The system is arranged so that all measurements are made on the stationary LIM primary under test. This simplifies measurement and recording of data, LIM power supply requirements and set-up procedure.

All test runs are made at constant speed. This is possible due to the speed regulating function performed by the voltage controller. Motor voltage (and hence thrust) are adjusted in response to a speed error signal, which is derived by comparing the selected speed to the measured speed.

Figure 5-22 schematically outlines the data measurement and reduction system. Details concerning test methods, instrumentation systems, test organization, data storage and analysis can be found in the LIM & Controls Variable Frequency Experiment Report (#454 700 003).

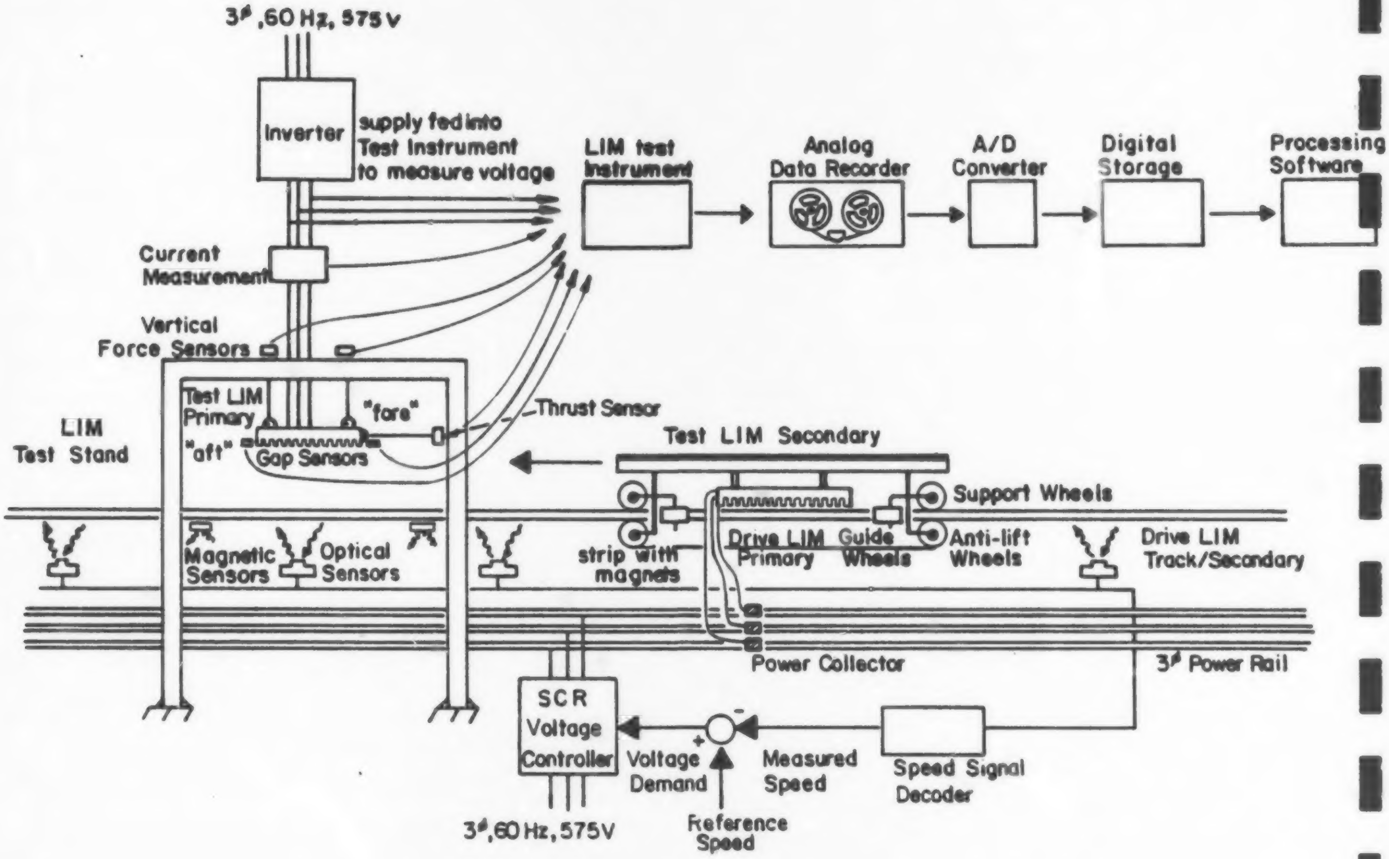
3ᶲ,60 Hz, 575 V
Inverter
supply fed into Test Instrument to measure voltage
LIM test instrument
Analog Data Recorder
A/D Converter
Digital Storage
Processing Software
Current Measurement
Vertical Force Sensors
Test LIM Primary
"fore"
"aft"
Gap Sensors
Thrust Sensor
LIM Test Stand
Test LIM Secondary
Support Wheels
Anti-lift Wheels
Guide Wheels
Drive LIM Primary
strip with magnets
Magnetic Sensors
Optical Sensors
Drive LIM Track/Secondary
Power Collector
3ᶲ Power Rail
SCR Voltage Controller
Voltage Demand
+
-
Measured Speed
Reference Speed
Speed Signal Decoder
3ᶲ,60 Hz, 575V

FIGURE 5-20: LIM DYNAMIC TEST SYSTEM

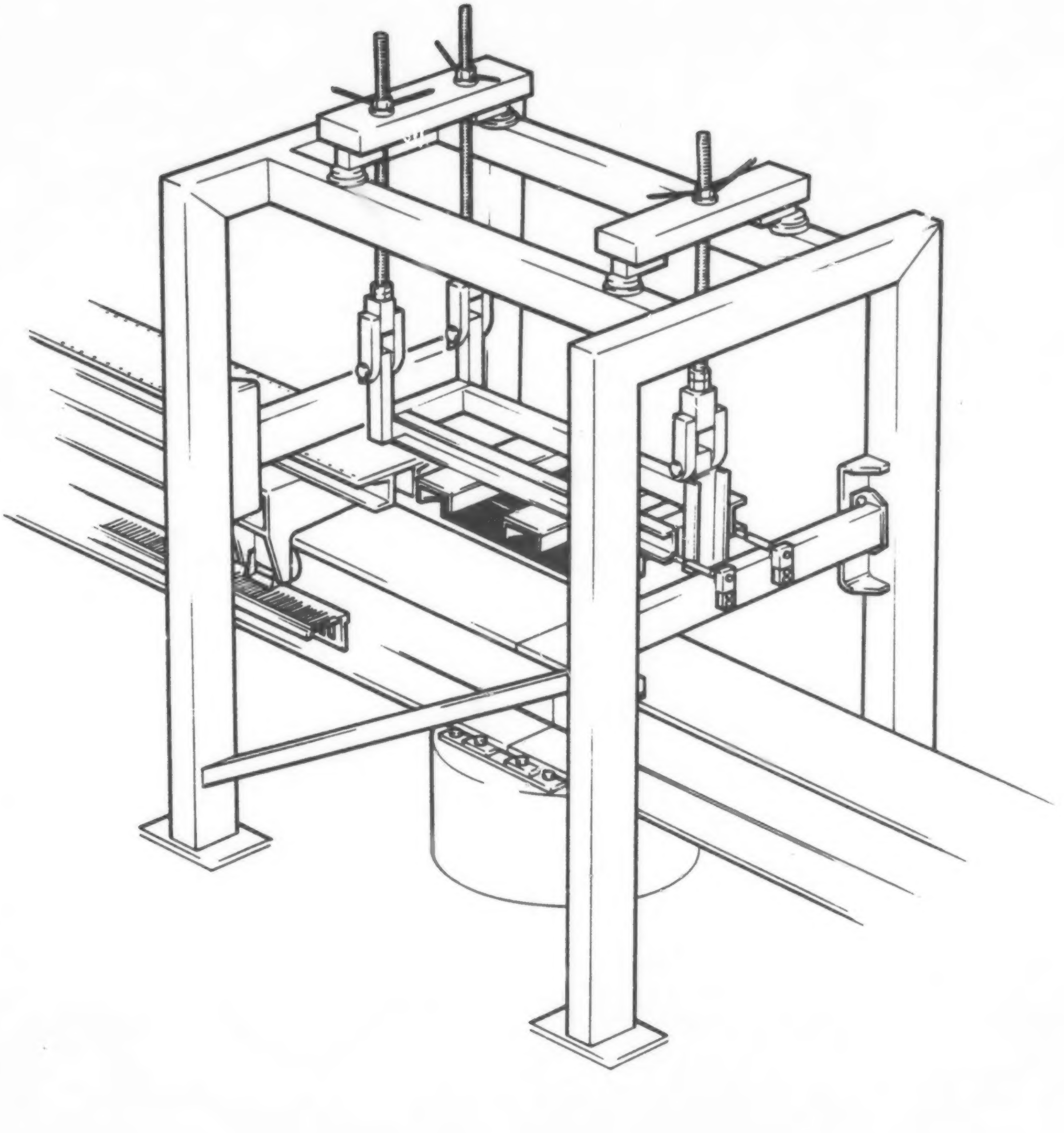

FIGURE 5-21: TEST STAND ILLUSTRATION

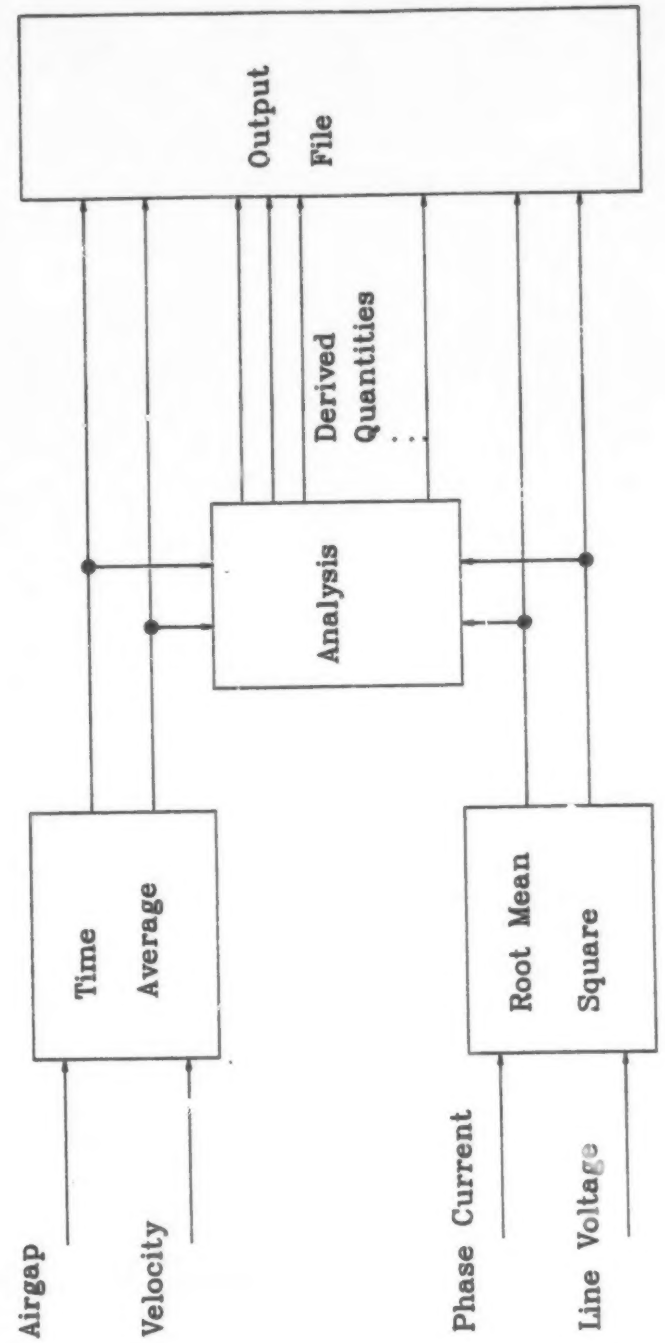
Airgap
Velocity
Phase Current
Line Voltage
Time Average
Root Mean Square
Analysis
Derived Quantities ...
Output File

FIGURE 5-22 SCHEMATIC DATA REDUCTION

5.4 EXPERIMENTAL RESULTS SUMMARY

An experimental test program was undertaken to create a data base of the performance information indicated in Figure 5-23.

Up to forty runsets were completed for each LIM with a runset configuration matrix of two top-cap thicknesses, four airgaps and five velocities. Each runset was made up of runs over a range of slip frequencies.

The test data was analysed using a procedure based on a Continuous Fourier Transform. The analysis program determines the conditions (airgap, velocity, dominant sequence current, frequency and slip frequency), use the resultant parameters (thrust, vertical force and dominant sequence voltage) and additional results (power factor, efficiency, etc) for each run.

Conclusions resulting from this activity were as follows:

1. The data collected from this series of tests has minimal scatter and appears to be consistent and repeatable. The quantifiable errors in the individual measurement systems are small and are within an acceptable range.

2. The test facility and data acquisition/analysis system performed well. They are valuable resources for future LIM testing.

3. The results obtained from these tests create a valuable data base of variable frequency LIM performance over a wide range of configurations.

4. The results are also useful to identify trends which can lead to further refinement and improvement of the analytical model and LIM design principles.

5. The test inverter presented certain difficulties during operation:

   - o poor regulation of load current over the complete range of frequency, velocity and LIM type,
   - o poor reliability of logic circuit leading to current offsets and phase imbalance,
   - o poor reliability of power circuit leading to several failures.

5.4.1 Sample Test Results

A complete record of test results may be found in the "LIM & CONTROLS VARIABLE FREQUENCY EXPERIMENT REPORT", Volumes I and II (UTDC Report 454 700 003). Some sample graphs are shown here to indicate the type of data collected in these experiments.

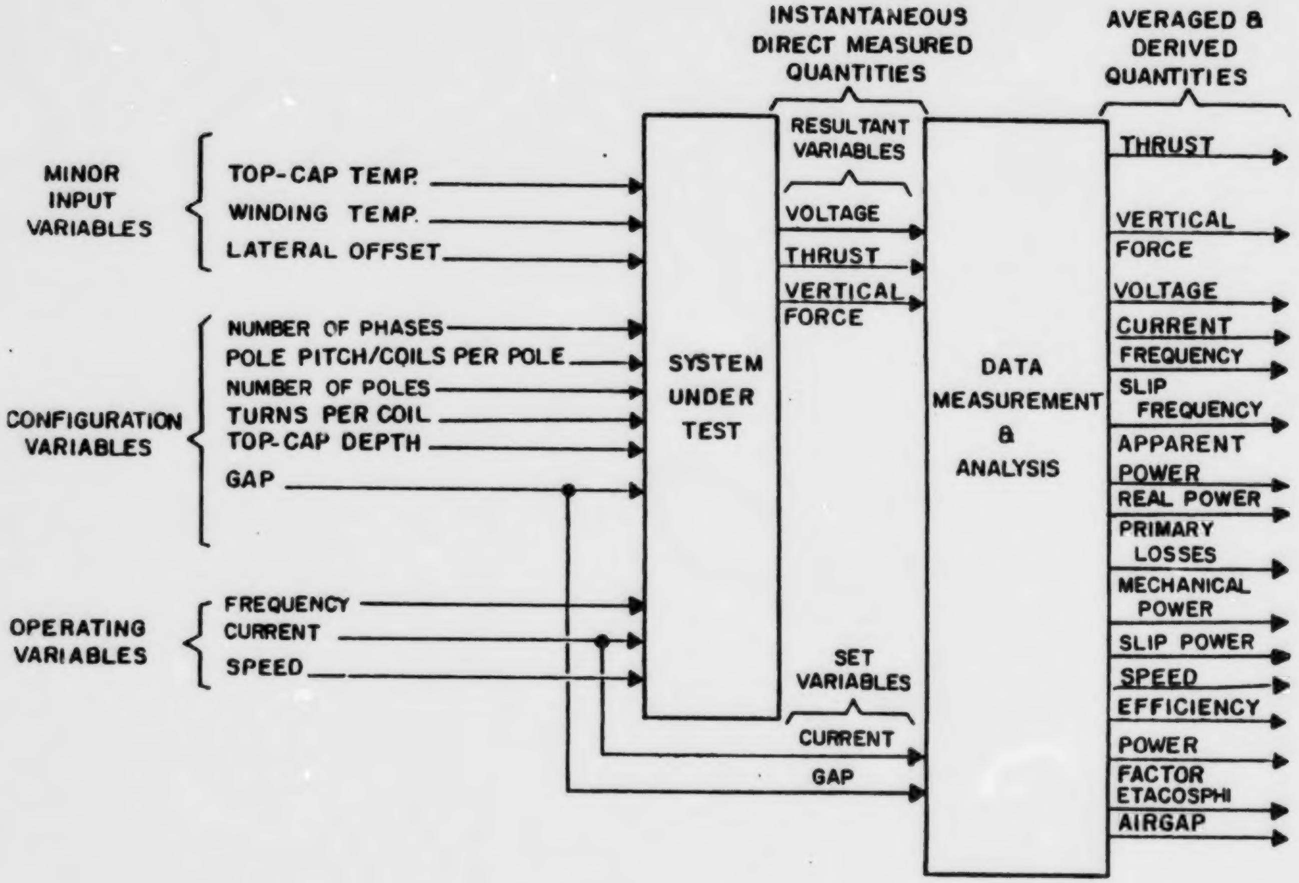
INSTANTANEOUS DIRECT MEASURED QUANTITIES
AVERAGED & DERIVED QUANTITIES
MINOR INPUT VARIABLES
TOP-CAP TEMP.
WINDING TEMP.
LATERAL OFFSET
CONFIGURATION VARIABLES
NUMBER OF PHASES
POLE PITCH/COILS PER POLE
NUMBER OF POLES
TURNS PER COIL
TOP-CAP DEPTH
GAP
OPERATING VARIABLES
FREQUENCY
CURRENT
SPEED
SYSTEM UNDER TEST
RESULTANT VARIABLES
VOLTAGE
THRUST
VERTICAL FORCE
SET VARIABLES
CURRENT
GAP
DATA MEASUREMENT & ANALYSIS
THRUST
VERTICAL FORCE
VOLTAGE
CURRENT
FREQUENCY
SLIP FREQUENCY
APPARENT POWER
REAL POWER
PRIMARY LOSSES
MECHANICAL POWER
SLIP POWER
SPEED
EFFICIENCY
POWER FACTOR
ETACOSPHI
AIRGAP

FIGURE 5-23: TEST SYSTEM BLOCK DIAGRAM INDICATING MEASURED AND DERIVED INFORMATION

Figure 5-24 a) through e) show LIM thrust, vertical force, efficiency, power factor and voltage for one LIM configuration for a range of slip frequencies and speeds. Similar test results were created to show the sensitivity of these same parameters to top cap depth and airgap.

5.5 MODEL PREDICTIONS

The LIM Equivalent Network model (see Appendix A-5) was used to generate curves that corresponded to the test data gathered in the Variable Frequency experiments. The exercise of comparing model data against experimental data was intended as the first step in a "model calibration" effort. LEN provides the user with a set of variables which can be specified in the input data file as "modification factors" to the basic equivalent network elements. By using these factors to force a match between the model and the LIM test data one creates a reasonably acurate model of that particular LIM configuration. By repeating this procedure over a range of LIM design configurations, one may begin to identify relationships between specific model errors and LIM design parameters. For example, it was found that the primary leakage inductance element, L1, needed to be increased (more than the model provided) as airgap increased. The reasons for this can be understood in a qualitative sense by recognizing that the formula used by LEN for L1 ignores "pole-to-pole" leakage in the airgap. What the model calibration procedure provides is a means of quantifying and correcting second-order errors.

Figures 5-25 through 5-29 show the comparison between model and experimental results for one sample of the LIM configurations tested. In this case the only element that required modification was L1, which was increased from the original model-calculated value by 40%. The resulting match in the curves is quite good over the complete range of speeds tested.

A point worth noting is the success of the model in predicting the attenuation in peak thrust with increasing speed. This is the "entry-end-effect" described in Section 5.2.4. In this particular example the change in peak thrust from 1 to 9 m/s exceeds 20%. LEN results display this same trend.

5.6 FIXED VS. VARIABLE FREQUENCY LIM PERFORMANCE COMPARISONS

There are several reasons why variable frequency (VF) LIM control results in superior performance than fixed frequency (FF) control:

1) When frequency is a controlled variable it is possible to operate a given LIM at a point which yields the most possible thrust for a given amount of real power, or apparent power, or stator dissipation, or vertical force, or any desired combination of these variables.

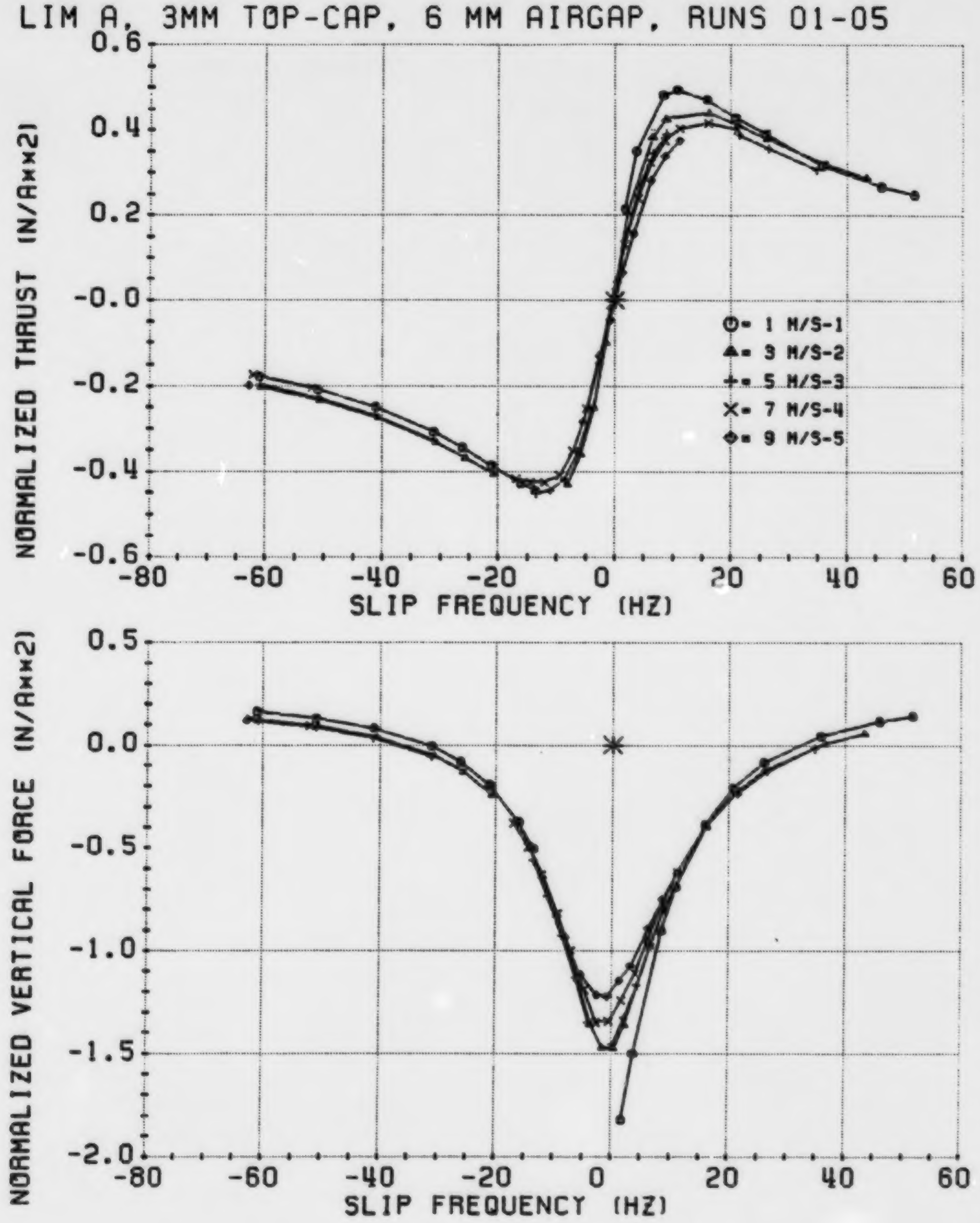

FIGURE 5-24: SAMPLE LIM TEST RESULTS

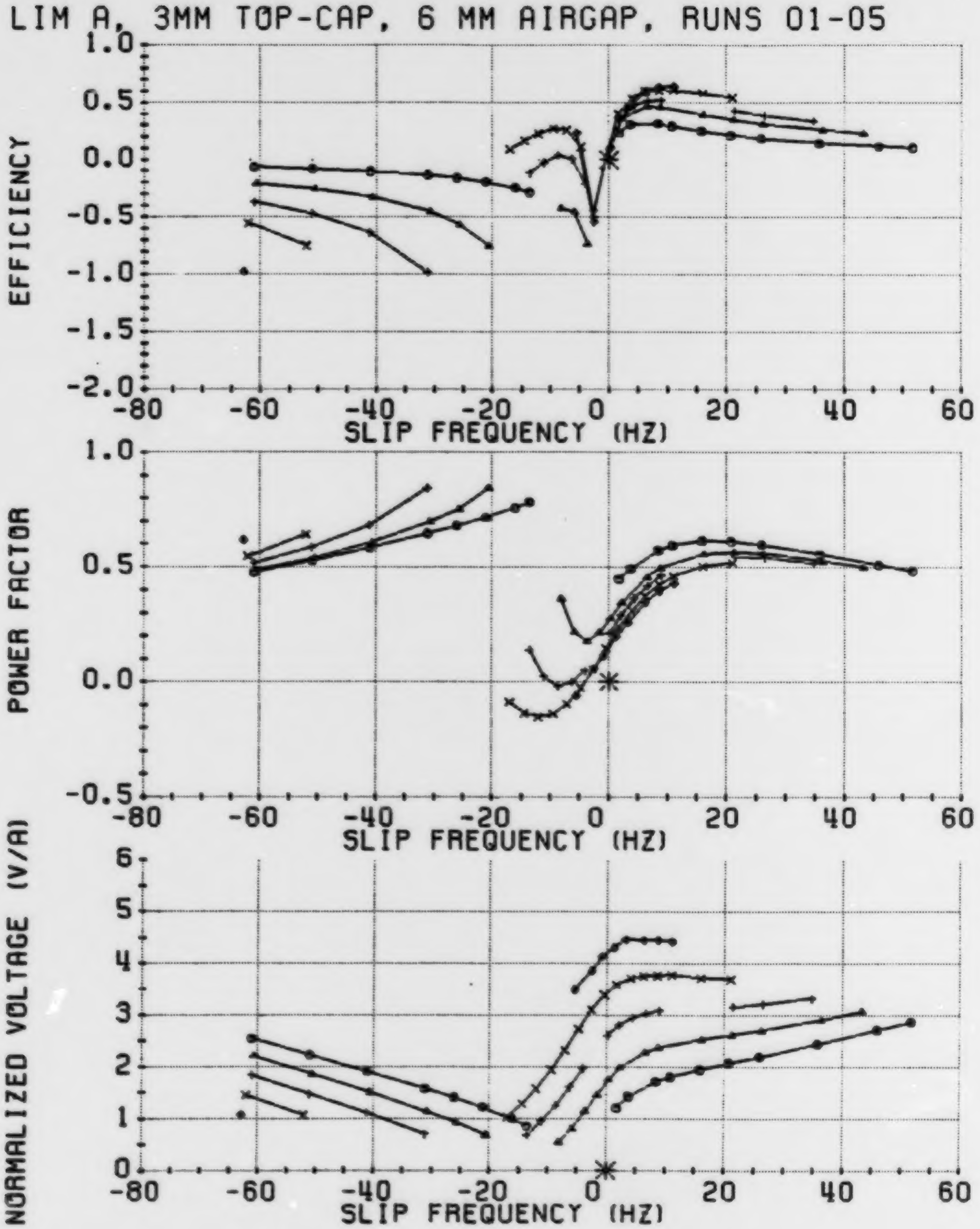

FIGURE 5-24 (Cont'd): SAMPLE LIM TEST RESULTS

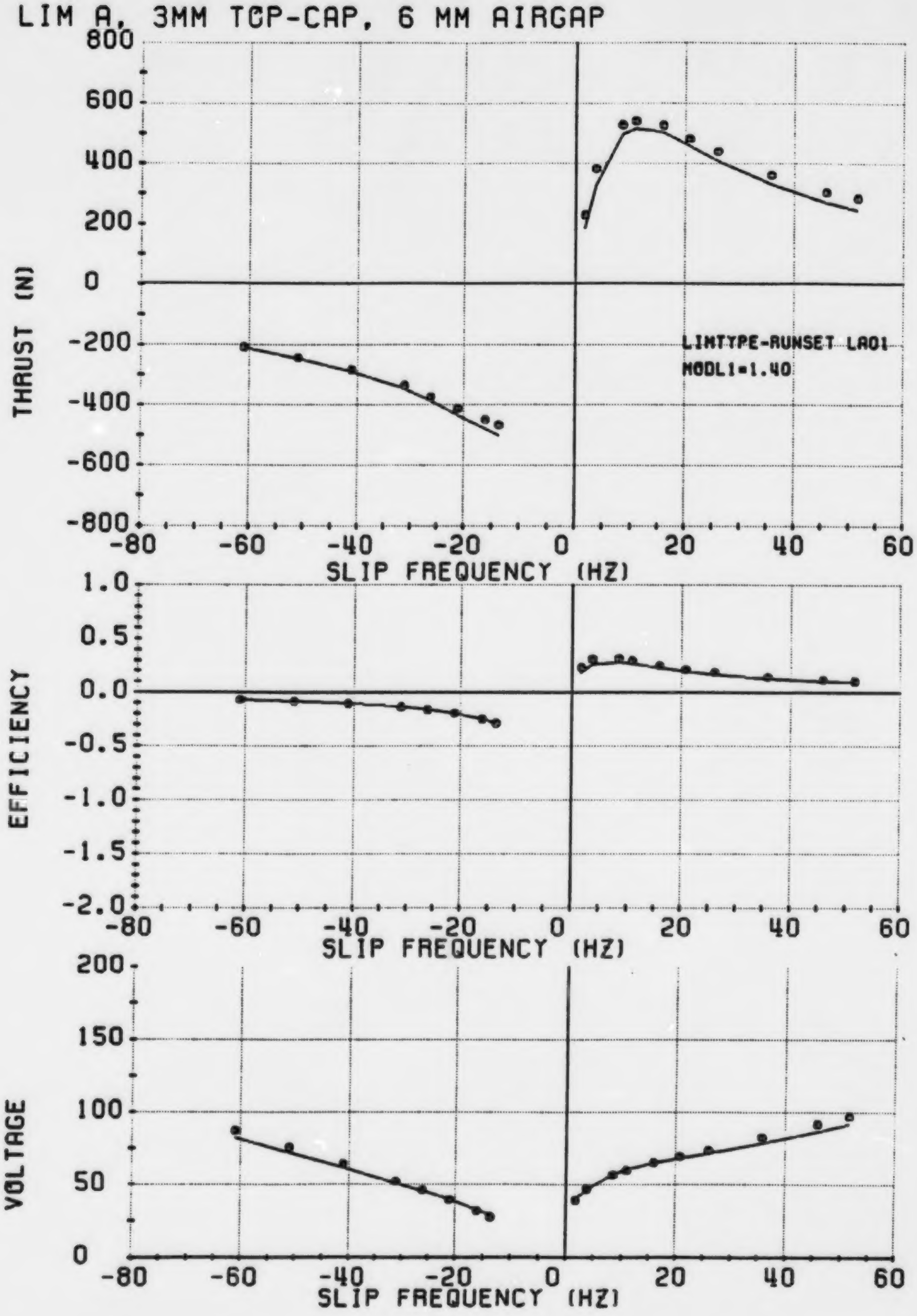

FIGURE 5-25: MODEL/TEST COMPARISON SAMPLE @ 1 M/S

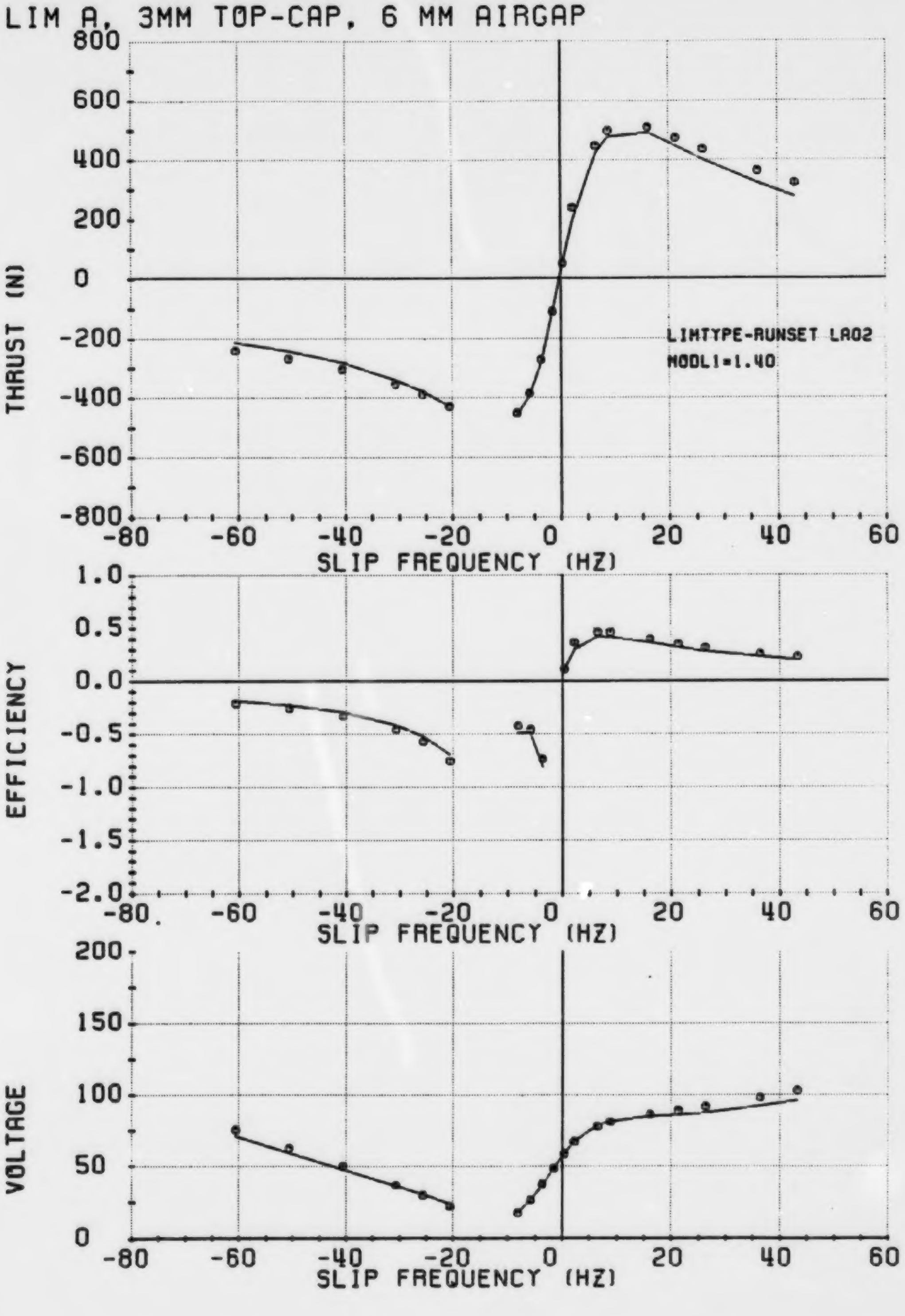

FIGURE 5-26: MODEL/TEST COMPARISON SAMPLE @ 3 M/S

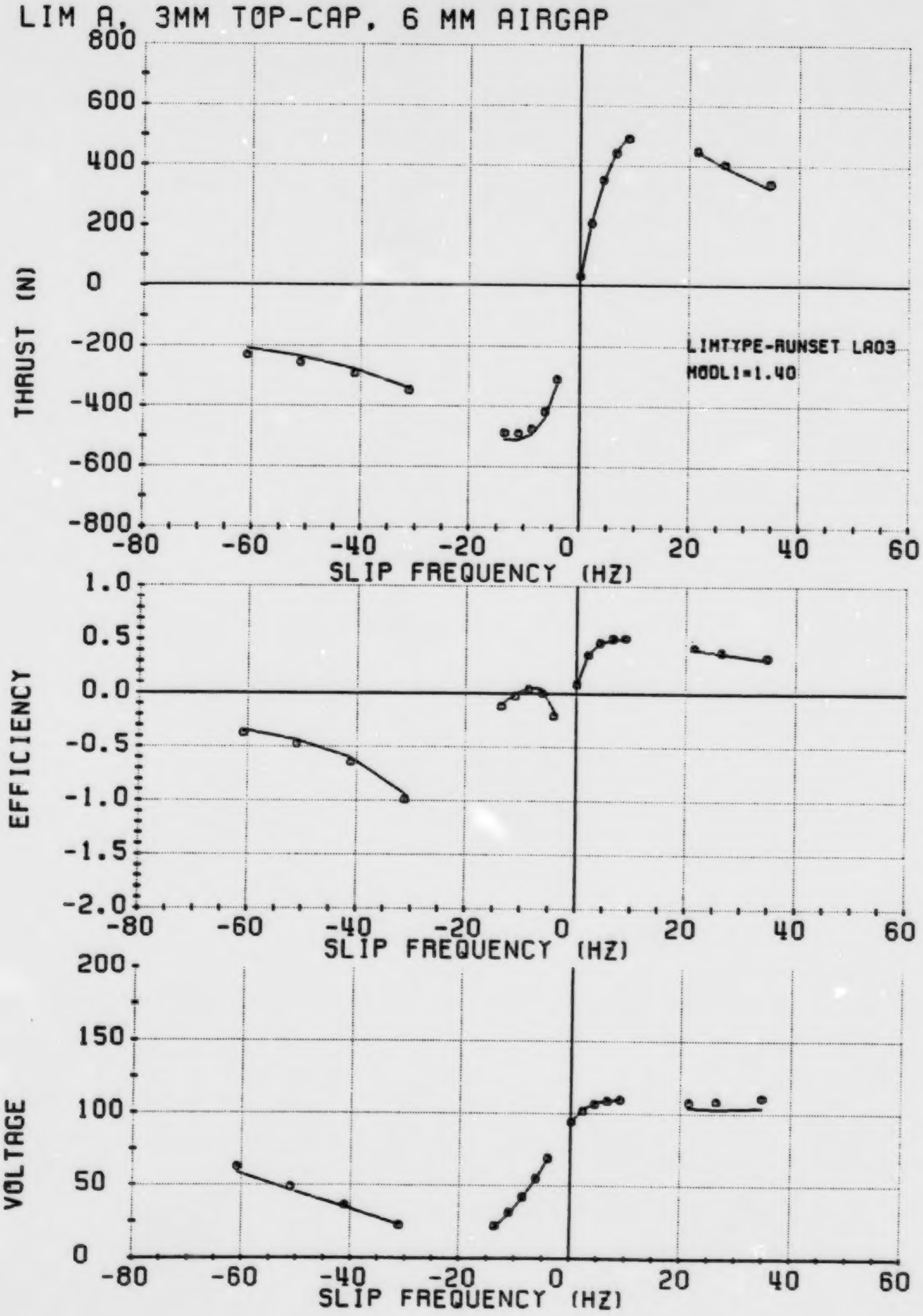

FIGURE 5-27: MODEL/TEST COMPARISON SAMPLE @ 5 M/S

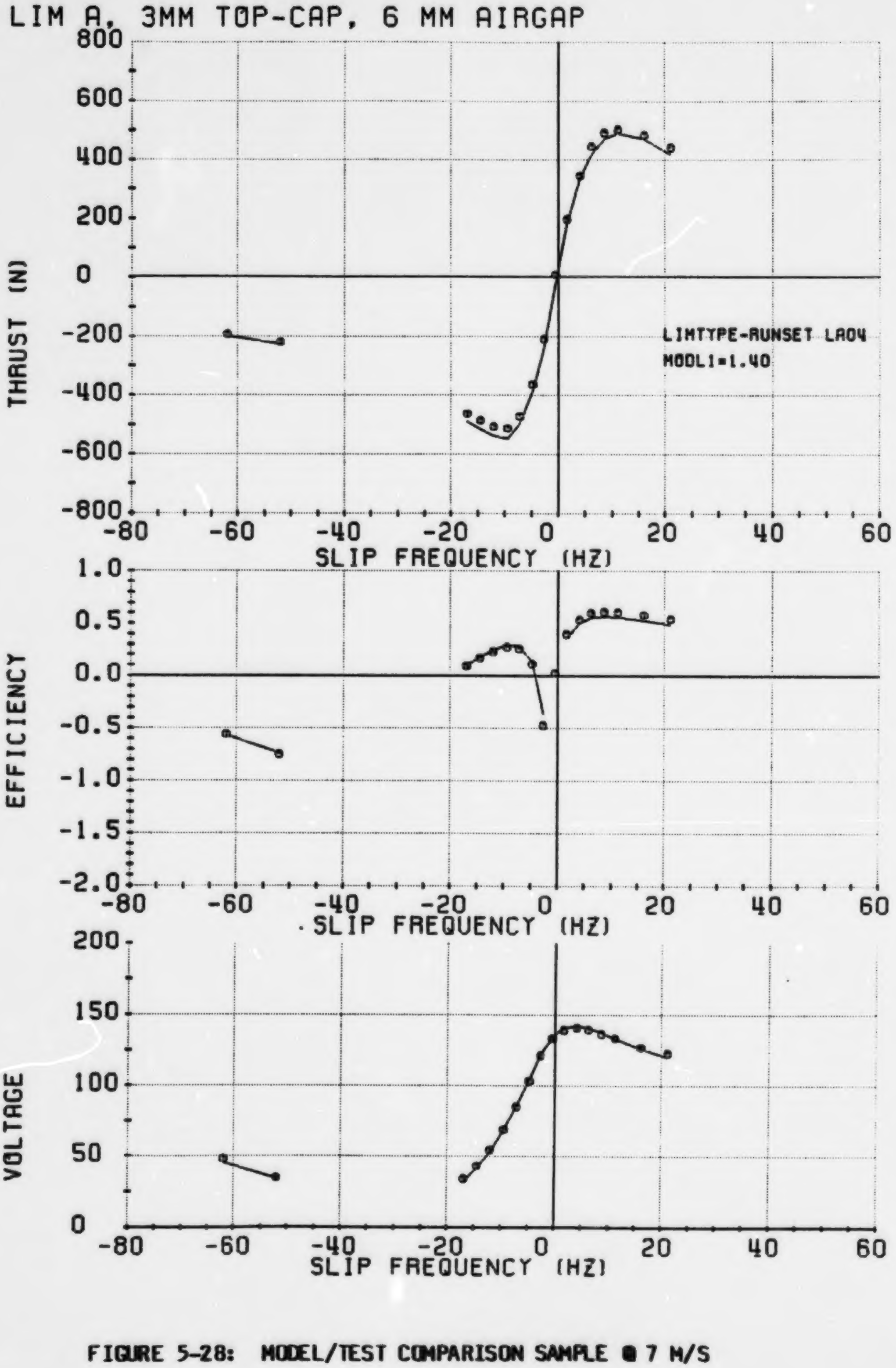

FIGURE 5-28: MODEL/TEST COMPARISON SAMPLE @ 7 M/S

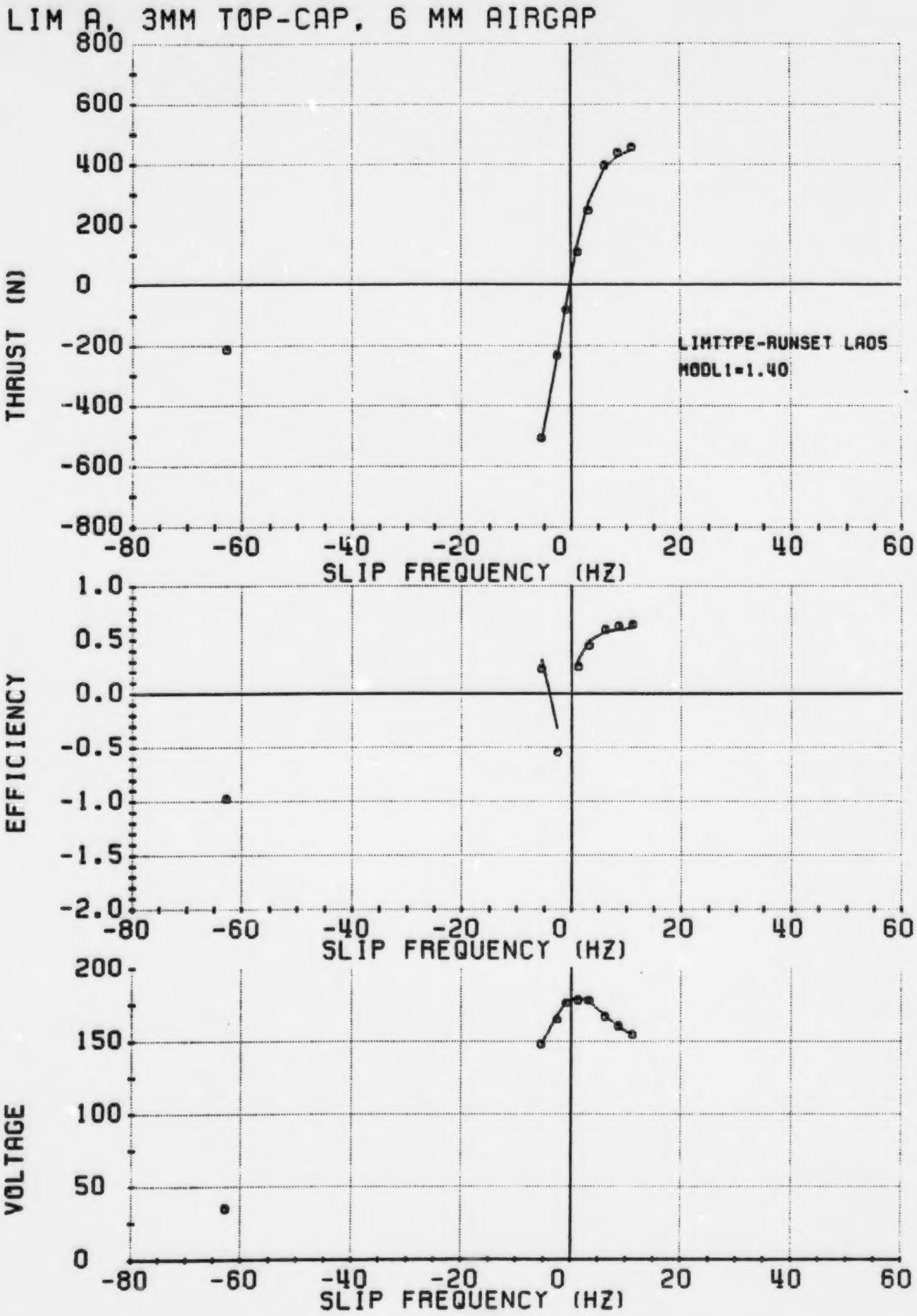

FIGURE 5-29: MODEL/TEST COMPARISON SAMPLE @ 9 M/S

2) When frequency is a controlled variable it is possible to brake in the so-called regenerative portion of the motor characteristic. This is in contrast to FF control which must employ "plugging"; a very inefficient form of braking.

3) An FF-controlled LIM must be designed with a pole-pitch that is consistent with the supply frequency (e.g. 60 Hz) and the maximum design speed. For many systems these constraints on pole pitch lead to serious compromises in the "electromagnetic design" of the LIM. VF-controlled LIMs are not so tightly constrained hence the design can often employ a longer pitch, which leads to general improvement.

4) FF-controlled LIMs use SCR voltage control which typically tends to reduce the overall power factor, particularly at lower control levels. VF-controlled LIMs use DC to AC conversion, so power factor is not a consideration.

In an attempt to quantify the effect of the above listed points in a way that is relevant for LIT applications, two types of study were undertaken:

1) Performance Comparison Study - A typical FF design and VF design, each with similar thrust capabilities, were experimentally characterized and their performance compared.

2) Design Comparison Study - A number of "paper designs" of VF and FF LIMs were created to meet a particular thrust/speed/duty specification and the designs were compared.

5.6.1 Performance Comparison Study

A typical FF-controlled and VF-controlled LIM were chosen for comparison. In this case "typical" means LIMs of about 1 kN thrust capability over the range of speeds from 0-6 m/s. The characteristics of each LIM were as follows:

PARAMETER	FF LIM	VF LIM
Pole Pitch	57 mm	114 mm
No. of Poles	8 mm	6 mm
Stator Width	152 mm	177 mm
Top Cap	3 mm	3 mm
Mech. Air Gap	6 mm	6 mm

The VF LIM was given twice the pole pitch of the FF LIM. This may seem somewhat of an arbitrary choice, but it makes the point that when VF is used, the designer can choose a longer pole pitch, i.e. he is not constrained to keep the pole pitch small in order to avoid excessive slip and the consequent inefficiency.

The stator widths differ slightly, (i.e. 16%) but this difference is irrelevant to the purposes or conclusions of the study.

After some consideration about what particular performance parameters would be meaningful in a comparison, it was decided to use Thrust vs. Speed, normalized to input real power and input apparent power respectively. Given that thrust and speed are what an application specifies, and that real and apparent power levels impact on system capital and operating costs in a general way, the choice of comparison parameters seems reasonable.

Figures 5-32 and 5-33 show the results of the comparison. Note that for both motoring and braking conditions over the complete speed range, VF displays better performance. The most dramatic differences are in braking, which is not surprising given that the VF LIM uses regenerative braking while the FF LIM uses plugging.

Also shown on Figure 5-32 is the characteristic of an FF LIM in combination with its voltage controller at about ½ of full thrust command. This condition is typical of the "real" case since in practice the nominal control thrust is well below the "full on" value.

5.6.2 Design Comparison Study

While it is clear that VF control can make a dramatic improvement over FF control in terms of Thrust per real and apparent power, it is not obvious how, if at all, this improvement affects the physical size and weight of the LIM stators. To try and get an idea of just how the VF vs FF trade off affects the design of the stator, a number of paper designs were produced. Three FF Designs and four VF designs were compared in terms of stator weight, real and apparent power consumption and reaction plate power dissipation.

5.6.2.1 Design Criteria

The seven LIMs were designed to the following criteria:

1) The LIM is required to produce motoring thrust only, at a level of exactly 3 kN, on a repetitive duty cycle of 5%.

2) The average "JA product", a measure of thermal loading, is designed to be 180 ± 10 A^2/mm^3 (see Sub-section 5.1.2.2).

3) The tooth, stator back-iron, and reaction plate back-iron peak flux densities are designed to be 1.5 ± 0.1 Tesla (see Sub-section 5.1.2.3).

These criteria were chosen in an attempt to eliminate issues that might complicate the comparison. For example, if it were specified that the LIM be able to produce a minimum value of motoring thrust

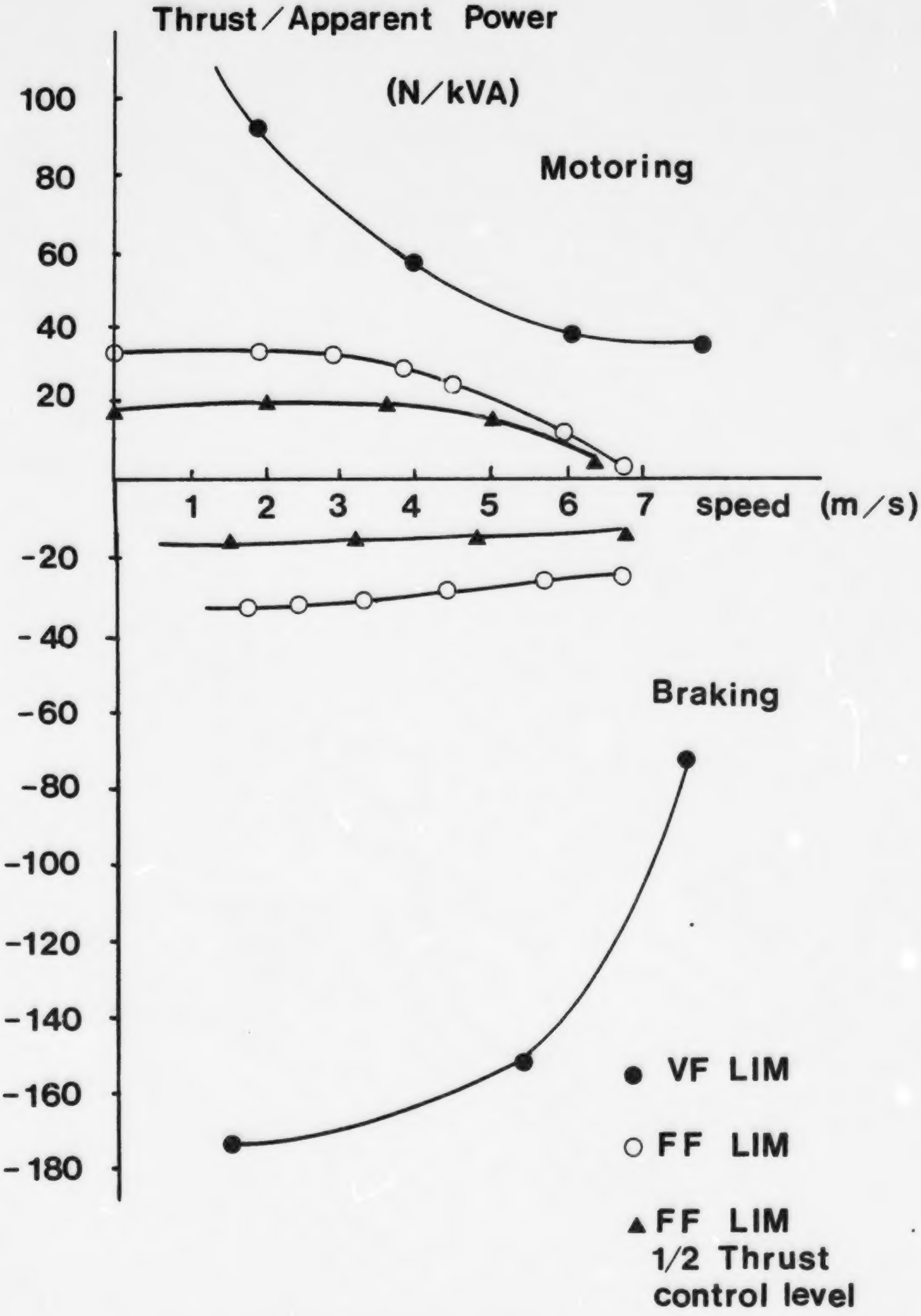

FIGURE 5-30: COMPARISON OF VF VS FF LIM PERFORMANCE: THRUST PER APPARENT POWER

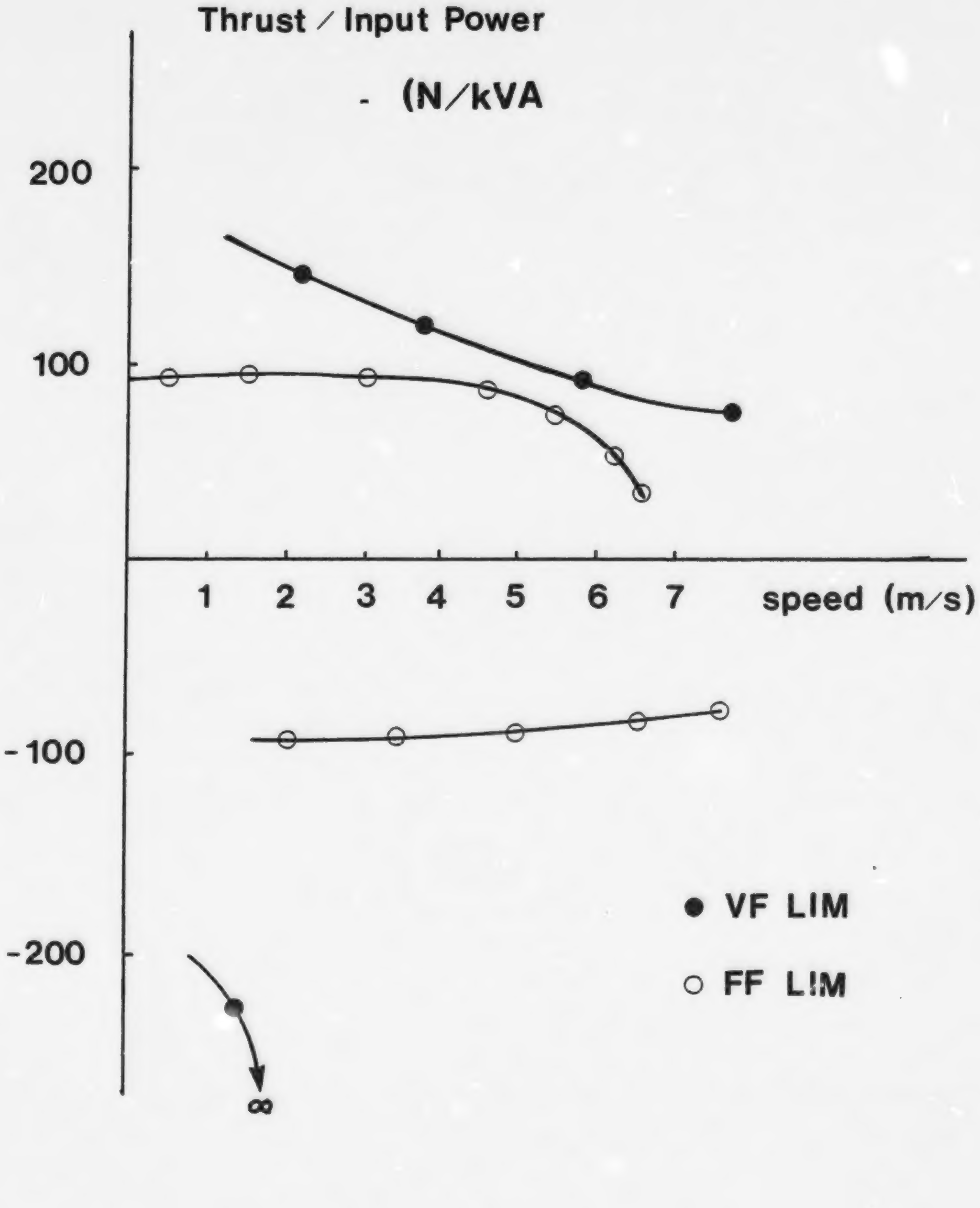

FIGURE 5-31: COMPARISON OF VF VS FF LIM PERFORMANCE: THRUST PER INPUT REAL POWER

and a minimum value of braking thrust the question of whether a given design is an optimum balance of motoring and braking performance becomes an issue.

Specifying the degree of thermal and magnetic loading as opposed to the allowable upper limits of each, promotes uniformity of comparison.

5.6.2.2 Design Variables

Besides the control mode, i.e. VF or FF, it was decided to vary the pole pitch and top cap depth in order to see the sensitivities of the performance and weight to each.

5.6.2.3 Summary of Results

The results of the seven design cases are shown in Table 5-4. An explanation of the choice of comparison variables is in order:

- o Stator Material - The separate and combined quantities of copper and steel used by a design are an indicator of the cost to produce it.
- o Supply - The quantity of real and apparent power required by the LIM are an indication of power distribution system costs and operating costs.
- o Reaction Plate - The power dissipated in the reaction plate can be a significant design factor if temperatures are likely to run high due to the nature of the application (e.g. long grades).

A number of trends are evident from the tabulated results and may be summarized as follows:

1) Top Cap Depth (or similarly, Top Cap material resistivity) has a strong effect on the real and apparent power that must be supplied for a given thrust. Interestingly, for the VF case, thinner top cap is reflected in the stator design as less copper. The trade off for the saving in copper is an increase in the supply requirement and an increase in reaction plate dissipation.

2) Pole Pitch, in the VF case, has a strong effect on apparent power. For example, doubling the pitch reduced the apparent power by a factor of two. The trade off for the reduced kVA is more steel.

3) Comparing "the best" FF and VF designs (i.e. best in terms of thrust per apparent power) there is about a 45% improvement in using VF for the particular design case studied.

Design				Stator Material			Supply		Reaction Plate
Pole Pitch (mm)	No. of Poles	Top Cap (mm)	Widtd (mm)	Cu (kg)	Cu (kg)	Cu+Fe (kg)	App. Power (kVA)	Real Power (kW)	Power Diss. (kW)
57	10	3	190	19	38	57	134	34	6
75	8	1	141	12	35	47	112	40	12
75	6	3	118	13	22	35	84	36	12
75	4	1	140	9	22	31	123	54	29
75	6	3	105	13	20	33	86	38	14
114	4	1	100	9	28	37	76	50	21
114	4	3	100	12	28	40	58	38	10

Design Criteria: 3 kN motoring @ 5 m/s, 5% duty, 6 mm mech. gap

TABLE 5-4: COMPARISON OF VARIOUS LIMs DESIGNED TO SATISFY COMMON PERFORMANCE CRITERIA

4) If "the best" is defined as minimum stator weight then for this particular design criteria there is little appreciable difference between the lowest weight FF and VF designs.

5.6.2.3 Remarks

The design studies presented here point to some tradeoffs with which the designer must be familiar. While only one performance target point was considered, the wide range of sensitivity to design parameter variation is clearly illustrated. Had a lower design speed (say, 1 m/s), or braking thrust been specified, the improvement in performance for the VF designs would have been even more pronounced, as per the trends observed in Section 5.6.1.

6.0 LIM DESIGN AND "EXPERT SYSTEM" SOLUTIONS

6.1 THE LIM DESIGN PROBLEM EXPLORED

Designing a LIM, or any other electric machine, is a complicated process. The number of design options that are available to the designer are almost limitless. The best LIM design is obtained by simultaneously choosing the optimal values for the following parameters.

1. Number of poles
2. Machine width
3. Pole pitch
4. Slot geometry
5. Primary yoke size
6. Air gap
7. Air gap, core, back iron flux densities
8. Top cap thickness and conductivity
9. Back iron size
10. Back iron lamination strategy
11. Primary electric loading.

Not listed are a number of second order effects and other parameters which could be considered. In order to select the appropriate parameter values, the LIT LIM designer would typically be provided with a required thrust, a duty cycle and a full range of line voltages available. Finding an optimal design from a null starting point would be a long and time consuming process. The design is usually expedited with the use of past design experience, analytical LIM models and Rules-of-Thumb. Motor configurations which worked well in the past are modified to fit the new application and problematic configurations are avoided. This implies that past designs must be documented in great detail and the Rules-of-Thumb must be put in writing if new designers are to learn the method without starting from scratch.

There is a tendency for some personnel to develop exclusive expertise in the design of motors. When these people retire or move to other employment, a scramble to regain lost corporate design capability may occur. While junior designers gain expertise, the ability of the firm to quickly design good machines may be compromised. In order to avoid the problem of exclusive expertise, UTDC and the Department of Electrical Engineering at Queen's University have been investigating the application of new computer techniques to the problem of LIM design [12].

6.2 EXPERT SYSTEM TECHNOLOGY

An expert system (ES) is a sophisticated data base management system which uses artificial intelligence (AI) techniques to explore relationships which link the data. The first use of ES was in diagnostic applications for complicated systems such as the human body or diesel electric locomotives. A recognized human expert (experienced physician, senior mechanic) "teaches" the ES program the symptoms of common problems and the most likely cures. Junior workers can then refer to the ES during their learning stage in order to solve problems more quickly and, at the same time, develop their own expertise. As new problems arise and new fixes are found, they can be added to the ES so that the base of experience grows. The attractiveness of this idea is obvious. As time goes on the experience bank grows and is immediately available to new employees. In addition the experience bank is transferable. Suppose that UTDC had been using an ES in their North American repair shops for several years. A street car sale is made overseas and a new repair shop is set up. By using the North American experience bank, the new shop could reach a high level of competence quickly. The North American and overseas ES could be merged periodically so that each could take advantage of the discoveries of the other.

A number of specialized computer languages have been developed for implementation of expert systems. The most common of these are LISP and PROLOG. PROLOG, for example, uses various algorithmns to search a data base for logical links between data or to draw interferences based on the data. The data base need not be in the form of numbers but can contain such information as:

(i) wheels are round
(ii) wheels are part of a car.

The inference that "a round part of a car is a wheel" could be drawn. The data base can also contain information in the form of numbers and formulas.

The amount of processing required in searching a large data base is considerable. In order to speed the search, some special computers have been designed especially for ES applications. These usually take advantage of multiple processors or parallel processing techniques. There are also implementations of ES systems and languages which can be run on a personal computer.

The nature of ESs is currently the subject of active debate among computer scientists. Some view ES as just good data base management, devoid of any sort of intelligence, while others support the view that ESs can actually learn and develop in an intelligent way.

6.3 FUTURE IMPLEMENTATION OF A LIM DESIGN EXPERT SYSTEM

The concept of an ES seems ideally suited to the task of accumulating the past experience and Rules-of-Thumb used in LIM designs. There are, however, limitations to the capabilities of an ES. The state of ES technology is not able to offer the capability required to propose, evaluate and recommend a LIM design to match a given set of requirements. There is some question if this approach is even desirable. It is likely that ES would never be able to explore new avenues as human designers often do.

If expert systems have a role in motor design it is most likely to be that of a design checker. A motor design along with the performance specification could be supplied to the ES for examination. The ES would then, based on the Rules-of-Thumb and past experience, warn of possible design problems. For example, the ES might infer that a particular design was prone to extreme normal forces, primary heating, mechanical problems, thrust attenuation due to lateral edge effects or other faults. This type of design advisor is often used in integrated circuit design in order to minimize prototype cycles.

The development of a LIM designer advisor is apt to be difficult. There are a large variety of machine parameters to consider and developing the ES software would consume a considerable number of man-hours. Adding the first set of information of the experience bank would also be a time consuming process. Limited application ES may be developed in a shorter time. Currently UTDC's largest motor demand is for small, fixed-frequency LIMs. These are typically made on a standard lamination geometry with adjustments made in length and width. With its reduced number of adjustable parameters, the small LIM design process is a subset of the general design process. A design advisor for this subset could be more easily implemented in the form of an ES. Based on current ES technology it appears unlikely that a working general design advisor could be implemented in less than five man-years. A restricted advisor for the small fixed frequency LIMs would most likely require at least two man-years of development.

7.0 DISTRIBUTED PROPULSION CONTROL CONCEPT

7.1 OVERVIEW

By definition, LIM-in-Track propulsion is "distributed". That is to say, the motors, rather than being located centrally, (i.e. on-board the vehicle) are distributed along the track. But what about the control of the motors? The various functional elements that make up a propulsion control system may be arranged in a variety of architectures.

In this chapter, a concept of distributed control and its underlying philosophy are presented. Figure 7-1 summarizes the major functions and places each of these within a "level". As a help to the reader, specific hardware items are identified with each level.

A characteristic feature, indeed, a principle of the control concept presented is that control functions which by nature are "fast acting" (time-critical) are associated with hardware (and software) which are situated nearby the devices they control. These are the "bottom level" functions, and are generally "self-contained" in the sense that they interact minimally with functions outside themselves.

Intermediate level functions provide the coordination between bottom level functions as required for moderately time-critical aspects of multi-vehicle management. This coordination is generally limited to relatively small, localized groups of LIM controllers, switch controllers and so on. That is, a given LIM controller would be functionally tied to other controllers in its near vicinity, but not to those located further away.

Top level functions provide management of those activities which by their nature are not localized and time-critical. Here, it is often appropriate to combine control functions in a single computer system.

Beyond the top level automatic control is yet another functional level; namely, the Operator Interface. Generally, any human operator functions are restorative or preventative measures and are initiated relatively infrequently. "Manual control" of the propulsion system is not provided at this, or any other level.

7.2 VELOCITY AND POSITIONING CONTROL

One of the major functions of an LIT propulsion system is to control the speed of vehicles at different points on the track. While "open loop" schemes involving either fixed- or variable-frequency power control are possible, closed loop approaches perform better and are more versatile. Open loop velocity control is discussed in reference [2] and will not be treated here.

LEVEL	FUNCTIONS	HARDWARE
OPERATOR CONTROL	o "cold" start o system failure recovery o backup/alternative modes selection o shutdown control o system status monitoring	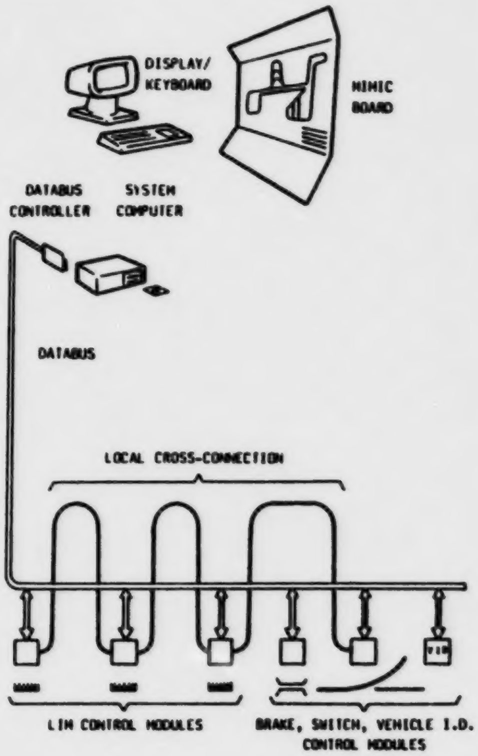 DISPLAY/ KEYBOARD MIMIC BOARD DATABUS CONTROLLER SYSTEM COMPUTER DATABUS LOCAL CROSS-CONNECTION LIM CONTROL MODULES BRAKE, SWITCH, VEHICLE I.D. CONTROL MODULES
TOP LEVEL AUTOMATIC CONTROL	o route selection o buffer management o Empty car management o System Health Monitoring o System Performance Monitoring	
INTERMEDIATE LEVEL AUTOMATIC CONTROL	o Collision Avoidance o Merge Control o Headway Control o Queing o Indexing	
BOTTOM LEVEL AUTOMATIC CONTROL	o Velocity & Stop Positioning Control o Station Control o Track Switch Control o Vehicle Identification o Emergency Stop Control o Local Malfunction Detection o Local Malfunction Protection & Backup	

FIGURE 7-1: DISTRIBUTED PROPULSION CONTROL CONCEPT

7.2.1 Sensing

Figure 7-2 is a functional block diagram of a velocity loop employing centralized control elements. More will be said of the particular configuration later, but first consider the problem of sensing vehicle velocity.

Velocity, rather than being sensed directly, is more conveniently determined by processing the digital output of devices which detect incremental changes in position. As might be expected, several means of processing such signals exist, but it is important to understand the limitations which may be inherent in a given approach. Consider, for example, the following list of concerns:

1) Direction Sensitivity - Does the sensing means provide discrimination of the direction of travel?

2) Stationary Presence - Can the sensing means detect a non-moving vehicle consistently and without ambiguity?

3) Inter-vehicle Gaps - In trains of vehicles there are necessarily gaps in the sensed target. Does the sensing means provide for a continuous signal regardless of these?

4) Low-Velocity Detection - Below what value do update delays render the signal useless for closed-loop control?

5) High-Velocity Detection - Above what value do processing speed limitations affect the velocity signal?

Please refer to Section 10 for a description of a practical sensing system.

7.2.2 Configuration

Figures 7-2, 7-3 and 7-4 illustrate three configurations of a closed-loop velocity control. The first two configurations are identical except for the physical locations of the switches which direct the controlled power to the appropriate LIM stator. Clearly, the first becomes problematic as the number of stators and/or the track distances grow larger. The second helps alleviate the problem of excessive power cabling by distributing the power switching locally.

The third scheme, which follows the "distributed" design philosophy to its full extent, offers considerably reduced lengths of cabling and eliminates the need for power switches. If these were its only advantages, it would possibly not be selected over the second alternative on a cost basis. However, there are other advantages inherent in the distributed configuration:

1) Where "coast-through" capability exists (see Section 4.4), distributed control offers a more complete functional

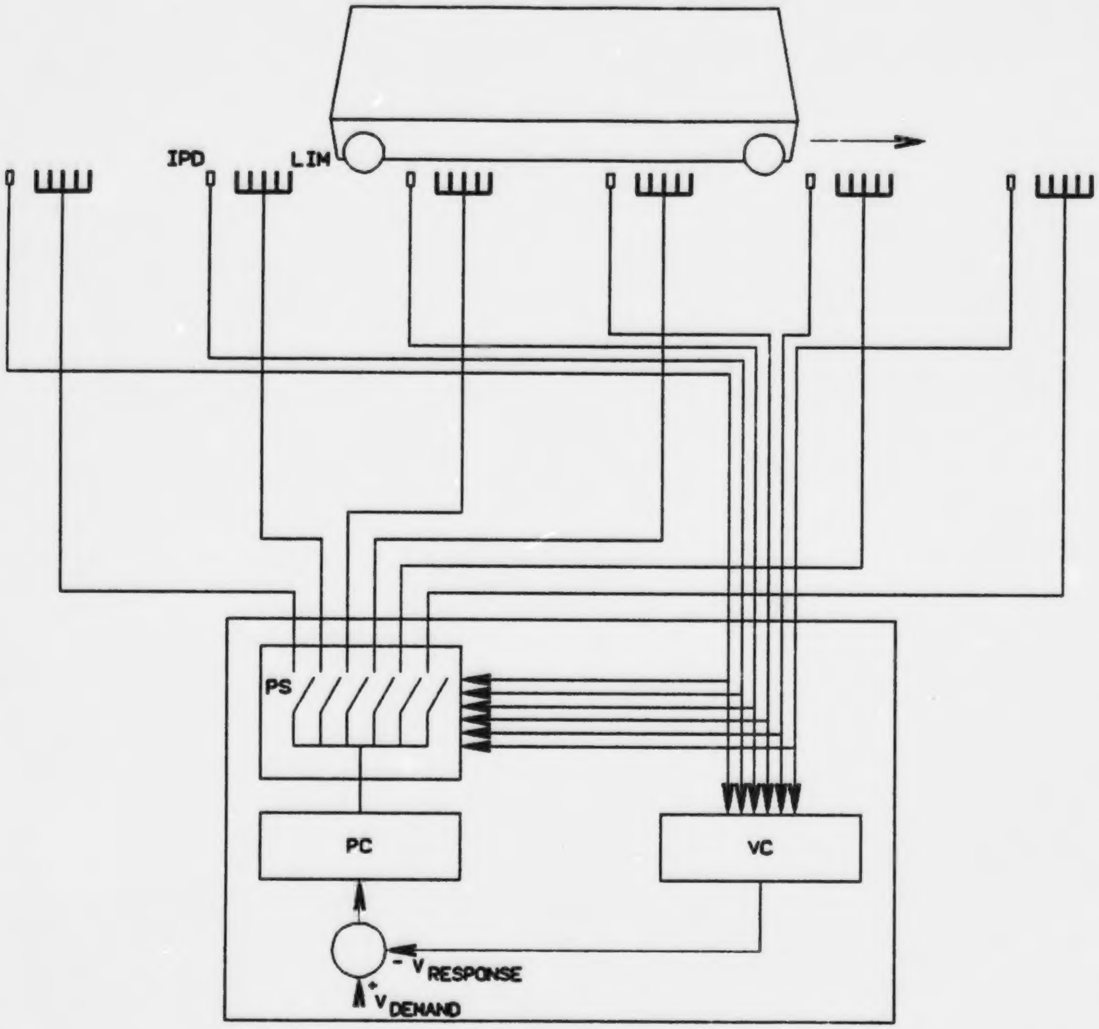
IPD
LIM
PS
PC
VC
- V RESPONSE
+ V DEMAND

IPD - INCREMENTAL POSITION DETECTOR

LIM - LINEAR INDUCTION MOTOR

PS - POWER SWITCH

PC - POWER CONTROLLER

VC - VELOCITY CALCULATOR

FIGURE 7-2: LIT VELOCITY LOOP WITH CENTRALIZED CONTROL AND POWER SWITCHING

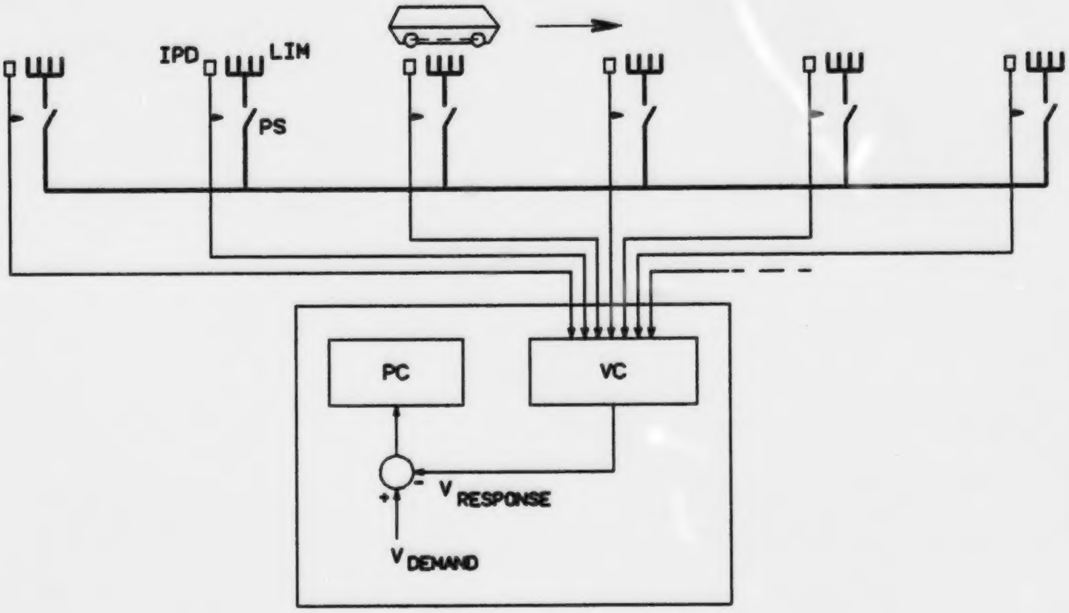
IPD
LIM
PS
PC
VC
+
-
$V_{RESPONSE}$
V_{DEMAND}

FIGURE 7-3: LIT VELOCITY LOOP WITH CENTRALIZED CONTROL AND DISTRIBUTED POWER SWITCHING

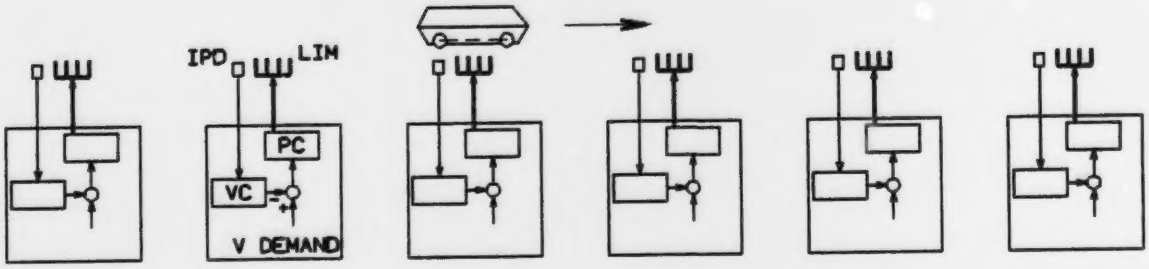
IPD
LIM
PC
VC
V DEMAND

FIGURE 7-4: LIT DISTRIBUTED VELOCITY CONTROL CONFIGURATION

redundancy than centralized control and is correspondingly more fault-tolerant.

2) Unlike centralized-control configurations which can only manage the control of one vehicle at any given time, distributed control can cope with multiple vehicles.

3) Other localized functions such as fault detection, fault correction, and protection are more easily realized in a distributed configuration.

7.3 MULTI-VEHICLE MANAGEMENT

Generally, LIT systems will have several vehicles operating at different points in the track network at any given time. Obviously, the potential for collision between vehicles exists, and except for certain special cases, must be avoided by some means of coordination and control.

Potential areas for collision are at stopping points and merge points, but also on straight track, since vehicles can be stopped or slowed through inadvertent failures and be hit from behind.

At least two approaches to multi-vehicle management can be identified for LIT systems. The first involves the time-coordinated release for vehicles from station points and the prediction of future state based on pre-determined vehicle speed-distance trajectories.

The second approach employs the protected block principle, which involves the designation of blocks, means of determining vehicle presence or absence within a block, and means of preventing vehicles from entering a block which is already occupied by another vehicle.

For some systems it may seem reasonable to employ both approaches, i.e. to use time-coordinated release as the first level collision avoidance mechanism and to overlay a protected block scheme for backup.

7.3.1 Time-Coordinated Release (TCR)

By its very nature, the TCR approach requires centralized control of moderate to high time-criticality. It therefore does not fit with the "distributed control" philosophy, which prefers centralized functions to be high level and non-time critical.

A major difficulty with TCR, besides its centralized nature, is that it relies on non-real-time predictions of system state and can be "fooled" by any system "hiccup" which influences vehicle travel times or dwell times.

Another disadvantage of TCR is that software algorithms for large multi-vehicle, multi-path systems can be exceedingly complicated to develop and test. By the same token, extensions to existing systems may require considerable rewriting of TCR software.

Lastly, the consequences of sudden failure in the computer which executes the TCR algorithms will almost certainly result in near-immediate suspension of system operation and will necessarily be followed by a tedious reinitializing procedure.

7.3.2 Protected Block (PB) Schemes

More in keeping with the distributed control philosophy than TCR is the Protected Block approach. Several variations of PB control are possible in LIT systems. Figures 7-5 and 7-6 compare two schemes. The first is known as a "fixed-block" system and the second could be described as a "trailing block" system. Both employ local cross connection of distributed "block controllers" but in the first the block controller is an intermediate level device which "oversees" a small group of LIM controllers while in the second, each LIM controller is its own block controller.

The purpose of the local cross connection is to transmit back to another block a signal which indicates the presence (or absence) of a "vehicle ahead". A presence indication would initiate appropriate control action, which depending on the relative location of the receiving controller to the sending controller could be to "slow" or "stop" any approaching vehicle.

Shown on both Figure 7-5 and 7-6 are the "protective buffer" and the "minimum following distance". The former is based on "worst case" stopping distance, i.e. it is the distance (rounded up to the nearest integral stator spacing) required to ensure that the vehicle can be completely stopped. The latter is the minimum distance that one vehicle can follow another without initiating the block protection mechanism. Minimum following distance is a significant parameter because it can impact on the ultimate throughput limits of the system. Note from the examples shown in Figures 7-5 and 7-6 the trailing block scheme has minimum following distance only slightly greater than the basic block length whereas the fixed block scheme minimum following distance is roughly twice the basic block length.

7.3.3 Vehicle Spacing Regulation

One inherent feature of the TCR approach which would seem to be lacking in protected block schemes is that vehicles are spaced apart and would not tend to bunch together except in the case of some malfunction. In protected block systems which do not employ some form of TCR one might expect the block protection mechanism to be exercised fairly regularly, and in some cases this would cause the system to behave not unlike "stop-and-go" rush hour traffic.

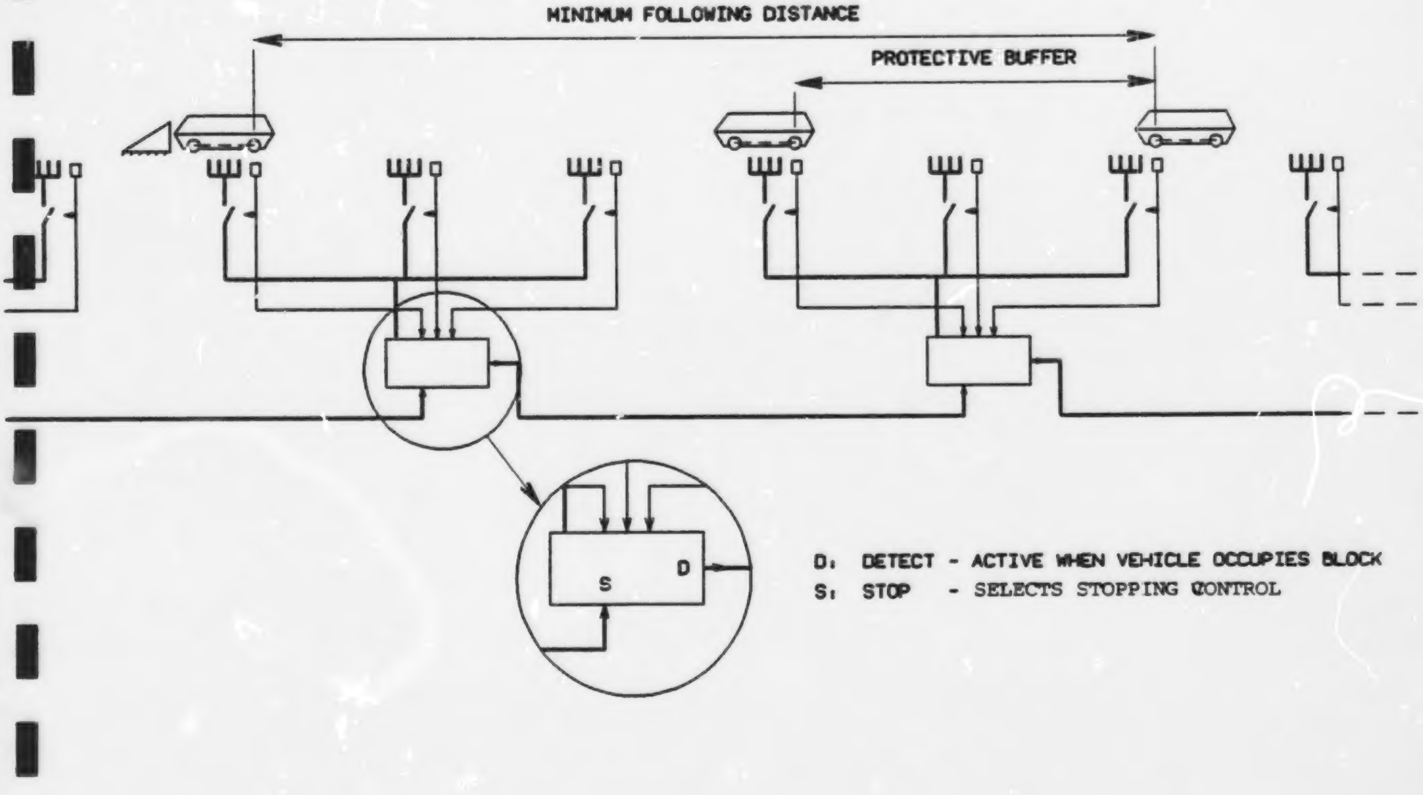
MINIMUM FOLLOWING DISTANCE
PROTECTIVE BUFFER
S
D
D: DETECT - ACTIVE WHEN VEHICLE OCCUPIES BLOCK
S: STOP - SELECTS STOPPING CONTROL

FIGURE 7-5: FIXED BLOCK SCHEME EMPLOYING LOCAL CROSS-CONNECTED BLOCK CONTROLLERS

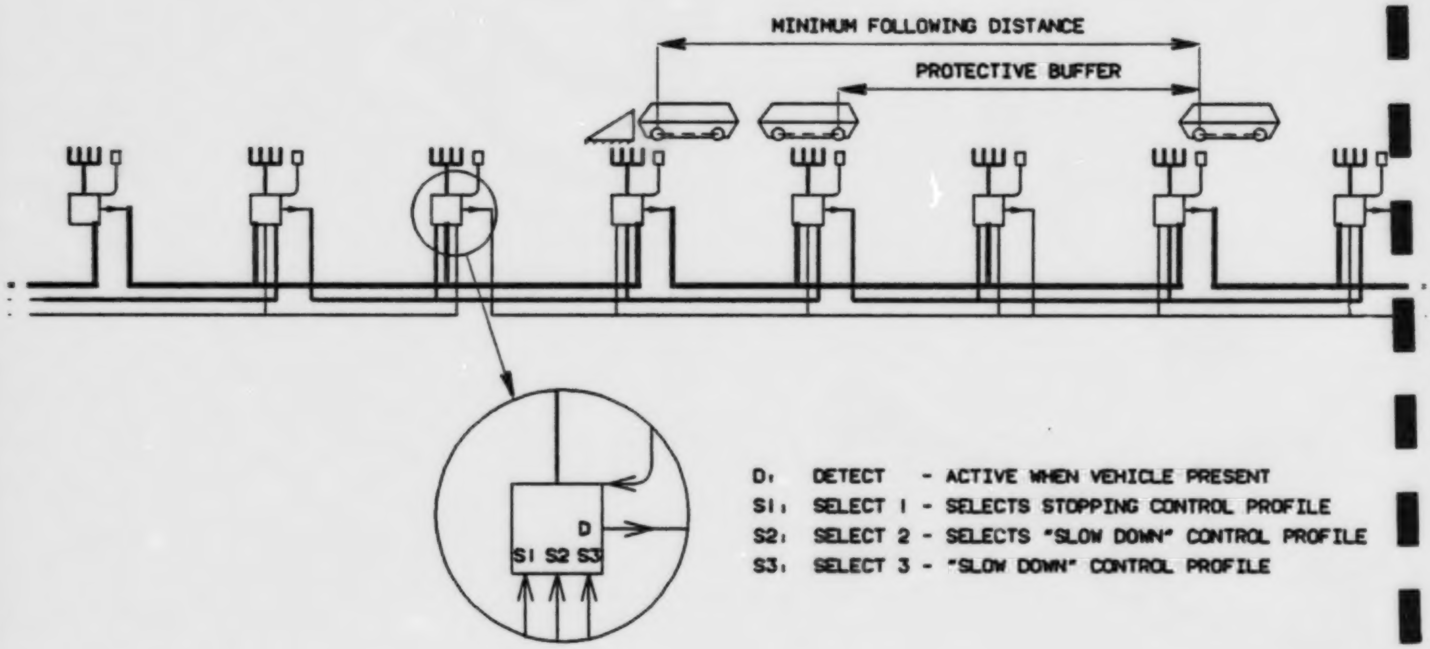
MINIMUM FOLLOWING DISTANCE
PROTECTIVE BUFFER
D
S1 S2 S3

D: DETECT - ACTIVE WHEN VEHICLE PRESENT

S1: SELECT 1 - SELECTS STOPPING CONTROL PROFILE

S2: SELECT 2 - SELECTS "SLOW DOWN" CONTROL PROFILE

S3: SELECT 3 - "SLOW DOWN" CONTROL PROFILE

FIGURE 7-6: TRAILING BLOCK SCHEME EMPLOYING LOCAL CROSS-CONNECTED LIM CONTROLLERS

It may be possible to avoid this situation by exploiting the distributed feature of the trailing block scheme to create "soft" block boundaries. In other words, a vehicle which begins to penetrate another vehicle's trailing block would be slowed down, but only marginally, causing the space between it and the leading vehicle to open up. With such a mechanism, it is not hard to imagine a sort of automatic regulation occurring. Throughout the system, vehicle spacing would be dynamically adjusted as required to maintain a minimum buffer.

7.3.4 Merge Control

The same type of mechanism which is shown in Figure 7-6 for collision avoidance on straight track may also be used to merge a vehicle into mainline traffic. In this case, vehicle detection signals from LIMs approaching a merge point are fed forward to "warn" the LIM controller responsible for accelerating the merging vehicle. The scheme is illustrated in Figure 7-7.

7.4 DESTINATION AND STATION CONTROL

In the previous section it was shown how management of collision avoidance in multi-vehicle systems could be achieved through local cross-connection of distributed LIM controllers, avoiding the need for any centralized coordination. It is somewhat harder to conceive of the functions of destination selection, routing, dispatch and loading/unloading being independent of a centralized controller, but a scheme exists that at least relieves the central processor from having to perform "real time" control.

The scheme referred to is based on a system of vehicle coding and automatic identification of these codes at specific locations on the track. For example, controllers located at stations can "know" which vehicle has just arrived, and based on stored information received earlier from the system computer, can make the appropriate action, i.e. whether to load or what to load. The local station controller is the "bottom level" device which handles the time-critical functions such as checking for proper vehicle docking, initiating and monitoring the load transfer operation and clearing the vehicle for release. The system computer is responsible only for the non-real-time action of downloading instructions, which can occur at any time prior to the vehicle arrival.

Figure 7-8 shows a system for controlling the routing of vehicles. Again, the system computer is relieved of making any real-time actions. Instead, it maintains a "routing table" which contains the track switch states required to direct a given vehicle to a given destination. A row of this table is downloaded to the corresponding switch controller sometime after an entry is changed, but before the vehicle is likely to arrive at the switch. The switch controller stores this information and "knows" which state to place the switch in at the moment it detects a given vehicle.

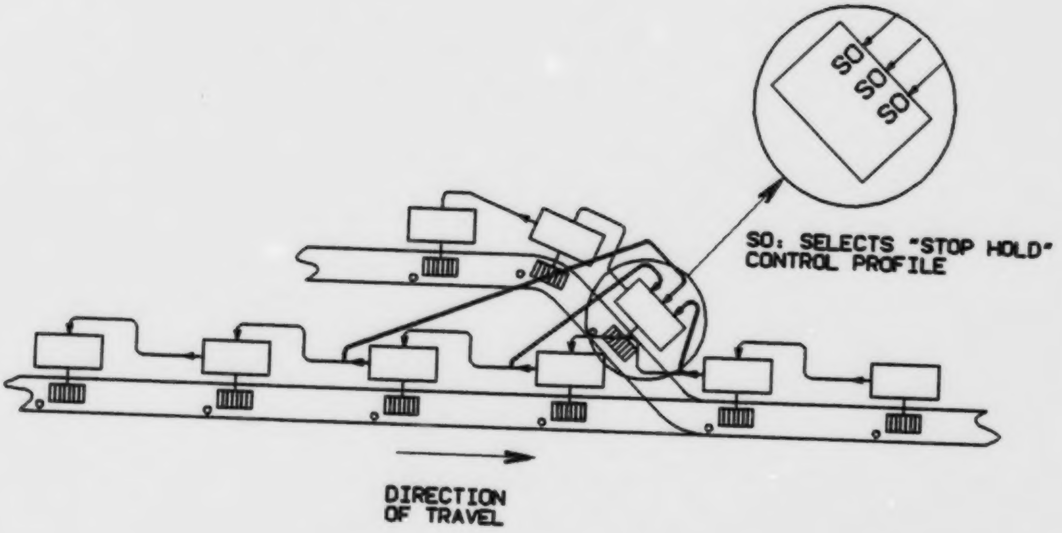
SO
SO
SO
SO: SELECTS "STOP HOLD" CONTROL PROFILE
DIRECTION OF TRAVEL

FIGURE 7-7: MERGE PROTECTION SCHEME EMPLOYING LOCAL CROSS CONNECTED LIM CONTROLLERS

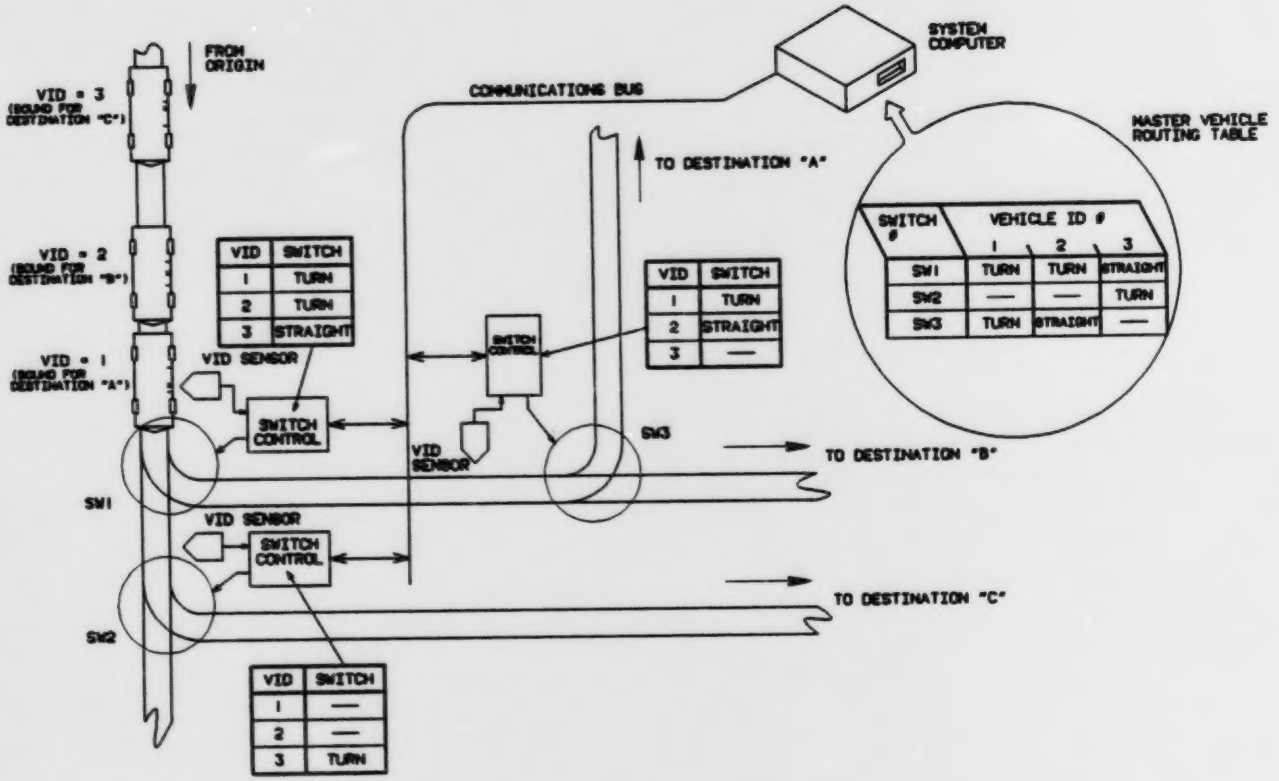
FROM ORIGIN
VID = 3 (BOUND FOR DESTINATION "C")
VID = 2 (BOUND FOR DESTINATION "B")
VID = 1 (BOUND FOR DESTINATION "A")
VID SENSOR
SWITCH CONTROL
SW1
VID SENSOR
SWITCH CONTROL
SW2
COMMUNICATIONS BUS
SYSTEM COMPUTER
MASTER VEHICLE ROUTING TABLE
TO DESTINATION "A"
SWITCH CONTROL
VID SENSOR
SW3
TO DESTINATION "B"
TO DESTINATION "C"

VID	SWITCH
1	TURN
2	TURN
3	STRAIGHT

VID	SWITCH
1	TURN
2	STRAIGHT
3	—

VID	SWITCH
1	—
2	—
3	TURN

SWITCH #	VEHICLE ID # 1	2	3
SW1	TURN	TURN	STRAIGHT
SW2	—	—	TURN
SW3	TURN	STRAIGHT	—

FIGURE 7-8: DESTINATION/ROUTING CONTROL

7.5 HEALTH MONITORING

A system containing hundreds of active components is unlikely to remain fault-free indefinitely. So, from the point of view of system safety, availability and maintainability, it is desirable to monitor as many functions as could go wrong. Clearly, LIT systems present a health-monitoring challenge. With LIMs, sensors, controllers, track switches, brakes and stations spread over several hundred metres of track, it is not hard to see that "distributed intelligence" and multiplexed communications is practically a necessity for effective health monitoring.

8.0 POWER SEMICONDUCTOR TECHNOLOGY

8.1 INTRODUCTION

The introduction of semiconductor switching devices caused a revolution in the control of electric machines. Previously, motors had been controlled using large resistor banks or complex machine sets such as the infamous Ward-Leonard set. Controlled power switching devices made the construction of frequency changing, voltage changing power supplies possible. As a result, compact and efficient AC and DC machine drive systems could be designed to operate from the AC mains. This chapter reviews how power semiconductors can be used to control a LIM-in-track system.

In the three decades since the first thyristor switches became available, a number of new devices have been developed. The characteristics and applications of the most common devices are outlined in Section 8.2.

Two power conditioning units (PCU's), intended for use with LIM in track systems, have been designed and tested during this program. The first was the AC Voltage Controller (ACVC) which produces a variable voltage fixed frequency (VVFF) output from an AC mains input. This unit achieves low capital cost and simplicity at the expense of LIM performance. The second unit investigated was a Pulse Width Modulated (PWM) Voltage Source Inverter (VSI). This device, which produces a variable voltage and variable frequency (VVVF) output, trades simplicity and cost for improved performance. The ACVC and PWM VSI are described in Sections 8.3 and 8.4 respectively.

Two alternative power conditioning units are described in Section 8.5 and future developments are discussed in Section 8.6.

8.2 POWER SEMICONDUCTOR DEVICES

Many types of power switching devices are presently available. Each of these has its own performance and capacity limits. Figure 8-1 shows the switching frequency and kVA capacity of the most popular devices. The following sections give a brief description of the characteristics of several switching devices.

8.2.1 Thyristors

The thyristor, also known as the Silicon Controlled Rectifier (SCR) can be thought of as a controlled diode. The standard SCR symbol is shown in Figure 8-2a.

An SCR can be made to conduct if the device is forward biased ($V_{ak} > 0$) and supplying a gate current. When an anode current is established, the device "latches" in the ON state and conduction continues after the removal of gate current.

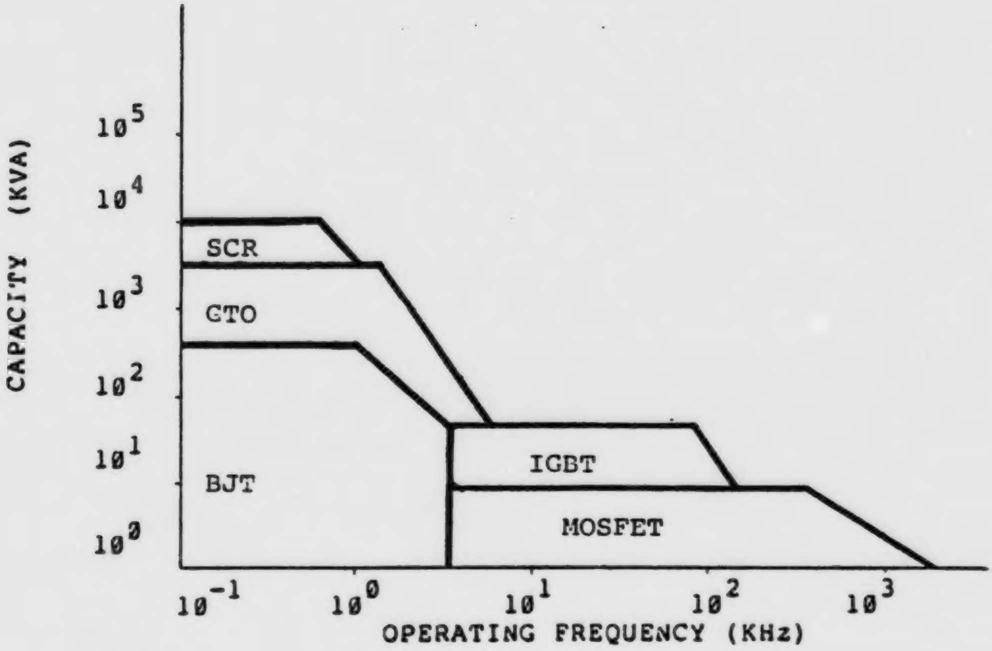

FIGURE 8-1: SWITCHING FREQUENCY AND kVA CAPACITY OF THE POWER SEMICONDUCTOR DEVICES

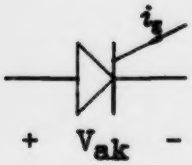

A) SCR

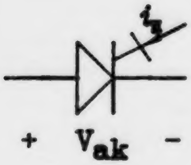

B) GTO

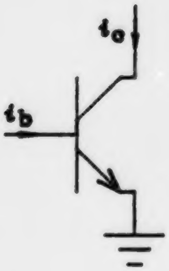

C) BJT

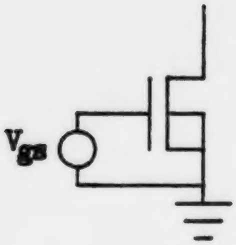

D) Power MOSFET

FIGURE 8-2: STANDARD SYMBOLS OF THE POWER SEMICONDUCTOR DEVICES

The SCR will turn OFF only when the anode current drops to zero or when V_{ak} becomes negative. In some applications the natural behaviour of the circuit shuts the SCR OFF at the correct time, while in others complex external circuitry is required to perform "forced commutation" of the device.

SCR's are available in very high current and voltage ratings and they are renowned for robustness and low cost. Because newer devices are more easily turned off, the SCR is now used only in applications where forced commutation is not required.

8.2.2 Gate Turnoff Thyristors

The Gate Turnoff Thyristor GTO (see Figure 8-2b) is a modified SCR which can be turned ON and OFF using gate current. A positive gate pulse latches the device ON while a negative pulse turns OFF the GTO. The turn off pulse is usually about 10% of the load current but lasts a very short time.

GTO's are available in approximately the same ratings as SCR's and are usually used in higher voltage, higher current applications where forced commutation is required.

8.2.3 Bipolar Junction Transistor

The power BJT (see Figure 8-2c) is a high power version of the bipolar transistor used in micro electronics. This device can be thought of as a current amplifier in which the base current is the input and the collector current is the output. Base current is supplied to turn the device ON and removed to return the device to OFF state.

In power BJT's the current gain I_c/I_b is about 10, so devices which switch large currents require substantial base drive capability.

8.2.3 Power FET's

Power MOSFET's (metal oxide semiconductor field effect transistors) (see Figure 8-2d) are the fastest switching devices available. These devices, which are manufactured in low voltage, low current ratings, are used in applications requiring high frequency operation such as a Switched Mode Power Supply.

The MOSFET is a voltage driven device, unlike the current driven GTO, SCR and BJT. The MOSFET is turned ON by applying a voltage between gate and source and OFF by setting Vgs=0. The gate impedance is extremely high so the gate drive can be a simple low power circuit. MOSFET gate characteristics make this device easy to interface with controller logic circuitry.

8.2.4 IGBT

The Insulated Gate Bipolar Transistor (IGBT) is a device which has the attractive gate characteristics of the MOSFET and the BJT's desirable output capability. The IGBT is a new device and is not yet widely available, however, if practical experience confirms the reliability and cost effectiveness of this device it will probably become a popular choice. The simplicity of the gate drive for this device would allow a significant reduction in the size and complexity of transitorized PCU's.

8.3 AC VOLTAGE CONTROLLER

The simplest way to control an induction machine is to control the RMS terminal voltage. A single phase ACVC is shown in Figure 8-3.

The switching of thyristors T1 and T2 are synchronized with the supply voltage, Vs, with a variable delay angle α . The operation of the controller can be illustrated with Figure 8-4 which is drawn assuming a purely resistive load. The result for a load containing inductance is somewhat different but the principle is the same. Note that the current periodically goes to zero because of the alternating line voltage. This natural commutation of the switching devices allows inexpensive SCR's to be used.

At the user selected delay angle α , T1 is gated and the supply voltage is applied to the load. At $wt = \pi$, the load current drops to zero and T1 goes to the OFF state. The RMS load voltage can be determined as a function of α and expressed as:

$$V_{RMS} = V\sqrt{1 - \frac{\alpha}{\pi} + \frac{\sin 2\alpha}{2\pi}}$$

line voltage $V_L = \sqrt{2}\ V \sin wt$

This simple circuit and switching strategy allows the user to gain control of the RMS voltage and thus control the thrust produced by the LIM.

Two major difficulties with the ACVC can be illustrated using Figure 8-4. First, note that the load current, which is also the line current, is nonsinusoidal. The harmonic content of the line current is of concern because it disturbs the power distribution system and necessitates the installation of filters. Current harmonics also cause thrust pulsations and increase heating in the LIM. When the harmonic component of the current is large, thrust pulsations could present noise and mechanical problems. It can be shown that the line current harmonic content increases with increasing α[13].

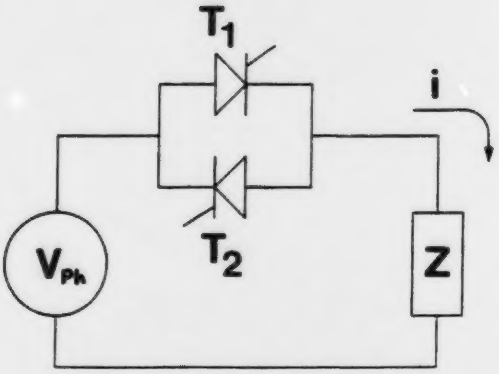

FIGURE 8-3: SINGLE PHASE ACVC

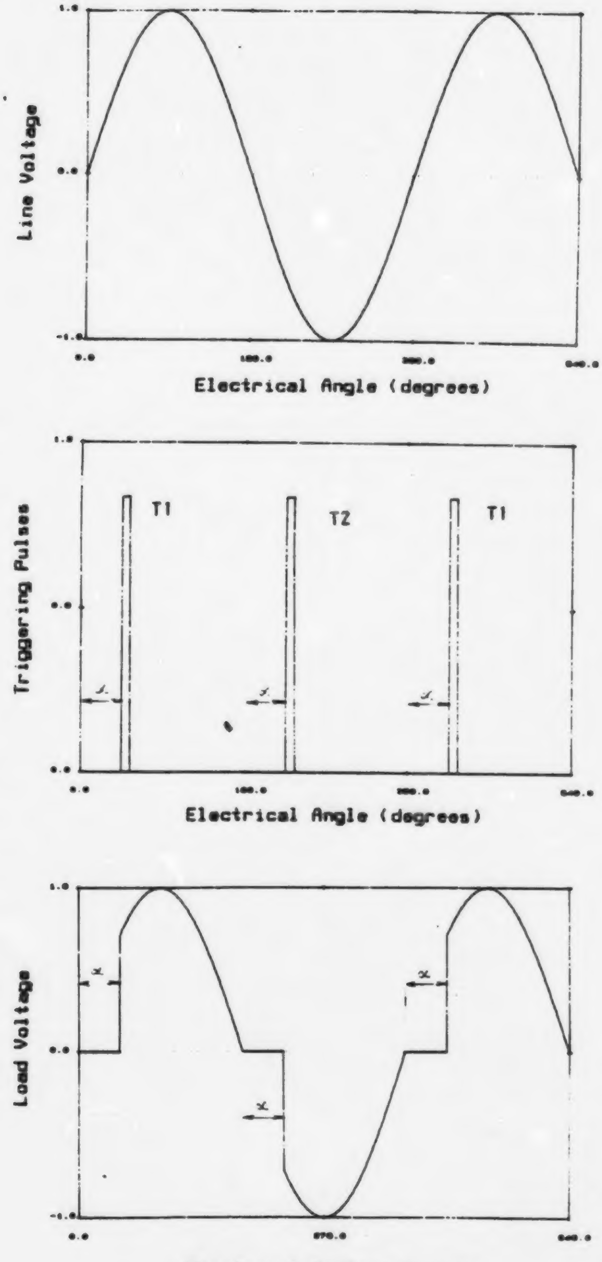

FIGURE 8-4: TYPICAL ACVC WAVEFORMS FOR RESISTIVE LOADS

The second difficulty with the ACVC involves the power factor of the controller/load pair. This index provides information about the current and voltage ratings of the distribution system relative to the power consumed. The power factor for this system can be expressed as:

$$pf = \sqrt{1 - \frac{\alpha}{\pi} + \frac{\sin 2\alpha}{2\pi}}$$

Note that even though the load is purely resistive, the combination has developed a lagging power factor. A similar phenomenon is observed when a load containing inductance is connected. A LIM operating alone typically has a low power factor and the addition of the ACVC pushes the power factor lower still. As a result, the power distribution equipment required for an ACVC controlled LIM in track system must be rated for a substantially higher voltage and current than the power consumed would indicate.

8.4 VOLTAGE SOURCE INVERTER

An inverter is a power conditioning unit which produces an AC supply from a DC source. The AC supply may approximate either a voltage source (VSI) or a current source (CSI), however only the VSI is considered here. A typical BJT based three phase VSI is shown in Figure 8.5. The switches of each phase segment are capable of connecting the load to either the positive or negative bus. An AC voltage is produced by alternately switching between positive and negative lines. The diodes D1-D6 allow the flow of reactive current in the PCU.

The most popular inverter switching scheme is known as PWM or pulse width modulation. A variable RMS voltage is produced by chopping the output voltage. Figure 8.6 illustrates this principle. Waveform A has a smaller ON pulse width than waveform B and it can be shown that A has a smaller RMS value. A popular method for generating PWM, sine-triangle comparison, is shown in Figure 8-7. The switching signal for a phase leg is determined by comparing a high frequency triangle carrier wave with a sine wave. When the sine wave is less than the triangle, the switching signal is high and vice versa. A high switching signal turns on the upper transitor (Q_1 of Figure 8-5) and turns off the lower transistor (Q_2 of Figure 8-5). A voltage known as the "pole voltage" is defined as the voltage between the output of the inverter and the halfway point in the DC bus, known as the "pole". The pole voltage takes on the same shape as the phase switching signal and it swings between $Vdc/_2$ and $-Vdc/2$. The load line to line voltage is determined by subtracting the pole voltages of adjacent phases ($V_{AP} - V_{BP} = V_{AP} - V_{PB} = V_{AB}$). The line to neutral load voltage depends on the load.

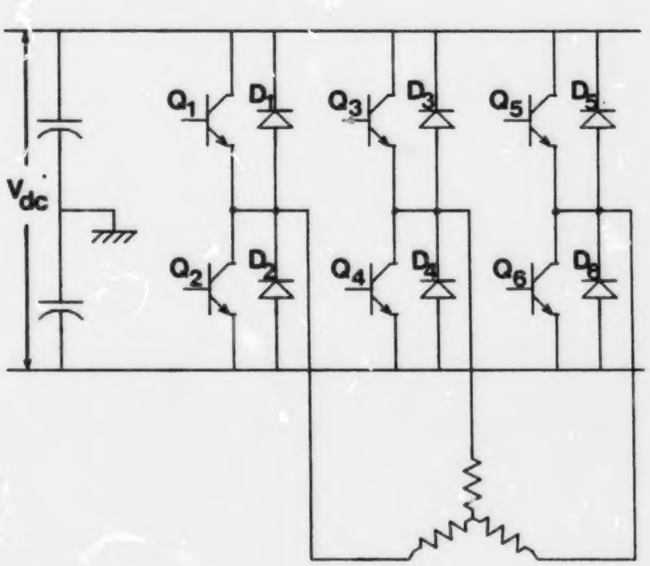
Q1
D1
Q3
D3
Q5
D5
Vdc
Q2
D2
Q4
D4
Q6
D6

FIGURE 8-5: TYPICAL BJT THREE PHASE VOLTAGE SERVICE INVERTER (VSI)

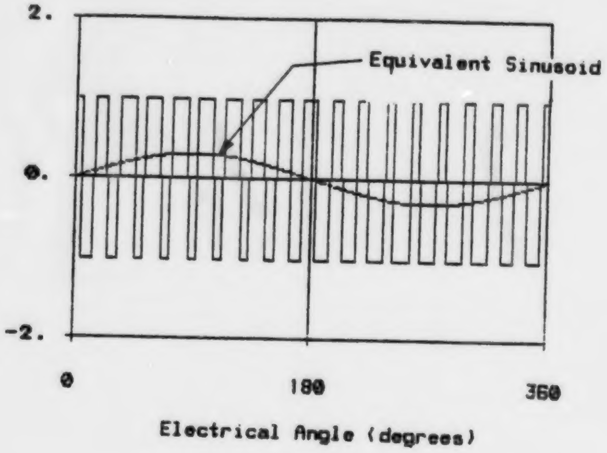

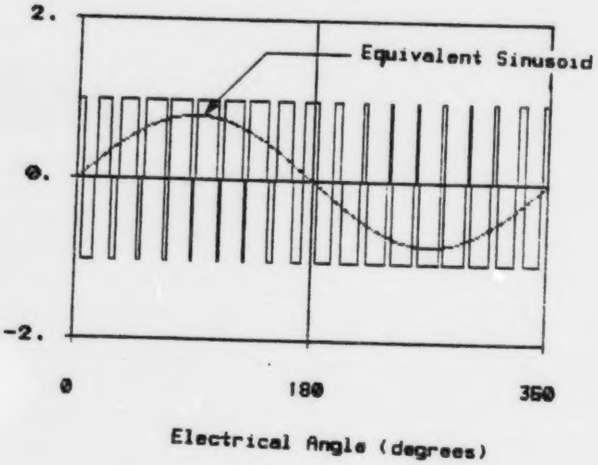

FIGURE 8-6: PULSE WIDTH MODULATION WAVEFORMS

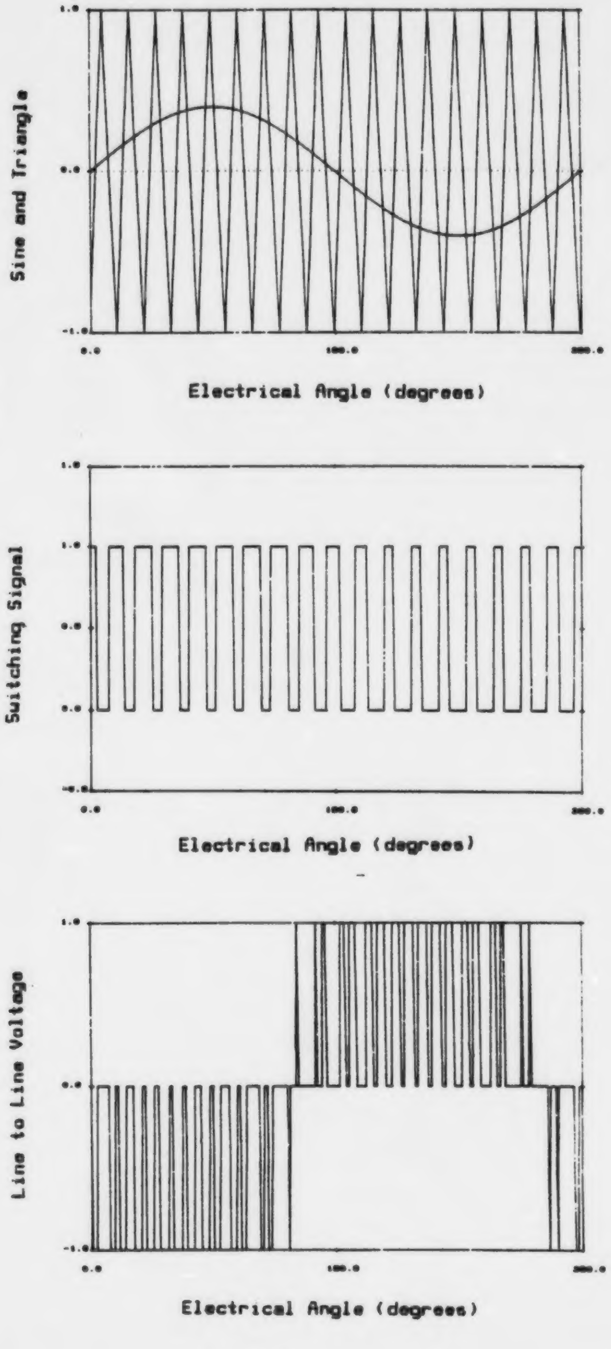

FIGURE 8-7: SINE-TRIANGLE COMPARISON METHOD FOR GENERATING PWM WAVEFORM

The inverter has a number of advantages over the ACVC. Firstly, the inverter output frequency is user selectable and thus LIM performance can be maximized over a wide speed range. This feature is used in many industrial and transportation induction drives, including UTDC's ICTS vehicle.

Secondly, reactive current required by the LIM flows in the anti-parallel diodes D1-D6 but not in the DC supply. As a result the inverter has a unity input power factor. This means that the power distribution can be designed for the LIM power instead of LIM apparent power as in the ACVC case. This can lead to a significant reduction in cable and distribution component size and cost.

The VSI also has several undesirable qualities. Forced commutation of the devices is usually required, consequently the power circuit is more complex and expensive than that of the ACVC. Capacitors required at the inverter input also add to the cost and dimensions of the VSI.

The switching logic required in an inverter is more complex than that of the ACVC. The logic must not only perform PWM generation and management but must also ensure that dangerous operating conditions do not arise. The cost of the logic circuitry will not be significantly greater than that of the ACVC but development costs are higher.

The choice of ACVC or PWM VSI for use in a LIM in track system must be made by considering the entire system cost. Typical systems are investigated under both schemes in Chapter 12.

8.5 ALTERNATIVE SCHEMES

There are a number of alternate schemes for applying controller excitation to a LIM. The first is a cyclo-converter supply. This power conditioning unit is a fixed frequency fixed voltage AC to VVVF AC converter which uses no intermediate DC link. A three phase cyclo-converter is shown in Figure 8-8.

A cyclo-converter operates by selecting pieces of the three phase input wave form and assembling them to approximate the required output voltage frequency and magnitude. The device count in a 3 phase to 3 phase cyclo-converter is rather large, however, inexpensive low frequency thyristors may be used. The quality of the output waveform decreases with increasing output frequency until the practical limit is reached to f out = f in/2. This means that a maximum frequency range of 0 to 30 Hz would be available using the 60 Hz mains. Presumably the system LIM's could be designed to operate correctly with this frequency range. If the reduced frequency range presents a problem, the distribution frequency could be increased using a single distribution inverter.

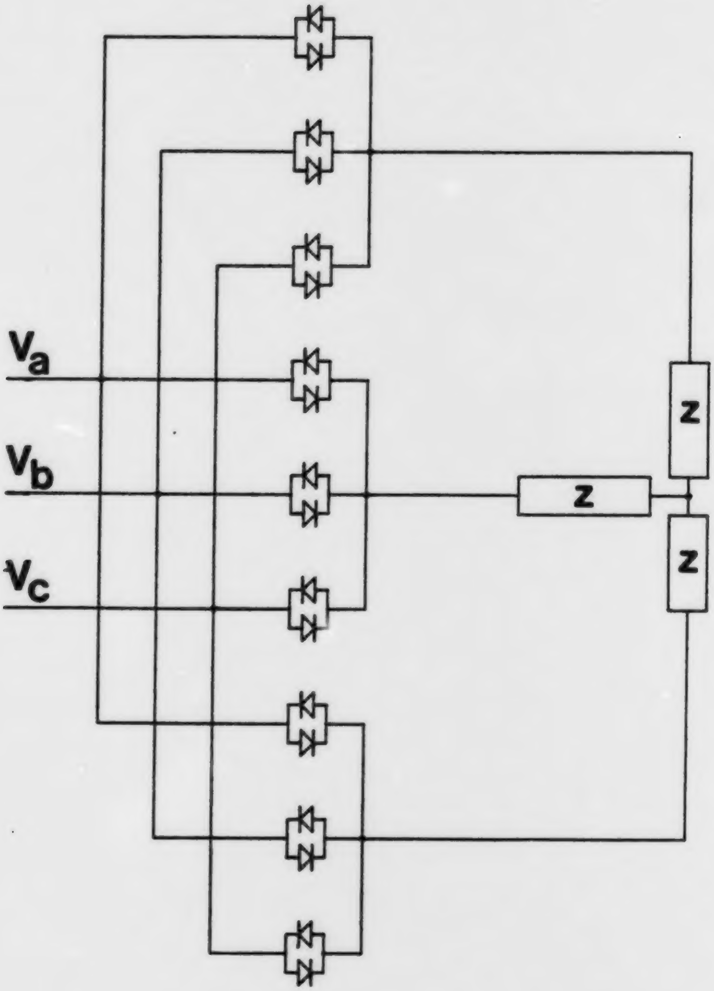

FIGURE 8-8: THREE PHASE CYCLO-CONVERTER

A second alternative is to implement AC voltage control using power transistors. Figure 8-9 illustrates a scheme proposed by [14] in which the mains voltage is chopped by the transistor pairs. The system power factor is not degraded as in the ACVC however the parts count for a three phase system is higher than that of a comparable inverter.

8.6 FUTURE DEVELOPMENTS

Current trends in power switching technologies indicate that in the future, switching devices will be more efficient, physically smaller, faster switching, and less expensive than those presently in use. Manufacturers are currently investigating ways of including some of the control logic in the device package. All of these developments would tend to make PCU's smaller and less complex than present units. The reduced complexity would probably result in increased reliability. The industry-wide trend toward higher performance lower cost microprocessors and microcontrollers will encourage the use of more sophisticated control algorithms.

The effect on PWM VSI units should be a significant reduction in size and cost accompanied by increased performance. The impact on ACVC technology will be limited. The ACVC will not benefit substantially from increased switching frequency and the SCR already has a small package, low price and high efficiency. The net effect will probably be to increase the attractiveness of PWM VSI's.

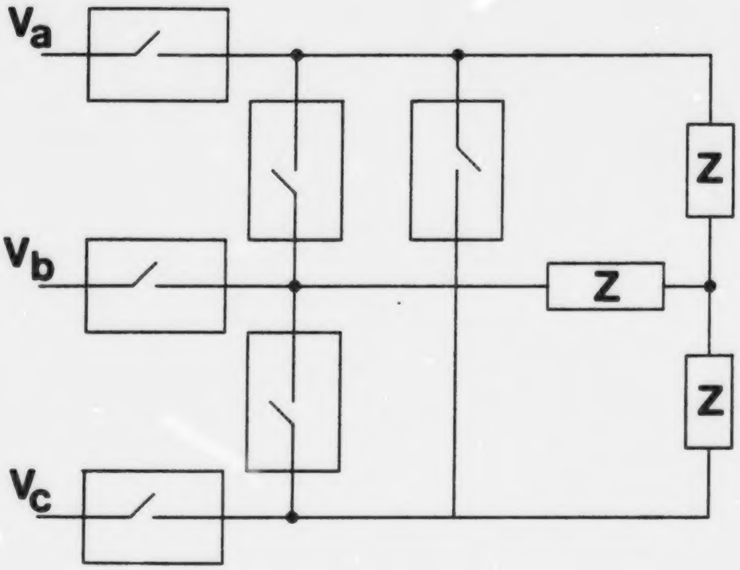

FIGURE 8-9: THREE PHASE POWER CONTROL CIRCUIT

9.0 COMMUNICATIONS

The "distributed control" concept outlined in Section 7.0 was based on the idea that LIT time-critical control functions can generally be decentralized, ie. carried out by local, semi-autonomous controllers. By following this idea through, configurations were developed for vehicle speed/position control, multi-vehicle management, station control, and vehicle-routing. In each case it was shown how the function could be achieved without relying on voluminous, real-time data transfer between local control points and the central computer system.

Though communications speed and throughput requirements may be minimized through design configuration, the requirement cannot be eliminated altogether. It is usually necessary to link local controllers into some form of communications network.

There are several forms of communications network. Indeed, so-called "standards" proliferate. Naturally, the performance, capabilities, and implementation costs of these standard networks vary widely. It is important when designing an LIT system to specify a communication standard which is appropriate. The following sub-sections review the fundamentals of some common approaches, outline the communications-dependent functions of typical LIT systems, and present an example of one commercial standard which has been applied successfully in an actual system.

9.1 COMMUNICATIONS APPROACHES

The term "communications" as used in the context of electronic data systems is very broad. It is therefore necessary to be more specific. Here, we consider communications systems with the following features:

- serial, binary data.
- use of a single cable "bus" (electrical or optical) as a medium for signal transmission over distance.
- multiple-point servicing (ie. medium is accessible to data transmitters/receivers at several points along its length).
- bi-directional data flow.
- transmission distances of the order 100 to 1,000 m.

In comparing standards, it is helpful to define generic descriptions as follows:

- Physical Signalling - The physical principle employed in signal representation and transmission.

- Bus Access Method - The means by which a given transmitter gains access to the bus so as to avoid inadvertent interference with other transmitters.
- Data Encoding - The technique by which information is represented on the physical signal.
- Data Transfer Protocol - The "rules" for packaging and unpackaging data which provide for source/destination identification, transmission error-checking, correction and failure-recovery.

9.1.1 Physical Signalling Approaches

The physical signalling principle employed determines certain ultimate system performance limitations:

- maximum transmission distance.
- maximum number of "drop points" (communicating devices) serviced by the communications bus.
- maximum data-handling capacity.

The trade-offs involved in choosing the physical signalling principle inevitably involve cost-related considerations:

- type of cable.
- type of terminations (connectors, isolating transformers).
- special provisions (impedance matching, use of repeaters).
- interfacing circuitry (receivers, drivers).

A comparison of four physical signalling approaches appears in Table 9-1.

9.1.2 Bus Access Methods

When several communicating devices "share" a common signal transmission medium, a means of keeping the various message transmissions separate is required. Techniques for managing multiple messages on a common medium are broadly subdivided as Time-Division-Multiplexing (TDM) and Frequency-Division-Multiplexing (FDM). Some bus standards employ FDM to create several "channels" on a medium, and then use TDM techniques to manage the data flow on a per channel basis. These standards, known as "broadband networks" are commonly employed in office and factory environments for linking localized computer systems together.

SIGNAL TYPE	CABLE TYPE	COMMENTS
Current Source	Two-Wire, Unshielded	Offers good noise immunity and low-cost cabling but tends to be low in bandwidth (10-100 kHz), is not well-suited to bi-directional data traffic, does not support "branch-tree" bus topology and is not easily expanded.
Voltage Source	Shielded, Twisted-pair	Offers moderate cost cabling, terminations and interfacing, moderate bandwidth (100 kHz-1 MHz), requires repeaters for long lines and/or large numbers of drop points.
Voltage Source	Co-Axial	Offers high bandwidth (10 MHz plus), supports long lines, but has higher cost cabling and terminations.
Light Source	Optical Fiber	Offers very high bandwidth (100 MHz plus), very long lines, but is highest in cabling, termination and interfacing circuitry costs.

TABLE 9-1: COMMUNICATIONS NETWORKS: PHYSICAL SIGNALLING APPROACHES

For LIT systems, broadband networks are not particularly suitable, the primary reason being cost of implementation. Single-channel networks based on TDM techniques are more suitable, but even among these, bus access methods vary. Three such methods are outlined in Table 9-2. Of the three, the Master/Slave would seem to be the most natural fit into the distributed control philosophy described in Chapter 7. the "slaves" correspond to the bottom level functional elements while the "master" is associated with the top-level automated functions. Unfortunately, the intermediate level functions, which require communication between bottom level elements, are not readily supported by the Master/Slave method, since slave-to-slave transmissions are generally too slow to be useful in time-critical situations such as vehicle collision avoidance.

An alternative to the Master/Slave arrangement which would support the intermediate level functions is the Carrier-Sensing/Collision Detection method. CSCD methods seem not be be a favoured choice in the industry though, and low cost, "off-the-shelf" hardware and software to support CSCD is not readily available.

Token passing methods have the same functional limitations of Master/Slave arrangements. Moreover, the principle lays a greater "responsibility", and hence processing-burden, on the bottom level elements.

9.1.3 Data Encoding

The information transmitted to and received from the communications bus is generally arranged as a signal containing a finite sequence of logical "1's" and "0's". The methods of representing a logical state in a signal vary. Table 9-3 identifies some common methods. To be received and decoded, signals like those is Table 9-3 generally require that a synchronizing reference be included with the signal. Sometimes this takes the form of a "clock" signal which is carried with the data signal on a separate pair of wires. Such data buses are dubbed "synchronous". Other times, the synchronizing reference signal can be recovered from the data signal by special techniques, eliminating the need for a separate clock signal. These are so-called "asynchronous" or "self-synchronous" data bases.

9.1.4 Data Transfer Protocol

Data is generally transmitted to the bus in finite-length sequences called "messages". The message contains not only the data which is intended to be transferred, but also source and destination addresses, sub-addresses, and other information used in synchronizing, error-checking and failure recovery.

Most systems employ a protocol; a sort of "exchange" between the sending and receiving stations. For example, the sender may wait for a reply from the receiver to be sure a message was received.

BUS ACCESS METHOD	PRINCIPLES OF OPERATION	COMMENTS
Master/ Slave	Only the bus master can initiate a transmission to or from any one of the several slaves connected to the bus. Master to slave transmissions can be selective, ie. to a particular slave, or in some systems "broadcast" to all slaves simultaneously. Slave to master transmissions are initiated by the master cyclically "polling" each slave to see if the slave has anything to report.	o Since the master has control, and the slaves can only "speak when spoken to" information coming "up" can only be as current as the polling cycle time permits. The more slaves, the less current the information. Selective, or prioritized polling can sometimes improve performance. o Slave-to-slave transmissions are only possible by employing the master as an intermediary. Again, information cannot be current, so time-critical functions should not rely on slave-to-slave communications.
Carrier Sensing/ Collision Detection (CSCD)	Every communicating station is permitted to initiate a transmission to any other station(s) if it senses no activity on the bus at the instant it wants to transmit. If by chance more than one station transmits simultaneously, the	o Since every station can access the bus when needed, information tends to be current. o As the bus gets "busier", collisions become more frequent, as do the resulting transmission delays. o Since a "busy" bus is less

TABLE 9-2: COMMUNICATIONS NETWORKS: BUS ACCESS METHODS

BUS ACCESS METHOD	PRINCIPLES OF OPERATION	COMMENTS
Carrier Sensing/ Collision Detection (CSCD) (cont'd)	resulting "collision" is detected by each of the sending stations and each station "tries again" some random amount of time later.	efficient in terms of transmission times, attempting to utilize the full physical capacity of the medium compromises performance.
Token Passing	Every communicating station is permitted to transmit when its turn comes to hold a special data item called the token. The token is passed from station to station giving each station momentary access on a fixed cycle. In some systems a station holding the token may grant another station access to the bus, thereby imitating the master/slave arrangement described above.	o Since stations must "wait their turn", information they provide is not current. As in the master/slave method, the more stations, the less current the information. o Since there is no fixed master, selective polling cannot be implemented as a performance improvement measure.

TABLE 9-2: COMMUNICATIONS NETWORKS: BUS ACCESS METHODS (CONT'D)

ENCODING METHOD	DESCRIPTION	1 | 0 | 1 | 0 | 0 | 1 | 1 | 0
Direct Encoding	"1" = signal high "0" = signal low	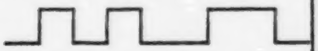
Manchester Encoding	"1" = low to high signal transition "0" = high to low signal transition	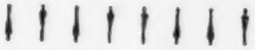
Amplitude Shift Keying	"1" = presence of high frequency carrier "0" = absence of carrier	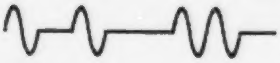
Frequency Shift Keying	"1" = carrier frequency high "0" = carrier frequency low	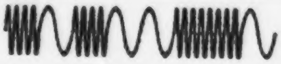
Phase Shift Keying	"1" = carrier "in phase" "0" = carrier 180° "out of phase"	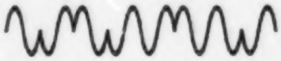
Non-Return to Zero (NRZ)	"1" = state change "0" = no state change	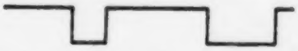

TABLE 9-3: COMMUNICATIONS NETWORKS: DATA ENCODING

In some systems, the reply contains some or all of the data that was originally sent, so that the sender can check the integrity of the transmission and "try again" in case of failure. Variations on protocols such as this abound. Some systems offer different modes of operation whch permit abbreviated protocols; means of trading off transmission integrity against messaging rate.

9.2 COMMUNICATIONS FUNCTIONAL AND CONTROL REQUIREMENTS

Some of the functions typically required in an LIT system which require the transfer of data between points are listed in Table 9-4. Note that those functions which are the most time-critical happen to involve the least volume of data. Conversely, those that are the least time critical involve the greatest volume of data. This situation was not arrived at so much be accident as by application of the distributed control principle. This principle is based on the recognition that functions requiring both high volume and high speed information flow can be localized so as not to require communication over distance.

9.3 SUITABILITY OF "BITBUS" DISTRIBUTED INTELLIGENCE NETWORK

"BITBUS" is a communications network standard developed by the INTEL Corp. for use in distributed intelligence applications. Products based on the BITBUS standard are being offered by a number of companies, both as Board-level products to Original Equipment Manufacturers and System products to end-users.

A brief characterization of BITBUS is as follows:

Physical Signalling - Voltage Source (Shielded, Twisted Pair)
Bus Access Method - Master/Slave
Data Encoding - Non-Return to Zero, Self-Synchronous
Data Transfer Protocol - Message/Response with Message Queuing and Retry Capability
Data Rates - 375 k Baud to 300 m between repeaters
- 62.5 k Baud to 1,200 m between repeaters

9.3.1 Controller to Controller Communications

BITBUS was not employed in functions requiring "lateral" data transfer ie. between local (bottom level) controllers, because of the time-critical nature of tasks such as collision avoidance and merge control. As was pointed out in Section 9.1.2, the delays involved in slave-to-slave transmissions are too large to support time-critical tasks.

Thanks to the low data volume and the localized nature of the tasks, it was practical to employ short, hardwired links carrying simple "static" logic in order to support collision avoidance and related functions (see Sections 7.3.2 and 7.3.4).

FUNCTION	DATAFLOW DIRECTION	DATA VOLUME	TIME CRITICALITY
Collision Avoidance/ Merge/Queuing Control	o LIM Controller to LIM Controller o Switch Controller to LIM Controller	very small, eg. less than 1 byte received/controller/ vehicle passage	high, eg. less than 100 ms delay
Route Selection	o System Computer to Switch Controllers	moderate, eg. 5 bytes sent/vehicle trip	moderate, eg. less than 15 sec. delay
System Health Monitoring	o Local Controllers to System Computer	high, eg. 200 bytes received/polling cycle	low, eg. 30 sec. delay following health status change
Alternative Modes Selection	o System Computer to Local Controllers	moderate, eg. 100 bytes to reconfigure	low, eg. 60 sec. delay following mode change
Real-Time Vehicle Tracking (ie. "Mimic Display")	o Local Controllers to System Computer	very small, eg. one byte/controller/ vehicle passage	high, eg. less than 1 sec. delay in tracking vehicle movement

TABLE 9-4: COMMUNICATIONS-DEPENDENT FUNCTIONS

9.3.2 System Computer to Controller Communications

BITBUS is well-suited to communications tasks involving the transfer of data "downwards" ie. from "Master" to "Slave".

Since the Master is "in control" of the communications bus it can effectively pre-empt it's less critical activities such as routine polling in order to get messages out quickly. An example is for the vehicle routing function in which it is essential that "fresh" instructions arrive at a local track switch controller ahead of the vehicle for which the change of routing is planned.

9.3.3 Controller to System Computer Communications

BITBUS is suited to "upwards" data transfers so long as they are not time-critical. For system health monitoring functions BITBUS is generally adequate, since is is usually not possible to respond to local faults immediately anyway.

BITBUS is not particularly well-suited for supporting the "mimic display" function, which requires fairly fast upward transfers. Since the mimic display concept is not actually a control function, but more of a convenience to human operators, one might argue that a real-time representation of vehicle locations is an unnecessary and complicating requirement.

9.4 SECTION CONCLUSION

An overview of communications approaches, LIT requirements, and suitability of a practical candidate system were reviewed. It should be stated that BITBUS distributed intelligence network, while providing for some of the required functions, is not ideal in every respect, though it is not clear at the present time that any of the other approaches would be either.

The weakest aspects of the BITBUS approach involve lateral and upward time-critical transfers. these are the areas in which a Carrier Sensing/Collision Detection method appear strongest. One can imagine a CS/CD technique working well with only a few vehicles in the LIT network: only the controllers in the immediate vicinity of the moving vehicles would need to be communicating to one another or to the system computer. However, as the number of vehicles in the system is increased, the probability of interfering, or "colliding" transmissions would increase, making data transfer inefficient at best, and "too slow" at worst. In the latter case, not only signals, but vehicles also, might find themselves colliding!

10.0 LIM VOLTAGE CONTROL MODULE

The LIM Voltage Control Module (LVCM) was conceived and designed as a key element of the Distributed Propulsion Control Concept described in Chapter 7. The LVCM fits into the "bottom level" of the control system hierarchy presented in Figure 7-1, and consistent with that classification is intended to fulfill time-critical functions semi-autonomously, thereby presenting a minimal communications burden to the system as a whole.

The LVCM design described in this chapter was prototyped in an earlier phase of the "LIMs and Their Control Systems" program. The design has since been refined and used in a "real world" application in Industrial Materials Handling. Designs are also underway for Airport Baggage Transport and People Moving Systems.

The following sections present a fairly detailed functional description of the LVCM, describe some of the experience gained through tests on the prototype Materials Handling System, and outline the refinements to the basic design that are being contemplated.

10.1 SYSTEM DESCRIPTION

Figure 10-1 and Table 10-1 provide a brief overview of the main functional capabilities of the LVCM. The following subsections detail the Hardware, Software, Motion Control algorithms and Built-In Monitoring features.

10.1.1 Hardware

10.1.1.1 INTEL 8044 Microcontroller

The distributed control module concept outlined in Chapter 7 is made practical through the application of recent microprocessor technology. The INTEL 8044 microcontroller is a single chip device which combines an 8-bit microprocessor with several additional functions intended for real-time control. "Firmware" resident in the 8044 provides a complete operating system with a multi-tasking executive which permits, among other things, communication to a "master" computer via the INTEL "Bitbus" serial data-bus system.

The LVCM employs a single INTEL 8044, external RAM and EPROM, an INTEL 8255A programmable peripheral interface (PPI) for I/O port expansion, and an INTEL 8254 programmable interval timer for functions related to SCR gate signal timing.

10.1.1.2 Sensors

Figure 10-2 illustrates the LVCM sensor arrangement. Note that there are two sensors used per LIM, one located near each end, so that detection of the train can be made from either direction of

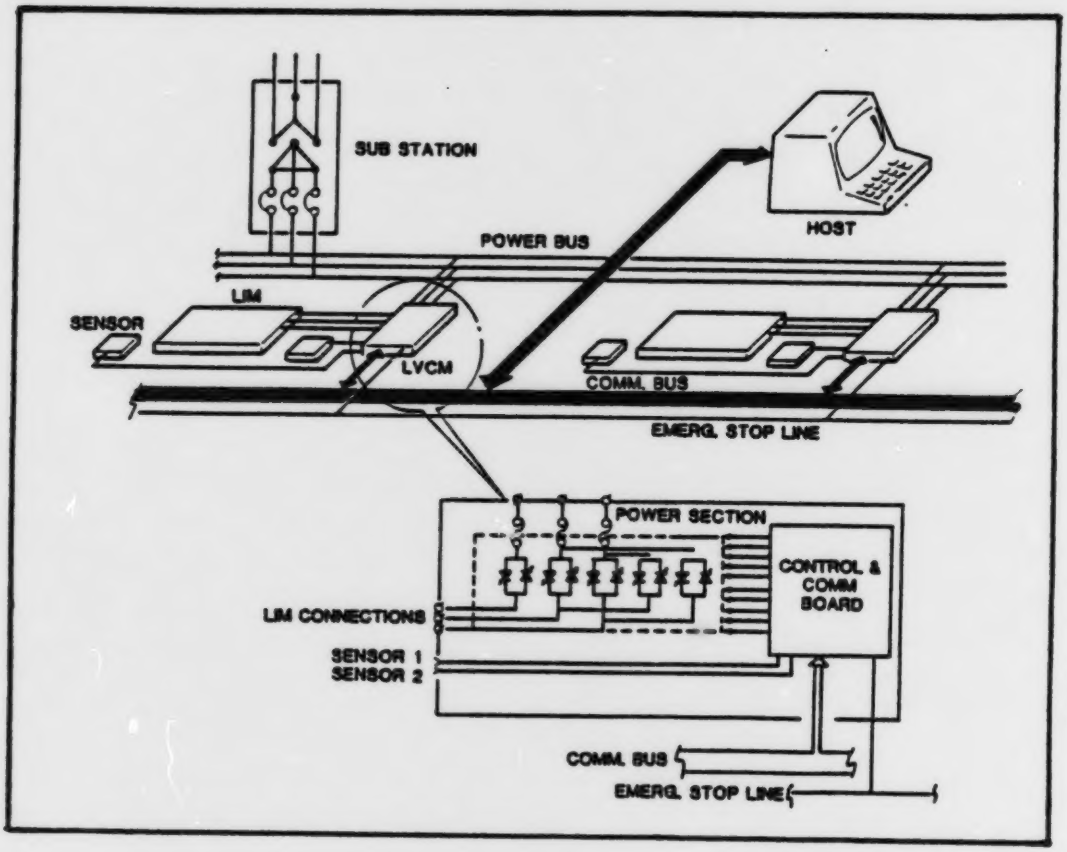
SUB STATION
HOST
POWER BUS
LIM
SENSOR
LVCM
COMM. BUS
EMERG. STOP LINE
POWER SECTION
CONTROL & COMM BOARD
LIM CONNECTIONS
SENSOR 1
SENSOR 2
COMM. BUS
EMERG. STOP LINE

FIGURE 10-1: LIM-IN-TRACK PROPULSION CONFIGURATION

FUNCTION	DESCRIPTION
LIM Thrust Control	o Variable voltage, fixed frequency method o Provides braking/motoring thrust o Provides forward/reverse travel
Vehicle Speed Control	o Closed-loop with programmable gain and compensation o Programmable speed/position profiling
Stop-Positioning Control	o Closed-loop with programmable gain and compensation o Programmable stop position
Communication	o BITBUS serial transmit/receive port provides two-way communication to system computer
Built-In Status Detection	o LIM overtemperature o SCR overtemperature o Under/overspeed o Sensor errors o Watchdog (processor failure) o Timed-out (failure to disable) o Vehicle detected o Emergency stop declared

TABLE 10-1: LIM VOLTAGE CONTROL MODULE FUNCTIONAL OVERVIEW

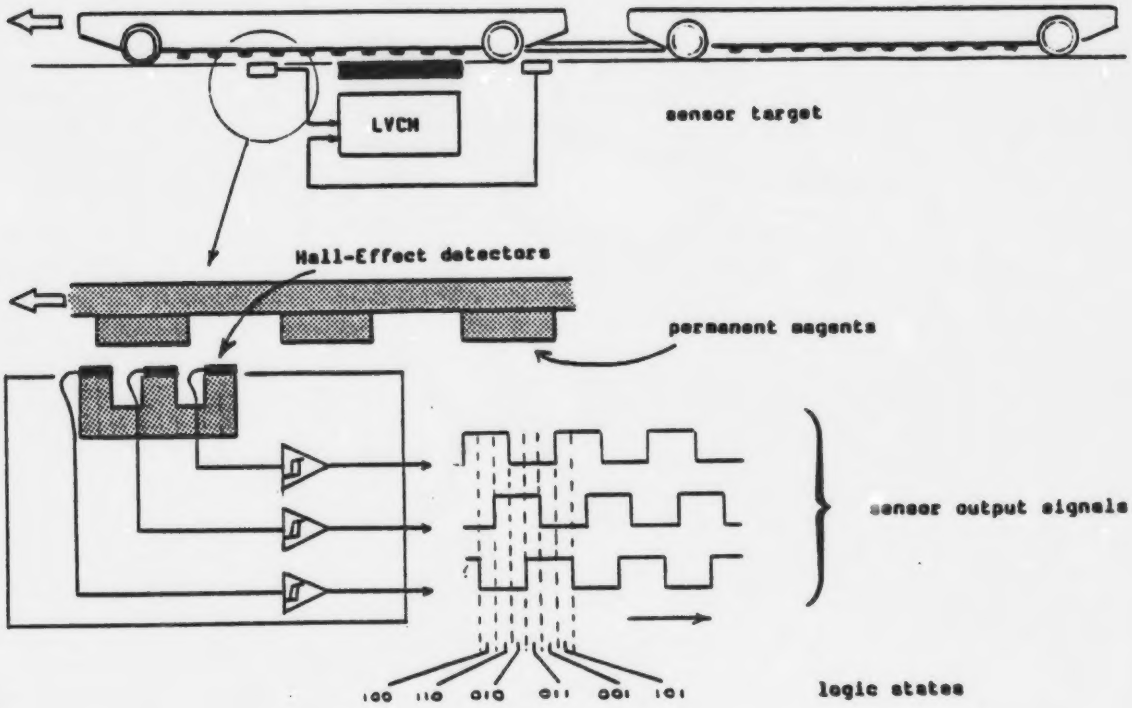
LVCM
sensor target
Hall-Effect detectors
permanent magents
sensor output signals
100
110
010
011
001
101
logic states

FIGURE 10-2: LVCM SENSOR ARRANGEMENT

approach before the LIM itself is encountered. Also, the two sensors are arranged such that one sensor continues to "see" while the other is temporarily "blinded" by the passage of an inter-vehicle gap.

The LVCM sensor is designed to work in conjunction with a vehicle-mounted sensing-rail. The sensing rail is comprised of a long steel strip onto which a series of evenly spaced magnetic strips are fixed. Hall-Effect magnetic flux detectors contained in the sensor respond to the presence of the magnetic strips as the rail passes by.

Each sensor uses three Hall-Effect detectors spatially-oriented with respect to the sensing rail strips so as to produce the output signal patterns shown in Figure 10-2. The three-detector arrangement facilitates the discernment of the travel direction, (which one detector alone cannot do), and stationary presence. (Two detector "quadrature" arrangements are ambiguous regarding the presence or absence of a non-moving target.)
The sensor has been designed to work with the sensor-rail over a gap of up to 12 mm, and provide resolution of position to 1 cm.

10.1.1.3 Sensor Interrupts

Figure 10-2 indicates the changing "bit pattern" which one would observe on the three output lines of the sensor during a passage of the sensing rail. (In this case, for movement from left to right).

The microcontroller monitors the sensor output lines through an input port, but as it is not practical to scan these ports continuously, a means is needed of "telling" when to sample. A hardwired discriminator circuit fulfills this need by sending an "interrupt pulse" to the microcontroller whenever the state of the sensor lines changes. Section 10.1.2.4 briefly describes the microcontroller program which is invoked upon the receipt of a sensor interrupt.

10.1.1.4 Power Section

Figure 10-3 is a simplified schematic of the circuit used to provide control of the magnitude and phase sequence of the applied LIM voltage. Of the five pairs of SCRs shown, only three pairs can be active at any given time. The choice of which three pairs are active determines the phase sequence seen by the LIM, and hence the direction of the LIM thrust.

An "active" SCR pair is one that is being repeatedly "gated" (once per 60 Hz cycle). The point in the cycle at which the gating occurs determines how much of the input voltage is applied to the load. In general, the later in the cycle the gating signal is applied, the smaller the voltage to the load will be. The measure of "how late" the gating signal is, is termed the "firing delay", t_{fd}, and is an

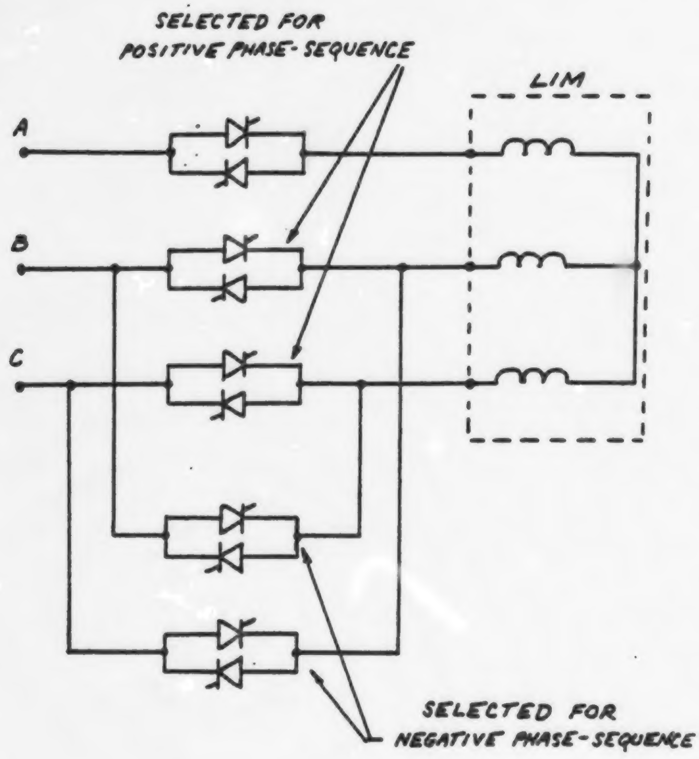
SELECTED FOR
POSITIVE PHASE-SEQUENCE
LIM
A
B
C
SELECTED FOR
NEGATIVE PHASE-SEQUENCE

FIGURE 10-3: LVCM POWER SECTION

important control parameter. The logic by which this and other key timing signals are generated is explained in the following sub-sections.

10.1.1.5 Gate Signal Timing

In order to correctly control the voltage to the LIM, it is necessary to generate a precisely-timed series of signals and direct these to the separate gates of the six active SCRs in the power circuit. The gating signals are made to follow a sequence which is completed once every cycle of the 60 Hz supply. The first gating signal of the sequence is released to gate "A" at a specified delay time, t_{fd}, following the detection of a zero-crossing in a line-derived, 60 Hz reference signal. Thereafter, gating signals are released at 60° (2.78 ms) intervals to gates -C, B, -A, C, and -B respectively.

Figure 10-4 is a simplified functional diagram of the gate signal timing and related logic. The basic functions are base-period determination, zero-crossing detection, pulse-delay, pulse-repetition, and shifting. Their operation is as follows:

- Upon power-up, a determination of the base period of the AC line voltage is made by timing subsequent positive zero-crossings. The resulting time value is then read by the microcontroller.

- The microcontroller averages the base period time over several cycles and divides by six to determine the pulse repetition time. This value is stored in a timer register and thereafter used for the purpose of repeating the first pulse of the cycle five more times during the cycle.

- The microcontroller writes the time value corresponding to the required "delay angle" to the pulse delay timer. The pulse delay timer causes the first pulse of the cycle to be released at the appropriate time following a positive zero-crossing of the reference signal.

- The first pulse loads the first bit of a six-bit shift register.

- The second pulse is released by the pulse-repetition timer and causes a shift such that the first and second bits of the register are full.

- Subsequent pulses released by the pulse-repetition timer shift the first and second bits to the third/fourth, fourth/fifth, and fifth/sixth positions before repeating the cycle again. The "two-bit wide" pulse corresponds to a gating signal duration of 120°.

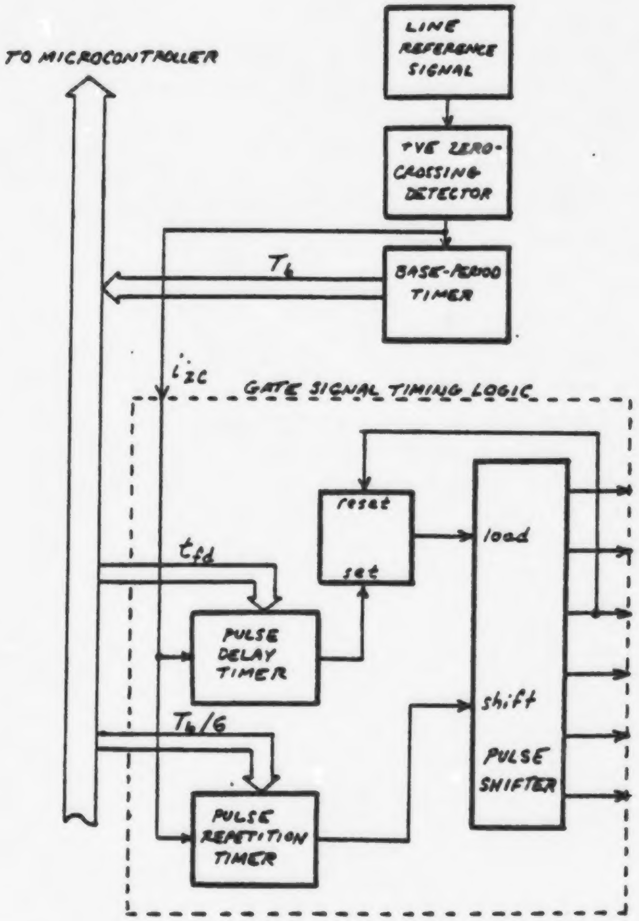
TO MICROCONTROLLER
LINE REFERENCE SIGNAL
+VE ZERO-CROSSING DETECTOR
T_b
BASE-PERIOD TIMER
i_{zc}
GATE SIGNAL TIMING LOGIC
reset
set
load
t_{fd}
PULSE DELAY TIMER
$T_b/6$
shift
PULSE SHIFTER
PULSE REPETITION TIMER

FIGURE 10-4: GATE SIGNAL TIMING AND RELATED LOGIC

10.1.1.6 Gate Signal Conditioning

The gating pulses which are "swept" across the six gate channels by the timing logic circuit undergo further conditioning by another circuit, one channel of which is shown in simplified form in Figure 10-5. Note the following:

- Logic gates are arranged so as to "steer" four of the six channels to the gates of the positive phase sequence SCR pairs if the PS (phase select) bit is high, or to the negative phase sequence SCR pairs if PS is low.
- Phase sequence changeover logic is included to ensure that when a transition from positive to negative phase sequence (or vice-versa) occurs, sufficient time is allowed for one set of SCRs to cease conducting before the other set is fired.
- Open-collector transistor stages provide the needed current-drive capability.
- Pulse transformers electrically isolate the SCR gates from the logic circuit.
- The basic gate pulses are modulated at a relatively high frequency so as to pass through to the secondary sides of the pulse transformers.
- The secondary sides of the pulse transformers each contain a rectifier circuit to demodulate the gate pulses.
- The primary feed to the gate drive circuit can be switched out so as to inhibit the gates from being fired. Control is via the GI (gate inhibit) bit.

10.1.2 Software

Most of the algorithms and logic functions of the LVCM are implemented in software. There are clear advantages in going to a software based design in a system of this type. These needn't be expounded upon here any more than to mention the flexibility in development and the simplification in electronic circuitry that can be had over a "hard-wired" approach.

The LVCM object code is stored in EPROM, except for the vendor-supplied "firmware" which is stored in the microcontroller chip itself. Data such as tables, constants, etc., which can be variable from time to time or from one LVCM to another are stored in RAM, and are reloaded by the host at every "power-up" of the system. The LVCM applications programs were created using assembly-language coding.

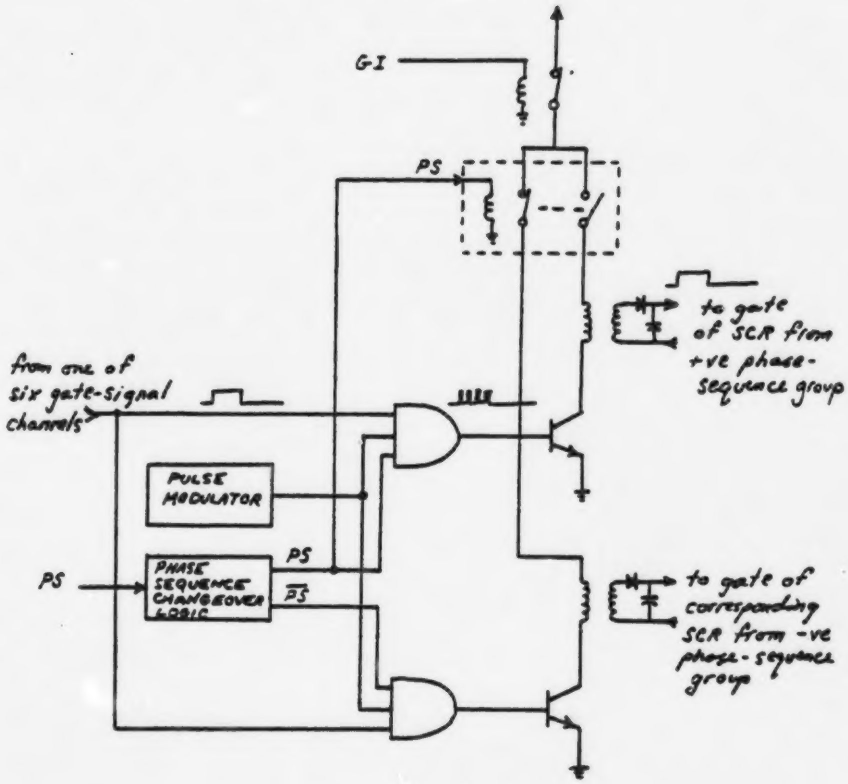
G I
PS
to gate of SCR from +ve phase-sequence group
from one of six gate-signal channels
PULSE MODULATOR
PS
PHASE SEQUENCE CHANGEOVER LOGIC
PS
$\overline{PS}$
to gate of corresponding SCR from -ve phase-sequence group

FIGURE 10-5: GATE SIGNAL CONDITIONING

10.1.2.1 "Task" Structure

The LVCM software is organized into various programs or "tasks", each of which corresponds to a broad functional area. Only one task can be executing at any given time but may be interrupted temporarily during execution in order to begin another task of higher priority. The RMX-51 Executive firmware, which resides in the 8044 microcontroller chip, manages task execution and interrupt handling through a multi-level priority structure. Those functions which require near immediate attention are placed within tasks of high priority. Other functions which are less time-critical are associated with lower priority tasks.

10.1.2.2 Remote Access and Control (RAC) Task

The 8044 microcontroller is intended specifically for applications in which it is linked to a host computer. The transfer of data between the host and the microcontroller is managed by a vendor-supplied program called the Remote Access and Control (RAC) task. Information to and from the host is organized in a "message" structure. RAC sends and receives these messages.

Through RAC, data such as tables and constants are downloaded to the LVCM memory. Another form of message handled by RAC contains commands which invoke the LVCM control task, as discussed in the next subsection.

Besides receiving data and commands from the host, RAC sends LVCM health status information to the host. This information is developed in various other tasks described in following subsections.

10.1.2.3 LVCM Control Task (LVCM-CONTROL)

LVCM-CONTROL is a message-driven task responsible for "preparing" the LVCM for activity by enabling the propulsion function, initializing certain control and logic variables, specifying the required direction of travel, and selecting the demand profile tables, and/or stop-position data from among the alternative sets stored in memory.

10.1.2.4 Sensor Handling Task (SENSOR-HANDLER)

SENSOR-HANDLER is an interrupt-driven task responsible for interpreting the sensor signals, so producing useful position and direction information. The invocation of SENSOR-HANDLER is synchronized to the basic sensor signals. Therefore, at higher speeds, when the sensor states are changing frequently, this task is at its "busiest". A functional block diagram of SENSOR-HANDLER appears in Figure 10-6. The major operations are as follows:

- It "looks for" and confirms the proper operation of the sensors.

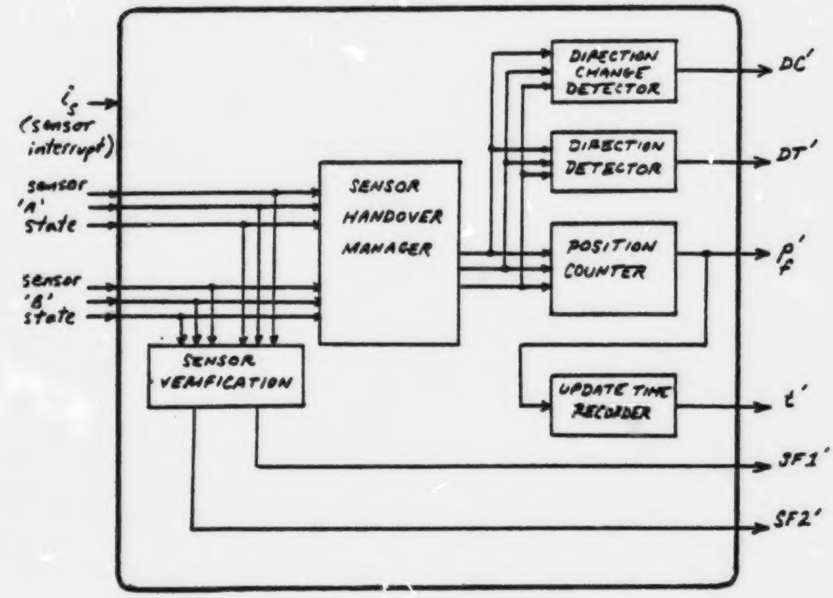
i_s
(sensor interrupt)
sensor 'A' state
sensor 'B' state
SENSOR HANDOVER MANAGER
SENSOR VERIFICATION
DIRECTION CHANGE DETECTOR
DIRECTION DETECTOR
POSITION COUNTER
UPDATE TIME RECORDER
DC'
DT'
p_f'
t'
SF1'
SF2'

FIGURE 10-6: SENSOR HANDLING LOGIC

- It determines which of the two sensors is currently active and manages the "handover" so that there are never any "gaps" in the position count.
- It compares every current sensor state to the previous state and deduces the direction of motion.
- It keeps track of current vehicle position by updating the position count at every second interrupt (every centimeter of travel).
- It monitors and flags invalid sensor states.
- It monitors and compensates for skipped states.
- It monitors and flags incidents of direction reversal.

SENSOR-HANDLER creates a number of variables which are used in other tasks. These are:

- p_f (feedback position)
- t (time associated with the most recent update of p_f)
- DC (direction change indicator)
- DT (direction travelled indicator)
- SFA, SFB (sensor failure indicators)

A more detailed description of these variables may be found in Table 10-2.

10.1.2.5 Thrust Control Task (THRUST-CONTROL)

THRUST-CONTROL is the least time-critical of the tasks. It is neither interrupt- or message-driven, but "runs in the background" continuously, pausing when any of the other tasks is invoked, and resuming once it is clear to do so.

THRUST-CONTROL is responsible for creating the basic control signals which specify the amount and direction of LIM thrust.
It creates these signals fresh every cycle of the task, thereby providing the dynamic manipulation necessary for control of vehicle motion.

Because THRUST-CONTROL is free-running, that is, not synchronized to some periodic event, measures are taken to make its execution time relatively constant and predictable. "Wait time" is deliberately introduced into the task so as to stretch-out the duration of an execution cycle to about 100 ms; long enough to ensure that it can be completed even during the microcontroller's "busiest" moments, yet not so long as to adversely affect system dynamic response.

		SYMBOL	NAME	RESOLUTION (bits)	SIGNED?	COMMENTS
A. Associated with LVCM-CONTROL (updated upon receipt of message from host)	1	N_{dp}	demand profile #	3	no	selects one of eight stored "demand velocity vs. position" tables
	2	DR	direction required	1	no	selects positive or negative travel direction
	3	CS	command start	1	no	prepares LVCM to operate in "normal" mode (closed-loop control)
	4	DS	dead start	1	no	prepares LVCM to operate in "dead start" mode (pre-set control for restarting a "stranded" vehicle)
B. Associated with MONITOR (updated by internal timer)	1	ES	emergency stop	1	no	indicates the occurrence of an emergency stop condition
	2	TO1	time out 1	1	no	declares the LVCM to have been "waiting" in a prepared state for too long
	3	TO2	time out 2	1	no	declares the LIM to have been energized for too long
	4	LT1	LIM temp. 1	1	no	indicates LIM "hot"
	5	LT2	LIM temp. 2	1	no	indicates LIM "very hot")
	6	FT	fin temp	1	no	indicates SCR's "hot"
	7	$T_p/6$	Pulse repetition time	16	no	average period of the 60 Hz reference signal divided by six
C. Associated with SENSOR-HANDLER (updated by sensor interrupt)	1	i_s	sensor interrupt	1	no	generated at every change in state of the position sensors outputs
	2	p_f'	feedback position	16	no	increment of 1 bit corresponds to a position change of 1 cm
	3	t'	event time	16	no	indicates the instant in time at which p_f' changed to its current value
	4	DT'	direction travelled	1	no	indicates the current travel direction
	5	DC'	direction change	1	no	flags the occurrence of a change in travel direction
	6	SF1	sensor failure	1	no	indicates correct sensor operation
	7	SF2	sensor failure	1	no	indicates correct sensor operation
	8	p_1	reference position	16	no	one of four reference values used to define a position frame
	9	p_2	reference position	16	no	one of four reference values used to define a position frame
	10	p_3	reference position	16	no	one of four reference values used to define a position frame
	11	p_4	reference position	16	no	one of four reference values used to define a position frame
D. Associated with THRUST-CONTROL (updated every 100 ms)	1	v_f	feedback velocity	8	yes	ranges from 0 to 10 m/s
	2	v_d	demand velocity	8	yes	ranges from 0 to 10 m/s
	3	e	velocity error	8	yes	difference in v_d and v_f
	4	e_p	proportional error	8	yes	
	5	e_i	integrated error	8	yes	
	6	c_v	control signal (velocity mode)	7	yes	combination of e_p and e_i
	7	p_{stop}	stopping position	16	no	stored constant representing required location
	8	p_{zone}	positioning zone	16	no	stored constant defining zone about p_{stop} where positioning mode applies
	9	q	position error	8	yes	
	10	q_p	proportional error	8	yes	
	11	q_i	integrated error	8	yes	reset to zero at each discrete change of position - overcomes "stiction" effect at
	12	q_d	damping signal	8	yes	derived from velocity feedback - stabilizes position loop response
	13	c_p	control signal (position mode)	7	yes	combination of q_p, q_i, and q_d
	14	c_c	control signal	7	yes	c_v or c_p - whichever mode is selected
	15	c	control signal	7	yes	jerk-limited version of c_c
	16	t_{fd}	gate firing delay	16	no	basic parameter controlling thyristor conduction time
	17	LS	loop select indicator	1	no	indicates whether control is velocity or position mode
	18	DT	direction travelled	1	no	see C.4
	19	DC	direction change	1	no	see C.5
	20	OS	overspeed	1	no	indicates velocity is greater than programmed demand
	21	US	underspeed	1	no	indicates velocity is less than programmed demand
	22	GI	gate inhibit	1	no	commands gates "off" stopping power flow to the LIM
	23	K_p	proportional gain	8	no	programmable constant for velocity loop
	24	K_i	integral gain	8	no	programmable constant for velocity loop
	25	J_p	proportional gain	8	no	programmable constant for velocity loop
	26	J_i	integral gain	8	no	programmable constant for position loop
	27	J_d	damping gain	8	no	programmable constant for position loop
	28	e_{max}	max. error	8	no	programmable constant defining tolerable velocity before declaring OS, US
	29	c_{start}	"dead start" control signal	7	yes	programmable constant defining thrust level for "dead start" condition
	30	J	jerk limit	8	no	programmable constant defining jerk rate limit
	31	c_{es}	emerg. stop control signal	7	no	programmable constant defining emerg. decel. rate
E. Associated with External Hardware	1	i_{zc}	zero-crossing interrupt	1	no	generated at every positive zero-crossing of the 60 Hz reference signal
	2	T_b	base period	16	no	time between significant occurrences of i_{zc}
	3	PS	phase select	1	no	selects forward or reverse sequence thyristors

TABLE 10-2: LVCM SIGNALS, CONSTANTS & LOGIC VARIABLES

The specific functions of THRUST-CONTROL are numerous, involving feedback control algorithms and various logic operations. A detailed description of these functions is presented in Section 10-1.3.

10.1.2.6 Monitor Task (MONITOR)

MONITOR is an interrupt-driven task responsible for various timer-related functions. It also performs periodic checks on certain external signals and keeps a "health status register".

The timing functions incorporated in MONITOR are as follows:

- Measurement of the time the LVCM spends "prepared" for activity prior to actually controlling a vehicle. If this time exceeds a preset limit, a "time-out" indication (TO1) is set in the health status register.
- Measurement of the time the power section feeding the LIM is "on". If this time exceeds a preset limit, a "timed-out" indicator (TO2) is set in the health status register.
- Calculation of the "pulse repetition time", t_{pr}, used for gate signal timing. This calculation is based on the averaging of several consecutive samplings of the external base-period timer. The resultant value is divided by six and loaded to another external programmable timer used in gate signal timing (Section 10.1.1.5).

MONITOR checks the external input ports which contain the various overtemperature indicator signals (FT, LT1 and LT2) and the emergency stop command (ES). These conditions are also stored in the health status register.

10.1.3 Motion Control

The main purpose of the LVCM is to see that a prescribed movement of the vehicle is effected during the time that the vehicle is within its zone of influence. "Prescribed movement" can involve the limiting of acceleration and deceleration, the regulation of velocity, and the fine control required in stop-positioning or indexing.

The motion control strategies employed in the LVCM are classical feedback techniques implemented in digital form. Two modes of closed-loop control are used: velocity-mode and position-mode. The former is used to generate the basic vehicle motion profile, the latter to provide fine control only.

Figure 10-7 is a functional block diagram of the LVCM. Though simplified, it attempts to indicate most of the important features

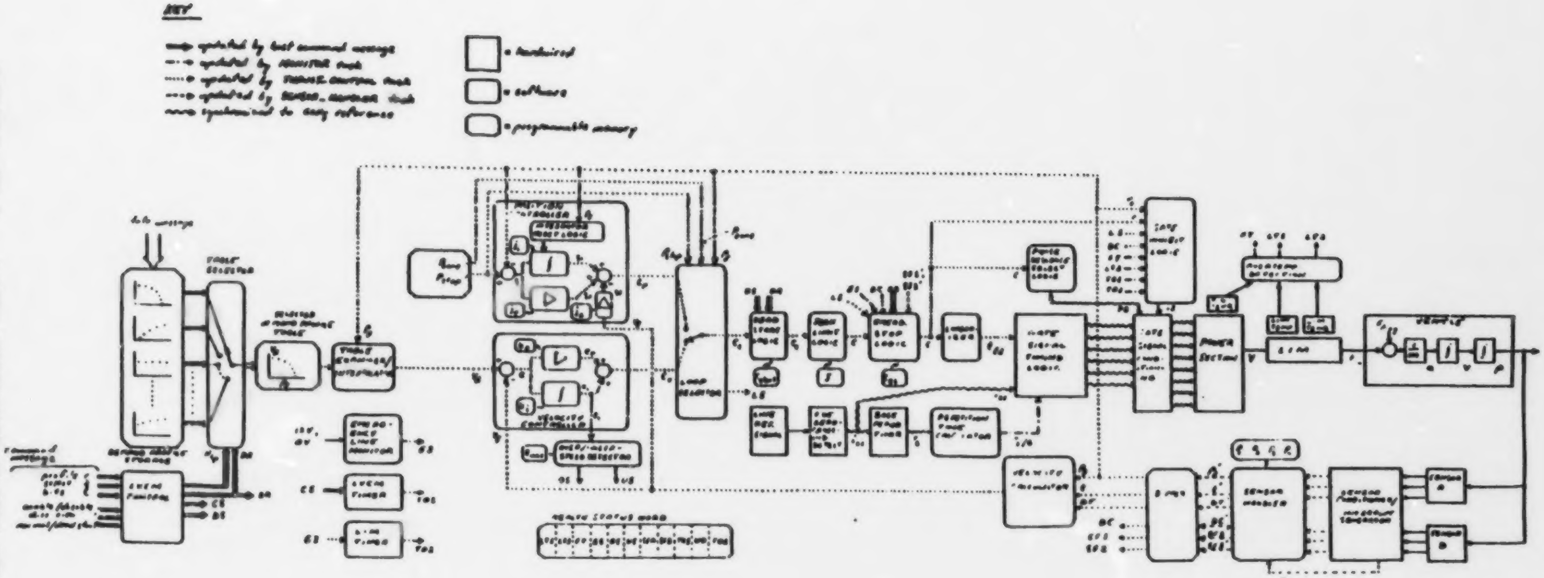
KEY
updated by last command message
= hardwired
= software
= programmable memory
Power Section

FIGURE 10-7: LVCM FUNCTION BLOCK DIAGRAM

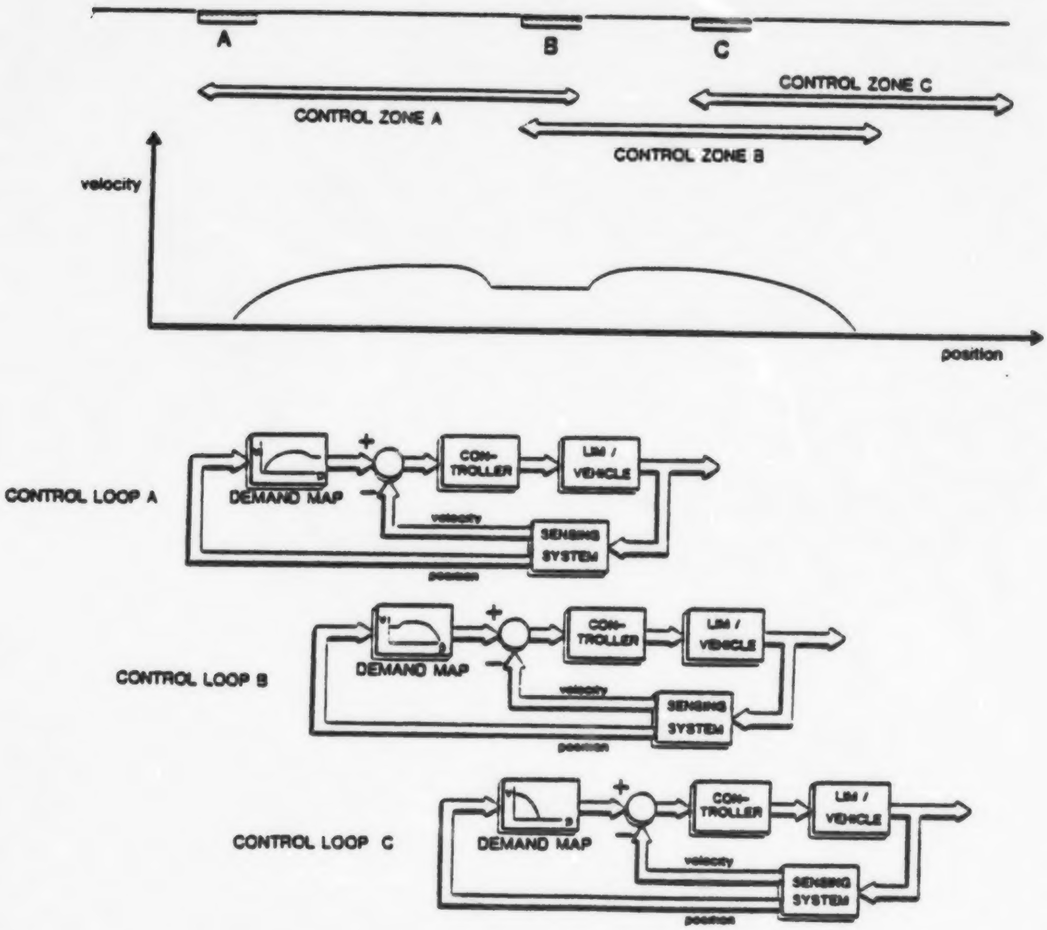
A
B
C
CONTROL ZONE C
CONTROL ZONE A
CONTROL ZONE B
velocity
position
CONTROL LOOP A
DEMAND MAP
+
-
CON-
TROLLER
LIM /
VEHICLE
velocity
SENSING
SYSTEM
position
CONTROL LOOP B
DEMAND MAP
+
-
CON-
TROLLER
LIM /
VEHICLE
velocity
SENSING
SYSTEM
position
CONTROL LOOP C
DEMAND MAP
+
-
CON-
TROLLER
LIM /
VEHICLE
velocity
SENSING
SYSTEM
position

FIGURE 10-8: OVERALL VELOCITY DISTANCE PROFILE AND CORRESPONDING LVCM DEMAND PROFILES

as well as to differentiate between "hardware" and "software". Table 10-2 summarizes the various signals, constants and logic variables found in the figure.

The following subsections should be read with frequent reference to Figure 10-7 and Table 10-2.

10.1.3.1 Velocity Control

The LVCM memory contains a table of "demand velocity" as a function of vehicle position with respect to the LIM. As the vehicle position advances, the demand signal changes according to the profile stored in this table. To the extent that the feedback controller can cause the vehicle velocity to follow the demand velocity profile, regulation of velocity is achieved. Furthermore, by properly tailoring the shape of the demand velocity profile, acceleration and deceleration may be kept within desired limits.

10.1.3.2 Demand Profile Table

The demand velocity profile is pre-calculated according to the requirements and constraints of the overall system, and then downloaded as a "table" of data to each of the LVCMs (see Figure 10-8). A single profile may contain up to ten points, a point consisting of two numerical values, i.e. demand velocity and its associated position.

10.1.3.3 Demand Profile Selector

Up to eight demand tables may be stored at once in the LVCM. This feature can save time by avoiding downloading. For example, consider an LVCM which is required to control a vehicle to a full stop, then subsequently to index the vehicle forward to another position, and finally to accelerate the vehicle back in the direction from whence it originally came. Three separate demand profiles would be needed for this particular sequence, but as these profiles are used over and over again, it makes sense to keep them stored locally in the LVCM rather than to call upon the host to download a "fresh" profile every time one is needed. Instead, the host need only transmit a short "profile select" code, and a "direction required" bit to the LVCM. The demand profile selector then uses this information to choose the particular demand velocity and demand effort profiles which it will control to. The selected table is written to an area of dedicated memory.

10.1.3.4 Table Examiner/Interpolator

Once per cycle of THRUST-CONTROL, the contents of the dedicated demand profile memory are examined to find those points which bracket the current position. A linear interpolation between these points determines the required demand velocity.

10.1.3.5 Velocity Controller

Once per cycle of THRUST-CONTROL, the velocity controller produces a velocity error signal, ev, by subtracting the feedback velocity from the latest demand velocity as dictated by the demand velocity profile. A corrected control signal, c_c, is derived from ev according to a formula which is expressed by the block diagram of Figure 10-9. The gain constants k_i (integral gain) and k_p (proportional gain) are stored in the LVCM memory and can be readily changed to suit the particular conditions (e.g., low speed or high speed) under which a given LVCM will operate.

10.1.3.6 Position Control

The regulation of velocity and the limiting of acceleration is achieved by means of a velocity-oriented algorithm, i.e. thrust is controlled so as to cause the vehicle velocity to "follow" a certain profile. This approach is also employed to provide some amount of control over vehicle stopping position, however, as vehicle velocity drops and approaches zero, the quality of the velocity feedback is diminished to the extent that it is no longer useful as a correction, and in fact would introduce error and instability in the control. As an aid to completing the deceleration trajectory "on target", a position regulator is introduced in the final moments prior to the vehicle coming to a full stop. This combination of velocity-oriented deceleration control and position-oriented final stopping control provide good stop-positioning accuracy in the shortest possible time.

10.1.3.7 Position Controller

Once per cycle of THRUST-CONTROL, the position controller calculates a control signal, c_p, based on the algorithm of Figure 10-10, which employs direct position feedback as well as velocity feedback for damping. The error-integrating function is introduced to overcome the "stiction" or static rolling friction which the vehicle experiences as its speed drops to zero. If the vehicle stops somewhere near, but not precisely on the targeted position, the control signal derived from the proportional error, q_p, alone may not be large enough to provide accelerating thrust. Under such conditions the integrated error, q_i, will build with time until the control signal is big enough to free the stuck vehicle. Note that the integrated error is reset at the first indication that the vehicle has moved. This is done to prevent instability in the control loop. The constants, j_p (proportional gain), j_i (integral gain) and j_d (damping constant) reside within LVCM memory.

10.1.3.8 Loop Selector

The loop selector "decides" when it is time to change from velocity-oriented control to position-oriented control. The decision is based on the value of the stop-position reference,

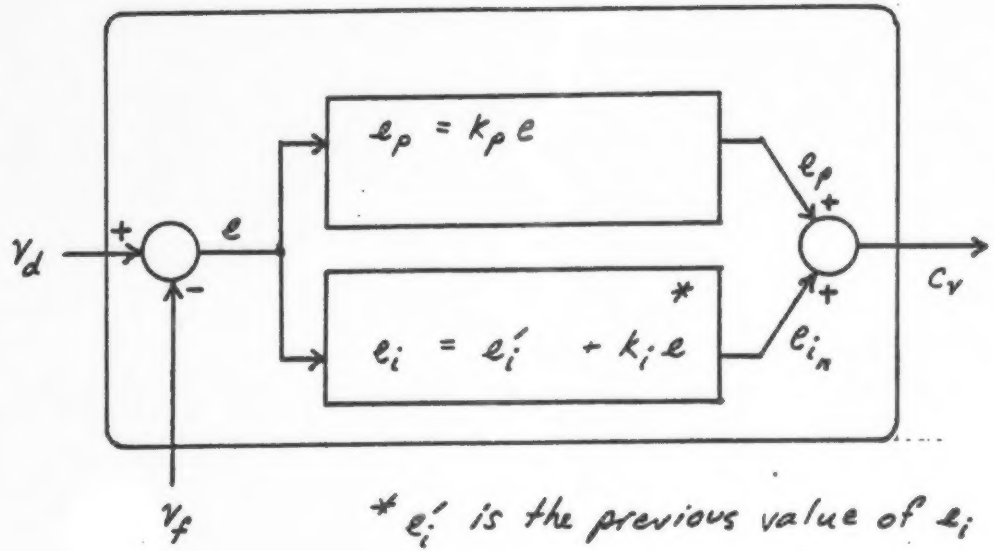
v_d
+
−
e
$e_p = k_p e$
$e_i = e_i' + k_i e$
*
e_p
+
+
e_{i_n}
c_v
v_f
* e_i' is the previous value of e_i

FIGURE 10-9: VELOCITY CONTROLLER

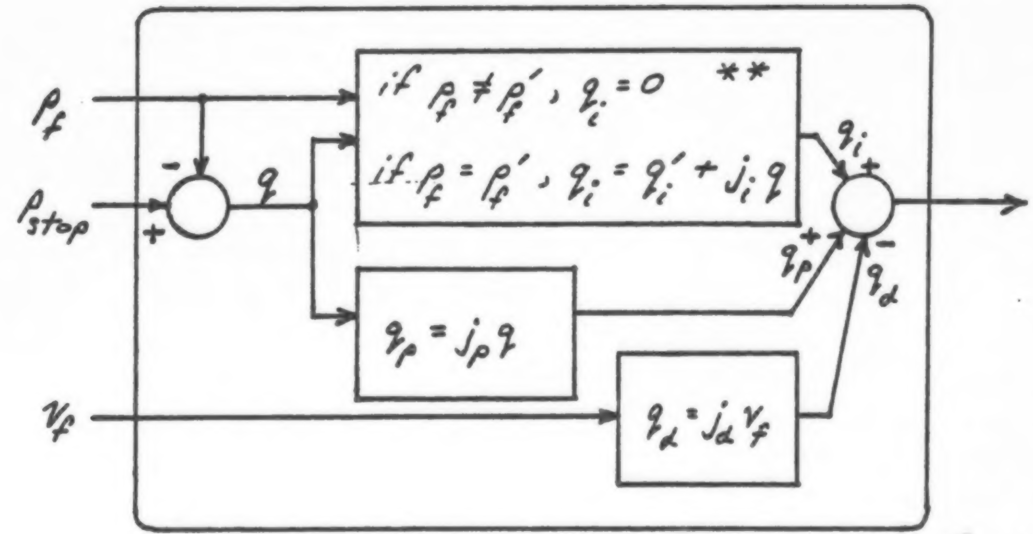
ρ_f
ρ_{stop}
v_f
-
+
q
if $\rho_f \neq \rho_f'$, $q_i = 0$ **
if $\rho_f = \rho_f'$, $q_i = q_i' + j_i q$
$q_p = j_p q$
$q_d = j_d v_f$
q_i
+
q_p
+
q_d
-

** ρ_f' is the previous value of ρ_f

FIGURE 10-10: POSITION CONTROLLER

p_{stop}, and the measured position, p_f. When the vehicle is within a fixed distance, p_{zone} of the final stop position, the position loop is selected. The constants p_{zone} and p_{stop} reside in the LVCM memory.

10.1.3.9 Dead Start Logic

At certain times a vehicle may be stopped at a location at which it is not normally intended to stop. This, for example, could occur following a power failure. Under such conditions, an LVCM which is normally used for cruising, for example, would be required to start a vehicle from standstill. In this situation the control signal is not derived from the demand tables and velocity feedback. Rather, it is a fixed signal of fixed duration initiated through the "dead start" logic. The dead start logic checks for the DR (direction required) and DS (dead start) command bits, both of which are sent by the host computer to all of the LVCMs in the system. Those LVCMs which detect the presence of a vehicle in their control zone then set the magnitude of the control signal, c_c, equal to a constant value, c_{start}. The sign of c_c depends on the direction required. The constant c_{start} resides in the LVCM memory.

10.1.3.10 Jerk Limiter

Jerk, or the time rate of change of acceleration, is not well controlled by the closed velocity-loop. Jerk-limiting logic is therefore introduced. The logic monitors the control signal and compares its rate of change to a limit constant, J, which resides in memory. If this limit is exceeded the control signal is modified such that its rate of change equals the limiting rate. Figure 10-10 illustrates the principle. Note that unlike a dynamic filter, which would "slow down" any signal, jerk limiting logic has no effect on the signal so long as its rate of change is lower than the pre-set limit.

10.1.3.11 Emergency Stop Logic

Each LVCM is "hard-wired" to a specially-dedicated emergency stop line. This line normally carries a "high" signal, but may be brought "low" (i.e. to zero volts) through the activation of wayside emergency pushbuttons. When the line goes low, an "emergency stop" bit is set in the LVCM and the emergency stop logic is activated. Its operation is simple. It first checks the "direction of travel" bit, DT, to determine which way the vehicle is moving (See Section 10.1.2.4), and then sets the control signal, c, to a fixed value, c_{es}, whose sign is chosen so as to provide retarding thrust. This thrust is maintained until a direction change is detected, at which point the gate inhibit logic (Section 10.1.3.14) disables the gate drive, turning off the LIM. The emergency stop logic bypasses the jerk limiter so as to obtain the fastest possible response.

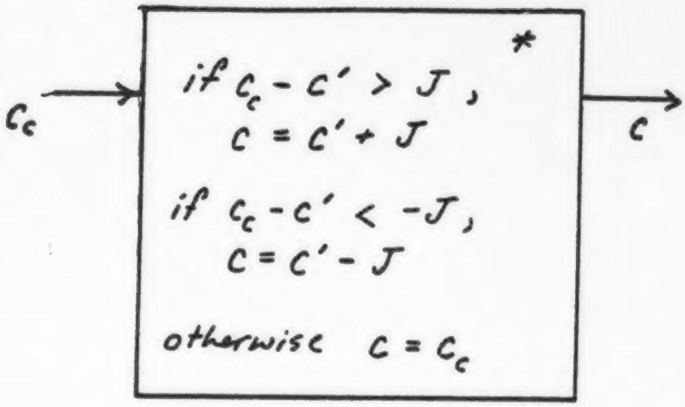
C_c
if $C_c - C' > J$,
$C = C' + J$
if $C_c - C' < -J$,
$C = C' - J$
otherwise $C = C_c$
*
C

* C' is the previous value of C

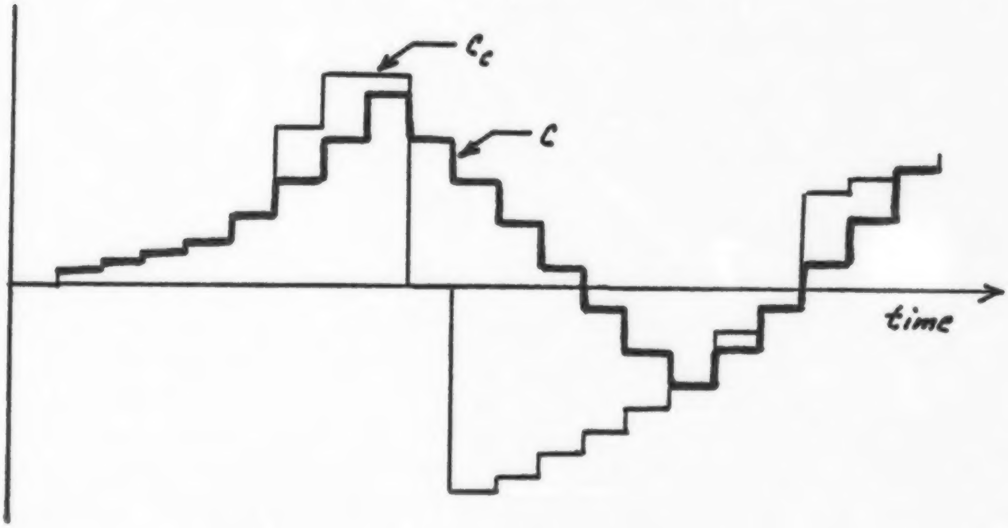

FIGURE 10-11: JERK LIMIT PRINCIPAL

A second condition that will result in setting the ES command is "disagreement" between the "direction travelling" and "direction required" bits, DT and DR. That is, a vehicle detected to be travelling in the wrong direction will be automatically stopped.

Lastly, the detection of a sensor failure, SF1 or SF2, in an LVCM configured for deceleration or stop-positioning will set the ES command.

10.1.3.12 Linearizer

The object of the linearizer is to make the relationship between the control signal, c, and the LIM thrust, F_{lim}, approximately linear. The requirement for such a function should be clear from Figure 10-12 which shows the natural relationship between the fire delay, t_{fd}, and the output voltage, V. A second non-linear influence is the square-law relationship between LIM thrust and voltage.

The linearization map of Figure 10-13 was derived empirically. The dashed line indicates the straight-line approximation to this curve as used in the linearizer routine. Since the control system is feedback corrected, this approximation is adequate.

10.1.3.13 Phase Sequence Select Logic

The phase sequence select bit, PS, is simply determined by the sign of the control signal, c. A negative control signal results in PS being low ("negative" phase sequence), while a positive control signal sets PS high ("positive" phase sequence). This rule holds regardless of the direction the vehicle is travelling.

10.1.3.14 Gate Inhibit Logic

Under certain conditions it is desired to stop power flow to the LIM. This is done by inhibiting the SCRs from turning on. The logic variable, GI, which commands the gate inhibit, is set if any one of the following conditions is true:

- P_f, the position feedback variable, is outside the "control zone" as defined by parameters stored in memory.
- c, the control signal variable, is zero.
- TO1 (LVCM time-out flag) is high. (Section 10.1.4.3)
- TO2 (LIM time-out flag) is high. (Section 10.1.4.4)
- DC (Direction Change flag) is high, and LS (Loop Select bit) is high (velocity mode). (Sections 10.1.2.4, 10.1.3.7)

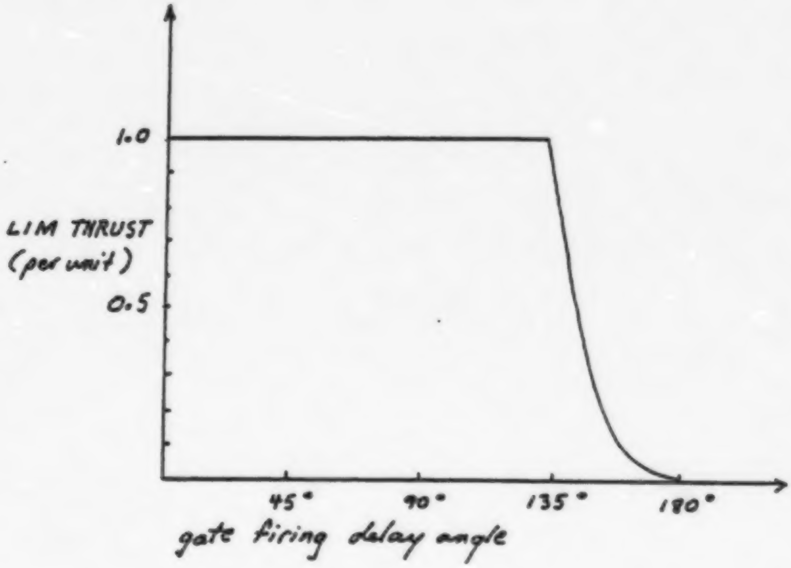

FIGURE 10-12: LIM THRUST VS. FIRING DELAY

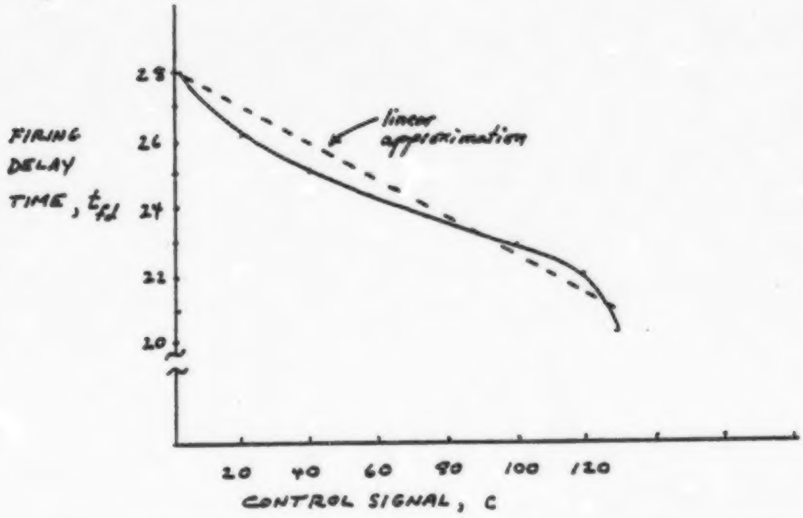

FIGURE 10-13: FIRING DELAY VS. CONTROL SIGNAL

- o LS (Loop Select) is low, P_f is at the required stop position, P_{stop}, and V_f (velocity feedback) is less than 0.1 m/s.
- o FT (Fin Temperature flag) is high. (Section 4.5.2)
- o LT2 (LIM Temperature 2 flag) is high (Section 4.5.2)

10.1.3.15 Position/Time Buffer

As explained in Section 10.1.2, the SENSOR-HANDLER and THRUST-CONTROL tasks are not synchronized, and therefore the transfer of data from the former to the latter requires a buffer. SENSOR HANDLER overwrites the position and time (p_f and t) memory locations with the most current p_f and t every second sensor interrupt (i.e. every centimeter of travel). THRUST-CONTROL reads the contents of the same memory locations once per cycle.

10.1.3.16 Velocity Calculator

While it is necessary to keep a running count of position, velocity needn't be updated any more frequently than once per cycle of THRUST-CONTROL. Hence, each cycle, the present and previous position/time pair are used to determine the average velocity over that cycle, so creating the velocity feedback signal v_f.

10.1.4 Monitoring System

The LVCM is designed to monitor several of its own functions and to respond in various ways to detected failures or irregularities. The design philosophy allows for "soft" failures, that is, malfunctions that can be tolerated for a limited time without need to disable the faulty LVCM. In other situations the LVCM failure response will result in a GI (gate inhibit - no LIM thrust) or ES (emergency stop - full reverse LIM thrust). In all cases the particular failure is flagged and communicated to the system host.

The monitoring system employs a "health status register". The contents of the register provide an "at a glance" update of the "health" of the LVCM. Each bit of the health status word corresponds to a potential failure state.

The host computer regularly reads and records the health status of each LVCM in the system, and depending on the location of the LVCM and the nature of the failure, raises the appropriate warning or alarm, and in some cases may shut down the system at the first opportunity.

10.1.4.1 Overspeed/Underspeed Detection (OS/US)

Normally, there will be some small difference between the vehicle speed as dictated by the LVCM demand profile and the speed as measured. However, if this difference becomes excessive it should be flagged, and the cause determined.

A "speed error" is detected if the magnitude of the integrated velocity error (Section 10.1.3.5) is greater than a predetermined amount, e_{max}, stored in the LVCM memory. If the sign of the error is positive, the condition is declared "OS" (overspeed); if negative, "US" (underspeed).

The LVCM does not initiate any form of shut-down upon detection of either speed error condition.

10.1.4.2 Overtemperature Detection (LT1, LT2, FT)

Critical components are instrumented with temperature sensors so that overtemperature conditions can be detected and flagged in the LVCM. The LIM winding contains two bi-metal strip sensors, one set at 110°C, the other at 130°C. The heat fin on which the SCRs are mounted is monitored by a single temperature sensor. The overtemperature flags are:

FT (Fin Temperature) - high above TBD°C
LT1 (LIM Temperature 1) - high above 110°C
LT2 (LIM Temperature 2) - high above 130°C

The LT1 condition is a "warning" but does not cause any form of shut down. LT2 and FT, however, indicate serious overtemperature conditions of the LIM and SCRs respectively. To protect these components from thermal damage the LVCM responds with a GI (gate inhibit) command.

10.1.4.3 "Time-out" Detection 1 (T01)

Once the LVCM receives a message from the host "preparing" it for a vehicle, it begins timing. If it does not "see" a vehicle within a predetermined period, t_{wait}, it sets the T01 (Time-out 1) flag.

There is no practical way to directly identify total failure of the sensing system, but the T01 condition serves as an indirect means, since normally, the sensing system would detect a vehicle before t_{wait} expires.

The T01 condition results in the GI (gate inhibit) command.

10.1.4.4 "Time-out" Detection 2 (T02)

Another timer is arranged to ensure that the GI (gate inhibit) command cannot be removed for any longer than a predetermined period, t_{max}. This precaution ensures that an LVCM cannot stay "on", as it might, for example, in attempting to move a vehicle blocked by some impediment. The T02 condition results in the GI (gate inhibit) command.

10.1.4.5 Sensor Failure (SF1, SF2)

The "health" of the position sensors (Section 10.1.1.2) is of obvious importance. Each LVCM has two sensors. Failure of a sensor is declared in any of the following situations:

- The sequence of signals coming from a sensor does not "match" any of the expected patterns.
- The three signals of a sensor are simultaneously "high".
- A change in direction is detected at a "high" speed (above 2.4 m/s).

The response to an SF (sensor failure) flag depends on how the LVCM is configured with respect to its demand profile. LVCMs used for accelerating or cruising are permitted to operate with only one sensor providing feedback.* LVCMs used for decelerating and stop-positioning respond by commanding an ES (emergency stop). This latter measure ensures that a sensor failure will not cause a vehicle to overshoot its stop location.

10.2 FIELD EXPERIENCE

The first "network" of LVCM's was installed on an Industrial Handling prototype system at UTDC, Kingston. The major features of the system were:

- approximately 80 metres of track.
- 14 LVCMs.
- 3.5 m radius curve.
- 11% grade.
- 5 m/s max. speed.
- Two-car "train".

---

*When the "leading" sensor is inoperative, thrust is not applied until the vehicle advances to the second sensor. Thereafter, control is maintained through "blind spots" by keeping thrust constant at the value which it had just prior to entering the region corresponding to the failed sensor.

- 1,500 kg/car load capacity.

A view of the prototype track is shown in Figure 10-14.

Commissioning and testing was conducted over a four month period in early 1987. During that time, a number of aspects of LVCM behaviour which had not been observed in the earlier tests on a single unit were discovered. The following subsections after a brief synopsis of what was learned during the commissioning period.

10.2.1 Communications Irregularities

Perhaps the most elusive and troublesome of the earlier commissioning problems were intermittent failures of the communications over the BITBUS network. While failures occurred under various operating circumstances, the most prevalent were during system "boot up", when the system computer was "downloading" program code and data to each LVCM in succession. As this was the "busiest" time in terms of communications densities the probability of a failed transmission was obviously at its greatest.

Over time, several steps were taken to attempt to improve communications integrity. No single measure alone "solved" the problem, but after implementing all of the following, communications errors were virtually eliminated.

- Ensure termination resistances are connected at either end of the bus only, and not at the host interface, which is at the bus midpoint.

- Bias the bus at 2.5 Vdc with a resistive divider and use diode clamps at each LVCM interface so as to avoid bus voltages outside the common mode range of the receiver.

- Add capacitive filtering to the switching circuit used to provide isolated 5V to the receiver/driver of each LVCM.

- Tie the shield of the bus to the neutral point of the isolated supply of the receiver/driver and not to the LVCM case.

- Replace the optocouplers which interface the receiver/driver to the LVCM micro-controller with a "faster" version of the device.

10.2.2 Watchdog Resets

A common design practice for microprocessor-based systems is to use a so-called "Watchdog Timer". The watchdog is preset to "bark" after a short interval of time unless the micro has issued a signal telling it not to. Failure to send the signal implies that the micro has somehow (ie. due to noise or other irregular condition)

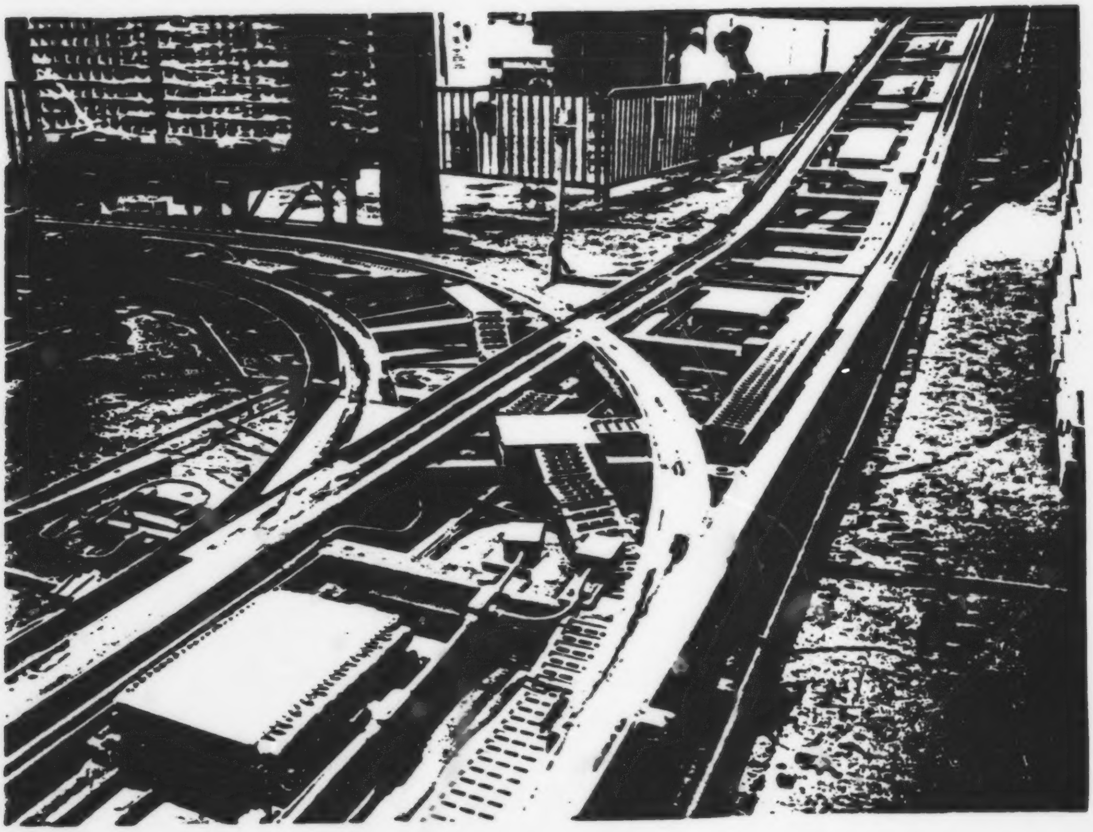

FIGURE 10-14: PROTOTYPE INDUSTRIAL HANDLING SYSTEM

got "hung up". The "bark" can be used as a trigger to reset the micro so that it can begin exercising its sequence of instructions properly once again.

During system commissioning, LVCM watchdog resets would occur more or less randomly on certain units and never on others. As these occurrences were in the order of one or two per eight hours of operation, catching the cause was all but impossible.

As the source of micro failure can be either due to hardware or software "bugs", both possibilities were investigated. Eventually, it was determined that the cause was in fact an "infinite loop" resident in the software code, and initiated by a particular vehicle sensor input pattern which never occurred "normally" but could occur if a sensor were to give an extraneous output. Hence, a bug which was actually caused by a combination of imperfect hardware and software.

10.2.3 PPI Resets

The PPI (Programmable Peripheral Interface) used in the LVCM assumes an "input" configuration on reset and must subsequently be initialized by the micro in order to configure any of its ports as outputs. Normally, this is done by a section of code that is invoked at a general "power on" reset. It was not foreseen during the original design that an inadvertent reset (eg. due to noise) of the PPI would result in a condition in which the micro is fully functional, but due to lack of a PPI output, absolutely unable to command thrust "on". This situation occurred several times during the commissioning period. A hardware design change was subsequently implemented which tied the PPI into the watchdog circuit so that, were the PPI to reset, it would result in a micro reset shortly thereafter, bringing about the needed re-initialization.

10.2.4 Sensor Calibration

The Hall-Effect detectors employed in the LVCM vehicle sensors differ one from another in their transfer characteristics; a variation which is noted in the manufacturers specifications. This necessitates circuitry which allows differences to be calibrated out when the sensor is assembled.

Properly calibrated, the sensor should remain functional provided the detectors are reasonably stable. Early experience however, was that the sensors tended to drift out of calibration with time. Subsequently, it was learned that the calibration technique used was not very effective in finding the centre of the tolerance band. Once an improved technique was adopted the sensors proved highly stable.

10.2.5 Control Zone Transitions

One of the questions which existed prior to the actual testing of a system of LVCMs was "how noticeable will the transitions be from one LVCM control zone to the next"? The answer, it was discovered, is that while on level track transitions are fairly smooth, however, such is not the case on inclined track.

The reason for this is that an LVCM operating on a grade depends heavily on the integrated term of the speed error signal to generate the appropriate control signal, but at the transition between zones, the "new" LVCM has not had the "history" to have generated any integrated error at all. Hence there exists a momentary reduction in thrust which is quite noticeable.

It was found that thrust pertubations at control zone transitions could in fact be made considerably lower by increasing the preset or "open loop" signal and reducing the integral gain.

10.3 FUTURE REFINEMENTS

As a result of the practical experience gained with using LVCMs in actual systems, and in response to a general requirement to improve the overall performance and applicability of the LVCM, a number of refinements were made to the design. These are highlighted in the following paragraphs.

10.3.1 Battery-Backed RAM

A key feature of the LVCM is that its control characteristics, ie. the demand profiles, gain constants, etc. (ref. Figure 10-7) are downloaded to each LVCM in the system as a unique data set, tailored to the particular track location to which they reside. These datasets are sent to the LVCMs when they are first powered up, eg. at the beginning of the day, or following a general system shut-down or power failure.

In practice it was discovered that the download procedure took enough time to be a "nuisance" in the operation of the system. It was decided that it would be beneficial to retain the contents of each LVCMs data memory so as to eliminate the necessity of downloading, except of course, the very first initialization of the system or after the replacement of a failed LVCM by a new one.

LVCMs in future applications therefore, will have a battery back-up for keeping the RAM (Random Access Memory) alive while the LVCM is powered down.

10.3.2 LXC Interface

"Local Cross-Connection", or LXC, is the name given to a method by which the intermediate level automatic control functions described in Section 7.3 are realized.

The principle of LXC is that an LVCM can relay the fact that it "sees" a vehicle to other LVCMs in its near vicinity over a simple, hardwired connection.

An LVCM receiving such information (which consists of a single bit wired in to the appropriate port) is triggered to select a particular demand profile, for example, a "stop" profile or a "slow down" profile.

The LXC interface then, consists of an output for the "vehicle present" indication, and several inputs, the meanings of which can be designated as required under control of the system computer.

Future LVCMs equipped with an LXC interface will be used in multi-vehicle systems for control of merging, queuing, collision avoidance and other functions involving the interaction of the vehicle with wayside brakes, track switches and stations.

10.3.3 Programmable Positioning Resolution

One of the design principles of LIT systems identified in Section 4.4 is to avoid "single point" system failures by using redundant LIMs and controllers wherever required.

It was discovered that in practice, this principle was difficult to follow at stopping points. It turned out that two LVCMs could effectively bring a vehicle close to the final stopping position under shared control, but that in the last centimeter or so they would "fight" in an attempt to make the final stop match their own particular command value. It appeared that no amount of fine-tuning could eliminate this situation 100% of the time.

In new LVCMs it will be possible to specify the resolution of the stop position command value so as to effectively place a "dead band" around it. In situations where two LVCMs share the positioning control, one would be programmed with a slightly coarser resolution than the other. This measure avoids the tendency to "fight".

10.3.4 Thrust Loss Sensing

A situation encountered during system trials was the absence of thrust even though the LVCM was commanding it. This occurred at various times for a variety of reasons and in some cases went virtually undetected because the vehicle was able to coast past the failed unit.

In order to detect and flag thrust loss and thereby avoid the "latent failure" situation, LVCMs will be equipped with a means of sensing motor current. The combination of a thrust command and no sensed current would trigger the "thrust loss" indication.

10.3.5 Phase Loss Sensing

Another potential latent failure is the loss of one of the three phase connections, either through faulty firing of the SCRs or a blown power fuse. Some thrust is still generated by a LIM with one phase gone, but the vibration imparted to the passing vehicle can be rather severe under such conditions.

Phase loss sensing would be achieved by a symmetry-check of the LVCM output voltage. Signals representing the three phase-to-neutral voltages would be summed electronically. An output other than "zero" would trigger the "phase loss" indication.

11.0 LIM FREQUENCY CONTROL MODULE

11.1 THE LFCM

The LFCM is a variable voltage, variable frequency motion control module designed for use in a LIT distributed control network. This model is a more sophisticated LIM control module than the LVCM described in Chapter 10. The addition of variable frequency capability allows the design of LIT systems with higher performance, lower kVA and higher efficiency.

The LFCM control software and hardware was designed around the INTEL 8097 micro controller. This device has expanded processing and input output (I/O) capabilities compared with the LVCM's 8044 controller and thus can perform more sophisticated control tasks. The algorithms and the majority of the software for the LFCM was developed at Queen's University under a statement of work for UTDC. Software documentation is included as Appendix B. A summary of this material is provided in Section 11.2.

The power condition unit planned for use in LFCM testing was a Gate Turnoff Thyristor based, Pulse Width Modulated, voltage source inverter developed by GEC Canada Ltd. and UTDC. The operation of this unit and its interface with the micro controller are described in Section 11.3.

The performance and stability of the LFCM software was tested extensively using an Inverter/load simulator. The results and analysis are presented in Section 11.4.

LFCM speed and position control performance analysis is presented in Section 11.5. Experimental results are not presented because the test inverter failed before positioning and speed control tests could begin. Satisfactory repair could not be effected in time to complete the experiments so a numerical simulation was used to investigate motion control. The details and results of the simulation are presented in Section 11.5.

11.2 LFCM CONTROL SOFTWARE

11.2.1 The INTEL 8097

The INTEL 8097 is a flexible single chip controller which operates at a high speed and has specialized I/O functions. The 8097 uses an internal number size of 16 bits allowing faster mathematical operations and making higher resolution easier. This micro controller has an onboard multichannel A/D converter which makes digitizing analog signals convenient. A set of six output lines (highspeed output lines) can be programmed to change state at a specific time. When a hardware timer reaches the appropriate time, the transition occurs without the intervention of the central processor. This leaves the processor free to carry on other tasks after it sets up the instructions for the transition. Another port can be used as high speed input lines. When any of these lines changes state, the new state and the transition time are recorded in a hardware stack. This information can be retrieved when the processor finds it convenient. These features are used to their full extent in the LFCM software.

11.2.2 PWM Generation and Current Control

The ultimate output of the LFCM to the LIM is an AC voltage and current supply to the LIM. It was decided to generate this supply using a voltage source inverter fed by a DC power distribution system. The inverter switching signals are generated by the 8097 micro controller using the regular sampling PWM generation scheme.

The most common analog PWM generation method, the sine-triangle scheme, was outlined in Section 8.4. In this scheme a continuous time sine wave is compared with a continuous time triangle wave at the desired switching frequency. This scheme works well when it is implemented in analog hardware, however it is incompatible with the micro controller environment in which continuous time signals do not exist.

Regular sampling PWM generation has some distinct advantages over natural sampling for digital implementation and it is particularly well suited for micro computer/controller implementation.

The principle of regular sampling can be illustrated by considering the comparison of a quantized sine function and a sychronized triangle wave (see Figure 11-1). When the quantitized sine wave is greater than the triangle wave, the switching signal is "high" and vice versa. A high signal closes the upper switch and a low opens the lower switch in the inverter leg (see Figure 8-5).

Because the sample lengths are fixed and the triangle wave is synchronized with the quantized wave, the position and width of the output pulses generated by this scheme are rigidly defined and therefore, predictable. This is not the case with natural sampling.

If the quantized sine wave has a 100% magnitude and a fundamental frequency w, the width of the k'th pulse can be expressed as:

$$W_k = \left[\frac{T}{2} + \left[\frac{T}{2} - W_N\right] \text{SIN}\,(wt_k)\right]$$

When the fundamental frequency, w, and the sample period T are chosen, the width and position of each pulse are defined. Equation (11.1) can be used to calculate pulse widths without the need for waveform comparisons. A list of pulse transition times can be calculated and used to generate the output waveform. If less than 100% voltage is required, each pulse width is scaled (eg. Wk = V% x Wk 100%).

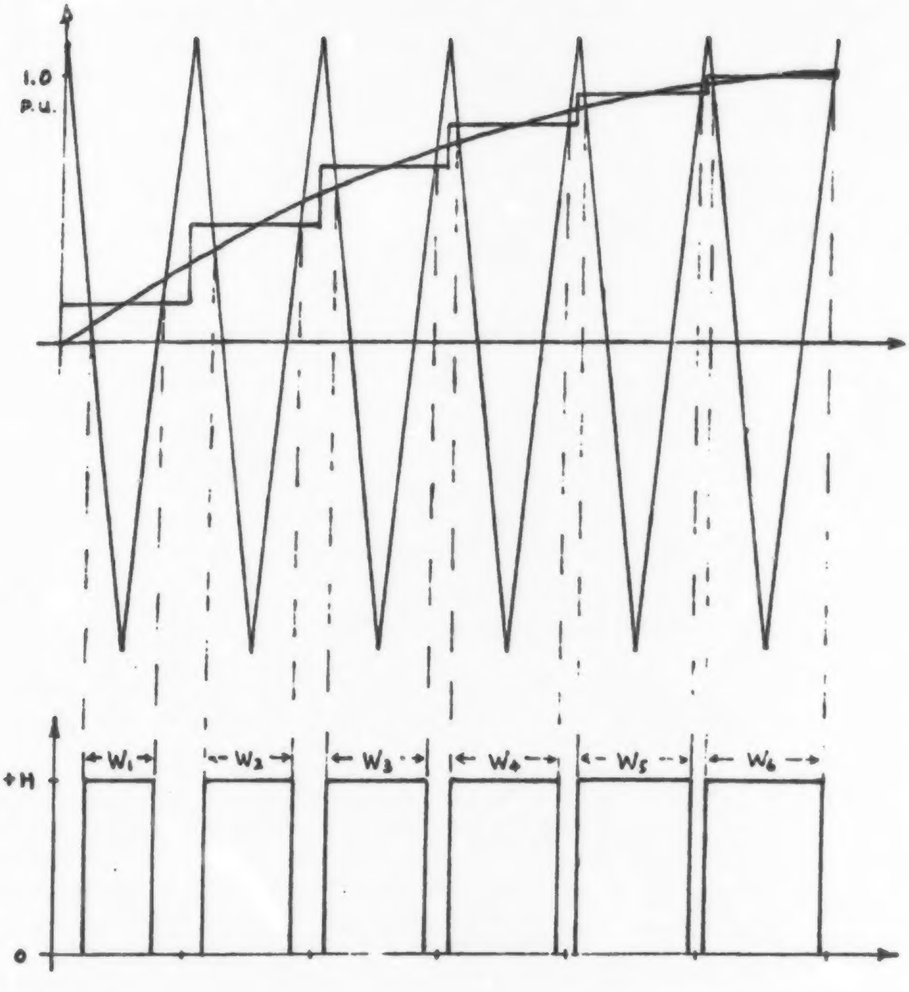
1.0
p.u.
+H
0
W₁
W₂
W₃
W₄
W₅
W₆

FIGURE 11-1: REGULAR SAMPLING

Regular sampled PWM generation is implemented in the 8097 as follows:

- o Upon start up and each time the fundamental output frequency is changed, equation 11.1 is used to generate a "look-up" table of pulse on and off times. The sine function is stored as look up table.
- o A crystal controlled internal timer is used to keep track of time to 2 u sec resolution. When a transition time arrives, the state of the off chip output line is set accordingly.
- o The width of each pulse is determined by scaling the value from the lookup table by the required voltage.

The three phase output is generated by moving three indices, separated by the equivalent of 120 electrical degrees, through the pulse width table.

Three lines of the high speed output port are used to produce the PWM gating signals.

In order to reduce transient stress in the inverter and motor, changes in frequency and phase sequence are mode in such a way that the voltages produced are continuous.

11.2.3 Current Sensing and Control

Motion control in electric drive systems is achieved by controlling the force or torque produced by the electric motor. The LFCM attempts to control LIM thrust by controlling phase current. If the machine is operating outside magnetic saturation there is a square relationship between thrust and current. If the three phase currents are balanced then the currents can be described mathematically as:

$$i_a = A \sin wt$$
$$i_b = A \sin (wt - 2II/3)$$
$$i_c = A \sin (wt - 4\ II/3)$$

It can be shown (see Appendix B) that A can be determined from the instantaneous values of two phases as:

$$A = 4/3 \sqrt{(i_a + i_b)^2 - i_a i_b}$$

The LFCM uses this method to determine the LIM phase current magnitude. The phase currents are measured using a Hall-Effect current transducer and converted to a digital representation by the 8097's on board A/D converter. The software calculates A using the equation (11.2) and compares it with a desired value and adjusts the voltage according to a PI control law. The process is illustrated in Figure 11.2.

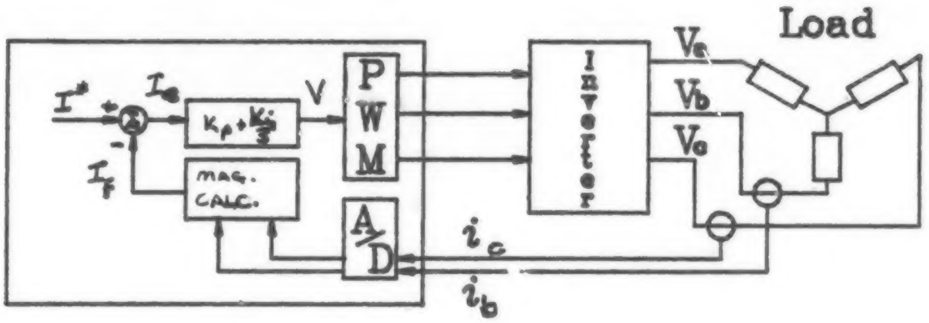
I*
+
-
Σ
I_e
K_p + K_i/s
V
PWM
I_f
MAG. CALC.
A/D
Inverter
V_a
V_b
V_c
Load
i_a
i_b

FIGURE 11-2: PI-CURRENT CONTROL PROCESS

11.2.4 Speed and Position Sensing

The speed and position sensing software receives signals from the magnetic position sensors developed for use with the LVCM. The signals from these sensors are XORed to create one signal which changes state whenever any one of the sensor lines changes state. This state change signal is used to drive one of the 8097's high speed input lines. The time of transitions is recorded and stored. Because of the sensor construction each transition corresponds to a distance increment of 0.5 cm. The LFCM software contains a fault tolerant position update routine which is designed to keep track of position correctly even if transitions are missed due to damaged or malfunctioning equipment.

11.2.5 Speed Determination

As described in Section 11.2.4 the LFCM software is provided with time updates at nominal distance increments of 0.5 cm. this suggests that the speed between sensor transitions could be calculated as $v = .005/\Delta t$ m/s. When this approach was tested the calculated velocity contained so much noise that it was virtually useless. The problem seems to be caused by tolerance in the nominal 0.5 cm distance increment. One factor affecting this parameter is variation in target rail to sensor vertical separation. Track imperfections, wheel wear or mechanical vibrations can change the sensor target gap. With a larger vertical gap, the sensor detects the magnets at a smaller horizontal separation. Figure 11.3 illustrates this problem.

The second velocity calculation approach examined was the application of sliding window averaging to the signal calculated using the first approach ($v = .005/\Delta t$). The velocity at the k'th time is calculated as:

$$v(kT) = \frac{v(kT-T) + v(kT-2T) + \frac{.005}{\Delta t}}{3} \qquad (11.3)$$

This method requires a moderate level of computation when implemented on the 8097 and produces a much cleaner signal that the first approach. Tests on the UTDC test track indicated that a velocity signal calculated using equation (11.3) still contained enough noise to disturb the LFCM's operating frequency calculation.

It can be shown that the sliding window average in equation (11.3) is a recursive digital filter. This observation lead to the third method for calculating velocity: explicit digital filtering of the incremental velocity. A standard second order low pass Butterworth digital filter was implemented and tested. It was found that the signal quality was very good but that the number of calculations required placed an excessive demand on the 8097's resources.

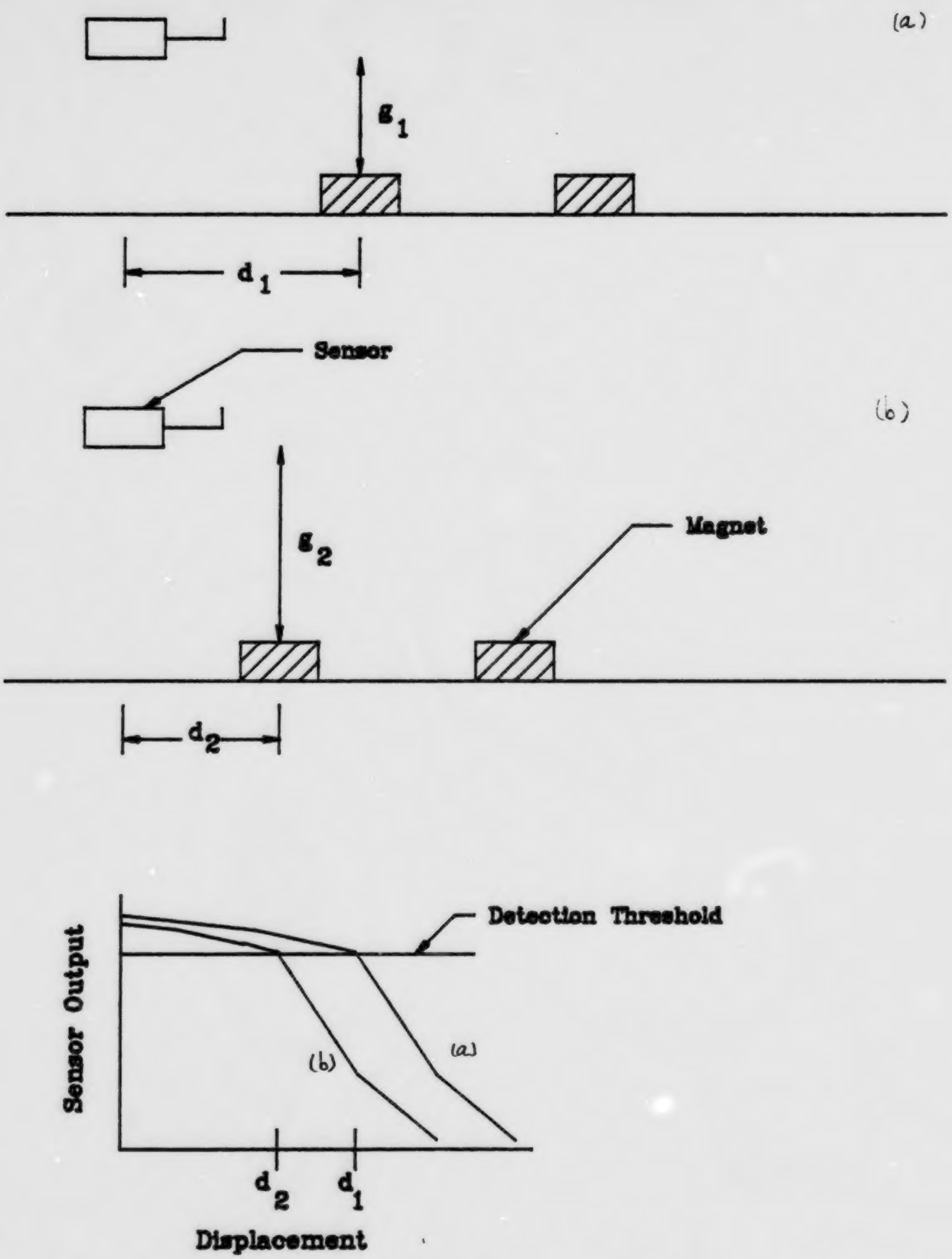
(a)
g_1
d_1
Sensor
(b)
g_2
Magnet
d_2
Detection Threshold
Sensor Output
(b)
(a)
d_2
d_1
Displacement

FIGURE 11-3: AIRGAP VARIATION EFFECTS ON SPEED DETERMINATION

The fourth and final approach is computationally simple and produces a signal quality almost as good as the digital filtering technique. In this approach the velocity calculation is tied to the system clock. At fixed time intervals the velocity is calculated by dividing the distance moved since the last calculation by the time increment. The time interval must be chosen large enough to achieve some averaging yet small enough that the vehicle speed changes by only a small amount between calculations. It was found that an interval of 16 was suitable for the UTDC test vehicle and track.

Test results are presented in Section 11.5.

11.3 MICRO-CONTROLLER INVERTER INTERFACE

The interface between the microcontroller and voltage source inverter is relatively simple because both the devices operate using digital signals. The primary function of the interface is to provide protection for the controller from the high potentials found in the inverter and to provide sufficient current capability to drive the switching devices.

The simplified interface for one phase is shown in Figure 11.4. The switching signal generated by the 8097 and its logical inverse are applied to a lock out circuit which ensures that the switching devices are not commanded to change state too rapidly. The gating signals also pass through an overtemperature circuit. When the switching devices become too hot, the gating signals are suppressed. A "shoot through" occurs in an inverter when both switching devices in a phase are ON at the same time. This situation presents a low impedance short circuit to the DC bus and the large current which results usually destroys one or both of the switching devices. The interface guards against shoot through's by monitoring the state of each switching device and screening dangerous signals. The last stage of the interface provides potential isolation via opto-isolation and current drive large enough to switch the GTO's.

11.4 TESTING THE LFCM

A number of tests were carried out at UTDC to determine the performance of the LFCM. These include investigation of the current control loop, testing of the position and speed sensing algorithms and positioning and speed control. The fault tolerant position algorithm was tested rigorously at Queen's University during development so these tests were not repeated. Some of the tests used the 8097 software and hardware while some used the algorithms in simulation. Tests done at Queen's University are presented in Appendix B.

11.4.2 Current Loop Performance

Testing and debugging an inverter firing circuit and its controller can be a challenging task. Small problems in timing and gain

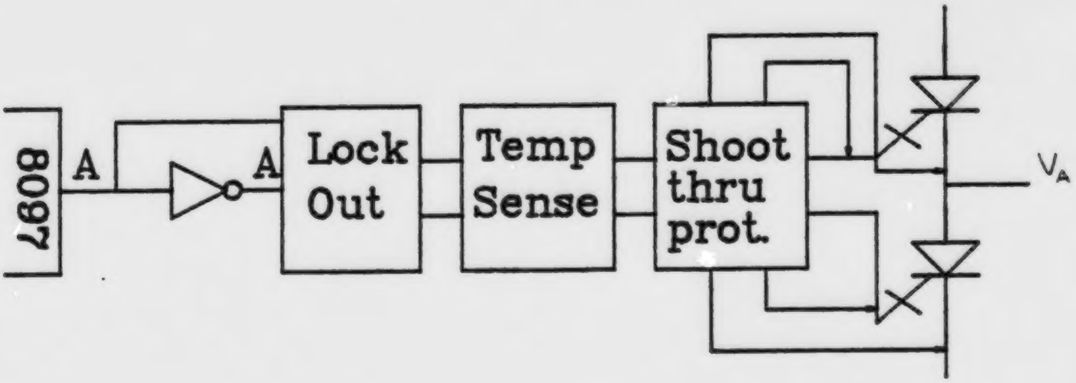
8097
A
A
Lock Out
Temp Sense
Shoot thru prot.
V_A

FIGURE 11-4: MICROCONTROLLER INVERTER INTERFACE

selection could result in instability or destructive failure of the inverter.

In order to speed and simplify the testing of the LFCM PWM generation and current control software, an inverter/load simulator was constructed. The circuit diagram for this device is shown in Figure 11.5. This unit allows the inverter software to be tested using low voltages and small currents. OP1-6 are opto-isolator devices which have a light emitting diode (LED) on the input and a photo transistor as the output. The application of approximately 1.5 V at the input of this device causes the output to conduct. The outputs of OP1-6 are connected to form a 3 phase bridge inverter.

The load simulator uses a steady state representation of a LIM in which the input impedance is modelled as a series inductor-resistor pair. Figure 11.6 shows this simplification along with the mathematical dual of the series inductor-resistor.

The dual network was used in the inverter/load simulator because it does not use cumbersome inductors. In addition, component values can be chosen to keep currents small while retaining a realistic dynamic response.

The LaPlace domain transfer function for the networks in Figure 11.6 are:

$$Iin(s) = \frac{V(s)}{s\ L+R} \qquad V_i\ (s) = \frac{V(s)}{CR1}\ \frac{1}{s + \frac{R1\ +R2}{R_1\ R_{2C}}}$$

$$Iin(s) = \frac{V/L(s)}{s\ +R/L}$$

The dynamic performance of these two networks will be the same (with the exception of scaling) if

$$\frac{R}{L} = \frac{R1 + R2}{R_1 R_2 C}$$

The values for the load used with the inverter simulator were:

R_1 = 10K
R_2 = 1K
C = .1μF

It should be noted that the simulated load is not meant to be an accurate dynamic LIM model but rather a tool for testing LFCM logic and control functions.

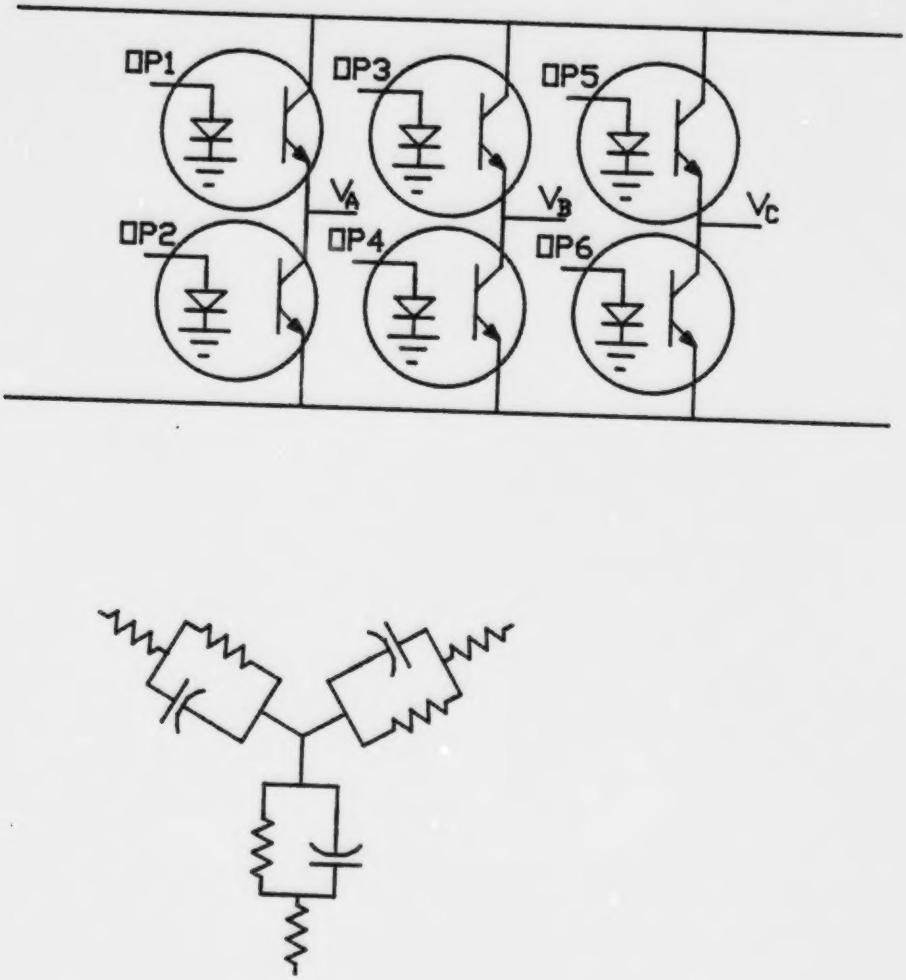
OP1
OP3
OP5
V_A
V_B
V_C
OP2
OP4
OP6

FIGURE 11-5: INVERTER/LOAD SIMULATOR

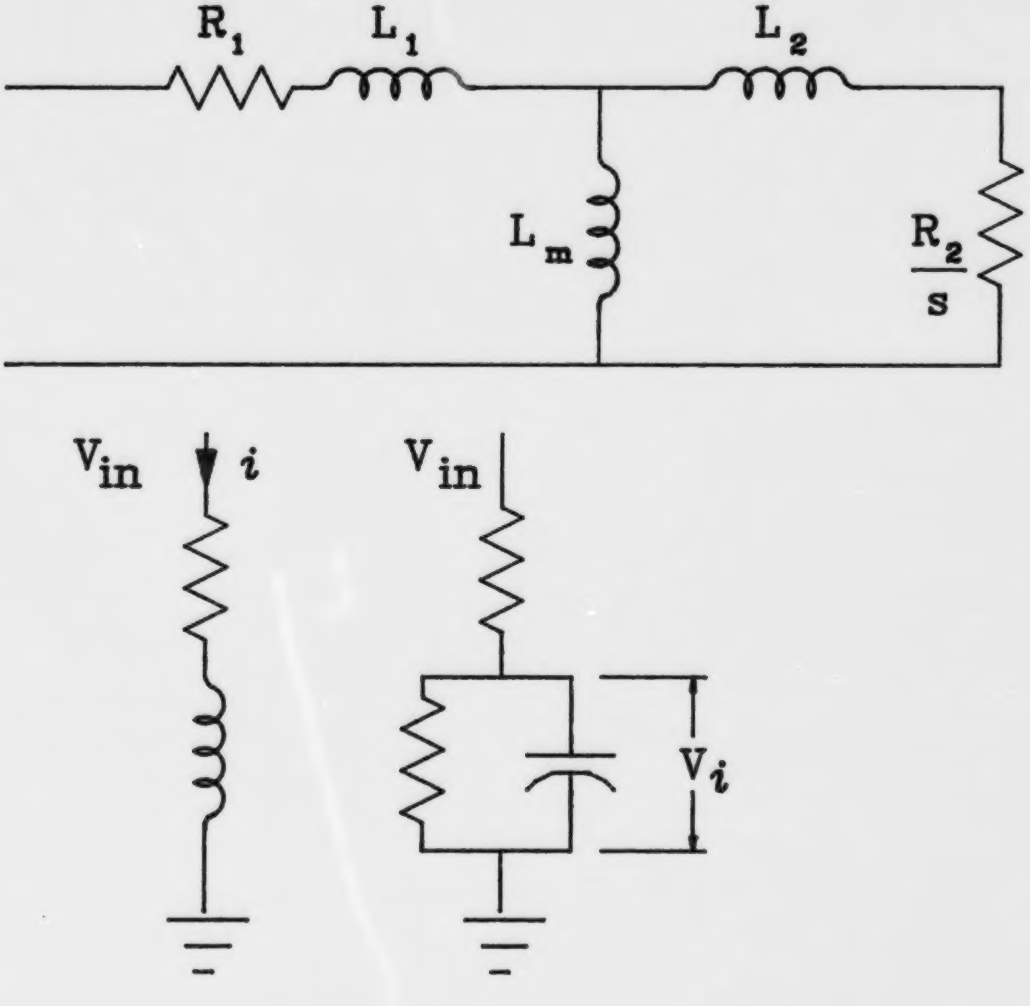
R_1
L_1
L_2
L_m
$\frac{R_2}{s}$
V_{in}
i
V_{in}
V_i

FIGURE 11-6: LOAD SIMULATION DEVELOPMENT

11.4.3 Current Loop Tests

A number of tests were carried out using the inverter/load simulator in order to determine the characteristics of the LFCM current control loop.

The demand current magnitude, phase sequence, fundamental output frequency and controller constants were chosen by the operator. The facility to cause step changes in one or more of these parameters was included in the test version of the LFCM software.

11.4.3.1 Performance as a Function of Controller Constants

The constants used in the PI current controller were chosen to minimize the step response time for minimal overshoot. Step responses using several controller gains are shown in Figure 11-7 and 11-8. The LFCM is driving the inverter simulator. The values chosen were $K_p=6/16$ and $K_i=4/64$ at 600 Hz sampling. The current values are in program units and do not represent any particular amperage. Program units are converted to amps with the current sensor calibration number when the LFCM controls a motor.

11.4.3.2 Current Control Loop Step Responses

In order to examine the stability of the LFCM's current control software, several tests using step changes in demand current were carried out. The results of these tests are shown in Figures 11-9 to 11-11. In each case the current magnitude reaches the demand value quickly and stably.

11.4.3.3 Steady State Behaviour

In the steady state the observed magnitude matched the demand. A set of typical steady state wave forms is shown in Figure 11-12. The small ripples on the magnitude signal are the result of a small DC offset in the output of the isolation amplifiers in the inverter simulator. This offset causes a disturbance in the current magnitude calculation.

11.4.3.4 Operation in the Presence of Phase Imbalance

The method used to calculate the current magnitude assumes a balanced three phase current set. Most rotary three phase machines are not perfectly balanced because of differences in winding paths and other small effects. Linear induction motors typically have much larger phase imbalances due to unsymmetrical winding and longitudinal end effects. It is important that the LFCM remains well behaved in the presence of this imbalance. In order to test the behaviour of the LFCM under unbalanced conditions the inverter simulator was modified to introduce a 15% imbalance in one phase impedance. Steady state operation resulting from a demand current of 256 units is shown in Figure 11-13. It can be seen that the currents are not balanced and that the current magnitude signal

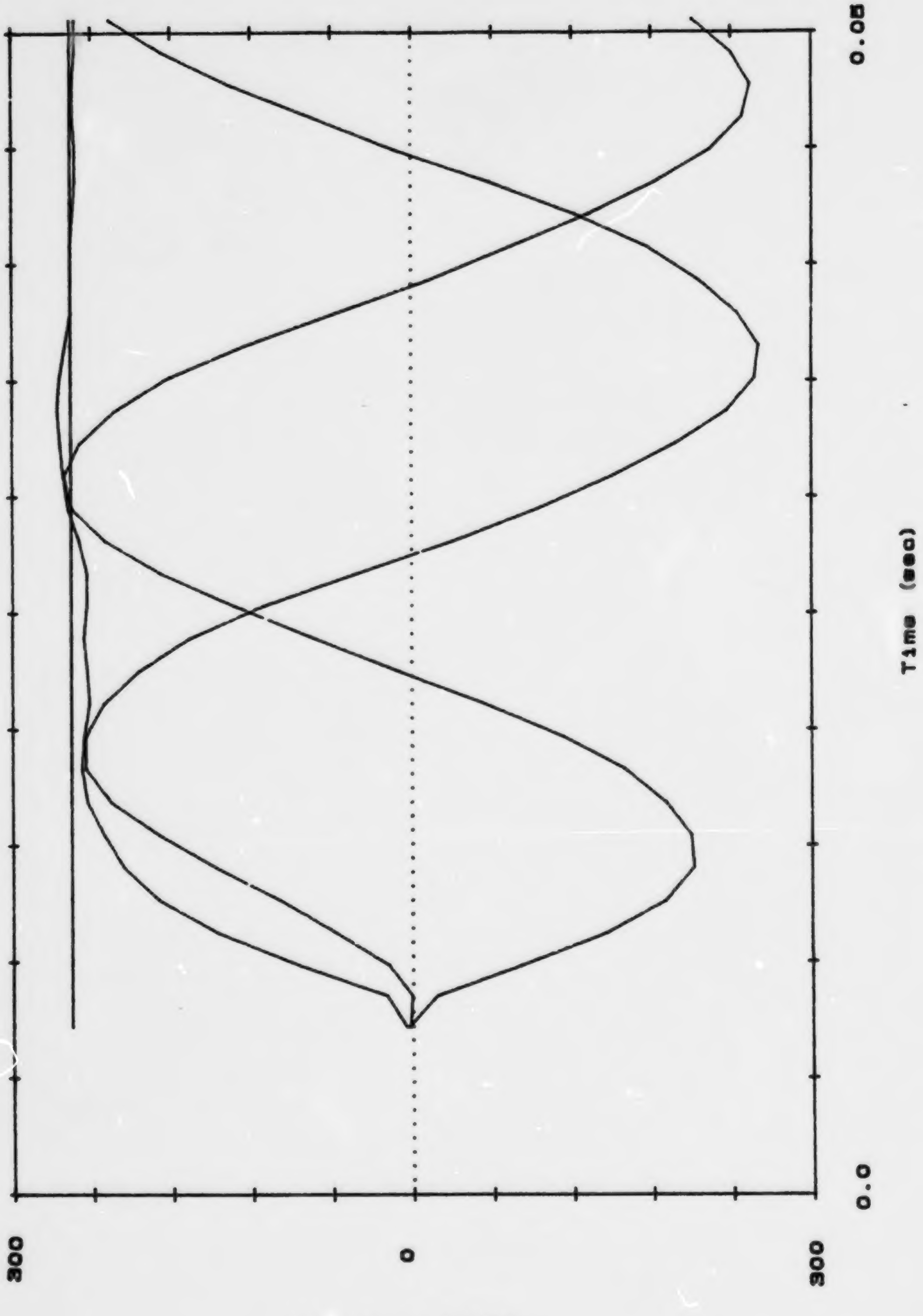

FIGURE 11-7: CURRENT CONTROLLER STEP RESPONSE - SMALL k_i

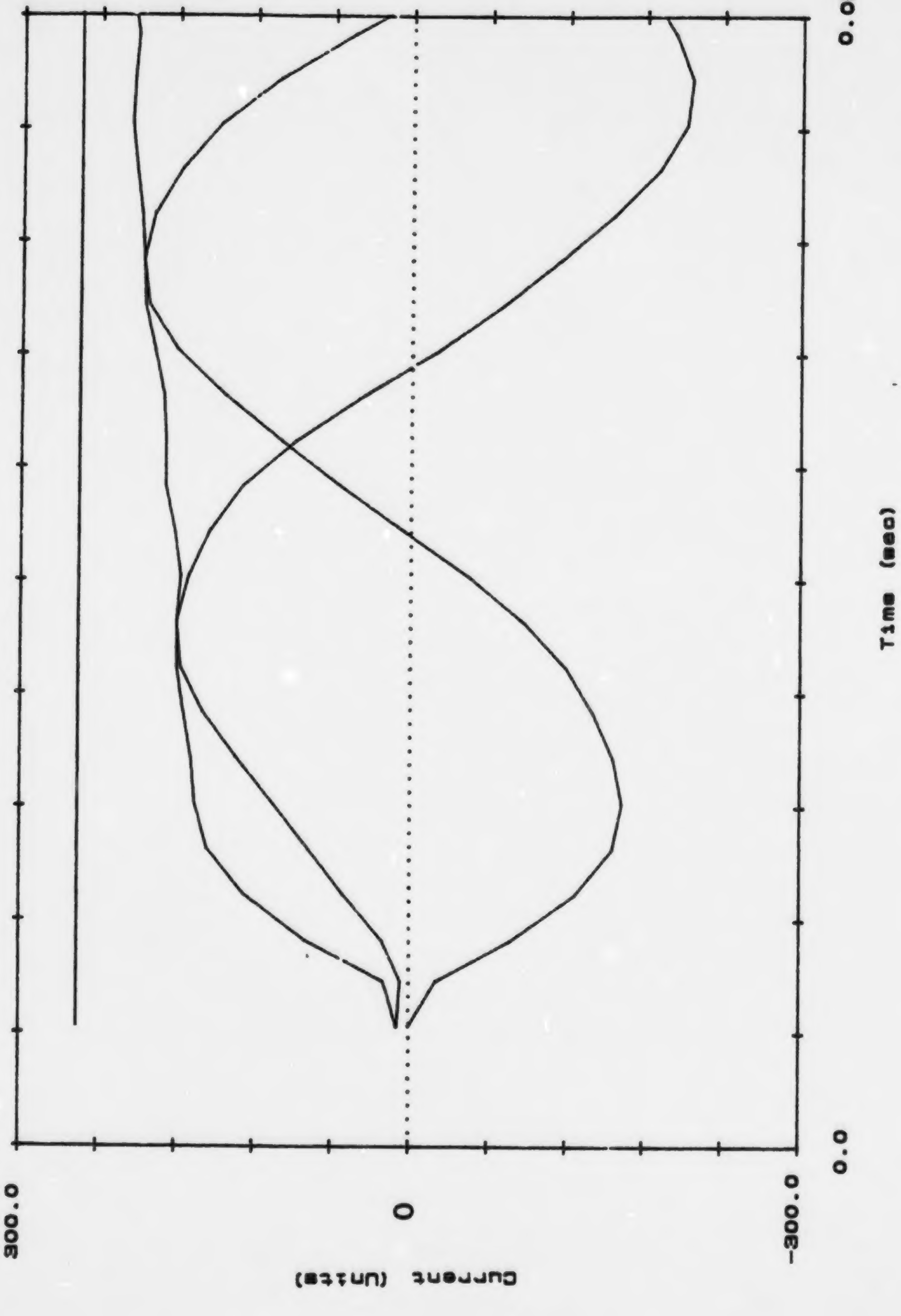

FIGURE 11-8: CURRENT CONTROLLER STEP RESPONSE - INCREASED k_i

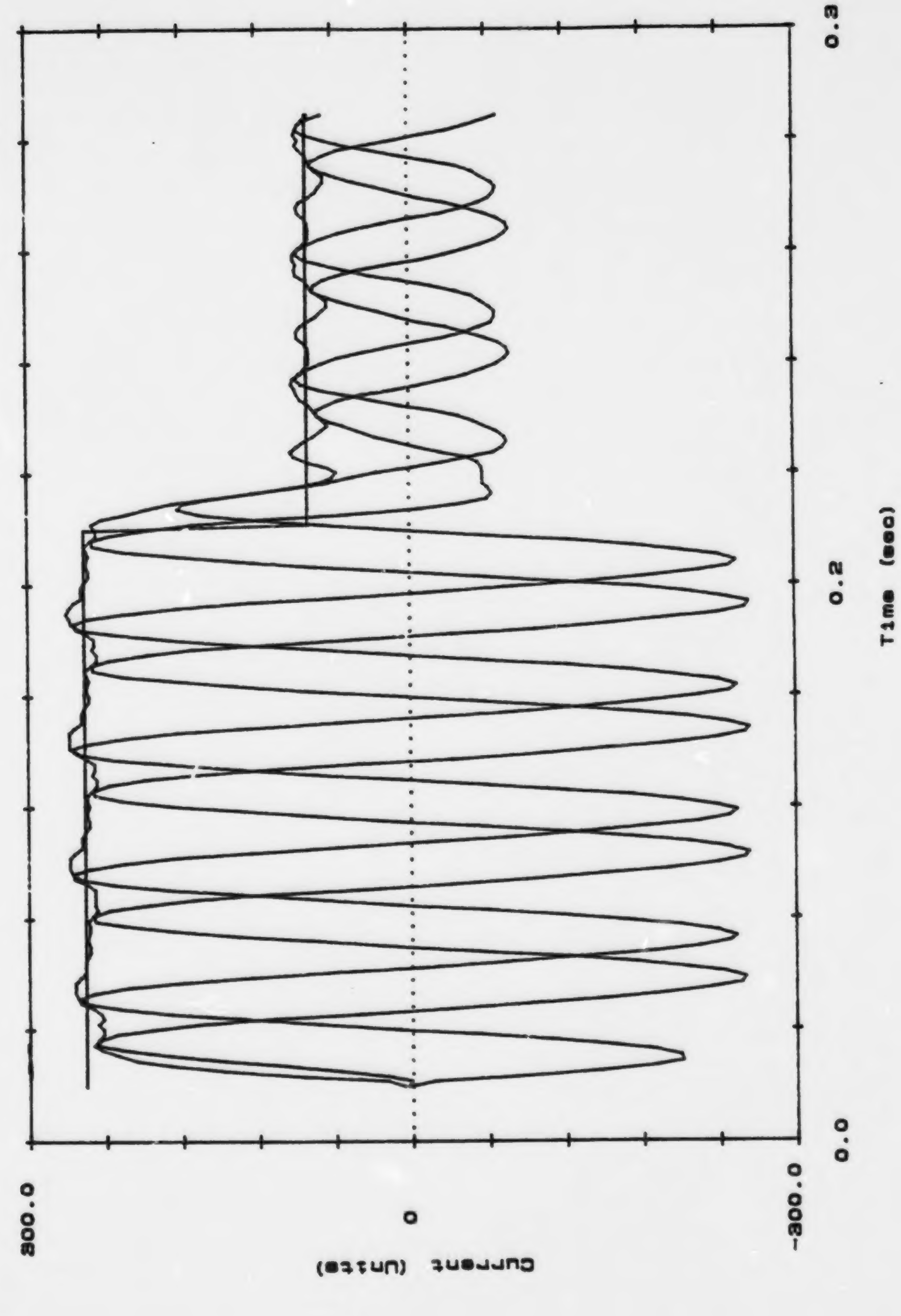

FIGURE 11-9: CURRENT CONTROLLER STEP RESPONSE - DEMAND 0-256-80

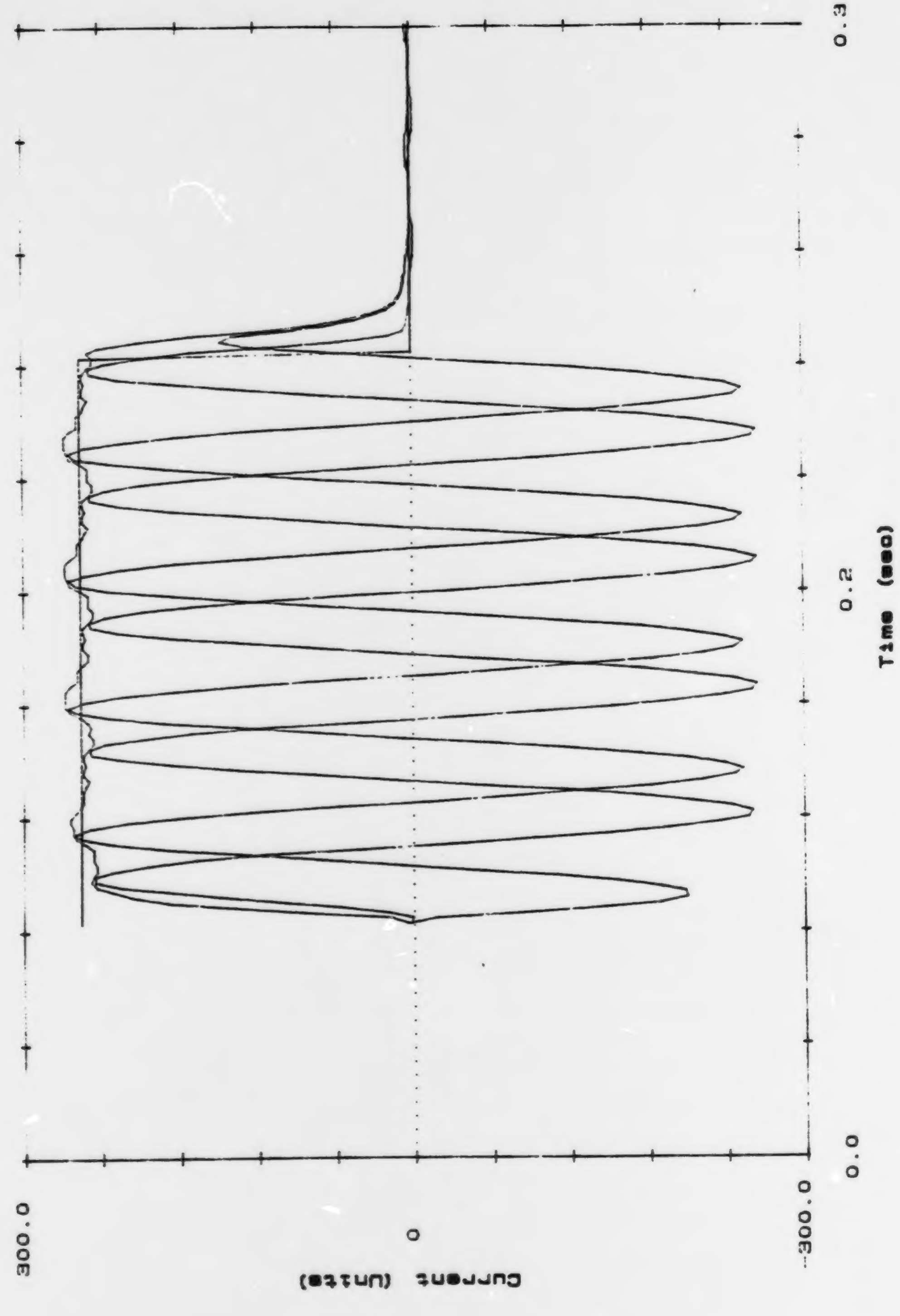

FIGURE 11-10: CURRENT CONTROLLER STEP RESPONSE - DEMAND 256-0 UNITS

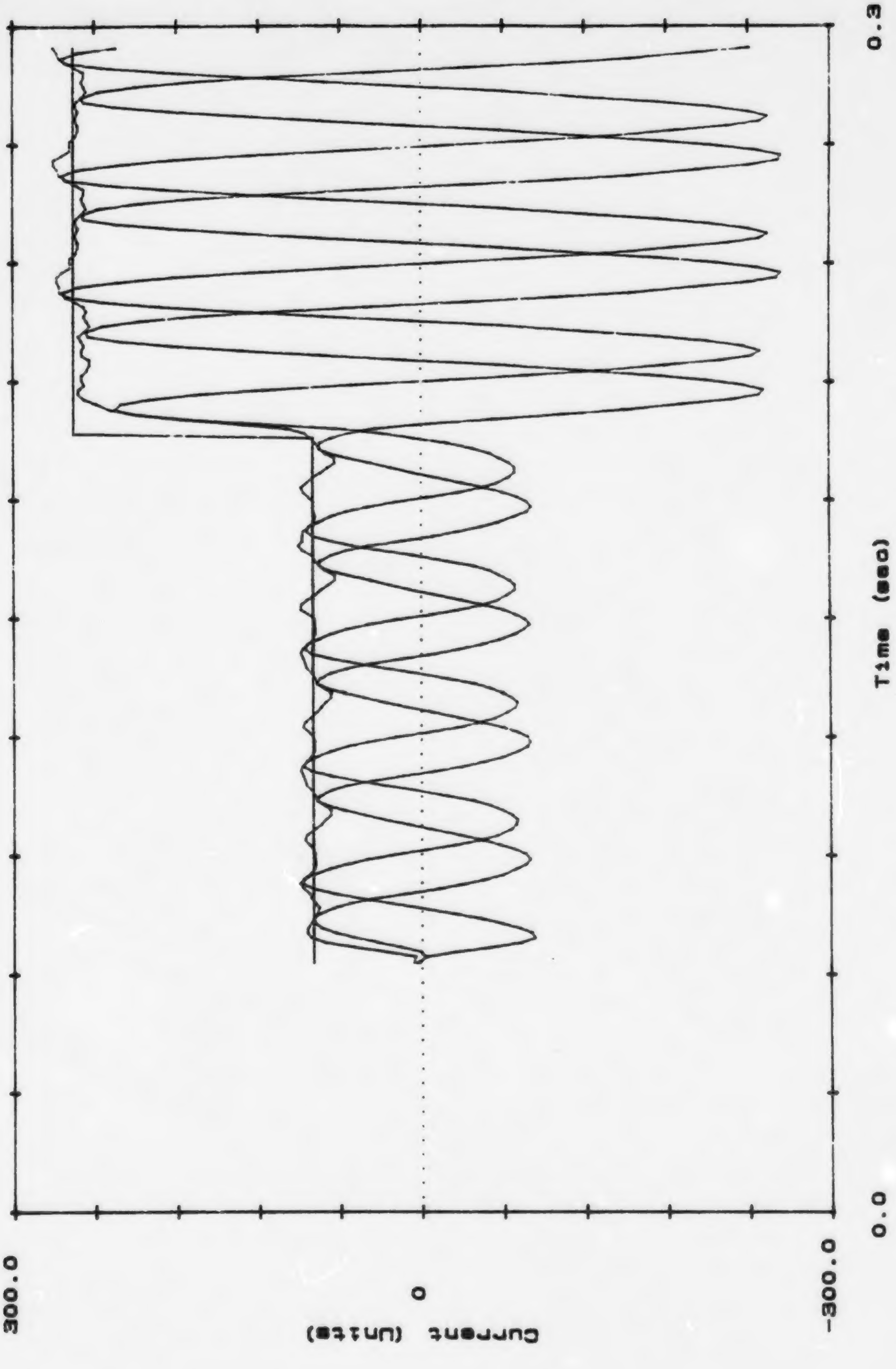

FIGURE 11-11: CURRENT LOOP RESPONSE: 0-80-256 DEMAND

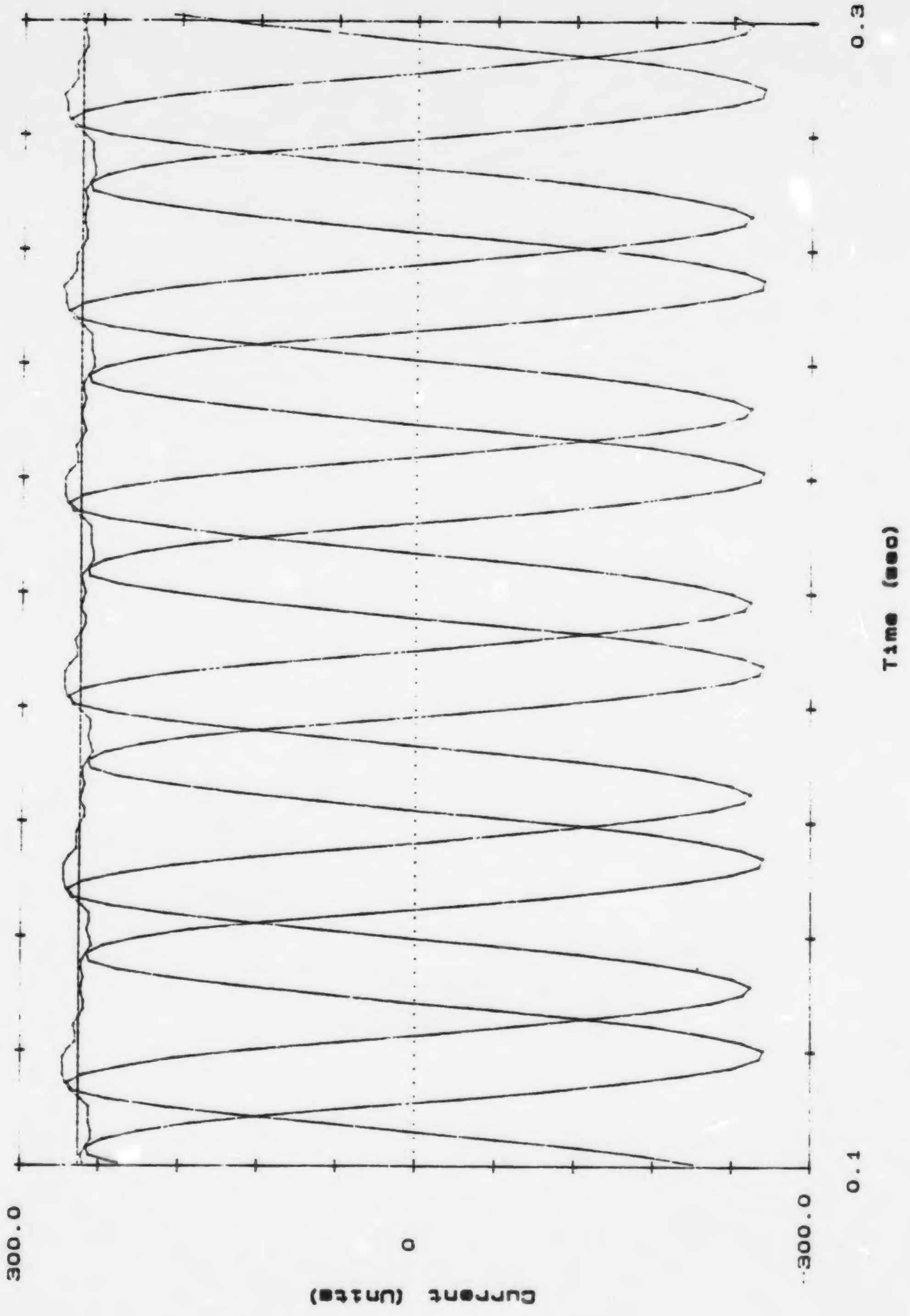

FIGURE 11-12: CURRENT CONTROLLER - STEADY STATE OPERATION

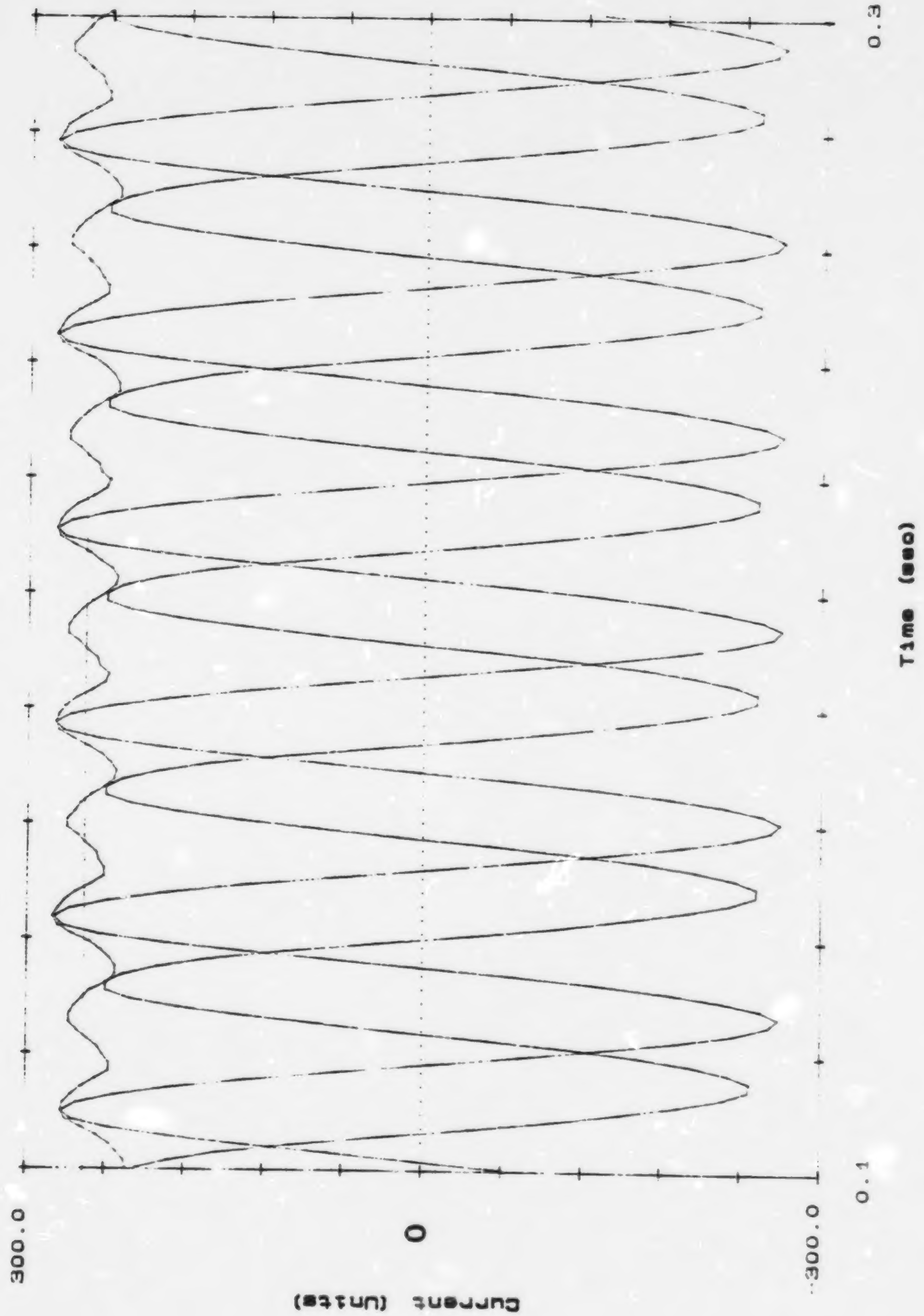

FIGURE 11-13: UNBALANCED LOAD - STEADY STATE

contains large ripples. The LFCM cannot correct a current imbalance because it produces a balanced three phase voltage. The second case investigated was a step demand change in the presence of imbalance. The results are shown in Figure 11-14. The time average of the calculated current magnitude meets the demand current and the system remains well behaved.

11.4.3.5 Transient Frequency Change

Under normal operation the LFCM will change the fundamental output frequency as the vehicle speed changes. It is necessary that this occurs in an orderly way. Figure 11-15 shows the result of a transient frequency change from 30 Hz to 15 Hz. As the frequency drops, the current rises quickly because of the reduced load impedance at the lower frequency. The current controller brings the current back to the demand level and steady state operation resumes at 15 Hz.

11.4.3.6 In manual operation the LFCM will be required to reverse the phase sequence. This change must occur quickly and in a controlled way. Figure 11.6 shows the result of a phase sequence reversal at 30 Hz. The change occurs quickly and without difficulty.

11.4.3.7 Comments on PWM Generation and Current Control Software

The results presented in this Chapter and those included in Appendix B indicate that the LFCM algorithms and software function correctly. Transient demand current, frequency and phase sequence changes were handled in an appropriate way. The system was well behaved in the presence of a substantial phase imbalance. The gating signals produced by the software appear to be safe and appropriate for application to and inverter gate base drive circuit (see Appendix B). Based on these observations it was concluded that it is appropriate to move to testing with an inverter and LIM.

11.5 SPEED AND POSITION SENSING

The speed and position sensing capability of the LFCM was tested using the dynamic test track and vehicle. In speed tests the vehicle was moved past the sensors at a known constant speed and while it was experiencing acceleration. The results of these tests are presented in Section 11.6.1. Position sensing was tested by moving the vehicle over the sensor, stopping and reversing the vehicle and by moving the vehicle past the sensor at a known speed. The results of these tests are presented in Section 11.5.2.

11.5.1 Speed Sensing

The velocity signal in the LFCM is scaled in order to increase resolution. One program speed unit is equal to 0.0256 m/s. The first speed test result, Figure 11-17, presented shows the signal obtained as the vehicle passed the sensor at 3 m/s. The signal contains some small variations but is relatively smooth. The signal magnitude indicates almost exactly 3 m/s. In the second speed test

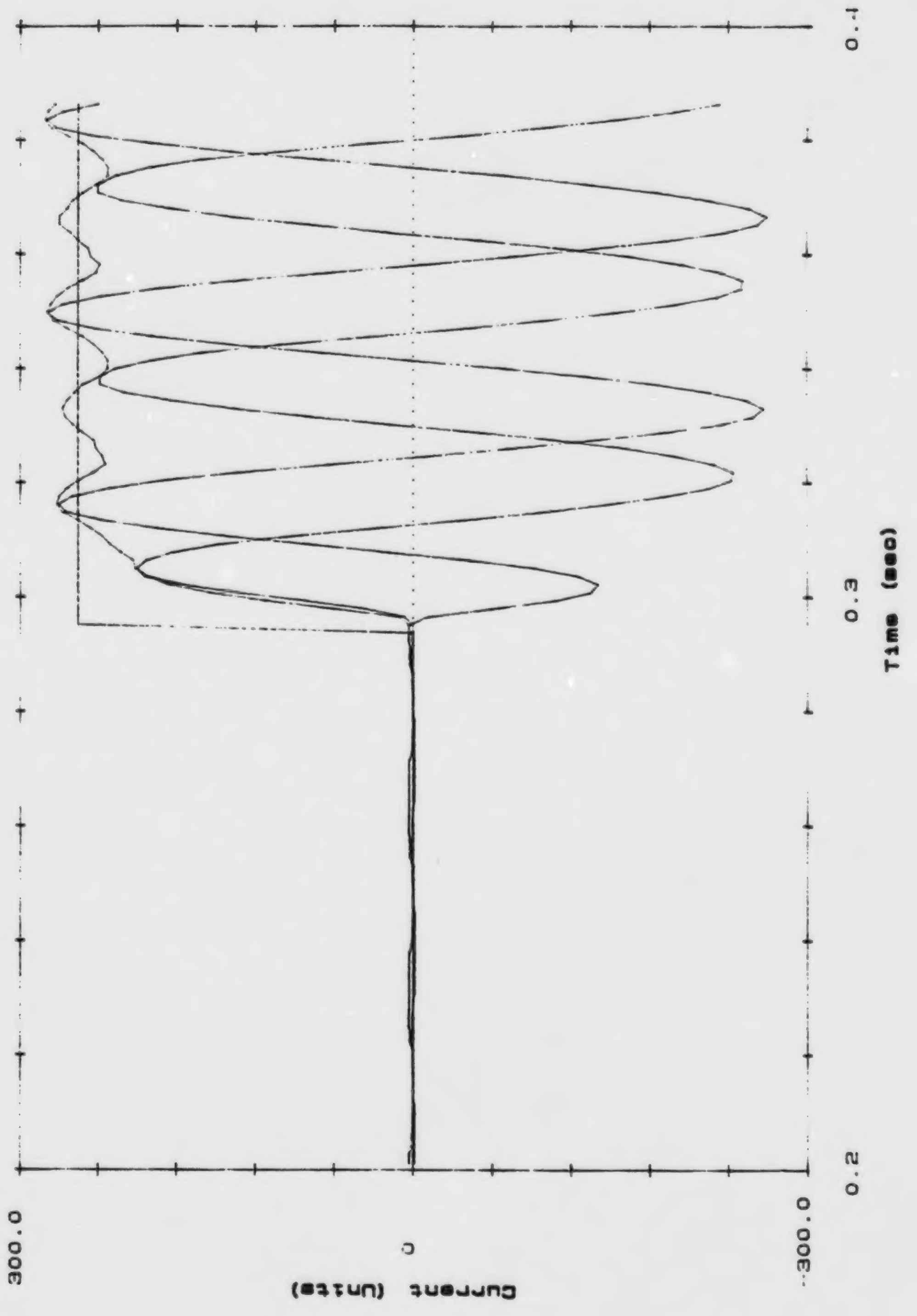

FIGURE 11-14: UNBALANCED LOAD - TRANSIENT

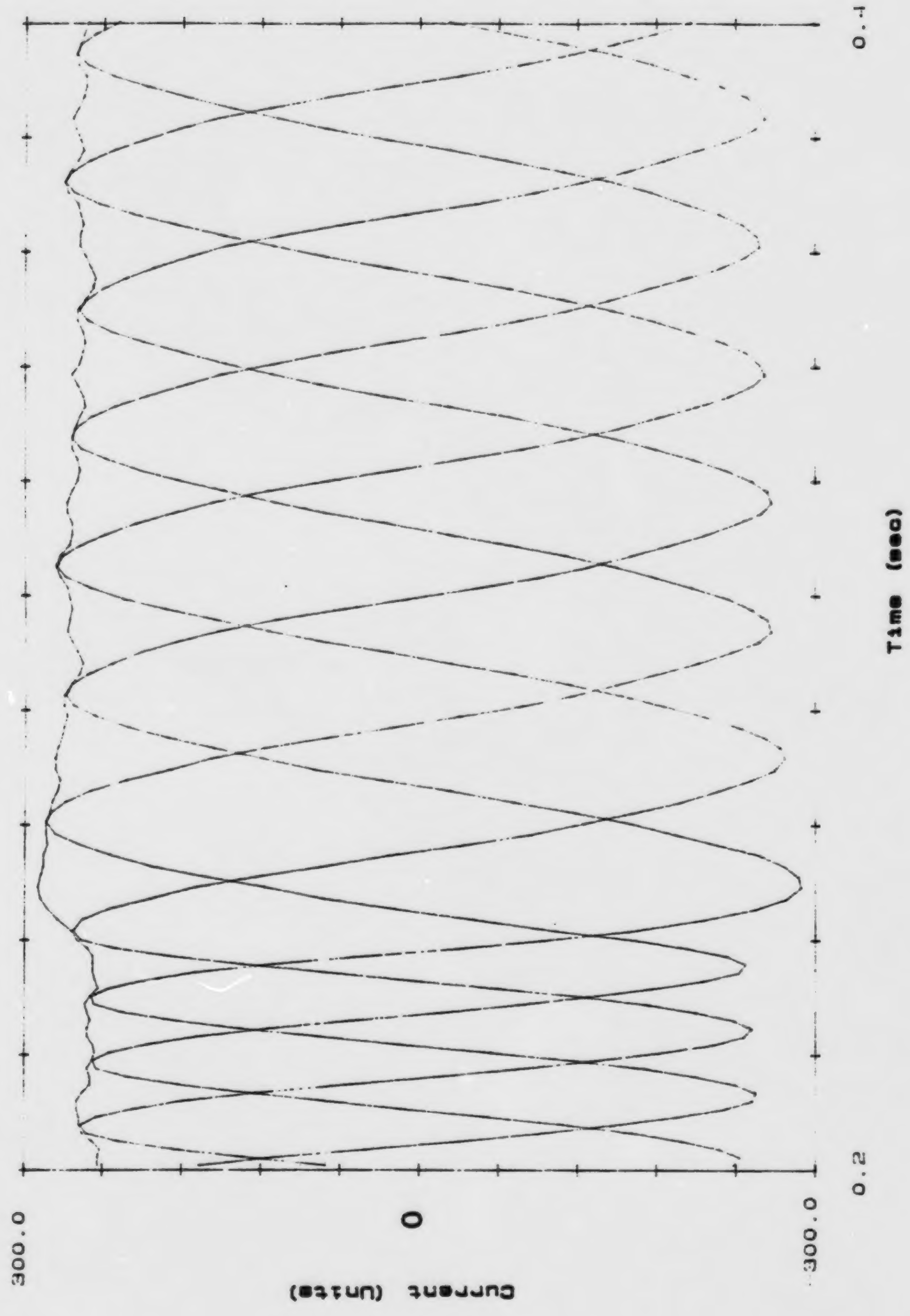

FIGURE 11-15: TRANSIENT FREQUENCY CHANGE

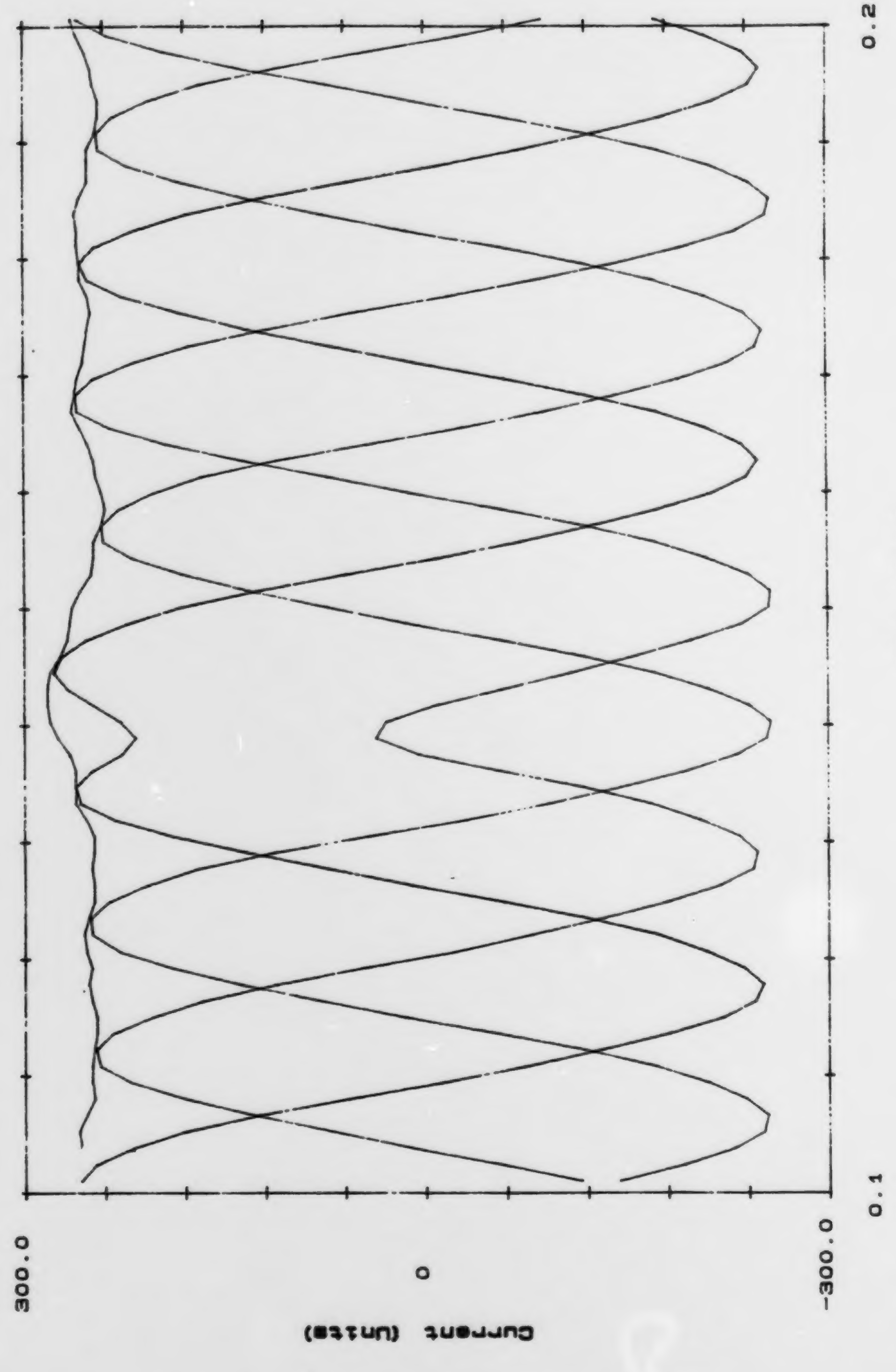

FIGURE 11-16: TRANSIENT PHASE SEQUENCE REVERSAL

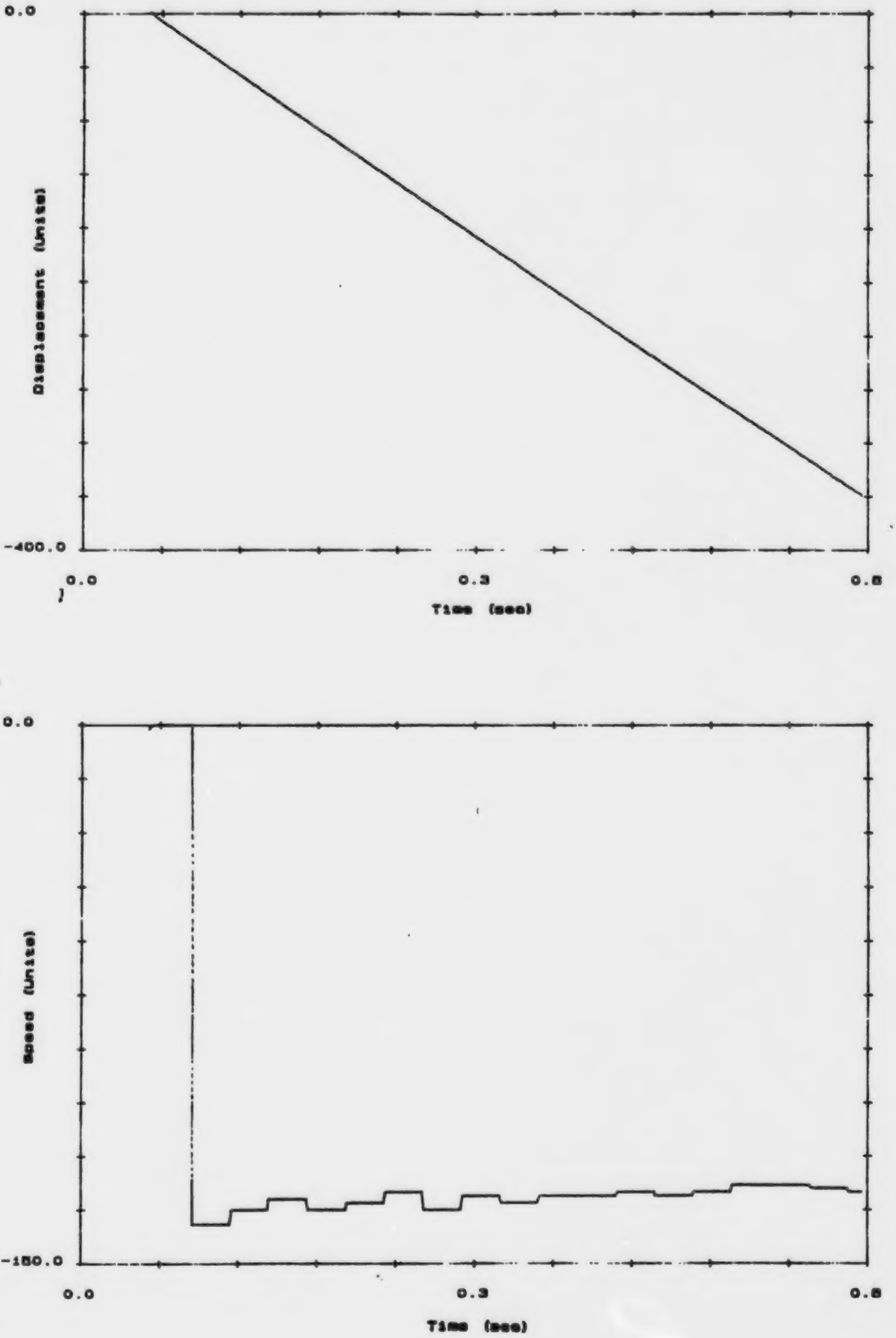

FIGURE 11-17: SPEED AND DISTANCE SIGNALS AT 3 M/S

the vehicle was positioned just out of sensor range and full thrust was applied to the vehicle. The resulting acceleration curve is presented in Figure 11-18. The position signal rises parabolically with time and the speed rises reasonably smoothly. The effect of time delayed velocity update is evident in the velocity signal. At fixed time increments the signal jumps to the average over the previous time interval. In each case the jump is small (maximum 0.3 m/s) thus confirming that the time interval has been chosen small enough to average the velocity but not unduly delay updates.

11.5.2 Position Sensing

The internal position maintained in the LFCM is in 0.5 cm units referenced to the leading edge of the test vehicle. If the vehicle travels in the reverse direction the count builds downward. Figure 11-19 shows the result of pushing the car over the sensor, stopping, and reversing the direction. The position count starts at zero, builds, levels off at the stopping point and decreases to zero as the vehicle backs out of the sensor zone. The position indicated is consistent with the vehicle position.

11.6 TESTING THE LFCM AND MOTOR COMBINATION

Unfortunately the test inverter planned for use with the LFCM failed and satisfactory repair could not be effected in time to complete testing before this report was to be completed. The LFCM software was tested using an inverter and rotary machine during the work done at Queen's University (see Appendix B). These tests covered steady state operation only and did not investigate positioning or speed control performance. It was decided to apply the LFCM control algorithms to a dynamic machine model in order to investigate positioning and speed control performance.

11.6.1 Machine Model

There is at present no good dynamic model for the LIM. Consequently these simulations employed the model for a rotary induction machine (RIM). The LIM and RIM are similar machines and the general results of simulations using the RIM would apply to the LIM.

The starting point for the model is the standard sixth order coupled differential equation set:

$$\begin{bmatrix} V_{as} \\ V_{bs} \\ V_{cs} \\ V_{ar} \\ V_{br} \\ V_{cr} \end{bmatrix} = \begin{bmatrix} R \end{bmatrix} \begin{bmatrix} i_{as} \\ i_{bs} \\ i_{cs} \\ i_{ar} \\ i_{br} \\ i_{cr} \end{bmatrix} + \begin{bmatrix} L \end{bmatrix} \begin{bmatrix} \dot{i} \end{bmatrix} + \begin{bmatrix} \dot{L} \end{bmatrix} \begin{bmatrix} i \end{bmatrix}$$

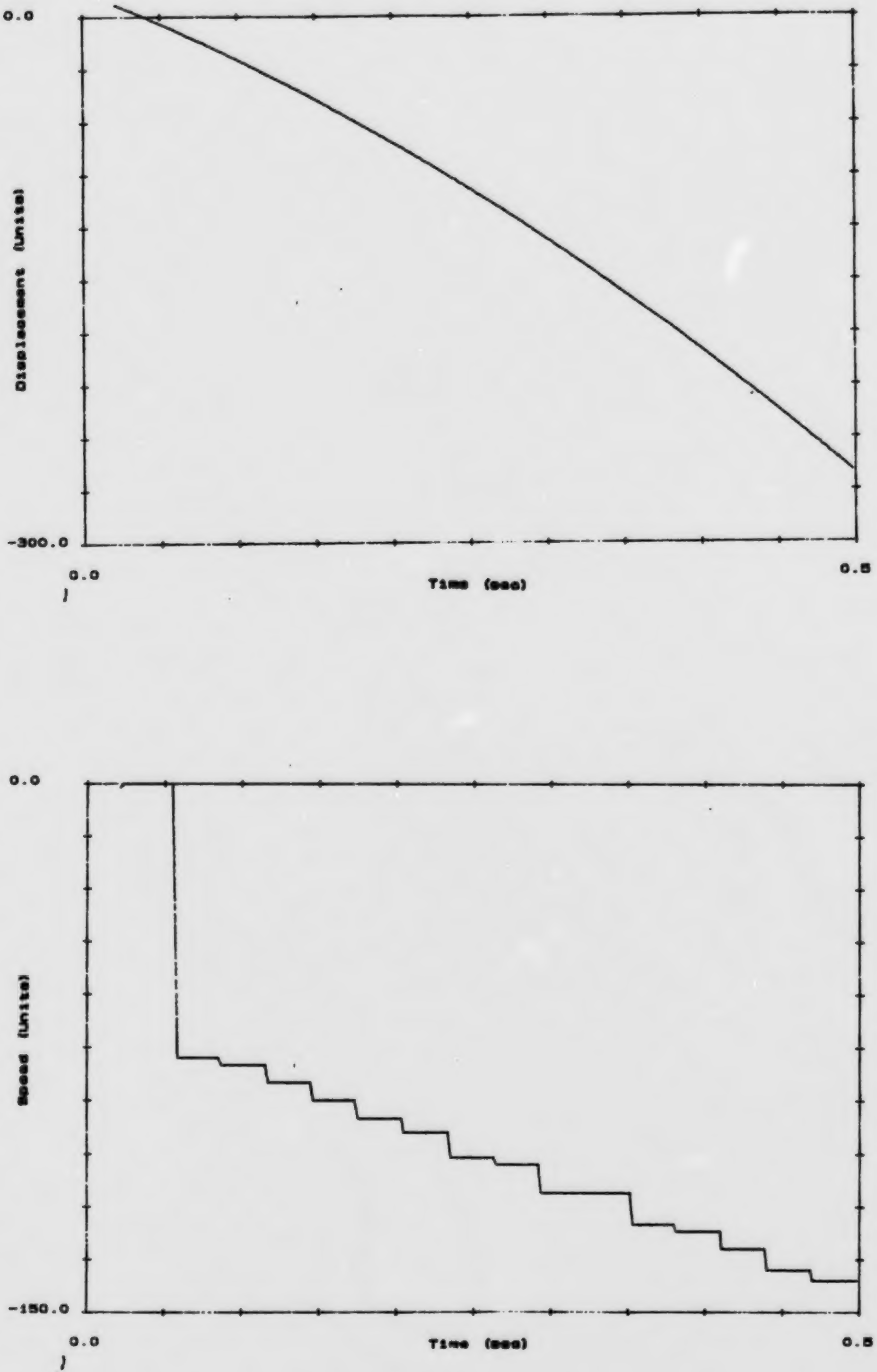

FIGURE 11-18: SPEED AND DISTANCE SIGNALS UNDER ACCELERATION

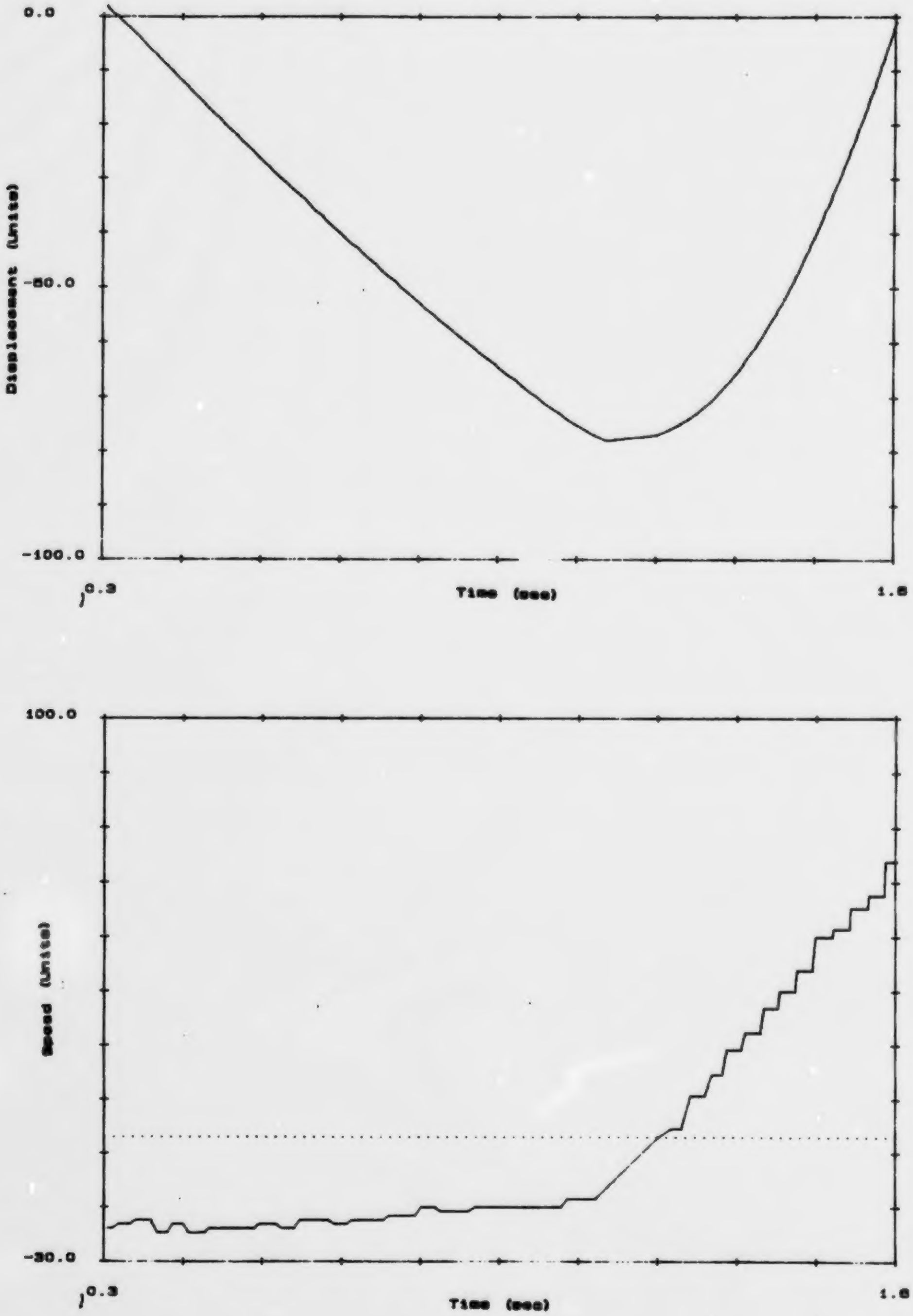

FIGURE 11-19: POSITION SIGNAL AS VEHICLE ENTERS CONTROL ZONE, STOPS AND EXITS

This equation can be rearranged to the state space form as:

$$\left[\dot{i}\right] = \left[L\right]^{-1} \Big[\left[v\right] - \left[R\right]\left[i\right] - \left[\dot{L}\right]\left[\dot{i}\right]\Big]$$

[L] is a full 6 by 6 matrix which depends on machine rotor angle. Equation (11.3) may be solved in a time stepping process by inverting [L] manually (a lot of work) and recalculating the inverse at each step or by calculating [L] at each step and then numerically inverting it (a lot of CPU time). An alternative is to use a set of linear transformations provided by the branch of machine analysis known as Generalized Machine theory to simplify the problem [15]. There exists a set of transformations which can move equation 11.3 from its present three phase reference system to a two phase reference frame attached to the primary. This transformation effectively reduces the system order by two. The remaining elements of [L] are either zero, constant, or functions of rotor speed. The form of the matrix makes manual inversion simple. Equation (11.3) has the same form in the new reference frame except that [L], [I], [V], are simple and the system is 4th order instead of 6th. Some entries in [L]' must be recalculated as the rotor speed changes. The transformed model is much easier to simulate and requires less simulation run time in the new reference frame.

If the details of three phase system are of interest, the following simulation procedure can be used:

- o Transform 3 phase voltages to 2 phase system.
- o Solve for 2 phase currents.
- o Calculate torque.
- o Determine rotor speed and position.
- o Transform currents to the 3 phase set.
- o Repeat for the next time increment.

In the present investigation the three phase system is not a primary interest: only the vehicle speed and position really matter. Consequently the control scheme can also be transformed into the two phase coordinate system. After transformation the PWM scheme generates two equal magnitude voltages separated in phase by 90°. The current magnitude is calculated by

$$|I| = \sqrt{i^2 + i^2_b}$$

The current is controlled using the same PI control strategy used in the LFCM. It has been determined that harmonic currents which flow in the machine are small (see Section B) so the high frequency components of the voltage are ignored and a sinusoidal voltage is applied to the simulated machine.

The LFCM motion control algorithms are implemented as follows:

- Whenever $v_{\alpha} = v_{\beta}$ the phase sequence is permitted to change.
- The frequency is allowed to change at any of 12 segmentation points in the waveform period (see Appendix B).
- Voltage magnitude may change continuously.
- Speed is updated every 16 m/sec.
- Position updates occur continuously.
- The demand torque is determined by a PI speed controller. The frequency is determined using fixed slip frequency control as $f = f_s + \frac{v}{2\pi}$, f_s = constant

The parameters used in this investigation were those of a 3 phase, 6 pole, 208 V machine presented in [16]. The rotor inertia was tripled and a coefficient of friction was introduce to represent a loaded vehicle. Time steps of 0.001 sec. were used in the simulation and the trapezoidal technique was used where integration was required. The maximum voltage magnitude was clamped at 300 V. The slip frequency used was 15 Hz with minimum allowed operating frequency of 1 Hz. It was found that the frequency and phase sequence update delay was too long if the frequency went below this value. The frequency was allowed to change in discrete steps of 1 rad/sec.

11.6.2 Simulation Results

The results of two simulations are presented here. First, shown in Figure 11-20, a vehicle enters the LFCM at 80 RPM when the demand speed is 120 RPM. The vehicle is accelerated rapidly and smoothly to the demand. In the initial transient the currents become unbalanced, the torque develops large ripples and the current magnitude signal is disturbed. As the machine reaches steady state the currents become balanced and the torque and current magnitude become smooth.

The second simulation was designed to test the positioning capability of the LFCM. A vehicle was sent into the LFCM control zone at a speed of 50 RPM. The LFCM has a position-speed profile which drops linearly from 50 RPM at 0 position to 0 RPM at the stopping point of 10 radians. If the speed profile were followed exactly the vehicle would slow to a stop without overshoot. The results shown in Figure 11-21 show the cart slow and stop with a negligible overshoot.

11.6.3 Interpretation

These simulation results indicate that the LFCM algorithms would be capable of controlling a rotary induction machine. Using the similarities of the RIM and LIM it is possible to say with good confidence that these algorithms would work with a LIM.

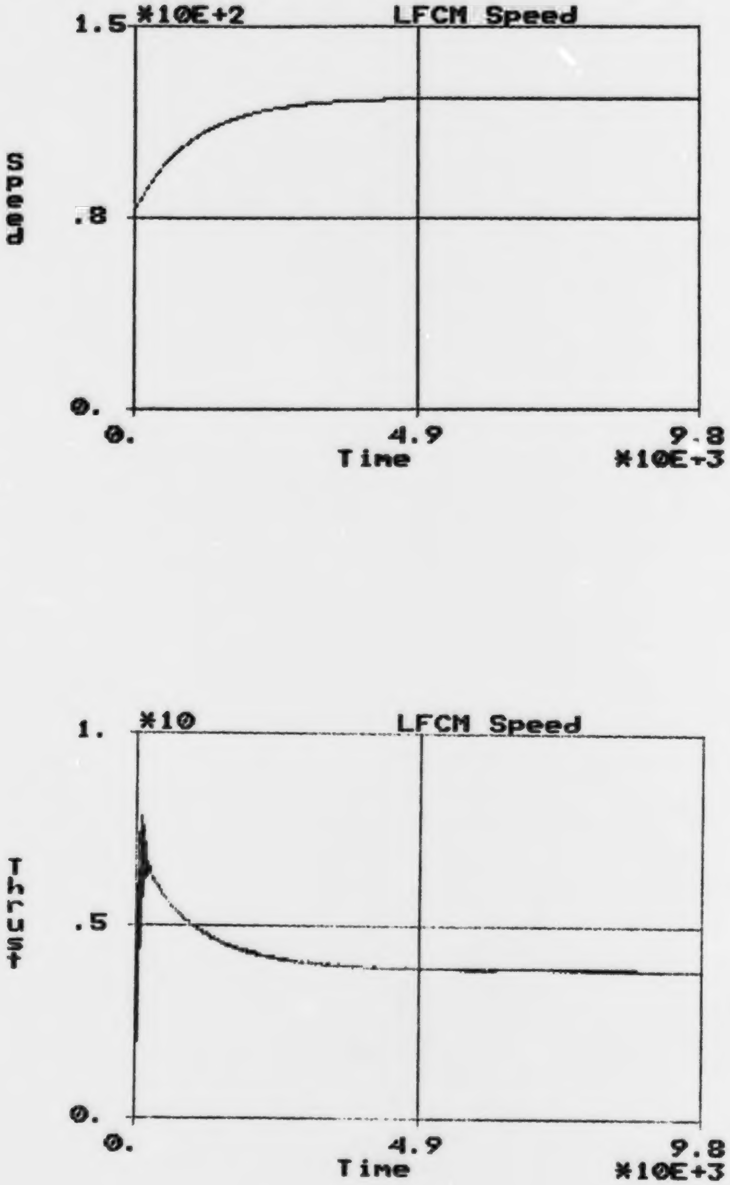

FIGURE 11-20: SIMULATED LFCM SPEED CONTROL

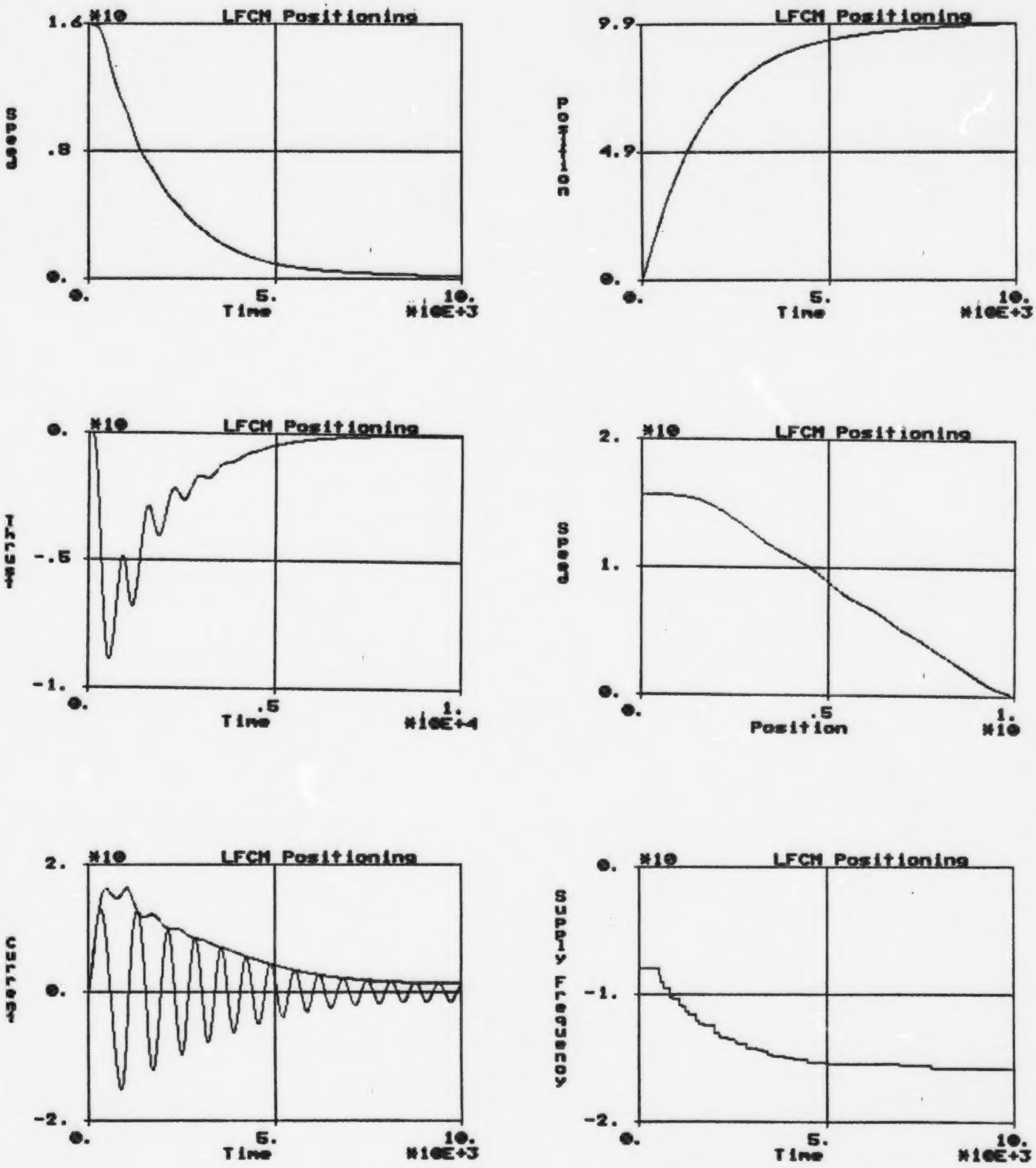

FIGURE 11-21: POSITION CONTROL

12.0 FIXED FREQUENCY VERSUS VARIABLE FREQUENCY SYSTEM TRADE-OFF

Variable Voltage Variable Frequency (VVVF) control has long been considered to provide superior performance compared to Variable Voltage Fixed Frequency (VVFF) control in industrial induction drive applications. The ability to vary the frequency allows maximum thrust to be obtained over the entire speed range, improves power factor and increases efficiency. In rotary machines VVFF is noted for the production of torque pulsations and increased heating due to harmonic components in the supply current and voltage. VVVF can be generated in such a way that the current and voltage harmonics are minimal and that torque pulsations are virtually eliminated. Experience has shown that similar benefits accrue to the LIM drives under VVVF control. The capital cost of VVVF power conditioning units is higher than that of VVFF units of a similar rating, however. This chapter presents a qualitative comparison of VVVF and VVFF schemes for LIT systems. Effects of the two schemes on the power distribution system, power conditioning unit and LIM reaction rail power are considered.

12.1 POWER DISTRIBUTION

The power distribution system for LIT system is typically extensive and complex. The head end of the system taps into the utility mains with breakers and perhaps a transformer. Power is then distributed to the track regions, and regional breakers protect the feeder cable. Each LIM controller is supplied through fuses from the region distribution panel. The LIM and controller are usually placed in close proximity so the cabling between them is short.

A common performance criterion used in power distribution for systems using LIM's is the power factor multiplied by the efficiency, known as "etacosphi". This figure provides an indication of how effectively the current and voltage are used to produce mechanical power. If etacosphi is low, the current is not being used to its full effect and distribution equipment will have to be sized larger than necessary. Because the LIM is a large airgap machine, its power factor is typically rather small and etacosphi is typically around 0.3 and sometimes less than 0.2, especially during braking. The addition of an AC voltage controller makes the combined power factor worse than the LIM alone. Power factor correction is difficult because the duty cycle of each LIM is so short. Capacitor banks could be added near the main feeder to improve the system power factor, however power factor correction can not be effectively applied at the LIM end of the distribution system. Capacitor bank effectiveness increases with the number of LIM's being simultaneously powered, which is to say effectiveness increases with the number of vehicles operating in the system.

Switching to a VVVF system has the potential to improve the only the real power consumed is distributed (mechanical power & losses). Reactive power required by the LIM is provided by the inverter and does not flow in the mains thus the power factor is unity.

In a system with many long runs of cable the saving in cost allowed by VVFF can be quite significant. This is particularly true in a system which moves heavy loads or requires large amounts of power.

12.2 POWER CONDITIONING UNITS

The power conditioning unit required for a VVFF LIM controller is very simple indeed. The three phase version is shown in Figure 10-7. The devices used are slow, low cost thyristors which are switched at the supply frequency (50, 60 Hz) and turned off by the natural behaviour of the circuit.

The power conditioning unit for a VVVF LIM controller is more complex and, for many applications, more expensive than that used in VVFF. The distribution system for LIT would probably be done at 250V dc making power BJT's the device of choice. Distribution above 250 V would require a special grade of apparatus while at 250 V or below, industrial standard equipment can be used. The PCU for VVVF would probably cost 1.5 to 2 times as much as a comparable VVFF controller would not be significantly different from its VVFF counterpart but the development cost would be higher.

In systems which require a maximum frequency of less than 30 Hz, for instance factory floor transportation systems where the maximum speed is 1 to 2 m/s, the VVVF PCU may employ a cycloconverter (see section 8.4). This PCU requires a three phase ac power supply and consumes both real and reactive power. The cycloconverter has, under some circumstances, a lower capital cost than an inverter but provides many of the performance advantages of an inverter fed system.

12.3 LIM AND REACTION RAIL

In fixed frequency systems, the LIM operates at one synchronous speed even though the speed of the vehicle varies. As a result the slip changes and is often large, particularly in braking. The power dissipated in the reaction rail is directly related to the slip, and can, because of the large slip, be significant in a fixed frequency system. As a result the reaction rail design is limited because of thermal consideration. In variable frequency systems the frequency is changed so as to keep the slip constant and relatively small. As a result the power dissipated in the reaction rail is smaller than that in fixed frequency systems. This allows the reaction rail to be small and mechanically simpler. In systems which move very large loads the reaction plate losses may rule out the use of fixed

Under fixed frequency operation, the LIM primary must be designed to provide a synchronous speed somewhat higher than the maximum operating speed using a commercial frequency supply. As a result, the pole pitch must be set at a small value. This has a number of consequences such as decreasing the power factor, increasing end effects and increasing sensitivity to air gap changes. In variable frequency operation the pole pitch may be set to a more desirable value because the designer also chooses the range of operating frequencies. A LIM designed for use under VVVF operation would most likely be smaller and less expensive than a LIM with the same performance characteristics used under VVFF. In VVVF the peak thrust is available at all speeds because of the ability to change operating frequency while in VVFF the peak thrust occurs at some fixed speed. The thrust available at other points is reduced. In order for the LIM to meet the design requirements at low speed it must be over designed for operation near the maximum thrust point. This results in a larger more expensive LIM.

12.4 CONCLUSIONS

At present it appears that VVVF systems would be more attractive in LIT systems which move heavy loads and require a large amount of power. In these systems the gains in power distribution and reaction rail design outweigh increase PCU costs. In systems which move very heavy loads VVVF may be the only feasible approach. Under some circumstances a cycloconverter may be used as a lower cost substitute for an inverter PCU in VVVF generation. For systems which are small or move light loads at high speeds, it appears that fixed frequency is still the approach of choice. Each system must be evaluated to determine which approach is the most appropriate.

13.0 SLIP POWER APPLICATIONS

Linear Induction Motors "waste" more power than conventional rotary induction motors. This statement doesn't follow from any one fundamental law, but rather from a number of practical differences between the two types of machine. For example, one of the major sites of lost power in either type is the secondary, i.e. the reaction plate for the LIM or rotor for the conventional motor. It turns out that for the LIM, in a variety of design cases, peak thrust per stator power input occurs at a higher slip frequency than is typical for rotary machines. Since secondary power loss is proportional to slip frequency, (refer to App. A-4) the LIM uses more secondary, or so-called "slip power" to produce a given amount of thrust.

Slip power is generally something one would wish to minimize. It contributes to a poor electromechanical efficiency figure, and causes reaction plate heating. Unfortunately, it is fundamentally impossible to eliminate slip power altogether. In induction motors, thrust cannot be produced without an associated slip power loss. Moreover, it is impractical to design to minimize slip power since that would require compromises in other aspects of performance (e.g. weight).

Given that the presence of slip power in a LIM reaction plate is inevitable, one might wonder if it can be "recovered" for practical use. Now normally, the power losses in a reaction plate are manifest as heat, which is ultimately transferred by convection to the passing air. However, the electrically conductive member of the reaction plate could be a winding, rather than the typical aluminum or copper sheet, and the slip currents could be routed through electrical circuits so that the power would be dissipated in a controlled, useful way. This is the LIM Slip Power Recovery proposition.

The concept of reaction plate slip power recovery is in some respects an excellent "fit" with the general concept of LIM-in-Track propulsion. It makes use of power which would otherwise be lost. More significantly, it offers a potential means of getting power to vehicles in systems which for one reason or another cannot use an exposed power rail/collector system.

In another sense, it could be argued that the slip power recovery proposal detracts from the simplicity and inherent reliability of the passive vehicle concept. That is, can LIT be justified in the first place if the requirement calls for anything more than the simplest form of vehicle? Do such vehicles need power on board?

These questions are not easily answered, nor is it intended to probe them further here. Instead, the concept, theory and application of reaction plate slip power recovery is developed. It may well be that having exposed the concept, more applications will be identified at some time in the future.

13.1 THEORETICAL PRINCIPLES

13.1.1 Slip Frequency

A good beginning to understanding "slip power" is to fully appreciate the concept of slip frequency in a LIM. Most textbooks introduce the idea of fractional slip but do not go the next step, which is to define the product of supply frequency and fractional slip, i.e. slip frequency. It is slip frequency which determines the motor behaviour, and unlike fractional slip, which is a derived quantity and rather abstract, slip frequency is measurable. It is the frequency one would detect if one were to measure currents or voltages induced in the reaction rail.

An excellent analogy for illustrating the importance of slip frequency is found in the wheel. Most people have direct experience operating automobiles and recognize the various conditions that influence the traction provided by their tires. It so happens that, in some senses, the behaviour of wheels and the behaviour of LIMs is very similar, even to the characteristic shapes of the force vs. slip frequency curves they exhibit.

Table 13-1 is a summary of the wheel slip analogy of LIM behaviour. Six distinct conditions of operation are observed. Most are within the realm of common experience. The last, which amounts to reversing the driving wheels while still moving in a forward direction, is hardly common, but not unimaginable.

13.1.2 Slip Power

In mechanical terms, power may be equated to the product of Force acting at a given velocity. One can imagine that power would be dissipated in the road surface as a passing tire tread applies force at a certain rate of slip. The power would in this case be termed "friction loss". Note that when the direction of the slip rate changes, so also does the direction of the applied force, hence the product, i.e. the power, remains positive. One way of looking at this result is that all force production, regardless of whether it is "braking" or "accelerating" force, requires that power be dissipated in the reactive surface.

Slip power in the LIM reaction rail is analogous to friction loss in a road surface. The power is the product of the applied force and the rate of slip, the latter term being the product of slip frequency and winding wavelength:

$$P_s = F f_s \tau$$

If one's goal is to minimize slip power per unit thrust, the means is clearly to keep the product $f_s \tau$ as small as possible. Unfortunately, it appears to be a general rule that motors with a small τ need a higher f_2 in order to produce reasonable thrust per stator current.

WHEEL SLIP ANALOGY		**LIM**	
1. 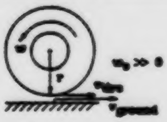 ω r $\omega_s \gg 0$ v_{tire} v_{ground}	Torque demanded is excessive. Wheels "spin". Accelerating force is present, but decreases as tire slip rate grows.	- Motoring - "Unstable" region	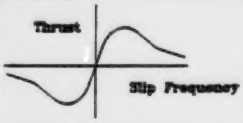
2. 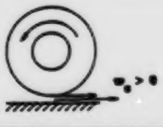	Torque demanded is normal. Wheel slip is imperceptible but finite. Increased torque results in increased slip rate.	- Motoring - "Stable" region	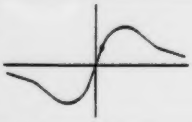
3. 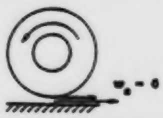	No torque demanded. Wheels "coast". Slip rate is essentially zero.	- Stator frequency is synchronized to mechanical speed - No thrust	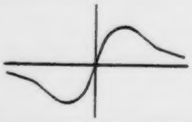
4. 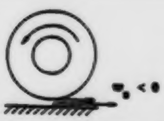	Braking torque demanded. Wheel slip rate is small, but opposite in direction to cases 1 and 2. Decelerating force is present.	- "Regenerative Braking"	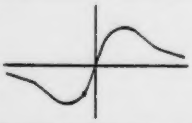
5. 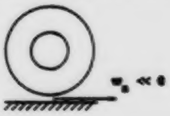	Braking torque demand is excessive. Wheels "lock up". Slip rate is large. Decelerating force is present.	- Stator current is D.C. - "Eddy Current Braking"	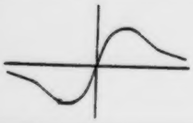
6. 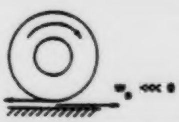	Wheels are suddenly "reversed" while still proceeding in forward direction. Slip rate is very large. Decelerating force is present.	- Stator current phase sequence is reversed. - "Plug Braking"	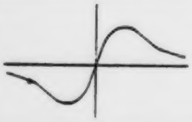

WHEEL (radius = r)

v_{ground} = velocity of the road surface with respect to an axle-fixed reference frame

= angular rate of wheel rotation
+ve denotes clockwise
-ve denotes counter-clockwise

$v_{tire} = r$ = tangential velocity of tire surface with respect to the axle-fixed reference

$s_{tire} = v_{tire} - v_{ground}$ = tire slip

$W_s = W S_{tire} = \frac{r \quad - v_{ground}}{r}$ = tire slip rate

LIM (wavelength = λ)

v = velocity of the reaction plate surface with respect to a stator-fixed reference frame

f = frequency of three-phase stator current
+ve denotes a, b, c sequence
-ve denotes a, c, b sequence

v_{field} = f = velocity of stator field with respect to the stator-fixed reference

$s = \frac{v_{field} - v}{v_{field}}$ = slip

$f_s = fs = \frac{\lambda f - v}{\lambda}$ = slip frequency

TABLE 13-1: Relationship between Variables in Wheel Slip Analogy of LIM Behaviour

recover it for use on board the vehicle, the parameters f_s and might be chosen so as to yield a certain amount of slip power. In other words, one would endeavour, through the selection of motor and power supply design parameters, (i.e. pole pitch and excitation frequency) to size the slip power output capability to the application requirement. In theory there is no upper limit to the amount of slip power that may be generated for a given thrust level. In practice, there are design issues which introduce constraints. These issues are identified in Section 13.2.

13.1.3 Circuit Considerations

If slip power is to be recovered then a means of accessing it is required. It is not inconceivable that some form of heat-exchanging mechanism could be used to extract heat energy from the reaction plate, and convert it into another form for storage or immediate use. However, a much more direct approach seems to be to employ a wound reaction plate connected to an electronic power-converter/battery charger. Figure 13-1A shows the basic physical configuration: The wound reaction plate replaces the conventional conducting sheet-over-steel plate. Connections are made between the reaction plate winding and a Slip Power Recovery Unit. The multiple, distributed connections are preferred to a single set of connections because they provide a tap into the particular area of the plate that happens to be receiving slip power at any given instant. Hence, current is not routed needlessly (and wastefully) through a series of coils which at that instant are not covering the in-track stator.

Figure 13-1B shows one possible electrical connection scheme. In this case, the primary poles are series connected and the three phases are configured in the "star" form. The secondary poles are separated into groups, each of which is also configured as a three-phase "star".

Alternatives to the connection scheme shown in Figure 13-1B are possible. For example, "delta" form connections could be used, though no "neutral" access would then be available. It is not actually mandatory to use a three-phase reaction plate winding just because the stator is three-phase. Two-phase space-quadrature windings or single-phase windings could also be used. It is not the number of phases, but the pole pitch which must be matched to the stator.

Figure 13-1C shows the per-phase equivalent circuit with secondary connected to a slip power recovery unit (SPRU). The SPRU, and the electrical loads which it provides power to, appear as a load impedance to the reaction plate winding, which conversely, acts as a source, V_m, with a series impedance, $R_2/s + jX_2$.

The source voltage V_m varies in both magnitude and frequency as the vehicle thrust and speed change. For example, during acceleration from a standstill the voltage will be relatively high and the

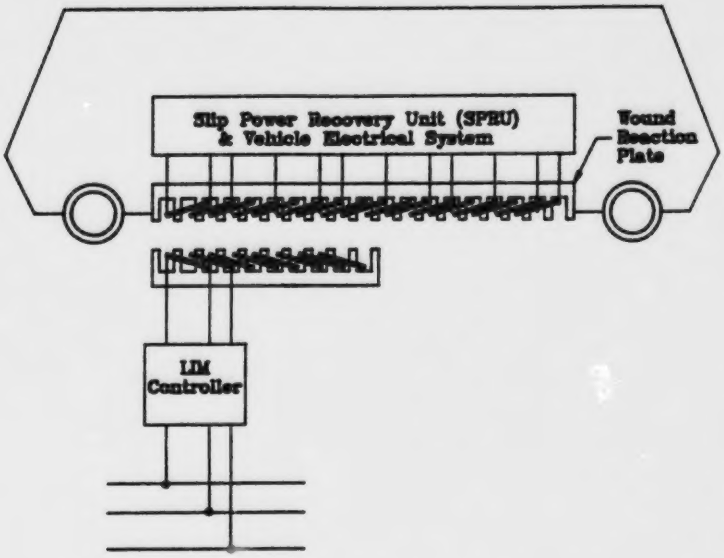
Slip Power Recovery Unit (SPRU)
& Vehicle Electrical System
Wound Reaction Plate
LIM Controller

A) Physical Configuration

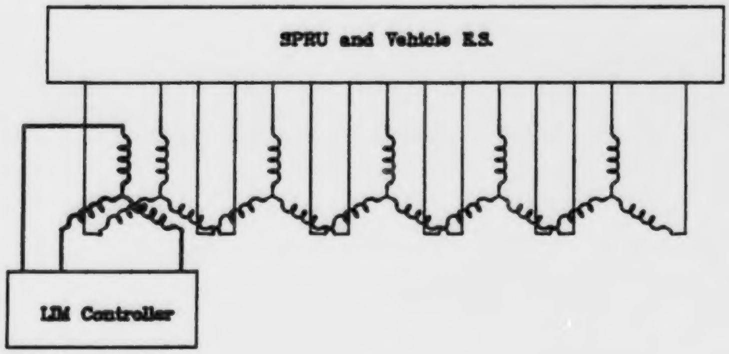
SPRU and Vehicle E.S.
LIM Controller

B) Electrical Representation

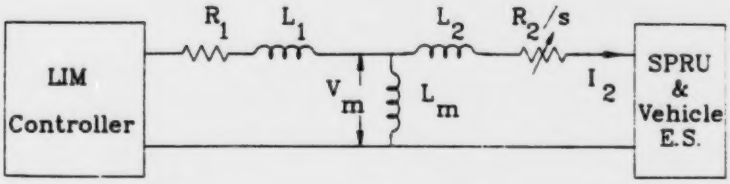
R1
L1
L2
R2/s
Vm
Lm
I2
LIM Controller
SPRU & Vehicle E.S.

C) Equivalent Circuit Model

FIGURE 13-1: RELATIONSHIPS BETWEEN VARIABLES IN SLIP POWER RECOVERY

frequency will begin to drop from 60 Hz as the speed increases. At cruise speed the voltage and frequency will be at their lowest. During phase reversal braking (plugging) the voltage will go to its highest and the frequency will exceed 60 Hz.

The large variation in the characteristics of the wound reaction plate source, V_m, almost certainly mean that the SPRU must contain a battery which will sink or source power as required in order to maintain a constant voltage output to the vehicle electrical loads.

The current, I_2, which flows in the reaction plate winding can do so only if the SPRU is receptive. Since the vehicle electrical loads are not necessarily constant and the battery can be in a fully-charged state, the SPRU must provide a parallel path for current to flow.

13.2 ANALYSIS OF TYPICAL SLIP POWER AVAILABILITY

13.2.1 Approach

To estimate the amount of slip power available for recovery the following method may be employed:

- o Define the speed, v, vs. time; and thrust, F, vs. time profiles (including station dwell time) for the vehicle.
- o Define the LIM pole pitch, τp
- o Define the LIM operating frequency, f (eg. 60 Hz)
- o Calculate the slip frequency, f_s vs. time profile using the formula:

  $$f_s = \frac{2\tau_p f - v}{2\tau_p f}$$

- o Calculate the slip power, P_s, vs. time profile using the formula:

  $$P_s = Ff_s 2\tau p$$

  (see Appendix A-4 for a derivation)

- o Calculate the time-averaged slip power

At this point, the total slip power has been estimated. This is the amount of power which must be dissipated on the reaction plate side of the airgap in order to achieve the thrust and speed profiles which were defined. For the particular motor pole pitch and supply frequency used, this power loss is inevitable regardless of the particular design or characteristics of the reaction plate.

Next, it is required to estimate the fraction of the total slip power that is recoverable. There are some practical issues to consider here:

- The resistance of the reaction plate winding acts as a source impedance to the Slip Power Recovery system, and some power must be lost in it. The proportion of power which is dissipated in the winding depends on the effective load impedance. Assuming our interest is in transferring the most power possible to the SPR system, the load impedance and source impedance must match. In this case, the power is split 50/50 between the winding resistance and the SPR loads.

- The power rectifier and power switching elements used in the SPR system have associated power losses.

- The battery storage used in the SPR system introduces power losses in both charging and discharging conditions.

13.2.2 Example

Consider a People-Mover type vehicle for which Slip Power Recovery is identified as a means of supplying the 2 kW auxiliary loads. The following characteristics and assumptions apply:

- 10 m/s cruising speed
- 1.3 m/s^2 accel/decel rate (constant)
- 600 m station spacing
- 5000 kg (nominal) vehicle mass
- 500 N drag (constant)
- no grades
- 20 sec. station dwell time

Using these data the speed and thrust vs. time profiles may be drawn as per Figure 13-2.

Next, the LIM pole pitch and supply frequency are chosen. Here, a 60 Hz supply is assumed and the pole pitch is chosen as 17 cm. The slip frequency and slip power profiles are then drawn.

In order to illustrate the effect of pole pitch on slip power, profiles were recalculated based on a 25 cm pole pitch. Both profiles are indicated in Figure 13-2.

The time-averaged slip power for the 17 cm pole pitch case is 32 kW, well in excess of the 2 kW required for the vehicle auxiliary

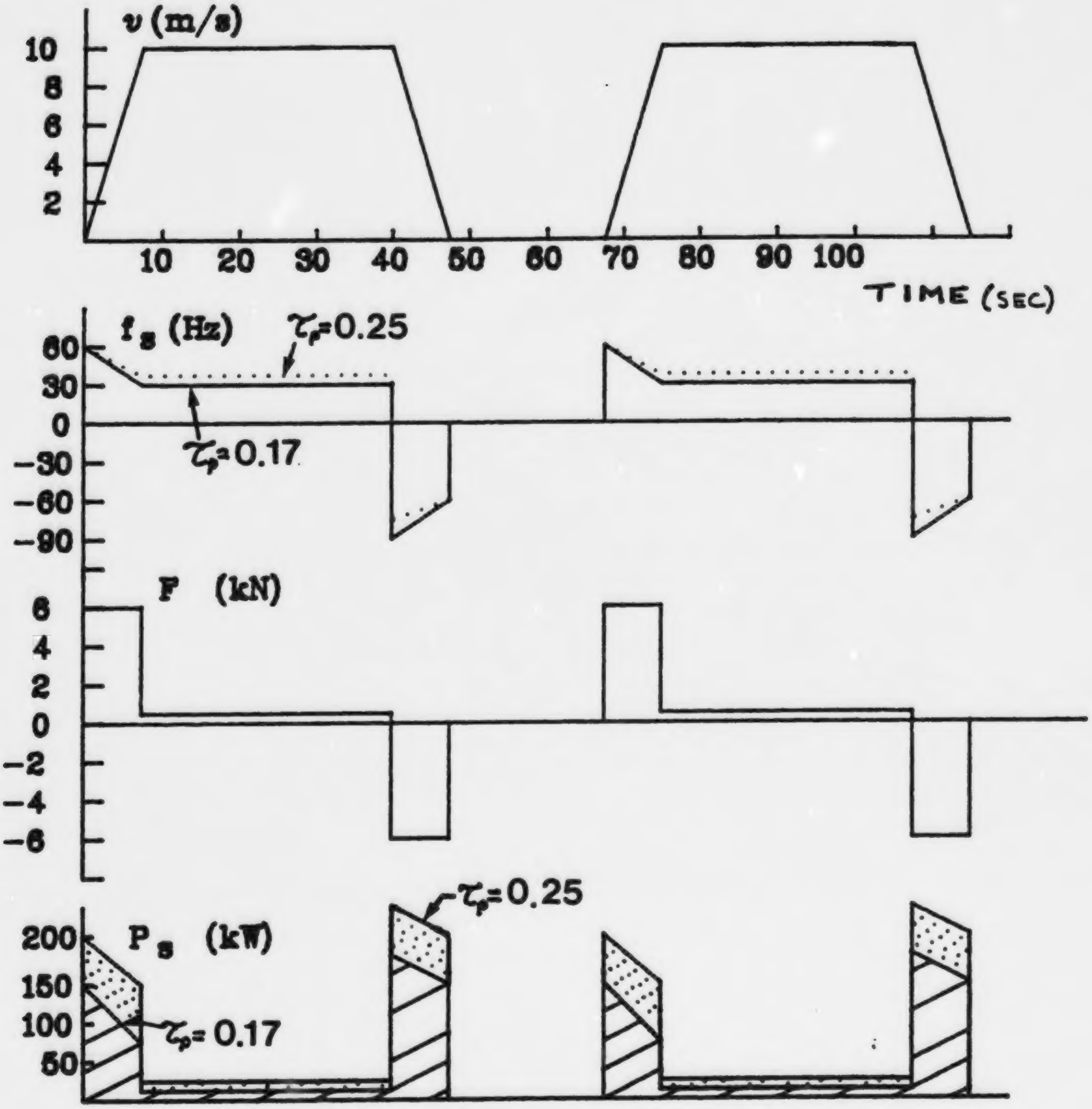

FIGURE 13-2: EXAMPLE SLIP POWER AVAILABILITY

loads. Of course, not all 32 kW could be recovered anyway. But how much could? To try and answer this, the following assumptions are made:

1) source and load impedances are matched, enabling maximum power transfer.

2) electronic rectification and power conversion processes have an average efficiency of 90%.

3) 75% of the averaged slip power is stored, then released, from the batteries in the process of regulating output voltage.

4) Battery charge/discharge efficiency (energy out vs. energy in) is 40%.

Following from the first assumption, half of the 32 kW is dissipated in the winding resistance. Of the remaining 16 kW, the power breakdown is as follows:

Power Electronic Components: 16 kW x (1-.9) = 1.6 kW
Battery: 16 kW x .75 x (1-.4) = 7.2 kW
Power to Auxiliary Loads: 16 kW - 1.6 kW - 7.2 kW = 7.2 kW

In summary, 7.2 kW out of a total average slip power of 32 kW could be delivered to the vehicle auxiliary loads, i.e. about 23%.

13.2.3 Power-Smoothing Considerations

The foregoing analysis assumes that it is practical to charge and discharge the batteries over short cycles (7 seconds charge followed by 30 seconds discharge.)

In order to avoid battery overheating it would be necessary to carry enough cells to keep the power dissipation per cell within allowable thermal limits. The simple analysis showed a battery dissipation loss of 7.2 kW. If the vehicle carried the equivalent of fourteen automobile batteries, each would need to dissipate about 500 W.

Are large arrays of batteries the only means of achieving power smoothing so that power can be regulated at the vehicle auxiliary loads? If so, the feasibility of SPR may rest on the practical weight and space restrictions imposed by the vehicle. Fortunately, not all vehicle loads require a steady supply. Some, in fact, may be switched in when it is convenient to draw power (i.e. during high thrust) and switched out when it is not. For example, heater loads could be so synchronized, so also could intermittently-required fans, pumps and air-compressors. These types of loads could therefore be managed in such a way as to achieve some degree of power smoothing. Other loads such as lighting and electronics would need a constant, regulated supply, but the battery storage requirements for these would be significantly less than for all the total load.

13.3 PRACTICAL SYSTEM DESIGN

13.3.1 Wound Reaction Plate Design

The wound reaction plate may take the form shown in Figure 13-1A, which is similar to the LIM stator. Alternatively, it could be "Gramme" - Surface-Wound as pictured in Figure 13-3. In either case, the following design principles apply:

1) Pole Pitch - The spacing of poles must be identical to that of the stator winding, otherwise the stator flux will not link in the most effective manner to the secondary circuit.

2) Number of Phases - The winding does not necessarily have to be three phase, however, the winding output must be rectified, and three phase rectification is generally preferred.

3) Copper Cross-Section - The efficiency of recovery, and the maximum possible transfer of slip power to the loads, are limited by the winding resistance. Hence, copper cross section is an important design parameter. In general, one would expect to use somewhat greater cross-section than is typical for sheet-type reaction plates which dissipate 100% of the slip power within the sheet.

4) Number of Turns - The number of turns on the reaction plate winding must be chosen to yield a range of output voltage which is compatible with the design of the SPR system.

13.3.2 SPR Circuit Design

Figure 13-4 outlines one potential concept for an SPR system. Note the following features:

1) Multiple Rectification Bridges with Paralleled Output

Since the slip voltage waveform alternates, (i.e. at the slip frequency) rectification is a necessary step in the conversion to a useful form. The paralleled output permits the energized segment(s) of the reaction plate winding to source power to a common bus. Note that the winding segments should not be parallel-connected on the input side of a single rectification bridge, otherwise power from an energized segment would "spill over" into the unenergized segments where it would not be recovered.

2) Load-Side Voltage Regulation

A step-down switching regulator keeps voltage constant to the batteries and vehicle auxiliary loads.

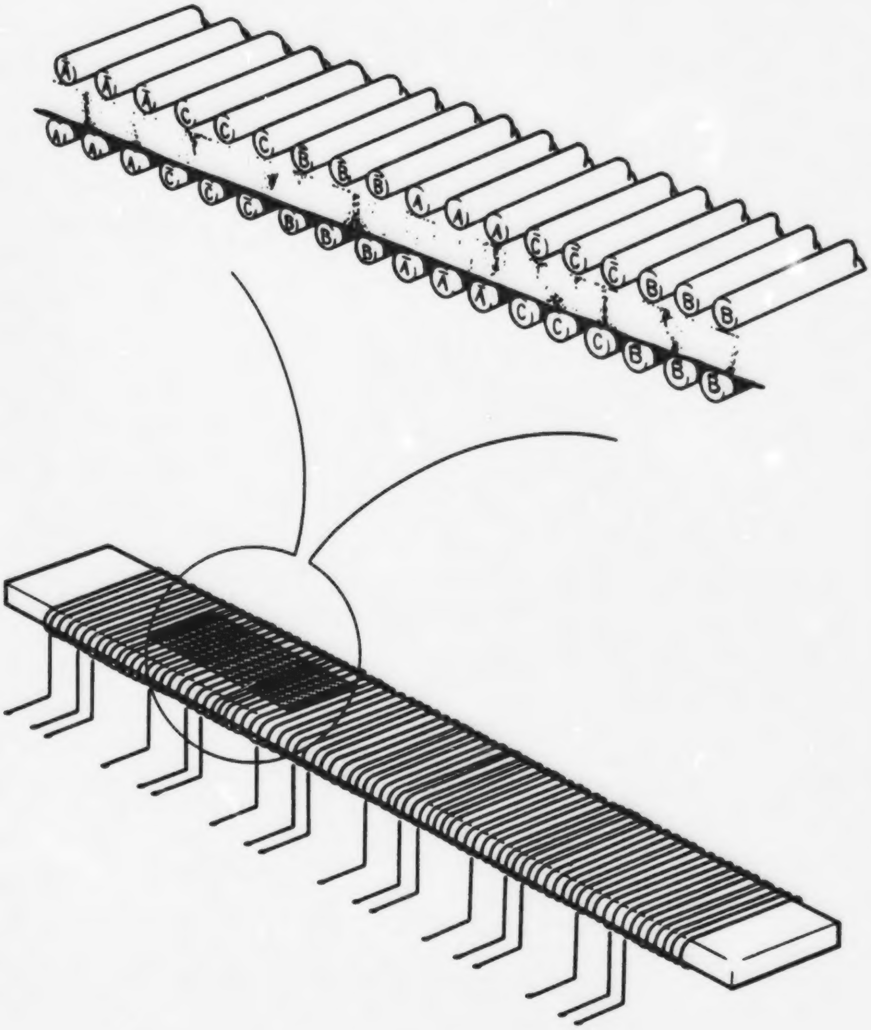
$\bar{A}$
$\bar{A}$
$\bar{A}$
C
C
C
$\bar{B}$
$\bar{B}$
$\bar{B}$
A
A
A
$\bar{C}$
$\bar{C}$
$\bar{C}$
B
B
B
A
A
A
$\bar{C}$
$\bar{C}$
$\bar{C}$
B
B
B
$\bar{A}$
$\bar{A}$
$\bar{A}$
C
C
C
$\bar{B}$
$\bar{B}$
$\bar{B}$

FIGURE 13-3: SURFACE-WOUND REACTION PLATE

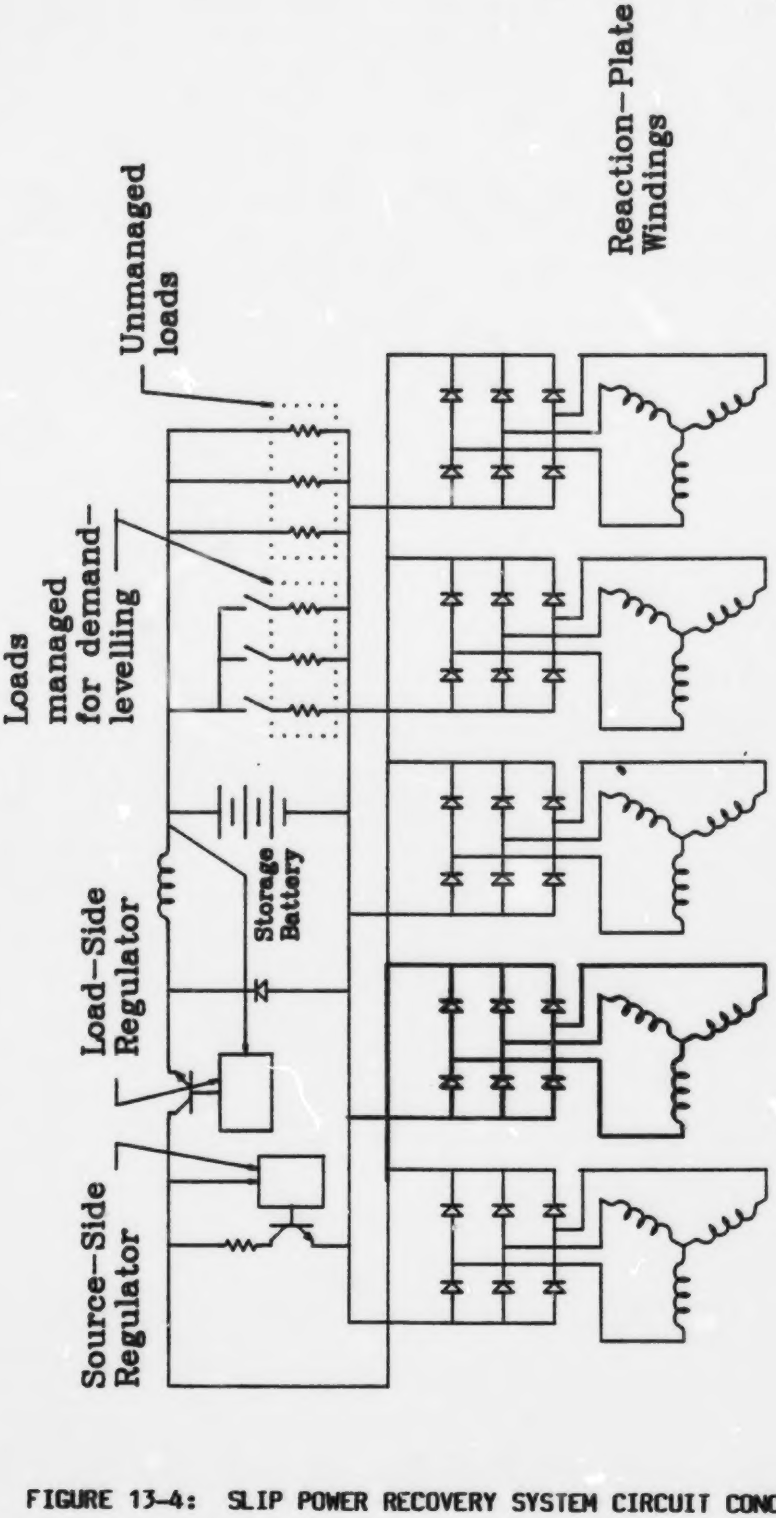
Reaction-Plate Windings
Unmanaged loads
Loads managed for demand-levelling
Load-Side Regulator
Storage Battery
Source-Side Regulator

FIGURE 13-4: SLIP POWER RECOVERY SYSTEM CIRCUIT CONCEPT

3) Source-Side Voltage Regulation

During periods of high slip power generation the battery and auxiliary loads may not present a sufficiently low resistance to the reaction plate winding to ensure power flow. Without slip power being dissipated of course, there can be no thrust. A possible means of ensuring a receptive load is to switch a "dummy load" across the rectified winding output with the appropriate "on/off" ratio to regulate at some fixed voltage.

4) Load-Managing Switching

Those loads which are only intermittently activated because of their functional nature, and which need not be instantly responsive to a control command could be permitted to switch-in only during periods when ample slip power is available. This type of load management would reduce the charging current to the batteries during charge cycles and reduce the amount of current supplied by the batteries during the discharge period.

13.4 BATTERY CHARGING WITH SLIP POWER RECOVERY

General

In order to make use of slip power recovered from a reaction plate of a lim-in-track propelled vehicle, the irregular nature of slip power must be overcome. A storage battery is a logical choice because its charge capacity versus mass and volume characteristics by far exceed those of capacitors and other electrical energy storage media. The basic problem is one of choosing the appropriate battery and designing a suitable charging system.

13.4.1 Battery Cycling

The method and frequency of charging a battery is important when designing such a system. Lead-acid batteries, in general, lend themselves more to buffer charging, where the battery charge is maintained often. One example is the car battery, which relies on the alternator to supply constant voltage, current limited charging power. Special deep-discharge lead-acid batteries, such as RV/marine batteries, are mechanically more robust, to handle deep-discharge, but have limited life compared to buffer charged lead-acid batteries.

Nickel-cadmium (Ni-Cad) batteries, on the other hand, typically have a 'memory', where, if they are only used to a fraction of their discharge capacity, they eventually become limited to that capacity. Newer Ni-Cad battery designs, however, include some that are capable of buffer and float charge at constant voltage, and fast charge at constant current.

13.4.2 Buffer Charging Techniques

While most battery manufacturers specify constant voltage buffer charging, or constant current fast charging, one manufacturer has shown a very novel approach.

It is a process involving high current charging bursts, in an effort to reduce thermal losses during charging, thereby increasing efficiency and speed. The result of fast charging is the production of gases. To rid the battery of gases, a technique referred to as 'burping',is used. Bursts of large negative current, which causes the battery to discharge the gas bubbles that were building up, as drawn from the battery. Using this method, it is claimed Ni-Cads can be fully charged in 20 minutes, where 7 to 8 hours is required at a constant current of 0.2 C_5A. (C_5 is the ampere-hour rating of a battery that is discharged to 1.00 volts/cell over a 5 hour period).

13.4.4 Battery Selection

In selecting the right size battery for use on a vehicle with slip power recovery, several factors are important:

a) The charge factor, "CF", which is the ratio of the number of ampere-hours required to fully charge the battery to the number of ampere-hours the battery can supply. For a standard Ni-Cad, using 0.2C_5A charging current, CF = 1.4 to 1.6. Burst charge batteries have a CF = 1.1.

b) The worst case capacity requirements of the vehicle electrical systems, "CV", expressed in ampere-hours. For example, if the longest trip the vehicle has to make between battery charges takes 10 minutes, and the average current requirement is 6 amps, CV = 6 x 10 amp-minutes = 1 Ah.

c) The charging current, "CI", which is the maximum current required by the charger during it's charging operation. For a standard Ni-Cad, CI = 0.2 C_5A. A burst charger, for a 20 min charge time, uses CI = 3.3 C_5A.

d) The charging time available, "CT", after the worst case discharge, as outlined in (b). For example, the time to charge after the 10 min discharge in (b) could be CT = 2 min = 0.033 hours.

Now, before selecting a battery, one has to check that the system can maintain a charge balance, by making sure that the long term average vehicle current requirement is less than the long term average slip power current available, times the charging factor of the battery.

Also, the current available must be greater than the charging current plus the vehicle's current requirements during the charging period.

Given the above criteria, we can then say that the short term charge balance is:

$$CI \times CT \geq CV \times CF$$

Using the example of a standard, constant current charging Ni-Cad system, with $CI = 0.2\ C_5A$ and $CF = 1.5$, and with A $CV = 1$ Ah and $CT = 0.033$ h, the equation is:

$$0.2\ C_5A \times 0.033\ h \geq 1\ Ah.1.5$$

$$0.0066\ C_5Ah \geq 1.5\ Ah$$

$$C_5 \geq 225$$

Now, for the same $CV = 1$ Ah, and $CT = 0.033$ h, if a reflex charging system is used, with $CF = 1.1$, and $CI = 3.3\ C_{5A}$, the equation is:

$$CI \times CT \geq CV \times CF$$

$$3.3\ C_{5A} \times 0.033\ h \geq 1\ Ah \times 1.1$$

$$0.11\ C_{5Ah} \geq 1.1\ Ah$$

$$C_5 \geq 10\ Ah$$

It can be seen from these two examples how important the charging current value is to the size of battery required for a vehicle.

13.5 AUTOMATIC GUIDANCE SYSTEM

The concept of a LIM-in-Track propulsion system with vehicle on-board automatic guidance has great potential as a replacement for factory floor AGVs. The important factors to consider are cost, flexibility, safety and reliability. The following sections outline the requirements and recommended solutions to the problems.

13.5.1 Steering Concept

The concept of four wheel steering best suits the requirements of LIM-in-Track propulsion, since it offers the capability to maintain minimum chording effects of a vehicle's reaction rail over a LIM in a curve. Also, if the vehicle was to be bi-directional, a steering mechanism would be required at each end of the vehicle.

To simplify the steering control requirements, totally autonomous controllers should be used at each end of the vehicle. This would be feasible if the guidance sensing system could supply suitable feedback for both ends of the vehicle. Also, the direction of longitudinal motion is a required input into the steering controller, since steering angle for error correction depends on the direction of travel.

The controller for such a system could be micro-processor based to allow maximum flexibility of the control algorithms, including non-linear functions, decision making, etc.

13.5.2 Sensing Systems

The two most common forms of guidance sensing are wire loop and infra-red reflective sensing, the latter being the more complicated, but more flexible. The advantage of the optical solution is that the vehicle path is determined by the placement of reflectors. This is ideal for AGVs, because it can be reprogrammed to take another path with reasonable ease, and does not involve burying a wire in the floor.

Unfortunately, optical systems can be interfered with by dirt, objects near reflectors and unusual lighting conditions. Wire guidance is more robust in this respect.

Establishment of a new path in flat floor LIT systems requires that the floor be excavated for installation of new LIMs and controllers. While this process is underway, a buried wire guidance system could easily be installed. Given its improved environmental tolerance and its ease of installation, wire guidance seems well suited to LIM applications.

13.5.3 Guidance Wire

While several types of wire guidance systems are in use, one type seemed particularly suitable for several reasons, which will become apparent.

For ease of installation, the two-wire guidance cable is advantageous, since it can be installed in one slot in the floor. The single-wire system needs a return path, or must follow a loop path, such as around an entire track.

The two-wire guidance cable can have reasonably close conductor spacing, so for experimentation purposes, common twin flat lead TV cable was judged suitable. It has a symmetrical magnetic field pattern, as in Figure 13-5a, which has a maximum strength directly over the centreline. The single wire has maximum (vertical component) strength to the sides, as in Figure 13-5b.

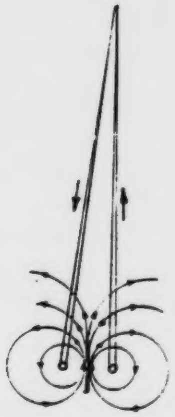

Figure 13-5a

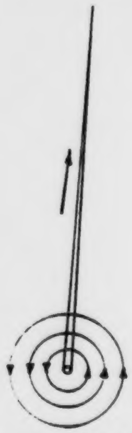

Figure 13-5b

13.5.4 Antenna Design

A loop antenna, with a width slightly wider than the conductor spacing of the guidance cable, and a reasonable length, could be expected to couple most of the field lines, as shown in Figure 13-6a. Alternatively, a loop antenna on either side could then be used to detect the return path of the field, as in Figure 13-6b.

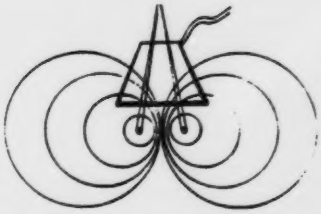

Figure 13-6a

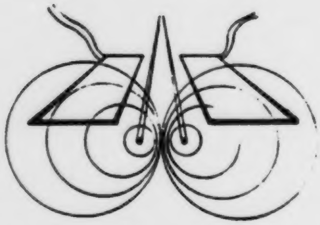

Figure 13-6b

Since the purpose of the antenna is to provide a signal which will help determine position error, the two loop design is more suitable. Addition of a ferrite core (see Figure 13-6c) would help concentrate flux lines through the loops, and addition of more loops would allow for easier "capture" of the signal should the vehicle be far off centre.

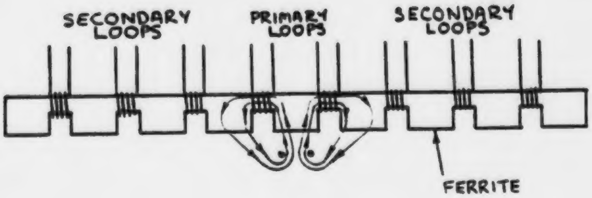
SECONDARY LOOPS
PRIMARY LOOPS
SECONDARY LOOPS
FERRITE

Figure 13-6c

Since the antenna must operate near a LIM, which has a large magnetic field output, it is recommended that the antenna length be an even number of LIM pole pitches, so that the net flux entering the antenna from a LIM will be small. This means, for example, that for a LIM with a 60 Hz synchronous speed of 6 m/s, the pole pitch is 50 mm, and the antenna could be 100 mm or 200 mm. See Figure 13-7a. The shorter length is recommended to minimize chording effects when the guidance cable has a sharp turning radius, as in Figure 13-7b.

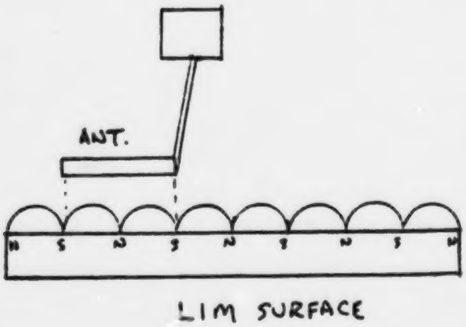
ANT.
N S N S N S N S N
LIM SURFACE

Figure 13-7a

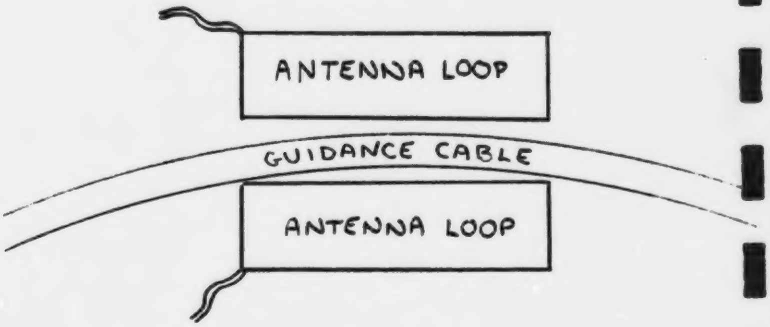
ANTENNA LOOP
GUIDANCE CABLE
ANTENNA LOOP

Figure 13-7b

It is also recommended that the guidance system transmission frequency be in the 20 kHz to 100 kHz range, but at a fixed frequency. Each loop antenna, with the addition of a capacitor, can form a tuned filter. The capacitor value can be chosen to maximize signal input and noise rejection, (see Figure 13-8). Such a simple second order filter arrangement can have a 40 dB per decade attenuation in the stop band. Therefore, a 60 kHz antenna will have 120 dB attenuation of a 60 Hz signal, without taking into consideration the filtering effects of a ferrite core.

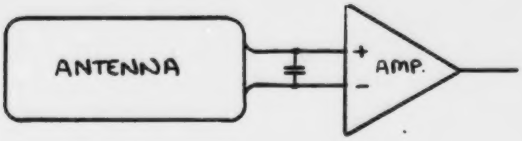

Figure 13.8

13.5.5 Antenna Signal Processing

Whether a two antenna system, as in Figure 13-6b, or multiple system, as in Figure 13-6c is used, the basic principle of guidance is the same. The vehicle is determined to be centred when the two (primary) antenna loops have equal signal levels. If one gets a stronger signal than the other, that is the one which as moved closer to the centre of the cable.

Either analog or digital circuitry could be used to derive a position error signal. While digital signal processing is more capable of producing a linear error output, the analog circuitry would be less expensive to develop and possibly to build. The lack of linearity in the error signal could be compensated for by using a micro-processor based steering controller.

13.5.6 Vehicle Path Selection

In a LIM-in-Track system using intelligent LIM controllers, such as LVCMs, each controller should each generate its own guidance transmission output, as in Figure 13-9. In fact, the frequency could be derived from the micro-processor clock in an LVCM, so that all LVCMs output almost identical frequencies, within the accuracy of the on-board crystals.

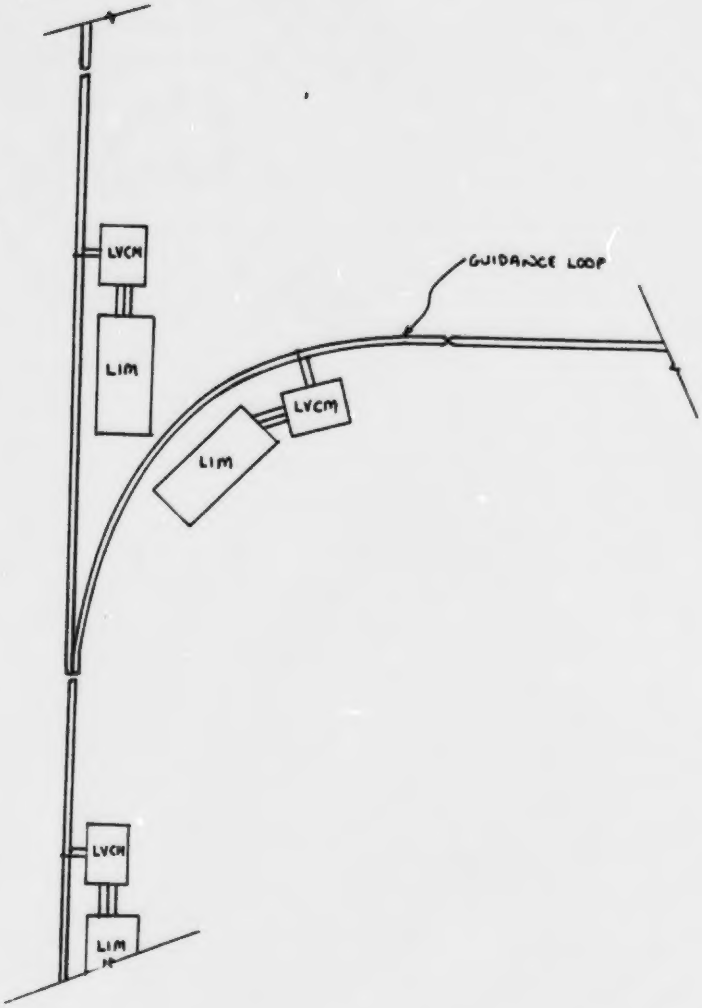
LVCM
LIM
GUIDANCE LOOP
LVCM
LIM
LVCM
LIM

FIGURE 13-9: WIRE GUIDED VEHICLE PATH SELECTION

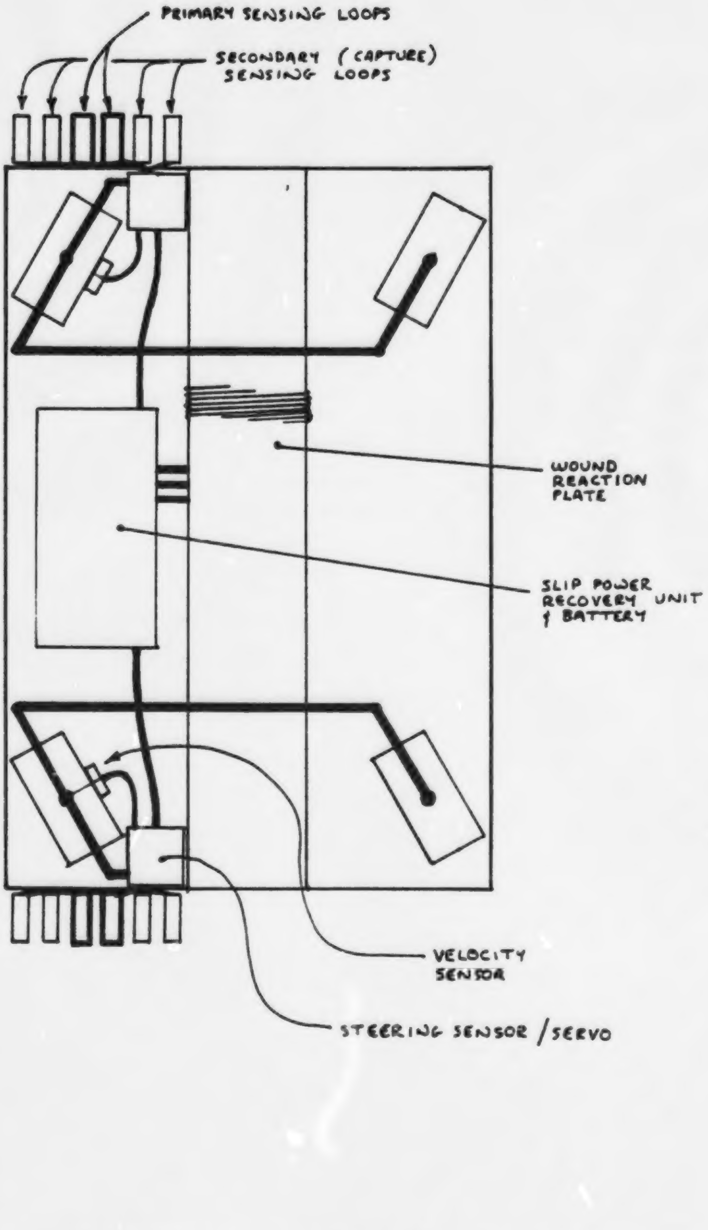
PRIMARY SENSING LOOPS
SECONDARY (CAPTURE) SENSING LOOPS
WOUND REACTION PLATE
SLIP POWER RECOVERY UNIT & BATTERY
VELOCITY SENSOR
STEERING SENSOR / SERVO

FIGURE 13-10: WIRE GUIDED VEHICLE UTILIZING SLIP POWER RECOVERY

Vehicle path selection is determined, then, by which LVCM has turned on it's guidance cable. This requires that each LVCM on the path the vehicle must take must know it has been selected as such by a supervisory level. With such a system in place, the wire guidance is complete.

13.5.7 Integrated Vehicle

Finally, with the guidance system in place, the vehicle requirements for an automatic guided LIM powered vehicle are known. As in Figure 13-10, the vehicle should have autonomous antenna and steering control equipment for each end of the vehicle, and a wound reaction plate with slip power recovery equipment to power the steering mechanism.

SUGGESTED FURTHER INFORMATION

Several areas mentioned require further investigation to help determine cost and technical feasibility of the slip powered automatic guided vehicle. These include:

a) Battery life for vehicles with heavy auxiliary current requirements or low charging duty cycles.

b) Antenna design to decrease cost and/or simplify signal processing equipment.

c) Vehicle steering dynamics, as they impact steering linkage and drive motor design, antenna and signal processing design, and velocity dependant steering algorithms.

d) Reliability and fault recovery for a guided vehicle steering system.

14.0 CONCLUSIONS AND RECOMMENDATIONS

14.1 RANGE OF APPLICATION

The basic LIT propulsion and control concepts described in this report are technically able to meet a very wide range of performance requirements.

The four applications specifically reviewed were:

1) a low speed industrial transport system
2) a high speed airport baggage transporter
3) an airport people mover
4) a container handling system

In each case, LIT with distributed control seems highly appropriate.

In fact, one might be at a loss to suggest any other technology that could satisfy the requirements of all four areas. Wheel adhesion limitations eliminate self-powered, wheel-driven alternatives. The power-rail hazard potential eliminates LIM-on-board, and belt or roller conveyor systems cannot achieve the required speeds.

While the four application areas studied exhibited widely varying requirements in terms of speeds, masses, grades and system lengths, they do not appear significantly different in terms of required functions. It is therefore likely that the key elements of the system, i.e. LIM controllers, communications network, sensors, etc., could be designed as "universal", mass-producable components.

14.2 LIM DESIGN

Design studies highlight the fact that there are key trade-offs in the areas of stator weight, and real and reactive power consumption. Assuming that appropriate weighting figures can be applied to these, optional designs may be sought so long as variable frequency control is employed. Fixed frequency control severely restricts one's opportunity to optimize.

There appears to be less to be gained by adapting VF control for "small" LIMs than for "big" LIMs. Below the range of 2-3 kN and 5% duty cycle it is not possible to effectively exploit longer pole pitch in a design, hence a key advantage of the VF approach is lost.

Above this range, LIMs designed for VF control are significantly better than FF-controlled LIM designs in terms of real and reactive power consumption.

Defining a methodology for LIM design has proven very difficult. A first step is to achieve an even balance of thermal and magnetic loading over the expected range of operating speeds and frequencies. Beyond this, judgement is required to achieve the appropriate trade-off balance of stator weight, reaction plate weight, real power and apparent power consumption. The trade-offs can be quite dramatic. For example, one design comparison was made in which a 29% stator weight increase resulted in a factor of two reduction in apparent power consumption.

Expert system software would not provide "answers" to trade-off dilemmas, but it may play a role in the "coaching" of inexperienced designers by explicitly highlighting the trade-off issues corresponding to any given step in the design process. For example, at the point where the designer selects a top cap depth the expert system might "suggest" that he try two slightly different depths and observe the sensitivities of weight, apparent power, etc. to this parameter.

14.3 MODELLING

The LIM model presented in this report predicts trends and performance reasonably well so long as the designs it models do not exhibit strong magnetic saturation or lateral edge effects. While better predictive tools are definitely available, it must be stressed that the utility of a model is determined as much or more by its "accessibility" as by its accuracy. Models that use involved mathematical constructions and which fail to link the abstract formulations with suitable physical pictures are likely to be more a hindrance than a help.

A technique which proved very useful was to augment the simple LIM model when necessary with Finite Element Analysis (FEA). FEA, when correctly employed and interpreted can produce a very accurate picture of the electromagnetic behaviour of a given LIM design. However, setting up the model and running variant design cases is relatively cumbersome. A combination of the simpler model and FEA works better than either alone.

14.4 DISTRIBUTED PROPULSION CONTROL

It is hard to overstate the significance of the distributed control concept in LIT applications. Besides resulting in an extremely robust arrangement in terms of failure tolerance, distributed control simplifies communications, health monitoring and multi-vehicle management. The costs of implementing distributed control have been kept within reason by adopting hardware developed for the industrial automation market. A future development area would be a version of the distributed network specifically tailored to LIT applications.

14.5 POWER CONTROL

The advance in the state of power semiconductor technology over the past decade has been quite rapid. Nevertheless, the cost differential between fixed and variable-frequency LIM control is still largely due to the differences in switching devices and associated circuitry. It is not at all unreasonable to expect that this differential will grow narrower over the coming decade as the applications of force-commutated power devices grow and demand increases. In the meantime, fixed frequency control is likely to prove most cost effective for "low-end" applications. It is recommended however that development of a variable frequency design be continued for use in large applications, e.g. above 3 kN thrust.

14.6 SLIP POWER APPLICATIONS

The Slip Power Recovery concept has been analyzed to the point where it appears technically feasible for applications such as the supply of 2 kW auxiliary loads on a People-Mover vehicle. There is some concern however, about the weight of batteries which may be required to be compatible with expected charging rates. This concern may be alleviated somewhat by employing "smart" load management control and/or advanced battery charging techniques.

Automated steering control supplied by slip power seems a worthwhile application as it provides a new degree of functionality; namely guidance.

The continued development of Slip Power Recovery is recommended, but should focus on the issues of battery-charging and load management in order to determine if these areas have reasonable technical solutions.

LIST OF REFERENCES

[1] D.B. Turner and W.L. Wolf, "Houston WEDway People Mover Control and Propulsion System", Conf. Proc. IEEE Vehicular Technology, May 1982.

[2] UTDC, "Transporter Development Program Phase II Final Report", UTDC Report #597 900 306.

[3] E.P. Steinmetz, "The Alternating Current Induction Motor", AIEE Trans., Vol. 14, pp. 185 - 217.

[4] E.M. Freeman, "Travelling Waves in Induction Machines: Input Impedance and Equivalent Circuits", IEEE Proc. Vol. 115, No. 12, Dec. 1968.

[5] F.W. Carter, "Air-Gap Induction", E.L. World and Engineering, 1901, pp. 884.

[6] B. Heller and V. Hamata, Harmonic Field Effects in Induction Machines, Elsevier, New York, 1965.

[7] P.L. Alger, The Nature of Induction Machines, Gordon and Breach, New York, 1965.

[8] R.L. Russell and K.H. Norsworthy, "Eddy Current and Wall Losses in Screened-Rotor Induction Motors", IEE Proc. 1958, pp. 163 - 175.

[9] D.E. Hesmondhalgh and D. Tipping, "Equivalent Rotor Impedance of Sheet-Rotor Induction Motors", IEE Proc., Vol. 130, Pt. B, No. 5, Sept. 1983.

[10] B.T. Ooi, "A Generalized Theory of the Linearized Induction Motor", IEEE Power Engineering Society Proc., Jan. 1973, pp. 1,252 - 1,259.

[11] E.R. Laithwaite, Induction Machines for Special Purposes, Newnes, London, 1968.

[12] G.E. Dawson and Gregory Ducharme, "Feasibility of an Expert System to Aid in LIM Design", Final Report to UTDC Inc. under SOW 330 001.

[13] S.D. Dewan and A. Straughen, Power Semiconductor Circuits, Wiley-Interscience, 1975.

[14] Alexander Mozdzer, J.R., and Bimal K. Bose, "Three Phase AC Power Control Using Power Transistors", IEEE Trans., Ind. App., Vol. IA-12, pp. 499 - 505, Sept./Oct. 1976.

[15] O. O'Kelly and S. Simmons, Introduction to Generalized Machine Theory, McGraw-Hill, 1968.

[16] Asish K. DeSarkar and Gunnar Berg, "Digital Simulation of Three-Phase Induction Motors", IEEE on Power Applications, Vol.-PAS-89, No. 6, July/August 1970.

APPENDIX A-1	DERIVATION OF MINIMUM ENTRY SPEED TO A VERTICAL TRANSITION
APPENDIX A-2	DERIVATION OF THE FORMULA FOR THE RMS FEEDER CURRENT IN L.I.T. SYSTEMS
APPENDIX A-3	STATOR SURFACES POWER DENSITY
APPENDIX A-4	REACTION PLATE POWER
APPENDIX A-5	LIM EQUIVALENT NETWORK COMPUTER MODEL
APPENDIX A-6	"FLUX BUNCHING" IN THE LIM CORE
APPENDIX A-7	FLUX DENSITY ESTIMATION FORMALAE
APPENDIX A-8	VERTICAL FORCE
APPENDIX A-9	SLIP FREQUENCY MAPPING

Appendix A-1 Derivation of Minimum Entry Speed to a Vertical Transition

Assumptions:

1. Vehicle can receive LIM thrust only after its trailing wheels are clear of the grade.
2. Drag effects are negligible.

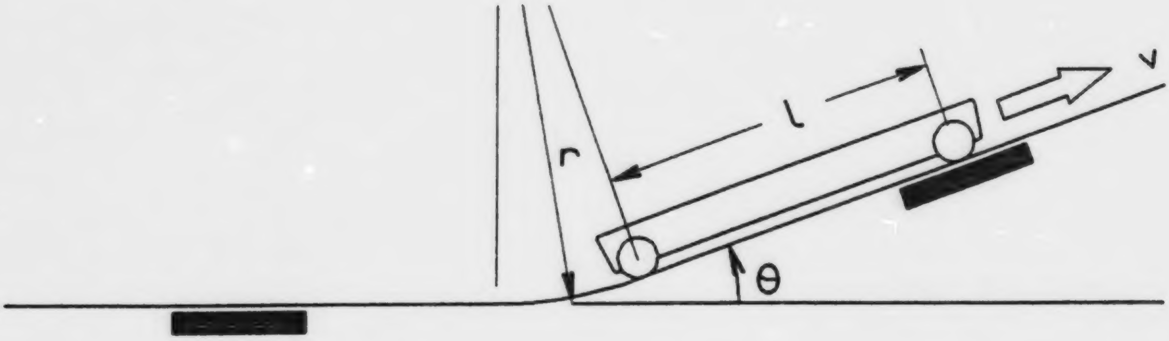

$$h_1 = r - r \cos \theta$$
$$h_2 = \frac{1}{2}\, l \sin \theta$$

$$\begin{aligned} h &= h_1 + h_2 \\ &= r\,(1 - \cos \theta) + \frac{l}{2} \sin \theta \end{aligned}$$

The energy of the vehicle at height h given an entry velocity of v_0 is :

$$\begin{aligned} E_h &= E - mgh \\ &= \frac{1}{2}\, m\, v_0^2 - mgh \\ &= m \left(\frac{v_0^2}{2} - g \left[r\,(1 - \cos \theta) + \frac{l}{2} \sin \theta \right] \right) \end{aligned}$$

The speed at height h can be determined from the kinetic energy as:

$$v_h = \sqrt{\frac{2\ E_h}{m}}$$

$$= \sqrt{2\left[\frac{v_0^2}{2}\quad g\left[r\left(1 - \cos\theta\right) + \frac{l}{2}\sin\theta\right]\right]}$$

Now v_h must be greater than zero to satisfy the "coast through" requirement. Hence:

$$v_{0\ \min} = \sqrt{2gr\left(1 - \cos\theta\right) + gl\sin\theta}$$

eg. suppose r = 3m, θ = 30°, l = 2m then $v_{0\ \min}$ = 4.2 m/s

Appendix A-2 Derivation of the Formula for the RMS Feeder Current in L.I.T. Systems

Notation: i_x -- instantaneous current
I_x -- long term RMS current

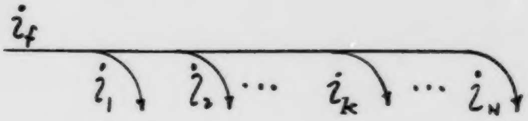

$$i_k = f_k(t) \sin(\omega t + \alpha_k)$$

Define $f_k(t) \equiv \dfrac{i_k(t)}{\sin(\omega t + \alpha_k)}$ for $x = 1, \ldots, N$

f_x is a periodic square wave function representing each LIM's "on" current magnitude.

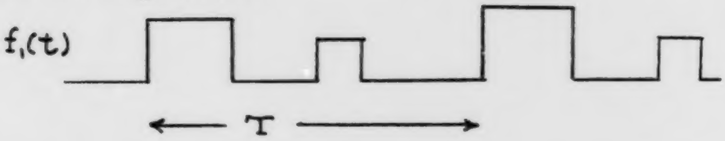

The RMS of $i_f(t)$ is:

$$I_f = \left[\frac{1}{T} \int_0^T \left[f_1(t) \sin(\omega t+\alpha_1) + f_2(t) \sin(\omega t+\alpha_2) + \ldots + f_N(t) \sin(\omega t+\alpha_N) \right]^2 dt \right]^{\frac{1}{2}}$$

$$= \left[\frac{1}{T} \int_0^T \left[\sum_{\substack{j=1 \\ k=1}}^{\substack{k=N \\ j=N}} f_j f_k \sin(\omega t+\alpha_j) \sin(\omega t+\alpha_k) \right] dt \right]^{\frac{1}{2}}$$

If there is no over lap between any of the LIM currents then the cross product terms $f_j f_k$, $j \neq k$ are all identically zero.

Using this simplification, the feeder current can be expressed as:

$$I_f = \left[\frac{1}{T} \int_0^T f_1^2 \sin^2(\omega t+\alpha_1) + f_2^2 \sin^2(\omega t+\alpha_2) + \ldots\right.$$

$$\left. + f_N^2 \sin^2(\omega t+\alpha_n)\, dt\right]^{\frac{1}{2}}$$

or

$$I_f = \sqrt{I_1^2 + I_2^2 + \ldots\ldots + I_N^2} \qquad 4B.1$$

In many L.I.T. systems the overlap between LIMs is negligible so feeder RMS current can be calculated using equation 4B.1. If there is a significant overlap, the feeder current can be corrected by including the cross product terms.

Appendix A-3 Stator Surface Power Density

Consider the power dissipated in a single slot of a LIM stator.

$$P_{slot} = (2NI)^2 R_{slot}$$

where $R_{slot} = \frac{\rho_{cu} W}{h_s w_s k_{fill}}$ = "bulk" slot resistance

Now $J = \frac{2NI}{h_s w_s k_{fill}}$ = slot current density

$A = \frac{2NI}{\tau_s}$ = surface current loading

$$P_{slot} = JA \rho_{cu} W \tau_s$$

The power density at the LIM surface is

$$P_{surface} = \frac{P_{slot}}{W \tau_s} = JA \rho_{cu}$$

Eg. If the JA product is 180 A^2/mm^3 and the copper resistivity is 225×10^{-7} then $P_{surface} = 4.05$ kW/m^2.

Appendix A-4 Reaction Plate Power

The power dissipated in the reaction plate is the product of the thrust on the plate and the speed of "slippage" of the travelling field wave across the surface of the plate. i.e.

$$P_2 = F (v_{field} - v) \qquad (1)$$

For fixed frequency systems the field velocity is a constant, and is twice the motor pole pitch times the frequency.

$$v_{field} = 2 \tau_p f \qquad (2)$$

It is important to note that in braking the field speed direction is reversed. A convention that handles this case is to assign a negative sense to frequency for negative phase sequence (plug mode) operation. The accompanying figure illustrates the use of the formula in plotting a power vs. time profile.

For variable frequency LIM control it may be convenient to express the reaction plate power in terms of slip frequency. It can be shown that the following form is equivalent to equation (1).

$$P_2 = F\, sf\, 2\, \tau_p \qquad (1a)$$

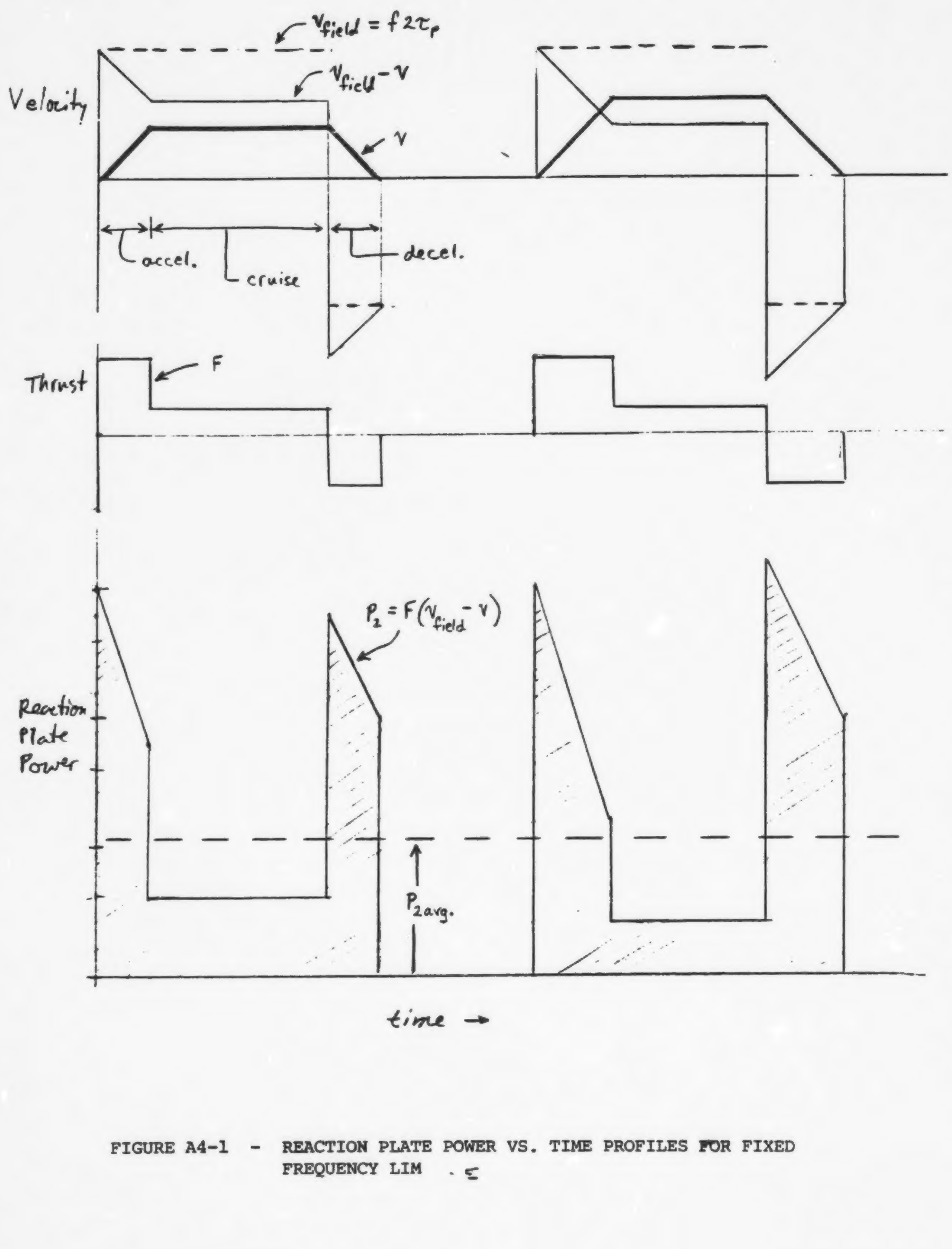

$v_{field} = f 2\tau_p$
$v_{field} - v$
Velocity
v
accel.
cruise
decel.
Thrust
F
$P_2 = F(v_{field} - v)$
Reaction Plate Power
$P_{2avg.}$
time →

FIGURE A4-1 - REACTION PLATE POWER VS. TIME PROFILES FOR FIXED FREQUENCY LIM

Appendix A-5 LIM Equivalent Network Computer Model

Introduction

The LIM Equivalent Network is an electric circuit analog of the linear induction motor. Two FORTRAN computer programs are employed to construct and solve the network based on user-supplied design and operating information. The first, WCA (Waveform Construction and Analysis) creates and applies Fourier analysis to the magnetomotive force (MMF) distribution for a LIM stator with given slot/tooth geometry, pole pitch, coil pitch and number of poles. The second, LEN (LIM Equivalent Network) uses the output of WCA along with the remaining LIM design variables to construct the equivalent circuit. It then applies the given operating conditions (terminal voltage or current, frequency and velocity) to solve the circuit, i.e. to calculate behaviour or "performance" of the LIM. Also derived from the circuit and input design variables are magnetic loading (flux density), electric loading and the amounts of copper and steel used in the design.

Figure A5-1 provides a block-diagram overview of the LIM Equivalent Network Computer program.

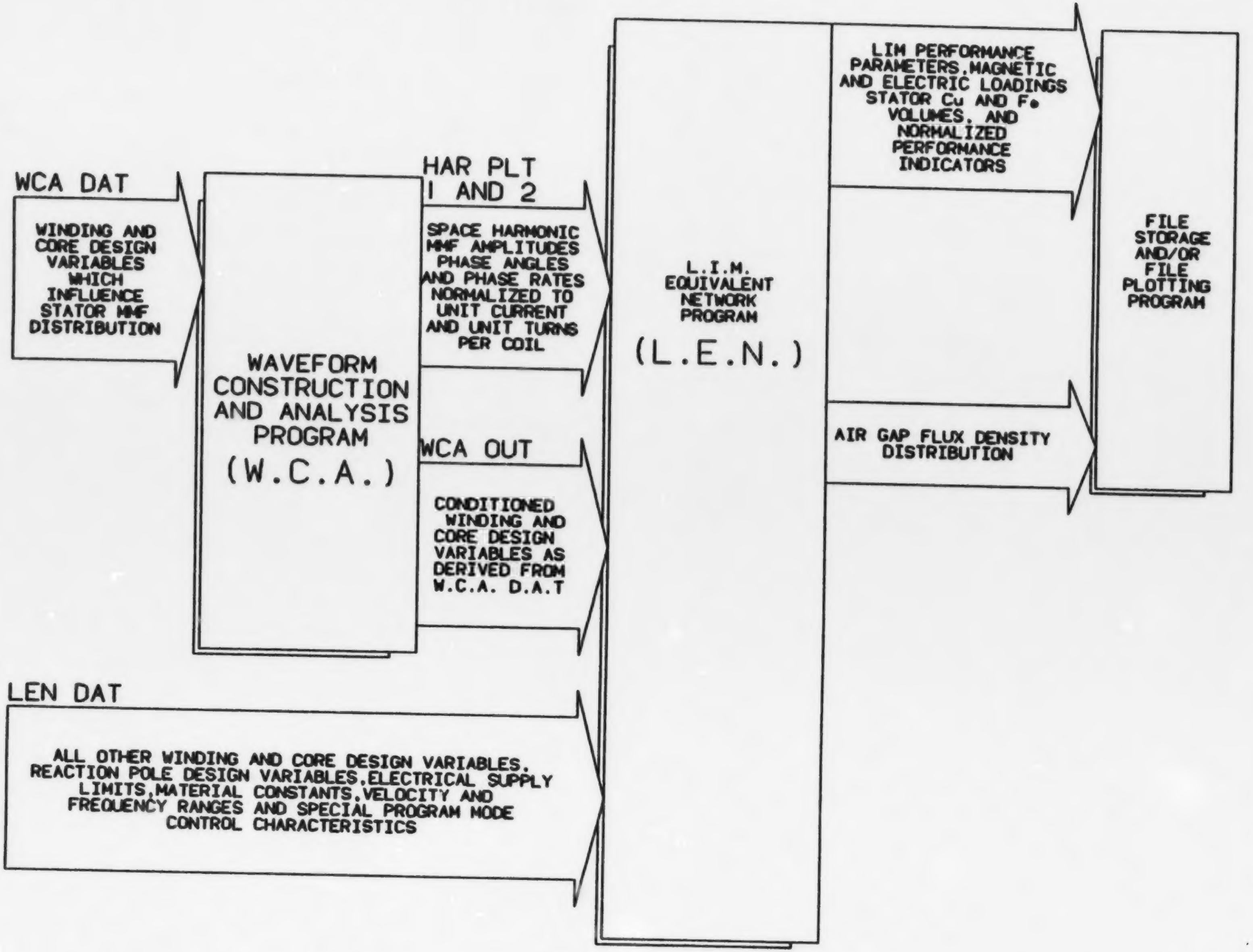
WCA DAT
WINDING AND CORE DESIGN VARIABLES WHICH INFLUENCE STATOR MMF DISTRIBUTION
WAVEFORM CONSTRUCTION AND ANALYSIS PROGRAM
(W.C.A.)
HAR PLT 1 AND 2
SPACE HARMONIC MMF AMPLITUDES PHASE ANGLES AND PHASE RATES NORMALIZED TO UNIT CURRENT AND UNIT TURNS PER COIL
WCA OUT
CONDITIONED WINDING AND CORE DESIGN VARIABLES AS DERIVED FROM W.C.A. D.A.T
LEN DAT
ALL OTHER WINDING AND CORE DESIGN VARIABLES, REACTION POLE DESIGN VARIABLES, ELECTRICAL SUPPLY LIMITS, MATERIAL CONSTANTS, VELOCITY AND FREQUENCY RANGES AND SPECIAL PROGRAM MODE CONTROL CHARACTERISTICS
L.I.M. EQUIVALENT NETWORK PROGRAM
(L.E.N.)
LIM PERFORMANCE PARAMETERS, MAGNETIC AND ELECTRIC LOADINGS STATOR Cu AND Fe VOLUMES, AND NORMALIZED PERFORMANCE INDICATORS
AIR GAP FLUX DENSITY DISTRIBUTION
FILE STORAGE AND/OR FILE PLOTTING PROGRAM

FIG A5-1 LIM EQUIVALENT NETWORK COMPUTER MODEL BLOCK DIAGRAM

Appendix A-6 "Flux Bunching" in the LIM Core

Equivalent magnetic circuits are a simplified but useful means of representing the behaviour of magnetic flux in a LIM. Reference [7] reviews the basic principles.

Figure A6-1 a) and b) illustrate the physical geometry and corresponding magnetic circuit for a ficticious LIM of infinite length. The magnetomotive force (MMF) sources, one per tooth, are shown with a direction and strength corresponding to a particular instant in time. At subsequent instants the pattern of these mmfs changes so as to bring about the "travelling" action of the flux wave.

Note that the instantaneous gap flux and core flux are distributed in space with the same wavelength. Over time these waveforms trace out envelopes of constant magnitude. Figure A6-1 e) illustrates the time averaged flux in the core.

The LIM depicted in Figure A6-1 does not represent the practical and very real effecto of finite length of the stator core. If the ends of the stator are thought of as inpenetrabble to flux then a section can be "chopped" out of the infinitely extending magnetic circuit and the current paths redrawn to conform to the new boundary constarints. This is done in Figure A6-1 b). Note that the gap flux waveform c) is identical to that in the infinitely long LIM but the core flux waveform d) has changed dramatically. Subsequent "snapshots" of the magnetic circuit behaviour over time, e), reveal that there are points in the core which never see flux, and points which see twice as much flux as the infinitely long LIM. This pattern is reminiscent of the nodes and antinodes in a standing wave.

In practice, the "bunching" of flux due to finite stator length has design implications. If a designer were to assume a uniform core flux distribution as exhibited in rotary motors he would fail to provide sufficient depth in the core to keep flux densities within reasonable limits.

It whould be recognized that the phenomenon of flux bunching as described for the stator core also occurs in the reaction plate core, and the save design cautions apply.

a) PHYSICAL GEOMETRY SHOWING FLUX LINES AT ONE INSTANT IN TIME

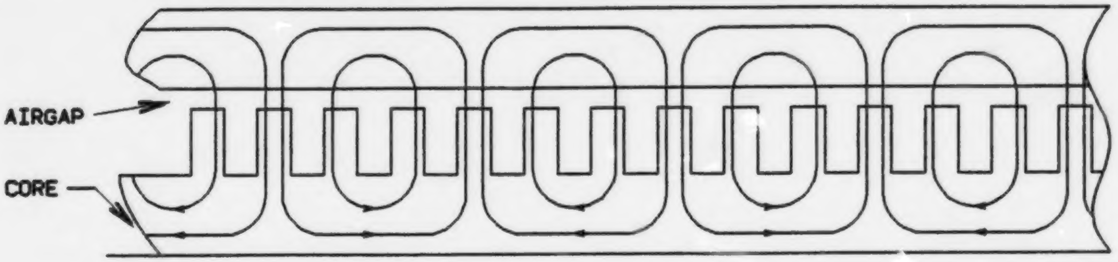

b) MAGNETIC CIRCUIT

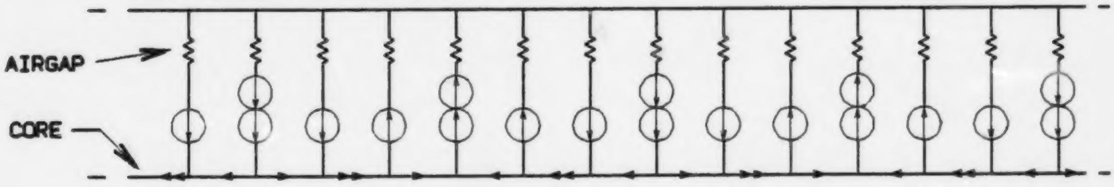

c) GAP FLUX

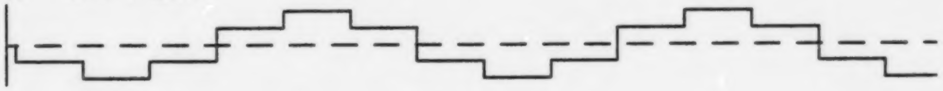

d) CORE FLUX

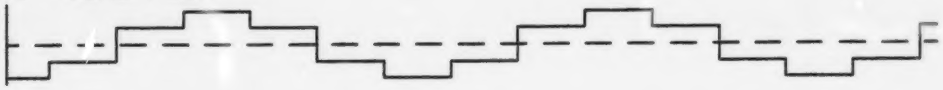

e) TIME AVERAGED CORE FLUX ENVELOPE (SHOWN HATCHED)

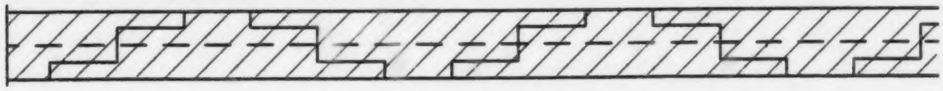

FIGURE A6-1 CORE FLUX DISTRIBUTION DEVELOPED FROM THE MAGNETIC CIRCUIT OF AN INFINITELY-EXTENDED LIM

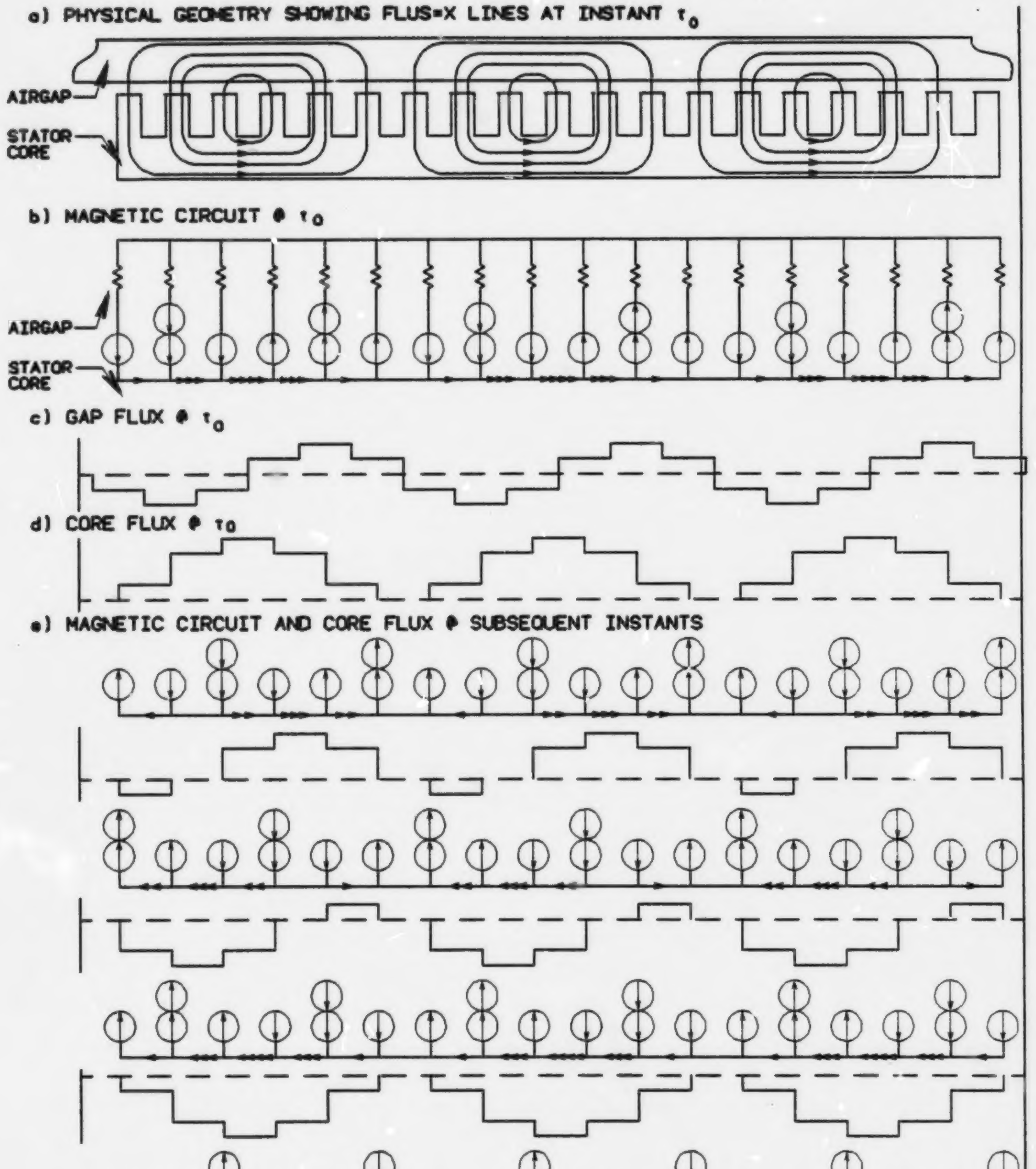

a) PHYSICAL GEOMETRY SHOWING FLUS=X LINES AT INSTANT t_0

b) MAGNETIC CIRCUIT @ t_0

c) GAP FLUX @ t_0

d) CORE FLUX @ t_0

e) MAGNETIC CIRCUIT AND CORE FLUX @ SUBSEQUENT INSTANTS

f) TIME-AVERAGED CORE FLUX ENVELOPE (SHOWN SHADED)

AIRGAP
STATOR CORE
AIRGAP
STATOR CORE

FIGURE A6-2: CORE FLUX DISTRIBUTION DEVELOPED FROM THE MAGNETIC CIRCUIT OF A FINITE-LENGTH STATOR

Appendix A7 Flux Density Estimation Formalæ

A7.1 Pole Flux

The effective or RMS airgap flux density is determined in the program LEN. This is the starting point for calculating the representative pole flux. An instantaneous, sinusoidal airgap flux density distribution can be constructed based on the RMS value as follows:

$$B(x) = \sqrt{2}\ B_{RMS} \sin \frac{\pi}{\tau_p} x \qquad (1)$$

Note that (1) is an idealized version of the actual distribution upon which B_{RMS} was based. The distrotions resulting from the entry-end effect, half filled end-slots , winding space harmonics and slot space harmonics are buried in the term B_{RMS} but not exhibited in the waveform of B(x).

The pole flux is obtained by integrating the flux density over the pole face. It is assumed that the flux density does not vary across the stator width.

$$\phi_{pole} = W \int_{\substack{pole\\start}}^{\substack{pole\\end}} B(x)\ dx$$

$$= W \int_0^{\tau_p} B_{RMS} \sin \frac{\pi}{\tau_p} x\ dx$$

$$= \frac{2\sqrt{2}}{\pi}\ W\ \tau_p\ B_{RMS} \qquad (2)$$

A7.2 Slot Leakabe Flux per Pole

The general expression relating flux, inductance and current is:

$$L = \frac{k_w\ Nb\phi}{i} \qquad (3)$$

The slot leakage flux for a single pole may be related to the slot leakage inductance term and the current that flows in it as follows:

$$\frac{\phi_{slot}}{2\,p} = \phi_{spole} = \frac{L_s \sqrt{2}\; I_1}{k_w\, N\, b\, 2\, p} \qquad (4)$$

A7.3 Reaction Plate Core Flux Density

The reaction plate core carries only the pole flux. Appendix 5D shows that unlike the infinitely extended stator, in which the pole flux splits so that the the core sees only half of the pole flux in any given cross-section, the LIM stator sees all the pole flux in some core sections and none is others. The peak reaction plate core fluxe density is therefore simply calculated as:

$$B_{R\ core} = \frac{\phi_{pole}}{W\, h_{R\ core}} \qquad (5)$$

The stator core sees both the pole flux and the per pole slot leakage flux. the spatial distribution of the slot leakage flux is such that under zero slip conditions the peaks of both fluxes are in phase in the core, and the peak flux density may be determined by the simple addition of the componenet fluxex divided by the stator core cross section.

$$B_{S\ core} = \frac{\phi_{pole} + \phi_{spole}}{W\, h_{S\ core}} \qquad (6)$$

At higher slip frequencies the effect of the back emf due to reaction plate currents tends to shifth the airgap flux distribution slightly so that the peaks of the pole flux and slot leakage flux do no coincide. Equation (6) will therefore tend to over predict as slip frequency increases. This effect may be noted in the LEN/FEA comparison plots of Figure 5-17.

Appendix A-8 Vertical Force

Magnetic (Attractive) Component

The airgap flux density in terms of the airgap mmf is:

$$B = \frac{\mu_0 \, F}{g}$$

Where B and F are effective or RMS values. The energy stored in the airgap is:

$$E = \frac{1}{2} \int_{vol} \frac{B^2}{\mu_0} \, dv$$

$$= \frac{1}{2} W \, g \, l \, \frac{B^2}{\mu_0}$$

$$= \frac{1}{2} W \, g \, l \, \mu_0 \, \frac{F^2}{g}$$

If the gap is changed an incremental amount, Δg, then the change in energy is

$$\Delta E = E - E'$$

$$= \frac{1}{2} W \, l \, \mu_0 \, \frac{F^2}{g} - \frac{1}{2} W \, l \, \mu_0 \, \frac{F^2}{g + \Delta g}$$

$$= \frac{1}{2} W \, l \, F \, \frac{\Delta g}{g^2 + g \, \Delta g}$$

if Δg is small, ie. $\Delta g << g$ then

$$\Delta E = \frac{1}{2} W \, l \, \mu_0 \, F^2 \, \frac{\Delta g}{g^2}$$

Now ΔEnergy = Force x ΔDistance so

$$F_{att} = \frac{\Delta E}{\Delta g}$$

$$= \frac{1}{2} W \, l \, \mu_0 \, \frac{F^2}{\Delta g}$$

$$= \frac{W \, l \, B^2}{2 \, \mu_0}$$

Electrical (Repulsive) Component

The second component of the LIM vertical force is a repulsive force due to an interaction between currents in the primary and secondary. This is a particularly complicated force to predict analytically. It has been found that this force can be approximated as:

$$F_{rep} = k\ I_1\ I_2$$

where I_1 and I_2 are the primary and secondary currents and k is an imperically derived constant of proportionality which depends on motor geometry.

The total vertical force is the algebraic sum of the repulsive and attractive forces.

Appendix A-9 Slip Frequency Mapping

Most of the literature dealing with induction machines presents plots of machine performance against slip or speed. Figure A9-1 shows the clossic thrust speed curve. This convention is quite adequate for fixed frequency applications but it becomes cumbersome when variable frequency supplies are used. For example suppose test were made at three frequencies. There would be three sets of synchronous speeds and three sets of slips. The thrust data would be plotted as in figure A9-2. The graph quickly fills up with lines and it becomes difficult to compare curves. An alternate approach is slip frequency mapping. Machine performance is plotted against slip frequency in this approach.

$$\text{slip frequency} = s\,f$$

$$= \left[\frac{v_s - v}{v_s}\right] f$$

$$= f - \frac{v}{2\tau}$$

Using this mapping, the data in figure A9-2 can be redrawn as figure A9-3 This mapping transforms the data in figure from a set of constant frequency lines to a set of constant speed lines. The curves are now drawn on a common horizontal axis and the effects of speed are readily seen. Slip frequency mapping has some interesting effects on the location of the familiar induction machine modes of plugging, regeneration and motoring. Figure A9-1 is redrawn in figure A9-4 shown the regions of operation.

Plugging and regeneration are both braking modes, however, plugging is characterized by high slip ($s > 1$). A slip frequency mapping is shown with theses regions marked in figure A9-5. The right half of the sf plane is unambiguously a motoring region because $T > 0$ and $v > 0$. The location of regeneration and plugging is not immediately obvious, however. Using equation A9-1, it can be seen that for every velocity there is some slip frequency at which the supply frequency must change sign. This occurs at

$$sf = \frac{-v}{2\tau}\ .$$

This point represents a phase reversal and a move to high slip operation. This is the division between regeneration and plugging.

The transition is perfectly smooth in the thrust characteristic but other machine characteristics have a discontinuity at the transition point. Power factor, efficiency and input impedance are all discontinuous because of the change in phase sequence. The speed dependence of the transition point is clearly shown in figure 5-28. As speed increases this point moves to the left.

FIGURE A9-1

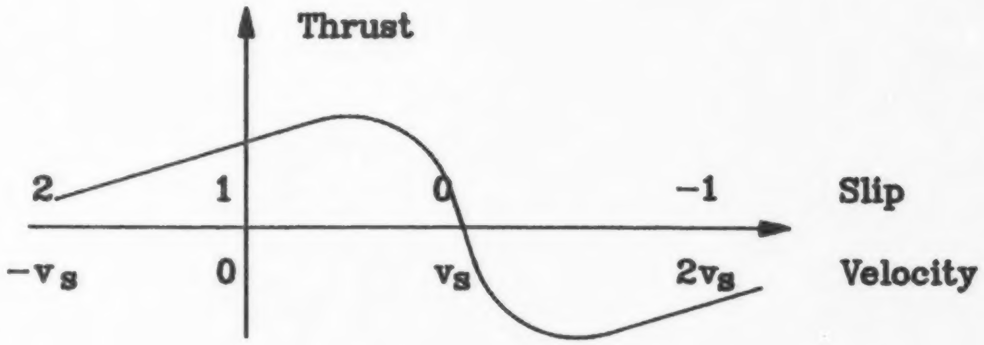

FIGURE A9-2

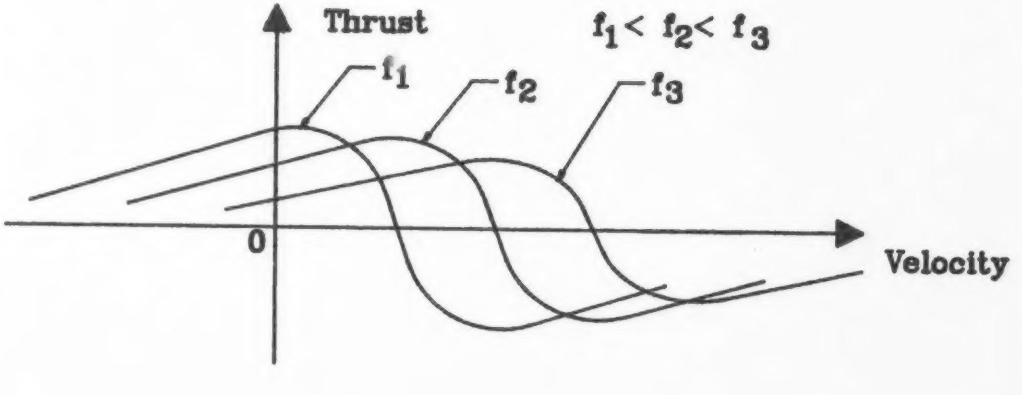

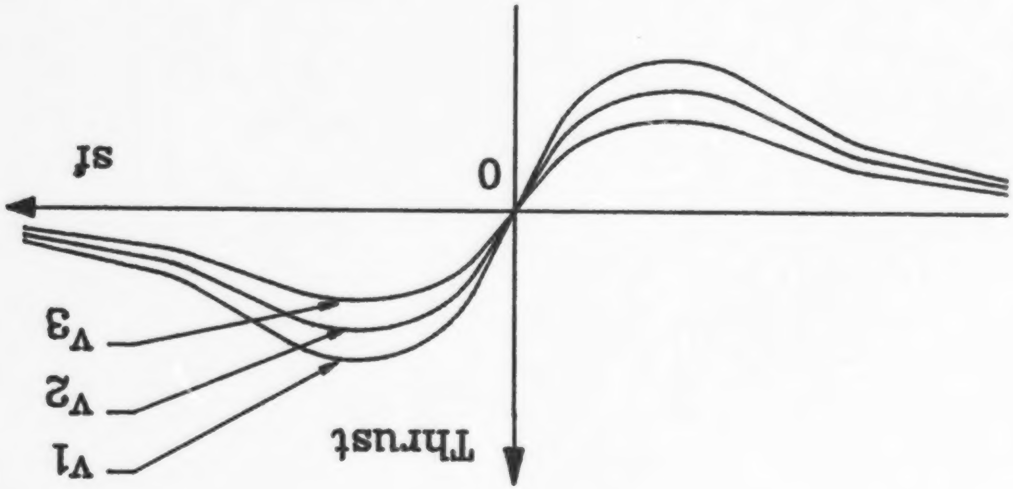

FIGURE A9-3

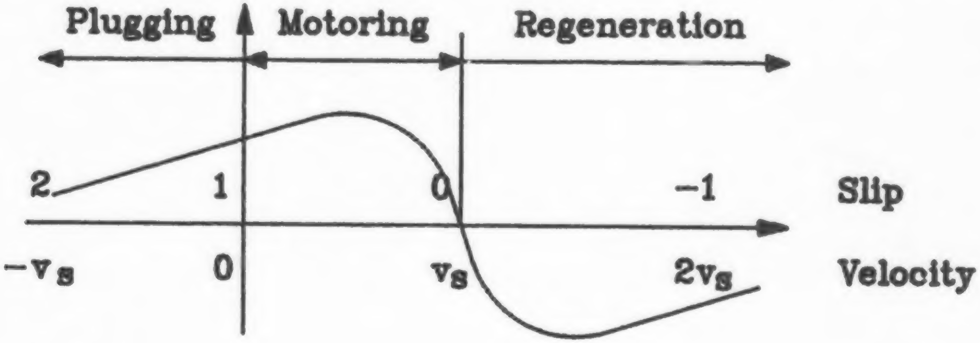

FIGURE A9-4

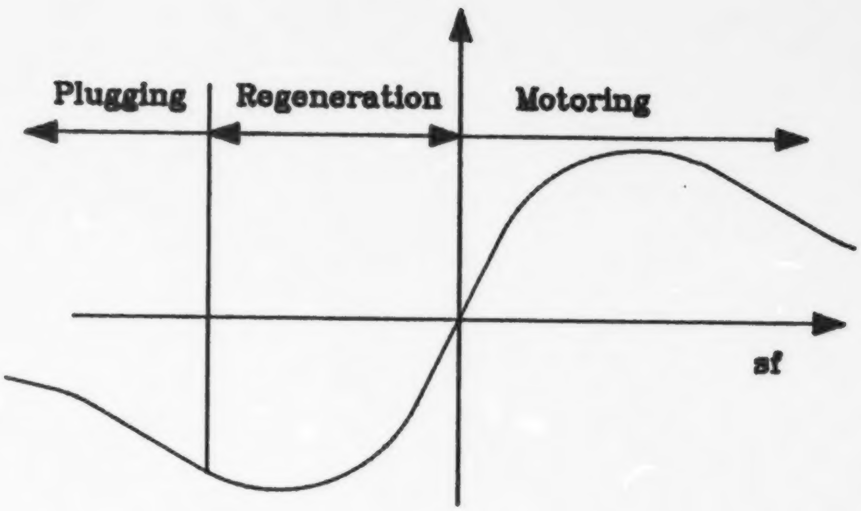
Plugging
Regeneration
Motoring
sf

FIGURE A9-5

APPENDIX B

SENSING, CONTROL AND COMMUNICATION
for
IN-TRACK LIM DRIVES

FINAL REPORT

L. Tong

G.E. Dawson

A.R. Eastham

This study was conducted for the Urban Transportation Development Corporation Research and Development Limited under Purchase Order No. 426-427.

Department of Electrical Engineering
Queen's University
Kingston, Ontario
K7L 3N6

January 1988.

MICROCONTROLLER CONTROL OF LINEAR INDUCTION MOTOR DRIVE SYSTEMS

by

Louis Tong

A thesis submitted to the
Department of Electrical Engineering
in conformity with the requirements for the
Degree of Master of Science

Queen's University
Kingston, Ontario, Canada
December, 1987

Copyright © Louis Tong, 1987

ABSTRACT

Louis Tong: Microcontroller control of linear induction motor drives, M.Sc. thesis, Queen's University at Kingston, December, 1987.

Linear induction motor (LIM) drives find wide appeal as propulsion drives in track-based transport systems, because of their ruggedness, low maintenance operation, adhesion independent propulsion thrust and low cost. This thesis concentrates on the control of an in-track LIM system developed at the Urban Transportation Development Corporation, Kingston, Ontario. The stator of the system is imbedded in the ground and the vehicle carries the passive reaction rail. The system is designed for low power applications such as material handling systems for automated factories or baggage carrying systems for airports. The benefits of this system compared to a conveyor system, are speed, a high degree of control over individual unit loads and a flexible layout. The control of the overall system is realized by a distributed control scheme. A single-chip microcontroller is used to provide local speed and position control at each stator. Each stator controller is linked to the host computer for overall system control. The Intel 8097 single-chip microcontroller is used to simplify the hardware complexity and to implement a sophisticated speed control algorithm, since it has enough capacity, CPU speed and I/O capability.

The speed control method investigated and the algorithm implemented in this thesis is a variable-voltage variable-frequency (VVVF) control scheme. Various VVVF control schemes and inverter switching techniques are discussed. In particular, the slip frequency stator current (SI) method is determined to be best suited for the LIM speed control operation. As well, the regular sampled pulsewidth modulation (PWM) technique is chosen as the inverter switching strategy. A LIM-in-track control system prototype was constructed to demonstrate the VVVF control of a LIM. Hardware and software implementation of the system prototype is presented. Design considerations and implementation techniques are discussed. Experimental results are presented to verify some of the control operations.

TABLE OF CONTENTS

Chapter 1 INTRODUCTION / BACKGROUND 1

1.1 Introduction 1

1.2 LIM-In-Track Propulsion Systems 2

1.3 Potential Performance Gain Using Variable-Voltage and Variable-Frequency Control 5

1.4 History of Inverter Drives 9

1.5 Thesis Scopes and Outline 12

1.5.1 Thesis Objectives 12

1.5.2 Thesis Outline 12

Chapter 2 PWM SCHEMES AND VVVF SPEED CONTROL METHODS 14

2.1 Introduction 14

2.2 Linear Induction Motor 16

2.2.1 LIM Stator 16

2.2.2 LIM Reaction Plate 18

2.3 PWM Inverter Drive 19

2.3.1 Advantages of PWM Inverter Drive 19

2.3.2 Development in PWM Techniques 20

2.3.2a Natural Sampled Modulation 21

2.3.2b Regular Sampled Modulation 23

2.3.2c Optimal PWM 25

2.4 VVVF Speed Control of LIM 26

2.4.1 Constant Volt/Hz Control 27

2.4.2 Field Oriented Control (FOC) 28

2.4.3 Slip Frequency Stator Current (SI) Control 30

Chapter 3 LIM-IN-TRACK THRUST/VELOCITY CONTROL 33
3.1 VVVF Speed Control of LIM 33
3.2 Velocity Control Loop 34
3.3 Current Control Loop 36
3.4 Slip Frequency Control Loop 41

Chapter 4 OVERALL SYSTEM DESIGN AND HARDWARE IMPLEMENTATION . . 47
4.1 Introduction 47
4.2 Hardware Overview 49
4.3 Hardware Implementation 50
4.3.1 Microcontroller Unit 50
4.3.2 Memory Unit 52
4.3.3 Current Sampling Interface 55
4.3.4 Position Sensor Interface 56
4.3.5 Inverter Gate Drive Interface 59
4.3.6 Reset Circuit 60

Chapter 5 SOFTWARE DESIGN AND IMPLEMENTATION 61
5.1 Software Overview 61
5.2 Software Implementation 64
5.2.1 PWM Module 64
5.2.1a PWM Interrupt Handler Routine 70
5.2.1b Frequency Changing Routine 73
5.2.2 Current Control Module 75
5.2.2a Current Sampling Interrupt Handler Routine 75
5.2.2b Square-Root Routine 78
5.2.3 Position Sensing Module 81
5.2.3a Sensor Interrupt Handler Routine 82
5.2.3b Sensor Reading Routine 85

5.2.3c Position Update Routine 87

5.2.4 Velocity/Thrust and Slip Frequency Control Module . . 91

5.2.4a Velocity/Thrust Control Routine 94

5.2.4b Slip Frequency Control Routine 95

Chapter 6 TESTING 99

6.1 Introduction 99

6.2 Software Development Facility 100

6.3 Preliminary Module Testing 102

6.4 Comprehensive Testing 108

6.4.1 Test Equipment 111

6.4.2 Testing and Results 115

Chapter 7 CONCLUSIONS 132

7.1 Introduction 132

7.2 Assessments of the System 133

7.3 Recommendations 136

REFERENCES 138

APPENDIX 140

A. Hardware Features of Intel 8097 Microcontroller 140

B. LFCM Prototype Board Layout and Schematic 142

C. Effect of DC Offset on Current Magnitude Calculation . . . 146

VITA 148

LIST OF FIGURES

1.1 LIM-In-Track propulsion system 3

1.2 Block diagram of the LIM-in-track propulsion system configuration 4

1.3 LIM voltage control module (LVCM) position/velocity control scheme 6

1.4 Comparison of LIM performance using VVVF and VVFF control . . 8

1.5 Diagram of a PWM inverter drive 10

2.1 LIM-in-track propulsion system configuration 15

2.2 In-track linear induction motor 17

2.3 Natural sampled PWM 22

2.4 Regular sampled PWM 24

2.5 Equivalent circuit model of one phase of induction motor . . 28

2.6 Stator current components in d-q frame 29

2.7 Slip frequency stator current (SI) method 31

2.8 Induction motor characteristics 31

3.1 Simplified block diagram of LFCM speed control scheme . . . 34

3.2 LIM thrust characteristics with an aluminum reaction plate . . 35

3.3 LFCM speed control scheme 37

3.4 LFCM speed control with a current feedback control loop . . 38

3.5 Thrust versus slip frequency characteristics of a LIM . . . 42

3.6 Power factor versus slip frequency characteristics of a LIM . 43

3.7 Efficiency versus slip frequency characteristics of a LIM . . 44

3.8 Complete block diagram of the LFCM speed control scheme for implementation using a microcontroller system 46

4.1 Block diagram of the LFCM microcontroller system 48

4.2 8097 microcontroller block diagram 52

4.3 LFCM memory map 54

4.4 Current sampling interface 55

4.5 LFCM sensor arrangement 57

4.6 Circuitry of the gate drive interface 59

4.7 Reset circuit 60

5.1 LFCM system software structure 62

5.2 LFCM software routine priority structure 63

5.3 Microcontroller implementation of regular sampled PWM . . . 66

5.4 Generation of a regular sampled width-modulated pulse . . . 67

5.5 PWM segmentation scheme 69

5.6 Simplified flowchart of the PWM Interrupt Handler Routine . . 72

5.7 Simplified flowchart of the Frequency Changing Routine . . . 74

5.8 Block diagram of the PI current controller 76

5.9 Simplified flowchart of the Current Sampling Interrupt Handler Routine 77

5.10 Linear lookup table for a square-root function 79

5.11 Hash table for a square-root function 79

5.12 Simplified flowchart diagram of the Square-Root Routine . . 80

5.13 LFCM system with a passing train 83

5.14 Bit representation of the LFCM sensor status register . . . 84

5.15 Simplified flowchart of the Sensor Interrupt Hardler Routine 86

5.16 Simplified flowchart diagram of the Sensor Reading Routine . . 88

5.17 Determination of vehicle position change 89

5.18 Simplified flowchart of the Position/Velocity Update Routine 92

5.19 Simplified flowchart diagram of the Velocity/Thrust and Slip Frequency Control Module 93

5.20 Determination of demand velocity by linear interpolation between two table points 94

5.21 Simplified flowchart diagram of the Velocity/Thrust Control Routine 96

5.22 Simplified flowchart diagram of the Slip Frequency Control Routine 98

6.1 Photograph of the LFCM prototype and the INTEL 8097 emulator board setup 101

6.2 Simulated 3-phase inverter and load circuit 103

6.3 Phase and pole voltages of one of the simulated 3-phase inverter/load circuits during change of frequency 104

6.4 Close-up phase and pole voltages of one of the simulated 3-phase inverter/load circuits during change of frequency . . 105

6.5 Phase voltage of two of the simulated 3-phase inverter/load circuits during a sequence reversal operation 106

6.6 Close-up phase and pole voltages of the reversed phase of the simulated inverter/load circuits during reversal 107

6.7 Plots of derived current magnitude (I) and phase current (I_a) versus time 109

6.8 Simulated inverter/load current response at $f = 10$ Hz . . . 110

6.9 Photograph of the LFCM experimental test setup 112

6.10 Schematic view of the test wheel 113

6.11 Photograph of the position sensor and magnetic strip 114

6.12 Schematic of the GTO 3-phase bridge inverter circuit 116

6.13 Photographs of the induction motor phase current and the inverter gating signal 117

6.14 Photographs of the phase current harmonic spectra 119

6.15 Photograph of the induction motor phase voltage 120

6.16 Photograph of two of the induction motor phase currents . . 120

6.17 LFCM controlled induction motor current response at $f = 10$ Hz, $K_P = 0.25$, $K_I = 0.625$ and $T_s = 1.67$ msec 121

6.18 LFCM controlled induction motor current response at $f = 10$ Hz, $K_P = 0.25$, $K_I = 0.5$ and $T_s = 1.67$ msec 122

6.19 LFCM controlled induction motor current response at $f = 10$ Hz, $K_P = 0.375$, $K_I = 0.5$ and $T_s = 1.67$ msec 123

6.20 LFCM controlled induction motor current response at $f = 20$ Hz, $K_P = 0.375$, $K_I = 0.5$ and $T_s = 1.39$ msec 124

6.21 LFCM controlled induction motor current response at $f = 60$ Hz, $K_P = 0.375$, $K_I = 0.5$ and $T_s = 1.39$ msec 125

6.22 LFCM position and velocity updates when vehicle travelling in the forward direction 127

6.23 LFCM position and velocity updates when vehicle travelling in the reverse direction 128

6.24 LFCM position and velocity updates during vehicle positioning operation 128

6.25 LFCM overall system operation at constant current and constant slip frequency 130

A.2 8097 external memory timings 141

B.1 LFCM prototype schematic 143

B.2 LFCM prototype board layout 144

B.3 LFCM prototype memory address map and chip select logic . . 145

C.1 Modified current sampling interface 147

LIST OF TABLES

5.1 LFCM event sequence of a passing train 83
6.1 Test condition summary for the LFCM current response test . . 126
A.1 8097 features and benefits summary 140

LIST OF SYMBOLS AND ABBREVIATIONS

A/D	analog to digital
CPU	central processing unit
CSI	current source inverter
EPROM	erasable/programmable read only memory
FOC	field oriented control
GTO	gate-turn-off thyristor
HSI	high speed input
HSO	high speed output
I/O	input/output
LIM	linear induction motor
LFCM	LIM frequency control module
LVCM	LIM voltage control module
PC	personal computer
PCU	power conditioning unit
PI	Proportional integral controller
PWM	pulsewidth modulation
RAM	random access memory
RC	resistor-capacitor load
ROMSIM	simulated read only memory
RMS	root mean square
S/H	sample-and-hold
SI	slip frequency stator current control
UTDC	Urban Transportation Development Corporation
VSI	voltage source inverter
VVFF	variable voltage fixed frequency

List of Symbols and Abbreviations

VVFF	variable voltage fixed frequency
VVVF	variable voltage variable frequency
V/F	constant volts/Hz control
a	train acceleration
a, b, c	suffixes denoting balanced 3-phase system
$0, \alpha, \beta$	suffixes denoting quadrature 2-phase system
$\alpha\beta$	stator-fixed frame
dq	synchronous rotating frame
Δt	time elapsed between interrupt
E_1	airgap voltage
E_I	integral error of PI controller
E_P	proportional error of PI controller
ϵ	error in position update
f	frequency
f_c	current frequency
f_d	demand frequency
f_m	mechanical frequency
g	airgap distance
G	goodness factor
η	efficiency
I_d	demand current
I_f	current feedback
e_I	current error
$\bar{I}_m$	magnetization current
$\bar{I}_1$	stator current
$\bar{I}_2$	rotor current
K_I	integral constant of PI controller

K_p	proportional constant of PI controller
L_1	stator leakage inductance
L_2	rotor leakage inductance
λ	stator wavelength
M	modulating waveform amplitude
μ_o	airgap permeability
P	train position
P_f	position feedback
ΔP	change of train position
ΔP_{calc}	calculated change of train position
R_2	rotor resistance
R_1	stator resistance
sf	slip frequency
sf_d	demand slip frequency
t_j	sample instant j
T	thrust
T_d	demand thrust
τ	pole-pitch
υ	train velocity
υ_d	demand velocity
υ_f	velocity feedback
e_υ	velocity error
V_1	stator voltage
V_{aN},V_{bN},V_{cN}	stator phase voltage
V_{AG},V_{BG},V_{CG}	inverter pole voltage
V_d	demand voltage
φ_r	surface resistivity

List of Symbols and Abbreviations

W	pulse width
W_N	minimum notch width
ω	fundamental frequency (rad/sec)
ω_m	modulating waveform frequency (rad/sec)

CHAPTER 1

INTRODUCTION / BACKGROUND

1.1 Introduction

It is only in the last fifteen years that linear motor drives have been seriously considered for industrial applications even though the technology has been developed since the turn of the century [4]. The range of recent applications is directly influenced by the advancement of solid state devices and the knowledge of speed control of ac machines. Although linear motor drives are presently finding wide appeal as propulsion drives for ground transportation, they are also finding increasing application for other industrial applications such as door actuators, aerodynamic disk-reading heads in computers, accelerators for high-velocity projectiles, and so on [1].

Recently, the Urban Transportation Development Corporation (UTDC) has established a research program to develop a low-speed material handling system, using linear induction motors (LIMs). The result of this program is a LIM-in-track propulsion system.

1.2 LIM-In-Track Propulsion System

Transport systems which employ track-based propulsion do not generally offer a high degree of control over individual unit loads. For example, conveyor, chain-drive and tow-line systems typically provide continuous, synchronous material flow, but possess no inherent facility to selectively manipulate one load independently of the others. This is because the drive system, based on a belt, chain, or cable drive shaft, mechanically couples all the loads together. In contrast, LIM-in-track propulsion [2] offers an opportunity to segment the drive-line into short, independently-controlled sections, thereby permitting a level of independent load management normally available only in systems employing self-powered carriers. Figure 1.1 illustrates this propulsion system, which is currently contracted for implementation in Toronto, Ontario for material handling. Figure 1.1a shows the system configuration, which is a series of LIM stators, situated in the ground between the tracks, to move and position material-carrying vehicles along a fixed guide-path. Figure 1.1b shows a close-up view of one of the LIM stators and its control module. This control module is known as the LIM Voltage Control Module (LVCM) and is described in the following sections.

Each in-track LIM module consists of special sensors that can detect the approach and passage of moving vehicles, a power conditioning unit, and a microprocessor based controller as shown in Figure 1.2. In addition, a communication link is established between these controllers

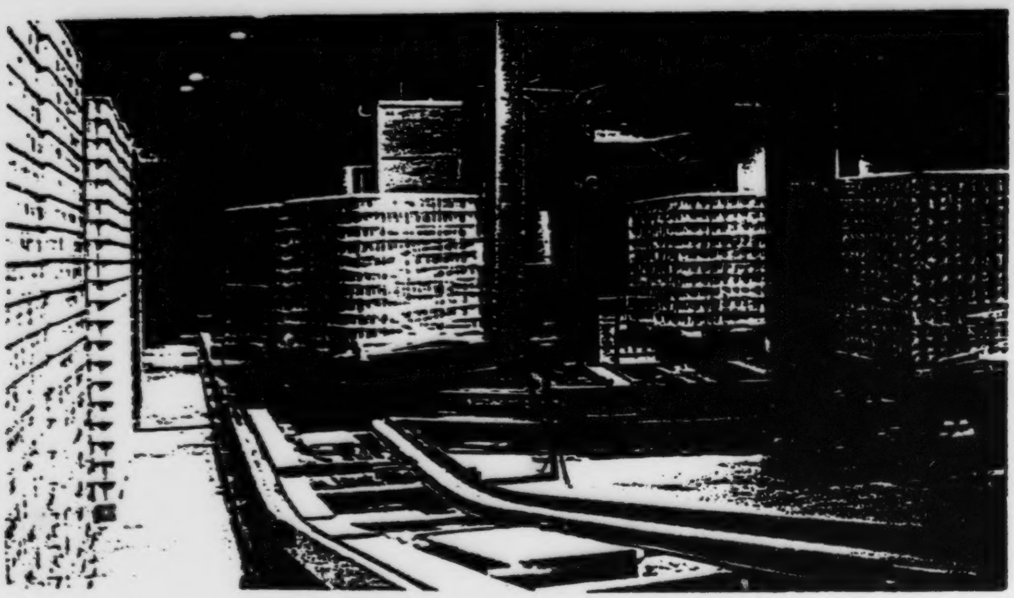

(a)

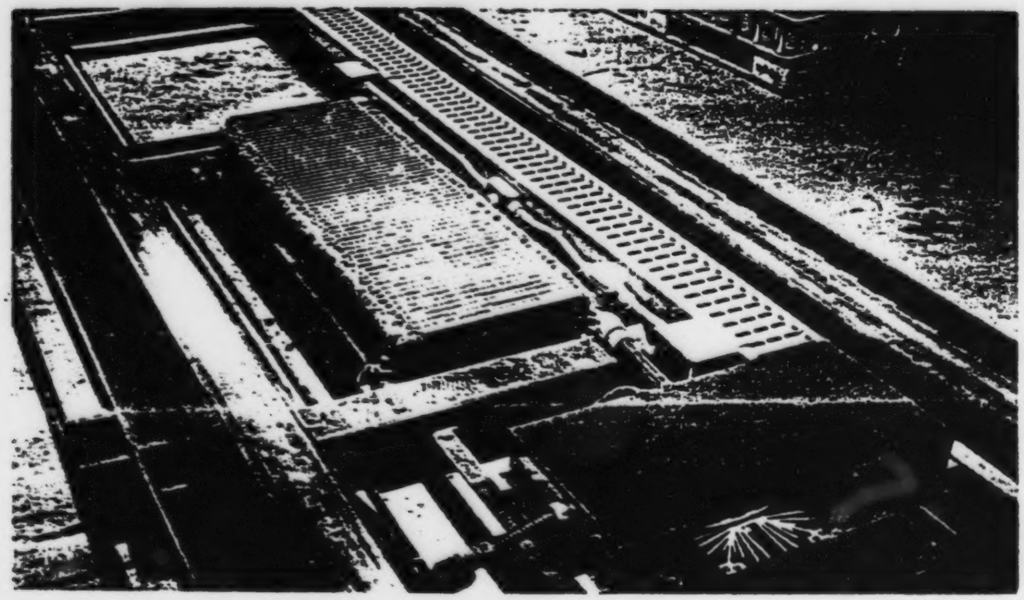

(b)

Figure 1.1 LIM-In-Track Propulsion System
a) Guidance track, in-track LIMs, and vehicles loaded with material.
b) Close-up of in-track LIM and voltage control module (LVCM).

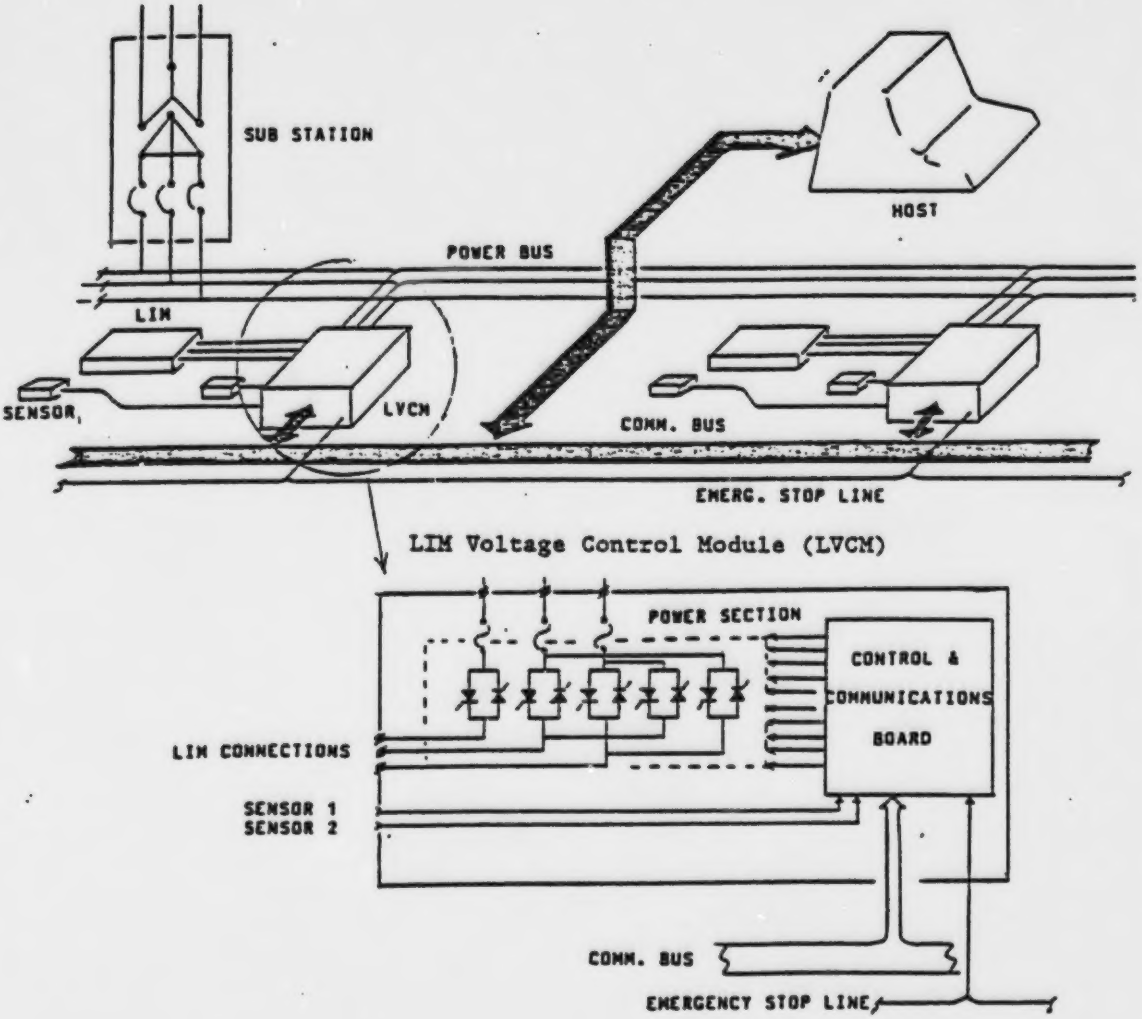
SUB STATION
HOST
POWER BUS
LIM
SENSOR
LVCM
COMM. BUS
EMERG. STOP LINE
LIM Voltage Control Module (LVCM)
POWER SECTION
CONTROL & COMMUNICATIONS BOARD
LIM CONNECTIONS
SENSOR 1
SENSOR 2
COMM. BUS
EMERGENCY STOP LINE

Figure 1.2 Block diagram of the LIM-in-track propulsion system configuration.

and a host computer in order to monitor the overall system operation. By means of local sensing, intelligence and motor control, the system possesses an inherent redundancy. That is, if any one of the distributed LIM modules fails, the system can still continue. Thus, the system is reliable, flexible and cost-effective.

The key element in this system is the LIM voltage control module (LVCM) [2], which is the microprocessor based controller. Each LVCM provides controlled voltage to the LIM in response to the difference between position/velocity feedback and the pre-programmed velocity demand profile as shown in Figure 1.3. The LVCM is a variable-voltage fixed-frequency (VVFF) controller, which controls the stator voltage at line frequency by symmetrically controlling the trigger angles of the three phase, line commutated, anti-parallel thyristors. This control scheme is simple, inexpensive and easily implemented with a microprocessor controlled circuit. However, an in-track LIM controlled by a VVFF speed controller has a performance which is characterized by a low power factor, low efficiency and limited speed range [3].

1.3 Potential Performance Gain Using Variable-Voltage and Variable-Frequency Control

Because of the limited range of performance of the VVFF speed control, other alternatives are investigated. The performance of a LIM

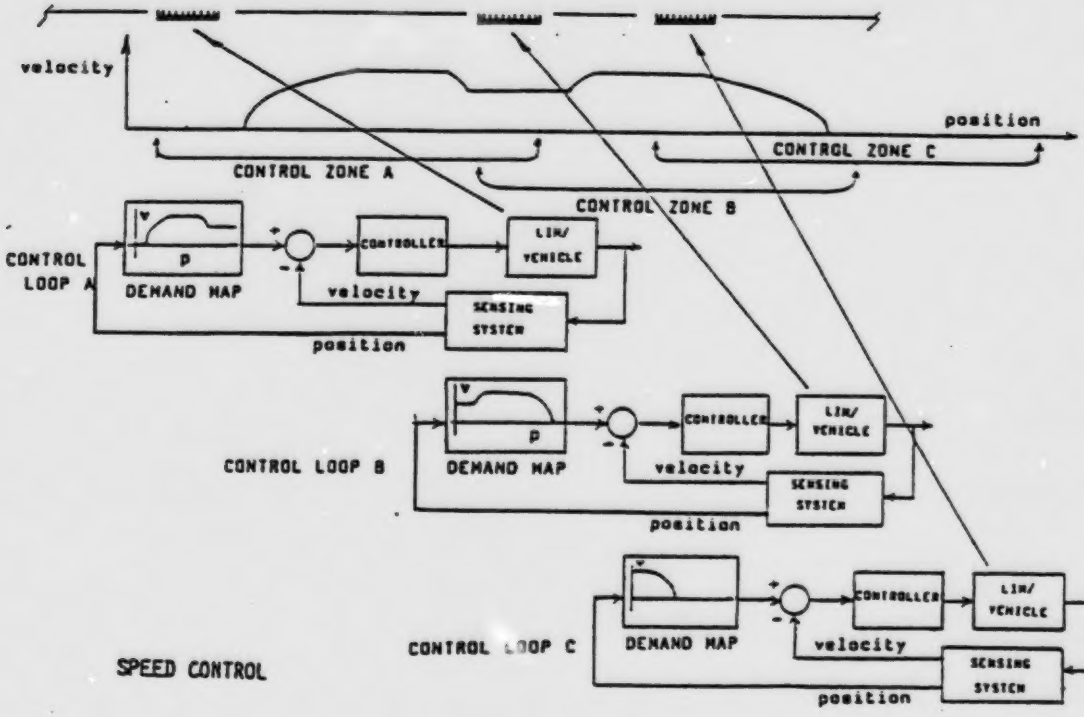
velocity
position
CONTROL ZONE A
CONTROL ZONE B
CONTROL ZONE C
CONTROL LOOP A
v
p
DEMAND MAP
+
-
CONTROLLER
LIM/ VEHICLE
velocity
SENSING SYSTEM
position
CONTROL LOOP B
v
p
DEMAND MAP
+
-
CONTROLLER
LIM/ VEHICLE
velocity
SENSING SYSTEM
position
CONTROL LOOP C
v
DEMAND MAP
+
-
CONTROLLER
LIM/ VEHICLE
velocity
SENSING SYSTEM
position
SPEED CONTROL

Figure 1.3 LIM voltage control module (LVCM) position/velocity control scheme; operation of three LIM modules at different positions.

can be greatly improved if fed from a variable-frequency source, and even further advantages can be realized if a variable-voltage variable-frequency (VVVF) speed control scheme is used. Hence, this thesis will investigate this mode of speed control for the in-track LIM system.

The advantages of using VVVF LIM speed control are:

(a) higher efficiency (η) due to lower slip [3], since slip of the motor can be controlled by varying the supply frequency, Figure 1.4a;

(b) higher power factor (pf) due to a higher value of Goodness Factor (G) [4], which expresses the ability of a motor to convert electrical power to mechanical power. As shown in Equation (1.1), G is directly proportional to the square of motor pole-pitch (τ) times frequency (f). With a controlled frequency, a lower frequency can be used and a longer pole-pitch can be employed. The result is that G increases;

(c) less sensitivity to airgap variation (Figure 1.4b), because G is not as sensitive to airgap distance, g, with a motor of longer pole-pitch as can be seen from the expression for Goodness Factor;

$$G = \frac{2\tau^2\mu_o f}{\pi\varphi_r g} \tag{1.1}$$

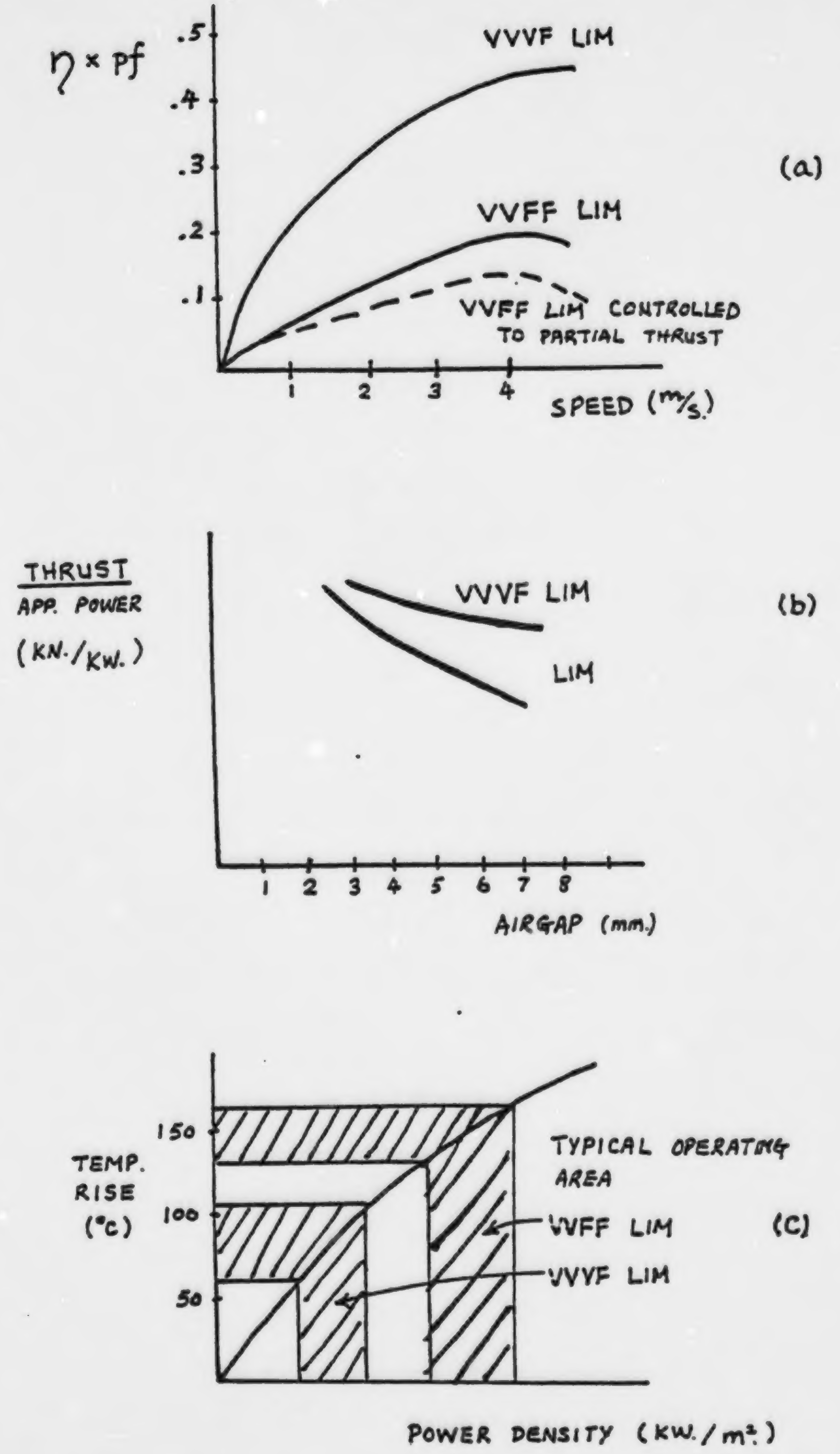

Figure 1.4 Comparison of LIM performance using VVVF and VVFF control
a) Power-factor x efficiency versus velocity.
b) Thrust per apparent power versus airgap.
c) Reaction plate temperature versus power density.

where μ_o - airgap permeability

φ_r - surface resistivity

τ - pole-pitch

f - frequency

g - airgap distance

(d) reduced reaction plate heating due to lower slip power [2], Figure 1.4c; and

(e) power factor is not affected by control level as in the VVFF scheme, where phase angle is affected by the variation of voltage level [3].

With these advantages, the VVVF scheme seems to be an attractive alternative. However, one must also be aware of its associated disadvantages, namely, the cost of the converters (eg. the costly GTO thyristors and their required gate drive circuits), complexity of control requirements, and harmonics introduced into the system [3]. Fortunately, these disadvantages are minor with the present trend of technology improvements in semiconductor devices.

1.4 History of Inverter Drives

When thyristors were introduced in the late 50's, they found immediate application in the development of inverter circuits for variable frequency drives. In the early 60's, several elegant force-commutation techniques were introduced, and among them, the pulse width modulation (PWM) technique [3,5,7] received the most attention because of its distinctive features. Figure 1.5 shows the diagram of a PWM inverter drive with the set of single-pole double-throw switches representing the force-commutated bridges. A fundamental frequency output voltage can be controlled by electronically activating these switches. The PWM drive obtains its dc input through simple uncontrolled rectification of the commercial ac line.

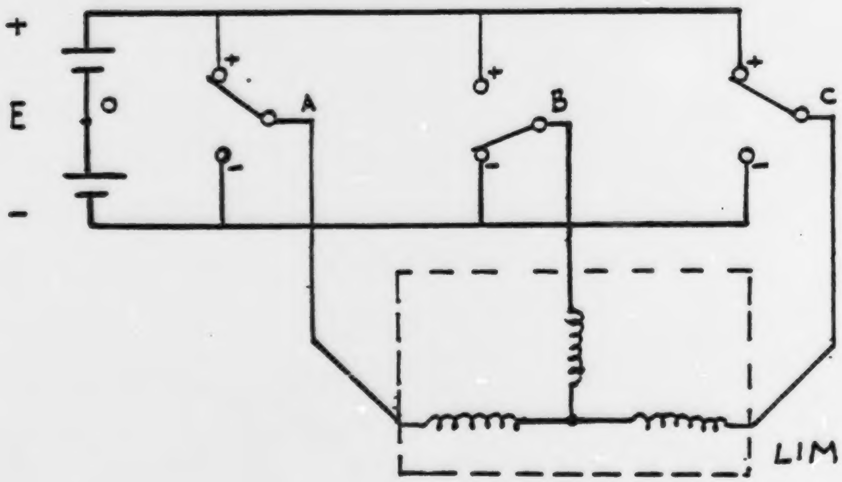

Figure 1.5 Diagram of a PWM inverter drive.

This type of inverter is favored for its high power factor, high efficiency, relative freedom from regulation problems, and particularly for its ability to operate a motor with nearly sinusoidal current waveform. These advantages are obtained at the cost of sophisticated control logic and hardwired analog/digital components. This sophistication is required to properly implement the mechanism of modulation for minimizing the unwanted harmonics at the motor terminal voltage.

With the advent of microprocessor technology in the mid 70's, some of these complicated control circuits were replaced by software implementation, thereby increasing reliability and flexibility. As well, software control allowed performance optimization of the drive system which could not be possible by hardwired control. However, because of the limited technology, only a small number of the functions could be performed by a single microprocessor. For a complicated motor control system, where several functions are to be performed, multi-processor arrangements were necessary (ie. dedicated microprocessors were used to perform different functions).

In the 80's, the semiconductor technology took another stride by introducing the highly integrated fast speed microcontroller [26], which incorporates many required features for motor control into a single chip. Hence, a single-chip microcontroller not only provides further simplification of hardware at a reduced cost, but also permits more complex and efficient motor control strategies through software development.

1.5 Thesis Scopes and Outline

1.5.1 Thesis Objectives

The objectives of this thesis are:

(a) To design and implement a VVVF controller, which incorporates all necessary LIM control functions;

(b) to develop algorithms which will lend themselves to microcontroller implementation; and

(c) to demonstrate the successful operations of the VVVF LIM controller.

1.5.2 Thesis Outline

In Chapter 1, the UTDC's LIM-in-track propulsion system was described. The advantages of using VVVF over VVFF control scheme in the LIM application were presented and discussed. The history of inverter drives was briefly reviewed. Finally, the objectives of the present studies are outlined.

In Chapter 2, the advantages of using PWM inverter drive for variable-voltage variable-frequency (VVVF) control are described, and various PWM strategies are reviewed. As well, several VVVF motor control schemes are presented.

In Chapter 3, a thrust/velocity control scheme for the VVVF excited in-track LIM system is described.

In Chapter 4, an overview of the system prototype is presented. The design and implementation of the hardware board - the microcontroller configuration and the various interface circuits - is described.

In Chapter 5, the system software implementation is presented. As well, the design considerations, options and implementation techniques are discussed.

In Chapter 6, the test setup and experimental results are included to verify some of the controller operations.

Finally, in Chapter 7, assessments and conclusions on the overall system are made, and future recommendations resulting from this research project are presented.

CHAPTER 2

PWM SCHEMES AND VVVF SPEED CONTROL METHODS

2.1 Introduction

LIM-in-track propulsion systems segment drive-lines into short, independently controlled sections, by means of localized sensing, intelligence and motor control [2]. A key element in this system is the "control module" concept. The control module functions as a local and autonomous regulator of LIM propulsive effort, and at the same time facilitates the integration of several LIMs into one or more drive lines.

Figure 2.1 presents the LIM-in-track propulsion concept; Figures 2.1a shows a block diagram representation of this LIM-in-track distributed control system, and Figure 2.1b shows the block diagram of the control module, which is referred to as the LIM frequency control module (LFCM). The control module is an adaptation of the variable-voltage variable-frequency (VVVF) control scheme where each module consists of a PWM inverter drive and a microcontroller controller and communications board. Each LFCM provides controlled voltage and frequency to the attached LIM in response to the difference between the

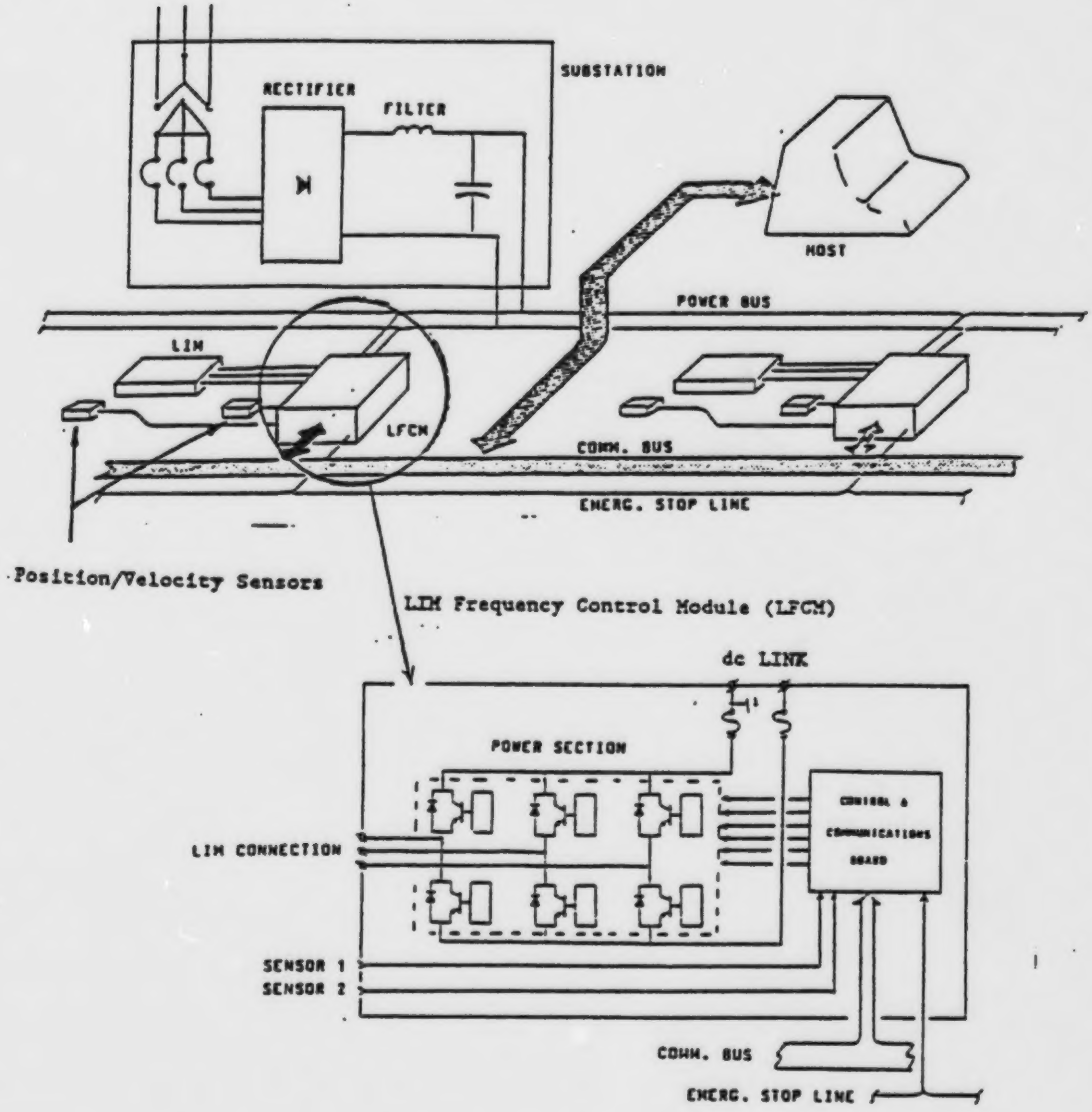
SUBSTATION
RECTIFIER
FILTER
HOST
POWER BUS
LIM
LFCM
COMM. BUS
EMERG. STOP LINE
Position/Velocity Sensors
LIM Frequency Control Module (LFCM)
dc LINK
POWER SECTION
CONTROL &
COMMUNICATIONS
BOARD
LIM CONNECTION
SENSOR 1
SENSOR 2
COMM. BUS
EMERG. STOP LINE

Figure 2.1 LIM-in-track propulsion system configuration
a) LIM-in-track, control module and position/velocity sensors.
b) LIM frequency control module (LFCM).

position/velocity feedback and the pre-programmed velocity profile. This is different than the LIM Voltage Control Module (LVCM) which only provides controlled voltage at line frequency (ie. 60Hz).

2.2 Linear Induction Motor

A linear induction motor (LIM) [1,4] can be described in simple terms, as a conventional rotary induction machine which has been cut along an axial plane and 'unrolled'. This results in a flat structure capable of producing motion in a straight line directly without the use of a crank or other mechanisms for converting rotary to linear motion. The LIM consists of three-phase stator windings and a conducting reaction plate. For LIM-in-track applications, the reaction plate is fixed to the vehicle and numerous stators are placed along the track as illustrated in Figure 1.1a.

2.2.1 LIM Stator

Figure 2.2 shows a LIM stator [2] typical of those used in LIM-in-track systems. It is designed and built by the Urban Transportation Development Corporation. The stator is of the single-sided variety, which is less efficient than a double-sided

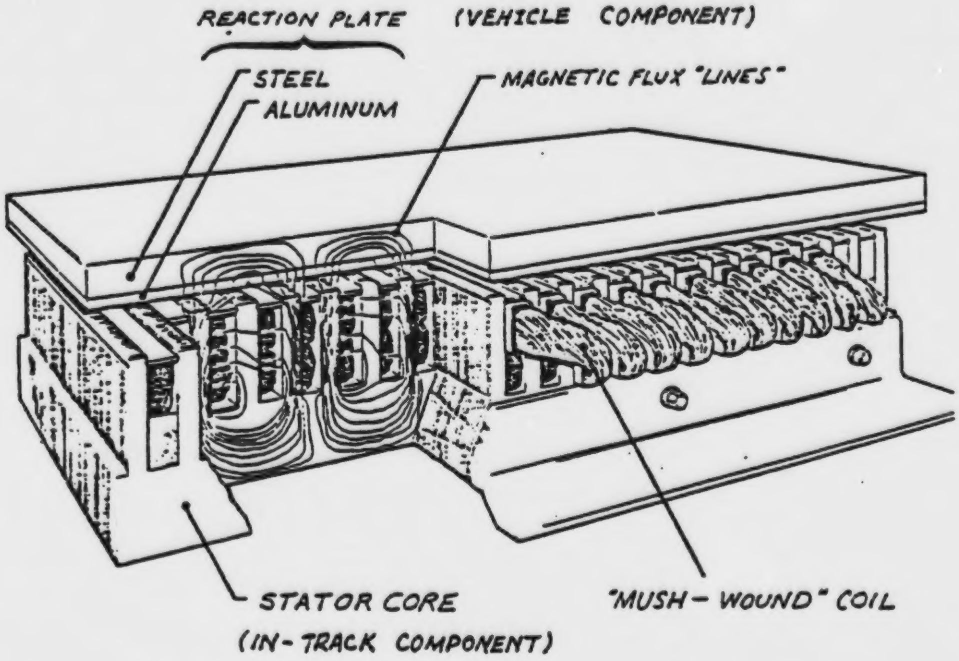
REACTION PLATE (VEHICLE COMPONENT)
STEEL
ALUMINUM
MAGNETIC FLUX "LINES"
STATOR CORE
(IN-TRACK COMPONENT)
"MUSH-WOUND" COIL

Figure 2.2 In-track linear induction motor.

configuration (which produces thrust on two surfaces) but generally more practical from the overall system perspective. The three-phase winding is a "mush-type", meaning that the coils are randomly wound with round wire as opposed to carefully formed with rectangular-section conductor. The lower cost mush winding is appropriate for in-track stators, where size constraints are less severe than for on-board stators. The LIM stators are sized according to the thrust/duty cycle requirement, so as to avoid motor over-heating.

The design of the LIM stators, as well as steel backed reaction plates, involve considerations in the areas of thermal, electrical, magnetic, and mechanical design.

2.2.2 LIM Reaction Plate

The LIM reaction plate [2] is a passive component, that is, it requires no power supply. This permits the vehicles to be simple, robust and unpowered compared to conventional motorized vehicles.

The reaction plate is of aluminum-over-steel construction. The aluminum provides a circuit for currents induced by the stator, and the steel provides a low reluctance magnetic path so that the airgap magnetic flux lines can link the primary and secondary electrical circuits as effectively as possible, see Figure 2.2. The basic geometry of the plate and the design of the LIM stator are determined by transient and steady-state performance requirements.

2.3 PWM Inverter Drive

For the past decade, especially after the advent of microprocessor technology, PWM inverter drives have been favored for speed control of ac machines because of high performance characteristics [6]. Figure 2.1b shows the power circuit of a conventional VVVF inverter. The dc link voltage can be supplied from an uncontrolled diode rectifier and the fundamental frequency output can be controlled electronically within the inverter by using a PWM technique. In this technique, the thyristors are switched on and off many times within a half cycle using switching strategy which generates a variable-voltage output with low harmonic content [3].

2.3.1 Advantages of PWM Inverter Drive

There are many advantages in using a PWM inverter drive. They are:

(a) output voltage and current waveforms have low harmonic content which results in less harmonic heating and thrust pulsations [3];

(b) speed control from standstill with full thrust capability because the thrust pulsations are low at low frequency [3];

(c) dynamic braking and regeneration are possible;

(d) PWM inverter supplies allow independent control of LIMs from a common dc feed (power bus); and

(e) the drive system can be made immune from possible ac line power failures by switching in a battery for the dc link voltage supply [3].

2.3.2 Development in PWM Techniques

The heart of any PWM inverter control scheme is undoubtedly the switching strategy used to generate the switching edges of the PWM control waveform [6,7,16]. In practice, there are three distinct approaches to formulate the switching strategy:

(a) natural sampled PWM,
(b) regular sampled PWM, and
(c) optimal PWM.

The modulating principles associated with each of these strategies are described below. Note that only sinusoidal modulating waves are considered even though there are others such as trapezoidal and triangular waves.

2.3.2a Natural Sampled Modulation [6,7,16]

This switching mode is generally implemented by comparing a triangular carrier waveform b with a sinusoidal modulating waveform a, as shown in Figure 2.3, to determine the switching instants, and therefore, the resultant pulse widths. Because the switching edge of the width-modulated pulse waveform c is determined by the instantaneous intersection of the two waveforms, the resultant pulse width t_p is proportional to the amplitude of the modulating wave at the instant that switching occurs.

This method of switching has been used widely in the past because of its inherent simplicity and ease of implementation using analogue techniques. It is, of course, possible to simulate this analogue process of natural sampling in the microprocessor software, and using the logic capabilities of the microprocessor to determine the pulse widths. But this is not a common practice because there is a heavy demand on processor computing time which makes real-time generation of the pulses difficult. Also, note that it is not possible to define the

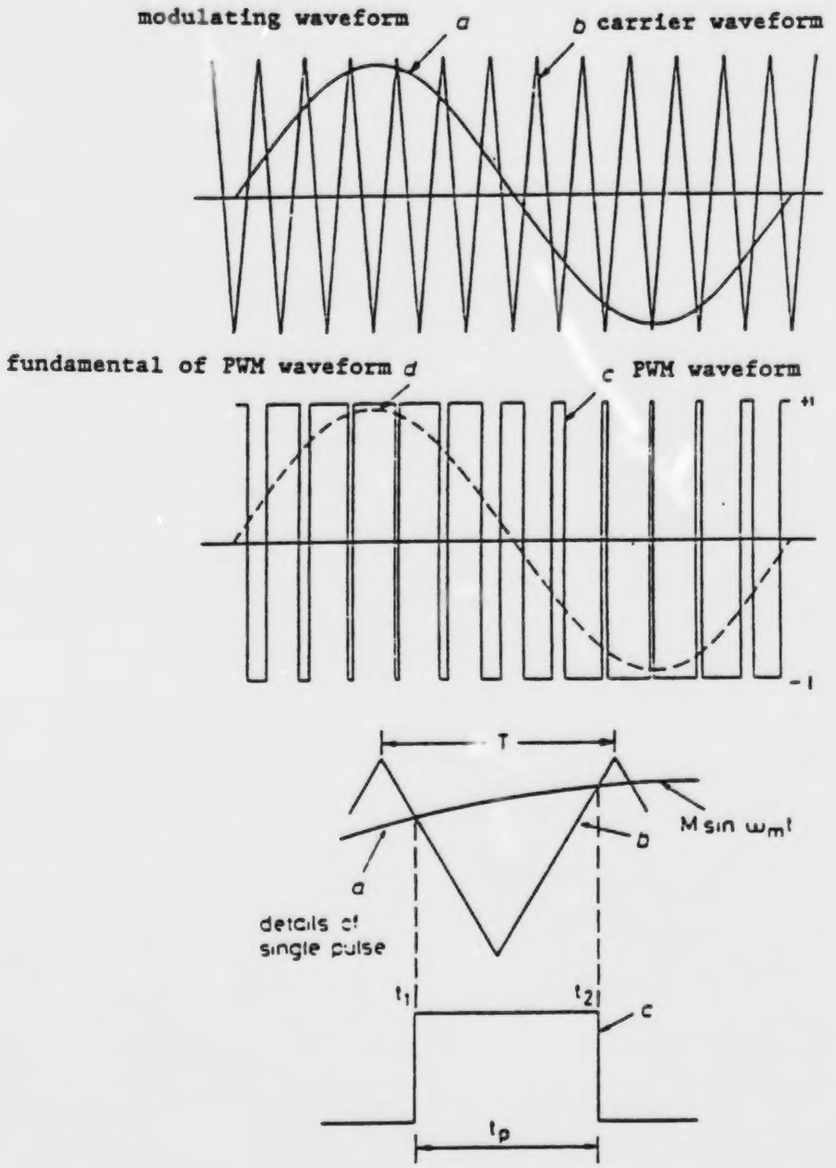
modulating waveform
a
b carrier waveform
fundamental of PWM waveform d
c PWM waveform
+1
-1
T
M sin ω_m t
b
a
details of single pulse
t1
t2
c
tp

Figure 2.3 Natural sampled PWM.

widths of the pulses using analytic expressions because the pulse centres in the resultant PWM are not uniformly spaced.

2.3.2b Regular Sampled Modulation [6,7,16]

Figure 2.4 illustrates the general features of this mode of switching. In this mode, the amplitude of the modulating waveform a at the sample instant t_1 is stored by a sample-and-hold circuit (operated at carrier frequency), and is maintained at a constant level during the inter-sample period t_1 and t_2, until the next sample is taken. This produces a sample-hold version of the modulating waveform b, which, when compared with the triangular carrier waveform c, defines the points of intersection used to determine the switching instants T1 and T2 of the width-modulated pulse waveform d.

In contrast with those of natural sampled modulation, the widths of the pulses from this process are proportional to the amplitude of the modulating waveform at uniformly spaced sampled time, and therefore, the sampled positions and sampled values can be defined precisely. The width of each pulse can be calculated directly from:

$$W_j = \frac{T}{2}\left[1 + M\sin(\omega_m t_j)\right] \qquad (2.1)$$

where W_j = the pulse width at the sampling instant t_j;

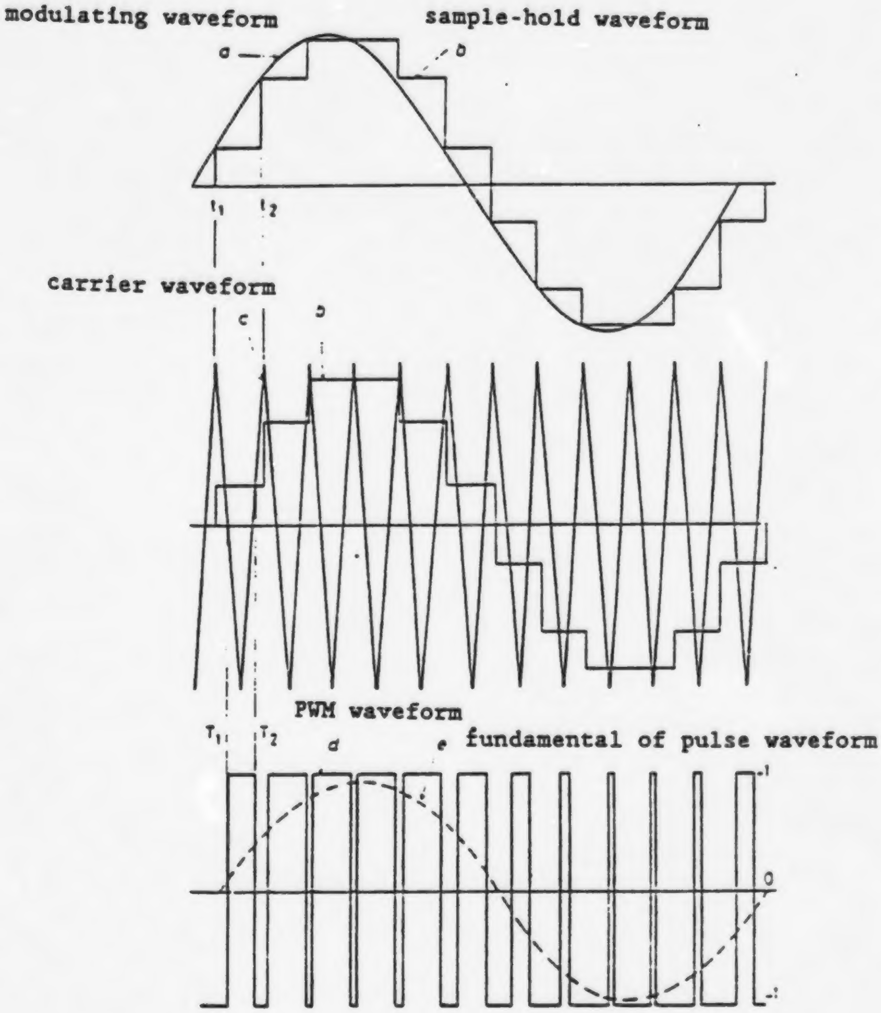
modulating waveform
sample-hold waveform
a
b
t1
t2
carrier waveform
c
b
PWM waveform
T1
T2
d
e
fundamental of pulse waveform
1
0
-1

Figure 2.4 Regular sampled PWM.

T - the period of the carrier waveform;

M - the amplitude of the modulating waveform, and

ω_m - the frequency of the modulated waveform.

It is important to note that this switching strategy is much easier to implement with digital or microprocessor techniques, and is, therefore, employed in the LFCM application. Further details of this scheme are described in Section 5.2.1.

2.3.2c Optimal PWM [7-9,13,14,16]

The so called "optimal" PWM switching strategies are all based upon the minimization of certain performance criteria [7,9,14] (eg. elimination of particular harmonics, or the minimization of harmonic-current distortion, torque ripple, etc.) to generate optimized PWM waveforms. These strategies involve the use of computer and minimization algorithms to determine the optimized switching angles. These angles can be subsequently pre-programmed into the memory of the microprocessor controlling the inverter and used to generate the PWM waveform in real-time.

Optimal PWM is particularly attractive at low frequency ratios [7,14] (ie. the ratio of switching frequency over fundamental frequency), where it has dramatic effect on harmonic content, and offers the possibility of extending the viable output-frequency range of the variable speed drive system. However, for this particular LIM-in-track application, where the frequency ratios are relatively high for the operating frequency range, optimal PWM strategy is not required.

2.4 VVVF Speed Control of LIM

As mentioned in Chapter 1, motor control with a VVVF scheme has a low slip characteristic which results in an improvement of efficiency. The speed of the motor can be varied by simply varying its synchronous speed, ie. by varying the inverter frequency. However, as the frequency is increased, the machine airgap flux falls causing reduced thrust capability [3,17]. Hence, in high performance drives, flux regulation is always required.

Presently, several control methods can be used to fulfill this requirement; namely, the constant volts/Hz (V/F) control, the slip frequency stator current (SI) control and the recently developed field oriented control (FOC).

2.4.1 Constant Volts/Hz Control [3,18]

The constant volts/Hz control method (V/F) has been popular in many industrial applications because of its good steady state performance and inherent simplicity. This control maintains approximately constant airgap flux, which in turn keeps the torque constant, as the motor speed varies by varying the inverter frequency. This control concept can be explained using the equivalent circuit model [17,18] of an induction motor, Figure 2.5. From the model, the airgap voltage (E_1), which is proportional to the airgap flux, is equal to the stator voltage (V_1) if the voltage drops at the stator resistance (R_1) and the leakage inductance (L_1) are ignored. Therefore, constant flux operation is ensured by keeping a constant ratio of stator voltage to frequency.

This scheme operates well at relatively high frequencies and for rotary induction motors. However, for LIMs, the approximation is no longer valid, because of the large stator leakage inductance (L_1) in the LIMs [1,19] Thus the L_1 drop is relatively high in comparison with V_1 even at low frequency operation. Hence, this control method is not very appropriate for LIM control applications.

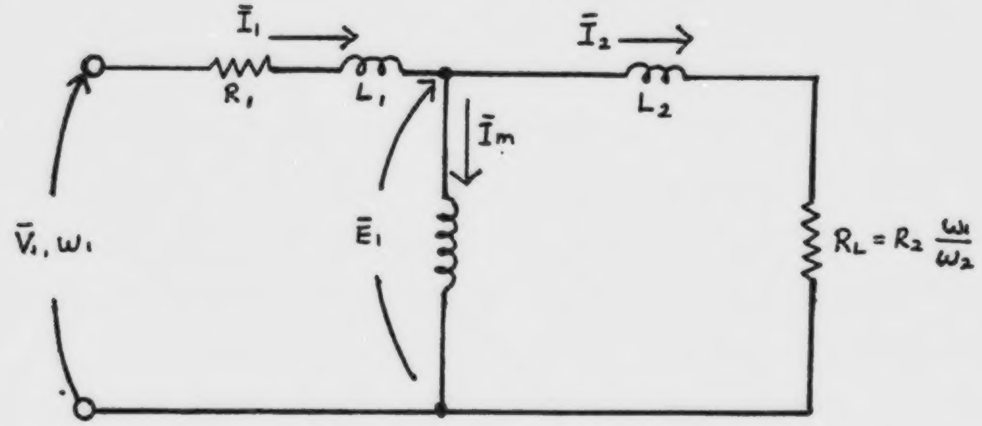

Figure 2.5 Equivalent circuit model of one phase of induction motor.

2.4.2 Field Oriented Control (FOC) [21-23]

The basic principle of field oriented control (FOC) is that the magnitude and phase of the stator current is controlled so that the machine flux is regulated during steady or transient torque conditions. In the FOC, the stator phase currents are transformed from a α-β stationary reference frame to the corresponding synchronously rotating d-q reference frame as shown in Fig. 2.6. The rotor flux vector is controlled to align along the d-axis of the d-q reference frame so that the q-component of rotor flux is zero. The torque then becomes proportional to the quadrature current component (i_{qs}) if the rotor flux is kept constant. Hence, the torque control is analogous to that of a dc machine, where i_{qs} and i_{ds} are similar to the armature current and the field excitation, respectively.

The FOC method permits optimum transient and steady state torque response, thereby offering high dynamic performance and torque control even down to zero speed. However, this method requires a flux sensing mechanism as well as complex software algorithms. The additional gain of motor performance does not justify the substantial increase of control complexity in this particular LIM application.

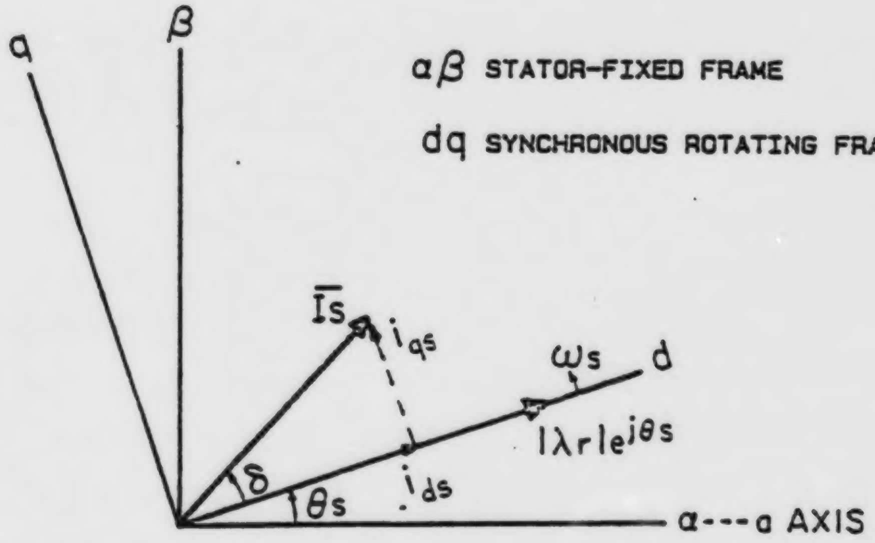

q
β
αβ STATOR-FIXED FRAME
dq SYNCHRONOUS ROTATING FRAME
$\bar{I}_s$
i_{qs}
ω_s
d
$|\lambda_r|e^{j\theta_s}$
δ
θ_s
i_{ds}
α---a AXIS

Figure 2.6 Stator current components in d-q frame.

2.4.2 Slip Frequency Stator Current (SI) Control [3,20,23]

In this control method, speed and torque control are performed by slip regulation according to the scheme outlined in Fig. 2.7. This control concept is based on the torque, current and slip relationship that exists when an induction motor is supplied from a fixed voltage as summarized in Fig. 2.8. These relationships apply for any supply frequency as long as the airgap flux remains constant. The motor requires some minimum value of current (I_{min}) to maintain synchronous speed with zero load torque. As the torque requirement increases, motor current must also increase.

This SI control scheme is sometimes implemented with a current-fed inverter (CSI) drive. With this scheme, the motor operation is controlled at its optimum torque/ampere rating point while enhancing rugged simplicity to achieve torque limit, fast response, regeneration, and wide speed range. However, two main limitations of CSI drives are, first, the large size of the dc link inductance and commutation capacitors which make the inverter somewhat bulky and expensive, and, second, the commutation dependence on machine sub-transient inductance which results in a large transient over-voltage at the machine terminal [3].

For this LIM-in-track application, the SI control scheme is adapted, and voltage source inverters with software implemented current

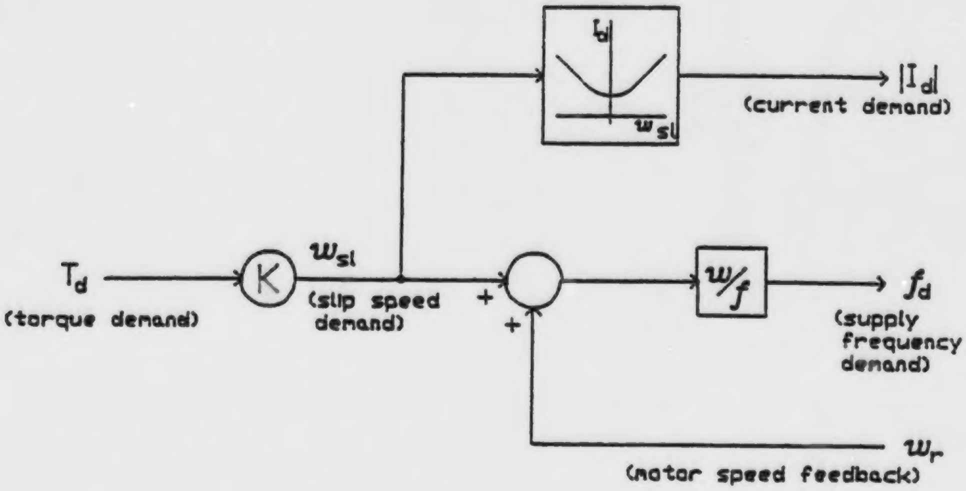
I_d
w_{sl}
$|I_d|$
(current demand)
T_d
(torque demand)
K
w_{sl}
(slip speed demand)
+
+
w/f
f_d
(supply frequency demand)
w_r
(motor speed feedback)

Figure 2.7 Slip frequency stator current (SI) method.

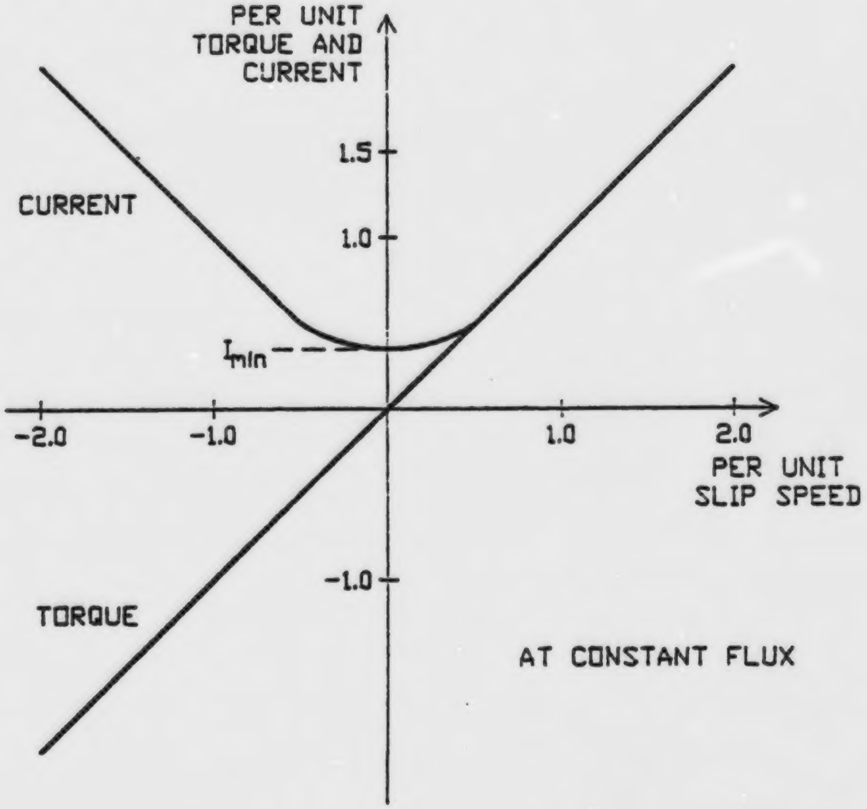

Figure 2.8 Induction motor characteristics.

control are used. Detailed descriptions of this control scheme implementation are presented in the following chapters.

CHAPTER 3:

LIM-IN-TRACK THRUST/VELOCITY CONTROL

3.1 VVVF Speed Control of LIM

The previous chapter outlined different methods of controlling induction motor drives. The tradeoff of the corresponding benefits in performance against the complexity of a particular control method should be evaluated for each application. For the LIM-in-track propulsion application, velocity governed by a set of velocity/position profiles is determined to be desirable. Depending on where each LIM module is located along the track, a specific profile is assigned. Hence, the LFCM control algorithm is similar to that of slip frequency stator current control. It is characterized by the hierarchy control loops where the velocity is controlled with outer loop feedback and the thrust, frequency and current are controlled with inner loop feedback. A simplified block diagram of the velocity control scheme is shown in Figure 3.1.

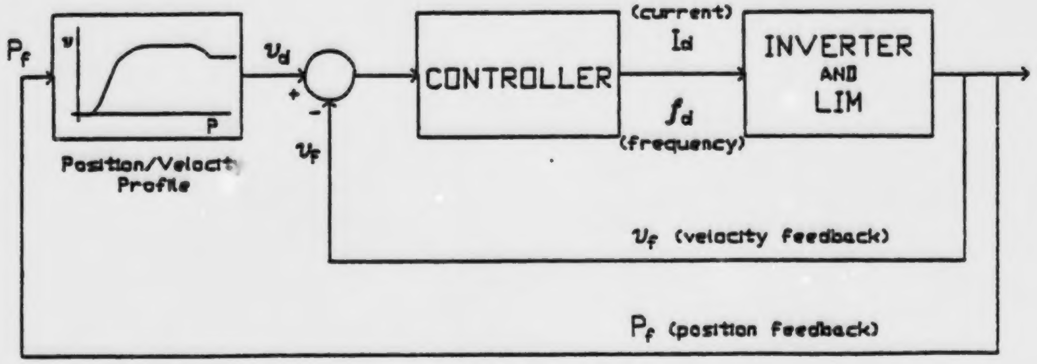
P_f
v
p
Position/Velocity Profile
v_d
+
-
v_f
CONTROLLER
(current)
I_d
f_d
(frequency)
INVERTER AND LIM
v_f (velocity feedback)
P_f (position feedback)

Figure 3.1 Simplified block diagram of LFCM speed control scheme.

3.2 Velocity Control Loop

The velocity control is implemented by first noting that thrust is non-linearly dependent on velocity or slip, and is proportional to the square of stator current [4,17], Figure 3.2. Figure 3.2a depicts a typical thrust-velocity curve for a LIM with an aluminum reaction plate operating at a particular frequency and voltage, and Figure 3.2b demonstrates the direct relationship of thrust and stator current squared. It is evident that a system operating with an open loop velocity control could easily result in an unstable condition, where the operating point is on the positive slope of the thrust/velocity curve. Hence, a closed loop velocity control is necessary.

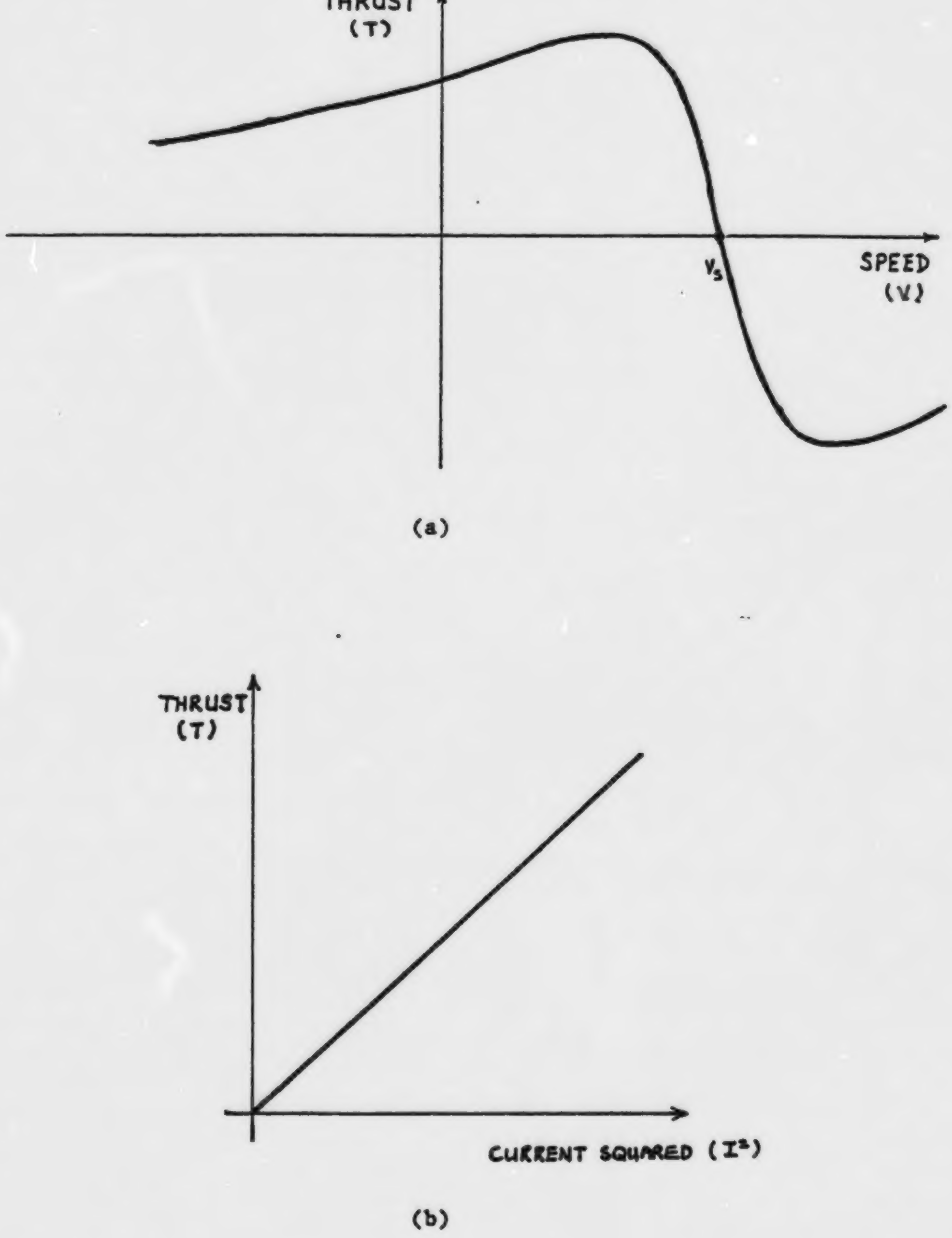

Figure 3.2 LIM thrust characteristics with an aluminum reaction plate
(a) Thrust versus speed.
(b) Thrust versus current squared.

Figure 3.3 shows the LIM frequency control module velocity control scheme. The actual velocity feedback signal (v_f), derived from the position feedback (P_f), is compared with that of the velocity demand signal (v_d) to generate an error signal (e_v) for the inner loops. A simple proportional integral (PI) controller is implemented to obtain the thrust demand (T_d) from the velocity error. A PI controller is chosen because of its ability to improve steady-state error and to control the transient response. This thrust demand is further processed to obtain a positive signal with an upper limit. The current demand (I_d) required for the inner loop control is derived by taking the square root of the thrust demand.

3.3 Current Control Loop

In the slip frequency stator current (SI) control scheme, a current source inverter (CSI) is normally employed for its direct control of motor current. However, for this LIM application, in which an individual inverter accompanies each LFCM, it is impractical to use a CSI because of its size and its relatively high cost. Hence, voltage source inverters (VSIs) with current feedback control loop are used instead.

The current control is implemented by a pseudo-current-impressed scheme, Figure 3.4, in which only the magnitude but not the phase is

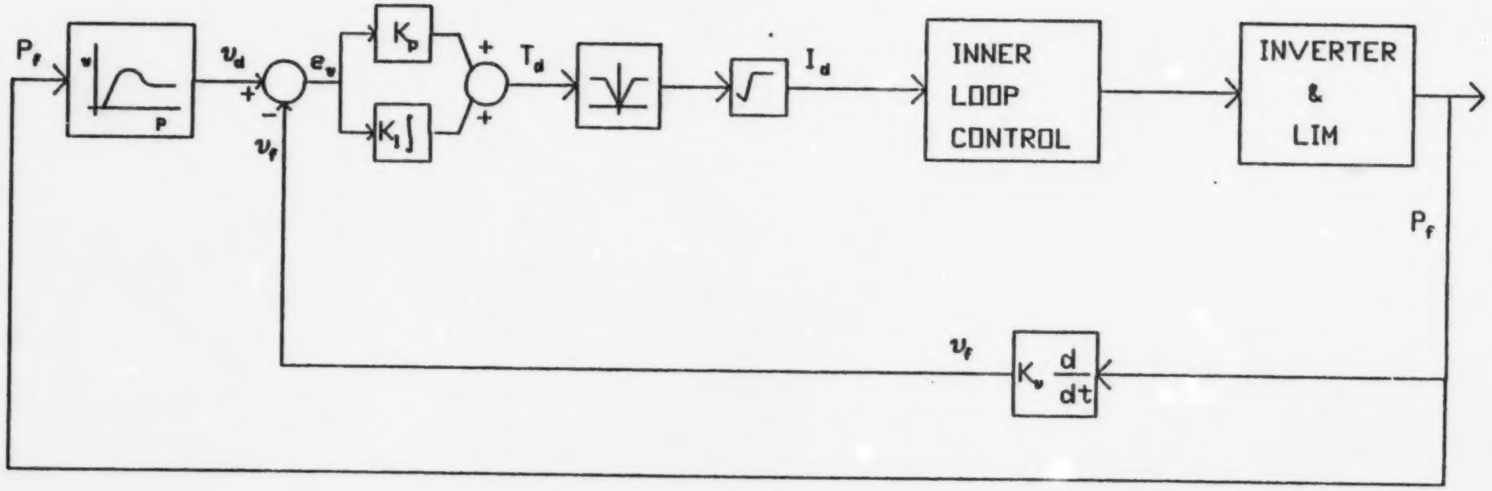
P_f
v
P
v_d
$+$
$-$
v_f
e_v
K_p
$K_I\int$
$+$
$+$
T_d
I_d
INNER
LOOP
CONTROL
INVERTER
&
LIM
P_f
v_f
$K_v \frac{d}{dt}$

Figure 3.3 LFCM speed control scheme.

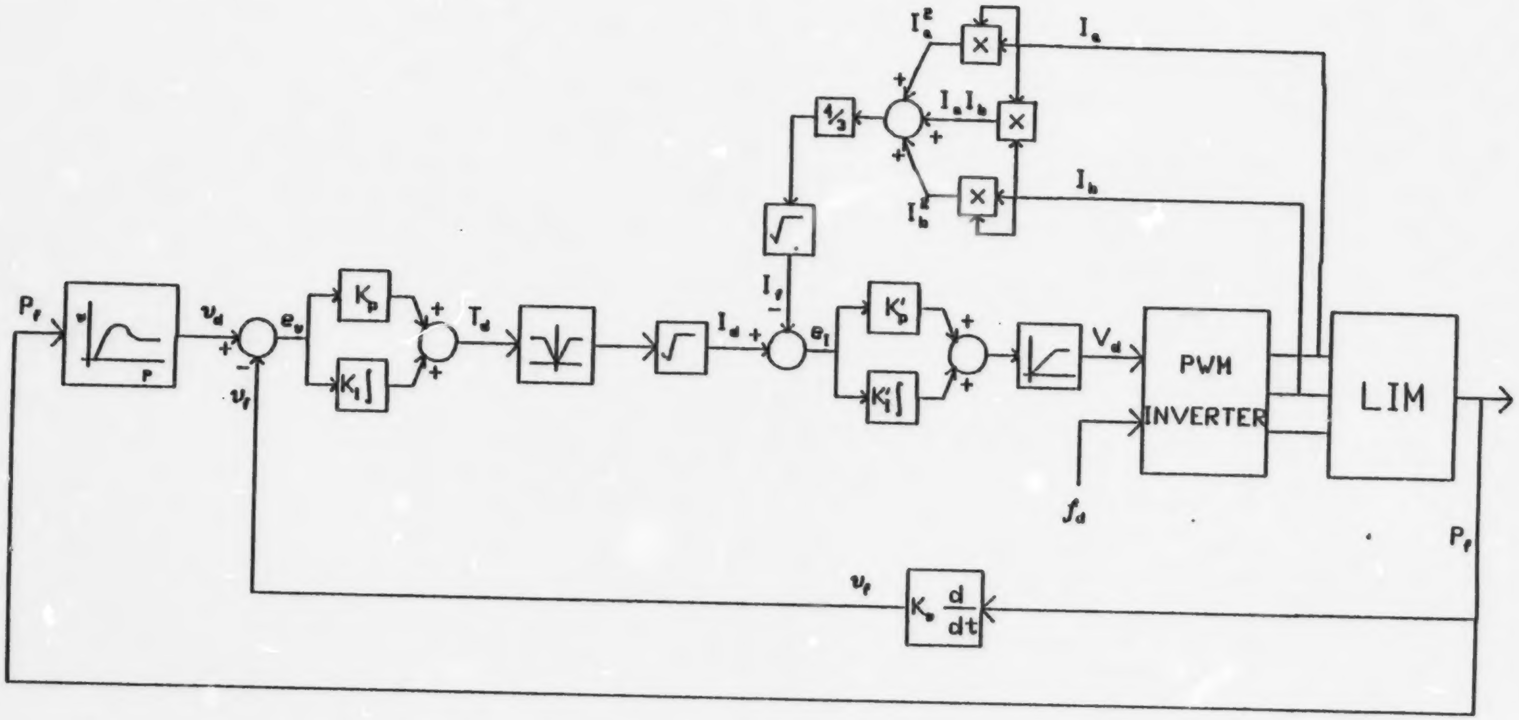
P_f
v_d
e_v
v_f
K_p
$K_I\int$
T_d
I_d
I_f
e_I
K_p'
$K_I'\int$
V_d
PWM INVERTER
LIM
f_d
P_f
v_f
$K_v\frac{d}{dt}$
I_a^2
I_aI_b
I_b^2
I_a
I_b
1/3
+
−

Figure 3.4 LFCM speed control with a current feedback control loop.

controlled. The current demand signal (I_d), generated by the velocity control loop, is compared with the current feedback signal (I_f) (ie. the peak value) to generate a current error signal for the inverter, again through a PI controller. Voltage clamping is implemented to prevent the voltage demand (V_d) from exceeding the inverter limit.

To obtain satisfactory performance from this system, a relatively fast current controller response is essential. The gain constants (K'_P and K'_I) of the PI controller and the current sampling period must be appropriately chosen to optimize the transient response. The conventional root mean square (RMS) method for determining the current magnitude for the current feedback is found unsuitable in this system, especially at low operating frequencies, because it normally requires integration over at least half a period of the fundamental frequency. Hence, the quadrature current method [24,25] is adopted. This method is implemented based on the knowledge that the current magnitude of a 2-phase machine can be obtained directly from the quadrature current components, and that a balanced 3-phase system can be represented by a 2-phase system using a matrix transformation. Equations (3.1) to (3.5), shows the transformation of balanced 3-phase currents (a,b,c) to 2-phase quadrature currents ($0,\alpha,\beta$), and the derivation of the current magnitude. The transformation can be written as:

$$\begin{bmatrix} i_0 \\ i_\alpha \\ i_\beta \end{bmatrix} = \begin{bmatrix} T \end{bmatrix} \times \begin{bmatrix} i_a \\ i_b \\ i_c \end{bmatrix} \qquad (3.1)$$

where the transformation matrix,

$$\begin{bmatrix} T \end{bmatrix} = \sqrt{2/3} \times \begin{bmatrix} 1/\sqrt{2} & 1/\sqrt{2} & 1/\sqrt{2} \\ 1 & -1/2 & -1/2 \\ 0 & -\sqrt{3}/2 & \sqrt{3}/2 \end{bmatrix} \tag{3.2}$$

and

$$\begin{bmatrix} i_a \\ i_b \\ i_c \end{bmatrix} = \begin{bmatrix} I\sin(\omega t) \\ I\sin(\omega t-120^\circ) \\ I\sin(\omega t-240^\circ) \end{bmatrix} \tag{3.3}$$

From the transformation, the 2-phase currents can be written as:

$$i_0 = 0 \tag{3.4a}$$

$$i_\alpha = \sqrt{2/3}\,(i_a - \frac{1}{2}\,i_b - \frac{1}{2}\,i_c) = \sqrt{3/2}\ I\sin(\omega t) \tag{3.4b}$$

$$i_\beta = 1/\sqrt{2}\,(-i_b + i_c) = \sqrt{3/2}\ I\cos(\omega t) \tag{3.4c}$$

Therefore, the current magnitude, expressed in quadrature components is:

$$I = \sqrt{2/3\,(i_\alpha^2 + i_\beta^2)} \tag{3.5}$$

However, further simplification can be achieved by rewriting (3.4b) and (3.4c) as:

$$i_\alpha = \sqrt{3/2}\ i_a \tag{3.6}$$

$$i_\beta = -1/\sqrt{2}\,(i_a + 2i_b) \tag{3.7}$$

because $(i_a + i_b + i_c) = 0$ for a balanced 3-phase system.

Hence, the current magnitude is:

$$I = \sqrt{4/3\,(i_a^2 + i_a i_b + i_b^2)} \tag{3.8}$$

Equation (3.8) shows that the current magnitude can be obtained instantaneously from the currents of any two phases of a balanced 3-phased system, which in turn, allows fast current control in the LIM. In fact, presently, the current is controlled at the inverter switching frequency, (ie. at every inverter switching instant), allowing synchronization with the PWM mechanism.

3.4 Slip Frequency Control Loop

In SI control, slip regulation is essential to optimize the LIM performance. Before analyzing the slip loop implementation, it is important to understand the LIM characteristics at various slip frequencies. The thrust, power factor and efficiency versus slip frequency, for a LIM operating at a fixed stator current are illustrated in Figures 3.5 - 3.7 respectively. (Note: these plots are obtained by UTDC from test measurements). From the plots, it can be determined that for either motoring or regenerating operation, optimum performance occurs within a narrow slip frequency range. For example, when the LIM operates in the motoring region, maximum thrust occurs around 10 Hz slip frequency, maximum power factor occurs around 15 Hz slip frequency, and maximum efficiency occurs around 8 Hz slip frequency.

It is evident that the motor performance can be optimized to different criteria, such as maximizing the thrust per ampere rating, the

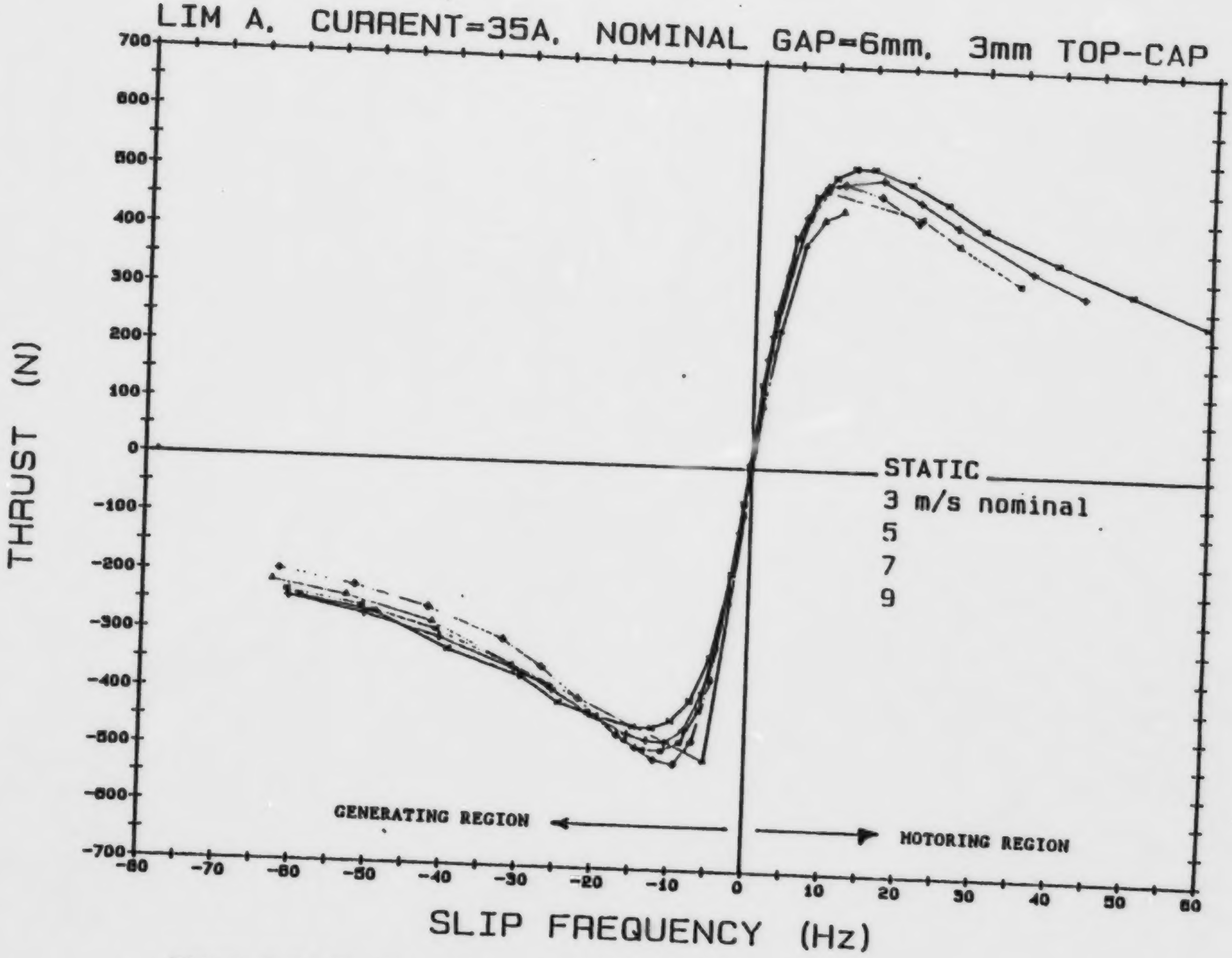

Figure 3.5 Thrust versus slip frequency characteristics of a LIM operating with solid steel, aluminum capped reaction rail at a constant stator current of 35 A, and an airgap of 6 mm.

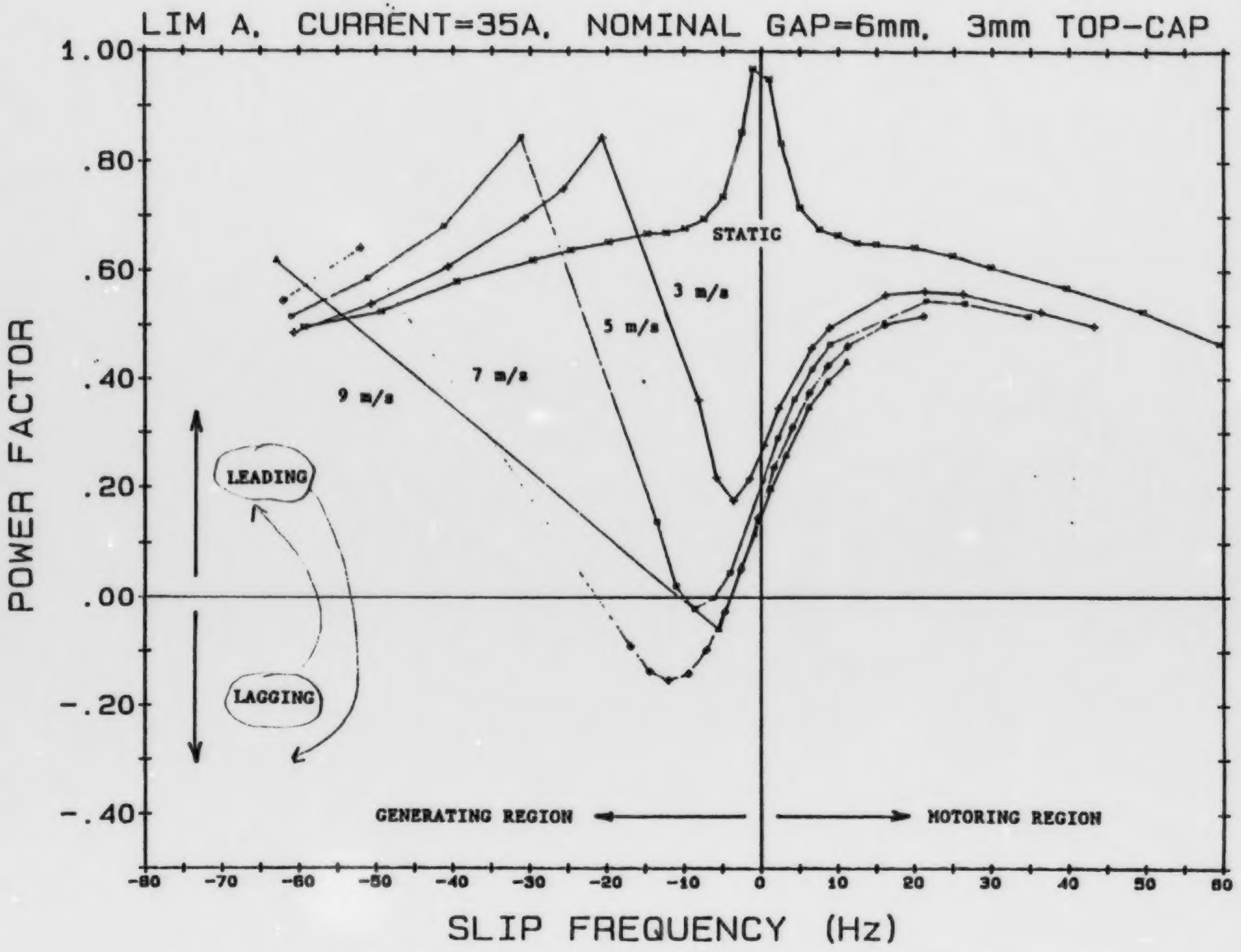

Figure 3.6 Power factor versus slip frequency characteristics of a LIM operating with solid steel, aluminum capped reaction rail at a constant stator current of 35 A, and an airgap of 6 mm.

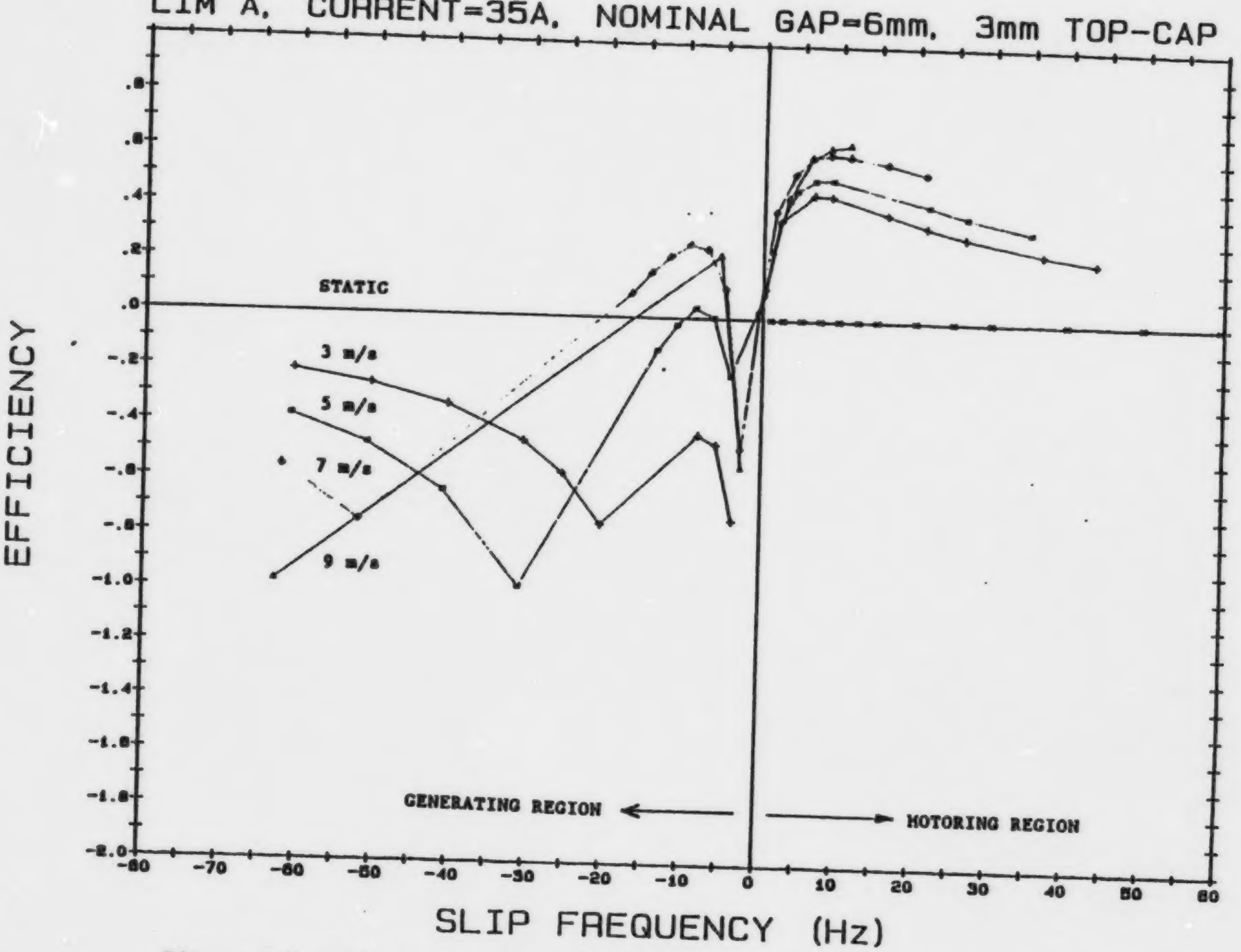

Figure 3.7 Efficiency versus slip frequency characteristics of a LIM operating with solid steel, aluminum capped reaction rail at a constant stator current of 35 A, and an airgap of 6 mm.

power factor or the efficiency, by controlling the slip frequency region in which the LIM operates. Hence, slip frequency control is implemented by using a slip frequency/velocity profile, Figure 3.8, similar to that of position/velocity profile, as shown in Figure 3.4. The frequency demand signal (f_d) for the inverter is produced by summing the optimized slip frequency demand signal (sf_d) of a particular velocity feedback (v_f) and the mechanical frequency (f_m) (ie. velocity feedback (v_f) divided by the the stator wavelength (λ = 2 times the pole pitch)). Note that the slip frequency demand signal (sf_d), determined by the slip-frequency/velocity profile, can either be a positive or negative value depending on whether motoring or braking is required.

Since the slip frequency control method is best suited to the present application, the control scheme of Figure 3.8 will be implemented. The details of the hardware and software requirements and method of implementation are presented in Chapters 4 and 5.

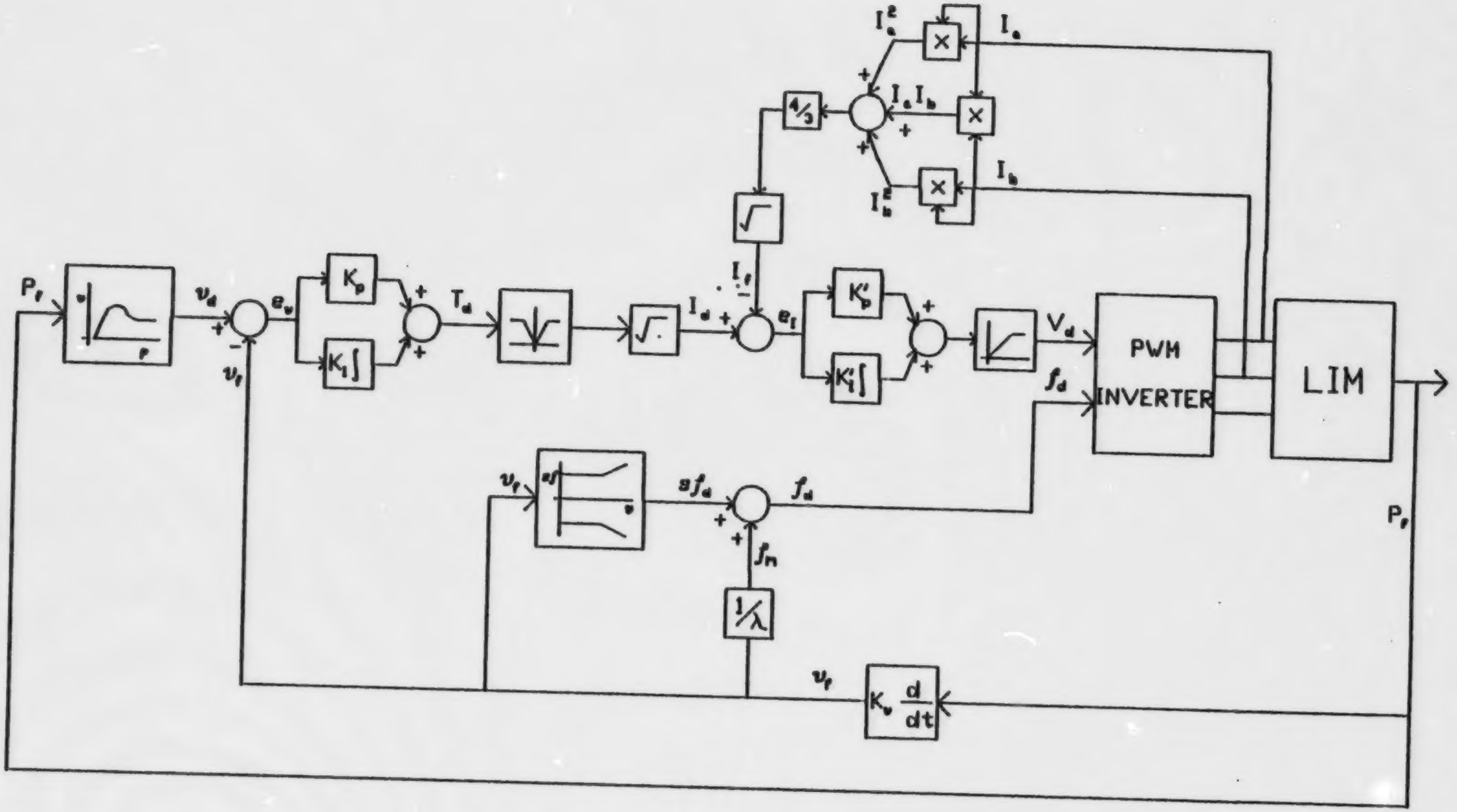
P_f
v_d
e_v
v_f
K_p
$K_I\int$
T_d
I_d
I_f
e_I
K'_p
$K'_I\int$
V_d
f_d
PWM
INVERTER
LIM
I_a^2
$I_a I_b$
I_b^2
I_a
I_b
×
4/3
sf_d
f_n
$1/\lambda$
$K_v \frac{d}{dt}$
P_f
+
−

Figure 3.8 Complete block diagram of the LFCM speed control scheme for implementation using a microcontroller system.

CHAPTER 4:

OVERALL SYSTEM DESIGN AND HARDWARE IMPLEMENTATION

4.1 Introduction

The LIM-in-track control module scheme and the motor control strategy have been discussed in the previous chapters. One of the objectives of this study is to implement the control scheme for the LIM frequency control module (LFCM) using a microcontroller system. In this chapter, the overview of the microcontroller system, as well as the hardware design and implementation are presented. The software control design and programming techniques will be presented in the following chapter.

Figure 4.1 illustrates the general overview of the microcontroller system. The system design is functionally divided into four areas. They are namely:

(a) the PWM control unit - consists of a software implemented PWM module which controls the timing of all the output pulses to the inverter, and a hardwired inverter gate-drive interface;

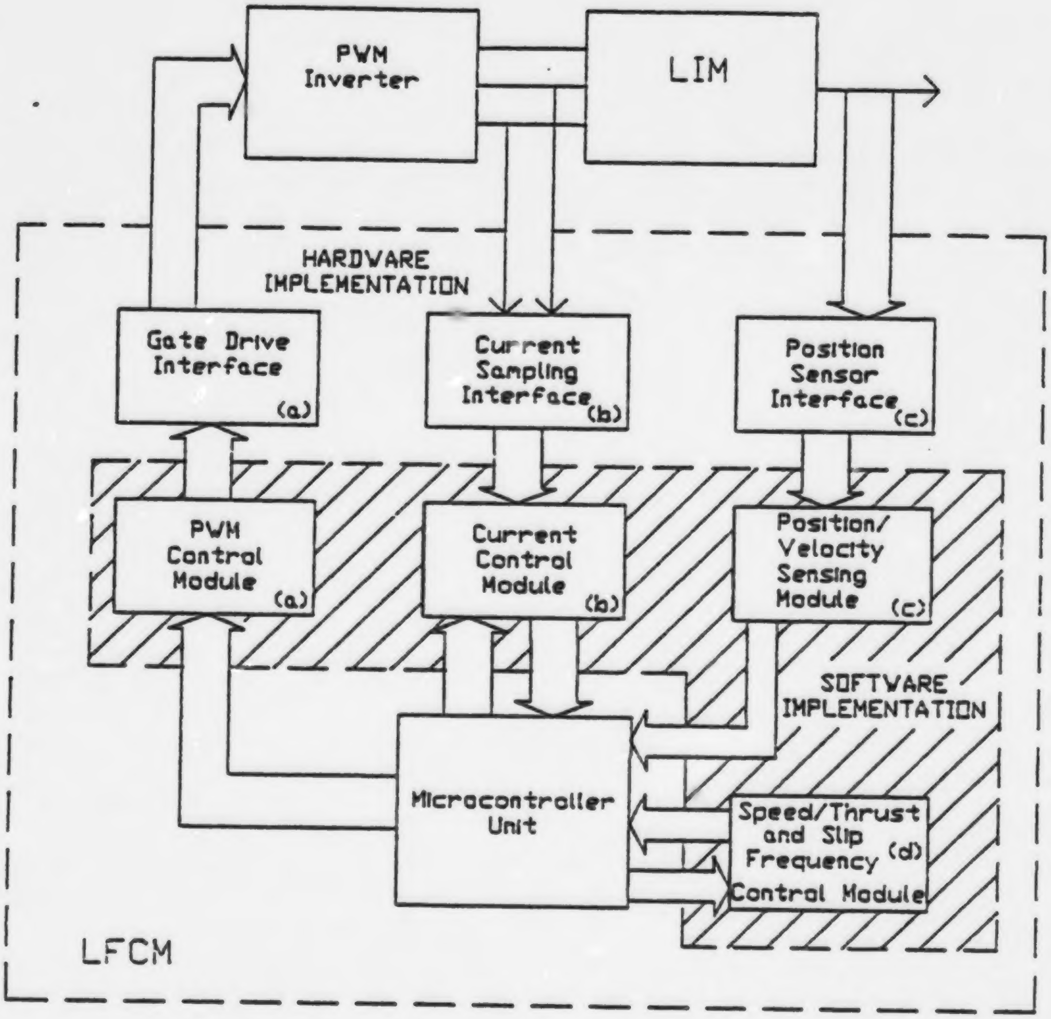
PWM
Inverter
LIM
HARDWARE
IMPLEMENTATION
Gate Drive
Interface
(a)
Current
Sampling
Interface
(b)
Position
Sensor
Interface
(c)
PWM
Control
Module
(a)
Current
Control
Module
(b)
Position/
Velocity
Sensing
Module
(c)
SOFTWARE
IMPLEMENTATION
Microcontroller
Unit
Speed/Thrust
and Slip
Frequency
Control Module
(d)
LFCM

Figure 4.1 Block diagram of the LFCM microcontroller system.

(b) the current control unit - consists of a software module for LIM current control and a hardware interface for current sampling;

(c) the position/velocity sensing unit - comprises of a position sensor circuit and a software module for deriving vehicle position and velocity according to sensor readings; and

(d) the speed/thrust and slip frequency control unit - a software module which generates the velocity demand signal and in turn, the current demand signal according to the position and velocity feedback information, and controls the frequency demand of the inverter.

4.2 Hardware Overview

Since LFCMs are situated in ground between the tracks, the two main criteria considered when designing the hardware are system compactness and cost. The hardware must be designed to accomplish the control task with as few components as possible. Hence, careful consideration in choosing hardware components for size, heat dissipation and cost is required.

The Intel 8097 single-chip microcontroller, part of the MCS-96 family chips, is specifically chosen to fulfill the task. The microcontroller, developed for distributed control applications, is equipped with all the features of a standard microprocessor, as well as many special hardware functions which are required in the LIM control system. These additional integrated features not only simplify the overall hardware design, but also reduce the number of external hardware components making the system compact, reliable and less costly.

The 8097 microcontroller is the heart of the LFCM system. It coordinates and supports all the necessary control functions described in the previous section. Hence, the remaining hardware design comprises mainly of an external memory unit, three I/O interfaces and a system reset circuit. The I/O interfaces are the current sampling interface, the inverter gate drive interface and the position sensor interface, Figure 4.1. These interfaces isolate the microcontroller from the external environment.

4.3 Hardware Implementation

4.3.1 Microcontroller Unit

The Intel 8097 microcontroller [26] is a high performance single chip device which combines a 16-bit powerful microprocessor with several additional I/O features. The specifications, as provided by the manufacturer, appear in Appendix A. Some of the features, such as a 10-bit A/D converter, high-speed I/O unit, 16-bit hardware timers, and parallel and serial ports, are found extremely useful in the LFCM hardware design. For example, the high-speed output (HSO) unit, which is a time-event triggering device, is used for controlling the inverter gate pulses; the high-speed input (HSI) unit, functioned as an external event-recorder, is used for position sensing, and the A/D converter, tightly coupled with the analog input channels, is used for measuring current feedback. Figure 4.2 shows a block diagram of the microcontroller.

The 8097 utilizes a 16-bit memory bus which allows fast external memory access and a large addressable memory space (ie. 64 kbytes). As well, the CPU incorporates a high-speed math processing capability which can perform a 16-bit addition in 1 usec., and 16-bit multiplication or 32-bit division in 6.5 usec. Table 1 of Appendix A summarizes all the microcontroller features. The high-speed CPU capability and I/O features, are ideally suited to the development and implementation of the complex real-time control algorithm for this LIM velocity control application.

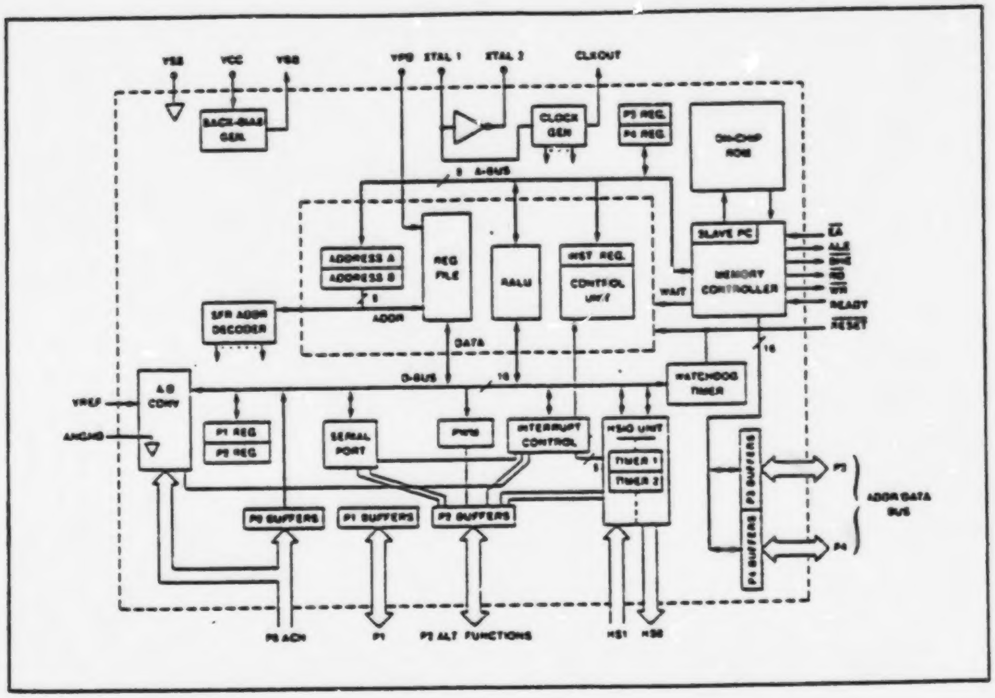
VSS
VCC
VSS
VPD
XTAL 1
XTAL 2
CLKOUT
BACK-BIAS GEN
CLOCK GEN
P3 REG.
P4 REG.
ON-CHIP ROM
8
A-BUS
ADDRESS A
ADDRESS B
REG FILE
RALU
INST REG.
CONTROL UNIT
SLAVE PC
MEMORY CONTROLLER
EA
ALE
BHE
RD
WR
READY
RESET
WAIT
SFR ADDR DECODER
8
ADDR
DATA
D-BUS
16
16
WATCHDOG TIMER
A/D CONV
VREF
ANGND
P1 REG
P2 REG
SERIAL PORT
PWM
INTERRUPT CONTROL
HSIO UNIT
TIMER 1
TIMER 2
5
P3 BUFFERS
P4 BUFFERS
P3
P4
ADDR/DATA BUS
P0 BUFFERS
P1 BUFFERS
P2 BUFFERS
P0 ACH
P1
P2 ALT FUNCTIONS
HSI
HSO

Figure 4.2 8097 microcontroller block diagram.

4.3.2 Memory Unit

Although the addressable memory space on the 8097 is 64 kbytes, only a small number of memory locations are provided internally by the microcontroller. External memory configuration is, therefore, needed for user program and data storage. However, before discussing the memory unit configuration, an understanding of the 8097 bus structure and timing is required, because an improper configuration will result in memory read/write failure.

The 8097 uses a 16-bit multiplexed address/data bus structure. This means that a memory interface is required for bus demultiplexing and memory alignment (ie. memory chips are aligned in pairs such that memory reads/writes are in a word boundary). Also, memory locations 0000H - 00FFH and 1FFEH - 2010H are reserved by the 8097 for special function registers, system stack, memory mapped I/O and interrupt vectors. Hence, when configuring the external memory unit, memory overlap must be avoided.

For the LFCM implementation, 32 kbytes of memory are required for system programs and data, and they are implemented on two 2764 EPROMs (8 kbyte static storage chips) and two HM6264LP RAMs (8 kbyte dynamic storage chips). Also, two transparent octal latches (74LS373) and two bus transceivers (74LS245) are implemented for the bus demultiplexing. Since there are numerous memory devices in the memory unit, a chip select logic is necessary to provide address decoding and device enabling. The logic is constructed according to a memory map, as shown in Figure 4.3. Figure B.3 of Appendix B illustrates a detailed configuration of the memory address map and the chip select logic.

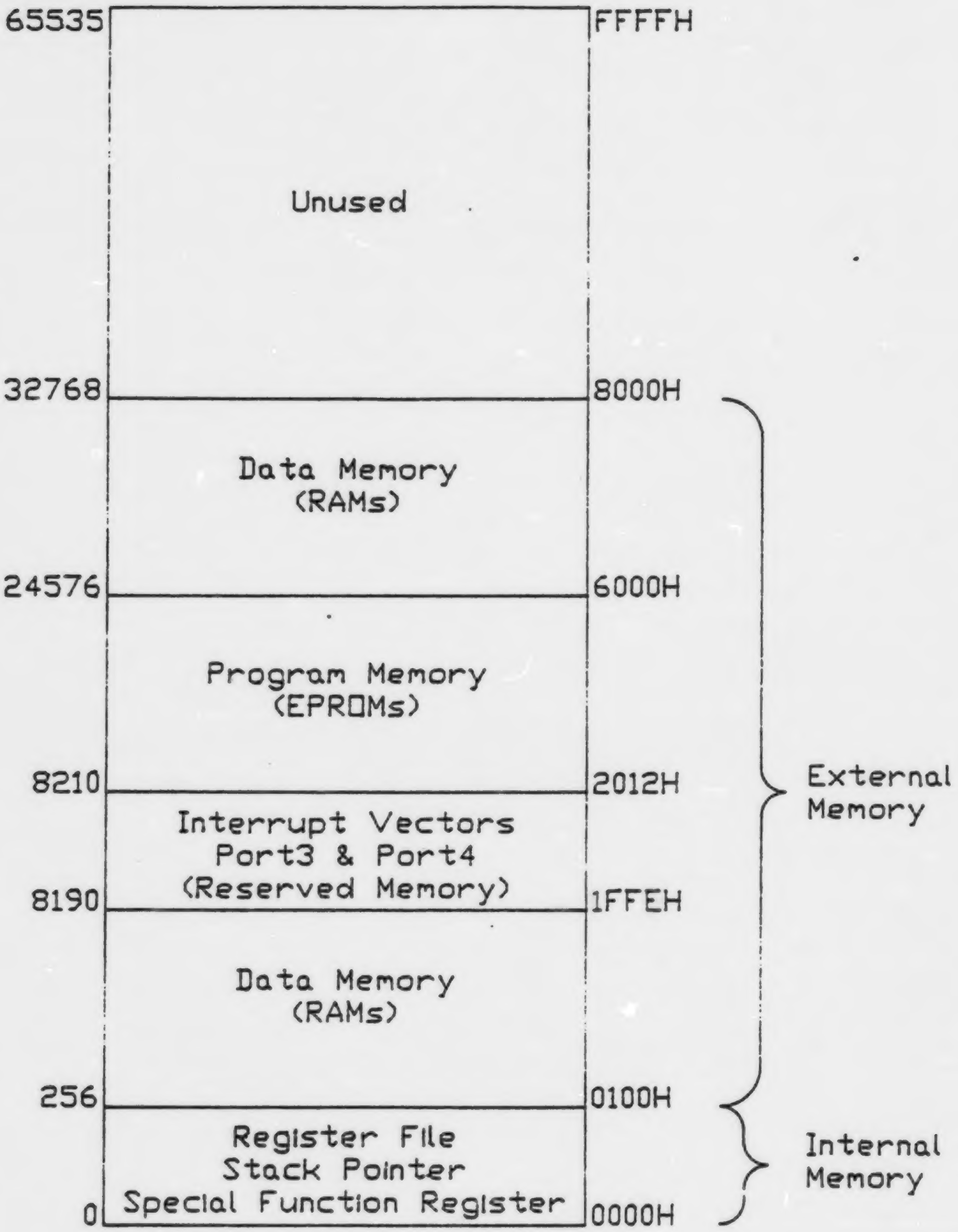
65535
FFFFH
Unused
32768
8000H
Data Memory
(RAMs)
24576
6000H
Program Memory
(EPROMs)
8210
2012H
Interrupt Vectors
Port3 & Port4
(Reserved Memory)
8190
1FFEH
Data Memory
(RAMs)
256
0100H
Register File
Stack Pointer
Special Function Register
0
0000H
External Memory
Internal Memory

Figure 4.3 LFCM memory map.

4.3.3 Current Sampling Interface

Because the A/D converter can only accept an analog signal between 0 to 5 volts, a current sampling interface is designed to protect the analog input channels from over-voltage damage when sampling currents. The interface consists of two identical protection circuits, each of which comprises a current sensor, an op-amp adder and a sample-hold circuit, as shown in Figure 4.4. The current sensors transform ac LIM current signals into small ac voltage signals (ie. within ±2.5 volts). The op-amps add 2.5 volts dc offset to the signals, to shift the signals into the required voltage range. A low-pass RC filter is used as a sample-and-hold (S/H) device for the A/D converter. The values of the RC components are chosen specifically to ensure that the voltage on the sample and hold circuit will not vary more than 0.05% [26]. The 1 Kohm trimpot, included in the op-amp adder, adjusts the gain to obtain equal magnitude current feedback from two of the three phases. This is essential for the current magnitude calculation, Section 5.2.2, because its derivation is based on the assumption of balanced 3-phase currents. However, with this gain control set up, one must be aware that there may be a possible error term introduced in the current magnitude calculation by the dc offset voltage. Please refer to Appendix C for the detailed derivation of this dc offset effect and and its possible solution.

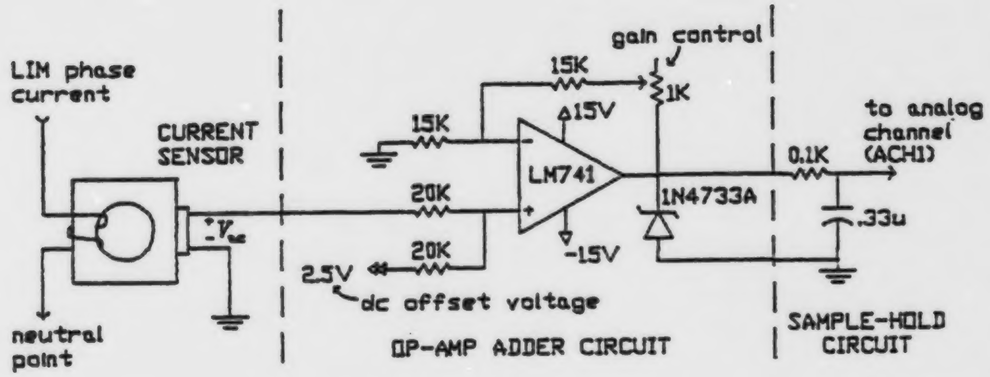
gain control
LIM phase current
15K
1K
15V
to analog channel (ACH1)
CURRENT SENSOR
15K
LM741
0.1K
20K
1N4733A
.33u
$\pm V_{oc}$
20K
-15V
2.5V
dc offset voltage
neutral point
OP-AMP ADDER CIRCUIT
SAMPLE-HOLD CIRCUIT

Figure 4.4 Current sampling interface.

4.3.4 Position Sensor Interface

The position sensor interface design is divided into 3 sections: a sensor circuit, an input protection circuit and a sensor transition-detector circuit. The sensor circuit consists of two sensors, one mounted near each end of the LIM, as shown in Figure 4.5, so that detection of the train can be made from either direction of approach. Note that the sensors are arranged such that one sensor will monitor vehicle position while the inter-vehicle gap is encountered by the other sensor.

The sensor, provided by UTDC, is designed to work in conjunction with a vehicle-mounted sensing rail. The sensing rail is comprised of a long steel strip onto which a series of evenly spaced permanent magnets are fixed. The sensor comprises of three hall-effect magnetic flux detectors mounted on an E-core, which is spatially oriented with respect to the sensing rail strips. In response to the presence of the magnetic strips as the rail passes by, the detectors produce the output signal patterns as shown in Figure 4.5. These signal patterns are dependent on the train travel direction. For positive train direction, the decoded 3 pulses appear in sequence with the values 1, 3, 2, 6, 4, 5, 1, 3, ... , 4, 5. For negative train direction, they appear in the reverse order of that of positive direction. The three detector arrangement facilitates the discernment of the train stationary presence and travel direction. The sensors and the sensing rail are designed to work with an airgap of up to 12 mm., and as well, each transition of the sensor represents a position change of 5 mm. However, the sensors are rather sensitive to the airgap distance. A slight increase in the airgap distance may lead to failure in detecting signal transitions.

The microcontroller monitors the sensor output lines through an input port. However, since it is not practical to scan these lines continuously, a means of detecting the sensor transition is needed. A hardwired discriminator circuit fulfills this need by generating an interrupt signal to the microcontroller whenever a state transition of the sensor occurs. Also, an input protection circuit is implemented between the microcontroller and the sensors to provide noise immunization. The details of this circuitry are presented in Appendix B, Figure B.1.

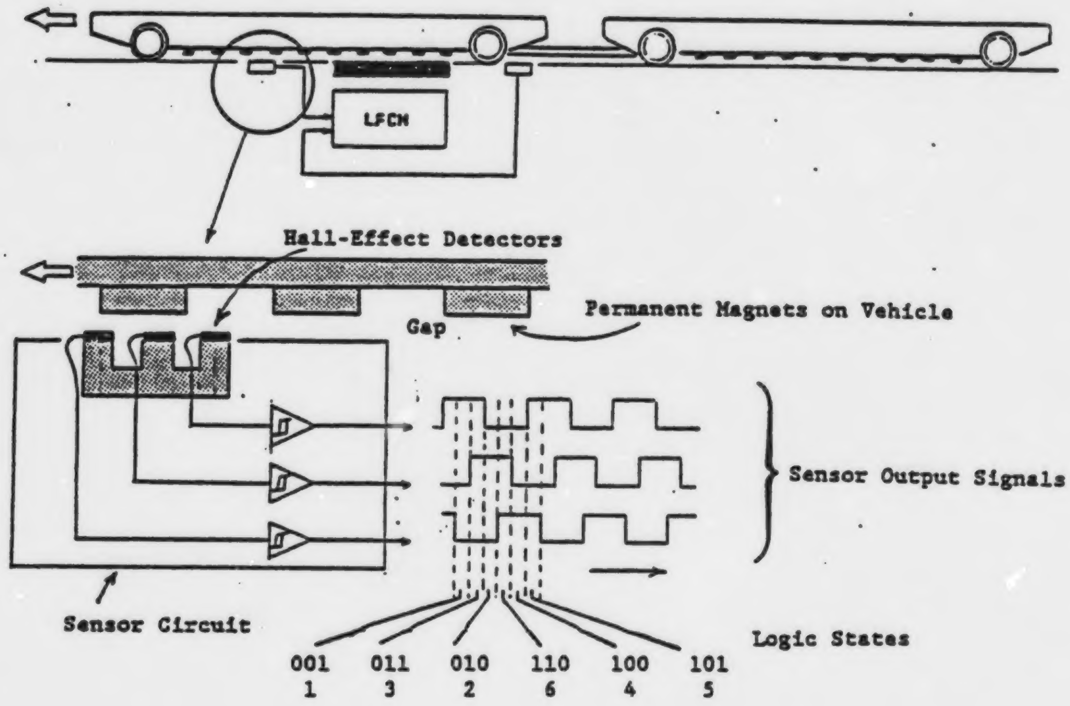
LFCM
Hall-Effect Detectors
Permanent Magnets on Vehicle
Gap
Sensor Output Signals
Sensor Circuit
Logic States
001
1
011
3
010
2
110
6
100
4
101
5

Figure 4.5 LFCM sensor arrangement.

4.3.5 Inverter Gate Drive Interface

In the inverter thyristor firing control, gating pulses are generated by the microcontroller via the HSO unit. Three pulse-width modulated gating signals are sent to the inverter firing circuits through an interface which consists of 3 pairs of complementary buffer circuits as shown in Figure 4.6. The complementary signals are correspondingly fed to each phase of the inverter bridge. This implementation ensures that only one thyristor of each inverter phase will conduct at any time, and hence, inverter short-circuits are prevented.

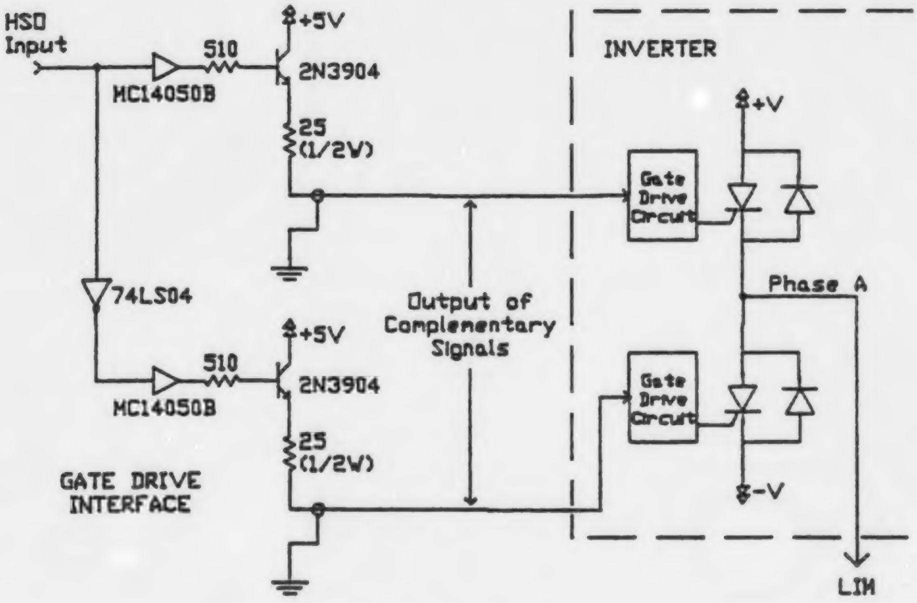
HSO Input
MC14050B
510
+5V
2N3904
25 (1/2W)
74LS04
+5V
MC14050B
510
2N3904
25 (1/2W)
GATE DRIVE INTERFACE
Output of Complementary Signals
INVERTER
+V
Gate Drive Circuit
Phase A
Gate Drive Circuit
-V
LIM

Figure 4.6 Circuitry of the gate drive interface (1 of the 3 phases).

4.3.6 Reset Circuit

Figure 4.7 shows a simple reset circuit, implemented on the LFCM control board. This is required for manual reset of the system whenever failure is detected. Upon each reset, the microcontroller will be re-initialized, and the I/O lines and special function registers will be in their reset state. Appendix B contains diagrams of the system board layout and schematic, and other information pertaining to the LFCM hardware configuration.

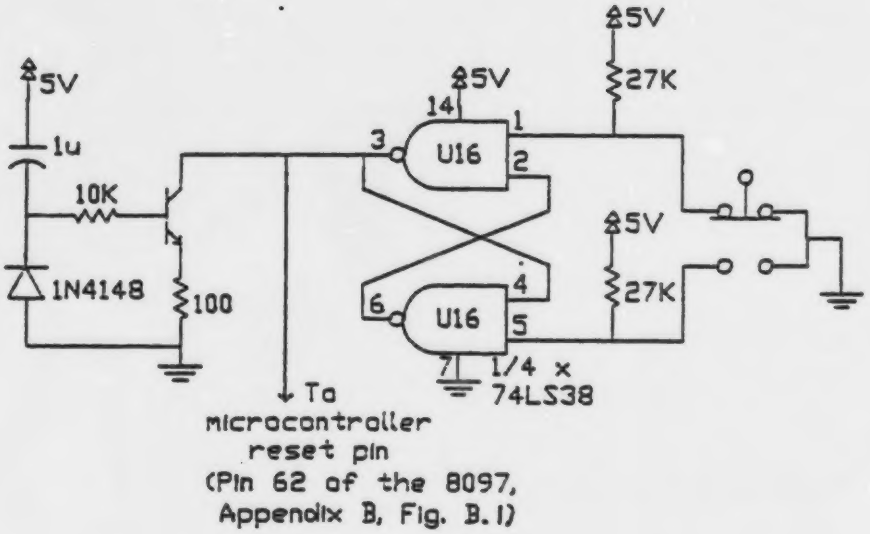
5V
1u
10K
1N4148
100
5V
14
3
U16
1
2
5V
27K
5V
27K
4
6
U16
5
7
1/4 x
74LS38
To
microcontroller
reset pin
(Pin 62 of the 8097,
Appendix B, Fig. B.1)

Figure 4.7 Reset circuit.

CHAPTER 5

SOFTWARE DESIGN AND IMPLEMENTATION

5.1 Software Overview

The software design of the LFCM represents the major portion of the system development, since the hardware design is constrained to a minimum number of components. The software algorithms coordinate and execute all the control tasks of the LFCM. The software design approach breaks the LFCM control tasks into four modules. They are:

(a) PWM Control Module;
(b) Current Sampling Module;
(c) Position/Velocity Sensing Module; and
(d) Speed/Thrust and Slip Frequency Control Module.

Each of these modules is responsible for particular control functions, and is made up of several routines. A block diagram of the system software structure is illustrated in Figure 5.1.

Since the LFCM system involves real-time interaction with the external environment, the software implementation is based on a priority

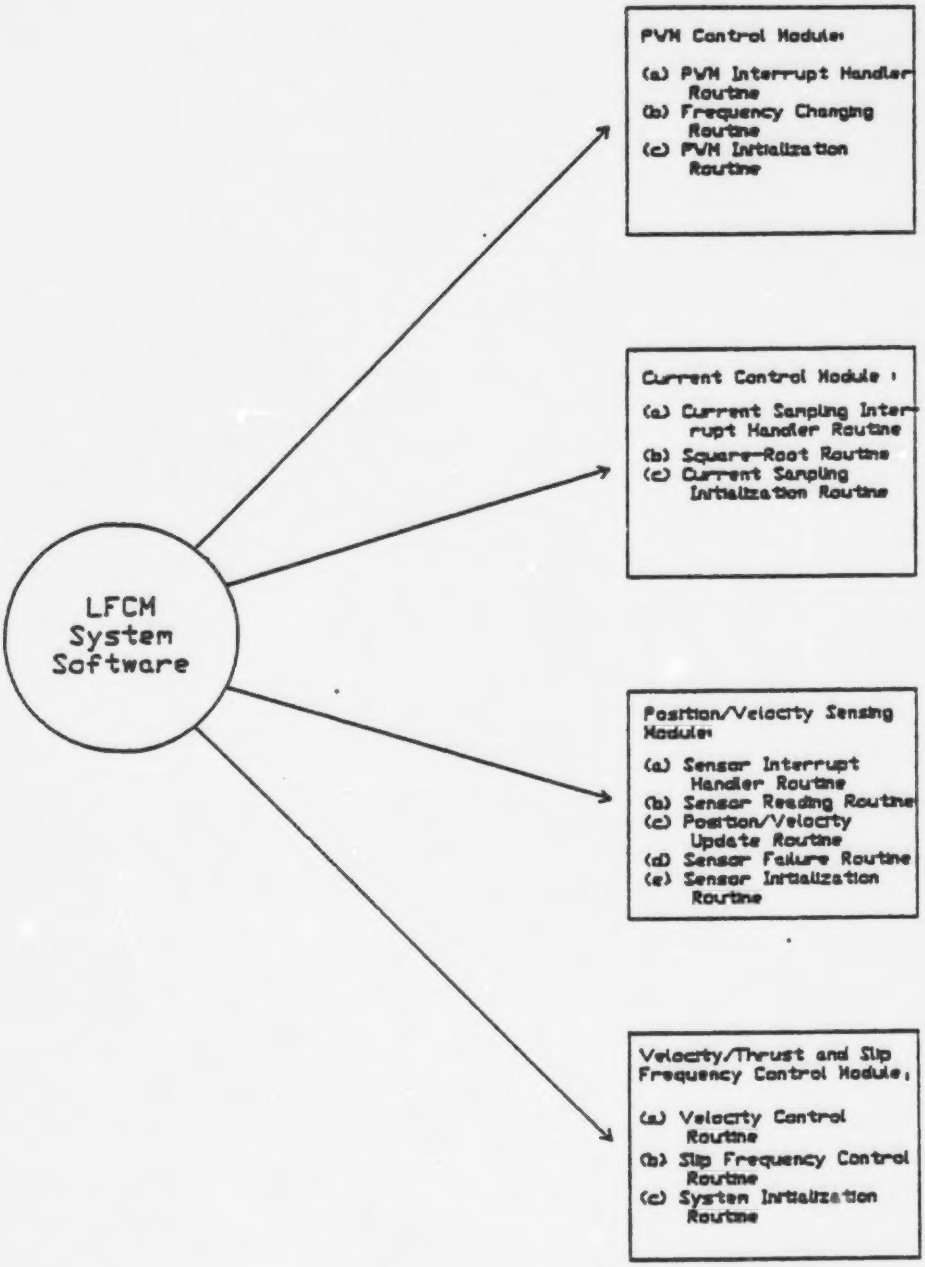
LFCM System Software
PWM Control Module:
(a) PWM Interrupt Handler Routine
(b) Frequency Changing Routine
(c) PWM Initialization Routine
Current Control Module :
(a) Current Sampling Interrupt Handler Routine
(b) Square-Root Routine
(c) Current Sampling Initialization Routine
Position/Velocity Sensing Module:
(a) Sensor Interrupt Handler Routine
(b) Sensor Reading Routine
(c) Position/Velocity Update Routine
(d) Sensor Failure Routine
(e) Sensor Initialization Routine
Velocity/Thrust and Slip Frequency Control Module:
(a) Velocity Control Routine
(b) Slip Frequency Control Routine
(c) System Initialization Routine

Figure 5.1 LFCM system software structure.

interrupt programming technique, with program tasks arranged in an hierarchical order. This means that, in term of execution sequence, programs of highest priority will always take precedence over those of lowest priority. For example, the velocity and slip frequency control routines are assigned to have the lowest priority because they are the least time critical function in the system. They are executed as a background task and can be interrupted whenever requested by the higher priority routines such as the PWM, current sampling or position sensing routines. Figure 5.2 depicts the LFCM routine priority structure.

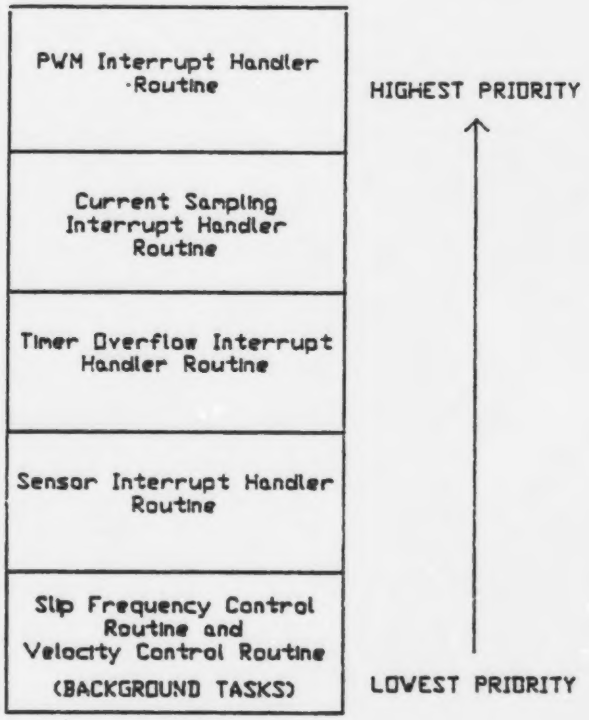
PWM Interrupt Handler Routine
Current Sampling Interrupt Handler Routine
Timer Overflow Interrupt Handler Routine
Sensor Interrupt Handler Routine
Slip Frequency Control Routine and Velocity Control Routine
(BACKGROUND TASKS)
HIGHEST PRIORITY
LOWEST PRIORITY

Figure 5.2 LFCM software routine priority structure.

Most of the system software is implemented with the high-level language, PL/M-96 [28]. This language is easy to understand which results in faster program development. However, its code execution is not as efficient as that of assembly language. Hence, for some time-critical tasks, the routines are written in ASM-96 assembly language [29].

5.2 Software Implementation

5.2.1 PWM Module

The most important consideration in the PWM control design is undoubtably the switching strategy used to generate PWM pulses. The design is based on the regular sampled switching method, and is implemented under the following requirements:

(a) 3-phase generation;
(b) independent control of output voltage and frequency;
(c) operation in the range of 0.5 - 60 Hz with a resolution of 0.5 Hz;
(d) control of frequency and modulation ratio; and
(e) maximum of 1000 Hz for the inverter switching frequency.

As well, the memory requirement, efficiency of operation, and the voltage and frequency accuracy of the output waveform are considered.

Since a real-time generation of PWM outputs using a software algorithm is time consuming, the module is developed principally on the basis of lookup tables [7]. Figure 5.3 shows the microcontroller implementation of the regular sampled PWM control. For a particular demand frequency (f_d), the microcontroller calculates all the pulsewidths of a 1 p.u. quarter-cycle sinusoidal modulating wave, and stores them as a lookup table in memory as shown. Because of the 120° phase difference between the phases and the quarter-cycle symmetry of a sine wave, the 3-phase PWM output information is read cyclically using 3 appropriately located address pointers. Hence, in the actual output operation, the microcontroller multiplies the voltage demand (V_d) with the three 1 p.u. pulsewidths, corresponding to the 3 phases of each sample instant, and outputs them to the inverter accordingly.

Figure 5.4 shows an expanded view of the pulsewidth synthesis. Each 1 p.u. pulsewidth is calculated according to the following equation;

$$W_j = \left[\frac{T}{2} + \left(\frac{T}{2} - W_N \right) \sin(\omega t_j) \right] \tag{5.1}$$

where

T = sample period (ie. 1 / switching-frequency);

t_j = sample instant j;

ω = fundamental demand frequency (rad/sec);

W_j = 1 p.u. pulsewidth at t_j, and

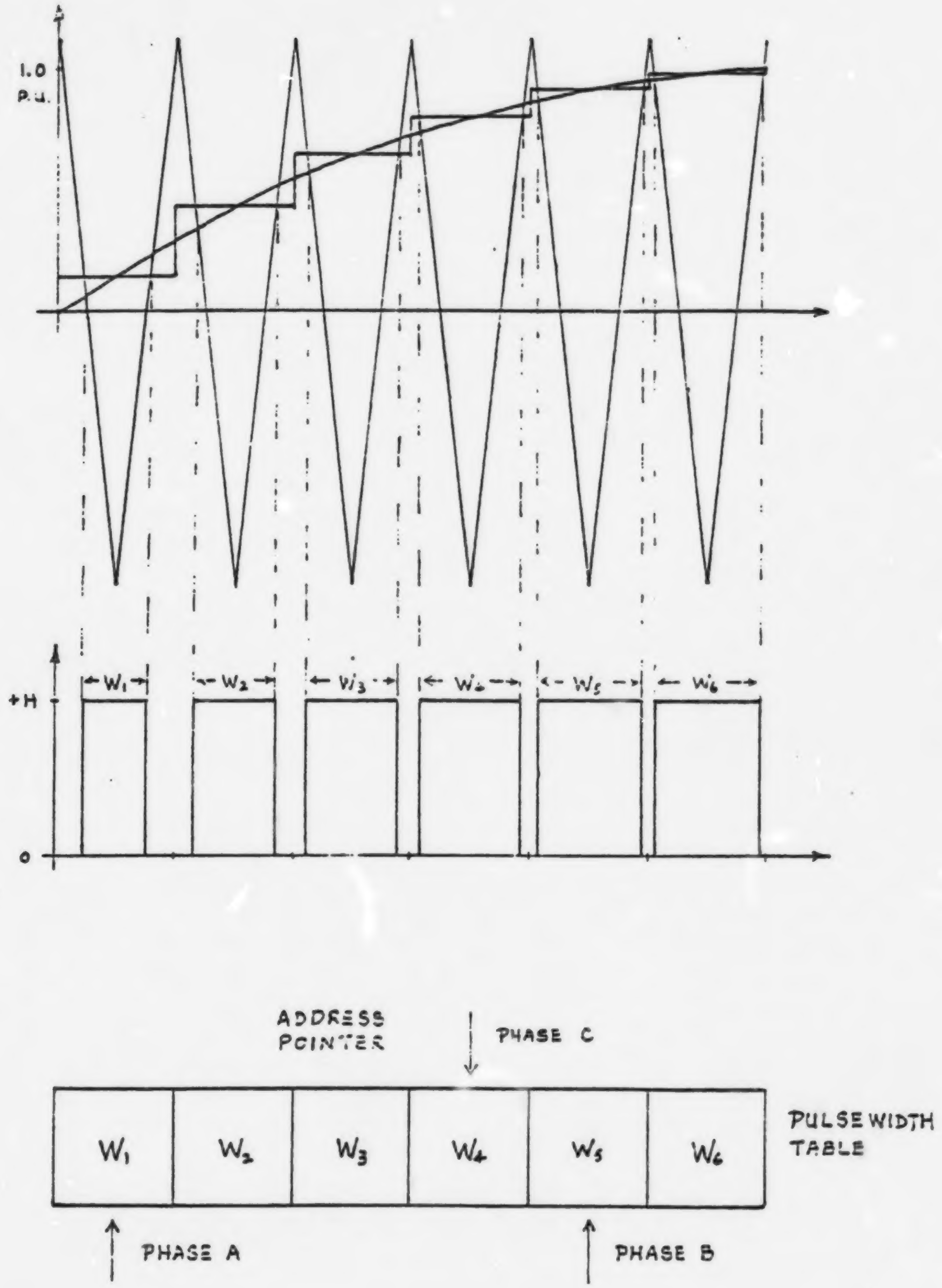
1.0
p.u.
+H
0
W₁
W₂
W₃
W₄
W₅
W₆
ADDRESS
POINTER
PHASE C
PULSE WIDTH
TABLE
PHASE A
PHASE B

Figure 5.3 Microcontroller implementation of regular sampled PWM.

W_N - minimum notch-width (ie. the minimum time for a given inverter output line to switch from one dc bus to the other and back).

All these variables are expressed in terms of the microcontroller clockticks. Each clocktick is equivalent to 2 μsec. The minimum notch width is included to ensure the modulation ratio (ie. the ratio of modulating signal amplitude over carrier signal amplitude) to be less than 1, and hence, provides a safeguard against inverter commutations which cause dc bus short circuits.

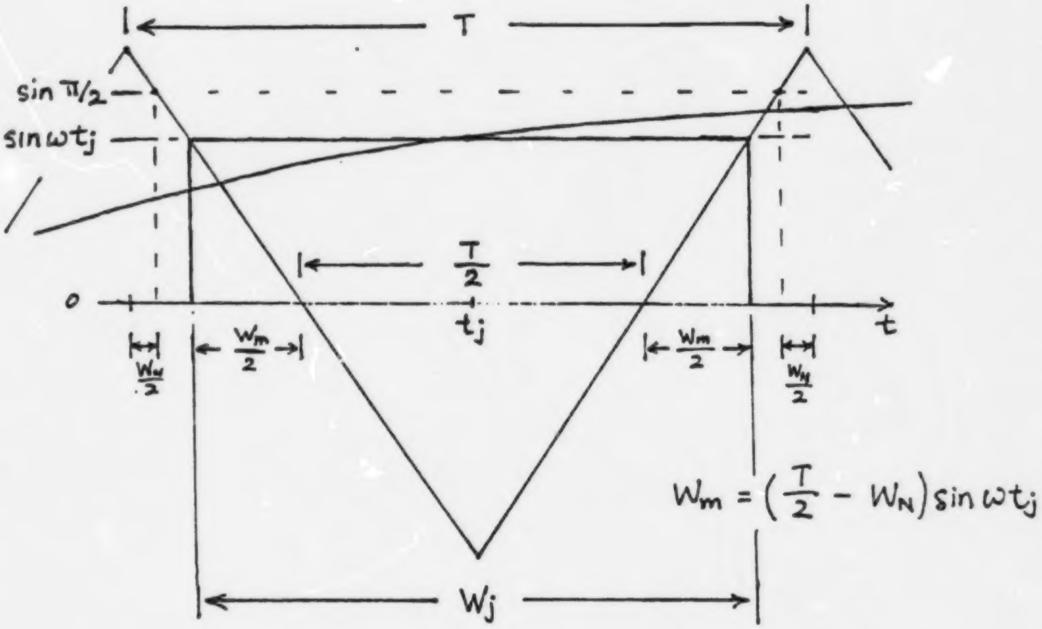

Figure 5.4 Generation of a regular sampled width-modulated pulse.

The number of pulses per quarter-cycle, or the sample period, is determined by the frequency ratio which is the ratio of switching frequency over fundamental output frequency. The choice of the frequency ratio is important, because it has a direct influence over the harmonic content of the PWM output. Normally, for optimum harmonic minimization, the frequency ratio is chosen to be as high as possible and to be an integer multiple of three, preferably greater than nine [8,16]. But for microprocessor implementation, it is desirable to have a ratio of multiple of four to maintain quarter-cycle symmetry, so that memory can be conserved. Hence, a discrete integer ratio [11] is chosen for each fundamental demand frequency to satisfy these criteria. These ratios are stored in the system memory as a lookup table. It is important to note that when changing the fundamental frequency, the frequency ratio is changed in integer steps. Therefore, care must be taken in order to prevent any significant inverter voltage transient.

Hence, a segmentation scheme is devised, as shown in Figure 5.5, in which the output waveforms are divided into segments, where each segment corresponds to 1/12 of a cycle and contains at least one PWM pulse. Figure 5.5a illustrates the frequency change operation at the beginning of segment 5 and segment 4. Frequency change is permitted only at the beginning of a segment. This is to ensure the matching of the fundamental voltages when changing frequency. A segment unit of '1/12' cycle is chosen so that the frequency ratio will be an integer multiple of three as well as maintaining quarter-cycle symmetry.

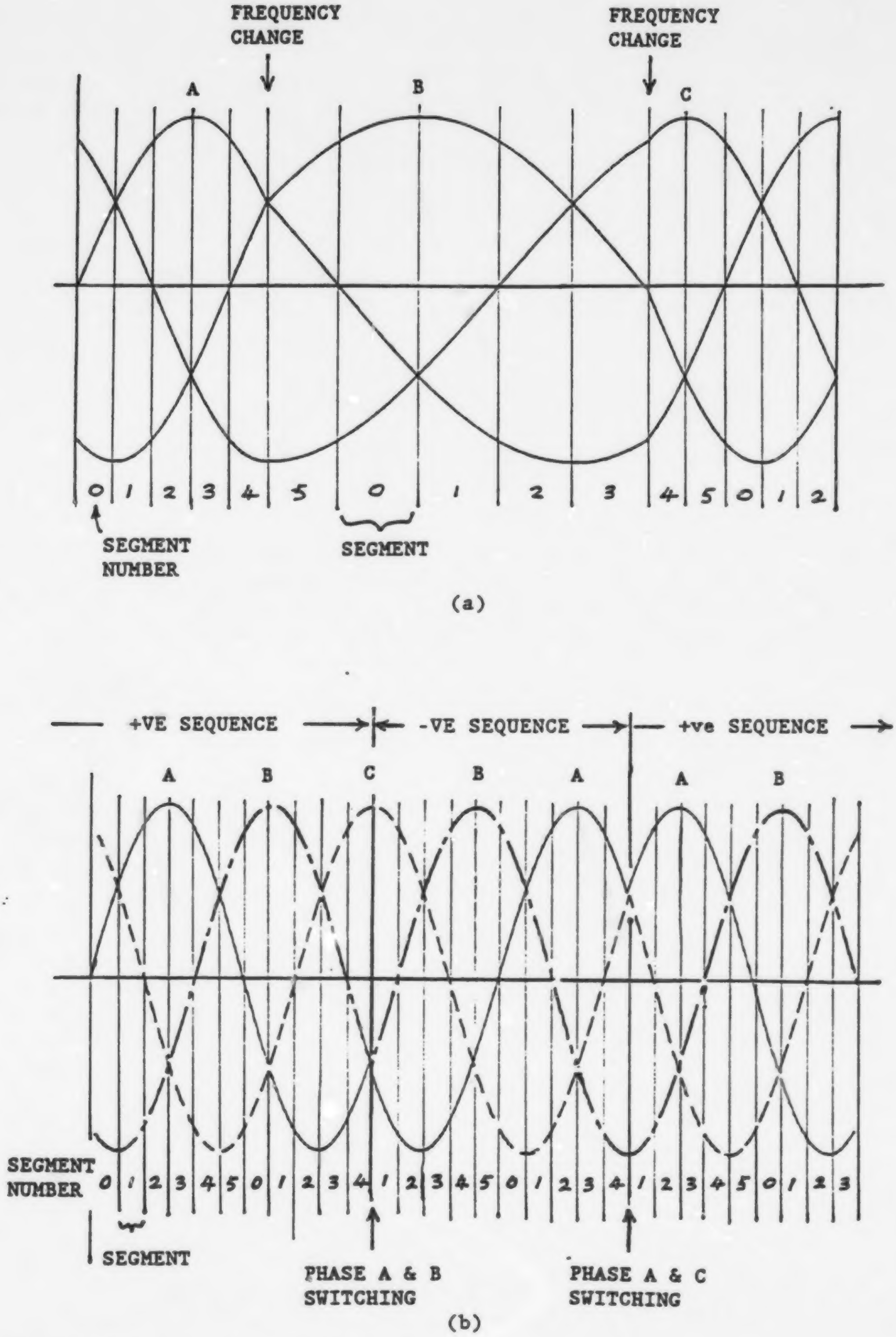
FREQUENCY CHANGE
FREQUENCY CHANGE
A
B
C
0 1 2 3 4 5 0 1 2 3 4 5 0 1 2
SEGMENT NUMBER
SEGMENT
(a)
+VE SEQUENCE
-VE SEQUENCE
+ve SEQUENCE
A
B
C
B
A
A
B
SEGMENT NUMBER
0 1 2 3 4 5 0 1 2 3 4 1 2 3 4 5 0 1 2 3 4 1 2 3 4 5 0 1 2 3
SEGMENT
PHASE A & B SWITCHING
PHASE A & C SWITCHING
(b)

Figure 5.5 PWM segmentation scheme
(a) Frequency change operation.
(b) Phase sequence reversal operation.

With this segmentation method, the implementation of phase sequence reversal is easily facilitated. Figure 5.5b shows the phase sequence reversal operation. The operation can be performed by merely switching the pulsewidth table address pointers of two particular phases at the appropriate segments. Note that each segment is identified by a number which is relative to phase A, and phase switching can only be done at the beginning of segment 1, 3 and 5. As shown, phase A pointer is switched with phase B pointer at the beginning of segment 1 to produce the negative sequence, and phase A with phase C at segment 1 to produce the positive sequence. The segment number is re-assigned if switching involves phase A, because it is relative to phase A.

The implementation of this module is divided into 3 parts, namely, (a) PWM Interrupt Handler Routine, (b) Frequency Changing Routine and (c) PWM Initialization Routine. The latter one is merely for module variable initialization, and therefore, is not discussed here.

5.2.1a PWM Interrupt Handler Routine

This routine is an interrupt driven routine, and is assigned to have the highest priority in the system because it controls all the PWM outputs. Hence, timing is very important and it should not be interrupted by other processes. The interrupt is triggered periodically by a software timer, and the period corresponds to the switching period (also known as sample period). During each execution of the routine, a new interrupt time is set to generate an interrupt at the next sample period. This software control of the interrupt period provides the flexibility of changing sample period, and thus, the switching frequency.

A simplified flowchart of the PWM routine is shown in Figure 5.6. Upon each execution, the pulsewidth information of the 3 phases is loaded into the high-speed output (HSO) unit, in which the 3 PWM pulses are output through the internal hardware. The pulsewidth information is obtained by multiplying the voltage demand value by the three 1 p.u. pulsewidths, fetched from the lookup table.

During each sample period, the address pointers and the related 'flag' variables are updated before fetching the 1 p.u. pulsewidths. These updates include checking if frequency or phase sequence is to be changed. If the frequency is to be changed, the current pulsewidth table will be replaced by a new one, which would have been prepared by the Frequency Changing Routine. However, these events are rather time consuming and could impose a problem in outputting the pulses, because during each sample period, there is a limited time before the pulses are sent out. Hence, to ensure proper pulse outputs, a one sample period delay is implemented. This means that at the beginning of each sample period, the pulsewidth information that is sent to the HSO unit for outputting, is pre-calculated during the previous sample period. For the remaining sample period, the necessary updates and the preparation of pulsewidth information for the next sample period are performed.

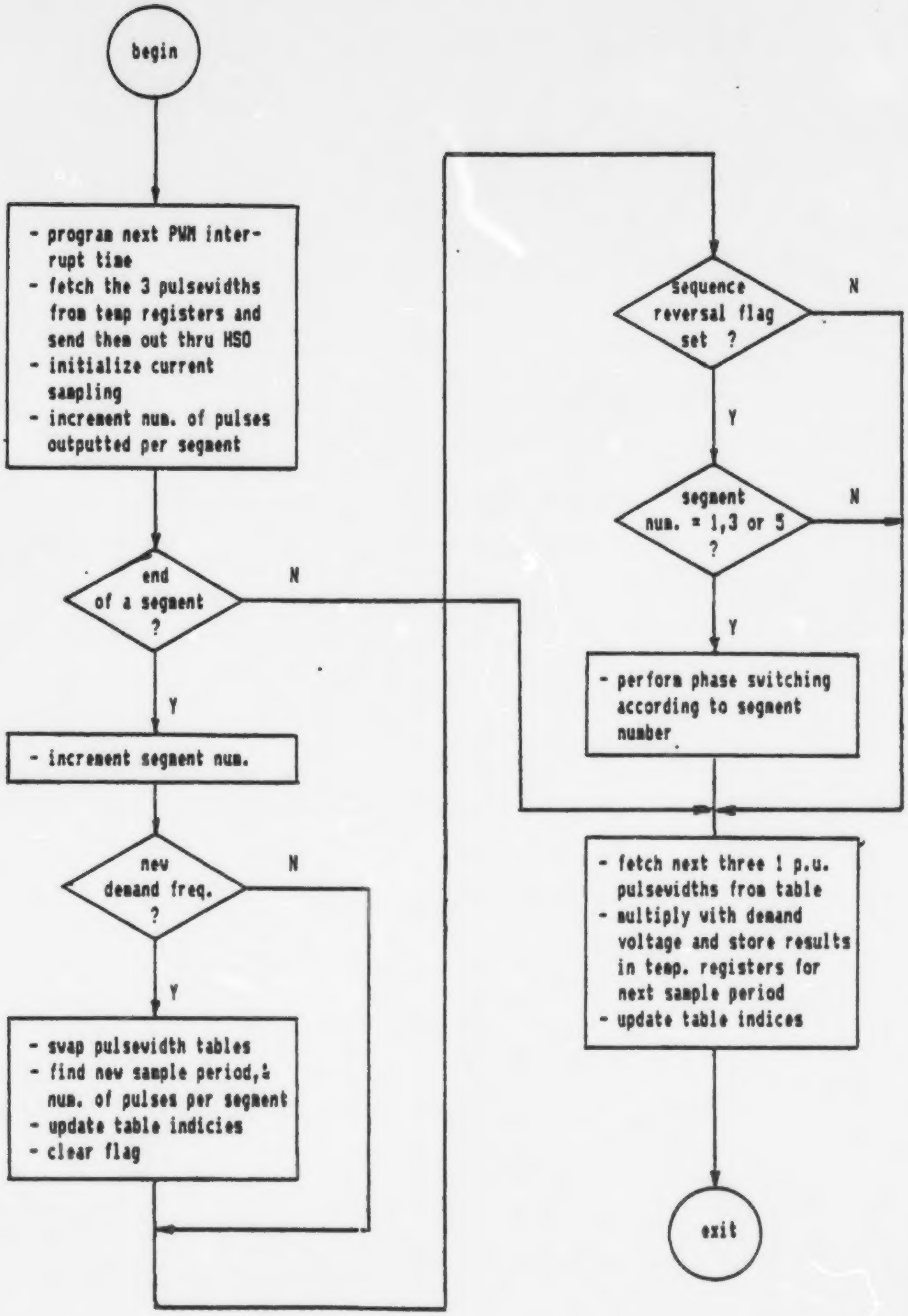
begin
- program next PWM interrupt time
- fetch the 3 pulsewidths from temp registers and send them out thru HSO
- initialize current sampling
- increment num. of pulses outputted per segment
end of a segment ?
N
Y
- increment segment num.
new demand freq. ?
N
Y
- swap pulsewidth tables
- find new sample period,& num. of pulses per segment
- update table indicies
- clear flag
sequence reversal flag set ?
N
Y
segment num. = 1,3 or 5 ?
N
Y
- perform phase switching according to segment number
- fetch next three 1 p.u. pulsewidths from table
- multiply with demand voltage and store results in temp. registers for next sample period
- update table indices
exit

Figure 5.6 Simplified flowchart of the PWM Interrupt Handler Routine.

5.2.1b Frequency Changing Routine

This is a non-interrupt driven subroutine program, and is designed to prepare a new pulsewidth lookup table when a new frequency is demanded. Note that it does not perform the actual change of frequency, which is done only in the PWM routine.

This routine is usually invoked by the Slip Frequency Control Routine when a new demand frequency is determined. Upon each request, the program is executed as a background task, and hence, can be interrupted by higher priority routines. It finds the frequency ratio of the new demand frequency and determines the new sample period and lookup table size. The pulsewidths of the 1 p.u. quarter-cycle modulating wave are calculated according to Equation 5.1, and stored in the table. Upon completion, a flag is set to indicate that frequency is ready to be changed. Figure 5.7 shows a flowchart of the routine.

Preparation of lookup table is time consuming, especially at low frequency where the number of pulses per cycle is large. In order to provide a quick change of frequency, assembly code programming is used. It is found that even for the largest lookup table (ie. when the demand frequency is 0.5 Hz), the maximum computation time is less than 5 msec, which is adequate for this system application.

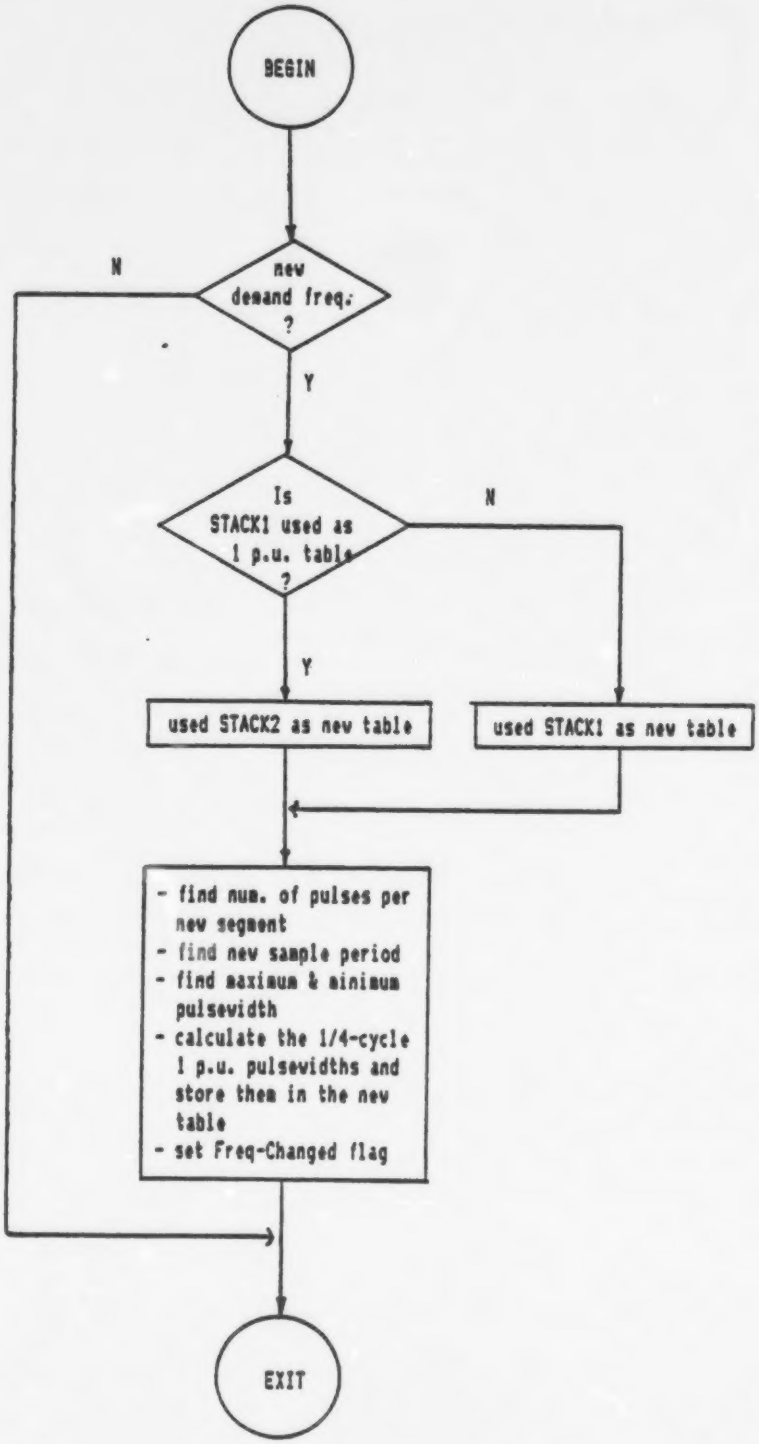
BEGIN
new demand freq. ?
N
Y
Is STACK1 used as 1 p.u. table ?
N
Y
used STACK2 as new table
used STACK1 as new table
- find num. of pulses per new segment
- find new sample period
- find maximum & minimum pulsewidth
- calculate the 1/4-cycle 1 p.u. pulsewidths and store them in the new table
- set Freq-Changed flag
EXIT

Figure 5.7 Simplified flowchart of the Frequency Changing Routine.

5.2.2 Current Control Module

This module provides LIM current control in the LFCM. The module is composed of 3 programs. They are: (a) Current Sampling Interrupt Handler Routine; (b) Square-Root Routine and (c) Current Sampling Initialization Routine.

5.2.2a Current Sampling Interrupt Handler Routine

This routine is an interrupt driven routine, and is invoked upon each completion of current sampling (ie. A/D conversion). The control algorithm is developed according to the current loop scheme discussed in Chapter 3. During each execution, the current controller derives the feedback current magnitude (I_f) from the three phase currents based on the following equation;

$$I_f = \sqrt{4/3\ [(I_a + I_b)^2 - I_a I_b]} \qquad (5.2)$$

which is equivalent to Equation 3.8. This feedback value subtracted from the demand current (I_d) produces an error signal (e_i). This error signal will, in turn, be passed through a PI controller shown in the block diagram of Figure 5.8. The result of this operation is the demand voltage signal (V_d), which is required by the PWM routine during each PWM sample period. The gain constants K_p (proportional gain) and K_I

(integral gain) are stored in memory, and hence, can be altered to allow control optimization. Also, an output voltage clamp is implemented for inverter protection. Hence, V_d is limited to be within a 8 bit binary value (ie. 0 - 512 decimal).

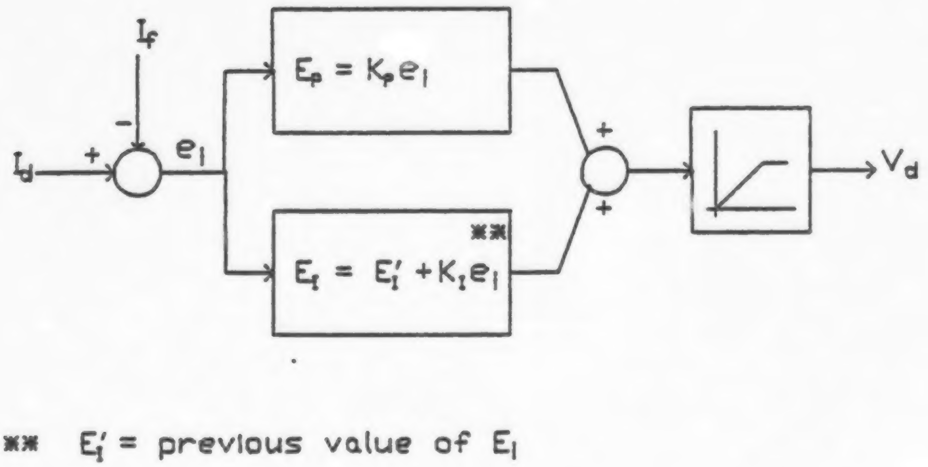

Figure 5.8 Block diagram of the PI current controller.

In order to control the current closely, this routine is operated in synchronization with the PWM mechanism, since voltage control is performed during each PWM sample period. Thus, each current sampling (ie. A/D conversion) is initiated by the PWM Interrupt Handler. A flowchart of the algorithm is shown in Figure 5.9.

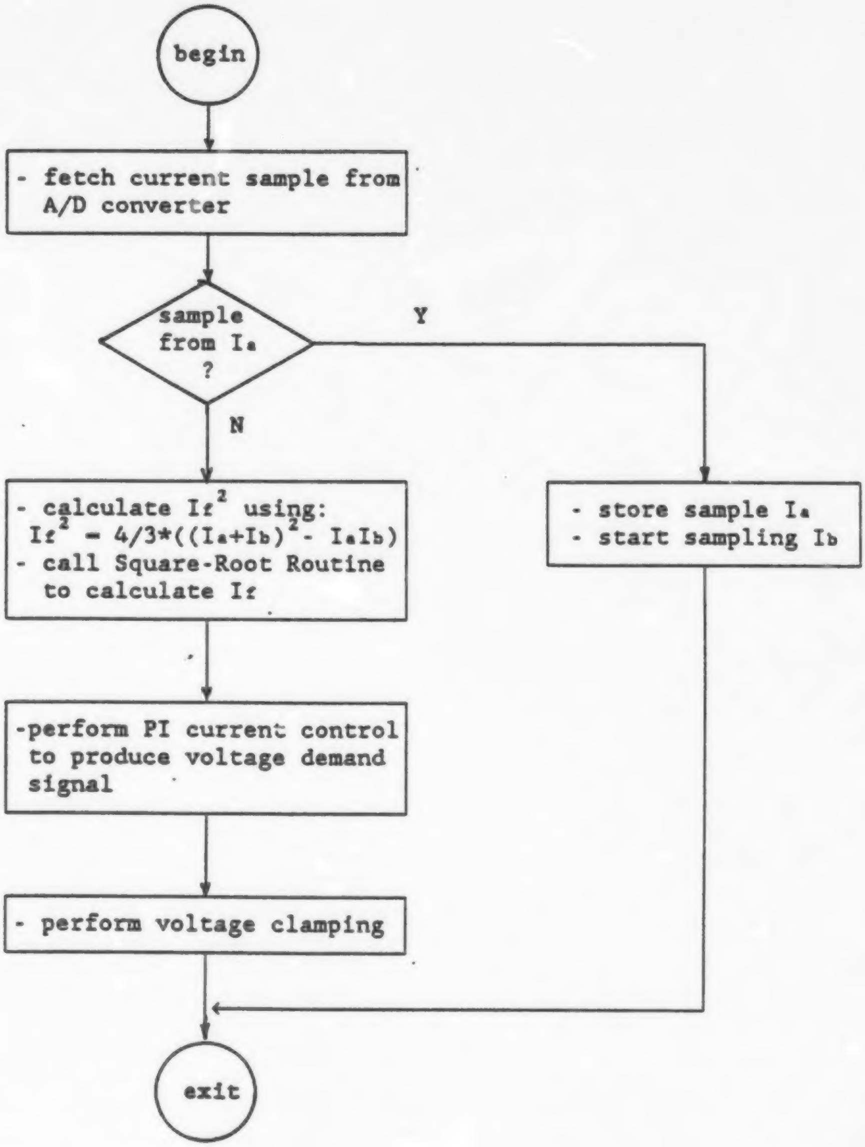
begin
- fetch current sample from A/D converter
sample from I_a ?
Y
N
- calculate I_f^2 using: $I_f^2 = 4/3*((I_a+I_b)^2 - I_aI_b)$
- call Square-Root Routine to calculate I_f
- store sample I_a
- start sampling I_b
-perform PI current control to produce voltage demand signal
- perform voltage clamping
exit

Figure 5.9 Simplified flowchart of the Current Sampling Interrupt Handler Routine.

5.2.2b Square-Root Routine

A square-root function is needed to find the current magnitude in Equation 5.2. To implement this function, the lookup table method is used, since it is fast and simple. Because of the 10-bit resolution of the A/D converter, the current magnitude is bounded between 0 and 512, and hence, the range of current square is 0 - 262144. Since it is such a large square range, the function is implemented with three lookup tables.

The first table is a linear table which stores the squares of numbers 0 - 52 as shown in Figure 5.10. To find the square root of a number (note: number must be within the range of 0 - 2704), a binary search is used to locate the element, and hence, the index of the searched element is the square root. However, with this type of lookup table, searching can be time consuming if table size is large. Hence, two other tables are used to find square roots for ranges of 2704 - 50176 and 50176 - 262144. These two tables are implemented as hash tables in which the table elements are the actual square roots, and the indices to these elements are determined by their square values according to the formula, shown in Figure 5.11. These hash table implementations [27], not only require a minimal amount of memory, but provide fast square-root lookups. On average, each evaluation takes approximately 0.35 msec, which is acceptable in this LIM application. Figure 5.12 illustrates a flowchart of the algorithm.

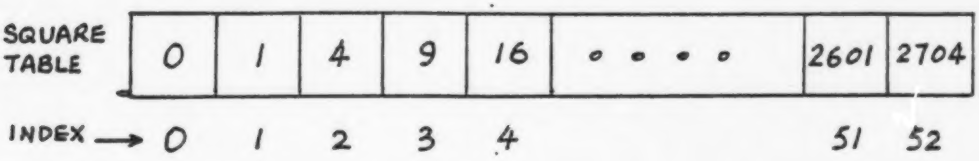
SQUARE TABLE
0
1
4
9
16
2601
2704
INDEX →
0
1
2
3
4
51
52

Figure 5.10 Linear lookup table for a square-root function.

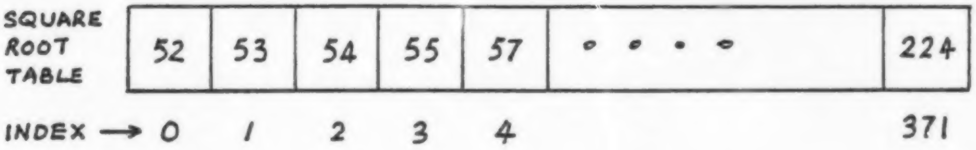
SQUARE ROOT TABLE
52
53
54
55
57
224
INDEX →
0
1
2
3
4
371

$$\text{INDEX} = \frac{X}{128} - 21$$

$$\sqrt{X} = \text{SQUARE ROOT TABLE [INDEX]}$$

Figure 5.11 Hash table for a square-root function.

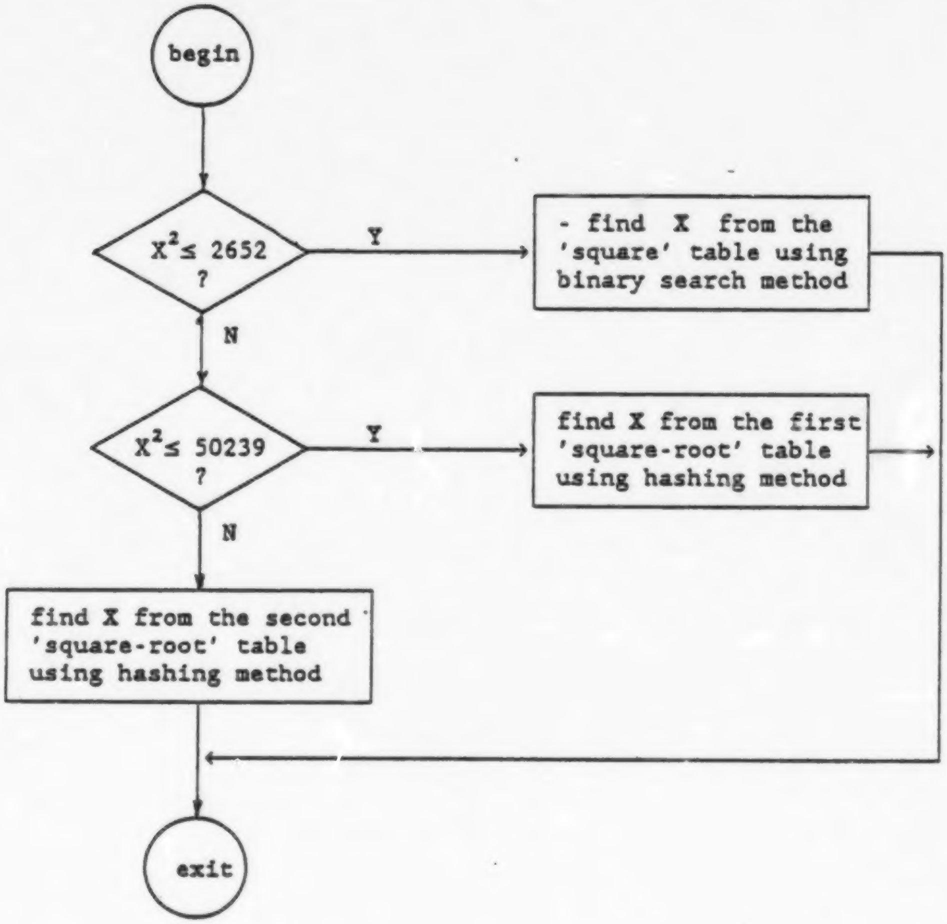
begin
$X^2 \leq 2652$?
Y
- find X from the 'square' table using binary search method
N
$X^2 \leq 50239$?
Y
find X from the first 'square-root' table using hashing method
N
find X from the second 'square-root' table using hashing method
exit

Figure 5.12 Simplified flowchart diagram of the Square-Root Routine.

Since the square-root function is also needed in the Velocity/Thrust and Slip Frequency Control Module, the routine is implemented as a function-called subroutine so that it can be shared among the modules. Hence, the number to be square-rooted is passed in as a parameter.

5.2.3 Position Sensing Module

The main functions of this module are to monitor the train position and velocity by decoding a series of 3-bit signals generated by the hall-effect magnetic flux sensors whenever a train passes by. These signal series consist of two set patterns. By continually recording these signals and the time of their occurrence, the train position and velocity can be accurately derived.

The design of this module is based on an interrupt driven routine, where interrupts are generated by the hardwired discriminator when sensor transitions are detected. This interrupt handler coordinates other subroutines to perform all the necessary module functions. The implementation of the module is divided into 6 parts. They are: (a) Sensor Interrupt Handler Routine, (b) Sensor Reading Routine, (c) Position Update Routine, (d) Sensor Failure Routine, (e) Timer Overflow Routine, and (f) Sensor Initialization Routine.

5.2.3a Sensor Interrupt Handler Routine

Since there are two sensors, one mounted near each end of the LIM, signal transitions can be detected from either one or both sensors (sensor A or sensor B). Thus, the main concern of this routine is to determine where the sensor interrupt originated and to decide which sensor reading is to be used for position update. Figure 5.13 and Table 5.1 illustrate the event sequence of a train (with two vehicles) passing through a LFCM. A sensor is referred to as 'active' when it is actively used for position update, otherwise it is referred to as 'passive'. Only one sensor is 'active' at any one time, and once it is determined 'active', it will remain in this mode until it detects an end of vehicle. This is to avoid duplicity in the position update when both sensors detect signal transitions. However, there are situations when the sensor modes are switched in the middle of a passing vehicle. For example, when the 'active' sensor fails to detect transitions due to external interferences or mechanical problems, the 'passive' sensor will take up the responsibility and become 'active'.

The software algorithm is developed based on the aforementioned scheme. A sensor status register, as shown in Figure 5.14, is employed to facilitate the 'active' sensor selection. This register is essential in the module, because it also determines what actions are to be taken during each sensor interrupt. Bit 0 and 1 of this register are to indicate, respectively, whether sensor A or sensor B have detected state transitions from the current sensor interrupt. Bit 2 and 3 are to

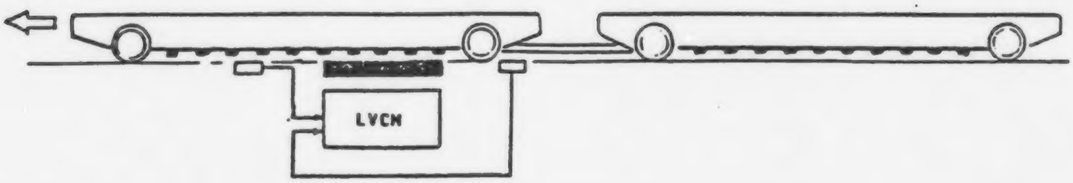

Figure 5.13 LFCM system with a passing train.

LFCM EVENT	SENSOR MODE **	
	Sensor A	Sensor B
Train approaches LFCM	P	P
Train encounters Sensor A	A	P
Train encounters Sensor B	A	P
End of vehicle #1 passes Sensor A, and vehicle #1 is on the top Sensor B	P	A
Vehicle #2 encounters Sensor A	P	A
End of vehicle #1 passes Sensor B, and		
Vehicle #2 is on the top of Sensor A	A	P
Vehicle #2 encounters Sensor B	A	P
End of vehicle #2 passes Sensor A, and vehicle #2 is on the top Sensor B	P	A
Vehicle #2 is on the top of Sensor B	P	A
End of vehicle #2 passes Sensor B	P	P

** Sensor Mode : A (active) or P (passive)

Table 5.1 LFCM event sequence of a passing train.

Sensor Status Register

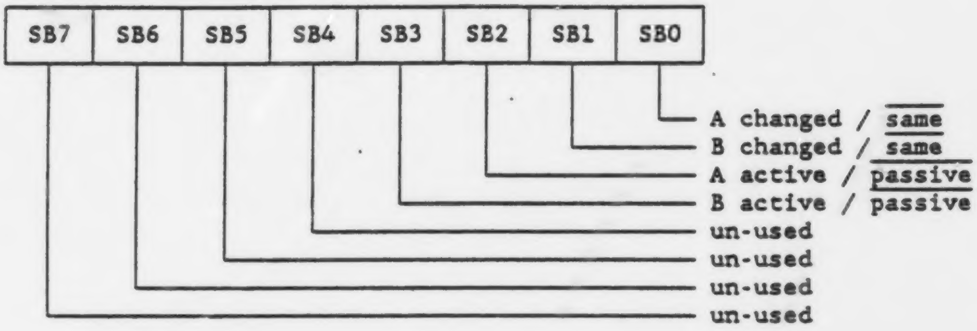
SB7
SB6
SB5
SB4
SB3
SB2
SB1
SB0
A changed / $\overline{\text{same}}$
B changed / $\overline{\text{same}}$
A active / $\overline{\text{passive}}$
B active / passive
un-used
un-used
un-used
un-used

case #	B active (SB3)	A active (SB2)	B changed (SB1)	A changed (SB0)	actions to be taken
0	0	0	0	0	——
1	0	0	0	1	set A active; call position update
2	0	0	1	0	set B active; call position update
3	0	0	1	1	error **
4	0	1	0	0	——
5	0	1	0	1	call position update
6	0	1	1	0	——
7	0	1	1	1	call position update
8	1	0	0	0	——
9	1	0	0	1	——
10	1	0	1	0	call position update
11	1	0	1	1	call position update
12	1	1	0	0	error
13	1	1	0	1	error
14	1	1	1	0	error
15	1	1	1	1	error

** If the train is started from stationary, case #3 is not an error.

Figure 5.14 Bit representation of the LFCM sensor status register.

indicate the sensors' mode, and bits 4 to 7 are un-used.

Hence, when a sensor interrupt occurs and the LFCM is enabled, the handler will first call on the Sensor Reading Routine to check if the interrupt is valid, and to record the sensors' states and the time of occurrence. Based on this information, it will then decide whether to call on the Position Update Routine to perform position and velocity update, to call on Sensor Failure to alarm error, or to exit from the routine when the interrupt is invalid due to noise. A flowchart of the handler is shown in Figure 5.15.

5.2.3b Sensor Reading Routine

The main function of this routine is to record the sensors' states and the time at which a sensor interrupt occurs. When the routine is invoked, it will immediately validate the sensors by ensuring that two consecutive readings are the same, by comparing the present state to that of the previous valid interrupt. This will filter out any false interrupts, which may be caused by noise glitches from the system. Also, the time elapsed between the present and the previous valid interrupts are checked against a time limit. This is to discern if the sensors have failed to detect state transitions for a long period of time, which may lead to errors in position update. The time limit is set according to the acceleration rate of the train. The details of

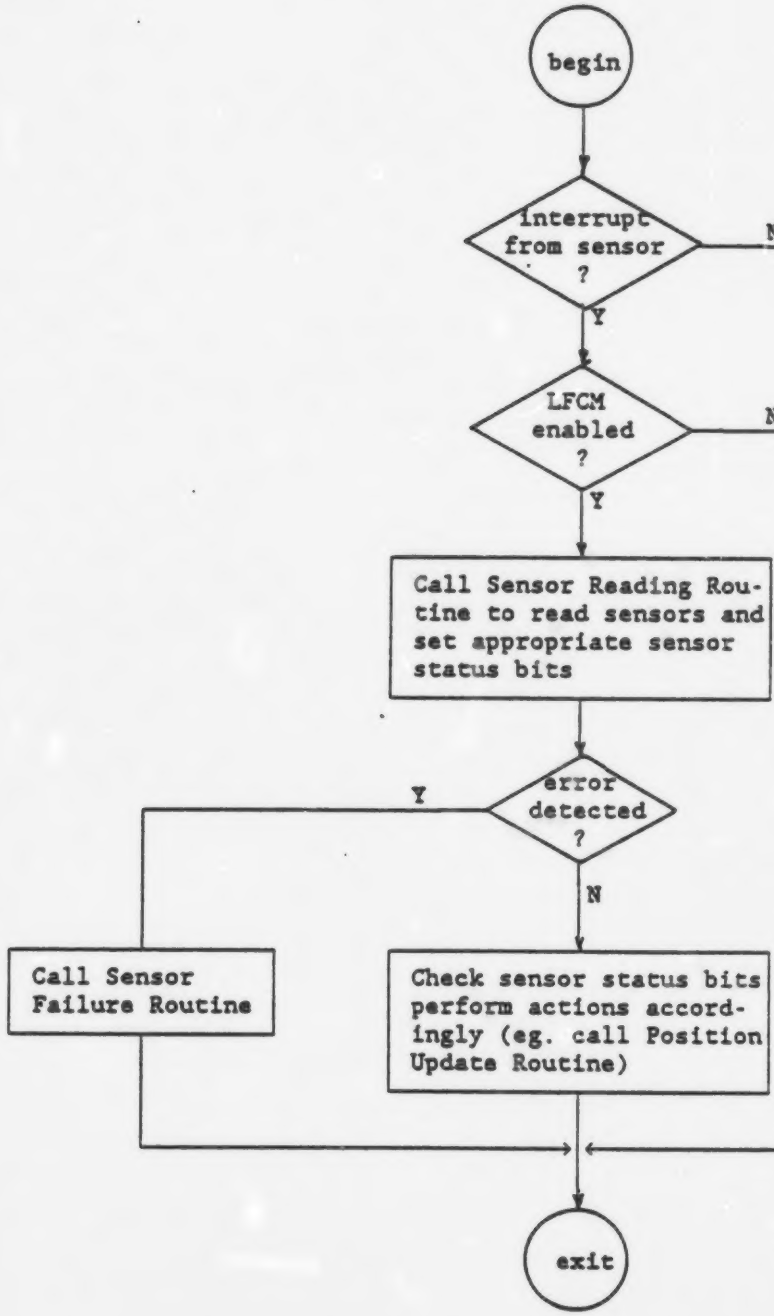
begin
interrupt from sensor ?
N
Y
LFCM enabled ?
N
Y
Call Sensor Reading Routine to read sensors and set appropriate sensor status bits
error detected ?
Y
N
Call Sensor Failure Routine
Check sensor status bits perform actions accordingly (eg. call Position Update Routine)
exit

Figure 5.15 Simplified flowchart of the Sensor Interrupt Handler Routine.

this time limit are further discussed in the Position Update Routine.

Once the interrupt is proven valid, appropriate bits of the sensor status register will be set according to where transitions have occurred (ie. sensor A or sensor B). This step is very important because, later on, position and velocity update will depend on this information. Figure 5.16 shows the flowchart of the routine algorithm.

5.2.3c Position Update Routine

This routine performs train position and velocity updates, based on the current and previous readings of the 'active' sensor. The train position (P) is monitored through the change of position between each sensor interrupt, and the velocity (v) is derived by dividing the position change by the time elapsed between the current and previous interrupts. Because of the sensor sensitivity to its airgap, which is liable to fluctuate during operations, the sensor readings are often unreliable. Thus, the algorithm of this routine is designed to be fault-tolerant to allow for occasional mis-detections of sensor transitions.

The position change, which is denoted as ΔP, is determined by comparing the current active sensor state to its previous interrupt

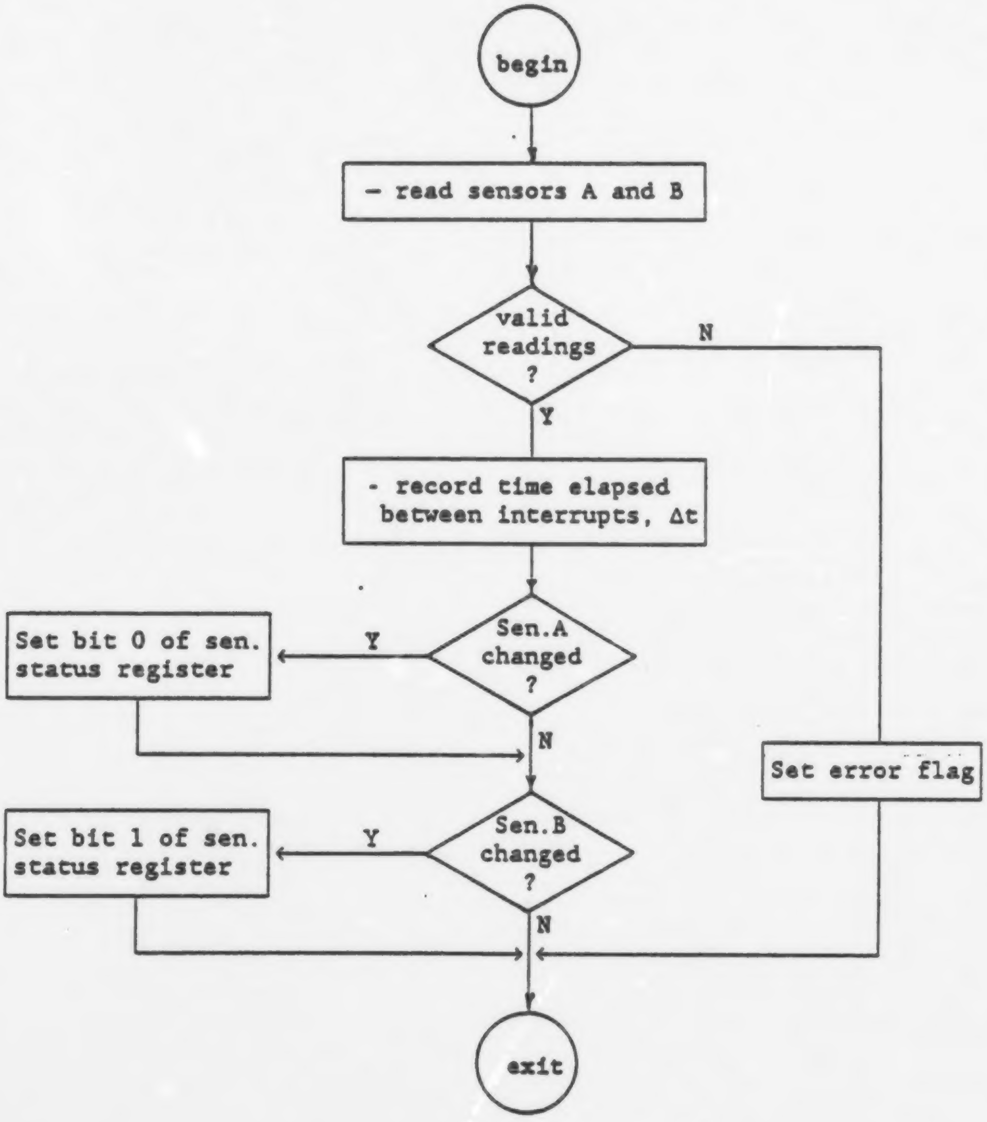
begin
- read sensors A and B
valid readings ?
N
Y
- record time elapsed between interrupts, Δt
Sen.A changed ?
Y
Set bit 0 of sen. status register
N
Set error flag
Sen.B changed ?
Y
Set bit 1 of sen. status register
N
exit

Figure 5.16 Simplified flowchart diagram of the Sensor Reading Routine.

state, since state transitions are of a set pattern (either the forward-direction pattern or the reverse-direction pattern). A 2-dimensional lookup table, as shown in Figure 5.17 provides quick determination of ΔP, which is expressed in the number of state transitions.

		CURRENT SENSOR READING						
	ΔP	0	1	2	3	4	5	6
PREVIOUS SENSOR READING	0	0	1	3	2	5	6	4
	1	5	0	2	1	4	5	3
	2	3	4	0	5	2	3	1
	3	4	5	1	0	3	4	2
	4	1	2	4	3	0	1	5
	5	6	1	3	2	5	0	4
	6	2	3	5	4	1	2	0

Figure 5.17 Determination of vehicle position change, using current and previous sensor readings.

However, from this comparison method, ΔP can, at the maximum, be equal to 6 state transitions. (Note: each transition is equivalent to 5mm) If there is a series of signal mis-detections prior to the current interrupt, the actual position change could be anything, although it must be equal to (ΔP + 6n) where n = 0, 1, 2, 3, ...etc. This is because the signal pattern repeats itself after every 6 transitions.

Hence, additional computations are required to determine the actual position change. ΔP_{calc} which denotes a calculated position change, is approximated by multiplying the last velocity update with the elapsed interrupt time, as determined by:

$$\Delta P_{calc} = \upsilon'\Delta t + \frac{1}{2} a\Delta t^2 \approx \upsilon'\Delta t \qquad (5.3)$$

where

υ' = train velocity at the previous interrupt;

a = train acceleration rate at the previous interrupt; and

Δt = time elapsed between interrupts.

This approximation is based on the assumption that the acceleration term, $1/2(a\Delta t^2)$, is small enough such that the distance contributed by this term is less than 6 transitions, and it can be corrected by rounding off ΔP_{calc} to the nearest $(\Delta P + 6n)$. (Note: ΔP_{calc} is rounded up to the nearest $(\Delta P + 6n)$, if the train is accelerating, otherwise, it is rounded down). Thus, the train position can be accurately determined.

As mentioned in the previous section, a time limit between interrupts is imposed to avoid errors (ϵ) in position update. This is to detect that the acceleration term, $1/2(a\Delta t^2)$, is greater than 6 transitions, which cannot be corrected by the round-off process. The formulae for determining the time limit for each sensor interrupt is given by:

$$\Delta t = \sqrt{2\epsilon/a} \qquad (5.4)$$

It is inversely proportional to the square-root of the train acceleration. Thus, if the train is at a constant velocity or at a small acceleration, the position change can still be accurately determined even after a long series of signal mis-detections.

Figure 5.18 shows a simplified flowchart of the routine algorithm. This routine can handle position and velocity updates when the vehicle is running at its top velocity (ie. 10 m/sec), and it is also capable of performing the required functions beyond this velocity limit.

5.2.4 Velocity/Thrust and Slip Frequency Control Module

The main functions of this module are to provide the velocity/thrust and slip frequency control based on the position and velocity feedback information. This module is designed to be a background task of the LFCM system, because it is the least time-critical among all the modules. The two control functions are implemented as two subroutines - the Velocity Control Routine and the Slip Frequency Control Routine. They are invoked at regular time intervals, approximately once every 0.1 second. Figure 5.19 shows a simplified flowchart diagram of the module algorithm.

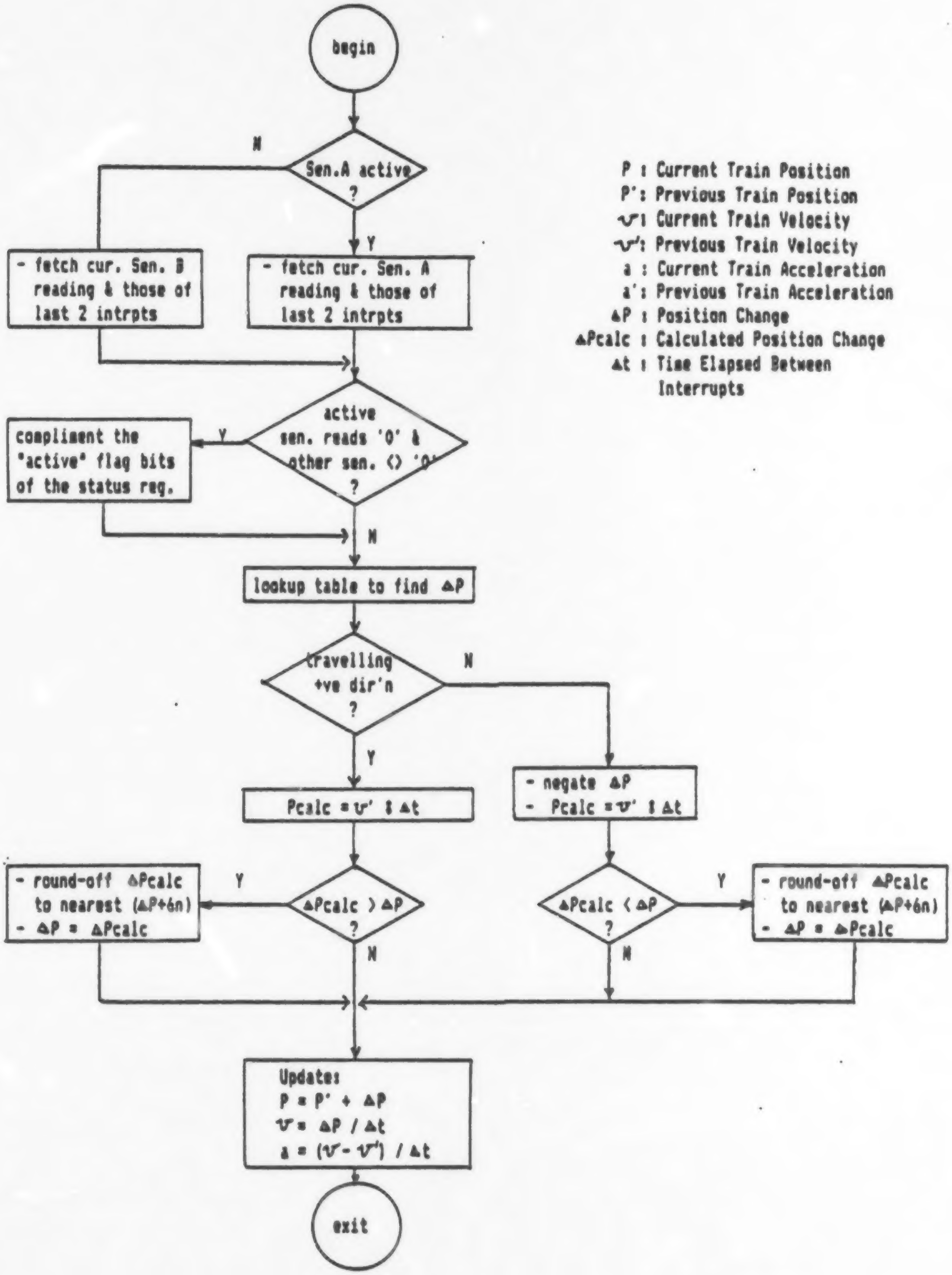
begin
Sen.A active ?
N
Y
- fetch cur. Sen. B reading & those of last 2 intrpts
- fetch cur. Sen. A reading & those of last 2 intrpts
active sen. reads '0' & other sen. <> '0' ?
Y
N
compliment the "active" flag bits of the status reg.
lookup table to find ΔP
travelling +ve dir'n ?
N
Y
Pcalc = v' * Δt
- negate ΔP
- Pcalc = v' * Δt
ΔPcalc > ΔP ?
Y
N
- round-off ΔPcalc to nearest (ΔP+6n)
- ΔP = ΔPcalc
ΔPcalc < ΔP ?
Y
N
- round-off ΔPcalc to nearest (ΔP+6n)
- ΔP = ΔPcalc
Update:
P = P' + ΔP
v = ΔP / Δt
a = (v - v') / Δt
exit
P : Current Train Position
P': Previous Train Position
v : Current Train Velocity
v': Previous Train Velocity
a : Current Train Acceleration
a': Previous Train Acceleration
ΔP : Position Change
ΔPcalc : Calculated Position Change
Δt : Time Elapsed Between Interrupts

Figure 5.18 Simplified flowchart of the Position/Velocity Update Routine.

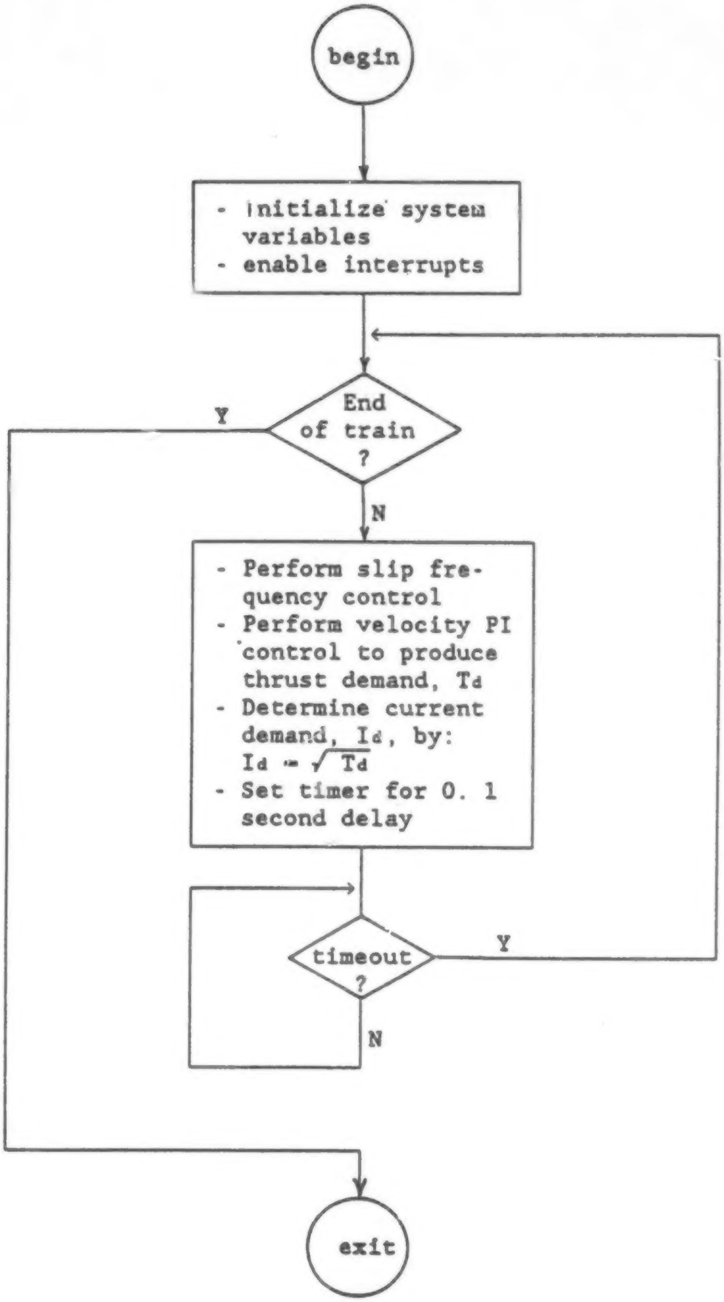
begin
- initialize system variables
- enable interrupts
End of train ?
Y
N
- Perform slip frequency control
- Perform velocity PI control to produce thrust demand, T_d
- Determine current demand, I_d, by: $I_d = \sqrt{T_d}$
- Set timer for 0. 1 second delay
timeout ?
Y
N
exit

Figure 5.19 Simplified flowchart of the Velocity/Thrust and Slip Frequency Control Routine.

5.2.4a Velocity/Thrust Control Routine

As described in Chapter 3, the regulation of velocity is achieved through a position/velocity profile and a PI controller, Figure 3.8. This profile is pre-calculated according to the system requirements and constraints, and is stored in the memory as a lookup table of demand velocity versus train position. Each table element stores a particular demand velocity (v_d) value and is indexed by the corresponding train position (P). Because of the memory constraint, only the major division points of the profile are stored in a table of 20 elements. Thus, for a position feedback (P_f) value that exists between two table points, the demand velocity (v_d) is determined by a linear interpolation of the two adjacent points as shown in Figure 5.20.

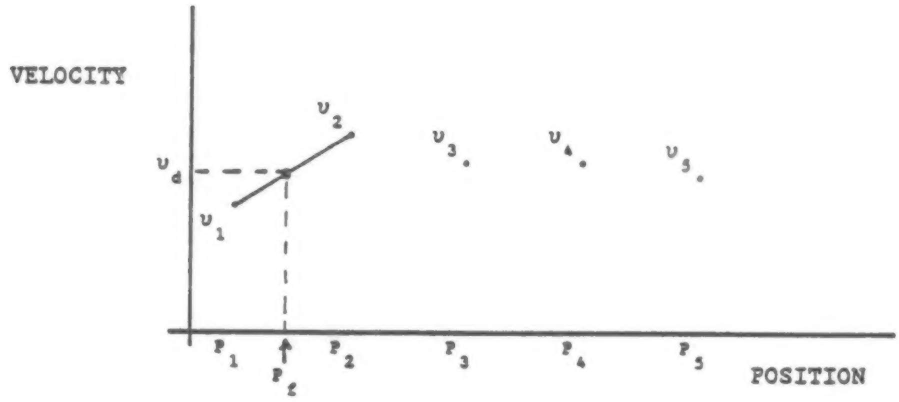

$$v_d = v_1 + (v_2 - v_1) \times \frac{(P_f - P_1)}{(P_2 - P_1)}$$

Figure 5.20 Determination of demand velocity by linear interpolation between two table points.

Once per cycle, the demand velocity (v_d) is determined from this lookup table. Then using a PI controller, the demand thrust (T_d) is derived from the velocity error (e_v), which is produced by subtracting the velocity feedback (v_f) from the demand velocity (v_d). The implementation of the PI controller is similar to that of Current Sampling Module, with the exception that the proportional and integral constants are chosen differently.

Finally, the demand current signal (I_d) required by the inner control loop is derived by taking the square root of the demand thrust (T_d). This is done based on the fact that thrust is directly proportional to the current squared. Note, that before invoking the Square Root Routine, the absolute value of the demand thrust (T_d) is taken, and it is clamped. This is to ensure the demand current signal (I_d) is within the limit (ie. 0 - 512). Figure 5.21 presents a simplified flowchart diagram of the routine algorithm.

5.2.4b Slip Frequency Control Routine

The demand slip frequency (sf_d) is determined from the slip frequency profile and the velocity feedback (v_f). This slip frequency profile is pre-calculated, based on a system optimization criteria such as power factor or efficiency optimization, and is stored in the memory as a lookup table of demand slip frequency as a function of velocity.

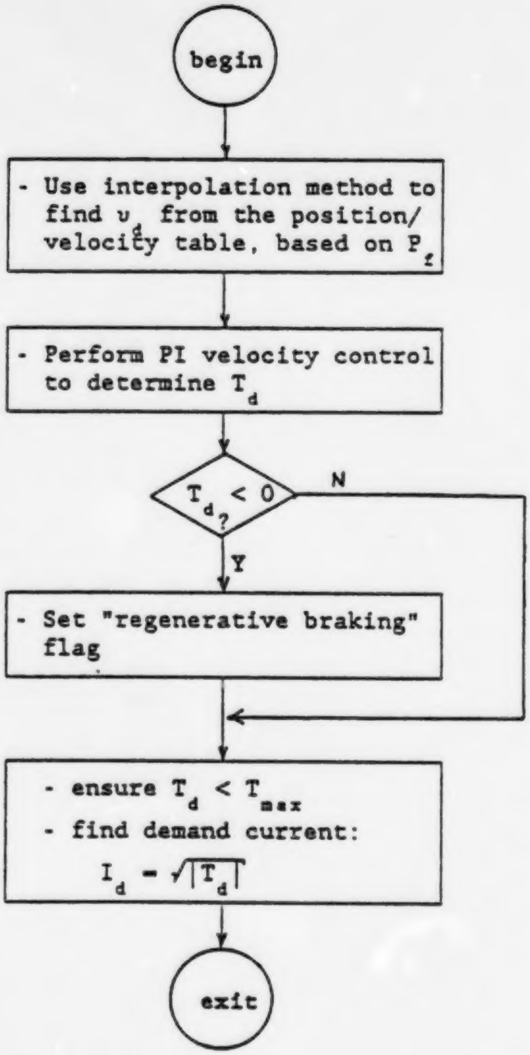
begin
- Use interpolation method to find v_d from the position/velocity table, based on P_f
- Perform PI velocity control to determine T_d
$T_d < 0$?
N
Y
- Set "regenerative braking" flag
- ensure $T_d < T_{max}$
- find demand current:
$I_d = \sqrt{|T_d|}$
exit

I_d : demand current

P_f : position feedback

T_d : demand thrust

v_d : demand velocity

Figure 5.21 Simplified flowchart diagram of the Velocity/Thrust Control Routine.

The table contains up to 25 points of information. Again, linear interpolation is used for values that are bracketed between points.

Once per cycle, after the Velocity Control Routine has been executed, this routine is invoked and the demand slip frequency (sf_d) is produced. To determine the demand frequency (f_d), the demand slip frequency (sf_d) is added to the mechanical frequency (f_m) if the LIM is in the motoring mode (ie. demand thrust > 0); and is subtracted from the mechanical frequency (f_m) if the LIM is in the regenerative braking mode. The mechanical frequency (f_m) is the velocity feedback (v_f) divided by the LIM wavelength (λ). If the demand frequency (f_d) is different from the current frequency (f_c), the Frequency Changing Routine will be invoked to prepare a new pulsewidth table. Figure 5.22 shows a simplified flowchart diagram of the Slip Frequency Control Routine.

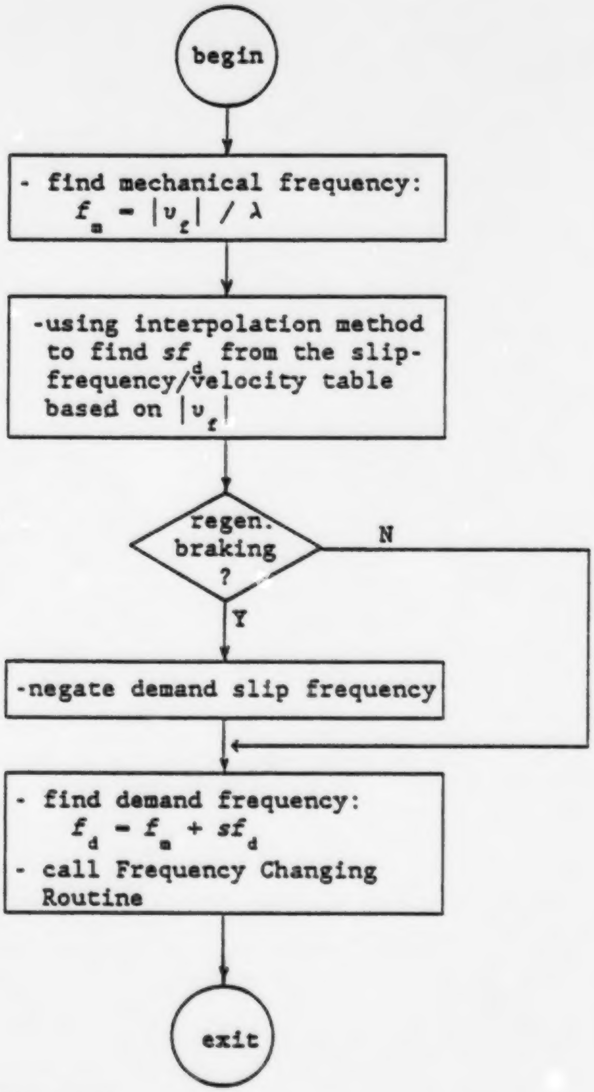
begin
- find mechanical frequency:
$f_m = |v_f| / \lambda$
-using interpolation method to find sf_d from the slip-frequency/velocity table based on $|v_f|$
regen. braking ?
N
Y
-negate demand slip frequency
- find demand frequency:
$f_d = f_m + sf_d$
- call Frequency Changing Routine
exit

f_d : demand frequency

f_m : mechanical frequency

λ : stator wavelength

sf_d : demand slip frequency

v_f : velocity feedback

Figure 5.22 Simplified flowchart diagram of the Slip Frequency Control Routine.

CHAPTER 6:

TESTING

6.1 Introduction

In the previous chapters, the control strategy of the LFCM system was discussed. The hardware and software implementation of the control scheme was also described in detail. One of the objectives of this thesis is to demonstrate the successful operation of the VVVF LIM controller. Hence, experimental results are presented in this chapter to verify the controller operation.

The testing of this VVVF controller is conducted in two stages. In the first stage, the PWM control unit and the current control unit are tested extensively using a 5 W transistorized switching inverter and a small 3-phase load. These tests are conducted to ensure that the software algorithms and the hardware circuits of these two vital control units are properly implemented. In the latter stage, with all the control units combined together, a complete test of the controller is performed on a 3 hp, 3-phase induction motor drive to ensure all the control units are synchronized.

6.2 Software Development Facility

A 'Zenith 158' personal computer (PC) and a 'Intel 8097' single board emulator (iSBE-96) are employed to facilitate the software development and the program downloading into the memory of the hardware prototype. The emulator board is a stand-alone microcontroller board, which consists of a 8097 microcontroller, 16 Kbyte of static RAMs (also known as ROMSIM), an 8-Kbyte EPROM, and some logic and peripheral devices. The emulator is linked to the computer via a RS-232 communication unit on board. As well, a 68-pin cable connector is provided which can be slotted directly into the 8097 chip socket of the prototype board, and hence allows direct interaction with the prototype hardware. The PC, though serving as a visual display terminal for the emulator, is also utilized for software development which includes program compilation and assembly. Figure 6.1 is a photograph of the emulator and the prototype board set up. With the emulator, software debugging tools such as single stepping, register examination and break-point setting are conveniently provided to aid in software development. Also, on-line assignment of program variables is permitted, which is particularly useful when fine-tuning the proportional and integral constants of the PI controller to obtain the desired response.

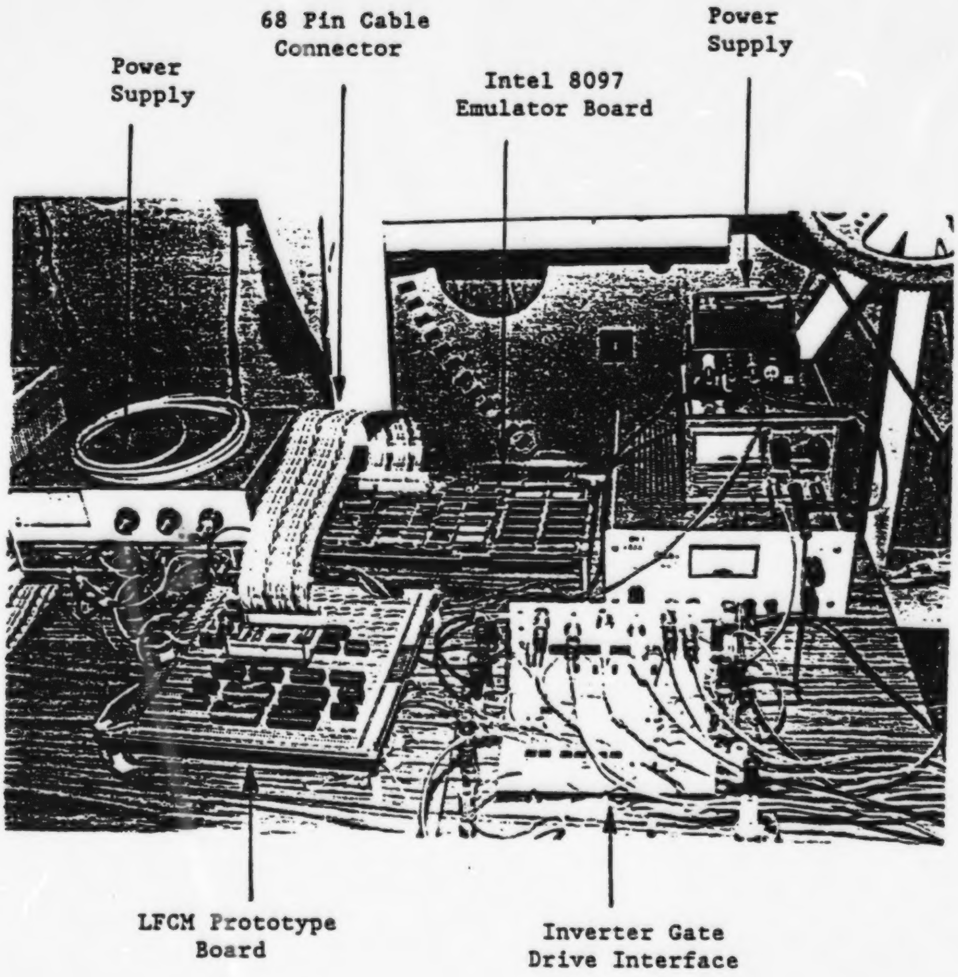
68 Pin Cable Connector
Power Supply
Power Supply
Intel 8097 Emulator Board
LFCM Prototype Board
Inverter Gate Drive Interface

Figure 6.1 Photograph of the LFCM prototype and the Intel 8097 emulator board setup.

6.3 Preliminary Module Testing

In order to properly test the PWM control unit, a 5 W, 3-phase inverter and load circuit is used to simulate the power conditioning unit (PCU) and the LIM. As shown in Figure 6.2, the inverter is constructed using diodes (1N4148) and opto-transistors (H11A1), and is loaded with a balanced 3-phase RC circuit (L) which resembles the low pass characteristic of a LIM. The PWM output timing, the operation of frequency switching, and sequence reversal are thoroughly examined during testing. Figure 6.3 shows the phase and pole voltage of one of the 3 phases during the changes of frequency from 20 Hz to 30 Hz to 40 Hz and then back to 30 Hz. A zoom of the transition for a frequency change from 30 Hz to 40 Hz is shown in Figure 6.4. Figure 6.5 shows the phase voltage of two of the 3 phases during a sequence reversal operation, and Figure 6.6 shows a close-up view of the phase and pole voltage of the reversed phase during reversal. This data is recorded by a digital storage scope, and subsequently plotted on a X-Y plotter. Note that, at the frequency transitions, there is very little voltage transient even when there is a step change of frequency ratio. Also, the voltage harmonics are reduced at the higher frequency ratio.

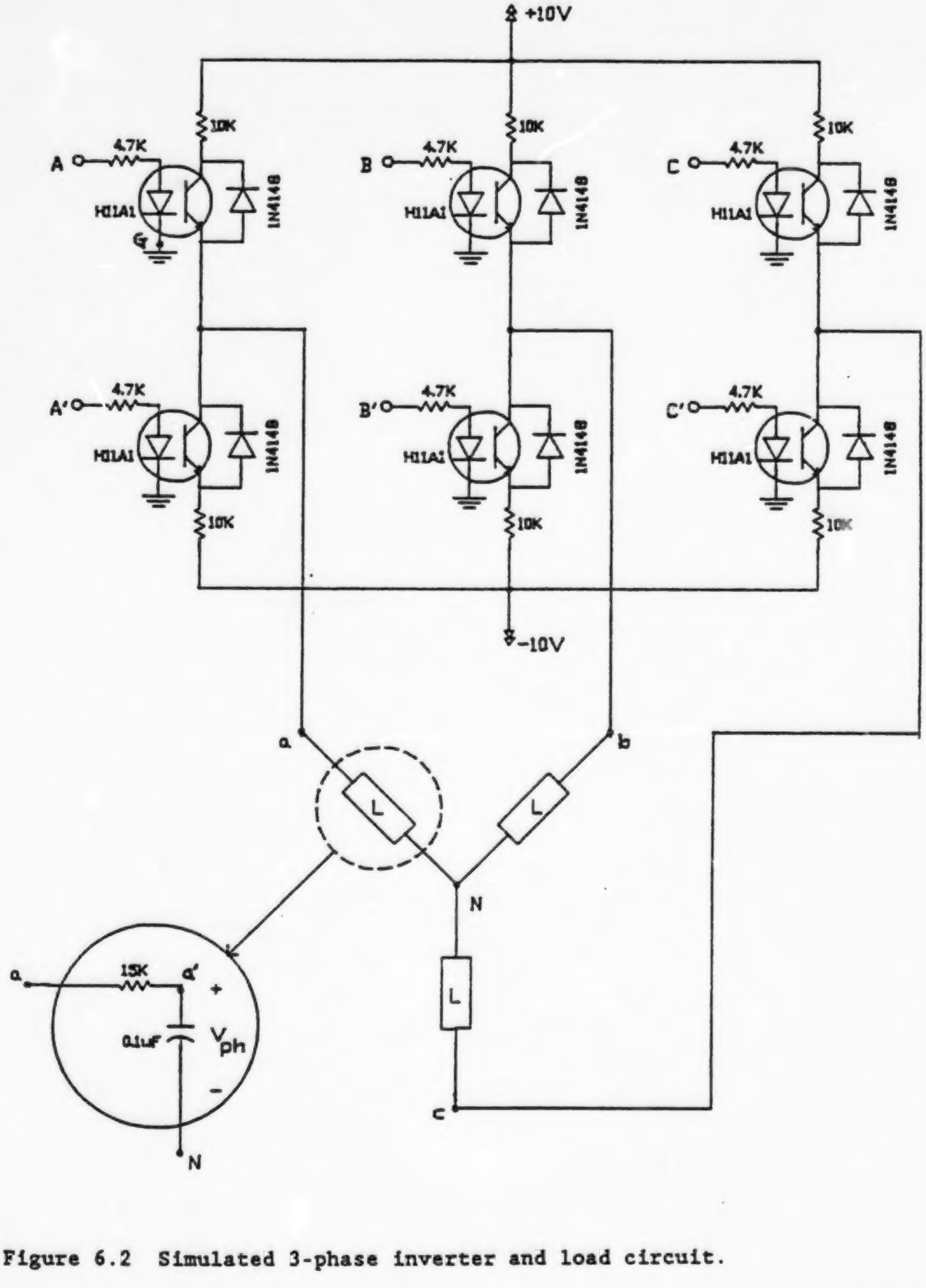
+10V
-10V
A
B
C
A'
B'
C'
4.7K
10K
H11A1
1N4148
G
a
b
c
N
L
15K
a'
0.1uF
V_ph
+
-

Figure 6.2 Simulated 3-phase inverter and load circuit.

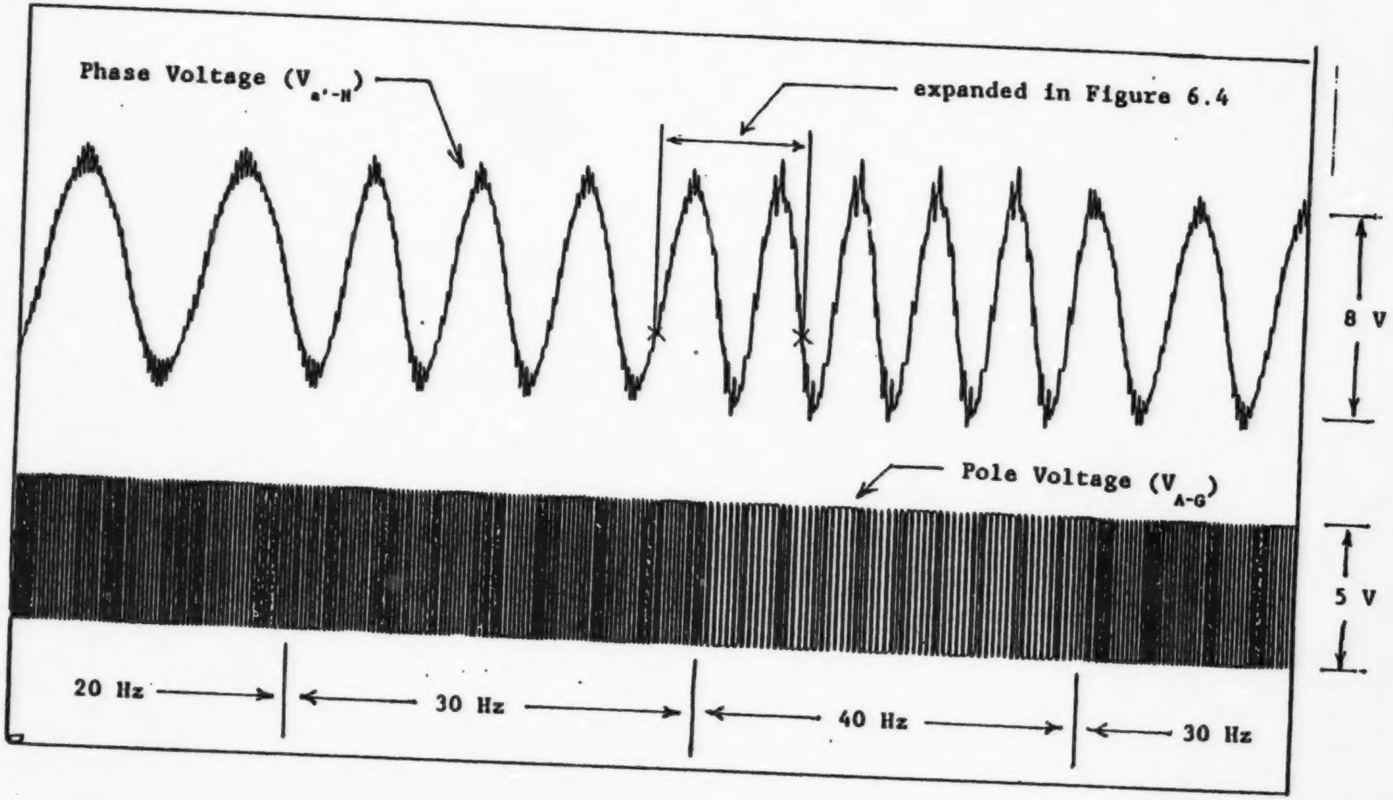

Figure 6.3 Phase and pole voltages of one of the simulated 3-phase inverter/load circuits, Figure 6.2, during the changes of frequency from 20 Hz to 30 Hz to 40 Hz and back to 30 Hz.

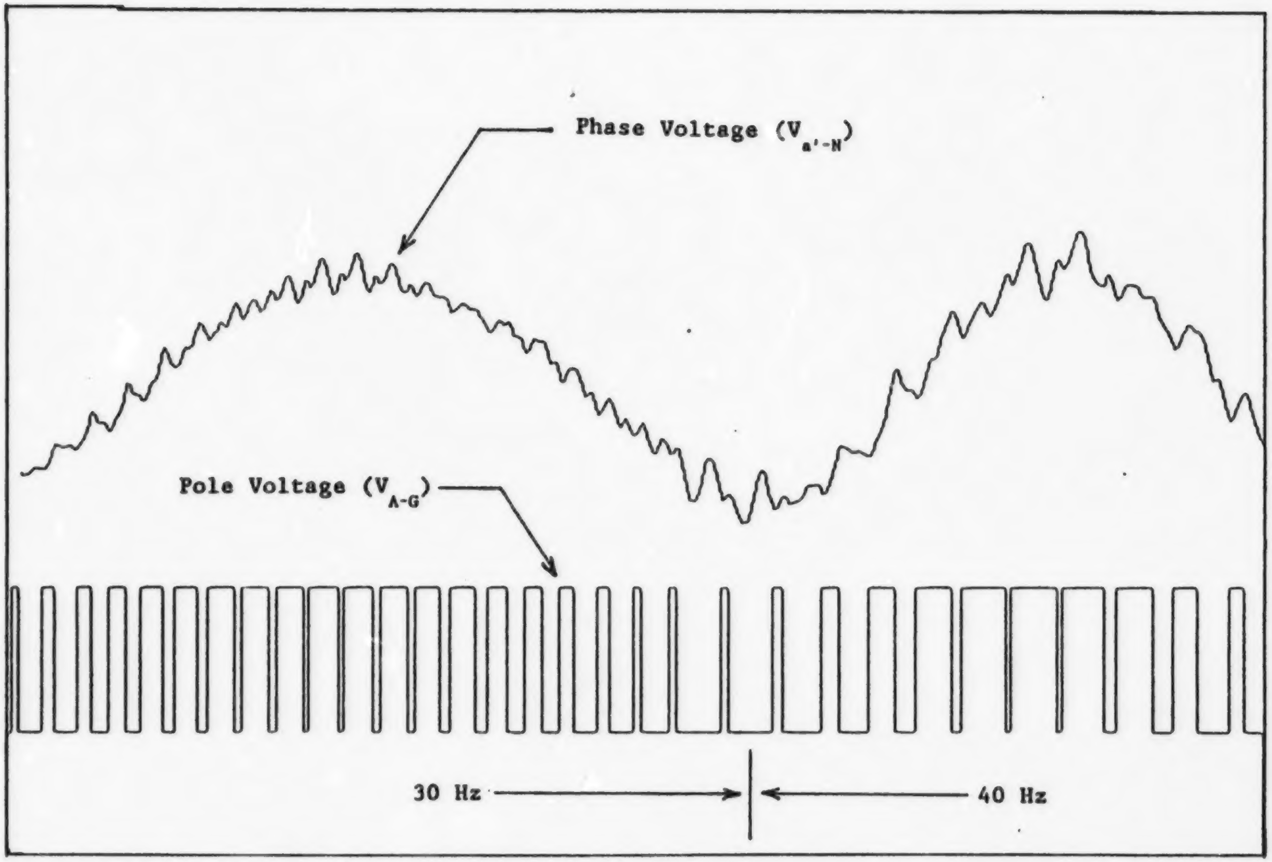

Figure 6.4 Close-up phase and pole voltages of one of the simulated 3-phase inverter/load circuits during the change of frequency from 30 Hz to 40 Hz.

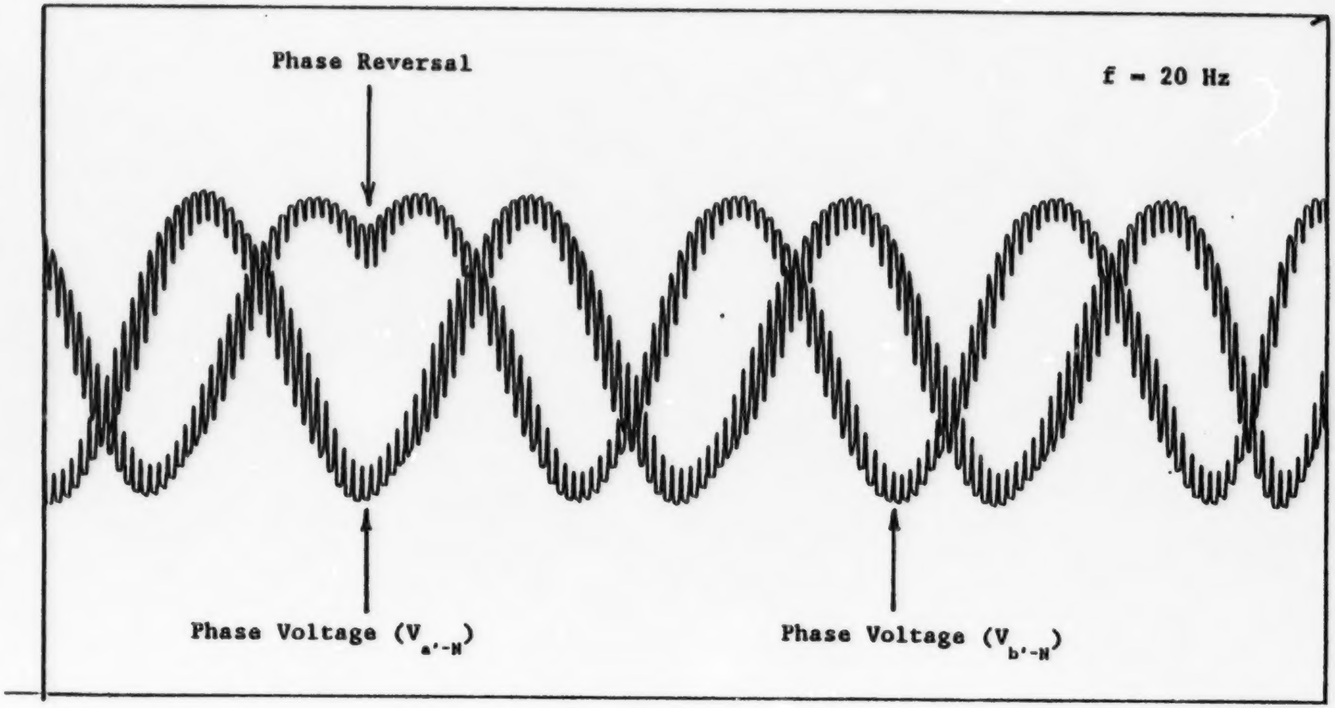

Figure 6.5 Phase voltage of two of the simulated 3-phase inverter/load circuits during a sequence reversal operation.

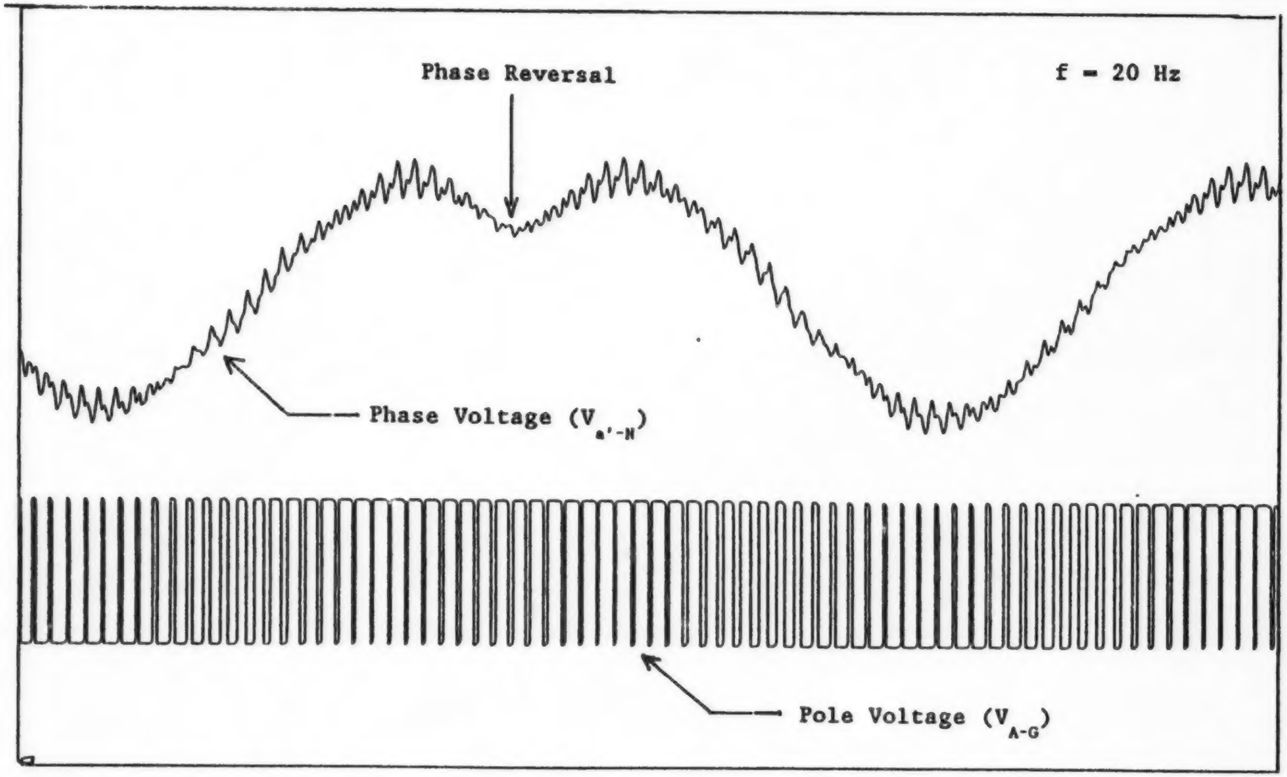

Figure 6.6 Close-up phase and pole voltages of the reversed phase of the simulated inverter/load circuits during reversal.

Two tests were performed on the current control unit. First, the algorithm developed for calculating the current magnitude, as well as the current sampling mechanism is tested using two known signals from a signal generator. These signals simulate two of the balanced 3-phase currents. As shown in Figure 6.7, the current magnitudes (I) derived from the instantaneous values agree well with the sampled current (I_s) magnitudes at various frequencies. Second, the entire current control loop is examined. This is done by running the current control unit together with the PWM control unit on the simulated inverter and load circuit. Figure 6.8 shows the current feedback response for different values of the proportional and integral constants. Note that there are ripples on the feedback current magnitude, which is caused by the slight unbalance of the phase currents. However, as shown, the controller alters the phase current waveforms in an attempt to correct the error.

6.4 Comprehensive Testing

A full size LIM and the controller developed in this thesis were originally planned to be tested at the Urban Transportation Development Corporation (UTDC) test facility. However, due to unexpected circumstances, UTDC was unable to provide the test equipment, which included the LIM test track and a LIM power conditioning unit. Hence, other alternatives were employed. A 3-phase rotary induction motor is used in place of the LIM since they have similar characteristics. The power conditioning unit to supply the motor, a laboratory-built 3-phase

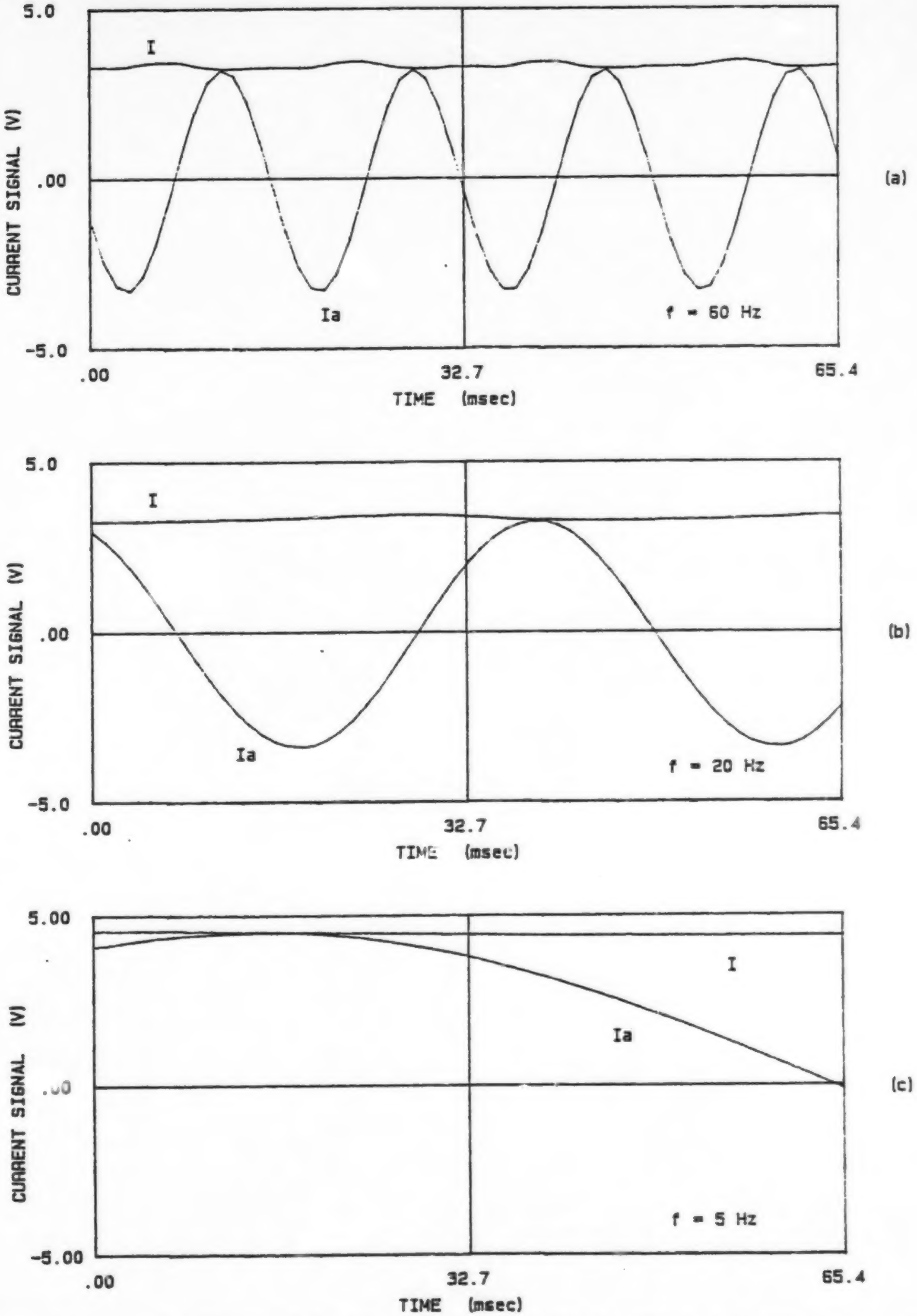

Figure 6.7 Plots of derived current magnitude (I) and phase current (I_a) versus time
(a) f = 60 Hz. (b) f = 20 Hz. (c) f = 5 Hz.

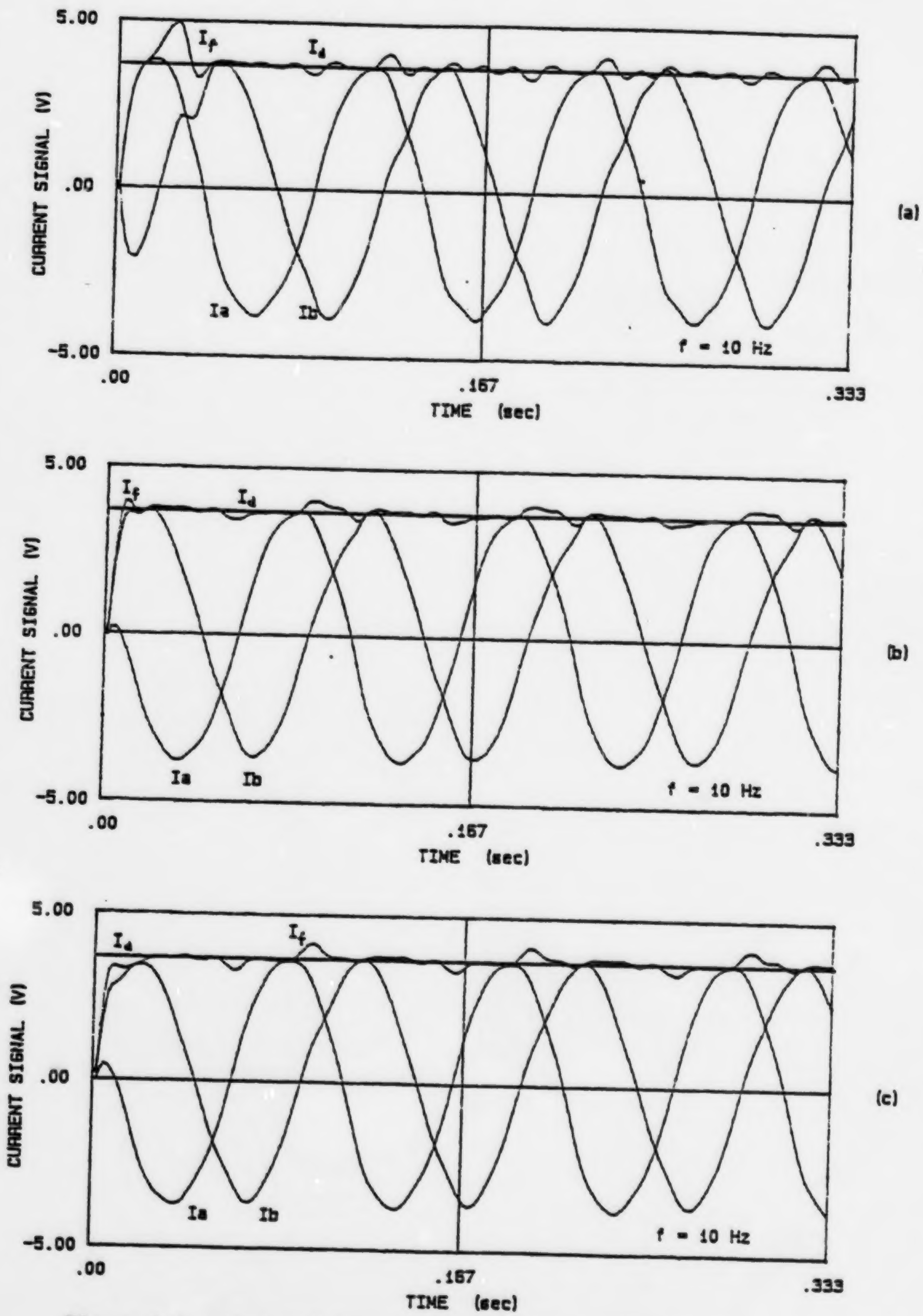

Figure 6.8 Simulated inverter/load current response at f = 10 Hz
(a) $K_I = 0.375$ and $K_P = 0.125$.
(b) $K_I = 0.188$ and $K_P = 0.125$.
(c) $K_I = 0.125$ and $K_P = 0.125$.

bridge inverter, was obtained from Queen's University. As well, a large rotating wheel, which was constructed for other research investigations, was utilized to simulate the action of passing vehicles. Figure 6.9 is a photograph of the experimental test setup. Again, the emulator and the PC are used to facilitate the testing. This experimental setup simulates the test track environment and permits verification of most of the system hardware and software operations.

6.4.1 Test Equipment

Figure 6.10 shows a schematic view of the rotating wheel. It was built several years ago as an experimental facility for linear motor research. It is used in this research project to simulate the magnetic strips mounted on vehicles passing over the position sensors. The wheel is 2 metres in diameter. On its side, evenly spaced magnetic strips are placed along half of the rim. Two sensors, sensor A and sensor B, are mounted next to the side of the wheel with an airgap distance of 5 mm from the magnetic strips. Figure 6.11 shows a close-up view of a sensor and the magnetic strip. Two sensors are set apart by a predetermined distance to resemble the front and back end sensors of the LIM.

The wheel is coupled with a 3 hp, 3-phase induction motor through a 6 to 1 gear mechanism. In the testing, the maximum speed of the wheel is 60 rpm (ie. rim speed = 4.7 m/sec), though for the LIM-in-track

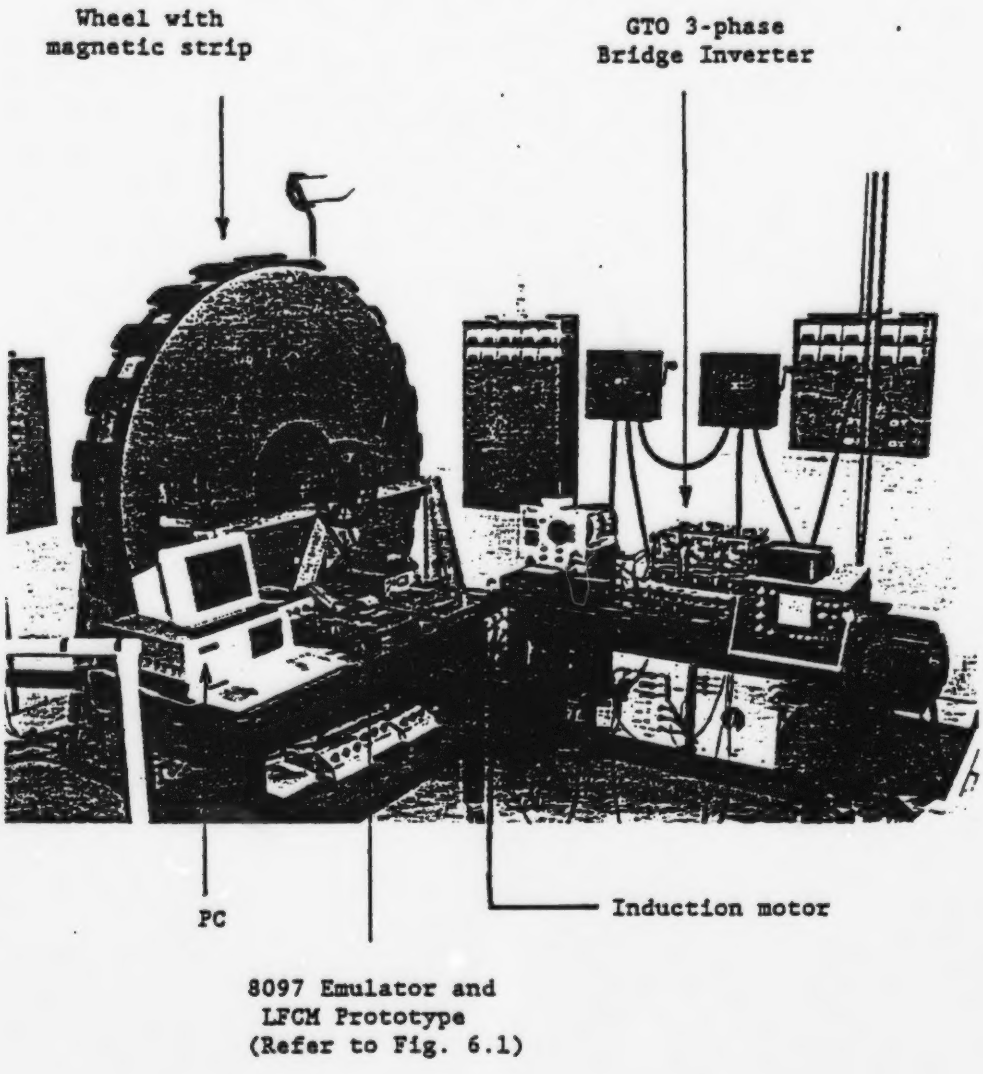
Wheel with
magnetic strip
GTO 3-phase
Bridge Inverter
PC
Induction motor
8097 Emulator and
LFCM Prototype
(Refer to Fig. 6.1)

Figure 6.9 Photograph of the LFCM experimental test setup - prototype and emulator boards, PC, 3-phase bridge inverter, induction motor and test wheel with magnetic strip.

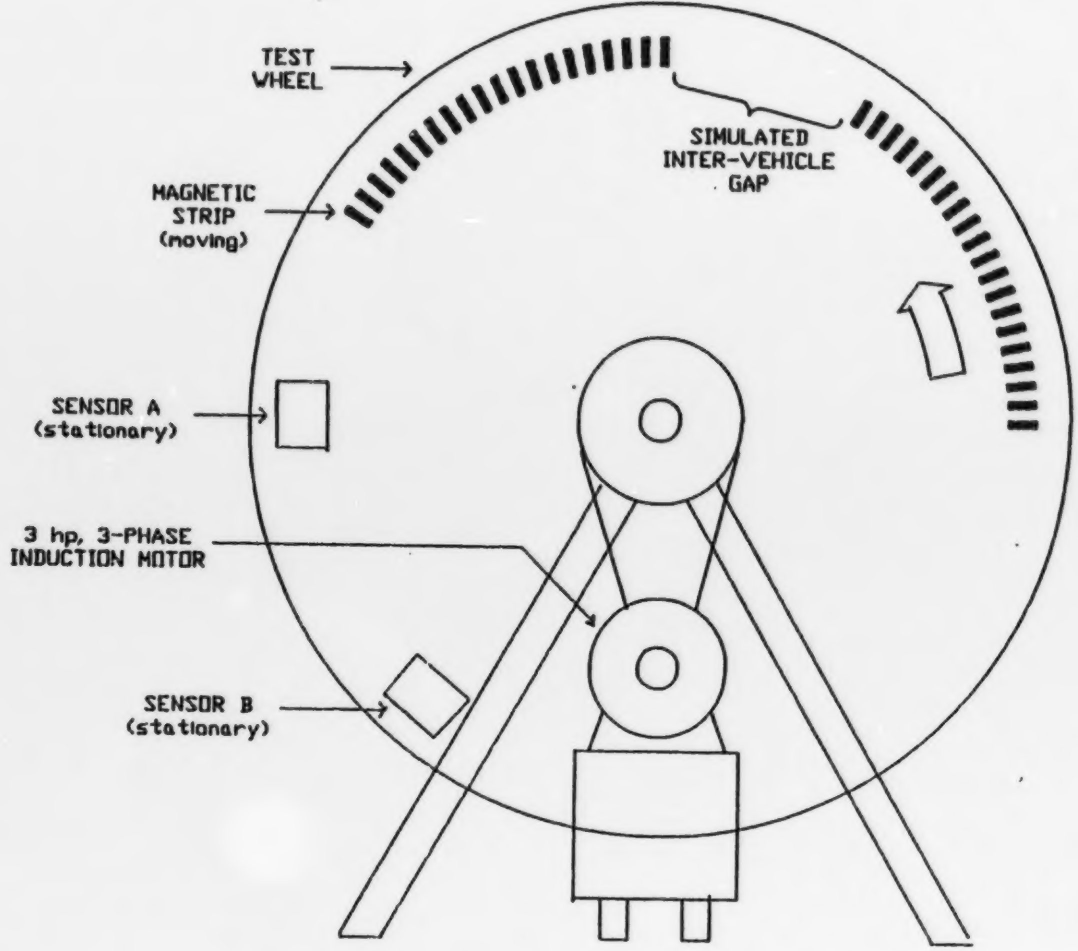
TEST WHEEL
MAGNETIC STRIP (moving)
SIMULATED INTER-VEHICLE GAP
SENSOR A (stationary)
3 hp, 3-PHASE INDUCTION MOTOR
SENSOR B (stationary)

Figure 6.10 Schematic view of the test wheel.

material handling application, the vehicles may be operating up to 10 m/sec. The large inertia of the wheel and the limited power produced by the motor resulted in a maximum speed limit. Wheel braking is achieved by induction motor regenerative braking or by induction motor plugging.

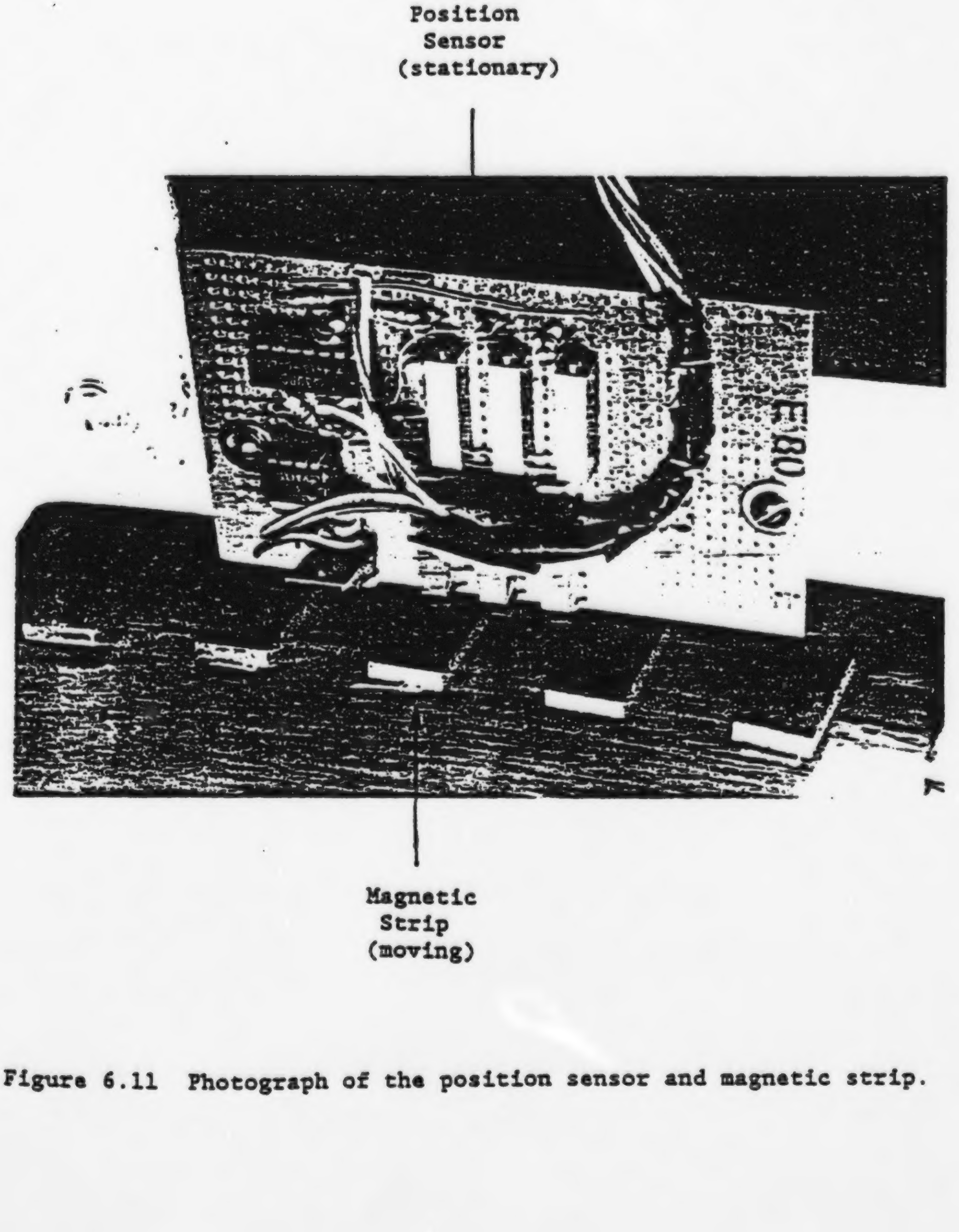
Position
Sensor
(stationary)
Magnetic
Strip
(moving)

Figure 6.11 Photograph of the position sensor and magnetic strip.

The 3-phase induction motor is power conditioned by a 3-phase GTO bridge inverter, which was built by the Department of Electrical Engineering at Queen's University for laboratory purposes. Figure 6.12 shows a schematic of the inverter power circuit. Details of the GTO gate drive and firing circuits are not included. The inverter, which obtains power from a dc main supply, is capable of supplying three kilowatts of power to the induction motor. The PWM signals are fed directly into the gate drive unit of the inverter from the PWM control unit of the prototype board.

6.4.2 Testing and Results

In testing the overall system operation, a 'building block' approach is adapted, in which the most fundamental unit, namely the PWM control unit, is tested first. Subsequently the remaining three control units, which constitute the three control loops described in Chapter 3, are added into the testing sequence one at a time.

To test the PWM control unit, the motor was driven at various voltages and frequencies. A selected portion of results are chosen to demonstrate the successful operation of the control unit. Figure 6.13 shows one phase of the PWM gating signals and its corresponding phase current. Figure 6.13a shows the results for 20 Hz operation, and figure 6.13b shows the results for 60 Hz operation. The gating signal is

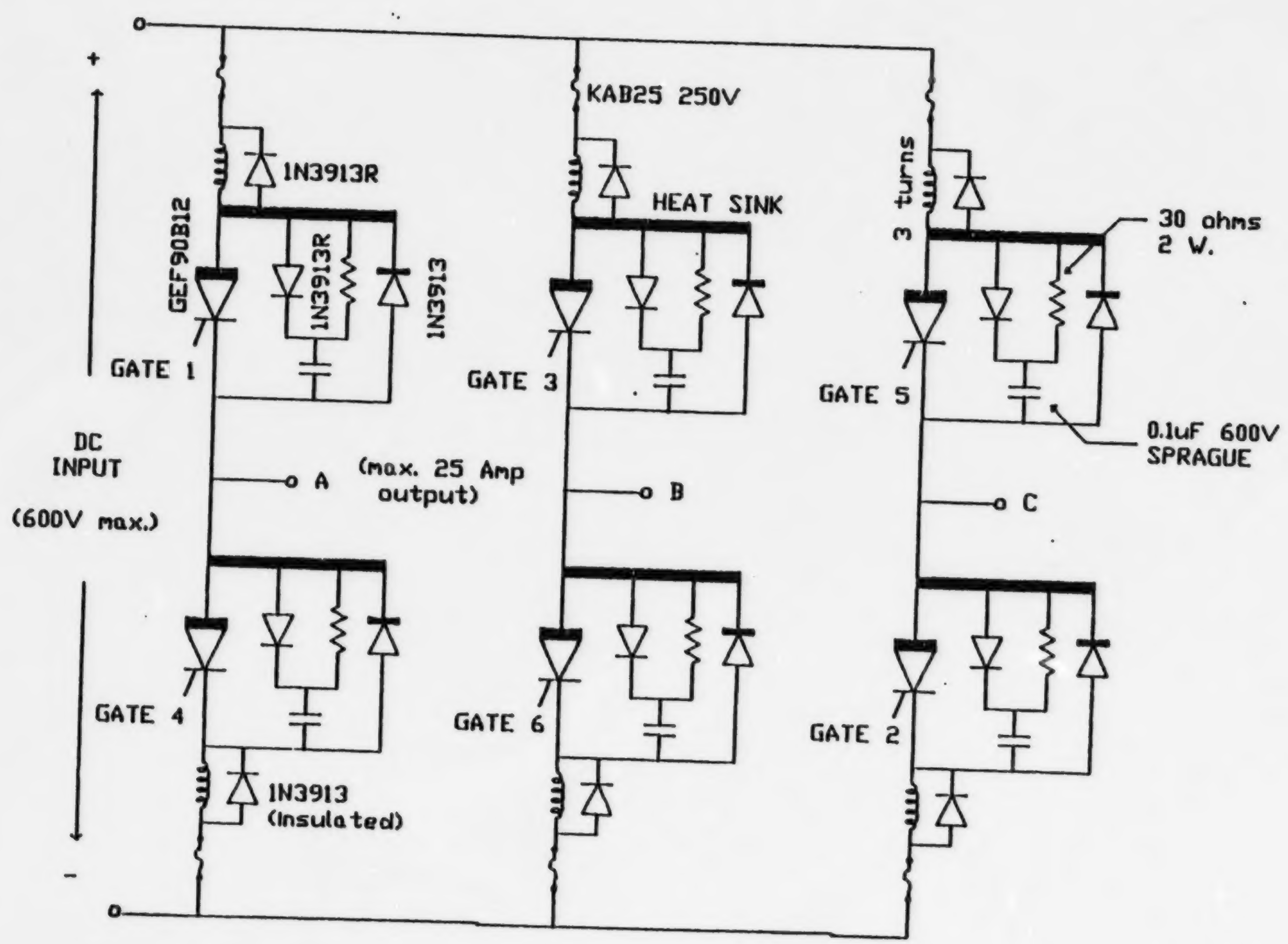
+
-
DC
INPUT
(600V max.)
KAB25 250V
1N3913R
GEF90B12
1N3913R
1N3913
HEAT SINK
3 turns
30 ohms
2 W.
0.1uF 600V
SPRAGUE
GATE 1
GATE 3
GATE 5
A
(max. 25 Amp
output)
B
C
GATE 4
GATE 6
GATE 2
1N3913
(insulated)

Figure 6.12 Schematic of the GTO 3-phase bridge inverter circuit.

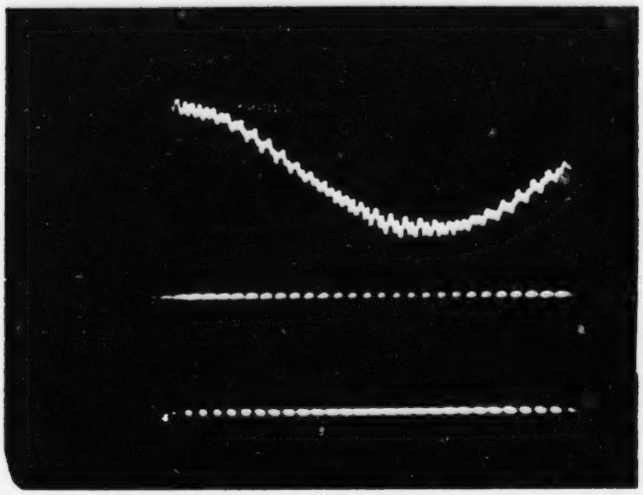

Vertical Scale: 5 Amp/div
(upper trace)

Vertical Scale: 2 V/div
(lower trace)

Horizontal Scale: 2 msec/div

(a)

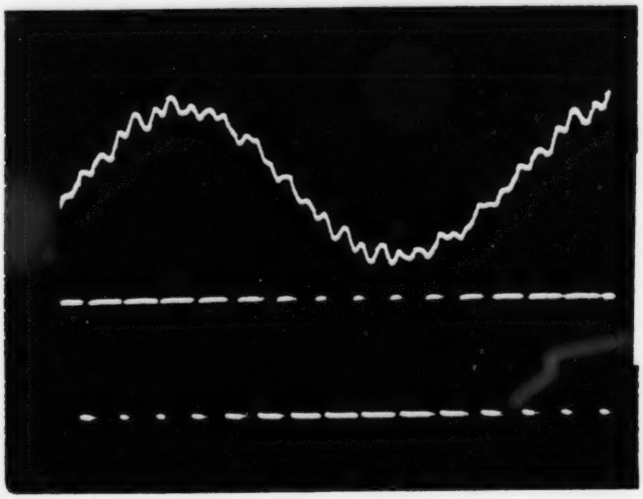

Vertical Scale: 5 Amp/div
(upper trace)

Vertical Scale: 2 V/div
(lower trace)

Horizontal Scale: 5 msec/div

(b)

Figure 6.13 Photographs of the induction motor phase current (upper trace) and the inverter gating signal (lower trace)
(a) Frequency = 20 Hz, PWM sampling frequency = 720 Hz.
(b) Frequency = 60 Hz, PWM sampling frequency = 720 Hz.

measured at the output of the microcontroller PWM output unit, and this signal directly corresponds to the pole voltage of the inverter. The phase current is measured at the current transducer output before sending it to the A/D unit. As shown, the phase current consists of a sinusoidal fundamental frequency waveform and some high frequency harmonic ripples. The phase current is lagging behind the gating signal because of the inductive load. Furthermore, the current harmonics obtained from a spectrum analyzer for the 20 Hz and 60 Hz operations are shown in Figure 6.14. Figure 6.14a shows the dominant 20 Hz fundamental and the low magnitude high frequency harmonics, which are centred around the switching frequency (ie. 720 Hz). Figure 6.14b shows the dominant 60 Hz fundamental and the low magnitude high frequency harmonics, which are also centred around the switching frequency. The low harmonic content of the current demonstrates the effectiveness of the PWM control technique. Figures 6.15 and 6.16. show the motor phase voltage and two of the balanced 3-phase currents respectively.

Once the PWM unit was shown to be performing as designed, the current control unit was included. This unit runs in conjunction with the PWM unit in a synchronized manner with the currents being sampled during each PWM sample period. In this part of the test program, the fine-tuning of the PI controller is also performed. Figures 6.17 to 6.21 depict the current response at various fundamental frequencies and PI constants. In each of these figures, parts (a) and (b) show the transient response of the motor current (I_f) and the demand voltage (V_d) to a step change of demand current (I_d), while part (c) shows the steady state response of the current (I_f). The demand voltage (V_d) shown is

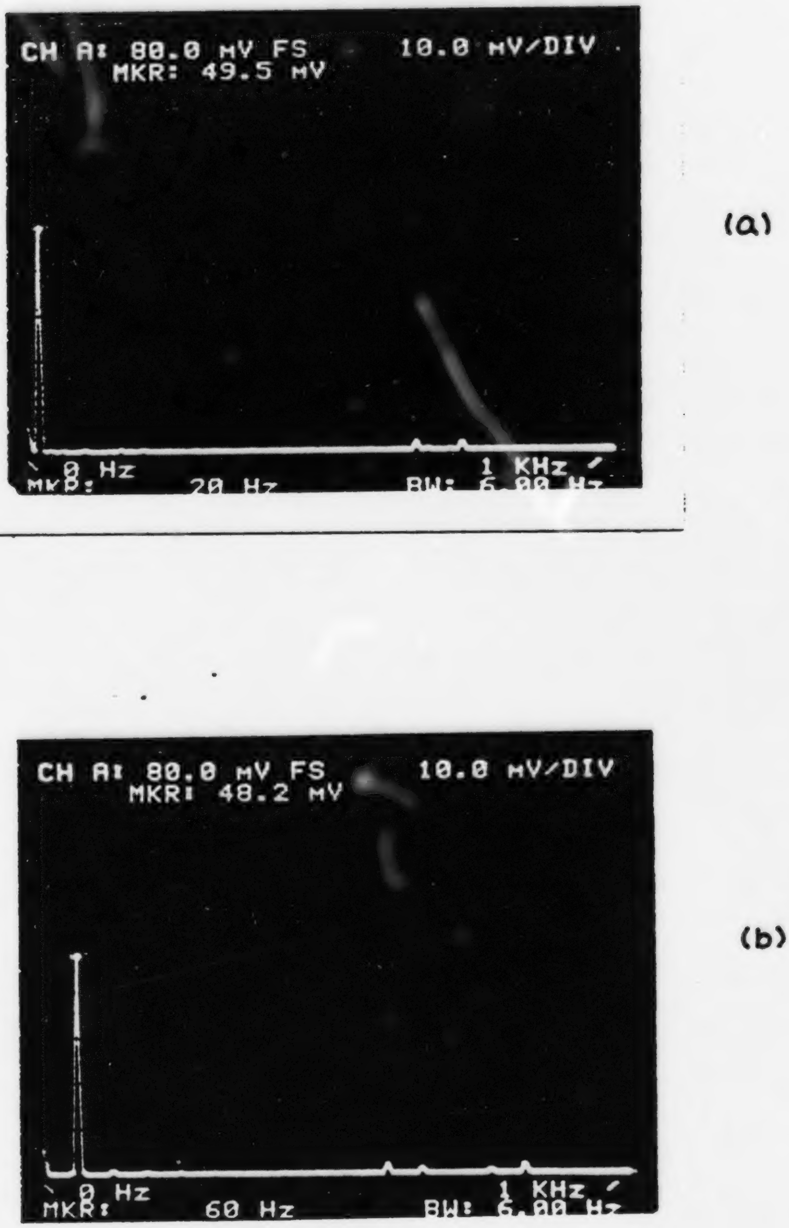

Figure 6.14 Photographs of the phase current harmonic spectra
(a) Frequency = 20 Hz, PWM sampling frequency = 720 Hz.
(b) Frequency = 60 Hz, PWM sampling frequency = 720 Hz.

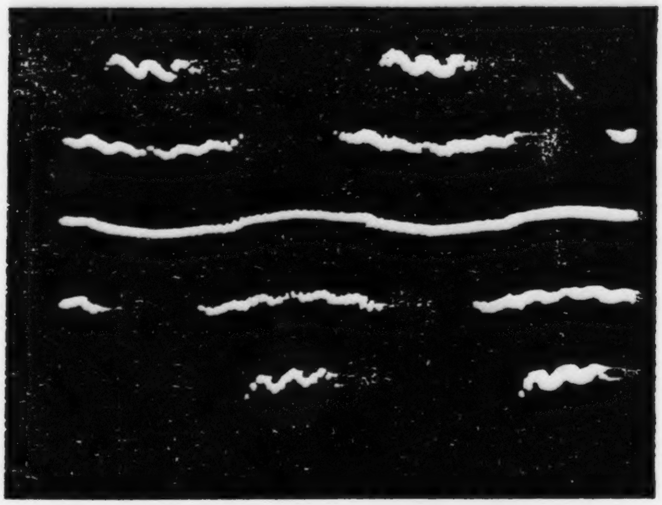

Vertical Scale: 10 V/div

Horizontal Scale: 10 msec/div

Figure 6.15 Photograph of the induction motor phase voltage at frequency = 20 Hzand PWM sampling frequency = 720 Hz.

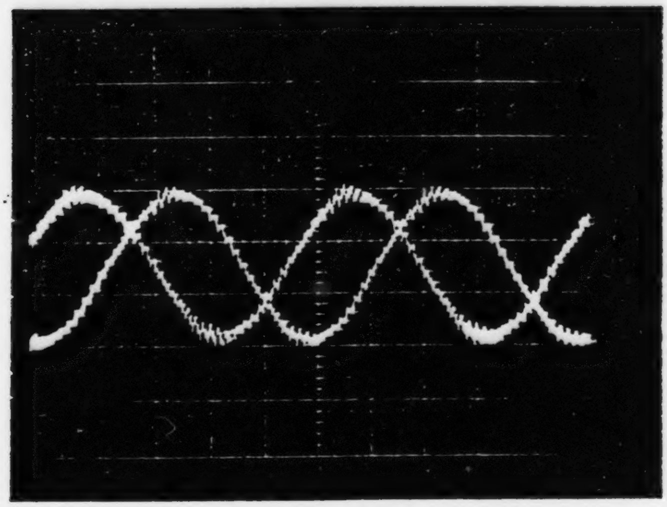

Vertical Scale: 5 Amp/div

Horizontal Scale: 10 msec/div

Figure 6.16 Photograph of two of the induction motor phase currents at frequency = 20 Hz and PWM sampling frequency = 720 Hz.

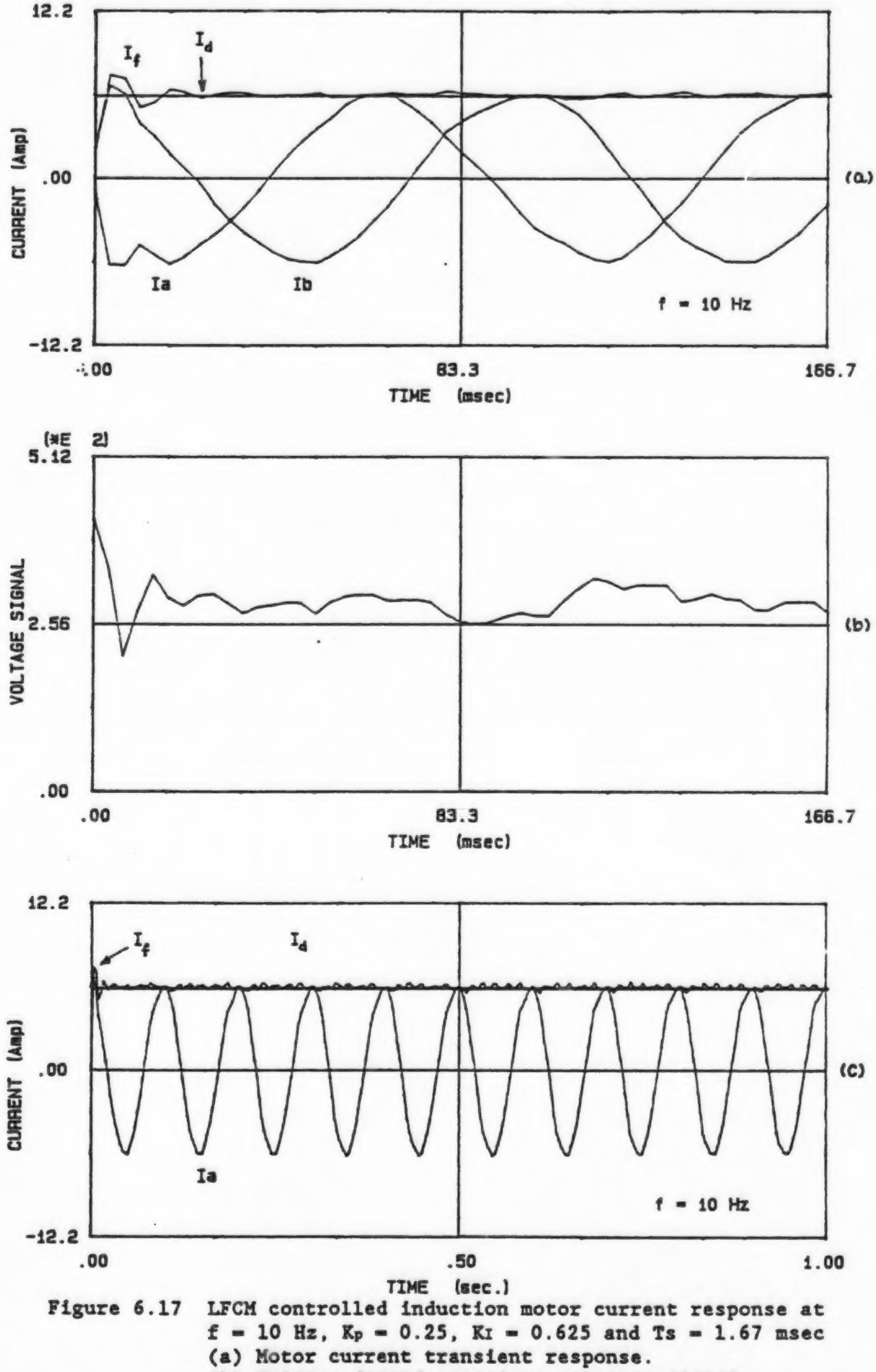

Figure 6.17 LFCM controlled induction motor current response at $f = 10$ Hz, $K_P = 0.25$, $K_I = 0.625$ and $T_s = 1.67$ msec
(a) Motor current transient response.
(b) Voltage demand transient response signal.
(c) Motor current steady state response.

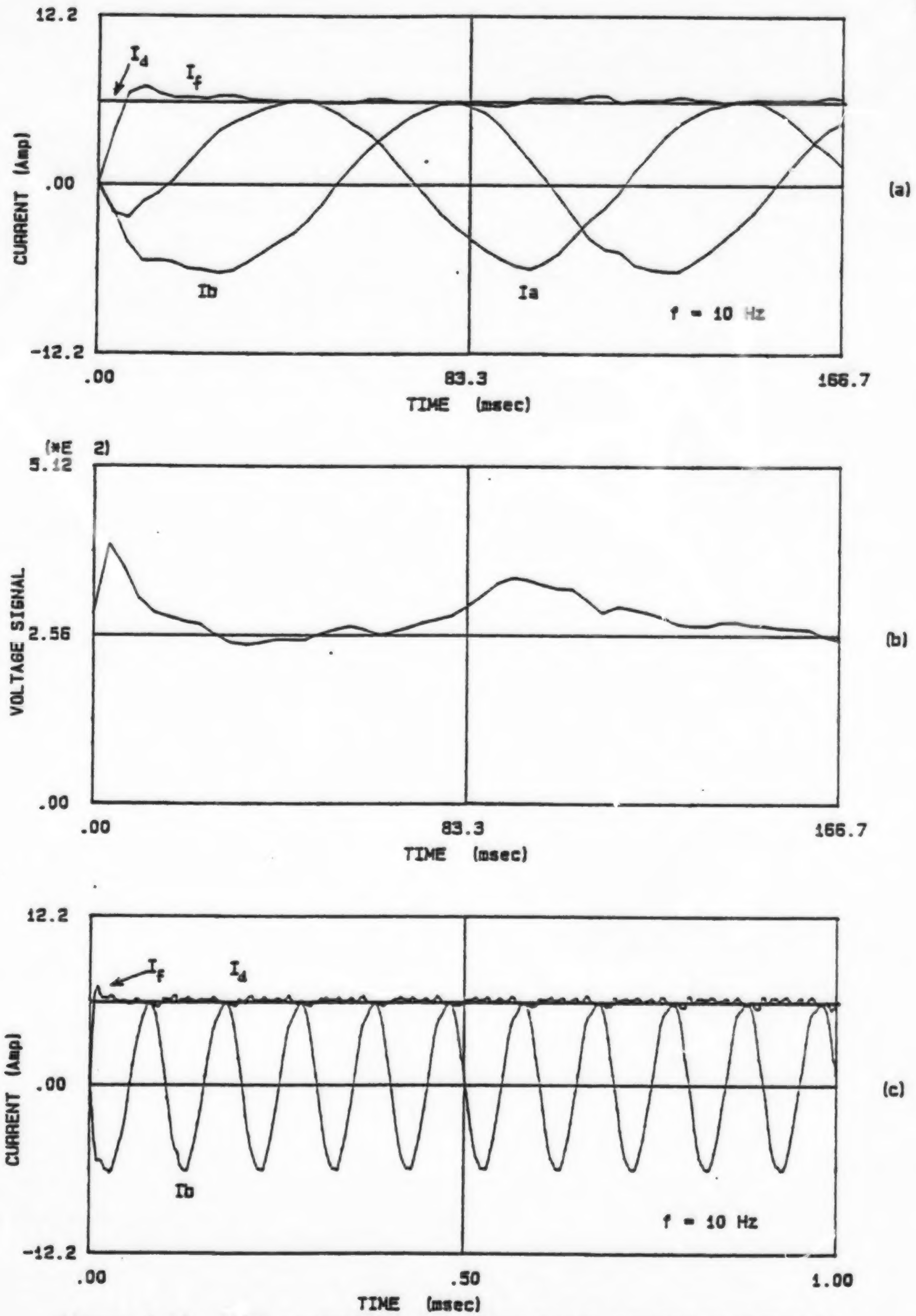

Figure 6.18 LFCM controlled induction motor current response at $f = 10$ Hz, $K_P = 0.25$, $K_I = 0.5$ and $T_S = 1.67$ msec
(a) Motor current transient response.
(b) Voltage demand transient response signal.
(c) Motor current steady state response.

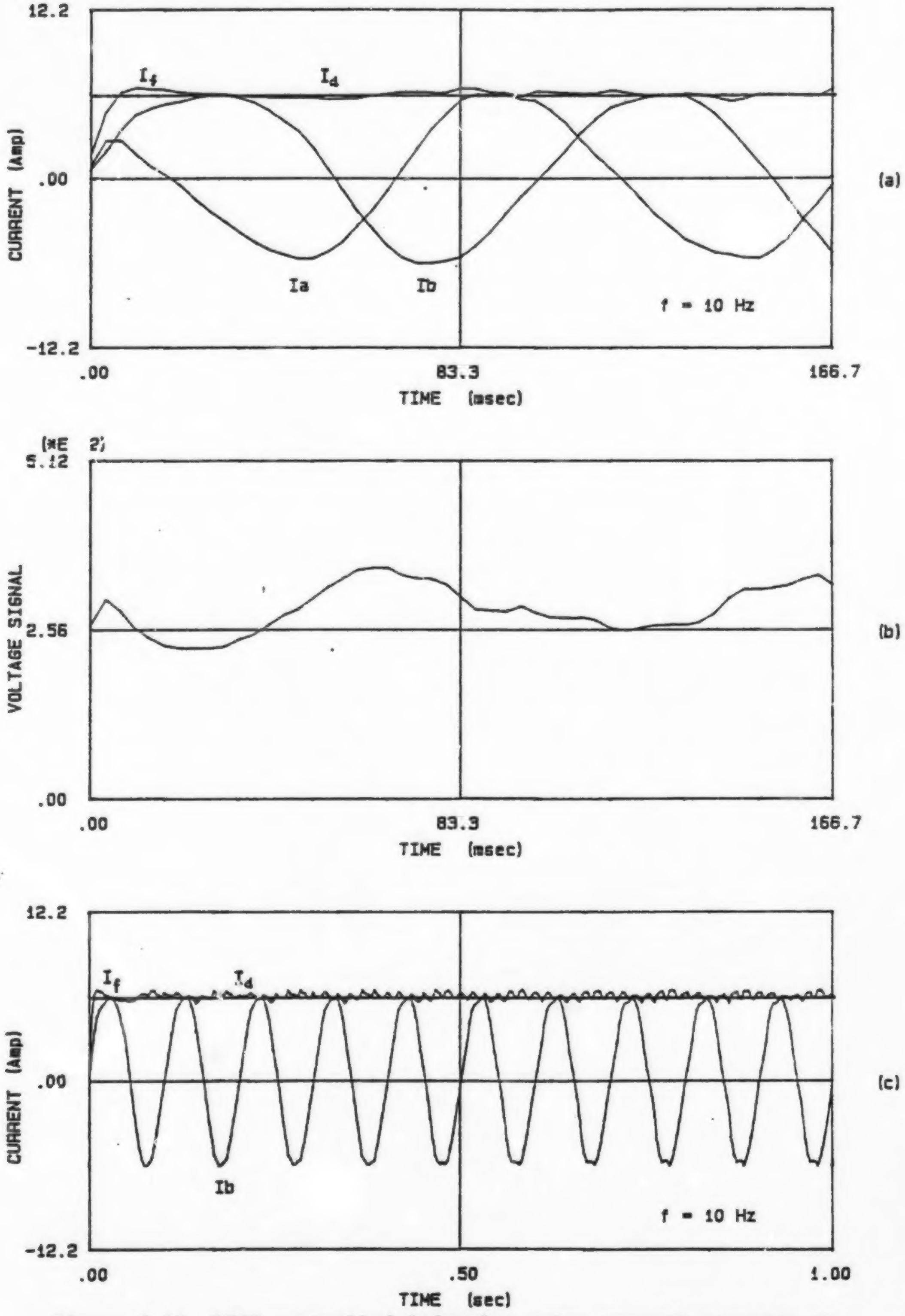

Figure 6.19 LFCM controlled induction motor current response at $f = 10$ Hz, $K_P = 0.375$, $K_I = 0.5$ and $Ts = 1.67$ msec;
(a) Motor current transient response.
(b) Voltage demand transient response signal.
(c) Motor current steady state response.

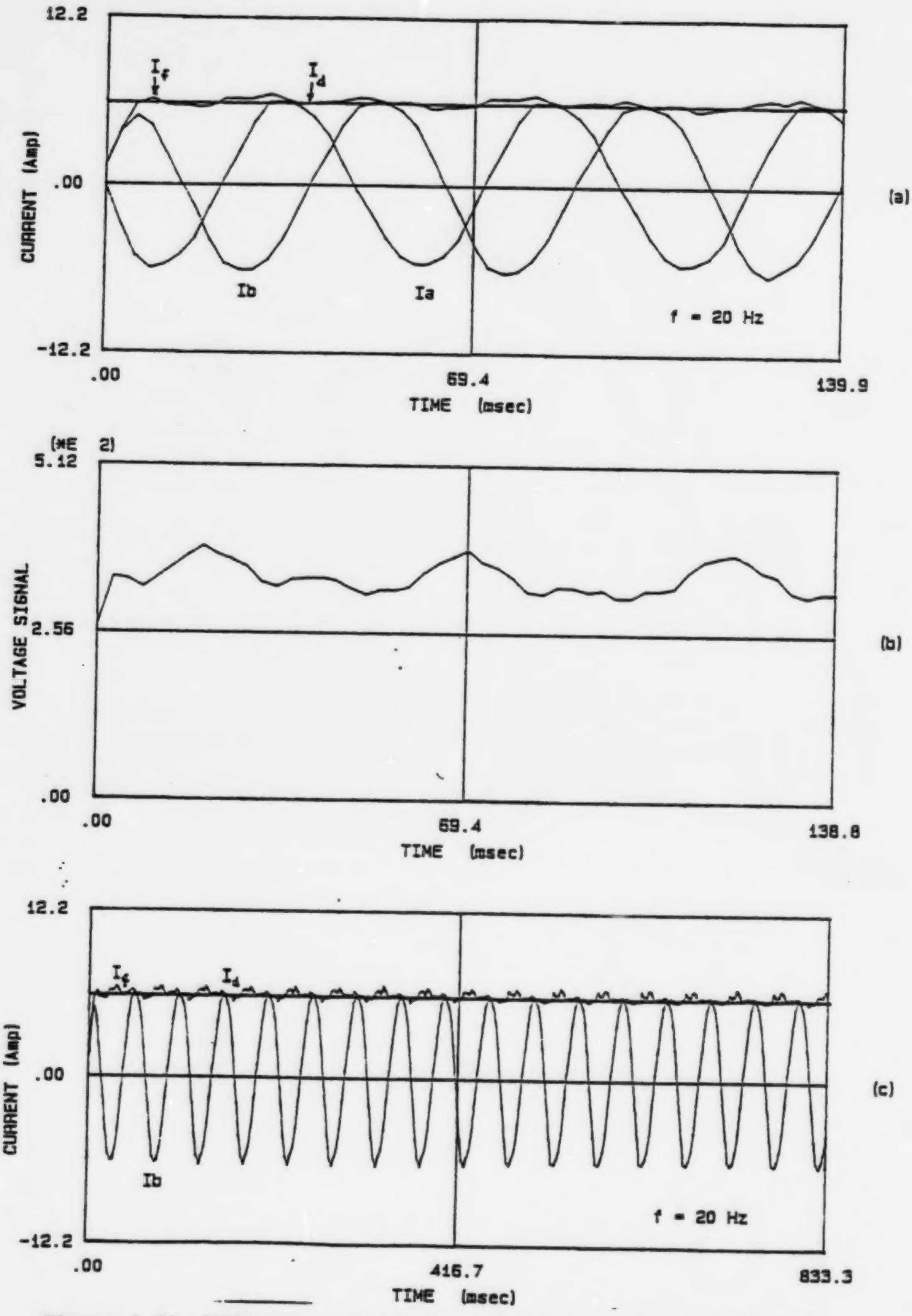

Figure 6.20 LFCM controlled induction motor current response at $f = 20$ Hz, $K_P = 0.375$, $K_I = 0.5$ and $T_s = 1.39$ msec;
(a) Motor current transient response.
(b) Voltage demand transient response signal.
(c) Motor current steady state response.

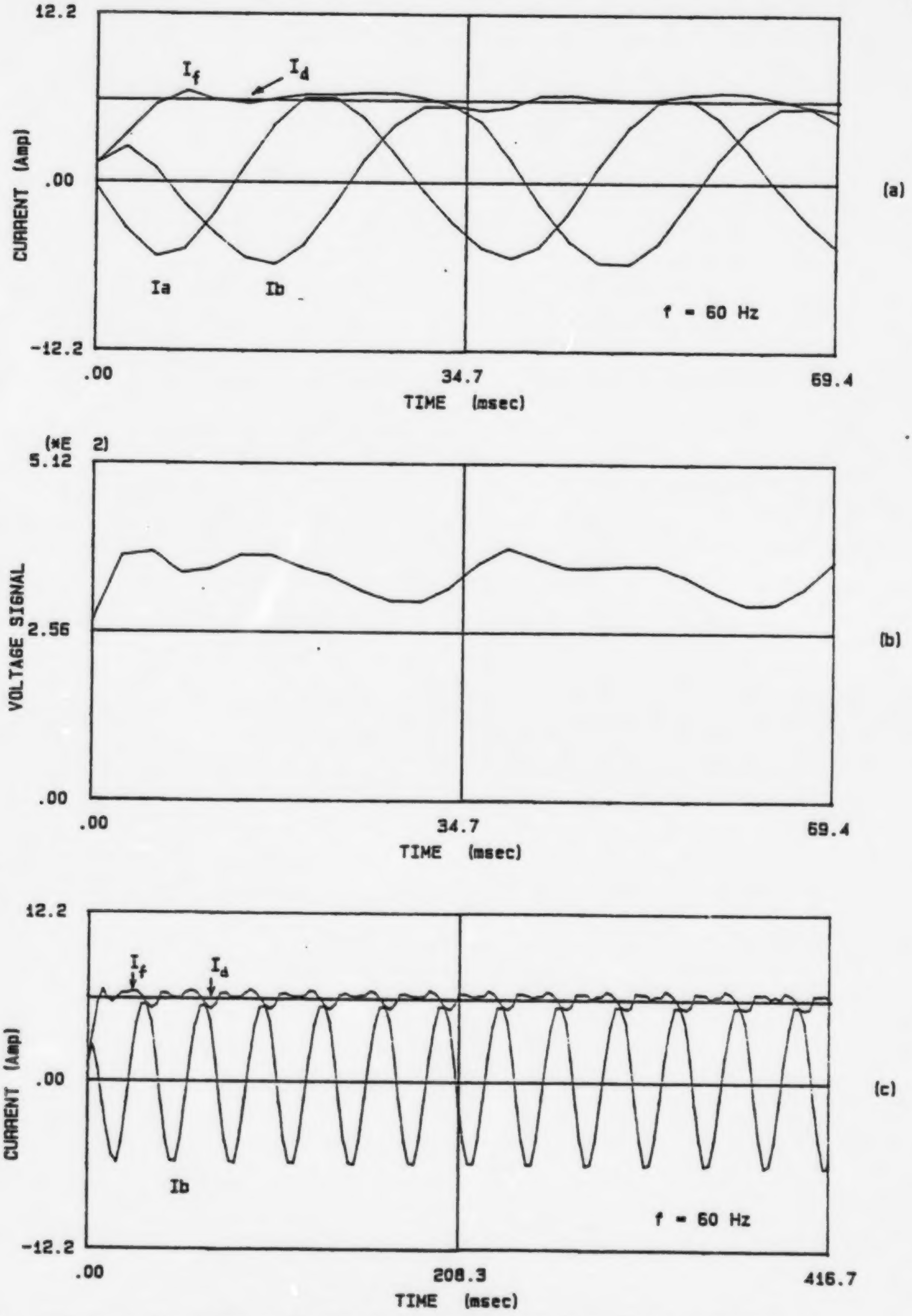

Figure 6.21 LFCM controlled induction motor current response at $f = 60$ Hz, $K_P = 0.375$, $K_I = 0.5$ and $T_s = 1.39$ msec
(a) Motor current transient response.
(b) Voltage demand transient response signal.
(c) Motor current steady state response.

essentially the control output of the PI controller, and it is used in the PWM unit to determine the pulsewidths. A summary of the test conditions for these test results is presented in Table 6.1.

Figure	Frequency (Hz)	Proportional Constant	Integral Constant	Sample Period (msec)
6.17	10	0.25	0.625	1.67
6.18	10	0.25	0.5	1.67
6.19	10	0.375	0.5	1.67
6.20	20	0.375	0.5	1.39
6.21	60	0.375	0.5	1.39

Table 6.1 Test condition summary for the LFCM current response test.

Figure 6.19 to 6.21 present the best current responses, where the proportional and integral constants are chosen to be 0.5 and 0.375 respectively. The responses are nearly at critical damping condition. These figures also illustrate that there is little effect on the current response even when the sample period is varied. In general, the current response of the system is fast. The rise time is approximately 6 msec, which is acceptable for the system application.

Before incorporating the position/velocity sensing unit into the group testing, the unit is examined individually to ensure the hardware interface and the software module are correctly implemented. Hence, the wheel is rotated manually to simulate the passing of vehicles, with position and velocity updates being performed accordingly. The testing is done at several different speeds, and for both the positive and negative travel directions. The velocity determined by the unit is corroborated by independent measurement. Figures 6.22 to 6.24 show some of the plots of vehicle position and velocity versus time. Figure 6.24, though it is different from the other two figures, delineates the operation of positioning a vehicle. The test results reveal that the position update is always within 5 mm accuracy, and the velocity update is within 10% of the independent measurement even though it appears slightly erratic in the velocity plots. The jittery result is primarily due to the inaccuracies in spacing between the magnetic strips on the wheel and the variations in the sensor airgap distance caused by the wobbling of the wheel.

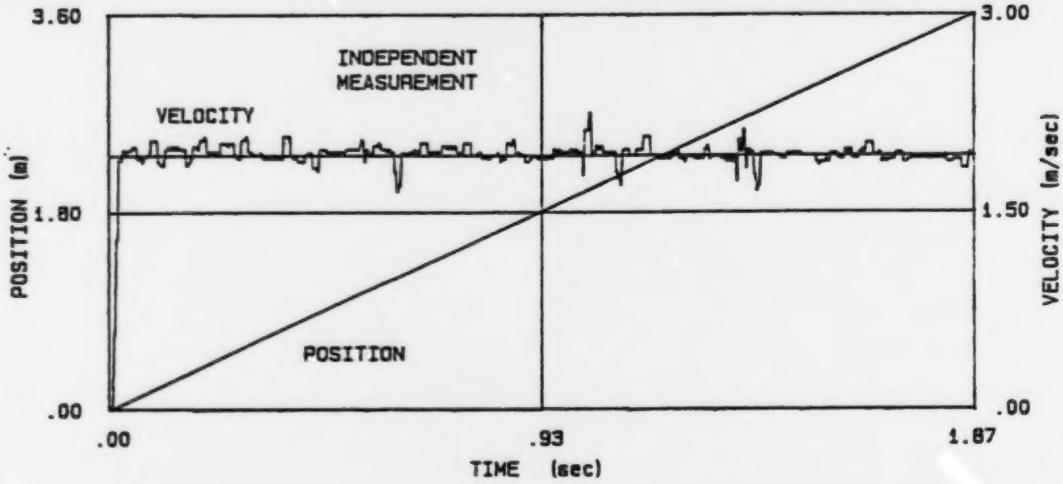

Figure 6.22 LFCM position and velocity updates when vehicle travelling in the forward direction.

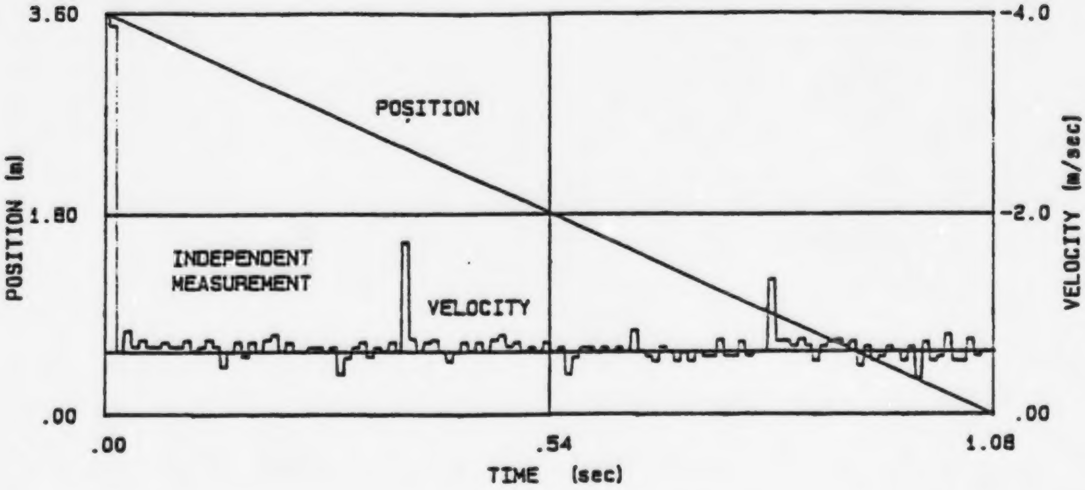

Figure 6.23 LFCM position and velocity updates when vehicle travelling in the reverse direction.

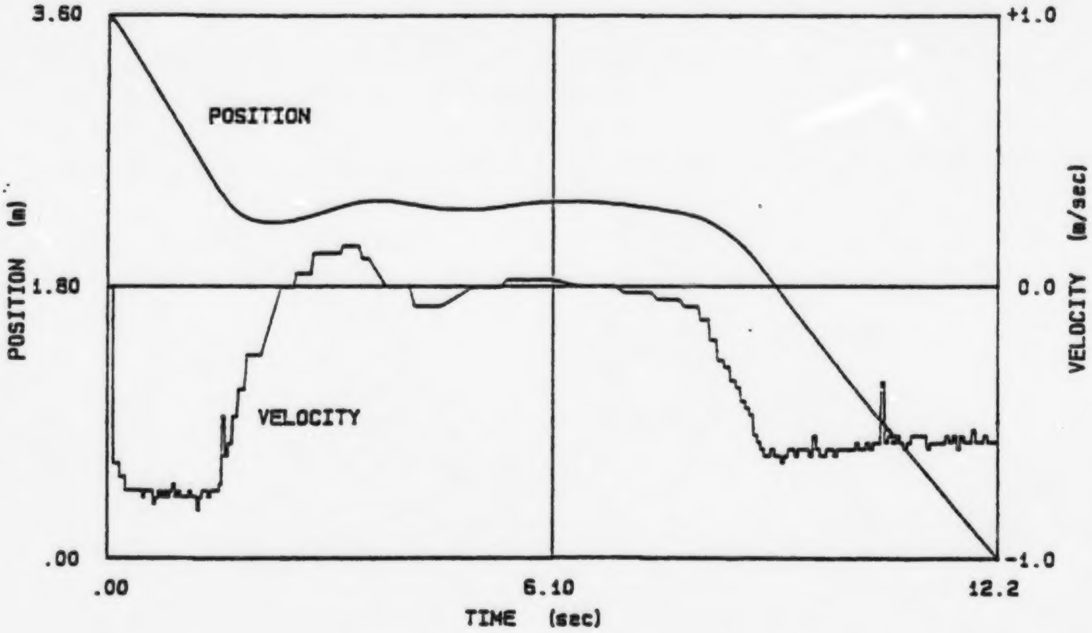

Figure 6.24 LFCM position and velocity updates during vehicle positioning operation.

As the final step in the test program sequence, all four control units, which are the entire control system as shown in Figure 3.5, are involved. However, because of the large inertia of the wheel and the low power PCU, precise speed control of the wheel is difficult. Hence, speed regulation tests are not included, and the open loop speed feedback means a constant demand torque is used. Also, the slip frequency control is arbitrarily set to 10 Hz for all velocities. However, in practice, the slip frequency/velocity profile would be determined from optimization analysis of the LIM performance.

Figure 6.25 illustrates the results of this overall system testing. Figure 6.25a shows the position and velocity updates from the time that the first magnetic strip is detected until the time that the last magnet is detected. Figure 6.25b shows the system operating frequency throughout the entire passage of the magnetec strips. As shown, when the sensor first detects the approach of a vehicle (ie. when the first magnetic strip is encountered), the motor is turned on with a constant demand current which is derived directly from the constant demand torque. The motor fundamental frequency was then set at 10 Hz, since it was zero initially and the demand slip-frequency was set at 10 Hz. In order to maintain the constant slip-frequency, the fundamental frequency increases in response to the increase of the wheel velocity. However, because of the low acceleration of the wheel due to its large inertia, the rate of the fundamental frequency change is rather small as depicted by the plot of demand slip-frequency versus time in Figure 6.25b. By the end of the vehicle passing (ie. when the last magnet is detected by the sensor), the motor frequency is at 11.5 Hz.

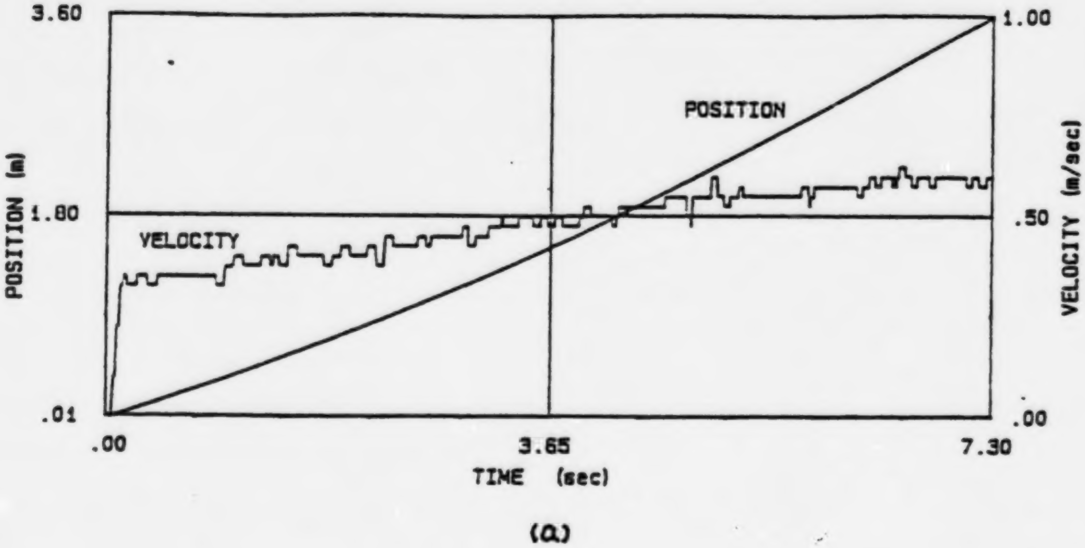

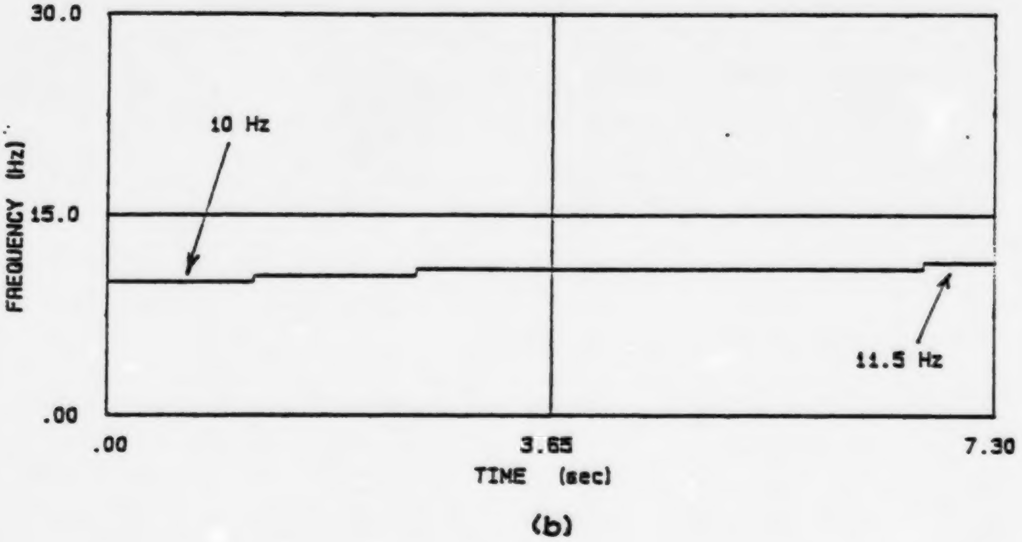

Figure 6.25 LFCM overall system operation at constant current and constant slip frequency
(a) Vehicle position and velocity versus time.
(b) Motor frequency versus time.

In summary, the comprehensive testing confirms the operation of the complete VVVF LIM controller, with the exception of the speed control loop. It demonstrates the successful operation of all the control unit functions. In general, the PWM unit is working satisfactorily and the harmonics of the system are low. The current response of the system is fast, and the position/velocity sensing unit produces accurate and reliable results.

CHAPTER 7:

CONCLUSIONS

7.1 Introduction

During the past ten years, linear motor drives have found wide appeal in propulsion drive applications, especially in the area of transit system. Recently, the Urban Transportation Development Corporation has developed a low-speed LIM-in-track propulsion system for material handling applications, using a variable-voltage fixed-frequency controller. The controller is known as the LIM voltage control module (LVCM). In this thesis work, a variable-voltage variable-frequency (VVVF) controller has been designed and implemented. The controller is known as the LIM frequency control module (LFCM). This controller improves the in-track LIM performance for material handling applications.

The objectives of the work reported in this thesis were:

(a) to design and implement a VVVF controller, which incorporates all necessary LIM control functions;

(b) to develop algorithms which will lend themselves to microcontroller implementation; and

(c) to demonstrate the successful operation of a VVVF controller.

In general, all of these objectives were successfully achieved. It is found that the microcontroller based LIM frequency control module (LFCM) is promising. Assessments and conclusions of the overall system are presented in the following section, and recommendations for the future work are considered in the final section of this chapter.

7.2 Assessments of the System

In this study, a microcontroller based LFCM has been successfully implemented. The control scheme is based on the slip frequency stator current method, in which the speed and thrust control of the motor are performed by slip regulation. A pulsewidth modulated (PWM) inverter drive is adapted in the implementation, and a regular sampled sinusoidal modulation scheme is chosen for the switching strategy. Independent control of inverter voltage and frequency are achieved for the system, in which the frequency demand is determined by a slip frequency control loop, and the voltage demand is generated by a current control loop. A frequency ratio is specifically assigned for each fundamental frequency, which ranges from 0.5 to 60 Hz in steps of 0.5 Hz, to meet the requirements for minimizing the voltage and current harmonics, and to facilitate the software implementation. The controller is capable of performing frequency switching up to every 1.4 msec (ie. every 1/12 cycle of a 60 Hz fundamental frequency, and phase sequence reversal every 2.8 msec (ie. every 1/6 cycle of the 60 Hz). This capability is required to obtain good dynamic control of the LIMs.

The inverter drive is a voltage source inverter (VSI), which though has no direct control over current as is the case of a current source inverter (CSI), but is more practical and economically feasible from the overall system perspective. Hence, a current feedback loop, using a PI controller, is applied to achieve a pseudo current control, and a quadrature current algorithm is employed to provide a quick determination of the feedback current magnitude. The current response of the system is generally fast; the rise time, in response to a step change of current demand, is approximately 6 msec.

For speed control, a closed loop control is implemented, again using a PI controller. The speed demand is governed by a position/velocity profile, which is pre-defined according the system requirement, and the position feedback. Slip regulation is achieved through the velocity feedback and a slip-frequency/velocity profile, which is pre-determined for optimum LIM performance characteristics. The slip and speed control tasks are running as the system background tasks at a interval of 0.1 second. The position and velocity feedback required by these two tasks are determined by a pair of Hall-effect sensors and some fault tolerant decoding logic. The results of the position and velocity updates are sufficient for good system operation. The position update is always within 5 mm accuracy, and the velocity update is mostly within 10% of the independent measurement.

A prototype of the system, which is based on the Intel 8097 microcontroller, has been successfully constructed. The prototype hardware has been kept to a minimum, and the majority of the system control is implemented by software programs. Hence, further changes or improvements in the system control scheme can be done simply by modifying the software programs, with minimal or no change to the hardware circuitry.

In this study, experimental results of the LFCM prototype have demonstrated the successful operation of the controller functions. In general, the system specifications are met; the transient response of the system is fast and the harmonic distortion of the system voltage and current are low. Although the closed loop speed control was not possible in the prototype testing, the work done in this thesis has shown great promise for the LIM-in-track application. Presently, research work is being carried out at UTDC to promote the system for the LIM-in-track applications.

7.3 Recommendations

Presently, the prototype LFCM is only designed for providing all the necessary LIM control functions. But in order to apply it in the LIM-in-track applications, there are many improvements needed to be made. Hence, possible future research areas and improvements are suggested as follow.

1. To investigate the implementation of a fault detection and alarm mechanism to detect sensor failures, inverter short-circuit or processor stalling.

2. To design a supervisory level of control for the LFCM, which would be responsible for all external communications, including communications with other LFCMs and a host computer, program downloading, system fault detection and emergency control. To implement this type of control, an additional microprocessor running in conjunction with the present microcontroller may be required.

3. To implement an emergency stop mechanism.

4. To finalize the circuit design and layout such that a printed circuit board can be used, and thus to reduce noise caused by the wiring connections.

5. To study the possibility of making the system more compact by integrating much of the digital circuitry into a custom VLSI chip.

6. To investigate a possible software implemented, short-circuit protection scheme for the inverter. Since most thyristors can normally withstand a current surge of 15 - 20 times of their rated values for one cycle, and the current response of the system is quite fast, the inverter may possibly be phased back [31] by the current controller when a current surge is detected.

7. To implement a more sophisticated digital low pass filter to reduce the noise from the velocity feedback.

8. To study the implementation of an adaptive control scheme for the PI current controller. Presently, the controller gains are carefully selected, under an assumption of a constant load condition, to provide a fast current response with little overshoot. However, in practice, the load time constant may vary during operation. Also, due to the 'end-effect' characteristics of LIMs, which is dependent on LIM speed, the motor parameters may vary at various speed. Thus, it is advantageous to have an adaptive control to adjust the controller gains at various operating conditions to maintain the desired current response.

REFERENCES

1. Boldea I. and Nasar S.A., "Linear Motion Electromagnetic Systems", John Wiley & Sons, Chapter 2, 1985.

2. Ballantyne W.J., "LIM-In-Track Propulsion System Description", Urban Transportation Development Corporation, Report No.454-810-001, pp.1-42, Aug. 1986.

3. Bose B.K., "Adjustable Speed AC Drive System", IEEE Press, pp.1-21, 1980.

4. Laithwaite E R., "Induction Machines For Special Purposes", George Newnes Limited, Chapter 1, 2 and 6, 1966.

5. Abbondanti A. and Zubek J., "Pulsewidth Modulated Inverter Motor Drives with Improved Modulation", IEEE Transactions on Industry Applications, Vol.IA-11, pp.695-703, Nov./Dec. 1975.

6. Bose B.K. and Sutherland H.A., "A High-Performance Pulsewidth Modulator for an Inverter-Fed Drive System Using a Microcomputer", IEEE Trans. Ind. Appl., Vol.IA-19, No.2, pp.235-243, Mar/Apr 1983.

7. Bowes S.R. and Mount M.J., "Microprocessor control of PWM inverters", IEE Proc., Vol.128, Pt.B, No.6, pp.293-305, Nov. 1981.

8. Grant T.L. and Barton T.H., "Control Strategies for PWM Drives", IEEE Trans. Ind. Appl., Vol.IA-16, No.2, pp.211-215, Mar./Apr. 1980.

9. Murphy J.M.D. and Egan M.G., "A Comparison of PWM Strategies for Inverter-Fed Induction Motors", IEEE Trans. Ind. Appl., Vol.IA-19, No.3, May/June 1983.

10. Pollmann A., "A Digital Pulsewidth Modulator Employing Advanced Modulating Techniques", IEEE Trans. Ind. Appl., Vol.IA-19, No.3, pp.409-414, May/June 1983.

11. Grant D.A. and Seidner R., "Ratio changing in pulse-width-modulated inverters", IEE Proc., Vol.128, Pt.B, No.5, pp.243-248, Sept. 1981.

12. Varnovitsky M., "A Microcomputer-Based control Signal Generator for a Three-Phase switching Power Inverter", IEEE Trans. Ind. Appl., Vol.IA-19, No.2, pp.228-234, Mar./Apr. 1983.

13. Acharya G.N., Shekhawat S.S., Shepherd W., Rao U.M. and Ng Y.M., "Microprocessor Based PWM Inverter Using Modified Regular Sampling Techniques", IEEE-IAS Annual Meeting, pp.1377-1385, 1984.

14. Deshpande V.V. and Doradla S.R., "Microprocessor (8085A) Based Multimode Pulsewidth Modulator", IEEE-IAS Conference Record, pp.3-11, 1986.

15. Pollmann A., "Software Pulse Width Modulation for μP Control of AC Drives",IEEE-IAS:26A Conference Record, pp.698-703, 1985.

16. John G., "Time Harmonics in Linear Induction Motors", Queen's University, Department of Electrical Engineering, M.Sc. Thesis, Chapter 2, 1985.

17. Fitzgerald A.E., Kingsley C.and Kusko A., "Electric Machinery", McGraw-Hill Book Company, Third Edition, Chapter 7 and 8, 1971.

18. Abbondanti A., "Method of Flux Control in Induction Motors Driven by Variable Frequency, Variable Voltage Supplies", IEEE-IAS International Semiconductor Power Converter Conference, pp.177-184, 1977.

19. Ballantyne J.W., "A Space-Harmonic Equivalent Network Model of the Linear Induction Motor", Queen's University, Master's Thesis, Chapter 2, 1985.

20. Phillips K.P., "Current-Source Converter for AC Motor Drives", IEEE Trans. Ind. Appl., Vol.IA-8, pp.679-683, Nov./Dec. 1972.

21. Blaschke F., "The Principle of Field Orientation as Applied to the New Transvector Closed-Loop Control System for Rotating-Field Machines, Siemens Review, Vol.34, pp.217-220, 1972.

22. Garbriel R., Leonhard W. and Nordby C., "Field-Oriented Control of a Standard AC Motor Using Microprocessors", IEEE Trans. Ind. Appl., Vol.IA-16, pp.186-192, Mar./Apr. 1980.

23. Ho E.Y.Y., "Decoupling Control of Induction Motor Drive System", Queen's University, Department of Electrical Engineering, M.Sc Thesis, Chapter 1 and 3, 1985.

24. Adkins B. and Harley R.G., "The General Theory of Alternating Current Machines", Chapman and Hall, Chapter 4, 1975.

25. O'Kelly O. and Simmons S., "Introduction to Generalized Electrical Machine Theory", McGraw-Hill, Chapter 7, 1968.

26. Intel, "Microcontroller Handbook", Intel Corporation, Chapter 1-6, 1985.

27. Reingold E. M. and Hansen W. J., "Data Structure", Little, Brown and Company, pp.332-339, 1983.

28. Intel, "PL/M-96 Programming Language User's Guide", Intel Corporation, 1985.

29. Intel, "ASM-96 Assemble Language User's Guide", Intel Corporation, 1985.

30. Intel, "iSBE-96 Single Board Emulator User's Guide", Intel Corporation, 1985.

31. Mok W.S., "Microcomputer Control of Induction Motor Drive Systems", Queen's University, Department of Electrical Engineering, M.Sc. Thesis, Chapter 4, 1980.

APPENDIX

Appendix A Hardware Features of Intel 8097 Microcontroller

The 8097 microcontroller consists of a 16-bit CPU coupled with data memory along with several I/O features all integrated onto a single piece of silicon. The CPU supports bit, byte and word operations. 32-bit double words are also supported for a subset of the instruction set. Table A.1 summaries the 8097 features and benefits. Figure A.2 shows the 8097 external memory timings.

FEATURES	BENEFITS
16-bit CPU	Efficient CPU with high throughput
232 bytes internal RAM	Large on-chip register file
Hardware MUL/DIV	Good math capability; 16 by 16 multiply or 32 by 16 divide in 6.5 μsec @ 12 MHz
6 addressing modes	Great programming flexibilty
High speed I/O unit - 4 dedicated I/O lines - 4 programmable I/O lines	Can mearsure and generate pulses with high resolution (2 μsec @ 12 MHz)
10-bit A/D converter	Allows external analog inputs
Full duplex serial port	Provides asynchronous serial link to other processors or systems
Up to 40 I/O ports	Provides TTL compatible digital data I/O including system expansion with standard 8 or 16-bit peripherals
Programmable 8 source priority interrupt system	Responds to asynchronous events and allows real-time programming
PWM output	Can generate analog output
2 16-bit timers	Synchronous events to real time
Watchdog timer	Ability to recover from software or hardware malfunction

Table A.1 8097 features and benefits summary.

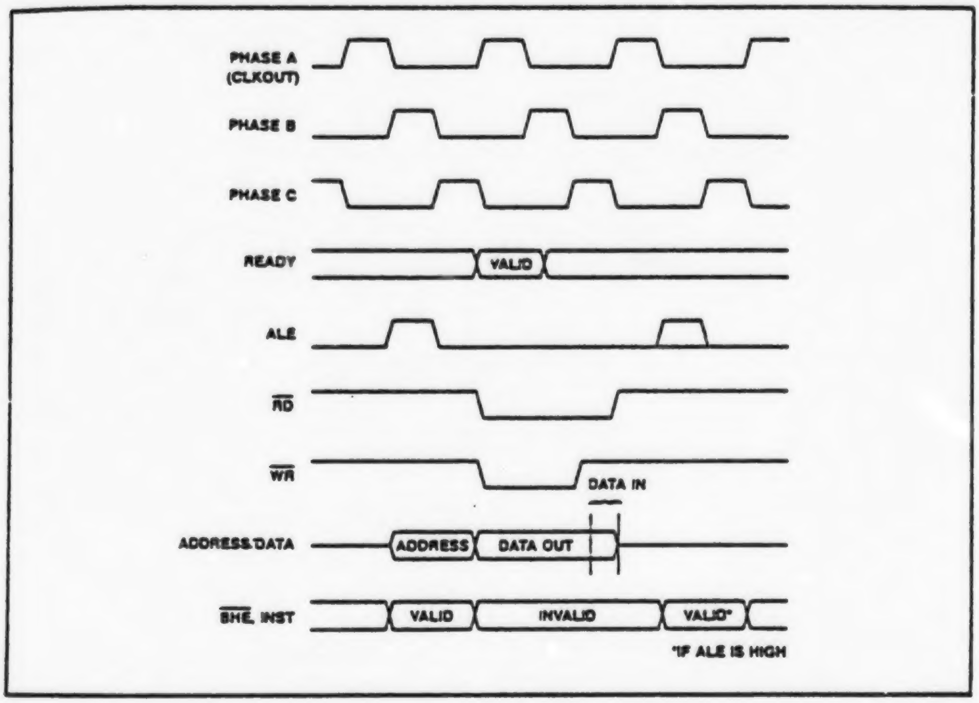
PHASE A
(CLKOUT)
PHASE B
PHASE C
READY
VALID
ALE
RD
WR
DATA IN
ADDRESS/DATA
ADDRESS
DATA OUT
BHE, INST
VALID
INVALID
VALID*
*IF ALE IS HIGH

Figure A.2 8097 external memory timings.

Appendix B LFCM Prototype Board Layout and Schematic

Figure B.1 presents the schematic diagram of the LFCM prototype and Figure B.2 illustrates the prototype board layout. As well, a detailed configuration of the memory address map and the chip select logic are shown in Figure B.3.

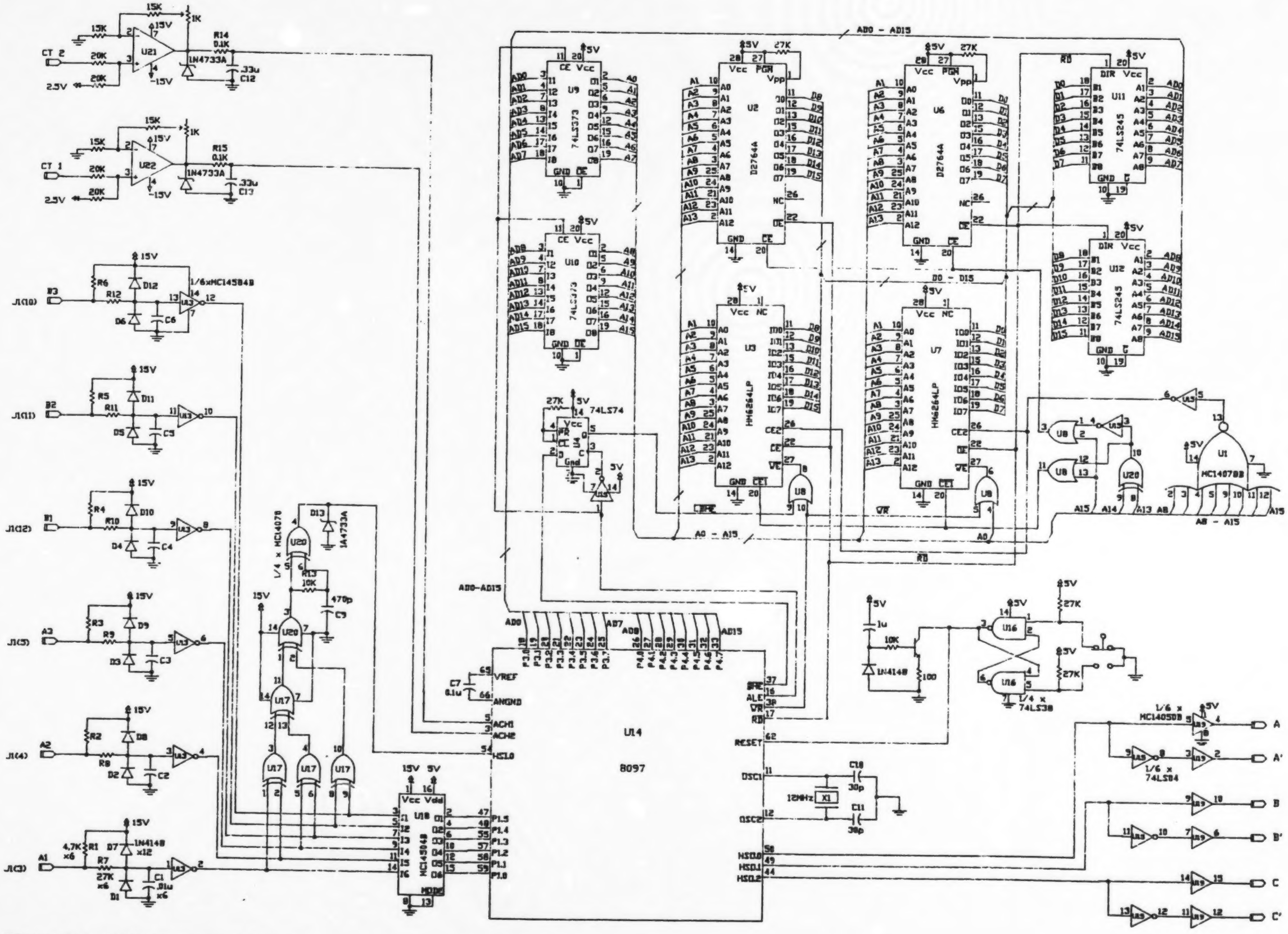
CT 2
CT 1
2.5V
U21
U22
1N4733A
R14
R15
C12
C13
J1(10)
J1(11)
J1(12)
J1(5)
J1(4)
J1(3)
B3
B2
B1
A3
A2
A1
1/6xMC14584B
U9
U10
74LS373
U2
U6
D2764A
U3
U7
HM6264LP
U11
U12
74LS245
74LS74
U4
U15
U8
U1
MC14078B
U16
1/4 x 74LS38
U17
U18
MC14504B
U20
1/4 x MC14070
U14
8097
12MHz
X1
1N4148
1/6 x MC14050B
1/6 x 74LS04
AD0 - AD15
A0 - A15
D0 - D15
A8 - A15
RESET
OSC1
OSC2
HSO.0
HSO.1
HSO.2
HSI.0
ACH1
ACH2
VREF
ANGND
ALE
WR
RD
A
A'
B
B'
C
C'

Figure B.1 LFCM prototype schematic.

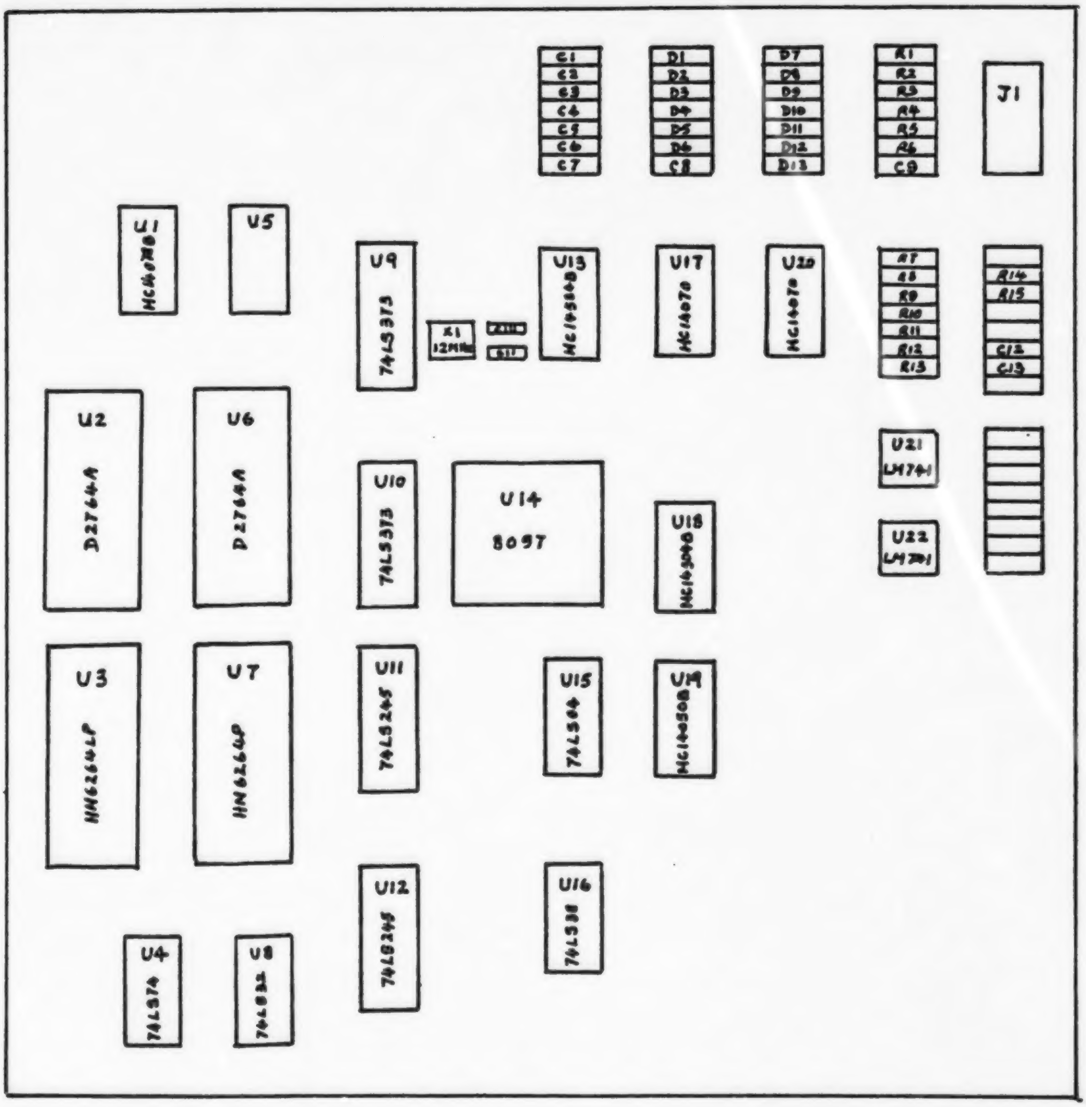
C1
C2
C3
C4
C5
C6
C7
D1
D2
D3
D4
D5
D6
C8
D7
D8
D9
D10
D11
D12
D13
R1
R2
R3
R4
R5
R6
C9
J1
U1
MC14070B
U5
U9
74LS373
X1
12MHz
U13
MC14508B
U17
MC14070
U20
MC14070
R7
R8
R9
R10
R11
R12
R13
R14
R15
C12
C13
U2
D2764A
U6
D2764A
U10
74LS373
U14
8097
U18
MC14504B
U21
LM741
U22
LM741
U3
HN6264LP
U7
HN6264LP
U11
74LS245
U15
74LS04
U19
MC14508B
U12
74LS245
U16
74LS38
U4
74LS74
U8
74LS32

Figure B.2 LFCM prototype board layout.

ADDRESS LINE	A15	A14	A13	A12	A11	A10	A9	A8	A7	A6	A5	A4	A3	A2	A1	A0	MEMORY LOCATION
INTERNAL RAM	0	0	0	0	0	0	0	0	X	X	X	X	X	X	X	X	$0000H-$00FFH
PORT 3 & PORT 4	0	0	0	1	1	1	1	1	1	1	1	1	1	1	1	X	$1FFEH-$0FFFH
RAM #1	0	0	0	X	X	X	X	X	X	X	X	X	X	X	X	0	$0000H-$0FFFH (EVEN BYTES-4Kb)
RAM #2	0	0	0	X	X	X	X	X	X	X	X	X	X	X	X	1	$0000H-$1FFFH (ODD BYTES-4Kb)
EPROM #1	0	0 1	1 0	X	X	X	X	X	X	X	X	X	X	X	X	0	$2000H-$5FFFH (EVEN BYTES-8Kb)
EPROM #2	0	0 1	1 0	X	X	X	X	X	X	X	X	X	X	X	X	1	$2000H-$5FFFH (ODD BYTES-8Kb)
RAM #1	0	1	1	X	X	X	X	X	X	X	X	X	X	X	X	0	$6000H-$7FFF (EVEN BYTES-4Kb)
RAM #2	0	1	1	X	X	X	X	X	X	X	X	X	X	X	X	1	$6000H-$7FFF (EVEN BYTES -4Kb)

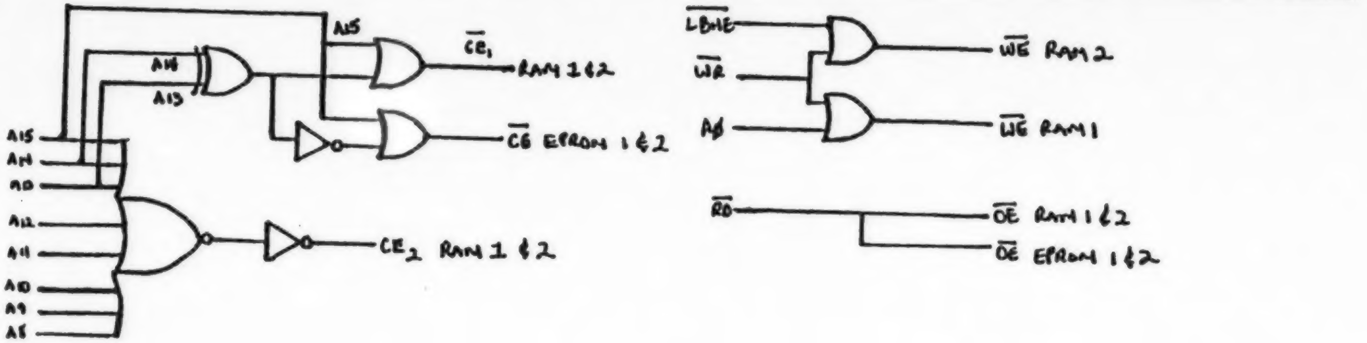
A15
A14
A13
A12
A11
A10
A9
A8
CE1 RAM 1&2
CE EPROM 1&2
CE2 RAM 1&2
LBHE
WR
A0
WE RAM 2
WE RAM 1
RD
OE RAM 1&2
OE EPROM 1&2

Figure B.3 LFCM prototype memory address map and chip select logic.

Appendix C Effect of DC Offset on Current Magnitude Calculation

Equation (C.1) shows the equation used in the control algorithm for the current magnitude calculation. The derivation of this equation is based on the assumption of balanced 3-phase currents.

$$I = \sqrt{4/3\ (I_a^2 + I_b^2 + I_a I_b)} \tag{C.1}$$

If the system is slightly unbalanced, the gains of the current sensor circuits should be adjusted appropriately to account for the difference. However, in doing so, the dc offset may be affected which may lead to errors in calculating current magnitudes. These errors can be derived as follows:

If only one dc offset is affected and the gain of one of the current sensor circuits is higher, the normalized current signals will become:

$$I_a = A \sin\theta \qquad \text{where} \quad A \approx 1 + \Delta$$

$$I_b = K_b + \sin(\theta - 120^\circ) \qquad K_b = \text{small}$$

and the terms used in the equation (C.1),

$$I_a^2 = A^2 \sin^2\theta$$

$$I_b^2 = K_b^2 + 2K_b \sin(\theta - 120^\circ) + \sin^2(\theta - 120^\circ)$$

$$I_a I_b = A\, K_b \sin\theta + A \sin\theta \sin(\theta - 120^\circ)$$

Therefore, the sum of these 3 terms becomes

$$\begin{aligned}\sum = {} & \sin^2\theta + \sin^2(\theta - 120^\circ) + \sin\theta \sin(\theta - 120^\circ) \\ & + K_b^2 + \Delta(\sin^2\theta + \sin\theta \sin(\theta - 120^\circ)) + 2K_b \sin(\theta - 120^\circ)\end{aligned}$$

where the first 3 terms are the desired ones for current calculation, and the last 3 three terms are the errors that may be introduced in the current calculation. In order to eliminate these errors, the hardware design of the current sensor interface should be modified. Instead of adding the dc offset to the incoming current signal and adjusting the control gain with the same op-amp circuit, two independent controls of dc offset and gain should be implemented as shown in Figure C.1. Also, to ensure that the circuit is functioning properly, a calibration procedure should be performed. The calibration procedure should be: (a) to adjust the dc offset signal such that the calculated current magnitude is zero when the two inputs to the sensor interface are grounded, and (b) to ensure that when two known magnitude signals from a balanced 3-phase system are input to the circuit, the calculated magnitude is the same.

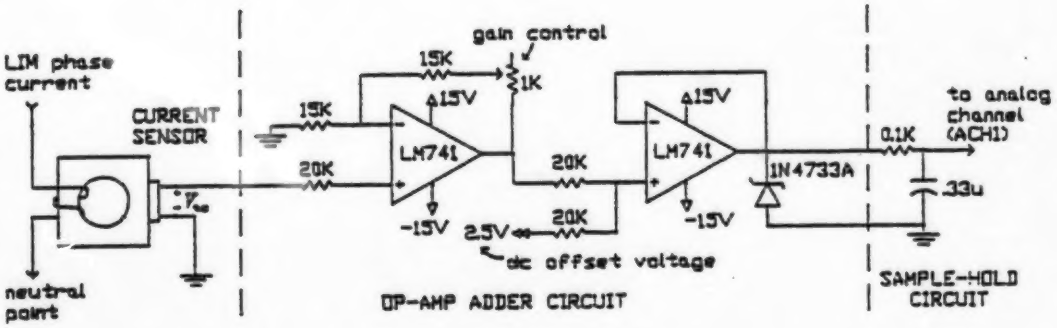
LIM phase current
CURRENT SENSOR
V_{oo}
neutral point
15K
15K
gain control
1K
20K
LM741
Δ15V
-15V
20K
20K
2.5V
dc offset voltage
LM741
Δ15V
-15V
1N4733A
OP-AMP ADDER CIRCUIT
0.1K
.33u
to analog channel (ACH1)
SAMPLE-HOLD CIRCUIT

Figure C.1 Modified current sampling interface.